THE ACADEMIC REGISTRAR
ROOM 261
UNIVERSITY OF LONDON
SENATE HOUSE
LONDON, WC1E 7HU

SAUDI ARABIA AND THE ARABIAN PLATE AS SHOWN

BY APOLLO 12 IMAGE OF THE EARTH

CAMERA USED : HASEL BLAD 70mm.

DETECTION OF SURFACE EVIDENCE OF SUB-SURFACE STRUCTURES BY INTERPRETATION METHODS OF LANDSAT IMAGERY IN THE SEDIMENTARY ROCKS OF CENTRAL SAUDI ARABIA

by

SHAHTA OMAR AL-KHATIEB

B.Sc., M.Sc.

DEPARTMENT OF GEOLOGY
ROYAL SCHOOL OF MINES
IMPERIAL COLLEGE OF SCIENCE AND TECHNOLOGY

A thesis submitted for the degree of Doctor of Philosophy in the University of London

1981

Dedicated to the memory of my late mother and grandmother.

To my dear father and my loving wife and to my dear son

and daughters Amre, Soad, Rana and Hadeel.

ABSTRACT

The application of different interpretation methods and techniques to Landsat multi-imagery in the analysis of lineaments of the gently easterly dipping sedimentary rocks of Najd Plateau and the eastern margin of the Arabian Shield have revealed the presence of a few important structures not known to occur in any previous literature and published maps of the area.

The quality, band, scale and processing techniques of images acquired under various atmospheric conditions proved to have some effect on the detection of subsurface structures. Selection of the right quality, processing and band of image depends to a great extent on the nature of the area and the surface evidence under investigation. The computer enhancement of band 7 increased the detectability of the images by at least 20%, while standard production of bands 5, 6 and 7 show some variations in their detectability if exposed under ideal atmospheric conditions where band 7 proved to be the best. Band 4 was found to be relatively less productive under the same conditions if some structural features are to be studied. The benefits of some interpretation methods, for example, fishing and systematic search are discussed.

The significance of the interpreted lineaments from images was analysed by directional frequency and length rose diagrams prepared by computer. The analysis in some areas was checked by field and other existing data.

The roughly N-S near meridional long, periodically spaced lineaments occupied by Precambrian intrusions, proved to be an old basement failure system extending across Saudi Arabia, such phenomenon also reported to occur in Nigeria, both seem to be a result of regional

scale crustal failure in the earth due to the effect of a great E-W stress if the E-W compressive stress field which produced both Hijaz and later Najd structures, is added. The Riyadh Fault System seems to be a result of a roughly N-S compressive stress field which took advantage of some of the pre-existing Najd faults and reversed their sense of movement.

The extension of Al-Amar-Idsas fault and the detection of the East Arabian Block which includes the majority of the giant hydrocarbon fields of Arabia, as well as some other detected structures such as Riyadh Tilted Block with its characteristic drainage pattern, Wadi Al-Atk and its related structures, are also revealed.

The sand dunes and sand cover with their characteristic nature which cover more than 30% of the area proved not to be a disadvantage always. Some subsurface failure zones of geological interest have been shown to have propagated upward through these sands and were clearly detected on the computer enhanced high pass filter images of band 7. The upward propagation of the deep seated structures seems to be affected by many variable factors in the different geological provinces of the area.

The detected structures in this study seem to highlight the structural framework of the Cover Rocks which may assist their evaluation as a host for mineral deposits.

ACKNOWLEDGEMENTS

The author wishes to thank many people and organizations who have generously provided academic, technical, financial and moral support during the course of this research. The author is very grateful for H.E. Sheikh Ahmed Zaki Yamani, his Deputy Minister for Mineral Resources, Sheikh Ghazi H. Sultan, A.R. Abu Rashid and staff of the Geology Department at the Directorate General of Mineral Resources for their help, support, and interest which made this research possible.

Thanks are also due to Mr. S. Rubaishi, Deputy Minister for Aerial Surveys and his staff for their continuous support in photographing necessary images for the research.

In particular, thanks to Dr.J.W. Norman for his supervision, guidance of the research and his encouragement with interesting discussions; also thanks to Professor G.R.Davis for his support and interest in the research. The author would like to thank Dr. K.J.Ackermann, General Manager of Riofinex Geological Mission,for his appreciated comments on English terminology and all his colleagues in Riofinex, Jeddah and London, especially Mr.K.Greenleaves and Mr.K.Clarke, for the great support received during the course of this research.

The author would also like to thank all the following: Department of Water Development at Ministry of Agriculture, Riyadh and their Contractors for their valuable bore hole data; Dr.J.Ferguson of the Imperial College for his complete support in computing the data; Professor D.J. Shearman for his remarks on English terminology on part of Chapter Three; Dr.P.L. Hancock and Dr. Kadhi for their interesting discussions on their work. Mrs. Pauline Lewis for typing the thesis. Thanks go to all my colleagues in the Photogeology Section, especially U.P. Dos Santos for his interesting and long lasting discussions.

CONTENTS

Chapter			Page No.
	Abstract		3
	Acknowledgement		5
	Contents		6
	List of Figures		14
	List of Tables		20
	List of Plates (in pocket)		22
	CHAPTER ONE		
	INTRODUCTION		
1.1	Description of the Area		23
	1.1.1	Location	23
	1.1.2	Accessibility	23
	1.1.3	Topography and geomorphology	25
	1.1.4	Climate	25
	1.1.5	Vegetation and human activities	27
1.2	The General Problem		28
1.3	Review of Previous Work		29
	1.3.1	Previous research	29
	1.3.2	Existing maps and data coverage	31
	1.3.2.1	Maps	31
	1.3.2.2	Aerial photographs	31
	1.3.2.2	Landsat images	33
	1.3.3	Previous research on the same field of study	33

Chapter			Page No.
1.4	Stratigraphy		33
	1.4.1	The Arabian Shield	35
	1.4.2	The Sedimentary Platform	36
1.5	Outline of the Structural Geology of the Arabian Peninsula		
	1.5.1	Tectonic setting of the Arabian Peninsula	37
	1.5.2	Regional structures of the Arabian Peninsula	40
	1.5.2.1	The Arabian Shield	42
	1.5.2.2	The Arabian Shelf	42
	1.5.2.2.1	The Interior Homocline	44
	1.5.2.2.2	The Interial Platform	45
1.6	Definitions of Terms and Abbreviations used in the Study		45

CHAPTER TWO

GENERAL CONSIDERATION OF IMAGERY INTERPRETATION

2.1	General Approach		50
2.2	Factors Controlling Image Interpretation		50
	2.2.1	Objective factors	51
	2.2.1.1	Scale of an image	51
	2.2.1.2	Resolution	51
	2.2.1.3	The quality of images	52
	2.2.1.4	Techniques of image viewing	52
	2.2.2	Subjective factors	53
	2.2.2.1	Physiological factors	54
	2.2.2.2	Psychological factors	54
	2.2.2.3	Human bias	56
	2.2.2.4	Repetitive interpretation	57

Chapter			Page No.
2.3	Imagery Used in the Study		58
	2.3.1	Standard production of bands 4,5 6,7 and infra-red colour composite	59
	2.3.1.1	Scale 1:1,000,000	60
	2.3.1.2	Scale 1:500,000	62
	2.3.2	Computer enhanced images	62
	2.3.3	Generated images	67
	2.3.3.1	Positive prints	68
	2.3.3.2	Negative prints	69
	2.3.4	Aerial photographs	69
	2.3.5	Application of landsat imagery	70
	2.3.5.1	Advantages of landsat images	70
	2.3.5.2	Disadvantages and limitations of landsat images	72
2.4	Atmospheric and Physical Factors Controlling Quality of Images (Seasonal Factors)		74
	2.4.1	Sun angle and Azimuth	75
	2.4.2	Soil moisture	77
	2.4.3	Temperature	77
	2.4.4	Rainfall (humidity in the atmosphere)	79
	2.4.5	Cloud coverage	82
	2.4.6	Winds and related dust and dust storms	82
	2.4.7	Other factors	83
2.5	Interpretation Procedures		84
	2.5.1	Preparation of images for analysis	85
	2.5.2	Interpretation methods	85
	2.5.2.1	Fishing method	86
	2.5.2.2	Systematic search	87

Chapter Page No.

	2.5.2.3	Application of multi-image technique	88
	2.5.3	Detection, identification and deduction of significance i.e. recognisability	90

CHAPTER THREE

METHODS OF PROCESSING, PRESENTATION AND ANALYSIS OF DATA

3.1	General Discussion		94
3.2	Presentation of Data		97
	3.2.1	Processing of data	97
	3.2.1.1	Advantages, limitations of computing	99
	3.2.2	Methods of presentation	101
	3.2.2.1	Directional rose diagrams	102
3.3	Analysis of Lineament Data		104
	3.3.1	Directional frequency rose diagrams	110
	3.3.1.1	General review	111
	3.3.1.2	Rose diagrams constructed from high pass filter 2nd generation and infra-red colour composites	118
	3.3.1.3	Correlations between rose diagrams of H.P.F.B.7 and I.R.C.C. images	123
3.4	Subtractions of Frequency Rose Diagrams		125
3.5	Effect of Various Factors on the Results		127
	3.5.1	Effects of objective factors	128
	3.5.1.1	Scale	128
	3.5.1.2	Effect of different multi-spectral bands	135

Chapter Page No.

	3.5.1.3	Effect of photographic processing (generated images)	138
	3.5.1.3.1	Negative prints	138
	3.5.1.3.2	Positive prints	143
	3.5.1.4	Computer enhancement	147
	3.5.1.4.1	First generation	147
	3.5.1.4.2	Second generation	148
	3.5.1.5	Effect of illumination source	148
	3.5.2	Effect of subjective factors	151
	3.5.2.1	Human bias	151
	3.5.2.1.1	Difference in human bias between two interpreters	152
	3.5.2.1.2	Difference in human bias between three interpreters	155
	3.5.2.2	Effect of experience by the same interpreter	158
	3.5.3	Effect of atmospheric factors	161
3.6	Correlation of Directional Frequency and Length Rose Diagrams		168

CHAPTER FOUR

DETECTED STRUCTURES

4.1	General Discussion		176
4.2	Extension of the Al-Amar-Idsas Basement Fault Under the Phanerozoic Cover Rocks		177
	4.2.1	Al-Amar-Idsas Fault in the basement	180
	4.2.2	Evidence of movement in the sedimentary rocks	184

Chapter | Page No.

4.3	Riyadh Tilted Block		189
	4.3.1	General discussion	189
	4.3.2	The photogeological phase	195
	4.3.3	Field investigations	200
	4.3.4	Trend surface computer programme	202
4.4	East Arabian Block		206
	4.4.1	Wadi Al-Batin segment	208
	4.4.2	Al-Hamudiyah arcuate lineament	210
	4.4.3	Central Arabian Graben and Trough System (C.A.G.T.S.)	214
4.5	Wadi Al-Atk and Related Structures		220
	4.5.1	Wadi Al-Atk	220
	4.5.2	Khashm Al-Haqaqa lineament	225
	4.5.3	Al-Butayn-Himar Sabha structure	226
4.6	The Riyadh Fault System		231
	4.6.1	General discussion	231
	4.6.2	Interpretation phase	233
	4.6.3	Current and previous ground investigations	236
4.7	North-South Periodically Spaced Lineaments		240
	4.7.1	Evidence in the Shield	250
	4.7.2	Evidence in the sedimentary rocks of the Arabian Shelf	252
4.8	Circular, Elliptical and Arcuate Features		259
	4.8.1	Circular, semi-circular and elliptical features	260
	4.8.1.1	Detectability of circular features on landsat images	260

Chapter Page No.

	4.8.1.1.1	Circular features in the Shield	262
	4.8.1.1.2	Circular features in sedimentary rocks near to the basement	263
	4.8.1.1.3	Circular features in relatively thick sedimentary rocks	264
	4.8.1.1.3.1	5 - 10 km radius	266
	4.8.1.1.3.2	10 - 30 km radius	266
	4.8.1.2	Detectability of circular features on different images	267
	4.8.1.3	Small circular features on aerial photographs	268
	4.8.2	Arcuate features	269
	4.8.2.1	Arcuate features in Precambrian rocks	270
	4.8.2.2	Arcuate features in sedimentary rocks	274
4.9	Detection of Lineaments Through Surface Sand Cover		275
	4.9.1	The northern extension of Al-Amar-Idsas Basement Fault	278
	4.9.2	Barrah and Majma'ah Grabens continuity	279
	4.9.3	Al-Hamudiyah arcuate and straight lineaments	280

CHAPTER FIVE

PROPAGATION OF SUBSURFACE FAILURES

5.1	General Discussion		284
5.2	Factors Enhancing Generation and Propagation of Lineaments		287
	5.2.1	Tectonic effect	287
	5.2.2	Fatigue effect	287

Chapter | Page No.

	5.2.2.1	Earth tides	287
	5.2.2.2	Seismic activity	288
	5.2.2.3	Rotational effect	291
	5.2.3	The gravitational effects	291
	5.2.3.1	Differential consolidation	292
	5.2.3.2	Isostatic adjustment	293
5.3	Factors Affecting and Controlling Propagation		293
	5.3.1	Inhomogenuity of tectonic history	294
	5.3.2	The general stratigraphy of the overlying rocks	294
	5.3.2.1	Summary of the stratigraphic sequence	295
	5.3.2.2	Nature and relations of rock types in a vertical succession	296
	5.3.2.3	Thickness of overlying sediments	296
	5.3.3	Unconformities	297
	5.3.4	Logged aquifers (hydraulic effect)	300
5.4	Summary of Propagation		301
5.5	Correlation of Basement and Sedimentary Rock Lineaments		302
	5.5.1	General discussion	302
	5.5.2	Lineaments in Precambrian rocks	304
	5.5.3	Lineaments in sedimentary rocks near the Basement	308
	5.5.4	Lineaments in sedimentary rocks away from Basement	309
	5.5.5	Summary of correlation	310
		References	312
		Appendix	318

LIST OF FIGURES

Figure		Page No
1.	Generalized map of Saudi Arabia showing location of thesis area. Approx. scale 1:20,000,000.	24
2.	Index map of 1:500,000 scale geological and topographical maps of Saudi Arabia.	32
3.	Arabian and surrounding lithospheric plates.	39
4.	Plate boundaries and the relative motions between plates.	41
5.	Plate boundaries and the relative motions of the Arabian, Nubian and Somalian Plates.	41
6.	Structural provinces of the Arabian Peninsula.	43
7.	Landsat index map of Saudi Arabia showing multi-imagery scale 1:1,000,000 used in the study.	61
8.	Landsat index map of Saudi Arabia showing multi-imagery scale 1:500,000 used in the study.	63
9.	Linear contrast stretch of portion of band 4.	66
10.	Localities where hydrological data over the area were collected.	78
11.	Total number of multi-imagery interpretations and dates of imaging.	78
12.	Average air temperatures.	80
13.	Average wind speed and directions.	80
14.	Average relative humidity.	81
15.	Average rainfall in millimeters.	81
16.	Interpretation procedure in the early stage of research.	92
17.	Outcrop traces of major faults of Najd Fault system in the Arabian Shield.	107
18.	Hijaz Fault System, mainly represented by the N-S trend.	109

Figure		Page No
19.	Lineament analysis of Himar-Sabha Structure.	132
20.a	Directional frequency rose diagrams of Khashm Al-Juair Area constructed from interpretations of aerial photomosaic scale 1:120,000 (left) and 1:1,000,000 scale Ce_2 image (right).	134
20.b	Directional frequency rose diagrams of Himar-Sabha area constructed from aerial photographs scale 1:60,000 (left) and part of I.R.C.C. image scale 1:500,000 (right).	134
21.	Directional frequency rose diagrams showing the possible effects of different MSS bands at two scales on the interpretation, scene 178/43.	136
22.	Directional frequency rose diagrams of interpretations of MSS bands of S.p. and N.p. images of the same scene 178/43.	141
23.	Directional frequency rose diagrams of interpretations of Ce_1(A) and images generated by photographic processing scale 1:1,000,000.	146
24.	Lineament analysis and their directional frequency rose diagrams of image 179/43 band 7 of scale 1:500,000 by two interpreters (A and B) showing human bias effect.	154
25.	Lineament analysis and their directional frequency rose diagrams of image 178/43 Ce_2, scale 1:1,000,000 by three interpreters (B, A and C) showing human bias effect.	156

Figure		Page No
26.	Directional frequency rose diagrams from interpretations of an image:	159
	a. covering a well known and structurally important area; images were available in the early stage of research.	159
	b. areas which do not include important structures, images were available later in the research.	159
27.	Directional frequency rose diagrams from interpretations of images covering the same areas acquired in the dry season (A) and the wet season(B).	163
28.	Basic data of lineament analysis as shown by a computer print out.	173
29.	Modified tectonic map - Kingdom of Saudi Arabia.(in pocket)	
30.	Structures(syncline and anticline) in the Jilh Formation at Khashm Al-Juair area : Effect of Al-Amar Idsas Basement Fault.	179
31.	Relative frequency rose diagrams on both sides of Al-Amar-Idsas Fault showing relatively less disturbing effect in the sedimentary rocks than in the basement.	181
32.	Extension of Al-Amar Idsas Fault in the sedimentary Cover Rocks.	183
33.	Metalliferous belt in Al-Amar-Idsas Fault Region scale 1:2,000,000.	185
34.	Lithogeochemistry of the Jilh Formation carbonates of Khashm Al-Juair Structure. The axial trace of anticline.	187
35.	The en echelon shaped structures of the Central Arabian Graben and Trough System.	190

Figure		Page No
36.	Riyadh Tilted Block with the structurally controlled drainage.	192
37.	Relative frequency rose diagrams showing lineament analysis of areas inside (A) and outside (B) The Riyadh Tilted Block.	195
38.	Wadi Waybayr Monocline.	197
39.	Topographic contour map of the Riyadh Tilted Block and the surroundings areas.	199
40.	Predicted surface of top of Dhruma and top of Marrat Formations indicating a tilt of 5° to the N63 ^{o}E.	201
41.	Assymetrical contours of residual values on the top of Dhruma and Marrat formations due to tilting of the Riyadh Block.	201
42.	Linear trend surface to top of Dhruma Formation.	203
43.	Linear trend surface to top of Marrat Formation.	205
44.	East Arabian Block and its present boundaries in relation to Arabian Plate.	207
45.	Geology of the East Arabian Block.	209
46.	Principal structural and photo-tectonic elements of the East Arabian Block.	211
47.	Wadi Al-Batin and its possible effect on the surrounding geology.	213
48.	Al-Hamudiyah lineaments A-B, C-D in relation to Wadi Al-Batin.	215
49.	Long arcuate features interpreted from Landsat imagery and geological maps.	217
50.	Possible mineralized basement areas under Cover Rocks.	219

Figure		Page No
51.	Wadi-Al-Atk and Khashm Al-Haqaqa structures.	221
52.	Al-Butayn-Himar Sabha structures.	227
53.	Riyadh Fault System.	232
54.	Arabian Shield and Red Sea structures.	234
55.	Linear fault traces in basement and Cover Rocks as revealed from Landsat imagery interpretations and aeromagnetic map of Wadi Addawasir area.	237
56.	Lineaments interpreted from Landsat images showing clear NE pattern in the Wadi Addawasir area.	238
57.	Map showing approximate N-S trend and characteristic spacing pattern of post-tectonic (gp) granites and Tertiary volcanic cones.	242
58.	N-S alignment of basic and ultrabasic intrusions with characteristic spacing pattern.	247
59.	Generalized geological map of Nigeria showing position of a N-S periodically spaced directions.	249
60.	Alternating 'highs' and 'lows' in the structural contours in the Arabian Shelf Region.	253
61.	Diameters of domal features related to bedrock in the Cover Rocks.	265
62.	Arcuate features interpreted from S.p. band 5 showing several overlapping impact effects.	271
63.	Arcuate features interpreted from Ce_2(A) and contrast stretched (B) images covering the same area as Figure 62, showing the effects of quality, band and processing on interpretation.	273

Figure		Page No
64.	Schematic cross section illustrating the behaviour of well rounded quartz grain sands during upward propagation of a subsurface linear feature.	282
	a. linear feature with a negative physiographic nature.	282
	b. linear feature with a positive physiographic nature.	282
65.	Seismic activity (distribution of earthquakes) around the Arabian Plate boundaries, recorded between 1961 - 1975.	289
66.	Generalized cross section in the sedimentary Cover Rocks.	298
67.	Directional frequency rose diagram map based on interpretations of 1:1,000,000 scale Ce_2 images.	303
68.	Directional frequency rose diagram map based on interpretations of 1:500,000 scale I.R.C.C. images.	305

LIST OF TABLES

TABLE		Page No.
1.	Generalised stratigraphy of sedimentary rocks, Central Saudi Arabia, after Powers et al (1966)	34
1.A	Colour composite images and true colours they represent on the ground.	60
2.	Summary of correlation between H.P.F.B7 and their derivatives with S.p. images bands 4,5,6,7 and I.R.C.C. of the thesis area.	71
2.A	Expected effects of wet and dry season factors on detectability and interpretability of images.	76
3.	Correlation of lineaments basic data acquired from interpretations of H.P.F.B7 and I.R.C.C. images scale 1:1,000,000 and 1:500,000 respectively.	124
4.	Correlation of lineaments basic data acquired from interpretation of S.p. images bands 4,5,6,7 and I.R.C.C. scale 1:1,000,000 and 1:500,000 (178/43 Riyadh area).	130
5.	Correlation of lineaments basic data acquired from interpretations of S.p. and N.p. bands 4,5,6,7 scale 1:1,000,000 (178/43 Riyadh area).	139
6.	Correlation of lineaments basic data acquired from interpretations of H.P.F.B7 first generation and images generated from them scale 1:1,000,000.	144
7.	Correlation of lineaments basic data acquired from interpretations of Ce_1 and Ce_2 images scale 1:1,000,000. (two S.p. images are included for further correlation).	148

TABLE		Page No.
8.	Lineaments basic data and background correlation showing the effect of human bias on interpretations of the same image 179/42 band 7 scale 1:500,000, by two interpreters A and B.	153
9.	Lineaments basic data and background correlation showing the effect of human bias on interpretations of the same image 178/43 Ce_2 scale 1:1,000,000, by three interpreters B, A and C.	157
10.	Correlation of lineaments basic data acquired from interpretations of images of the same scenes exposed under dry and wet season conditions scale 1:1,000,000.	166
11.	Correlation of the nature of N-S periodically spaced lineaments in Saudi Arabia and Nigeria.	256
12.	Correlation of lineaments basic data acquired from interpretations of H.P.F.B7 images covering areas in different geological provinces.	307

LIST OF PLATES

Plate

1. General rose diagrams (relative fracture frequency)

   A - 1:1,000,000 scale interpretation overlays (multi-imagery)

   B - 1:500,000 scale interpretation overlays (multi-imagery)

2. General rose diagrams (relative fracture length)

   A - 1:1,000,000 scale interpretation overlays (multi-imagery)

   B - 1:500,000 scale interpretation overlays (multi-imagery)

3. Selected rose diagrams (fracture frequency)

   A - 1:1,000,000 scale Ce_2 images

   B - 1:500,000 scale I.R.C.C. images

4. Selected rose diagrams (fracture length)

   A - 1:1,000,000 scale Ce_2 images

   B - 1:500,000 scale I.R.C.C. images

*5. Selected rose diagrams (relative fracture frequency)

*6. Selected rose diagrams (relative fracture length).

7. Geological map of the Arabian Peninsula, scale 1:4,000,000 (D.G.M.R.)

---

* Included for further correlation. The rose diagrams are exactly the same as in 3 and 4 but showing frequency and length in percentages rather than absolute number.

CHAPTER ONE

INTRODUCTION

1.1 DESCRIPTION OF THE AREA

The Kingdom of Saudi Arabia is a large country of about 2.2 million km^2, occupying about three fourths of the Arabian Peninsula.

The country has a great range of relief, climate, geology, and scenery, from the temperate heights of the rugged mountains and hills which occur on the Precambrian Shield in the west, to the great, dry, sandy Rub'al Khali desert in the southeast, and the slightly tilted Najd Plateau in the central and eastern parts.

1.1.1 Location

This research deals mainly with the area of Phanerozoic sedimentary rocks of central Saudi Arabia and partly with the eastern edge of the Precambrian shield.

The study area includes the main part of the Najd Plateau, in the Najd Province, and western and northern regions of the eastern (Hassa) Province. The latter includes the giant Saudi Arabian oil fields. (Figure 1)

1.1.2 Accessibility

The study area generally has low relief. A national highway system provides easy access in to the area, and numerous

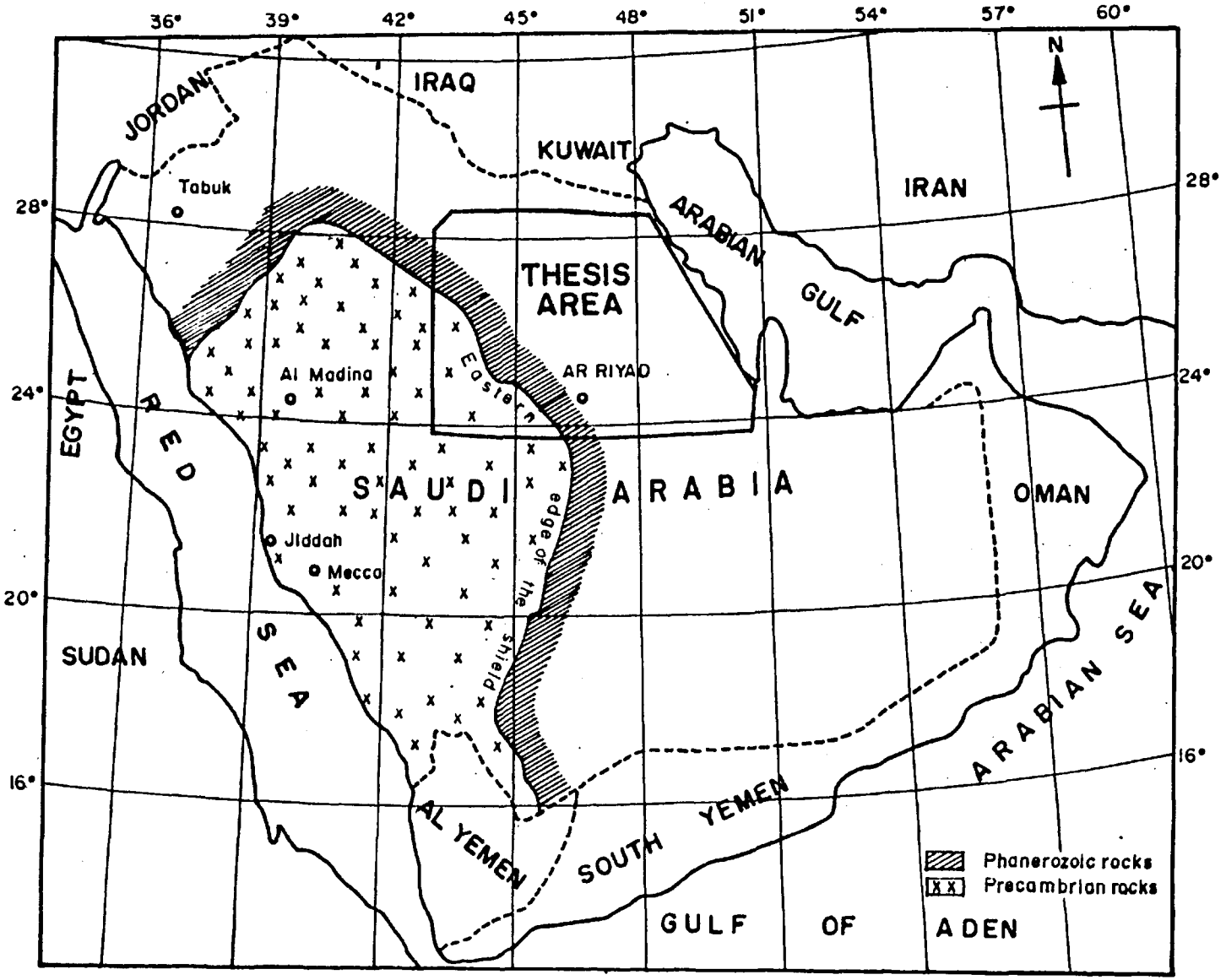


Figure (1) : Generalized map of Saudi Arabia showing location of thesis area.
Approx. scale 1:20,000,000.

secondary roads and desert tracks allow mobility within the area, especially to four-wheel-drive vehicles. Additional access was provided to the writer and his supervisor by DGMR helicopter support, which saved much time in field investigation of the more remote parts.

1.1.3 Topography and geomorphology

Generally, relief in the area ranges from 400 to 800m and grades from 700m above sea level at Riyadh to sea level along the western shore of the Arabian Gulf.

The central part of Saudi Arabia, the geology of which comprises a belt of several Phanerozoic sedimentary formations consists of west-facing limestone escarpments separated by long sand-filled basins which form the nafuds. The escarpments are arranged in a series of concentric arcs, concave to the west and sub-parallel to the eastern edge of the Precambrian Sheild. The system of scarps and basins is mainly divided along lat 24°N into a northern, northwesterly-trending, and southern, southwesterly-trending segment around the Central Arabian Arch.

The work described in this thesis mainly considers the area around the C.A.G.T.S. and the northern segment of the Arabian Platform.

1.1.4 Climate

Saudi Arabia has a wide variety of climatic conditions ranging from temperate regions in the south west to continental, hot

regions in the central parts and to relatively hot and humid conditions in the coastal areas. On the whole the country is dominated by an arid to semi-arid climate.

The main part of the study area falls in the semi-arid region where it is hot and dry in summer, but cold and relatively humid in winter time. Temperatures in summer range between 40° to 55°C in the day time and drop to 20° to 25°C at night, while in winter they range between 0° to 15°C during the day and are slightly lower at night. Such a drastic change in seasonal or diurnal temperatures affect the general erosional pattern of the rocks and rock fracturing.

The rainfall over the main part of the area is low, with an average of around 10cm/year, mostly falling between November and April. Winds in Saudi Arabia vary greatly, being affected by the surrounding seas and deserts, the best known wind is the shamal (north) typical of the eastern and central part of the country.

These winds create some sandstorms but still leave the land somewhat cool. So the shamal winds and sandstorms together with other less prevailing winds, mainly in Summer, dominate the area and leaves the atmosphere dusty for a few days. Some images indicate the effect of wind and storms in a pattern of concentric curves or Curvilinear pattern together with the control of sand dunes migration.

The atmospheric factors of dust, rainfall, temperature, humidity, wind direction and speed, together with sun angles and azimuth control to a certain extent the quality and

detectability of the images. These will be discussed in more detail under factors affecting the quality of images.

1.1.5 Vegetation and human activities

Vegetation in the area is sparse and widely scattered, oasis and shade are limited to some major wadis. The flora is not diverse, probably the most widespread trees are few species of acasia and camel thorn trees which grow under a variety of conditions. The important feature of some of these plants is that they reflect varying degrees of soil moisture: some of them grow in the major wadis which flood during heavy rain showers. The other common plants are shrubs which provide grazing after intermittent rain. Some sabkhas are present; these are characterised by halophytic vegetation which are easily detected on images. Particular plants, such as sidr, are easily detected by I.R.C.C. images.

The nafuds (sand seas) are characterised by plants such as obal and a white barked bush which has deep roots which help in places to stabilize the sands.

The sparse and widely scattered vegetation is an unfortunate situation from the pastoral point of view, is in fact fortunate from the photo-geological point of view where images in fact indicate almost hundred percent exposures of the terrain.

Human pastoral activity within the study area is very limited, and only major features such as towns and cities, paved roads, and pipelines can be detected by imagery. Desert tracks formed by bedouin vehicular traffic can be misleading on imagery,

because they can trap local winter rain and the resulting vegetation produces an unnatural pattern which does not necessarily reflect topographic features: (Photoplate 33).

1.2 THE GENERAL PROBLEM

This thesis deals with the detection and study of surface evidence of certain structures which might be of subsurface origin, by applying different interpretative methods and by using images of different scales and qualities, and by field investigation. The identification of those criteria which might represent structural evidence also formed part of this task.

One approach has been a general analysis of lineaments, where the surface of some Phanerozoic rocks involved displays fractures which are suitable for study from Landsat images.

The sedimentary rocks of Central Saudi Arabia have been studied in some detail by the petroleum industry, but very little attention has been given to their potential as host rocks for metallic ore deposits. To deal with such a task over a relatively wide area, it has been necessary to carry out a structural analyses programme supported by small scale Landsat imagery of different qualities,scales and bands and using processing techniques and interpretation and identification techniques.

One of the problems in this region is that little or no work of this type has been carried out. The eastern part of the relatively well studied Shield and its well known structures are included in the study area in order to examine the possibility

of the extension of these known structures through the overlying sedimentary rocks. To achieve these aims, field reconnaissance visits and helicopter traverses were carried out in selected localities, in order to collect necessary field data. This was considered as ground base data, necessary before the interpretation could be completed. Due to the accumulation of relatively large amounts of data, especially during the lineaments analysis, some computing programmes of rose diagrams and surface trend programmes were involved.

1.3 REVIEW OF PREVIOUS WORK

1.3.1 Previous Research

Although Precambrian rocks underlie the whole thesis area, some four fifths of this basement is overlain by Phanerozoic sediments.(Figure 1) Accordingly, reference has been made largely to previous work on the Phanerozoic rocks, with only passing reference where necessary to that on the Precambrian.

The first glimpse of the geology of Central Arabia was provided by Philby during his camel trip across the Arabian Peninsula between 1929 and 1939. However, the real geological research in the area started in 1933, when ARAMCO (Arabian American Oil Company) was granted oil concessions. This company's work has included a geological reconnaissance of most of the area overlain by Phanerozoic rocks, besides extensive geological mapping, regional and local geophysical surveys and the drilling of many thousands of boreholes. Structural

test wells were drilled for the better understanding of stratigraphic and structural problems. From 1933 to date, ARAMCO personnel and others have published several papers on specialised aspects of Phanerozoic geology. The most important of these is Powers et al (1966), which summarizes all the basic stratigraphic and structural information known at the time.

Besides this work, G.F. Brown (1947) described the ground water conditions in the Kharj area near Riyadh and subsequently, R. Kell studied the Jurassic rocks of the mountains surrounding Jabal Tuwaiq. The Ministry of Agriculture and Water Resources has investigated most of this area with its water well drilling programme; this work has provided interested scientists with a great deal of subsurface data regarding formational thicknesses, lithofacies and other information. Some of their water well logs have been used as sources of data for this research.

The Ministry of Petroleum and Mineral Resources, and though their contractors have prepared a wealth of reports on some structural aspects of certain parts of the region and also carried out hydrological studies. Kadhi, (1976) in an unpublished Ph.D. thesis studied in detail the geology and structure of part of the C.A.G.T.S.

A review of Cover Rock geology by Davis and Morrisey (1976) in a feasibility study commissioned by the DGMR to assess the potential for base metals, reviewed most of the data provided by ARAMCO, the Ministries of Agriculture and Petroleum and Mineral Resources, and all existing geophysical maps. These authors also examined few cuttings from chosen wells.

The writer submitted in 1977 a progress report on the DGMR Cover Rock project. This presented data derived from borehole cuttings and surface geochemistry and was a first step in the search for lead and zinc in the Cover Rocks. Lastly, in 1978, the Riofinex Geological Mission, under contract to DGMR, commenced a regional study of the Cover Rocks. Work started on rocks of the Aruma Formation.

1.3.2 Existing Maps and Data Coverage

1.3.2.1 Maps

In collaboration with the USGS, ARAMCO consolidated its regional topographic and geological information in published form. The first maps to be published were in the 1:500,000 topographic series; later, geological maps were prepared at the same scale (Figure 2). The third and most important series of maps were topographic and geological maps at the scale of 1:2000,000 and these include the most up-to-date material. A tectonic map of Saudi Arabia was published in 1972 by Brown, who based his work mainly on geophysical and borehole data.

1.3.2.2 Aerial Photography

Saudi Arabia is one of the few countries in the world that has been completely covered by relatively high altitude air photography. Starting in 1949, this work was carried out under photogrammetric specifications and was published at a scale of 1:60,000. More recently, a new programme of photography has been commenced which, it is hoped, will result

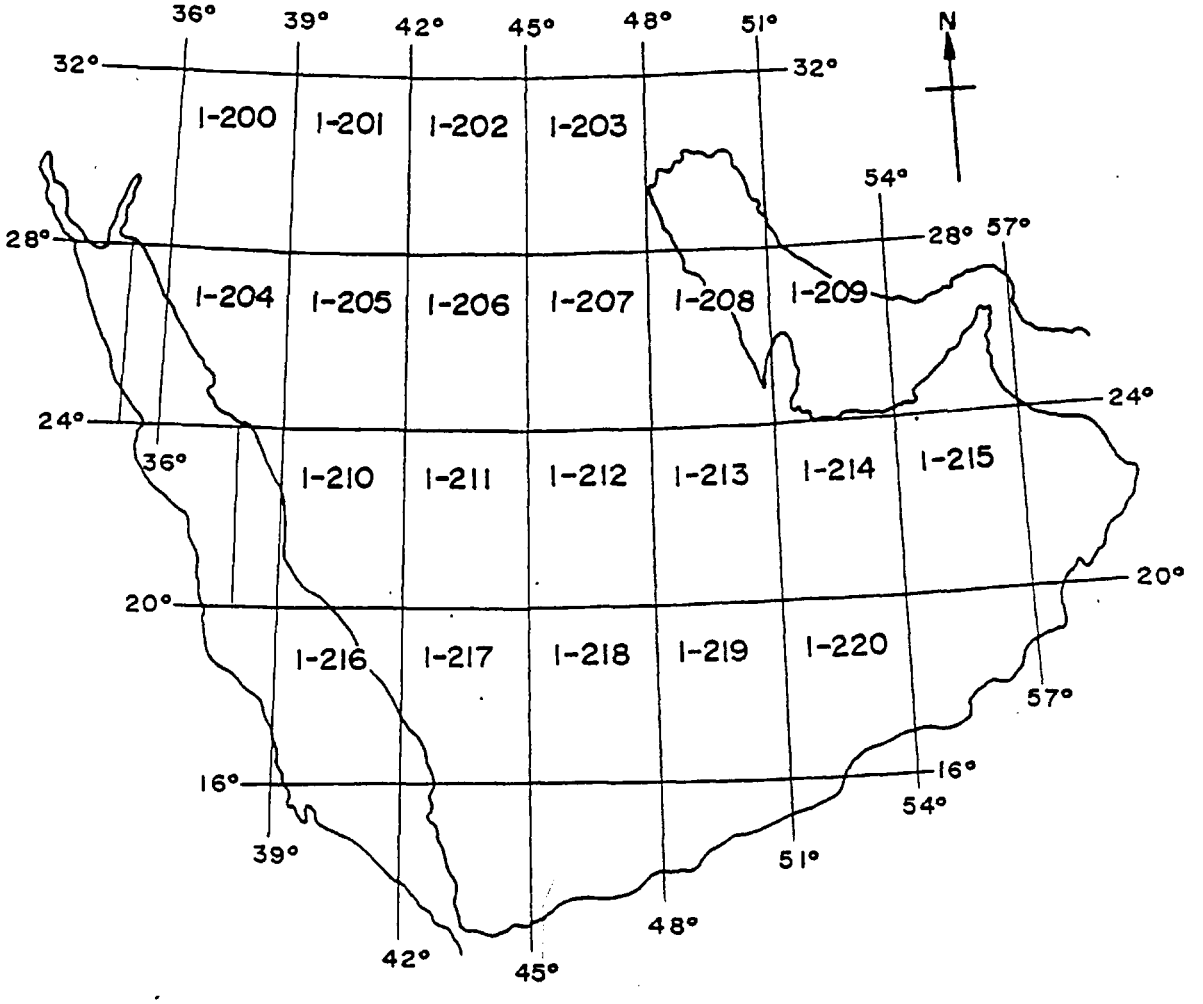


Figure (2): Index map of 1:500,000 scale geological and topographical maps of Saudi Arabia (after index map on I-270-A).

in complete coverage of orthotopographic maps and controlled mosaics, both at a scale of 1:50,000.

1.3.2.3 Landsat Images

Landsat image coverage is complete for the country [and is available from the Ministry of Petroleum and Mineral Resources]. Forms available include standard production of bands 4, 5, 6 and 7 and H.P.F.B.7 images.

1.3.3 Previous Research in the Same Field as the Study

Such research, the application of different interpretation techniques of Landsat images to detect the surface expression of subsurface structures, has not been carried out in Saudi Arabia hitherto.

In other parts of the world, however, this work has been commenced, but apparently only at air photograph scales. Norman, Price and Peters, for example, took the lead in this research when in 1977 they published results of their photogeological fracture trace study which elucidated the controls of Kimberlite intrusion in Lesotho. Later, Norman and Partridge in 1978 published the results of similar work which aimed to determine sub-Karroo structures in South Africa.

1.4 STRATIGRAPHY

The stratigraphy of the Phanerozoic rocks is well established; in varying detail for the Mesozoic and Tertiary, either in their outcrop or below surface in oil field areas, (Table 1).

Age			Formation	Generalized lithologic description	Thickness (Type or reference section)	Major stratigraphic divisions
CENOZOIC	QUATERNARY AND TERTIARY		Surficial deposits	Gravel, sand, and silt		
	TERTIARY	Miocene and Pliocene	Kharj	Limestone, lacustrine limestone, gypsum, and gravel	28 m	Miocene and Pliocene Clastic Rocks
			Hofuf	Sandy marl and sandy limestone; subordinate calcareous sandstone. Local gravel beds in lower part	95 m	
			Dam	Marl and shale; subordinate sandstone, chalky limestone, and coquina	91 m	
			Hadrukh	Calcareous, silty sandstone, sandy limestone; local chert	84 m	
		Eocene — Lutetian	Dammam	Limestone, dolomite, marl, and shale	33 m	Upper Cretaceous to Eocene Carbonate Rocks
		Eocene — Ypresian	Rus	Marl, chalky limestone, and gypsum; common chert and geodal quartz in lower part. Dominantly anhydrite in subsurface	56 m	
		Paleocene — Thanetian / Montian(?)	Umm er Radhuma	Limestone, dolomitic limestone, and dolomite	243 m	
			Possible disconformity			
MESOZOIC	CRETACEOUS	Maestrichtian / Campanian	Aruma	Limestone; subordinate dolomite and shale. Lower part grades to sandstone in northwestern and southern areas of outcrop	142 m	
		Turonian(?) / Cenomanian	Wasia (Sakaka Sandstone of northwest Arabia)	Sandstone; subordinate shale, rare dolomite lenses	42 m	Middle Cretaceous Clastic Rocks
		Aptian / Barremian	Biyad.	Sandstone; subordinate shale	425 m	Late Lower Cretaceous Clastic Rocks
		Hauterivian	Buwaib	Biogenic calcarenite and calcarenitic limestone interbedded with fine sandstone in upper part	18 m	
		Valanginian	Yamama	Biogenic-pellet calcarenite; subordinate aphanitic limestone and biogenic calcarenitic limestone	46 m	Upper Jurassic and early Lower Cretaceous Carbonate Rocks
		Berriasian	Sulaiy	Chalky aphanitic limestone; rare biogenic calcarenite and calcarenite limestone	170 m	
	JURASSIC	Tithonian	Hith	Anhydrite	90 m	
			Arab	Calcarenite, calcarenitic and aphanitic limestone, dolomite and some anhydrite. Solution-collapse carbonate breccia on outcrop due to loss of interbedded anhydrite	124 m	
		Kimmeridgian	Jubaila	Aphanitic limestone and dolomite; subordinate calcarenite and calcarenitic limestone. Lower part sandstone between 20° N. and 22° N.	±118 m	
			Hanifa	Aphanitic limestone, calcarenitic limestone, and calcarenite	113 m	
		Oxfordian / Callovian	Tuwaiq Mountain	Aphanitic limestone; subordinate calcarenitic limestone and calcarenite. Abundant corals and stromatoporoids in upper part	203 m	
		Callovian(?) / Bathonian / Bajocian	Dhruma	Aphanitic limestone and shale; subordinate calcarenite. Dominantly sandstone south of 22° N. and north of 26° N.	375 m	Lower and Middle Jurassic Clastic and Carbonate Rocks
		Toarcian	Marrat	Shale and aphanitic limestone; subordinate sandstone	103 m	
	TRIASSIC	Upper	Minjur	Sandstone; some shale	315 m	Permian and Triassic Clastic Rocks
		Middle	Jilh	Sandstone, aphanitic limestone, and shale; subordinate gypsum	±326 m	
		Lower	Sudair	Red and green shale	116 m	
PALEOZOIC	PERMIAN	Upper	Khuff	Limestone and shale; dominantly sandstone south of 21°N.	171 m	
	?	Lower / undated	Wajid	Sandstone, gravel, and basement erratics (Recognized only in southwestern Saudi Arabia and northern Yemen)	950 m calculated	Lower Paleozoic Clastic Rocks
			Precambrian basement complex			
	DEVONIAN	Lower	Jauf	Limestone, shale, and sandstone	299 m	
	ORDOVICIAN AND SILURIAN		Tabuk	Sandstone and shale	1,072 m	
	CAMBRIAN		Saq — Umm Sahm, Ram, Quweira, Siq	Sandstone	+600 m	
			Precambrian basement complex			

TABLE (1) GENERALISED STRATIGRAPHY OF SEDIMENTARY ROCKS CENTRAL SAUDI ARABIA, AFTER POWERS etal (1966).

This has been advantageous to the present study where the interest centred on rocks of Mesozoic age. However, the stratigraphy of the Palaeozoic rocks is less well known and locally, especially east of longitude 47°, becomes problematical.

Any review of Cover Rocks stratigraphy tends to be based on the data contained in USGS Professional Paper 560/D. The writer has drawn on this and also on numerous unpublished hydrological reports made available by the Ministry of Agriculture and Water Resources. In addition field visits have been made to some important localities. These were chosen so as to lie within certain structural regions, such as the Riyadh tilted block, where the rocks involved range from the Tuwaiq up to the Arab Formations. In order to understand the stratigraphic controls relevant to Phanerozoic geology, however, it is necessary first to pay brief attention to the rocks on which they lie: the Arabian Shield.

1.4.1 The Arabian Shield

This is composed of a complex of igneous and metamorphic rocks and is considered to be the continuation of the Nubian Shield from which it is now separated by the Red Sea and the Gulf of Aden. (Plate 7)

The importance of these Precambrian shield rocks to the current work is shown by the following. First, the sedimentary rocks of the Phanerozoic cover were largely derived from erosion of the Shield. Second, the Shield in its structural and geometric position has formed the basement to the deposition

of the Phanerozoic rocks. Third, and most important, elements of the complicated structural pattern of the Shield can be detected in the overlying sedimentary cover. An example of this and part of the original results of this study is the extension of a major shield fracture, the Al Amar-Idsas Fault. This was detected within the Palaeozoic rocks and followed up to the Jurassic Tuwaiq Mountain Limestone, where it is interrupted by the Al Majma'ah Graben.

Despite this ghost-like imprint, however, the stability of the Shield since cratonisation has led to the almost relatively undisturbed flat-lying regime of the Phanerozoic cover.

1.4.2 The Sedimentary Platform

This occupies two thirds of the country and is composed of a very gently tilted sedimentary sequence ranging from the Cambrian to the Neogene which overlies the shield rocks. Locally well exposed, these rocks are often hidden beneath a cover of unconsolidated gravel, alluvium, and sand dunes.

The thickness of the sedimentary pile was estimated by Powers, et. al (1966) to aggregate 5500 metres. Subsequent investigations, such as those of Kadhi (1976), supported by borehole data, have shown that this thickness is far from uniform. Part of the current work has sought to demonstrate that such variations have resulted from the local movement of structural blocks during sedimentation.

One third of these sedimentary rocks are of clastic origin, the remainder being carbonates and minor evaporites. It had been contended by the writer that such compositional variation has resulted in a variation in the effects of the upward propagation of deep-seated structural failures, (Kadhi (1976) and unpublished reports of M.A.W.

1.5 OUTLINE OF THE STRUCTURAL GEOLOGY OF THE ARABIAN PENINSULA

The structural pattern of the Arabian Peninsula was set in Precambrian times with the stabilisation of the Arabian Shield. By the beginning of the Palaeozoic, the rocks of the Shield had been fused into a rigid land mass and their surface had been reduced to a nearly level plain.

From the Cambrian onwards, a vast epicontinental sea moved back and forth across the lower parts of this stable basement and deposited the comparatively thin succession of almost flat-lying strata. This epicontinental sea was flanked on the northeast by a great sedimentary basin, the Tethyan Trough.

1.5.1 Tectonic Setting of the Arabian Peninsula

There is a general consensus of opinion shown, for example, by the work of McKenzie (1972) and Dewy et al. (1973) that the Arabian Plate was once a part of the African Plate until their separation by the Red Sea Rift. There is less general agreement on the time of this initial separation, however, although the Red Sea appears to be primarily a late

Tertiary feature. Girdler and Styles (1974) have suggested that separation occurred in the late Eocene. More recent work, supported by radioisotope dating, has also indicated an Eocene age, in this case 28 ± 1 m.y. (Al Shanti and colleagues, pers. comm.).

The Arabian Plate is bounded by various important structural features, each of which played a role in forming its internal structural pattern (Figure 3). West of the Arabian Plate, this boundary is the Red Sea/Dead Sea Rift. Analysing these structures, Nowrouzi (1972) related the development of this rift to the more rapid northward motion of the Arabian Plate compared with the African Plate. Earlier, in 1970, McKenzie et al. attempted to show that the Red Sea opened from a series of enchelon ridges (at a rate of 1cm per year)[1] and that the Arabian Plate rotated by about 7 - 8° anti-clockwise relative to the African Plate, about a pole located near Cyprus (Figures 4,5)[2] Since this rotation would have caused the two margins of the Red Sea to overlap in south, McKenzie and his colleagues argued that the Afar Depression of Ethiopia was largely created from mantle material during the separation.[3]

Eastwards, the Arabian Plate is bounded by the Arabian Gulf and Iran. Stocklin (1974) has argued that, during Palaeozoic times, Iran was part of an "Arabian Platform" with a "Palaeotethys" bordering to the north.

---

[1] This is supported by recent work by the Saudi Arabian/Sudanese/Red Sea Commission (DGMR miscellaneous Studies, 1979)which also indicates that the Red Sea is widening by 1cm per year.

[2] Girdler (1966) calculated a rotation of 6°.

[3] Similarly, in an unpublished report for the DGMR, Shearman(1979) postulated a similar accumulation of mantle material around a small plate in the vacinity of the Gulf of Akaba,which rotated independently at the north-western extremity of the Arabian Plate.

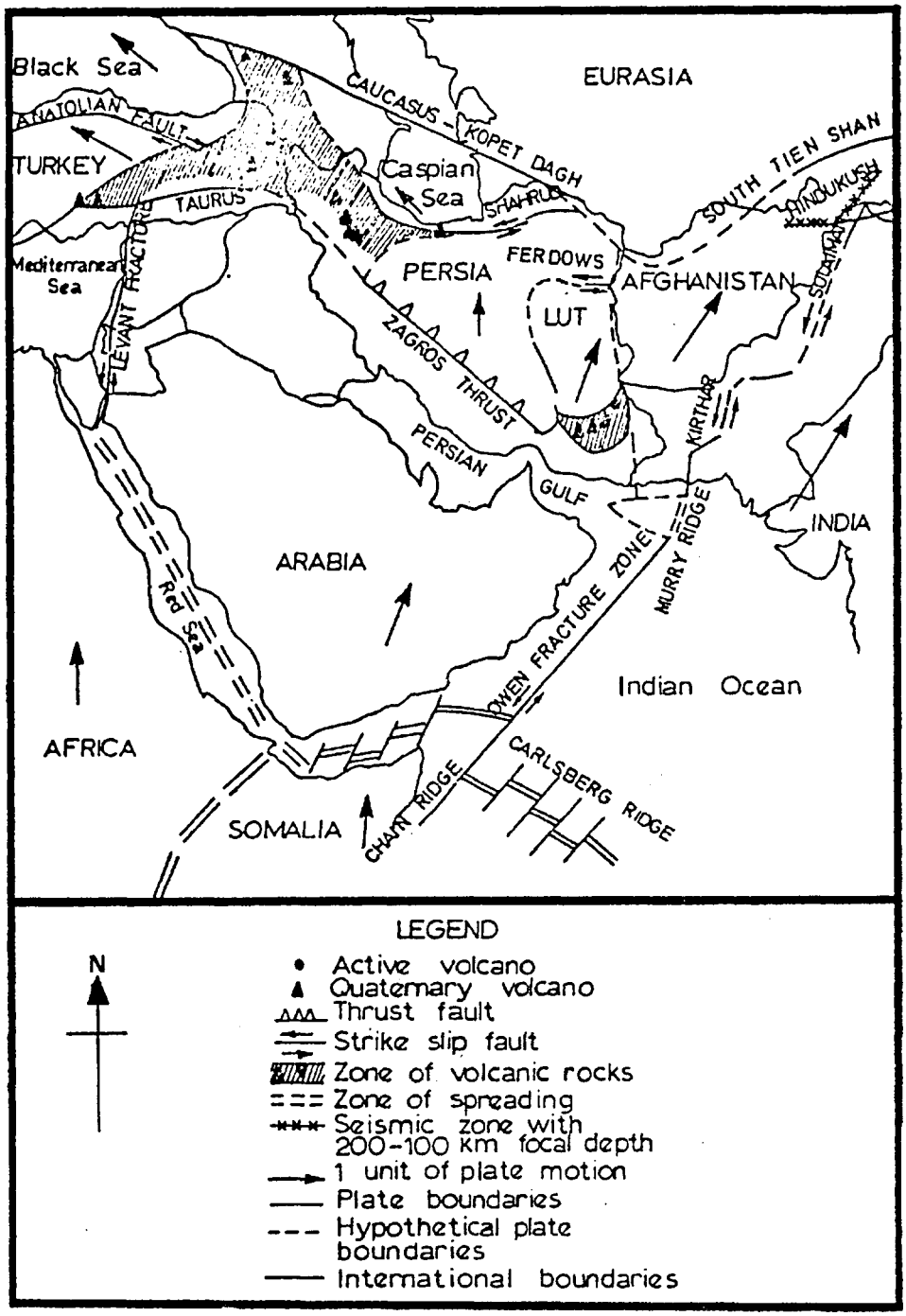


Figure (3) : Arabian and surrounding Lithospheric Plates after Nowroozi, 1972).

This "Palaeotethys", he believes, was closed during the Hercynian Orogeny by the northward subduction of Iran beneath the Scytho-Touronian Plate, thereby leaving the Southern Caspian Depression as a possible modern relict. Simultaneous to this, he thinks, was the creation of a "Neotethys" south of Iran as Arabia separated along the main Zagros thrust line.

Recently, Farhoudi (1978) has suggested a relationship between the Zagros displays and arc system which has controlled to a certain extent the shape of the Arabian Shield.

Much work has been done on the analyses of the relationship of the Arabian Plate to adjacent plates to the north and east in order to set Arabia in its tectonic framework. Associated with this work have been Allen (1969), Ambraseys (1970), Friend (1970), Dewy et al (1973), McKenzie (1970/1976), Stocklin (1974), Tchalenko (1974), Tarling (1970), Arpat and Sarouh (1972), Richardson et al (1976) and Girdler et al (1972/1974), as cited by Kadhi (1976).

1.5.2 Regional Structures of the Arabian Peninsula

The destruction of Tethys, which took place in the Cretaceous with orogenic movements that have been recorded from Turkey to Iran and which extend into Arabia, together with the Alpine Orogeny in the Zagros region, together outline the real tectonic framework of the Arabian Plate. Within this framework, two major structure provinces may be recognized:

1. the comparatively stable interior region whose rigidity is controlled by the Precambrian basement;

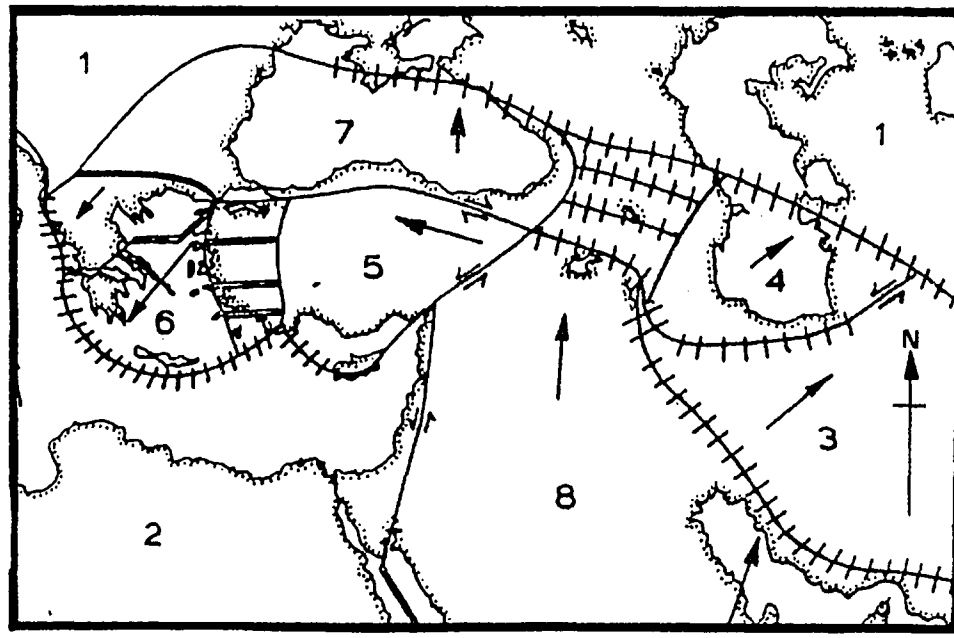


Figure (4): Plate boundaries and the relative motions between plates (after Mckenzie 1972).

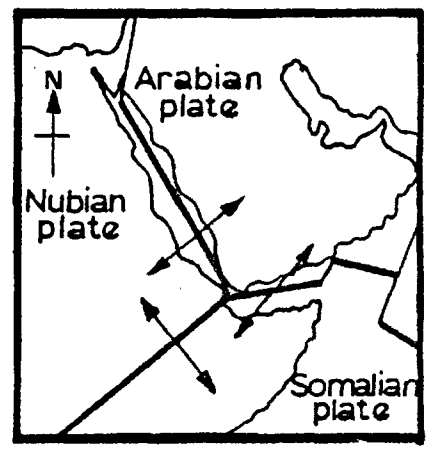


Figure (5): Plate boundaries and the relative motions of the Arabian, Nubian and Somalian Plates (after Mckenzie etal 1972).

2. the great mobile belt, peripheral to the stable region and made up of the Taurus, Zagros and Oman Mountain Systems. Saudi Arabia lies entirely within the stable region (Figure 6).

1.5.2.1 The Arabian Shield

This occupies about one third of the Arabian Peninsula and until recently, until separated from it by the Red Sea Rift, was a projection of the Nubian Shield. The Arabian Shield, composed mainly of igneous and metamorphic rocks, shows evidence of strong deformation. However, once rigid, these rocks resisted further deformation thereby protecting the overlying sedimentary blanket from significant disturbance.

The rigidity and the irregular shape of the Shield have been discussed by Farhoudi (1978) in his comparison of Zagros geology to that of island arcs. He suggested that Zagros displays an arc system, different stages of the development of which had been brought about by the convergence of the continental Arabian Shield.

1.5.2.2 The Arabian Shelf

Following its cratonisation, the Shield underwent peneplanation, after which it was slightly tilted to the northeast towards the ancestral Tethys where marine and non-marine sediments were deposited. This area of deposition is now known as the Arabian Shelf; it displays little evidence

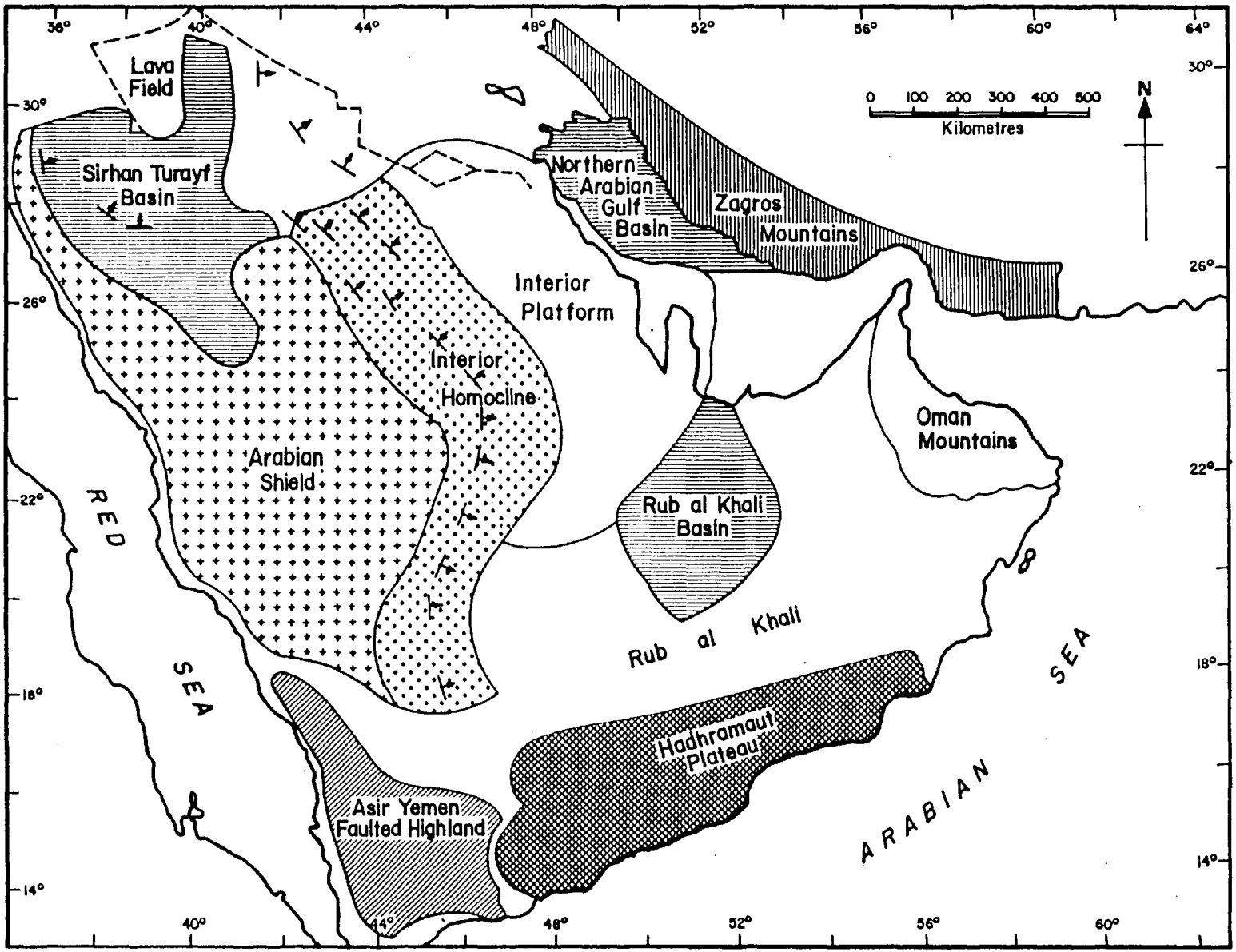


Figure (6) : Structural provinces of the Arabian Peninsula. (modified after Powers etal 1966, Kadhi 1976).

of disturbance although the Phanerozoic cover was affected by unconformities and disconformities brought about by the alternating transgression and regression of the sea. The present research has shown that, within the Shield, relatively large blocks have been separated by north-northwest trending faults and tilted gently to the northeast (with an average inclination of 5°). Subsidence within the Shelf persisted with few interruptions from the Palaeozoic until Recent times; however, the geological history of the Shelf is not homogeneous over the area. Accordingly, it has been divided as follows:

1.5.2.2.1 Interior Homocline

The rocks of the homocline are everywhere marginal to the Shield. They represent rocks of Palaeozoic, Mesozoic and Cenozoic age, and form the main object of this study.

The principal structural complication within the interior homocline is the Central Arabian Arch which affected all rocks, including those of the basement, up to those of Eocene age (Kadhi and Hancock, 1979). The Arch extends across Central Arabia, approximately along latitude 24°N, and as far east as Qatar (Brown, 1972). The area of the present study lies completely north of the Arch where the regional dip of the rocks lies between 1 - 2° to the north and northeast.

1.5.2.2.2 The Interior Platform and Adjacent Basins

The Interior Platform borders the Interior Homocline to the east; adjacent to it there are some basinal areas which, together with it, form an unstable shelf.

The generally flat-lying sedimentary rocks are disturbed by several major north-south anticlines which include some of the major oil reservoir structures in Saudi Arabia. These structures were evolved during the Mesozoic and Cenozoic sedimentation (Powers et al., 1966). The main basins adjacent to the Interior Platform include the Rub'al Khali, Northern Arabian Gulf and Sirhan-Turayf Basins.

1.6 DEFINITIONS OF TERMS AND ABBREVIATIONS USED IN THE STUDY

Some of the terms used in this thesis have been defined and used by previous authors. Other terms have been modified by the writer to suit the requirements of this research.

Absorption: The process by which EMR (electro-magnetic radiation) is assimilated and converted into other forms of energy, primarily heat.

Band: A wave length interval in the electromagnetic spectrum defined by two wave lengths or frequencies.

Brightness: Magnitude of the response produced in the eye by light from an image.

Colour Composite: A colour image produced by assigning a colour to a particular spectral band 4, 5 and 7 to form a picture closely approximating a colour infra-red photograph.

Contact print: A print made from a negative or diapositive in direct contact with the sensitised material.

Contrast: The difference in light intensity between the brightness, highlights and the deepest shadows.

Detectability: The ability of an imaging system to record the characteristics of an object on the ground although its identity may be unknown.

Frequency rose diagram: The total manifested number of lineaments expressed as a percentage of the whole or part of an image where azimuth occurs within the directional class intervals of 10°. (N.B. see also Length rose diagram).

Gray scale: A calibrated sequence of gray tones ranging from black to white.

Ground data: Information derived from the field and surveys to support interpretations of remotely sensed areas.

Haze: Minute solid particles of dust, smoke etc. in the atmosphere near the earth's surface.

Interpretation: The science-based skill by which variable information can be extracted by the study of photographs and images.

Image: The recorded representation of an object produced from it's EMR by a suitable method.

Image enhancement: Any of several processes used to improve the interpretability of an image.

Lambert conical projection: A map projection on which all geographic meridians are represented by straight lines which meet at a common point outside the map.

Landsat: An unmanned earth orbiting statellite which transmits multispectral images in the 0.4 - 1.1 μm region to ground receiving stations.

Length rose diagram: The total manifested length of lineaments expressed as a percentage of the whole or part of an image in 10° directional class intervals.

Lineament: A linear topographic or tonal feature on the terrain and/or images, where parts are aligned in a straight line or slightly curving. This may represent a zone of structural weakness and presumable reflects a subsurface phenomenon.

Linear: An adjective used to describe the straight-line nature of a feature on the ground or on images.

Manifested length: Simply refers to that part of the lineament detectable on the image or in other words the portion which is propagated to the surface and visible.

Multispectral scanning system (MSS): A scanner system which simultaneously acquires images in various bands (wave lengths) of regions of the same scene.

Noise: Any unwanted disturbance within a useful frequency.

Overlay: A transparent sheet giving information which more or less resembles that shown on the original image.

Path: The longitudinal centre line of a Landsat scene corresponding to the centre of an orbital track.

Pixel: Abbreviation of an image element; a ground energy source.

Recognizability: The ability to identify an object on an image without any quantitative measures.

Remote sensing: The collection of information about an object, through a recording device, without being in physical contact with the object.

Row: The latitude centre line of a series of Landsat scenes.

Resolution: The size of the smallest detectable and measurable feature of an image.

Scene: The area on the ground which is covered by an image.

Sun angle: The angle of the sun above the horizon.

Texture: The frequency of change and arrangement of tones on images.

Tone: Each distinguishable shade of grey, from white to black on an image.

ABBREVIATIONS

C.A.G.T.S.	Central Arabian Graben and Trough System
C.C.T.	Computer Compatible Tapes
Ce_1	Computer Enhanced 1st Generation
Ce_2	Computer Enhanced 2nd Generation
D.G.M.R.	Directorate General of Mineral Resources Jeddah, Saudi Arabia
DN	Digital Number
E.A.B.	East Arabian Block
E.M.R.	Electro Magnetic Radiation
H.P.F.B.7	High Pass Filter Band 7
I.R.C.C.	Infra-red Colour Composite
M.A.W.	Ministry of Agriculture and Water Riyadh, Saudi Arabia
U.S.G.S.	United States Geological Survey (Saudi Arabian project)
S.p.	Standard production
N.p.	Negative print

CHAPTER TWO

General Consideration of Imagery Interpretation

2.1 GENERAL APPROACH

Landsat imagery provides a coverage of wide areas with minimum photographic distortion. The MSS with its four bands technique is of great help to many fields of the study of natural resources.

The repeated coverage by Landsat imagery enables interpreters to select images for their purpose from either the most suitable season or from almost regular intervals. For example, winter images, which display a minimum sun elevation, provide maximum enhancement of lineaments with topographic features,and is unlimited by political or security restrictions, and is available to all at reasonable cost.

Although valuable, Landsat is best used in conjunction with other data sources. During the course of this research existing geological and topographical maps were examined also to identify such geological features as the linear orientation of post-tectonic granites together with the alignment of Tertiary volcanic cones. (Figure 57).

2.2 FACTORS CONTROLLING IMAGE INTERPRETATION

With Landsat images, interpretation still demands a scientific background and rests largely on probabilities. Few things are unambiguous; many interpretations must therefore be regarded as probable until all the visible evidence has been considered. Such a process is also affected by

subjective and objective factors and in order to attain good results one must carefully understand these factors and be aware of their effect on the results.

2.2.1 Objective Factors

2.2.1.1 Scale of an Image:

This study covers the relatively large area of approximately 300,000 square kilometres, and requires the use of relatively small scale images. It was therefore decided to use computer enhanced 1:1,000,000 scale band 7 images. In order to determine the effect of scale on the analysis, images of certain areas were studied on the scale of 1:500,000. This study has indicated differences, both in quality and quantity of data obtained from the two sets. Such differences will be carefully discussed in the coming chapters, and it can merely be said now that the optimum scale of images used is determined by the nature of the interpretation project.

2.2.1.2 Resolution:

The ability of an imaging system to record find details in a distinguishable manner is referred to as the resolution, or resolving power of the system. It is sometimes expressed as the number of detectable lines that would occupy the distance of 1mm on the image. It is influenced by a number of factors such as scale, contrast, acuity of vision etc.

2.2.1.3 The Quality of Images:

"Quality" tends to be a vague but useful concept, difficult to define closely, involves numerous criteria and is judged in different ways by different interpreters. Many different types of imagery have been used in this research. These include the standard spectral bands 4, 5, 6 and 7, infra red colour composites, and computer enhanced images with others generated from them.

This imagery cover was acquired at different times of the day, month and year so that it is affected by several variables, such as atmospheric effects. Generally, the quality of the images that have been used varies from average to excellent. Some display very high contrast, thereby obscuring certain internal details of geological features. Other images lack sufficient contrast; this results in some geological data being confused with their background and reduces the detectability of certain features on these images. Such a variety of imagery and variety of qualities will affect the analysis. Quality is influenced by tone, contrast, sun angle, sharpness, shadow, cloud cover and sand brightness. This heterogeneity mitigates against the possibility of common measure.

2.2.1.4 Techniques of Image Viewing:

Techniques of image viewing simply means the technique by which images are interpreted and not the viewing itself. When the interpreter analyses an image, he knows that sound

conclusions cannot be made until some relatively important data have been obtained from such an image. Thus, photogeologists have always tried to diversify and discover new techniques for viewing images. This attempt is made possible by the wealth of stored information that can be extracted from the images. The principal method of viewing images which has been used in this research is the unaided eye, for no stereoscopic coverage of Landsat images is available. This might be considered as one of the limitations of Landsat imagery, despite the fact that some three-dimensional views can be generated through computing devices.

As the interpreter has to perceive differences or nuances of tone, and texture, he should have the best possible lighting arrangements, constant and uniform for consistency of interpretation. Throughout this research some interpretations have been carried out using different lighting sources. These included clear sunlight, cloudy sunlight, artificial light only, in order to study the effect of such different sources of illumination on the interpretation.

2.2.2 Subjective Factors:

There is a general consensus of opinion amongst users of different types of imagery, whatever their field of interest, that there are factors affecting their interpretation other than the objective factors and yet of equal importance. These are the subjective or human factors. There is less general agreement, however, on the definition of these factors

and their relative role in interpretation, since they are basically dependent on human characteristics.

2.2.2.1 Physiological Factors:

These hinge upon the physical fitness of the interpreter to do his interpretation, assuming that interpreters have the basic requirements of sound health.

Factors affecting fitness include physical strain; for example, the interpreter may sit with his head and back in an unsuitable position, and strain muscles and affect the blood supply to the head. Another is visual ability, particularly the effectiveness of recognising tonal changes and colour contrast.

Visual power is extremely important. Moreover, with experience and practice, individual interpreters acquire the ability of both conscious and subconscious recognition of features of significance to their own particular field.

Normal colour vision is of critical importance especially, as in this study, where such images as infra-red colour composites are used.

2.2.2.2 Psychological Factors:

Despite their importance in interpretation, psychological factors are ill-defined and controversial; this is because they include personal feelings, disposition and individual reaction to images.

Previous experience of this area and familiarity with the previous literature give the interpreter confidence in his research. Psychologists believe that knowledge of the nature of objects before they are perceived and examined, creates a feeling of security and confidence which is bound to produce a steady successful performance. Another important psychological factor is the duration of image examination. During this research it has been found that one or two hours is a suitable period before eye strain sets in. This fatigue and consequent confusion, lack of variety and monotonous working conditions create boredom; this situation can be avoided by viewing discontinuously and at irregular time intervals. Working with other colleagues tends to be encouraging and avoids boredom. During this study, image interpretation has been carried out at different times of the day under different degrees of illumination, with quiet music or preferably songs in the background. This has proved useful in keeping the working atmosphere more cheerful.

A large amount of experimental work has been carried out by psychologists to investigate the effect on the observers' work of such emotional states as depression or anxiety. One's memory is affected by many factors also, such as the time of day in which observation is made.

Clarity and good general quality of images used in this study proved to have increased the writer's interest in the work during interpretation process.

In conclusion, the writer finds it worth mentioning that, during this research, a psychologically stressed situation makes perception rather difficult. Identification of features becomes doubtful and as the process of interpretation goes on the observer begins to over-use imagination which may adversely affect the quality and the validity of the results. For this reason the writer has been very careful not to become bored, and it has been noticeable that the quality and clarity of the images used have tended to hold the writer's interest and confidence.

2.2.2.3 Human Bias:

Since interpretation is mainly carried out by human interpreters, human bias is to be expected. Perceptive bias differs from one person to another, demonstrable, for example, in the case of the height measurement formula using stereopair and parallax bar a constant factor is inferred (in this case referred to as the K factor or personal factor).

It is believed that in some images, the presence of clearly artificial lines or linear patterns, such as highways or railways and scanning lines in standard MSS bands, biasses the interpreter into preferentially observing other lineaments more or less parallel to them. This situation has been avoided by using computer enhanced images on which scanning lines are eliminated.

Any interpreter being left-handed or right-handed will find it easier to trace certain directions on images than others.

The writer, being right-handed, has for example,found it easier to trace NE-SW, N-S, and NW-SE lineament respectively. The experience of an interpreter in his field plays a role in his interpretation result and preferentially in plotting some features easier than others. To demonstrate this point besides others, the image 178/43 high pass filter band 7, of 1:1,000,000 scale, has been interpreted by three different interpreters each on his own. Table (9) indicates the experience background and the result of interpretations.

Interpreter B, having few years experience in detecting arcuate or circular features from images, traced two or three curved lines which were not perceived by interpreter A and C. Variation is common in lineament pattern interpretations of the same scene by different observers. Agreement is limited to certain features only (Table 9).

2.2.2.4 Repetitive Interpretation

It is generally agreed that variations in lineament pattern interpretation do occur between separate interpretations of the same scene by the same observer. Where spectral band and geology are the same and the physiological and psychological factors are more or less standard, the different data sources of the same scene prove to be of direct effect on the final data gathered from the interpretation.

In the course of this research, some computer enhanced of band 7 images were used free of scanning lines. These presented good content and very clear lineaments or lineament

patterns were detected. If later, during the repetitive interpretation of the same scene but using standard bands 4, 5, 6 or 7 at the same or at different scales, then clear patterns were inferred in their interpretation although those lineaments or patterns are not clearly or only faintly represented. Later interpretations in general will be overshadowed by memory of the computer-enhanced imagery data and there is a little chance of avoiding such a factor. Computer enhanced images (H.P.F.B 7) have not replaced the standard MSS bands but simply improved the final presentation of the same data.

2.3 IMAGERY USED IN THE STUDY

Growing interest in Landsat images among earth scientists in several disciplines has led to the production of different types of imagery ranging from the standard production of MSS bands to the up-to-date H.P.F.B 7 imagery.

For the purpose of this research images compiled of different spectral bands, or those of a single band taken at different seasons of the year, or from different altitudes, or generated from the same scene by different image processing methods have been found to vary considerably in their information content. (Figures 7 and 8).

On this occasion and supported by the experience gained within this research attention is drawn to the fact that publishing interpretation based on a single image might be

misleading and presenting only part of the information available.

Scale influence has been encountered in this research, and two main scales were used namely, 1:1,000,000 and 1:500,000. Differences or resemblances will be discussed by means of either frequency or length rose diagrams.

2.3.1 Standard production of bands 4, 5, 6, 7 and infra-red Coloured Composites

Standard production images are images which are a direct production of MSS are derived from the CCT without going through any enhancement techniques. This represents the four spectral bands as shown in the following table:

MSS BAND	WAVE LENGTH μm	COLOUR	COLOUR NORMALLY USED FOR PROJECTION
4	0.5 - 0.6	Green	Blue
5	0.6 - 0.7	Red	Green
6	0.7 - 0.8	Photo IR	Red
7	0.8 - 1.1	Photo IR	Red

In some parts of the thesis area the four bands of the same scene were used because each single band (wavelength) has its own physical characters and its own reaction with the atmosphere and the objects on the terrain.

The other standard production images are the "coloured composite" images. A standard Landsat colour composite image has the spectral colour characteristic of an infra-red colour photograph. The infra-red colour composites used in this study are a combination of bands 4, 5 and 7 respectively. For better understanding of the coloured composite imagery and what true colours they represent on the ground see Table 1.A which illustrates the following:

TABLE 1.A

OBJECT ON THE GROUND	COLOUR ON FALSE COLOURED IMAGES
Vegetation	different shades of red
Water	dark blue (factor of depth)
Suspended sediments	white to light blue
Red beds	yellow
Limestones	bluish-blue
Bare soil	blue
Eolian sand (dunes)	white to yellow (yellowish)
Cities (urban)	blue
Clouds	white

2.3.1.1 Scale 1:1,000,000 images

As shown in Figure 7, the coverage of standard production images is not uniform over the thesis area. Some justification for this situation might be the following:

a) the purpose is research and not a systematic study

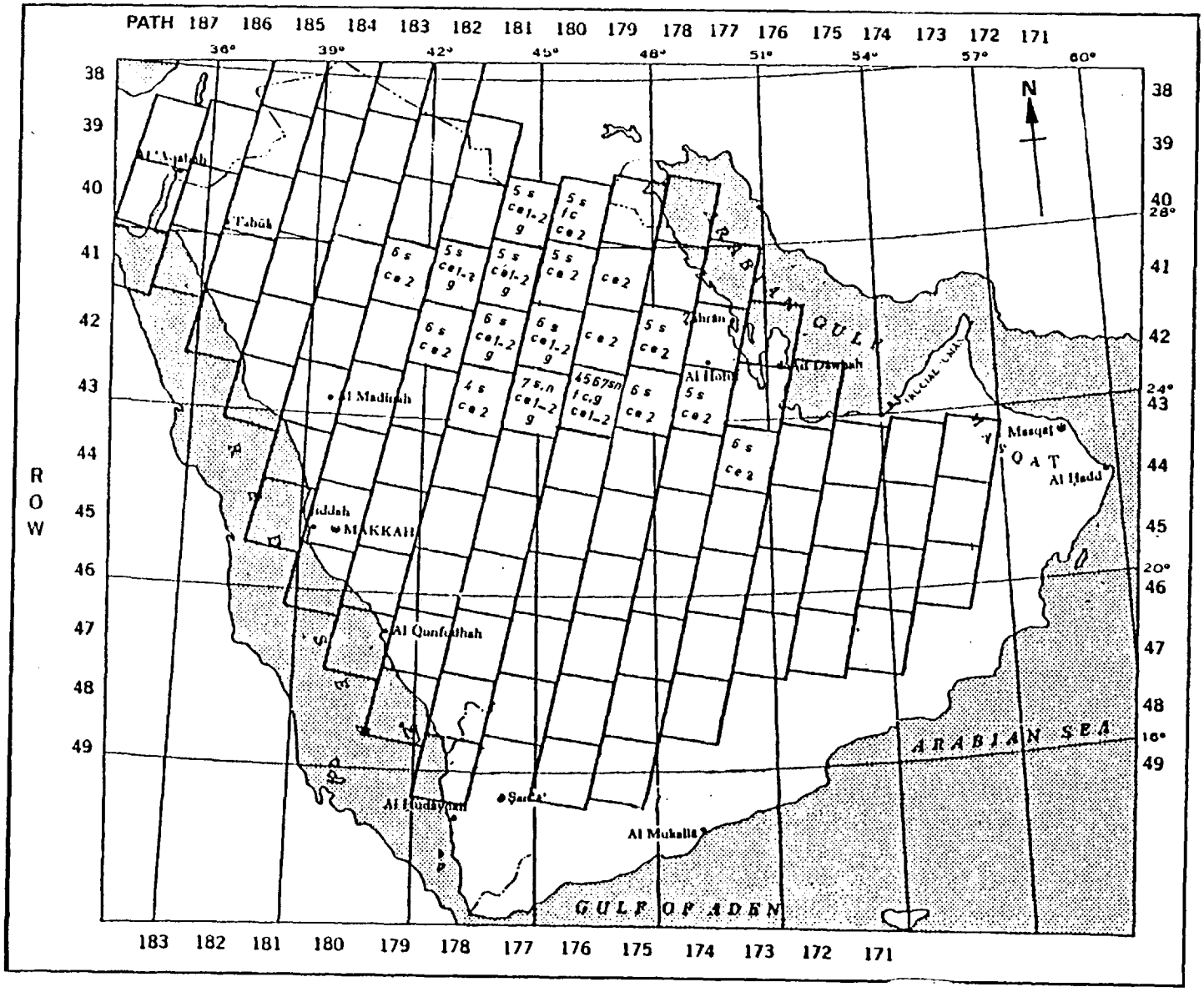


Figure (7) : Landsat index map of Saudi Arabia showing multi-imagery at scale 1:1,000,000 used in the study.

Key

4,5,6	MSS bands
S	Standard production
n	Negative print
fc	Infra-red colour composite
ce_1	Computer enhanced (1st generation)
ce_2	Computer enhanced (2nd generation)
g	Generated from ce_1 by photographic process

b) the availability of the images within a reasonable time

c) the fact that within the thesis area some smaller areas are relatively more important than others from the geological, structural and geographical point of view, for example Riyadh area 178/43.

2.3.1.2 Scale 1:500,000 images

Standard production images of this scale used in the research are mainly of infra-red colour composites together with few individual bands where the latter are restricted to key areas. (Figure 8).

The images at this scale were the first available to the writer and although some of the relatively important structures detected were a direct production of interpretations of these images, the general trends of lineaments were not well shown, and when the 1:1,000,000 computer enhanced images were available, and later the 1:500,000 images, the lineaments were interpreted again on a more confident basis.

2.3.2 Computer Enhanced Images

Image enhancement is defined as the modification of an image to alter its impact on the viewer.

Recently, computerised processing of images (enhancement), when used to maximize image content and quality for direct

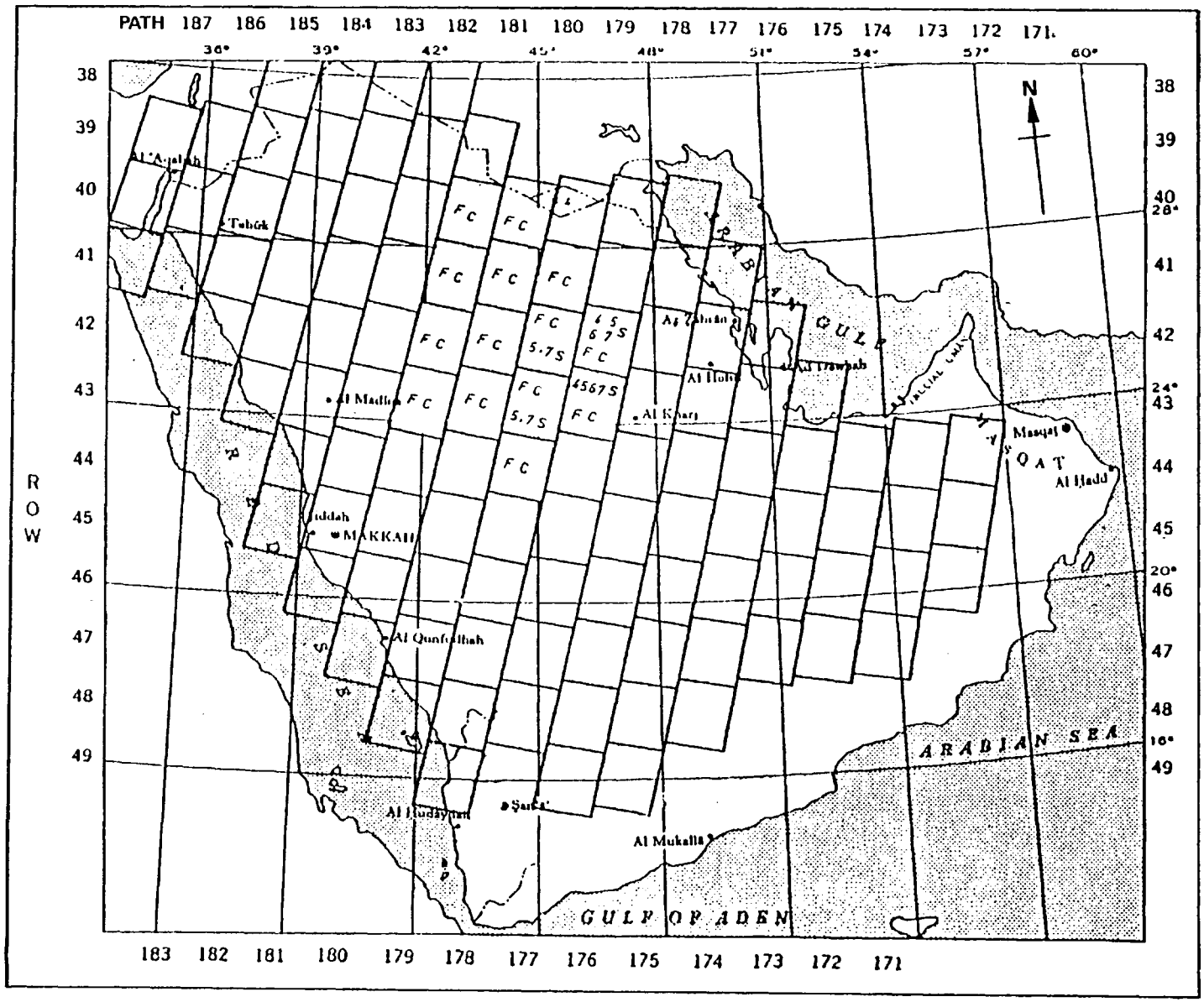


Figure (8) : Landsat index map of Saudi Arabia showing multi-imagery at scale 1:500,000 in the study

Key

4,5,6 MSS bands

FC Infra-red colour composite

S Standard production

interpretation by analysts, has proved to be a valuable tool for geologists.

Among the several established computer enhancing techniques, the high pass filtering of Band 7 was used. The reason behind this selection is firstly and, more important, the fact that high pass filter technique has proved to be the most valuable in enhancing certain lineaments and linear features and sharpen and amplify certain details in the image smaller than the array of pixels and secondly, the availability of these images within reasonable time factor.

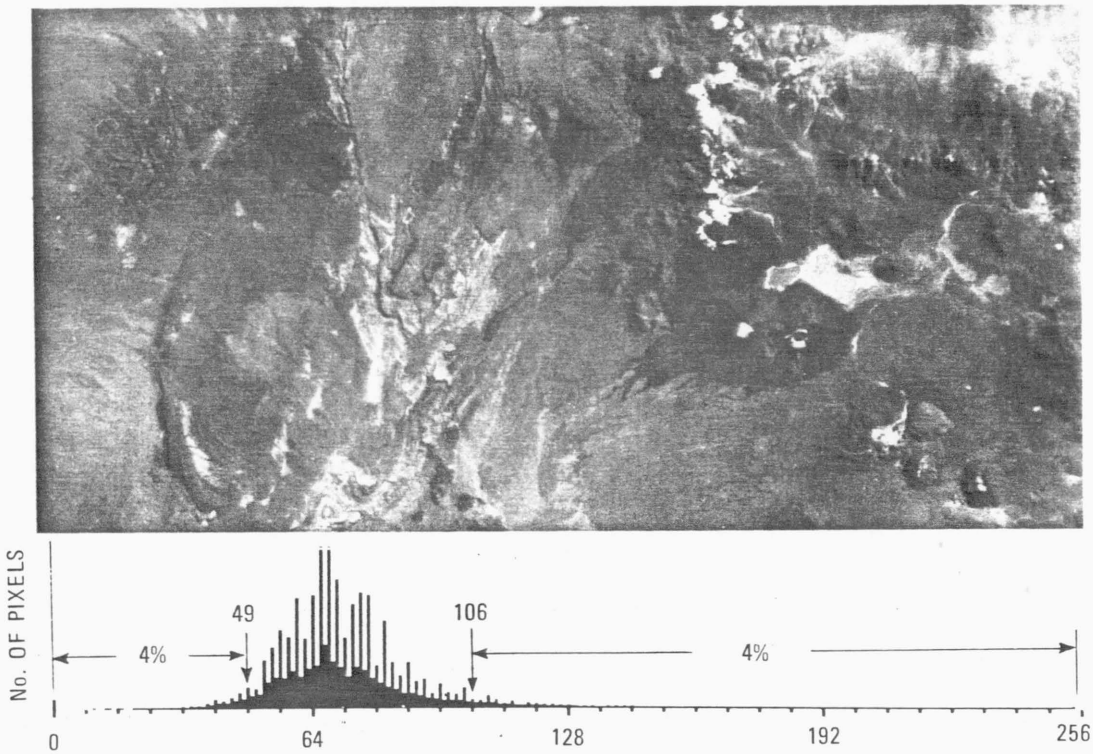
The high pass filtering of an image is achieved by subtracting the neighbourhood average (defined by used as odd number of N x M pixels) of the DN values around a particular pixel from the original value of this pixel, in other words, is simply achieved by generating a smooth image (low pass filtering) and then subtracting it from an original image such a subtraction isolates the details on the high frequencies, Condit, (1979). Filters are designated high, medium and low pass depending on the spatial frequency of the terrain features which are to be enhanced. Since this research is mainly concerned with lineament analysis which has a high spatial frequency measured in tens or hundreds of meters high pass filtering was used to enhance these geological features.

It is known that each image consists of tiny equal areas (picture elements) known as pixels, the brightness of each pixel has a numerical value (DN) ranging from zero for black to 256 for white.

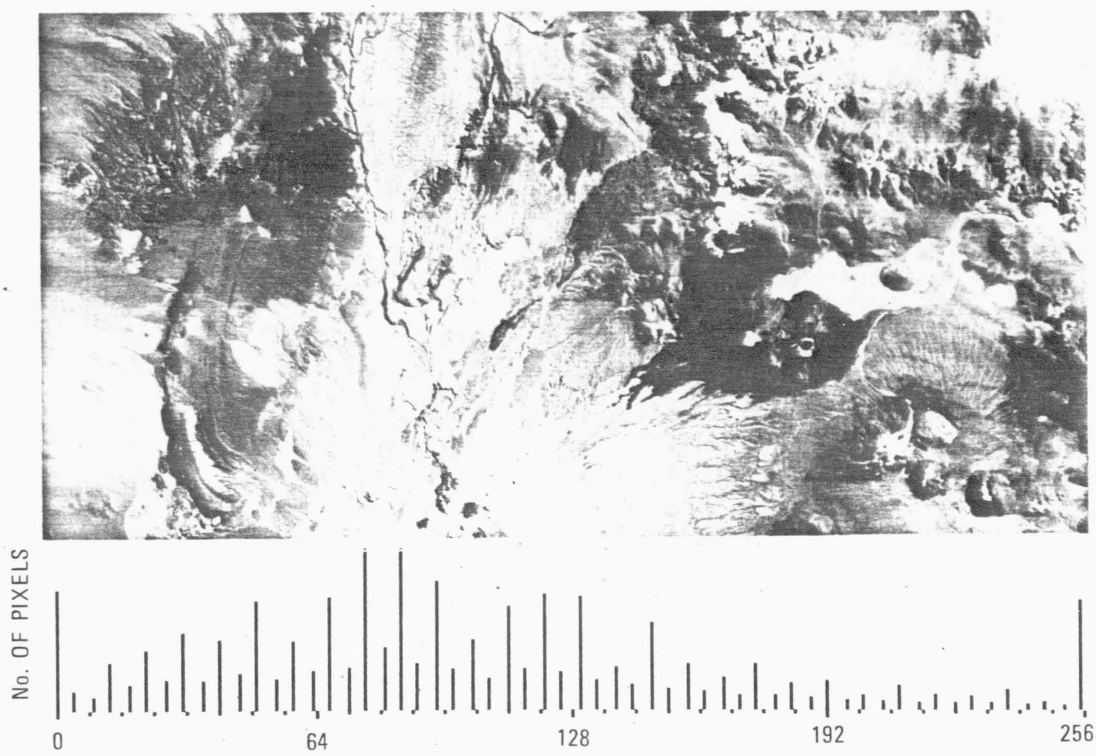
After the high pass filtering process of the image has been prepared, the DN values of the image pixels and the surrounding pixels are subjected to contrast stretching. This process can be summarised as follows: The Landsat MSS was designed with a sufficient dynamic range to image earth at low and high sun angles of the arctic and desert regions respectively. Consequently most images occupy only a fraction of the dynamic range and, therefore, have relatively low contrast. Although contrast can be increased by photographic means, manipulating digital data directly in the computer has the advantage that the stretching or increasing contrast is absolutely controlled. Contrast stretching begins with the formation of a histogram of the number of picture elements (pixels) versus the brightness or digital number (DN). The maximum of the histogram is shifted to the centre of the output picture gray level distribution. The brightness range of interest, which may be all a part of the data displayed in the histogram, is then expanded to fill the entire black white range of the output film.(Figure 9)

The advantages of computer enhancement, including high pass filtering and contrast stretching proved to be much better for precise geological analysis by improving the resolving power and detectability of images (modified after Goetz (1974) Sabin (1978).

The computer enhanced high pass filter Band 7 imagery used in this study are of two different generations in respect of their stretching parameters. The first generation which are



A. ORIGINAL iMAGE WITH NO CONTRAST ENHANCEMENT.



B. LINEAR CONTRAST STRETCH WITH LOWER AND UPPER FOUR PERCENT OF PIXELS SATURATED TO BLACK AND WHITE RESPECTIVELY.

Figure (9): Linear contrast stretch of portion of band 4 (after Sabin 1978).

represented by seven scenes(Figure 7)have a stretching parameter of the following values: 0-0, 112-0, 142-255, 255-255. The second generation of images which relatively covers the whole thesis area have different stretching parameters as follows: 0-20, 102-20, 152-235, 255-235. For correlation of the quality and tonal distribution within these two different stretching parameters and a third photographic enhanced image of the same scene (Photoplates 1, 2 and 3).

The computer enhanced images in this thesis are prints of negatives made from the original negatives by a direct contact processing to avoid as much as possible of the optical distortion in the conventional optical photography.

2.3.3 Generated images

This type of imagery can be defined as: images produced from pre-existing images by various photographing techniques.

The reason for using generated images is based on the need to achieve some of the thesis tasks in applying different methods of image interpretation, and the fact that there is a frequent need to facilitate the photointerpreter's task of gleaning the necessary and appropriate information, that is contained or can be generated either in a set of original multi-band images or their derivations by different means of photographic processing.

This involves modifying some of the pre-existing images to change (increase or decrease) their resolving power and detection capability. Photographic enhancement, through

photographic duplication, may result in relative loss of information but at the same time it has proved to enhance the contrast in certain areas of the image when it has been applied to each band of multi-spectral image, enabling the extraction of more information.

Since these images are produced through many steps of photographing techniques the following factors must be considered:

a) resolving power of the camera (can be eliminated by contact printing)

b) resolving power of the film

c) quality of paper prints

d) technician experience (if electronic scanning is not used)

2.3.3.1 Positive prints

This type of image covers only certain areas within the thesis area and are referred to with a letter g (Figure 7).

The positive prints used are a photographic production of existing prints of high pass filter Band 7 of the first generation. A negative of each of these prints was prepared by photographic processes and new prints were made from each negative , a process which may be referred to as photographic

multi-enhancement.

The produced prints indicated some change of contrast than that of the original images. Accordingly, some local structures in the generated images seemed to be enhanced and sharpened than in the originals.

2.3.3.2 Negative prints

This type of imagery used covers some limited parts of the thesis area (Figure 7) and is referred to by the letter n. Negative prints were made by preparing paper prints from a standard production positive transparency and since it is a paper print and not a transparency the term negative print is used.

2.3.4 Aerial photography

A few aerial photographs scale 1:60,000 and one photomosaic scale 1:50,000 and 1:120,000(Photoplate 5) were used for correlation with certain Landsat images regarding detectability of lineaments and their continuity, frequency and patterns. Some aerial photographs also showed either a characteristic pattern of drainage which may reveal variations in the composition of rocks involved or some degree of structural control.(Photoplate 32).

The presentation and correlation of the data achieved from all the different imagery used in the study will be discussed in detail in Chapter three. Before correlating the data achieved from each type of imagery used in the study the writer

thinks that correlation of the characters of these images in a brief table may be of interest. Table 2 summarizes the advantages of one type over another.

2.3.5 Application of Landsat imagery:

For better understanding of the role of landsat imagery in this research or any other research of the same nature, the advantages of landsat images and precautions or limited applications are to be taken in consideration in any evaluation of a study.

2.3.5.1 Advantages of landsat images:

The main advantages of landsat images can be summarized as follows (not in order of priority):

1. Repetitive coverage at different seasons and illumination conditions (sun angle, azimuth) is available

2. Cloud free images can be selected

3. Low to intermediate sun angle can enhance subtle geological features (in this study mainly certain lineaments)

4. Image distortion is negligible

	COMPUTER ENHANCED (HIGH PASS FILTER BAND 7) AND GENERATED IMAGES	STANDARD PRODUCTION OF BANDS OF 4, 5, 6, 7 AND INFRA RED COLOUR COMPOSITES
Contrast	Sharp,enhanced mainly for certain lineaments	Varies from one band to another but generally less sharp than computer enhanced images
Detection of lineaments	Mainly clear and traced with confidence	Less clear and bands 7, 6 are better than others under the same condition
Contrast between water and land	Clear	Band 7 is recommended, while bands 4, 5 can penetrate shallow waters for detection of suspended sediments
Detection of vegetation	Relatively clear	Colour composites are the best
Application in different fields of interest	Only limited to 0.8 - 1.1μm wave length	Has wide range of wavelength 0.4 - 1.1μm, can apply to wider range of fields of interest
Atmospheric effect(haze dust)	Less affected by haze, dust and recommended for desert areas	Varies according to wavelength band 7. Is the best, other bands react differently to atmosphere under different conditions
Basic data, sun angle, Azimuth exp. data	Some data available (disadvantage)	All available (advantage)
Co-ordinates	Not available (disadvantage) and hopefully to be considered in future production	All shown (advantage)
Scanning lines	Eliminated during enhancement process	Shown on all bands and f.c. and suppressed the interpretation of lineaments parallel to them (disadvantage)
Preparation of colour composites	Cannot be prepared	Can be prepared by many ways by the combination of three bands for example 4, 5 and 7.

TABLE (2) SUMMARY OF CORRELATION BETWEEN H.P.F.B.7 AND THEIR DERIVATIVES WITH THE S.P. IMAGES OF THE THESIS AREA

5. Cost is relatively low (this does not include computer enhanced coloured and black and white sets).

6. No political or security restrictions are involved.

7. I.R.C.C. images can be prepared by many processes.

8. Digital/computer enhanced images can be made available by computer processing techniques.

9. Different scales of imagery can be made available ranging from 1:4.700000 to 1:100,000

10. Images can be made available by different forms i.e. paper prints, transparencies either positive or negative with different sizes, for example, 70mm chips or 9" x 9" in size and larger.

2.3.5.2 The disadvantages and limitations of Landsat images:

Landsat images have a few limitations:

1. Low spatial resolution

2. Lack of adequate stereocoverage

3. Restricted spectral range

4. The poles are not covered by Landsat images because of the Landsat launching design

5. Lack of shadow free images which are important for certain projects

From this study one can add the following limitations:

1. Images are exposed only at a limited time of the day (09.30 - 10.00 a.m. local sun time in Saudi Arabia)

2. The repetitive coverage of images of the same scene with relative time span do not represent the same area geographically due to satellite orbit decay.

3. The use of Landsat images in areas of highly complicated geology, results are to be considered with some caution.

4. The computerized imagery of certain specifications are still relatively expensive. (The writer does not fully agree with F. Sabin (1978) that computerized imagery is an advantage of Landsat images in the absolute meaning. For example a complete set of true coloured images and black and white set of the multi-band of any given scene costs a few thousand US dollars.

These limitations are to be expected because Landsat programme was designed mainly as an experimental programme intended for many applications and was not specifically designed for geology.

2.4 ATMOSPHERIC AND PHYSICAL FACTORS CONTROLLING QUALITY OF IMAGES (SEASONAL FACTORS)

Landsat images are a direct representation of the earth's surface in the four MSS bands recorded by the sensors on the satellite by recording the reflected EMR through the atmosphere.

The EMR reflected or radiated from the earth's surface experiences interaction with the atmosphere as travels to the remote sensor, and the information it carries from the ground surface can be altered or degraded considerably.

The extent of this interaction is a function of the atmosphere and it constituents, and the wavelength. The atmospheric effects exhibit both fixed and variable attenuation factors. The fixed effects are the result of molecular absorption, while the variable effect, which are relatively more important, are related to local weather conditions.

Saudi Arabia is dominated by arid semi-arid weather conditions which have their own atmospheric effect. To summarize representative atmospheric conditions over the thesis area, the hydrologic data from three different regions were

obtained (Figure10).The atmospheric effects of these factors are discussed in the following section , and (Table 2a).

2.4.1 Sun Angle and Azimuth

Since sun provides most of the EMR that is incident or reflected from the earth's surface through the atmosphere, the relative position of the sun to the remote objects and the sun angle (from the horizon) play an important role in determining the reflected form of that object on the images. This reflection is a component of many factors, among them in order of importance are the following: soil moisture and surface roughness, particle size density (grain size), colour and chemical composition. Since this research deals to some extent with lineament analysis, the sun angle and azimuth both play an important role in such an aspect (Figure 11).

It has been found that certain linear features may be enhanced or suppressed on Landsat images depending upon their orientation to sun azimuth. Those features trending normal or at high angles to the sun azimuth are enhanced by shadows or highlights, those trending parallel with the azimuth are less visible and not easy to recognise as for example the linear features parallel to the MSS scanning lines.

The imagery used in the study were acquired at variable times of the year which show different sun azimuth with different effects. Sun angle which is related to the time of the year,where summer images have a relatively higher angle 57°-64°, so shadows have a minimum real extent leaving almost

Factor	Wet season	Effect on image and results.	Dry Season	Effect on image and result.
Sun Angle	31° - 45°	Enhance lineaments which have topgraphic expression.	46° - 61°	Supress and less enhance the same directions.
Sun Azimuth	134° - 148°	Enhance NE-SW lineaments.	085° - 095°	Supress the NW-SE lineaments and the E-W and may enhance N-S lineaments if other conditions are favourable.
Air Temperature	$10^{o}C$ - $25^{o}C$	Minimum haze.	$25^{o}C$ - $45^{o}C$	Maximum haze.
Rainfall	40 - 70 mm / month	Eliminate haze and dust, enhance vegetation along lineaments, clean rock surfaces and increase the validity of 4, 5 bands and more lineaments are detected.	0 - 5 mm	Accelerate haze and dust Limited to band 7 which can penetrate, minimize the number of detected lineaments.
Relative Humidity	50 - 70%	Enhance band 7 specially over vegetated areas	20 - 40%	Effect is minimized by other dry season factors.
Speed and Direction of Wind	5 - 7 km/h NW - variable	Generate dust and as a result random lineament pattern of non-geologic nature which may be eliminated by showers of rain in any time.	8 - 13 km/h variable - SE	Create dust and supress the detection of structures, random and non random patterns of sands and sand dunes specially in open desert or sand filled grabens. Migration of sands may obscure segments of known lineaments thus minimize length and increase frequency (together with scale).

TABLE (2A) EXPECTED EFFECTS OF WET AND DRY SEASON FACTORS ON DETECTABILITY AND INTERPRETABILITY OF IMAGES.

unobscured terrain. Winter, Spring and Autumn images have relatively lower sun angles 34° - 44° which proved useful in geological interpretations and enhanced some of the lineaments and linear features mainly those which possess topographic expressions.

2.4.2 Soil Moisture

Soil or rock moisture is one of the main factors which affect E.M.R. reflectance together with other parameters. The complex nature of the earth's surface blends these parameters in an infinite variety of combinations and predictions cannot be made without understanding the individual cases of variability, such a detailed study is beyond the scope of this research.

What is of interest for this research is the fact that differences of soil moisture along a lineament or in the main course of a wadi generally overshadows tonal colour differences, this is not the case when the lineament is covered by a thin film of water, which varies in reflectance depending on the spectral band involved. Relative humidity or moisture along some lineaments enhanced certain kinds of vegetation and are more striking on coloured photographs (Photo plate 43) and bands 6,7 images (Photo plates 8,9), while the same features are relatively less clear and are not easily detected on band 4 of the same scene (Photo plates 11, 12), under the same atsmopheric conditions.

2.4.3 Temperature

This factor includes the surface temperature of the soil and rocks, i.e. the diurnal surface temperature and the atmospheric temperatures (Figure 12). The effect of the diurnal temperature of the rocks surface is regarded as the absorbed

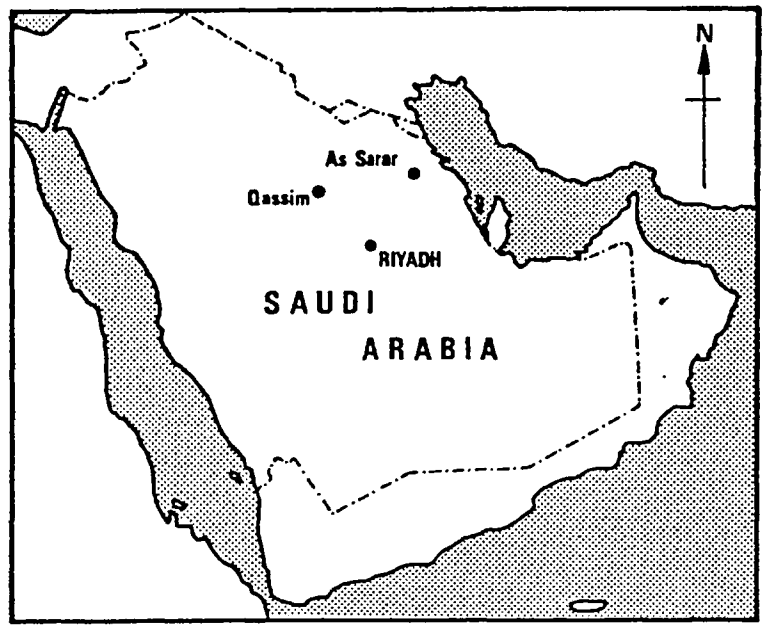


Figure (10) : Localities where hydrological data over the area were collected (years 1972, 1973). (after unpublished data of Ministry of Agriculture and Water - Riyadh).

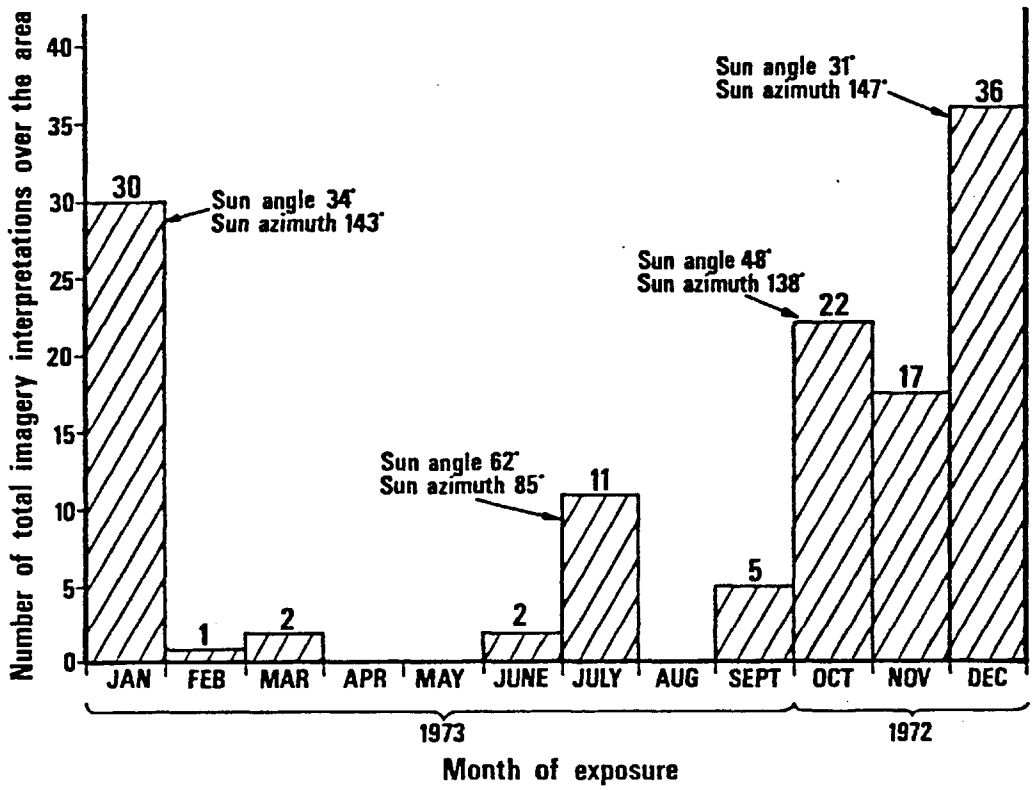


Figure (11) : Total number of multi-imagery interpretations and dates of imaging.

and the reflected solar energy which affects the tonal distribution of these rocks on the image. Dark shales in this aspect should behave differently from light coloured limestones where the first will look darker than limestones in a given image if the other atmospheric factors are constant.

The atmospheric temperature (air temperature) has an indirect effect on image quality, the higher temperatures in summer normally increase haze in the atmosphere which in turn decreases the quality of the images especially when sands and sand dune covered areas are involved. (Photo plates 45,46)

2.4.4 Rainfall (Humidity in the Atmosphere)

Rainfall is a factor controlled by seasonal influence. Within the thesis area rainfall (Figure 15) is expected between December and April. The quality and the amount of data acquired from winter images proved to be superior to the summer images in general for many reasons, but the rainfall or wet climate improvements are the following:

a) Atmospheric haze caused by wind blown dust during summer temperatures produces light scattering, but is removed by rain giving a clear atmosphere resulting in a good image contrast.(Figure 13).

b) Heavy showers, which occur occasionally in the area, wash away the surface dust areas over the bedrock and the bedrock character is well exposed.

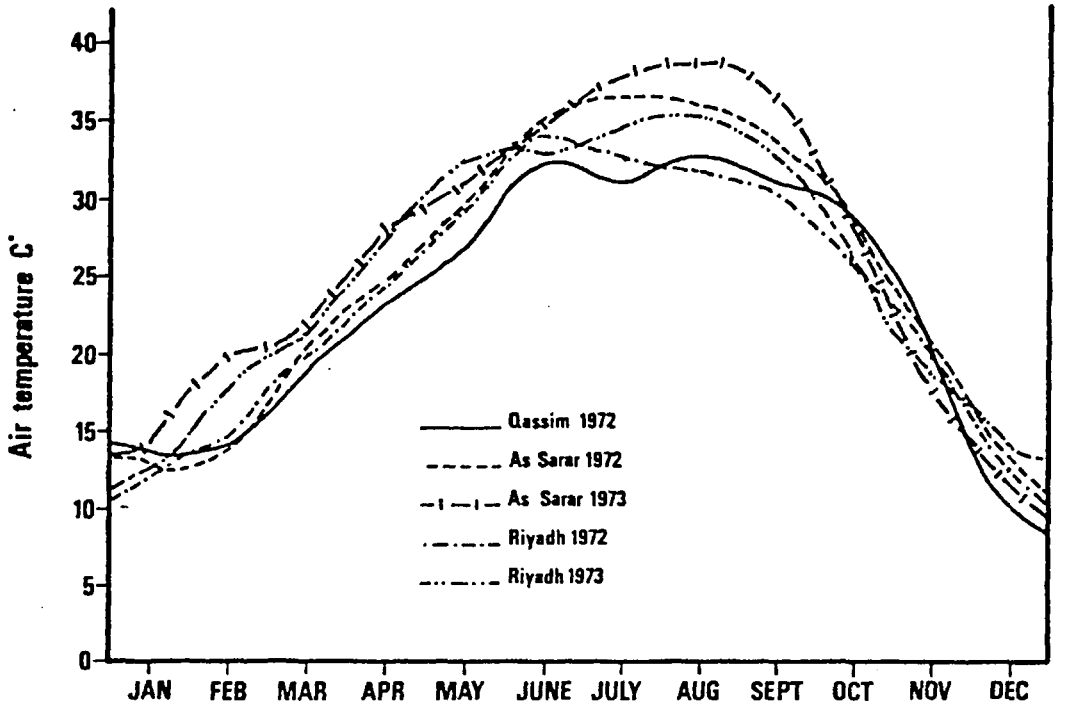
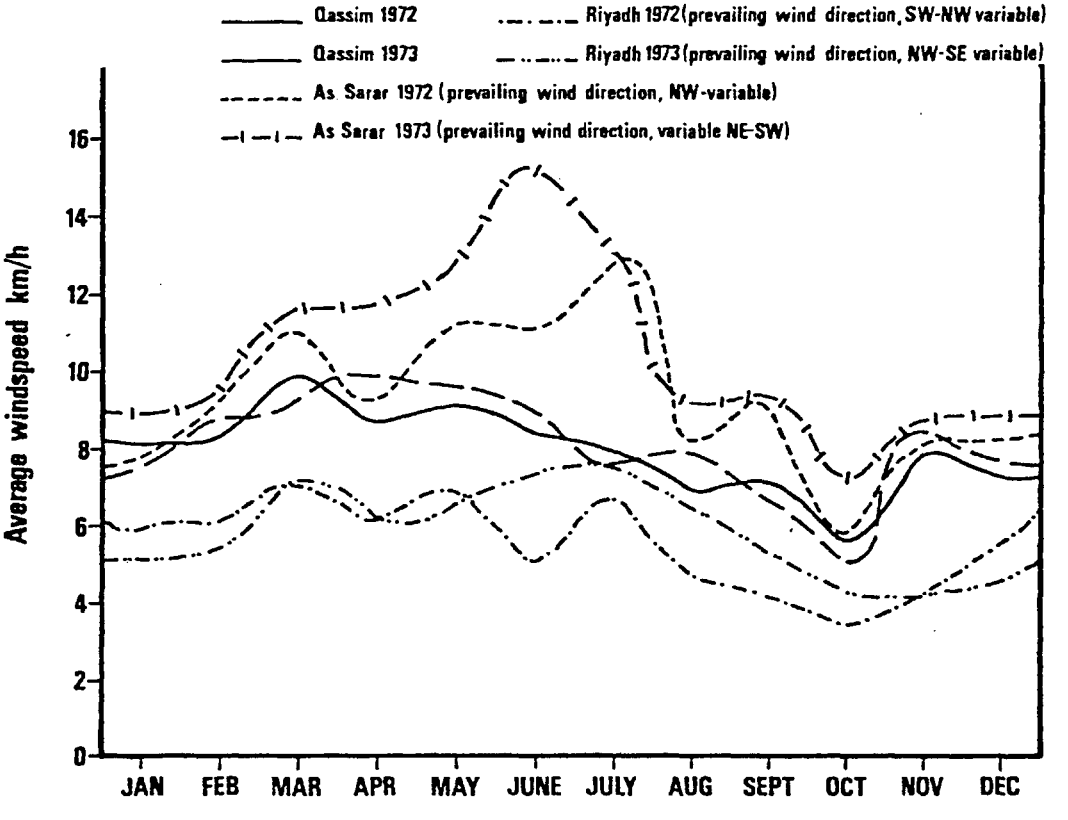


Figure 12 : Average air temperature.



	JAN	FEB	MAR	APR	MAY	JUNE	JULY	AUG	SEPT	OCT	NOV	DEC	
DAY OF MAX WIND	29	7	1	23	17	9	12	5	16	3	3	28	RIYADH 1972
TIME OF MAX WIND p.m. unless stated	12-1	2-5	12-1	2-3	3-9	1-2	12-1	1-2	1-2	1-2	10-11am	2-3	

Figure (13) : Average wind speed and directions.

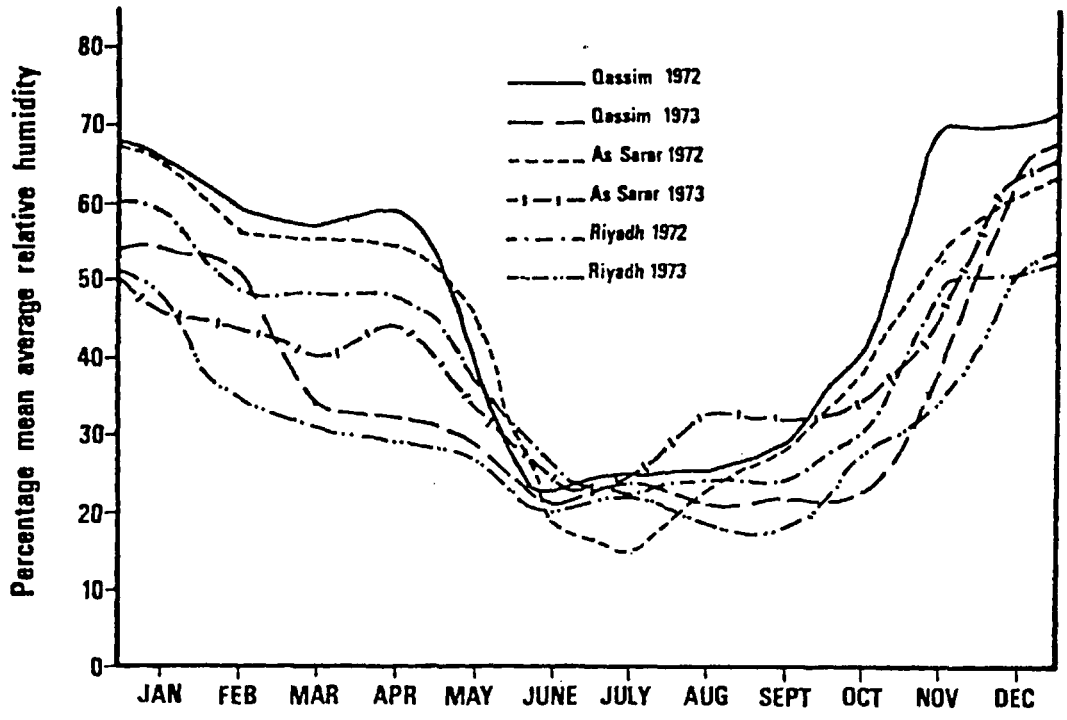


Figure (14) : Average relative humidity.

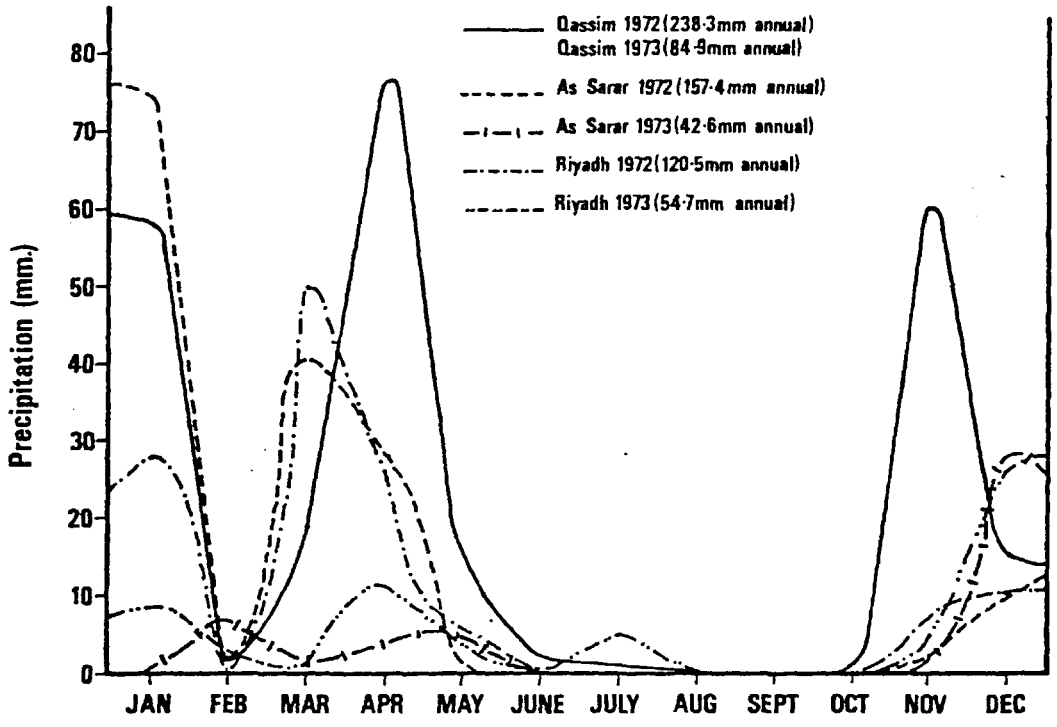


Figure (15) : Average rainfall (mms).

Humidity or water droplets, which are mainly related to rainy periods, have a relative effect on the scattering and reflectance of the EMR. (Figure 14).

The concentration of water vapour is highly variable around the year, but increases in the wet season in the lower atmospheric layers which are also affected by other seasonal factors outside the rainy season. The thesis area possess normally very low humidity, which is almost negligible except where vegetation occurs. Some water vapour accumulates on the top of the plants and results in enhancement of tonal differences in the image.

2.4.5 Cloud Coverage

This is not an important factor within this research since most of the available imagery are cloud free. Few images have 10 - 15% cloud coverage obscuring parts of the ground in the four used multi-spectral bands, but clear images also exist with different acquisition dates. Cloud coverage and fogs do occur occasionally in the thesis area and are related to the season of the year and even the time of day. (Photo plate 13)

2.4.6 Winds and Related Dust and Dust Storms

Despite the fact that the area is dominated by variable directions of wind, the shamal wind(from the north) is the dominant. It slightly cools the surface in summer, and also generates some dust storms which result in a dusty, hazy climate for a few days. The relationship between winds, their

direction and speed, and the dust in the atmosphere is well established in Saudi Arabia.

The prevailing winds in general might be responsible to the non random nongeological patterns of certain ground featuring features such as streaks which is not an uncommon feature on some of the images (Photo plate 34)

Dust and haze (± 0.25μm) in the atmosphere selectively scatters the shorter wavelengths of the EMR and as a result MSS band 4 (0.5 - 0.6 μm) is not recommended in the dusty hazy climate since it possesses the highest component of scattering. Band 7 (0.8 - 1.1 μm) on the contrary is thought to be better used in such climatic conditions where it possesses the lowest component of scattering especially in summer images where dust and haze are at their maximum.

2.4.7 Other Factors

Other factors have less effect on the quality of images. Among these are the roughness of the terrain, the mineralogy and organic content of rocks, and thirdly the vegetation coverage. These factors are not of much important effect in the thesis area since it is flat lying rock with little or no differences in mineralogical and biological constituents, while vegetation is sparse and widely scattered, chiefly restricted to the main wadis in winter time.

Seasonal variations of climate makes an advantage of one MSS band over another and the optimum band for one season is not necessarily the optimum for another. The nature and the

magnitude of the examined object adds another variable parameter.

Details of the seasonal and atmospheric factors and their effect on image quality and interpretation results will be presented in Chapter Three.

2.5 INTERPRETATION PROCEDURES

Procedures and/or methods of interpretation of Landsat images are determined by the objective of the interpreter, although in this thesis some methods are used or stressed to enhance the detection of the necessary data to achieve the research task.

Despite the fact that Landsat images are acquired by advanced technology, they were at first interpreted in much the same simple manner as aerial photography during which examination of different types of images with the unaided eye constituted the crucial interpretation phase. Spectral analysis is now becoming of additional importance.

The disadvantage of the presence of MSS scanning lines within the standard production of images and the confusion they may create has been overcome by determining whether or not a feature in question appears on more than a single band image or by using images free of scanning lines, but surely this means debased original data and a feature might be removed by the computer enhancement and other photographic processing techniques.

2.5.1 Preparation of Images for Analysis

The whole interpretation in this research has been accomplished using images in the form of prints (either positive or negative).

A clear, smooth overlay was laid over each print to draw the interpretation, the transparency of the overlay was found to be important since the interpretation was carried out monoscopically and the use of any textured overlays would have obscured some image details. The smooth surface of the overlay and the type of pen used proved to ease the moving of ones hand during interpretation - such factors are of relative importance to the result of interpretation. Attention was paid to handling images properly avoiding folding or artificial scratching or other defects which later might be mistaken for natural features.

2.5.2 Interpretation Methods

The images were handled in many ways during the course of interpretation. The 1:500,000 images being of relatively large size were laid down on a table and were interpreted by looking at them either from a short distance or relatively longer distance.

The 1:1,000,000 images being smaller in size and more handy were interpreted by holding the image with an inclination angle of 15° - 50° away from the interpreter, and then the image was rotated clockwise and anti-clockwise while changing the inclination angle during rotation. Most of the

interpreted lineaments in this research were detected by this method under suitable illumination conditions.

Interpretation was started by a quick examination of all available images of both scales, depending on their sequence of availability.

Interpretations have been carried out by inspecting the whole or a large part of the imagery. After the inspection stage the images were prepared for more detailed selection and study.

Two methods of interpretation were used in this study. It is believed that both together proved to be practical.

These methods are fishing and systematic search.

2.5.2.1 Fishing Method

This term has been defined in a broad sense in manual of remote sensing as "image interpreters have learned that aerial imagery is full of surprises, and they are often tempted to examine every object in every photograph so as not to miss anything."

It has been found that this is rather a broad non representative definition and does not cover the usage of the term in this study.

For this thesis, the Fishing method is defined as "searching for and attempting to detect some interpretation criteria for certain features expected to occur in a given image but not previously reported". The interpretation of certain Landsat images of the thesis area proved to be full of unexpected phenomena

and this encouraged the writer to examine them for the detecting of previously unknown structures despite the relatively long time required. In this research, this method was applied mainly in those areas where features of interest are expected to be found as for example the images covering areas adjacent or near a previously known structure.

For example, the northern part of a well known Pre-cambrian fault and its related structures where it impinges on the sedimentary cover, as shown on the pre-existing maps, research by this method which has proved that this structurally and economically important fault extends through (beneath) the sedimentary cover with very clear surface evidence (Photo plate 1)

More details of this fault and other important structures detected by the fishing approach during the interpretation process are given in Chapter Four. During certain stages of this method a few images which are not expected to contain desirable information were disregarded and then subjected to the second method which proved to be of more significance.

2.5.2.2 Systematic Search

This method can be regarded as a combination of both quick inspection and later intensive study. It requires better understanding of interpretation techniques and interpreter background, together with the main factors which control to a certain extent the quality and the validity of any interpretation process. The knowledge of some geological background of the area under investigation is necessary for interpretation by this method.

The amount of time spent in this intensive study varied from one image to another. Some images of certain key areas required close scrutiny of the entire image whereas as a result some important structural lineaments and other elements of both surface and subsurface nature were discovered.

2.5.2.3 Application of multi-image techniques

Some multiple images were used in the course of interpretation to verify the general approach of this research.

This was based on the fact that the scale or the approach to the lineament analysis to be carried has a direct bearing on the choice of suitable imagery for such a project. It is generally agreed that using different scales and different parts of the spectrum (i.e. 'bands', in the case of Landsat) one can obtain different information. For this reason, among others, two scales and many different qualities and types of imagery were used in this research.

The definition of multiple images means the application of multi-band, multi-date and multi-processing imagery techniques. Detailed description of these images has been discussed earlier in the chapter.

The application of this multi-image technique proved to increase the amount of information and knowledge of certain structures during the process of interpretation. This technique required establishing a documentation system to organise the data used in such an easy way to refer to any

information in the following way: a sheet was prepared with all required information of any image,as the example set out below:

JOB NO.	PATH/ROW	DATES OF INTERPRETATION	DATE OF EXPOSURE	SCALE
1	178/43	26.6.78 19.10.79	6 Dec.72	1:1,000,00

GEOLOGICAL ENV.	THE NEAR KNOWN STRUCTURE	OTHER REQUIREMENTS	COMPUTING REQUIREMENTS
Sedim.+Pre cambrian	C.A.G.T.S.	Statistical subtraction of Job No.1 from Job No.2	Freq.Rose Diagram Length Rose Diagram N-S Lineament spacing

This documentation system proved to be helpful in the interpretation of results and their significance.

A relatively new technique of correlating frequency and length rose diagrams of the interpreted lineaments was used.

In this technique, both frequency and length rose diagrams of the same interpretation of a given image are superimposed on each other to detect the relation of frequency and length of the lineaments and to identify whether or not a certain maxima of frequency coincides with that of length, and generally to study any relation, if it occurs, between the length and frequency of the lineaments of any area. This correlation has been carried out in two methods:

a) graphical (superimposition of rose diagrams)

b) statistical where frequency /Length ratio of each of the class intervals of some rose diagrams were

studied in detail.

It is hoped that this will help in solving some of the long lasting arguments among photogeologists on how to understand the lineaments nature either by their frequency or their length in a given area under investigation.

All the previously mentioned methods of interpretation were mainly carried out in this research under relatively consistent and uniform interpretation methodology and trying to keep constant standards throughout the whole process of interpretation which proved not to be an easy task.

2.5.3 Detection, Identification and deduction of significance i.e. recognisability

Image interpretation which is normally regarded as qualitative and quantitative, is basically a deductive process in which features that can be identified and then recognised, and thus lead the image interpreter to the identification and location of other features. To achieve better results, the interpreter should be able to integrate the different characteristics which make up the area under investigation. This requires the following two steps :

a) Detection and the identification of the remotely sensed feature and,

b) the deduction of its significance

Detection is merely the act of discovering the existence of an object, while identification is the revealing of its

true identity. Detection and identification do not necessarily occur in time according to the sequence suggested above. But in fact it depends to a certain extent on the interpreter background and experience, he might be able to detect and identify at the same time.

Identification is primarily a photographic problem affected to a certain extent by psychological components. In the process of interpretation in the early stages of this research the detected and/or identified lineaments were drawn on the overlay using different colours to designate each direction class of lineament.(Figure 16)

Later in the process when the writer was familiar with the patterns of lineaments it was found that this process of colouring individual lineaments was not required.

At this stage interpretation entered another state of deducing the significance of these interpreted structures.

Deduction of the significance (recognisability) of the identified feature however, is more of an intellectual problem, in no way dependent on the image but on the training, experience, background and intelligence of the interpreter. It requires amongst other processes the conscious or unconscious consideration of the elements of image and their relation to the terrain they cover, the interpreter's ability to integrate the different information gathered from the image and those gathered in the field (i.e. ground data) It is recommended from this research work that systematic consideration of the image interpretation elements should precede integrated

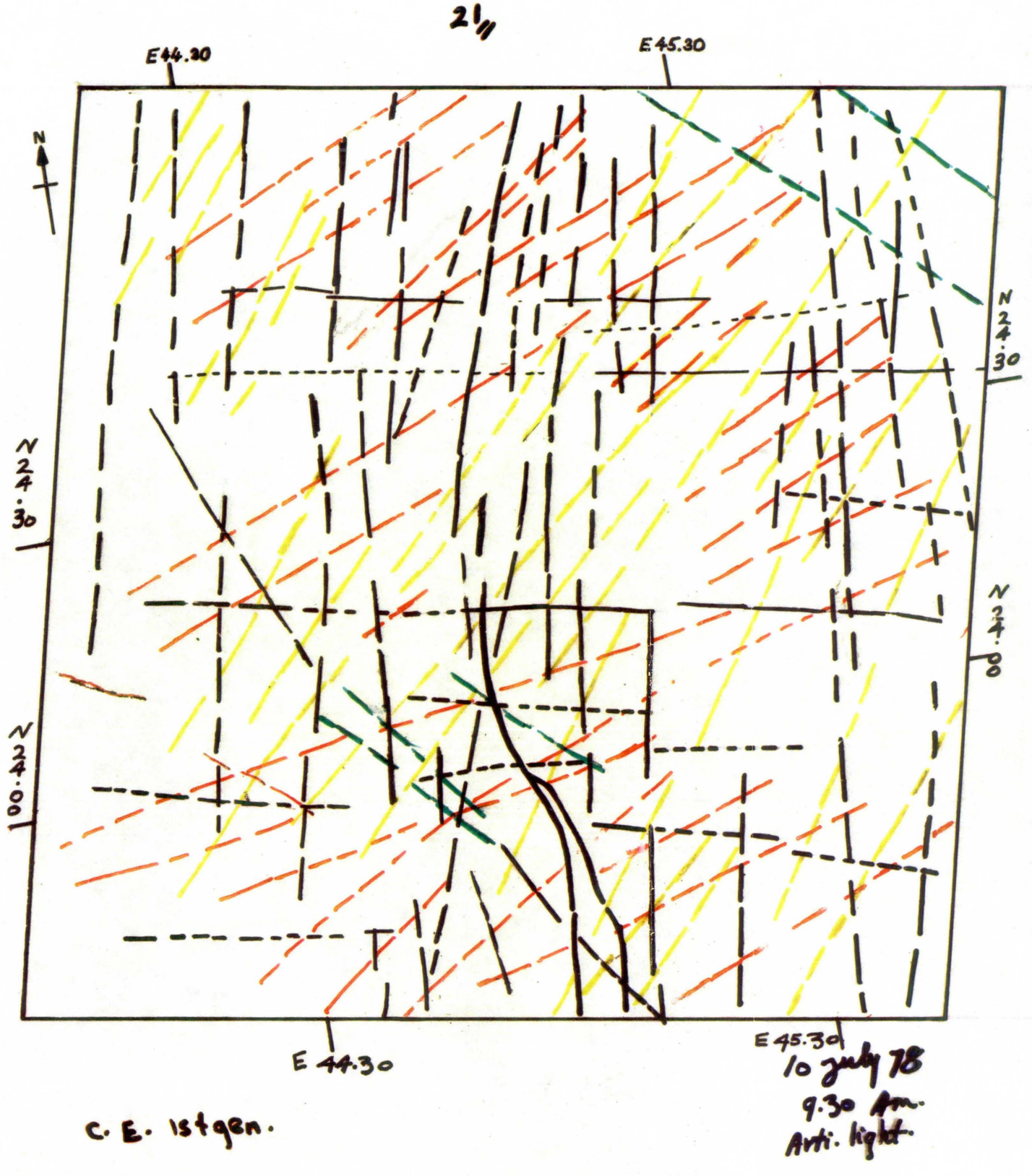


Figure (16) : Interpretation procedure in the early stage of research.

terrain interpretations.

This was exercised by the writer after field visits collecting ground information for the verification of interpretation data.

CHAPTER THREE

METHODS OF PROCESSING, PRESENTATION AND ANALYSIS OF DATA

3.1 GENERAL DISCUSSION

This study, which deals mainly with analysis of Landsat images, has little or no direct connection with the numerous previous studies of fracture trace analysis from aerial photographs. The only connection is that the same terminology is used in both studies, and the results are presented as directional rose diagrams of frequency and length. The writer agrees with the conclusion of Blanchet (1957) and other authors that fracture traces represent the surface expression of joints and small faults, whilst longer lineaments represent more fundamental and deep-seated structural elements which originated at the level of the basement. However the writer would prefer to modify this statement slightly because some lineaments, although deep-seated do not necessarily arise from the basement.

One of the assumptions in this study is that the propagation and development of some linear features in particular geological provinces are probably related to a specific cycle or cycles of tectonic events. Thus it should be possible to establish a relationship between some of these lineaments and other structures or structural events which can

then serve as a tool in solving other geological problems in areas of the same region where little was previously known about the detail of the geology.

A difficulty which arises in any imagery analysis is that some spurious lineaments of non-geological origin might be included.

In this research images of different bands, qualities and scale, exposed under different atmospheric conditions, were interpreted under various subjective factors. This procedure is advantageous but it is subject to some limitations if the techniques of preparation, enhancing and processing of the images are not clearly understood. For example, the direction of placing of the filter in order to produce the high pass filter band 7 images can have a profound effect on the enhancement or suppression of lineaments which are normal to, or parallel to, that direction, (Sabin, 1978). Also the procedure of using multi-imagery and multi-interpretations may have added non-geological lineaments. Such doubts are always present. To minimise these doubts care was exercised during interpretation to use the maximum number of criteria to support the identification of any lineament. Nevertheless not all of the lineaments were inferred with equal degrees of confidence. A general look at some of the interpreted overlays indicates that the lineaments are mainly represented in the following ways:-

(i) Most are directly or indirectly related to some regional geological events.

(ii) Some tend to cluster into groups which can be related to specific geological feature in that image.

(iii) Others occur in a seemingly random fashion which is not easily related to any known event. This latter group might be a direct or indirect result of one or more of the following factors.

(a) The use of multiple images and techniques;

(b) Human bias;

(c) The nature of the ground surface;

(d) The influence of a prevailing wind on lineaments of both geological and non-geological origin.

(e) The lineament may be genuine, but the cause has not been detected or understood.

To further minimise doubt, other information such as that gained from water well logs and existing maps were consulted.

The idea behind this is, that whilst absolute accuracy of interpretation of local detail in a regional study may not be that important, and is not easily achieved, relative accuracy and uniformity of the processes of interpretation are.

3.2 PRESENTATION OF DATA

The success of lineament analysis depends to a large extent on the methods of presentation and ease of correlation for better understanding of the results.

The aims of this analysis are mainly :

(i) The identification of significant similarities and/or differences between trends of lineaments as manifested at the surface.

(ii) Their possible relation to geological events, to help in detecting anomalies versus background, and to assist in the recognition of the latter.

3.2.1 Processing of Data

Because the thesis area is large and the amount of data is also large, it has been necessary to apply data processing techniques.

The decision to employ computer data processing techniques in any study depends to some extent on the aim of the study, the size of the project and the budget where the latter is of importance. In this present research an agreement was made with Dr. J. Ferguson, who carried out the processes of digitizing and computing the data. The costs of the arrangement were covered by the writer's fellowship. (The writer is of course aware of the systematic processes used in computing, and of how to prepare rose diagrams and the other methods which were used to handle the raw data.)

Dr. Ferguson suggested to the writer that the raw data for digitizing and computing should be prepared in the following manner :-

(i) The image frame must be clearly drawn on a transparent overlay of the interpretation.

(ii) Lineaments should be drawn clearly with an indication of their degree of continuity.

(iii) The co-ordinates of the images are to be clearly designated.

(iv) All necessary data are to be recorded on the overlays: e.g. path/row, date of exposure, type of band and the nature of processing of the image.

(v) Each overlay must be given a serial number, known as the job number, to refer to during data processing and later discussions.

To fulfill the requirements of the research the writer requested the preparation of two types of rose diagrams:

(i) Rose diagrams of 10° class intervals which show both directional frequency and length for each overlay. The class interval of 10 degrees was selected as this would smooth the results and eliminate too much noise.

(ii) Relative directional frequency rose diagrams using the same 10° class intervals: i.e. percentage rose diagrams,

The latter are required for structurally important areas or subdivisions of them, such as areas on both sides of a known or inferred fault. These rose diagrams were only prepared for images of 1:500,000 scale and they will be discussed in Chapter 4 under the headline of "Detected Structures".

Requisition was also made for preparation of a trend surface programme for a certain area using four water well logs (stratigraphic logs) to confirm the presence of what was thought to be a tilted block northwest of Riyadh. Some statistical analyses were required which included the periodical spacing of N-S lineaments and the subtraction of the data for certain rose diagrams. Statistical treatment was given to the latter because they deal with inferred regional patterns of lineaments which result from the acquisition of large amounts of information.

3.2.1.1 Advantages and Limitations of Computing

The application of computing programmes and digitizing techniques proved to be satisfactory in handling and processing the data and offered a practical means of elucidating the relationships of the thousands of lineaments which had been recorded.

Some of the advantages of data processing techniques with respect to analysis of lineaments are:

(i) The time factor: (The rapidity with which data can be handled through digital computers is invaluable).

(ii) The ease of cross-correlation and the filtering of information.

(iii) The reproducibility of data at any required time.

Some of the precautions which have to be taken in the study of lineaments are :-

(i) To achieve a relatively good reasonable result certain minimum numbers of lineaments should be used, i.e. sample areas have certain requirements.

(ii) Registration of data. There are several registration effect which may cause small variations of lineament directions. The first of these is registration or annotation of a given lineament on the film inaccurately. The second is that lineaments may be inaccurately located during normal digitizing. In each of these cases the annotations are mis-registered with respect to adjacent lineaments. The effect is that the digitizing of curvilinear or non-straight lineaments requires the operator to break them into smaller straight segments.

In this research the percentage of the curvilinear lineaments fortunately is very small, and the application of 10° class intervals possibly smooths any discrepancies.

3.2.2 Methods of Presentation

The methods of presentation of data are of a fundamental importance to the success of any study. Improper presentation of data can to a certain extent influence the recognition of both significant and insignificant trends.

In geological studies such as imagery lineament analysis there are usually two principal approaches. These are the quantitative and qualitative methods. In certain studies a combination of both approaches is used. For the particular nature and scope of this study, together with the large amount of data, the quantitative approach is preferable. This is because it is possible to recognise and correlate a greater number of characteristics of detected lineaments and their expressed patterns by quantitative rather than qualitative terms. On the other hand more than 95% of the lineaments possess rectilinear shape which drops the need for shape classification of lineament.

So, choice of the method of presentation of data in this research aimed for the following :-

First, the ease with which data can be described in numerical and graphical form. Second, the facility with which additional or indirect information can be derived from

the data.

To achieve such objectives it was thought that presentation of the data by directional rose diagrams offered the best method.

3.2.2.1 Directional Rose Diagrams

The most important properties of one of any lineament, is its direction or azimuth. Besides this, the direction is the least susceptible to human bias and the least affected by lithological or superficial variations. Further, direction is the variable least affected by scale whereas lineament characteristics can be.

It is regarded by many image interpreters that graphical presentation is vital for easy comprehension and comparison with other data. The most commonly used two dimensional graphical method for statistical presentation of data in lineament studies is the directional rose diagram. Rose diagrams in general are more meaningful, because of their representation in compass-like form, which allows immediate recognition of directional peaks in either frequency or lenght, together with their range and amount of variation.

Also, it has been found in this research project that the comparison of rose diagrams constructed from different images is most easily made. An additional advantage of using directional rose diagrams is that higher frequencies are given greater visual weighting because of their increase in arc length. To obtain better results, rose diagrams of both

frequency and length are presented either as individual roses or as groups of roses and as rose maps. The latter are prepared to present the general pattern of lineaments, and they enable one to examine the geographical variation of directional data, the extent of uniformity and the migration of particular trends across the area. The variations on certain factors such as lithology, geological setting (i.e. igneous or sedimentary), structural events and other subjective and objective factors in interpretation.

Also the presentation of data in any one of the two types of directional rose diagrams (frequency or length) allows the interpreter to effectively understand the behaviour, variability, and uniformity of the lineaments over part of or all of the study area. Further the operator can conclude information such as: the dominant trends of lineaments; any relationships which exist between certain numbers of long or short lineaments in particular directions, or, whether or not the total picture is uniform ?

The data of both types of directional rose diagrams will be presented and analysed,first, by dealing with the frequency rose diagrams with a general discussion of the data over the whole thesis area. Specific roses will then be dealt with , for example those of the high pass filter band 7 images and the infra-red colour composite images which completely cover the thesis area. Later, certain individual roses and groups of roses will be discussed. The effects of objective, subjective and atmospheric factors on the results will be

discussed.

Comparisons of frequency and length roses by superimposing one over another have been made and some interesting relationships established.

Subtractions of certain frequency rose diagrams will be dealt with where appropriate. Finally, relative rose diagrams will be considered within later chapters.

3.3 ANALYSIS OF LINEAMENT DATA

The information derived from the analysis provides background study of the lineaments in the thesis area, but it also provides a background for studying regional structures beyond the study area and thus identifies critical areas worthy of subsequent detailed study.

The writer believes that briefing in the important regional-structural events which operated in the area is a necessity for better interpretation and understanding of the local results which otherwise will be of little significance.

Besides the previously mentioned information regarding the general history of the Arabian Shield and the Interior Homocline, other important geological events took place which affected both structures and sedimentation regionally. The most important of these are the following:

(i) The Central Arabian Axis

The Central Arabian Axis, referred to by Powers and co-workers (1966) as the Central Arabian Arch is a zone of grabens, troughs, and normal faults which extends roughly east-west just south of Riyadh, and then swings north-north-west around to north-north-east in Al-majmaah area. This axis seems to have played a succession of key roles in the evolution of the cover rocks. Image 178/43 (Photoplate 6) displays parts of the structure with both 'emerging' and relatively stable or 'subsiding' areas on its south and north sides respectively. Powers et al (1966), Hancock and Kadhi (1978), in different interpretations, concluded that the Arabian Axis hinge line is a result of extension over a basement structure and have played a major role in the production of the tensional tectonic structures in its vicinity. This suggestion is supported by the results of this present research, where the roughly N-S direction might be a result of this tensional process before being followed again by a N-S compressive stress.

(ii) The Ha'il Arch

The Ha'il Arch (sometimes referred to as the Hail Axis) is represented by a pronounced northward bulge along the northern margin of the contact between the shield and the cover rocks. Previous studies indicate that the axis records a north trending headland of basement rocks

which had different effects on early and late Palaeozoic strata. During deposition of the latter it acted as a hinge line between what appears to have been an emerging or passive area to the west and a pronounced sag to the east. The arch may be a residual high between the Dibdiba Basin to the east and the Surhan-Turaif basin on the west (Powers et al., 1966). But Bureck (1969) and Greenwood (1973) regarded it as the consequence of a series of uplifts.(Plate 7)

(iii) The Najd Fault System

The Najd system is a complex of major sinistral transcurrent faults of Proterozoic age in the Arabian Shield. It is some 300 kms wide and extends 1,100 kms inland from the Red Sea. The system is a braided one parallel and curved en-echelon faults (Figure 17) which was produced by an E-W compressive stress field (Brown, 1972).

Complex arrays of secondary structures including accessory strike-slip (transcurrent), thrust, and normal faults together with some folds and dyke swarms, are associated with some of the major faults, particularly near their terminations. These secondary structures indicate that dilation and extensional conditions existed synchronously in different parts of the fault zone. What concerns the writer in this research is that some of these Najd faults at their extremities impinge

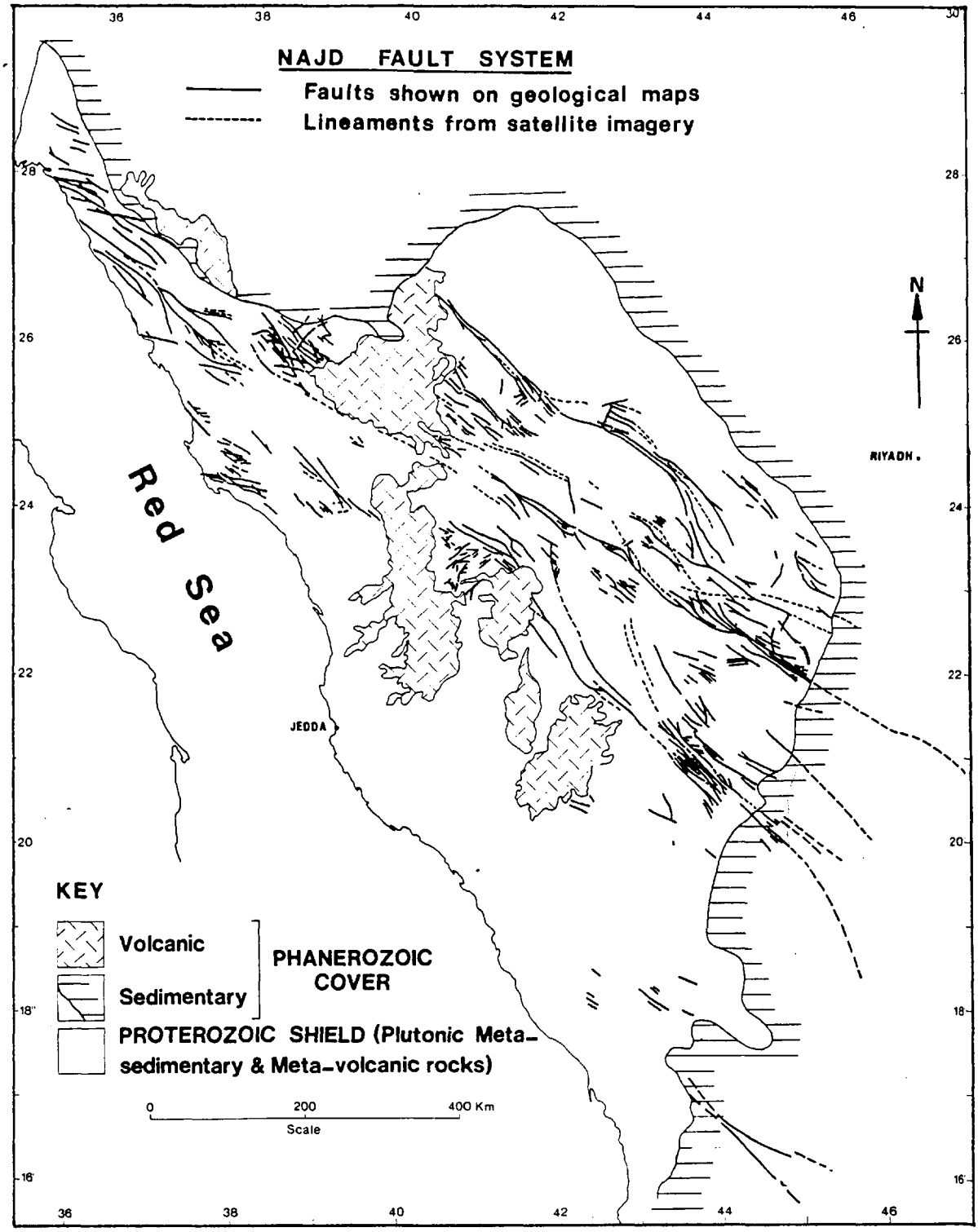


Figure (17) : Outcrop traces of major faults of Najd Fault System in the Arabian Shield (after Moore 1979).

on the cover rocks in certain localities. It is therefore pertinent to enquire whether these faults and their secondary structures played a role during sedimentation and also influenced the structural events in certain parts of the cover rock region ?
Fleck et al,(1976) dated the Najd Fault System as Late Proterozoic to Early Phanerozoic 580.530 million years ago. However the faults were probably re-activated several times up until the Tertiary. The late movements are revealed by displacement of Tertiary dykes, Moore (1979).

(iv) The Hijaz Fault System

The Hijaz tectonic fabric is predominantly north-south with a less conspicuous northeast-southwest trend. (Figure 18).

After the Hijaz events culminated there was dislocation of the Arabian Shield complex by the strike-slip faults of the Najd System in Late Proterozoic and Early Phanerozoic times, (Brown and Jackson, 1960).

Brown (1972) argued that the Hijaz faulting took place at relatively greater depths than the Najd Fault System.

The four important structures outlined above, together with other regional or local events of both structural and stratigraphical nature, would be expected to have

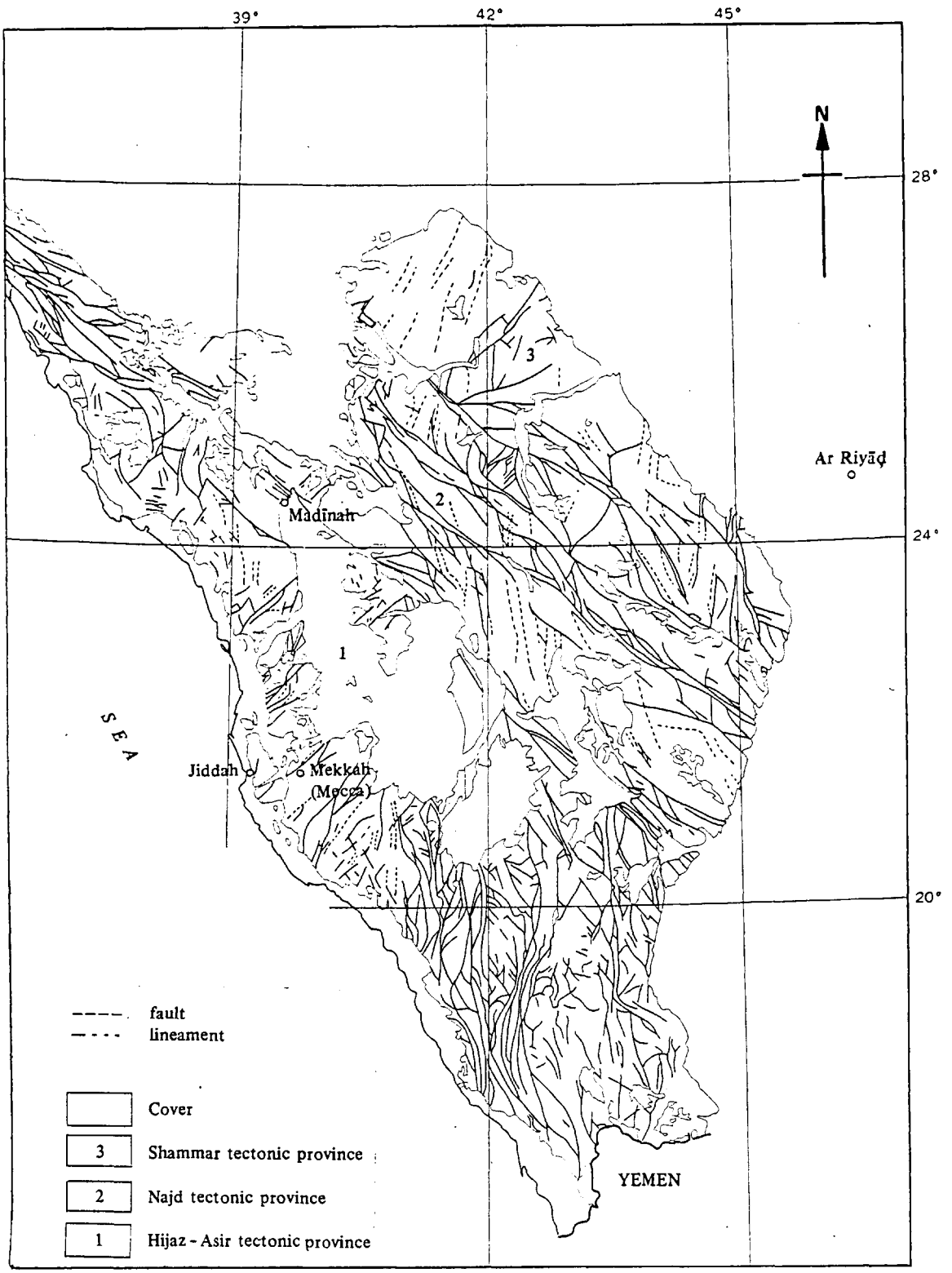


Figure (18) : Hijaz Fault System, mainly represented by the N-S trend, approx 1:7,500,000 scale (after Greenwood etal 1980).

played a role in shaping the structural patterns within the study area particularly with respect to the detected lineaments.

3.3.1 Directional Frequency Rose Diagrams

One of the outcomes of the research is that a total of one hundred and twenty-nine interpretation overlays have been prepared. Each overlay is represented by a frequency rose diagram. All are compiled on the same sheet (Plate 1 A-B) which represent 1:1,000,000 and 1:500,000 images respectively. Regardless of the differences in scale, the roses will be discussed together in general, because such a procedure facilitates correlation of the two scales under various and variable parameters.

Because of these parameters involved in the analysis and for ease of presentation, the writer believes that repetition of certain information can hardly be avoided. This information will be summarised and presented later.

In the interpretation of the results and discussion of their significance minor details at an early stage will not be involved. It is more useful to start by dealing with the dominant and obvious facts and their significance, before proceeding to the detail. This procedure will help the better understanding by a reader and the easy flow of information.

Generally, the rose diagrams of the whole of the thesis area indicate a spread of values (maximum and minimum) of both the same and different class intervals (trends) of certain directions over others which are less dominant. This is no doubt a result of the interaction of various factors. Firstly, the size of the study area and the different structural, and stratigraphical provinces which it includes. Secondly, the multiplicity of the factors involved and the ways in which they mutually interefere in the interpretation process. The dominant characteristics of the roses will be summarised and, during the general review the reasons for the important patterns will be discussed where possible. This is because the writer believes that, although there is agreement among users of Landsat imagery, that lineaments are the most prominent features interpretable from images, these would be meaningless if their origins and/or relations to other features are not established.

3.3.1.1 General Review

The following are amongst the most clearly defined characteristics of the general rose maps, (plate 1 A-B).

(i) There is a prominent mode which trends north 10° east, but which locally swings few degrees to the east or the west. This mode is a maxima in 69% of the roses. The values of these modes ranges from 7% to 28% of the total number of lineaments in each diagram. Where the percentage decreases to 7% or below, but still represents

a maxima in certain diagrams, it indicates that some other trends of varying frequency have started to impress themselves through the data.

In the rest of the diagrams, where this direction is not the maximum, it is also not the minimum. The fact that this direction is prominent and frequent all over the area and across different geological provinces and controlled old intrusives of Precambrian and younger rocks, indicates that it is an old trend which has been partially rejuvinated and propagated upward through the sedimentary cover. It should therefore be regarded as a regional feature.

Because of the dominance and importance of this N 10°E trend it will be discussed in detail under a special section in Chapter four, (Section 4.7).

(ii) Another general feature of the rose plate is the dominance of north-east trends over north-west trends which with few exceptions only are poorly represented.

The north-east trends are present as maxima in 95% of the roses and represent more than 80% of the total lineaments. The NE trends are distributed over a range of maxima which includes that of the N 10°E trend. These maxima are: N40°-50°E, N50°-60°E, N30°-40°E and N70°-80°E respectively.

The N30°-40°E directions probably represents the northeastern part of the Riyadh Fault System. This general trend swings across the area due, either to the presence of some structural control, or, some subsurface factors which modified the upward propagation of the now deeply buried Najd Faults.

The dominance of the northeast lineaments over those which trend northwest is to be regarded as a result of one or more of a complex of factors which involve photogeological, geological and atmospheric conditions. Amongst these are the following :-

a. The average NE direction is normal to or at high angle to the general strike of the stratigraphy in the area, and in consequence they can be more obvious and interpreted with confidence.

b. Most of the lineaments have some topographic expression, being either positive or negative in cross-section. These lineaments are enhanced in the winter by relatively low sun angles (31°-40°) and the sun azimuth (SE-NW). It is therefore fortunate that the majority of the imagery used was exposed in winter time.(Figure 11).

c. The trend might be a direct or indirect expression of Precambrian features , for example the Hijaz

and Najd Systems, which because of erosion are poorly expressed topographically in the rocks of the Shield but are well expressed in the Cover Rocks through which they were later propagated.

d. The majority of the interpretation overlays were produced from high pass filter band 7 images which represent 80% of the 1:1,000,000 images and 51% of the total images. It is possible that the position in which the filter is placed during the processing of the images might have the effect of either enhancing or suppressing particular lineaments, depending on the position of the filter relative to the trend of the lineaments.

(iii) The NW-SE trends, which comprises an average of 5-15% of the total lineaments (although it occasionally reaches 30%) are poorly represented. The trends are in general represented as maxima only in 3% of the total roses. The reason for this relatively low representation has already been discussed. In the few cases where this direction represents either a maximum or higher frequency than the background (Plate1 A-B) it was found to be a result of two important factors.

a. The majority of the roses represent interpretations of images which cover areas of mainly Pre-cambrian rocks where the direction includes the

prominent Najd Fault System and other related structures (roses 75, 87, 68, 61).

The poor representation of this direction over the outcrop of the sedimentary rocks is due to the fact that the rigid blocks of basement reduced the deformation and thus did to a certain extent protect the sedimentary blanket from significant disturbance. (Modified after Dunnington 1958).

b. The rest of the roses of higher values were found to occur in areas which fall in different sedimentary and structural provinces. There they are covered by sabkhas and alluvium where the effect of the NW direction of strike is not an ambiguous factor. Some of these areas are also located in the vicinity of relatively young tectonic provinces. These include the Arabian Gulf, the Zagros belt, and Wadi Al-Batin where it joins Al Majmaah Graben to build up the inferred Eastern Arabian Block. Other similar roses are located in the vicinity of Ha'il Arch.

(iv) The E-W trend is also one of the poorly represented directions, and it is expressed by less than 3% of the total lineaments, with a few exceptions where the value

increases to 10%. The latter are mainly restricted either to high pass filter images or to those which cover Precambrian terraines.

This low representation of the E-W direction may be due to the following factors :-

(a) The standard production images (which represent 50% of the total roses of both scales) exhibit the E-W scanning lines of the MSS which could mask any real E-W lineaments which might be present. Accordingly E-W lineaments were only designated where the evidence for their existance is unequivocal.

(b) In certain areas, where both sedimentary and igneous rocks occur, it was found that the projections of some E-W lineaments seen over sedimentary rocks match up with the direction of dykes and fissures in the igneous rocks. This relationship probably indicates the tensional nature of this trend.

(v) In the few roses (Plate 1, A-B) where the NW direction is represented by several maxima or relatively higher frequencies, some trends of different values spread over the N10^{o}-80°W and gives rise to a rose diagram with a more complex radial pattern. Among the roses which show such a phenomenon are : 57, 73, 121, 122.

In general this pattern is represented in 15% of the total roses in which the values differ slightly due to differences in both scale and quality of the images.

This important and significant feature might be a result of one of the following :-

a. The majority of these roses were constructed from images of certain parts of the basement where different types and sizes of acidic and basic rocks are intruded into the older metamorphic and volcanic rocks. These intrusions, either on their own, or as a part of greater batholiths generated radial patterns of lineaments.

b. The rest of the radial roses are located in areas of sedimentary cover where relatively clear circular, semi-circular and curvilinear patterns occur. Depending on their position relative to the stratigraphic sequence they may represent either, surface propagation or settlement over Precambrian intrusions at depth, or, sedimentary domal structures, such as evaporite domes. Such features are not uncommon in the eastern and north-eastern parts of the area.

(vi) In few roses the relative increase in the NW direction does not produce a radial pattern with the NE directions. Instead some of the trends represent conjugate sets in which the acute angle is directed mainly N-S. The two directions are mainly the N30°-40E° and N40°-50°W. They possibly record the newly discovered Riyadh Fault System (Section 4.6)

The pattern is represented in 11% of the total roses, but it is best displayed by the 1:1,000,000 scale images. The reasons for this are not only those of scale but also the multi-imagery in the 1:1,000,000 series. The roses which illustrate this best are 68, 61, 126 and 87; where the first three represent areas within the sedimentary sequence in the vicinity of Wadi A-Batin and Hail Arch. Rose No. 87 covers a Precambrian part of the shield where the NW direction, i.e. Najd Fault System and related structures are normally expected.

3.3.1.2 Rose Diagrams constructed from high pass filter 2nd generation and infra red colour composites.

The presentation of data will now proceed to details in the analysis of those rose diagrams which were constructed from high pass filter 2nd generation and infra red colour composites of 1:1,000,000 and 1:500,000 respectively.

In these roses interference of variable parameters is minimised and the data are relatively homogeneous.

The thesis area is completely covered by both types of images: the high pass filter band 7 2nd generation, and, the infra-red colour composites. The data from these images are presented all together (Plate 3 A-B). By using this procedure the effects of some objective factors are almost cancelled. In order to minimize the effect of some subjective factors, single interpretations which have been interpreted at closer time intervals were selected. Since the majority of the selected images were exposed in winter time, i.e. the wet season, the effects of the atmospheric factors are minimized.

The same six aspects which were discussed in the general presentation will be dealt with again, and any significant differences or similarities of results will be illustrated and their possible reason discussed where necessary. To avoid repetition the reasons will be mentioned at the end of the presentation.

(i) The prominent N10°-20°E direction is again present represented as the maximum in 73% of the total rose diagrams (Plate 3).

(ii) The dominance of the NE directions over the NW directions is also maintained, but it is less dominant than in the general presentation. These directions vary in their trends across the N10°-80°E arc in the

majority of roses and are present as maxima in 88% of the roses and represent 75-85% of the total lineaments. N5°-6°E is the dominant trend within the NE directions in general and is a maxima in 40% of the roses.

Other directions, N3°-4°E, N4°-5°E and N6°-7°E are present as maxima in 27%, 17% and 7% of the roses respectively.

A point of particular interest in the NE modes (Plate 3) is the relative dominance of the N7°-8°E in 28% of the total roses. This is restricted to the high pass filter band 7 images and is completely missing from the infra-red colour composite images. (Table 3) Such a case strongly supports the idea that enhancement of these images by the filtering processes improved the detectability in that direction.

(iii) The NW directions (N1°-8°W) are more pronounced and represent maxima in 12% of the total roses, and the percentage of the total lineament varies from 15 - 25% in general but in certain roses (77, 58, 87, 122 and 123) this ratio jumps to 48%. In a limited number of roses it is still represented by relatively lower values: 5-10% of the total lineament, e.g. rose 95.

(iv) The E-W model direction (N80°-90°E and S80°-90°E) is increased in this representation where it comprises an average of 5% of the total lineaments. Occasionally

the value increases to 13% in the high pass filter images. The only rose where this direction is represented as a maxima (122) is an infra-red colour composite image covering an area within the Precambrian part of the area.

(v) Roses which indicate radial arrangements of lineaments are also more pronounced in this presentation where they represent 37% of the total roses. The increase is due to the relative increase of the NW directions previously mentioned.

(vi) The NE-NW conjugate sets are also present but are less abundant than the radial trends. They are present in 16% of the total roses. Contrary to the radial patterns, the conjugate sets are more dominant in the interpretations of the high pass filter images. The two directions which form the conjugate set are mainly the N30°-40°E and N40°-50°W with only a few instances where they deviate from these directions.

In summary rose diagrams in Plate 3 show some variations from those in Plate 1 but there are also many similarities.

Regarding the six points which have been discussed in both Plates 1 and 3 the second clearly shows varying degrees of higher values of the whole trends with the exception of the NE directions. These variations are due to many factors the

most important of which are : photographic, photogeological, geological and atmospheric.

The photographing process or some processing techniques have to a certain extent improved the detectability of certain images over the standard production. This is true in the case where the E-W and the N70°-80°E directions are more dominant in the high pass filter images in they are of relative high values in 60% of the total number of its images.

The elimination of repetative interpretations covering wide range of time intervals, and , the selection of those interpretations of closer time intervals, modified the results where the selected interpretations were all done after the writer has gained experience in the use of different types of imagery of different qualities. Thus photogeological factors assisted the detectability of lineaments with greater confidence.

The geological factors, which include both structural and stratigraphical provinces, played an important role because some of the anomalous rose diagrams represent areas which are located in different structural and/or stratigraphical provinces. Some are in the vicinity of previously known structures or of structures discovered in this research. Such anomalous diagrams do in fact provide corroborative evidence for the inferred structures.

The atmospheric factors have in general improved the quality and the detectability of the images included in the second presentation. The majority were exposed in the wet

season which involves a low to moderate sun angle, higher relative humidity and because of higher rainfall less dust. These four factors either individually or together appear to have effects on the final results of the analysis.

3.3.1.3 Correlations between Rose Diagrams of H.P.F.B7 and I.R.C.C Images

To proceed to further detail,(Table 3) includes a correlation between the twenty images of the high pass filter and the twelve images of the infra-red colour composites of Plate 3. The Table allows both results to be correlated in more detail, while, at the same time, the effects of scale and/or type of imagery under variable parameters can be assessed.

Meanwhile, this correlation will prepare the reader for discussion on the effects of scale under constant parameters.

In this table, the same six aspects used in previous correlations are dealt with. In the H.P.F.B7 images rose diagrams the relative increase of the roughly N-S, E-W and N70^{o}-80°W trends and the decrease of the N50^{o}-60°E is probably due to the effect of the filtering process and the elimination of the E-W scanning lines. Relative increase and/or decrease in the number of rose diagrams which indicate radial patterns or conjugate sets is restricted to areas of either Precambrian rocks in the shield or sedimentary provinces where the effect of a northwest strike restriction is insignificant.

	H. P. F. B. 7			I. R. C. C.			
Directions of Lineaments	% of Total No. of Lineaments	% As Maximum	Explanation	% of Total No. of Lineament	% As Maximum	Explanation	General Remarks
Approx. N-S		78%			67%		
N30°-40°E		26	Riyadh Fault System		18		Excluding N10°-20°E
N40°-50°E		33	Riyadh Fault System		17		N20°-30°E is almost missing in both.
N50°-60°E		19			49	Enhanced because of atmospheric factors	
N60°-70°E		13			13		
N70°-80°E		9			3		
N10°-20°W	3.1			2.5			Lower values in both is due to the swing of strike direction.
N20°-30°W	2.7			1.6			
N30°-40°W	3.4		Maxi. in Rd 87	3.4			
N40°-50°W	2			2.8			
N50°-60°W	3.9			2.8		Max in Rd 122	
N60°-70°W	4.7			3.7			
N70°-80°W	4.2			4.3			
TOTAL	24%			21.1%			
N80°-90°W	5.2		Scanning lines eliminated	3.3			Scanning lines included but mainly represent Precambrian areas
Radial Patterns		in 37% of Rose diagrams			in 55% of Rose diagrams		Mainly Precambrian intrusions and strike restriction is invalid
Conjugate Sets		in 27% of the roses			8%		Mainly Precambrian intrusions and strike restriction is invalid
Average Total No. of Lineaments	125				274		

TABLE (3) CORRELATION OF LINEAMENTS BASIC DATA ACQUIRED FROM INTERPRETATIONS OF H.P.F.B 7 ce_2 AND I.R.C.C. IMAGES SCALE 1:1,000,000 AND 1:500,000 RESPECTIVELY.

Since the available H.P.F.B7 images cover relatively wider areas than I.R.C.C these values vary accordingly. Another point of importance in this aspect, is that the relatively higher values in the I.R.C.C are not completely a result of the capability of this type of image to show lineaments. The detectability is improved by the prevailing atmospheric conditions during the wet season where vegetation along some wadis or lineaments can easily be detected by I.R.C.C images. Another clear difference in this correlation is the average total number of the detected lineaments. In the case of the I.R.C.C , an average of 274 lineaments were detected in contrast to the H.P.F.B7 which have an average of 125. This is no doubt due to the scale effect, together with other objective, subjective and atmospheric factors. The effects of each of these factors on the results will be described in detail, but before doing so it is convenient to summarize how the differences between these effects were detected and the technique used.

3.4 SUBTRACTIONS OF FREQUENCY ROSE DIAGRAMS

To test the effect of the various factors on the results of the interpretation process of an image, the raw data of the two interpretations are dealt with. In general, the differences, if any, between any two selected frequency rose diagrams have been subtracted and the significance of the observed differences have been assessed using the Chi-square test.

Thus:-

$$\chi^2 = \frac{(oi - Ei)^2}{Ei}$$

$$i = 1.18$$

where (oi - Ei) is the difference between two rose diagrams for each of the class intervals (0° - 180°) and Ei is the expected distribution. Since the knowledge of this expected distribution is not known, the subtracted distribution is used instead. Thus if we compare rose diagrams of images X and Y then :

$$\chi^2 = \frac{(Xi - Yi)^2}{Yi}$$

$$i = 1.18$$

in this case the observed distribution of the second image data is used as the expected distribution. To cross check the results, some image data subtractions were reversed, for example Rose No. 100-5, then 5-100. In the cases where this test was carried out the final subtractions were the same, that is to say, were either significant or not significant. Nevertheless, it is important to notice that the Chi-square test can only give an approximate idea of the significance of the differences. For this reason, during presentation of any subtracted roses, both rose diagrams will be shown for

further correlation. Also in most cases tables which include the whole lineament raw data, or the main part of it, is shown as well. In certain cases where it is clear that if the differences are not significant, this does not imply that there are no differences but simply that the differences are not of any significance to that particular factor.

It has been noticed that in certain subtractions, that a high or low count value for a particular single class interval is responsible for the observed differences being significant. This was found to be mainly a result of subtracting roses of images exposed under different atmospheric conditions or produced by different enhancement techniques of either photographic or computer processes, rather than the effect of different scales or different MSS bands.

A comparison of some other roses, which represent certain sub areas thought to be of some structural significance, indicated statistically significant differences. These differences were found to lie mainly in the class intervals between N30^{o} - 60°E.This sector seems to be a critical one and it is occupied by more than 40% of the total lineament in the area (Plates 1, 2, 3, 4).

3.5 EFFECT OF VARIOUS FACTORS ON THE RESULTS

It is agreed by most photo-interpreters that objective, subjective and atmospheric factors have various effects on the outcome of any remote sensing study. These effects may be a

result of either, one factor or mutual interference of more than one factor and/or their elements. For this reason, it must be emphasised that if the effect of a particular factor is to be properly understood, then the effects of the other factors must, ideally, be constant.

3.5.1 EFFECTS OF OBJECTIVE FACTORS

3.5.1.1 Scale

Scale is one of the important factors which plays a role in the analysis of the qualitative and quantitative aspects of lineaments. In this study the various qualitative aspects, except direction of lineaments, are not included.

The effects of scale have been dealt with in two ways, viz:

(a) The effects of scale where other factors are variable

(b) The effects where other factors are mainly constant.

(a) The effect of scale where other factors are variable is well demonstrated in Plates 1 and 3 and (Table 3). Despite the heterogenity of other factors, the effects of scale are mainly restricted to the total number of detected lineaments and their lengths. In plates 1 and 3 an average of 180 detected lineaments occurs in each of the 129 rose diagrams plotted for both scales. This average results in

fact mainly from the contribution made by the thirty roses of the 1:500,000 images. These latter have an average of 238 interpreted lineaments and is almost twice that of the 1:1,000,000 images which have an average of 122 lineaments per interpretation. Among the 1:500,000 images the I.R.C.C. image interpretations have an average of 274 lineaments per interpretation. This is almost double that of the 1:1,000,000 H.P.F.B7 which have an average of 125 lineaments per interpretation. These relationships can be seen in (Table 3).

(b) The effects of scale under constant factors include a correlation of five rose diagrams which represent 1:1,000,000 and 1:500,000 image interpretations (Table 4, Figure 21). Types of bands and exposure dates are constant, and other subjective factors are roughly the same with some minor variations. The differences which the table show are in the total number of detected lineaments and their interpreted lengths in kilometres. The average total number of detected lineaments on the 1:500,000 scale is 258, but the number decreases to 112 for the 1:1,000,000 images. The average length of lineament on the 1:500,000 scale images is 31 km, and is almost half that of the 1:1,000,000 scale images which averages 57 kilometres. The other points of correlation in the table are in good agreement, and the slight variations which do occur are probably the effects of subjective factors. The reason for the difference in the lengths and number of lineaments detected using the two different scales is that where two disconnected

Type of Imagery	1:1,000,000 Images Standard Production						1:500,000 Images Standard Production					
Rose Diagram No. MSS Band	2 4	3 5	4 6	5 7	7 F.C.	Average	96 4	98 5	99 6	100 7	95 F.C.	Average
Exposure Date	10-1-73	10-1-73	10-1-73	10-1-73	10-1-73		10-1-73	10-1-73	10-1-73	10-1-73	10-1-73	
Interp. Date	7-9-79	22-4-79	6-6-79	5-6-79	6-6-79		7-6-79	6-6-79	6-6-79	7-6-79	7-6-69	
Interp. Time	1 pm	6 pm	10 am	11 am	8.30 am		9 am	7 pm	12.30 pm	6 pm	9 pm	
Illumination Source	Sun light	Artifi. light + poor sun light	Sun light	Sun light	Artifi. + sun light		Poor sun light + Artifi light	Artifi. light	Sun light	Artifi. + sun light	Artifi. light	
Total No. of Lineaments	106	140 *	97	102	115	112	279	211	285	237	279	258
Total length of Lineaments in km	6442	7839	5372	6365	5364	6276.4	8097.5	6997.5	8339.5	8359	9040.5	8166.8
Average Length of Lineament in km	60	60	55.4	62.4	46.6	57	29	33	29.2	35.3	32.4	31.65
N0°-10°E%	9.4%	4.3%	5.2%	9.8%	11.3%	8%	11.8%	12.8%	13%	8.9%	9.7%	11.2%
N10°-20°E)Graphic)repres.)Total No %	maxim. 26 24.5%	maxim. 26 18.6%	maxim. 26 26.8%	maxim. 15 14.7%	maxim. 19 16.5%	maxim. 22 20.2%	maxim. 53 19%	maxim. 37 17.5%	maxim. 41 14.4%	maxim. 56 23.6%	maxim. 76 28.3%	maxim. 52 20.5%
N20°-30°E	0%	5%	2%	5.9%	5.2%	3.6%	1.4%	4.3%	5.3%	5.11%	3%	3.8%
N30°-40°E	12.3%	12.9%	11.3%	12.7%	14.8%	12.8%	14%	10.9%	10.9%	11.4%	18.6%	13%
N40°-50°E	13.2%	6.4%	7.2%	5.9%	7.8%	8.1%	8.6%	11.8%	7%	9.7%	7.4%	8.9%
E - W	1.9%	3.6%	1%	3.4%	2.1%	2.4%	2.2%	2.3%	2.1%	2.6%	1.3%	2.1%
N40°-50°W	4.7%	3.6%	7.2%	5.9%	5.2%	5.3%	4.3%	5.2%	3.5%	5.1%	1.9%	4%

TABLE (4) CORRELATION OF LINEAMENTS BASIC DATA ACQUIRED FROM INTERPRETATIONS OF S.P. IMAGES BANDS 4, 5, 6, 7 AND I.R.C.C. SCALE 1:1,000,000 AND 1:500,000 (178/43 RIYADH AREA)

segments of a given lineament occur, they would be recorded as two separate lineaments on the 1:500,000 image, but, because of scale would tend to be recorded as one lineament of the same total length on the 1:1,000,000 image.

As previously mentioned aerial photographs of 1:60,000 scale were used to study the effect of relatively large scale on lineament interpretations and to be correlated with Landsat images. In Himar Sabha Area i.e. domal feature (Figure 19) , an uncontrolled aerial photo-mosaic was correlated with a portion of Landsat image 1:500,000 scale roughly covering the same structure.

The lineament analysis of both scales are shown in (Figure 19) and the constructed rose diagrams for this data are shown on (Figure 20-b)

The correlation indicated the following:-

1. The aerial photograph analysis indicated almost four times more lineaments than the Landsat portion.

2. The maximum direction on the aerial photograph frequency rose diagram is the E-W and the N30°-50°W (Najd Fault System), while the maximum on the image rose diagram is the N10°-20°E which is in full agreement with the other Landsat image interpretations. This direction is represented on the aerial photograph frequency rose diagram but with relatively lower value.

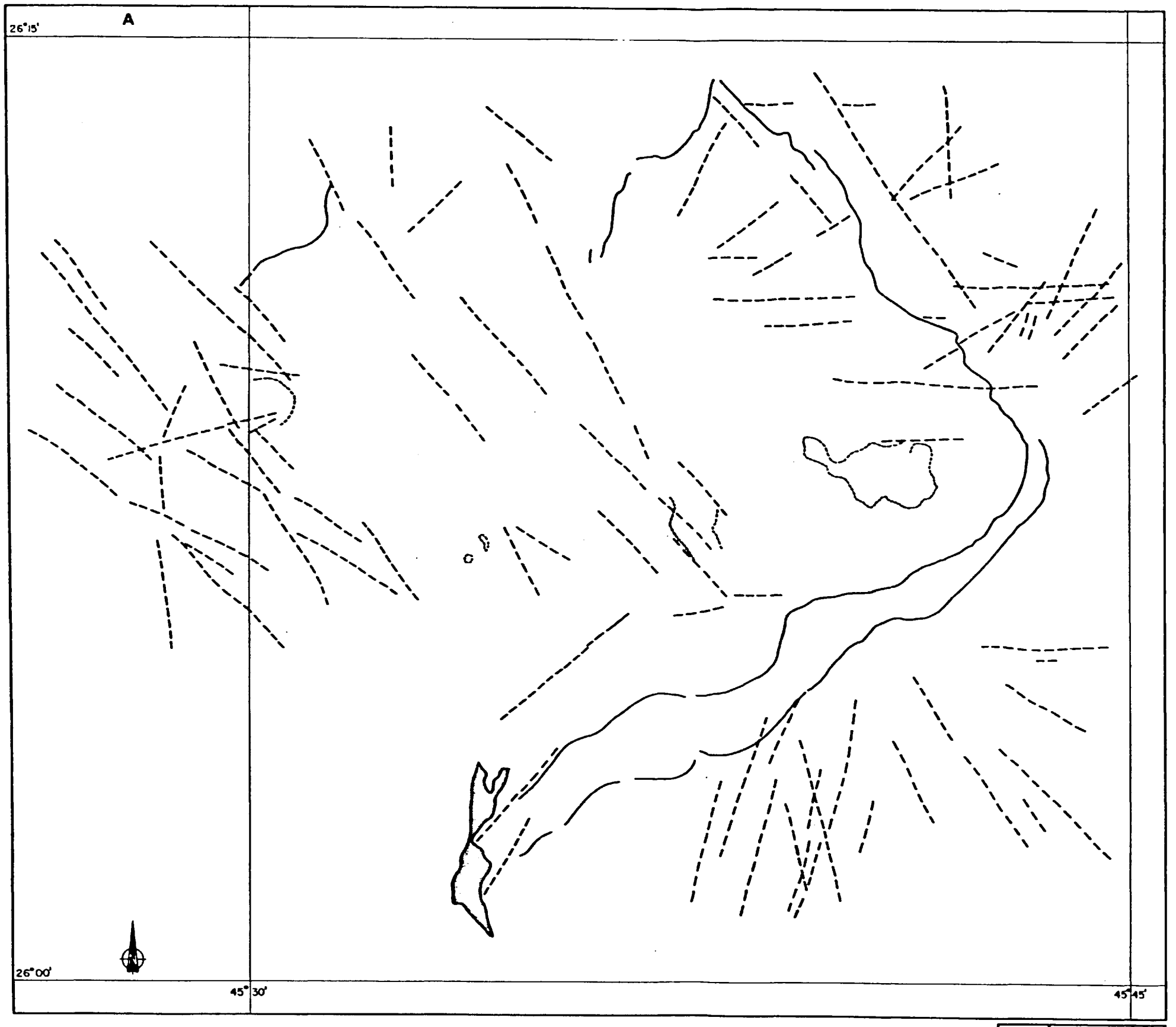


FIGURE 19: ANALYSIS OF HIMAR SABHA STRUCTURE

Based on photo-interpretation by: SHAHTA AL-KHATIEB
A Based on 1:60,000 aerial photographs

3. Some directions which are missing on the image frequency rose diagram for example the N20°-30°E (which is the case on the majority of Landsat images), is represented on the aerial photograph frequency rose diagram with relatively lower values.

4. The correlation between the aerial photograph lineaments in both frequency and length rose diagrams indicate an agreement of 80 - 85%. Such a result generally agrees with the frequency/ length relationship on Landsat images. It can be concluded, however, that under various scales the frequency/length relationship is expected to be almost the same if other factors are constant.

5. On the relative length rose diagrams the N30°-50°W direction of the aerial photograph indicates the maximum and is represented by 14% of the total length, while on the Landsat image portion this trend is represented by 6%, and the maximum length instead is the N50°-60°E direction which in turn is poorly represented on the aerial photograph relative length rose diagram by less than 2%.

From these points of detailed correlation rose diagrams of both scales in this and other examples in Al Amar-Idsas Area, (Figure 20a) it can be concluded that both scales of aerial photographs or mosaics and Landsat images indicate an

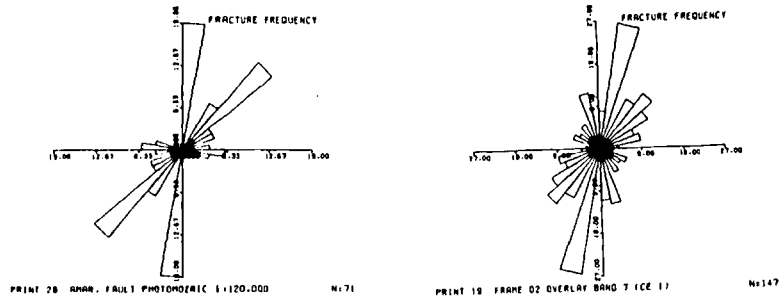


Figure (20 a) : Directional frequency rose diagrams of Khashm Al-Juair Area. Constructed from interpretations of aerial photomosaic, scale 1:120,000 (left) and 1:1,000,000 scale ce_2 image (right).

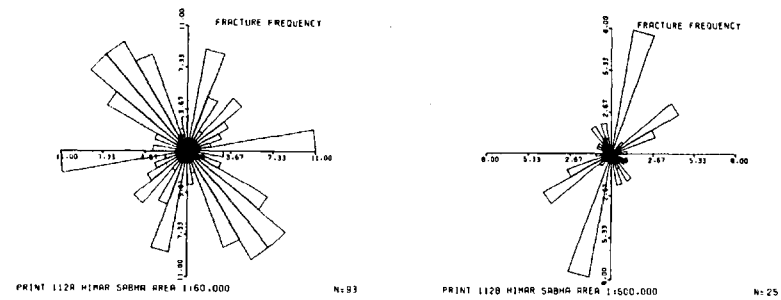


Figure 20 b) : Directional frequency rose diagrams of Himar-Sabha Area, constructed from aerial photographs 1:60,000 scale (left) and part of I.R.C.C. image scale 1:500,000 (right).

almost constant frequency/length relationship of lineaments and provide different and complementary types of geological information regarding lineament analysis.

3.5.1.2 Effect of different multi-spectral bands

Each single band of the MSS image has its own specific wave length which interact with the components of the atmosphere. This means that the validity of any one band and its advantage over other bands is closely related to atmospheric conditions as well as to the aim and the nature of the project under study. In this research one of the objectives was to study the application of multi-band imagery and to investigate any differences the individual bands might have in aiding detection of lineaments or other structural features.

Table 4,Figure 21 indicate a correlation between the four multi-spectral bands 4, 5, 6, 7 and the I.R.C.C. of the same scene (178/43). These images were exposed during the same day, so that atmospheric conditions were constant. They were made in January when the atmospheric conditions in Saudi Arabia are the most favourable for imaging and have the least variable effect on different wave lengths (Figures 12,13,14,15). Under these atmospheric factors various bands indicate less differences regarding their capability of detecting either individual lineaments or trends. This does not apply to the I.R.C.C image which is included here for scale correlation only. Generally speaking, the quality

scale 1:1,000,000 1:500,000

Band

4

5

6

7

I.R.C.C.

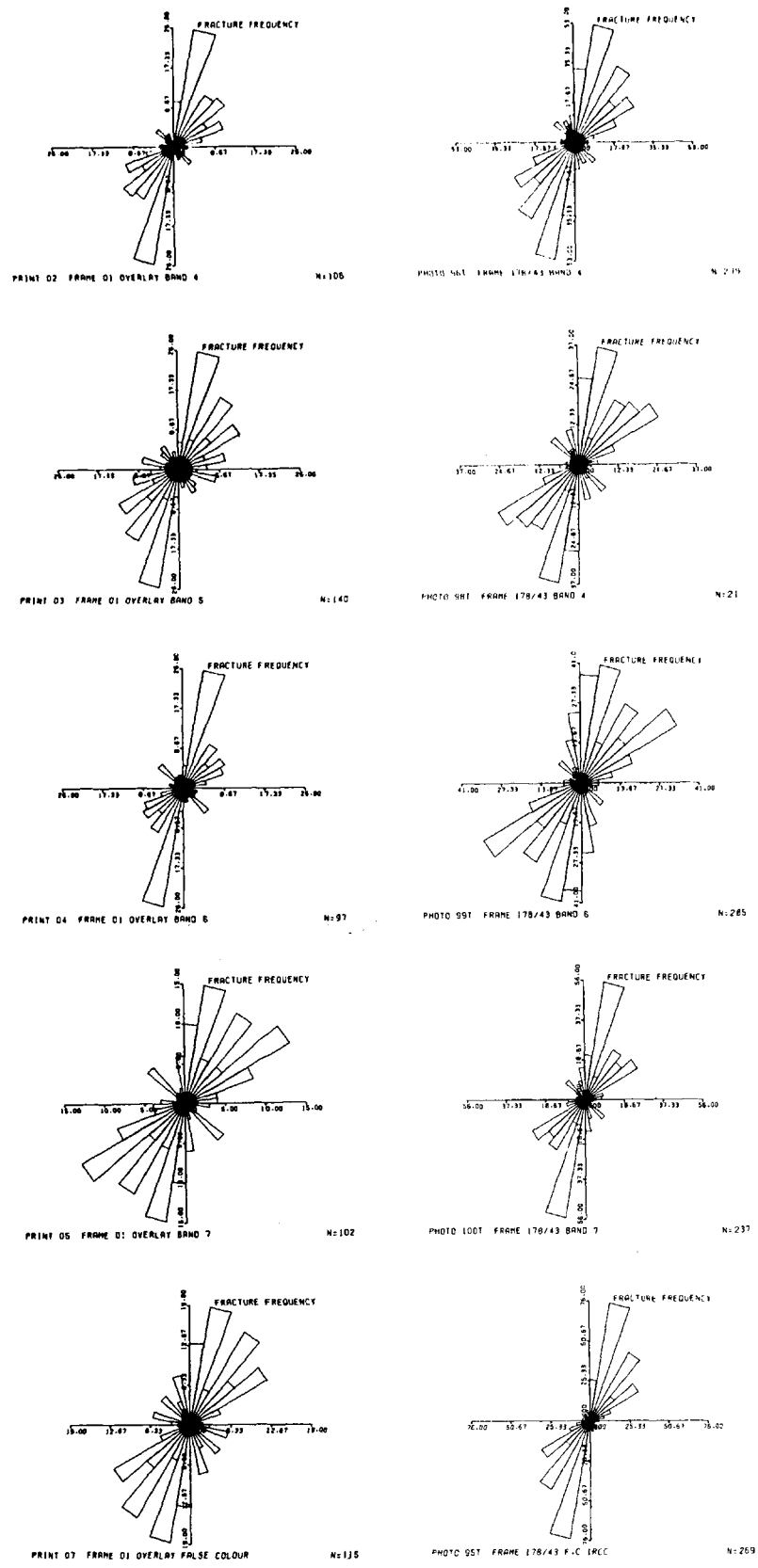


Figure (21) : Directional frequency rose diagrams showing the possible effects of different MSS bands at two scales of scene 178/43 (complementary to Table 4).

of this image and its capability of showing lineaments has been greatly improved by the directly or indirectly prevailing atmospheric conditions of the wet season where it indicates an agreement with 86% of the average background. This conclusion is supported by the following :-
For the correlation of the ratio of each single band to the background average indicated almost the following values :

BAND 4	BAND 5	BAND 6	BAND 7	AVERAGE BACKGROUND
77.3%	78%	77%	82.5%	100%

these values, as well as Table 6 both indicate that Band 7 has a relatively higher value than the other bands. Band 7 being the least sensitive to humidity either in atmosphere or over the vegetation along wadis or lineaments and also sensitive to moisture of soils filling lineaments may have preferably helped in detecting more lineaments in certain trends.

In general it is believed that there is no absolute advantage of one band over another, if atmospheric factors are constant, but rather the favourable band can be selected depending on the nature of the project and the season of the year. For example, if the contacts between water and land is to be drawn with confidence bands 6 and 7 are recommended. If on the other hand, the nature of turbidity currents or suspended sediments at shallow depths in this water are to be studied, bands 4, 5 proved to be the best (Sabin, 1978). This is supported by the case of the Wadi Awsat Graben (Photo plate 12).

This phenomenon is clearly demonstrated in the area in some 1:500,000 images exposed in winter time where few water ponds do exist.

From the structural point of view, image 178/43 includes part of the C.A.G.T.S and some of the related structures. One of these is the Awsat Graben (Photo plate 5, 6, 8, 12) is displaced by scissor-like faults. This displacement is clearly demonstrated by Bands 7, 6, 5 but Band 4 failed to show such a displacement. Instead images of this band indicated other lineaments of mainly the NO^{o}-$10^{o}E$ direction, which is relatively less dominant in the images of Band 5 and 6. This band is not the best if structural displacement and other structural features are to be investigated. Also, during the research it has been found that improving the quality of an image can, to a certain extent, compensate defects of the band involved if Landsat imagery lineaments are to be studied.

3.5.1.3 Effect of Photographic Processing (generated images)

3.5.1.3.1 Negative prints:-

Table 5, Figure 22 indicate data prepared from four interpreted standard production images of Bands 4, 5, 6 and 7 of the scene 178/43 compared with data interpreted from the same bands and the same scene but using negative print images (Photo plate 12.A) and atmospheric factors in both cases are constant. For detailed investigation and for the purpose of cross checking, data is correlated in three ways :

	STANDARD PRODUCTION					NEGATIVE PRINTS				
Rose Diagram No. MSS Band	2 4	3 5	4 6	5 7	Average	9 4	10 5	11 6	12 7	Average
Exposure Date	10.1.73	10.1.73	10.1.73	10.1.73	10.1.73	10.1.73	10.1.73	10.1.73	10.1.73	10.1.73
Interpretation Date	7.9.79	22.4.79	6.6.79	5.6.79	Mid 79	5.9.79	3.9.79	3.9.79	28.8.79	9.79
Interpretation Time	1 pm	6 pm	10 am	11 am	Mainly day time	10.30 am	3.30 pm	11 am	10 am	Day time
Illumination Source	Sun light	Mainly artifi. light	Sun light	Sun light	Mainly sun light	Average sun light	Sun light	Artifi. light + sun light	Sun light	Sunlight + artifi light
Total No. of Lineaments	106	140 *	97	102	111	95	132	159 *	130	129
Total Length of Lineaments (cm)	664.2	783.9	537.2	636.5	650.45	623.9	852.8	848.6	785.8	777.5
Average Length of Lineament (cm)	6	6	5.5	6.2	6	6.56	6.46	5.34	6	6
N0°-10°E%	9.4%	4.3%	5.2%	9.8%	7.2%	11.6%	7.6%	6.9%	6.9%	8.25%
N10°-20°E) Graphic) Repres.) Total No.) %	maxim. 26 24.5%	maxim. 26 18.6%	maxim. 26 26.8%	maxim. 15 14.7%	maxim. 23 21%	maxim. 19 20%	maxim. 26 19.5%	maxim. 27 17%	maxim. 20 15.4%	maxim. 23 18%
N20°-30°E	0%	5%	2%	5.9%	4%	1.1%	3.8%	1.9%	3.8%	2.7%
N30°-40°E	12.3%	12.9%	11.3%	12.7%	12.2%	3.2%	12.1%	15.7%	16.9%	12%
N40°-50°E	13.2%	6.4%	7.2%	5.9%	8.2%	6.3%	4.5%	9.4%	3.1%	5.8%
E - W	1.9%	3.6%	1%	3.9%	2.7%	1.6%	3%	2.5%	2.6%	2.42%
N40°-50°W	4.7%	3.6%	7.2%	5.9%	5.5%	9.5%	3.8%	3.8%	5.4%	5.6%

TABLE (5) CORRELATION OF LINEAMENTS BASIC DATA ACQUIRED FROM INTERPRETATIONS OF S.P. IMAGES BANDS 4, 5, 6, 7 AND N.P. IMAGES SCALE 1:1,000,000 (178/43 RIYADH AREA)

(i) The two types i.e. standard production and negative prints of images of the same band with each other.

(ii) A single band of the standard production against the average background of the four negative print images.

(iii) The average background of both types of images against each other.

In the first correlation, bands 4, 5, 6 and 7 indicated an agreement of 66%, 86%, 72% and 78% respectively. In the second correlation, bands 4, 5, 6 and 7 indicated 75%, 81.5%, 75% and 81% respectively.

In the third correlation, bands 4, 5, 6 and 7 of both types of images agreed with 88% of the total data results.

In the three correlations, some specific trends of lineaments indicated more agreement than others. Amongst them are the following:-

1. The average length of lineament in the three correlations indicated an agreement of 95%, 97% 100% respectively.
2. The prominant N10^{o}-20°E direction indicates an agreement of 86%, 83%, 100% respectively.
3. The N30^{o}-40°E (NE Riyadh Fault System) indicates 67%. 95% and 98%.

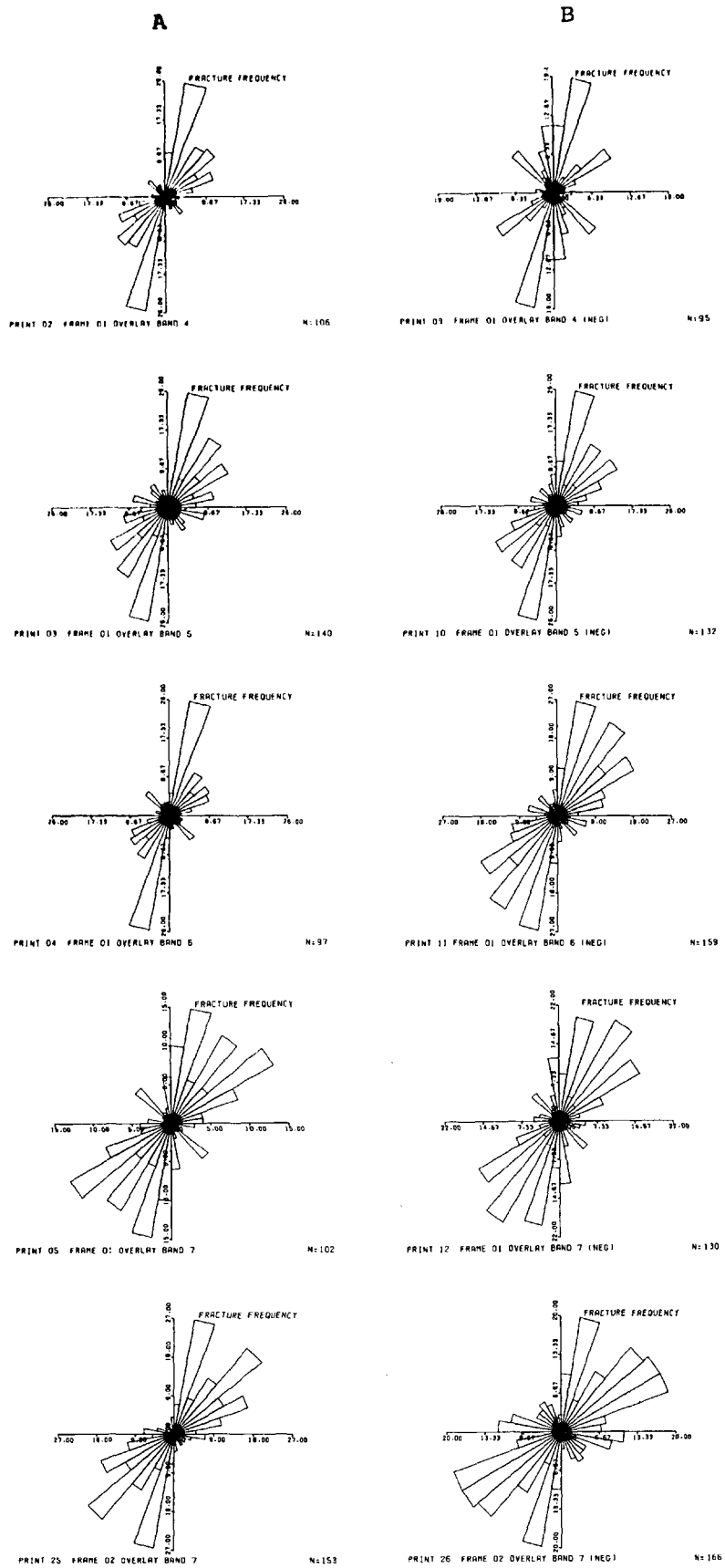


Figure (22) : Directional frequency rose diagrams of interpretations of S.P. images (A) and N.P. images (B) of the same scene, 178/43, scale 1:1,000,000 (complementary to Table 5).

4. The N40°-50°W (NW Riyadh Fault System) indicates 72%, 80% and 98% respectively. The lower value in the first correlation, i.e. 66%, is due to the difference between values of band 4 in both types of images. It can be concluded that this process of generating images by negative prints have affected band 4 more than other bands, by reducing its clarity to show lineaments.

Despite the devaluation of band 4 by this process, it has proved that the mainly prominant trends in the previous examples are still preserved by this process.

The rest of the trends in various bands still indicate relatively high values of agreement ranging from 57% to 90%. These lower values of agreement in the less dominant trends might be due to one or more of the following :-

1. Factors of photographic processing such as amount and homogenuity of light (Zeiss photographing method).

2. Objective factors such as source of illumination used during interpretation, where in Table 5 band 5 S.P and band 6 N.P indicated higher total number of lineaments. (see under Section 3.5.1.5).

3. Subjective factors such as varying date of interpretations which include effect of experience where difference of four months may increase or occasionally decrease number of lineaments in one or more class intervals.

3.5.1.3.2 Positive prints:

Table 6 represents data prepared from interpretations of seven scenes of H.P.F.B7 1st generation images and those generated from them by scanning photographic processes. These seven images have been made available in an early stage of the research. Some include areas of important structures 178/43, 179/43, 179/42,(Photoplates 6,1,13)respectively, and, accordingly they were frequently interpreted, consulted and referred to in most of the discussions. As a result the contents of lineaments and other structures were well recognised and became well known. So the memory of these images directly or indirectly may have improved other types and bands of images of the same scenes in varying degrees.

In table 6 the interpreted data in the two types of images in general have an agreement of 84% with average backgrounds. In detailed correlation of some important class intervals (trends) the following have been noticed:

1. In regard to the average length of lineament, frequency percentage of N20°-30°E, N30°-40°E, both types of images agree by 97%, 98%, 97% respectively.

2. Despite the fact that interpretations of generated images have shown more lineaments in general, the percentage of the prominent N10°-20°E in these images is relatively lower than the H.P.F.B7 images.

3. The average percentage frequency of N0°-10°E,

Type of Imagery	Computer Enhanced (HPFB 7 1st generation)								Generated Images by Photographic Processes							
Path Row	178/43	179/43	180/40	180/41	180/42	179/42	181/41		178/43	179/43	180/40	180/41	180/42	179/42	181/41	
Rose Diagram No.	15	20	32	41	46	51	65	Average	16	19	33	42	47	52	66	Average
Exposure Date all in 1972	10-1-73	6-12	14-10	14-10	14-10	6-12	20-11	wet season	10-1-73	6-12	14-10	14-10	14-10	6-12	20-11	wet season
Interpretation Date all in 1979	5-6	21-8	15-8	7-8	3-8	12-6	17-9		10-6	13-9	15-8	6-9	6-9	12-6	3-9	
Geological Province	Interia homocline	shield + inter. homo.	inter. homo.	inter. homo-cline	shield	inter. homo-cline	shield		Interior homo-cline	shield + int. homo.	inter. homo.	Interia homo-cline	shield	Inter homo-cline	shield	
Interpretation Time	1 pm	1 pm	11 am	12.30 pm	11 am	10.30 am	4.30 pm	day interpre.	8 am	11.30 am	12.30 pm	11 am	3 pm	12 pm	4.30 pm	day interp.
Illumination Source	Sun light	Sun light	Sun light	Artifi. light	Sun light	Sun light	Artifi. light	Sun light	Sun light	Good sun light	Sun light	Good sun light	Sun light	Sun light	Sun light	Sun light
Total No. of Lineaments	113	117	82	129	88	187	127	120	149	147	111	158	163	156	135	146
Total Length of Lineaments (cm)	738.3	686.7	684.8	782.9	447.3	928.9	1110.7	768.5	911	857.4	890.7	863.5	945.5	786.9	1082.1	905
Average Length of Lineament (cm)	6.5	5.9	8.4	6	5.1	5	8.7	6.5	6.1	5.8	8	5.5	5.8	5	8	6.3
N0° - 10°E	16.8%	7.7%	2.4%	3.9%	2.3%	11.2%	4.7%	7%	10.1%	5.4%	0.9%	6.3%	C%	13.5%	3.7%	5.7%
N10°-20°E) Graphic Repres.	maxim	high value	maxim	maxim	maxim	high value	maxim	maxim	maxim	maxim	maxim	maxim		high value	maxim	maxim
N10°-20°E) Total No.	23	14	29	34	21	26	24	24	20	27	18	29	26	17	20	22
N10°-20°E) %	20%	12%	35%	26.5%	24%	14%	19%	21.5%	13.5%	18.5%	16%	18.5%	16%	11%	15%	15.5%
N20°-30°E	0.9%	4.3%	3.7%	5.4%	9.1%	6.4%	0.8%	4.8%	4.7%	1.4%	3.6%	3.2%	5.5%	8.3%	5.9%	4.7%
N30°-40°E	11.5%	9.4%	3.7%	3.1%	4.5%	16.6%	3.9%	7.5%	6.7%	8.2%	9.9%	7.6%	3.7%	14.7%	3%	7.7%
N40°-50°E	8%	12.8%	8.5%	6.2%	11.4%	9.1%	7.1%	9%	7.4%	10.2%	13.5%	12.7%	11.7%	11.5%	14.1%	11.6%
E - W	5.7%	7.2%	3.6%	5.1%	2.8%	2.1%	2.8%	3.3%	9.4%	2.7%	2.7%	2%	6.7%	1.3%	3.9%	4.8%
N40°-50W	4.5%	2.6%	1.2%	0%	3.4%	0.5%	3.1%	2.8%	6.7%	2%	2.7%	0%	1.2%	0.6%	1.5%	2.1%

TABLE (6) CORRELATION OF LINEAMENTS BASIC DATA ACQUIRED FROM INTERPRETATIONS OF H.P.F.B. 7 FIRST GENERATION AND IMAGES GENERATED FROM THEM, SCALE 1:1,000,000.

N10°-20°E, N40°-50°E, E-W, N40°-50°W only agree by 81%, 72%, 78%, 69% and 75% respectively, the first two are higher in the H.P.F.B7 images while the others are lower.

4. Average total numbers of detected lineaments agreed by 82% where the generated images indicated higher values. From the process of high pass filtering it is clear that the direction in which the filters passed across the image determines which linear features are enchanced; those trending normal (or with high angle) to the filter direction are enhanced while lineaments parallel with the filter direction are suppressed (modified after Sabin,1978).

In this (Table 6)despite the increase in the number of lineaments in the generated images, the H.P.F.B7 images indicate higher relative values (percentages) of roughly N-S directions (or other directions which range from 10°-30° degrees to the east or to the west) over the E-W (or other directions which range from 10°-30° degrees to the north or south). Rose diagrams are shown in Figure 23.

From these results it might be concluded that during the process of filtering, the filter was placed in an E-W direction. This conclusion was later supported by Joe Morgan of the U.S.G.S Remote Sensing Department, Virginina (personal communication). The generated images, have been prepared by a scanning photographic process which seems to have changed

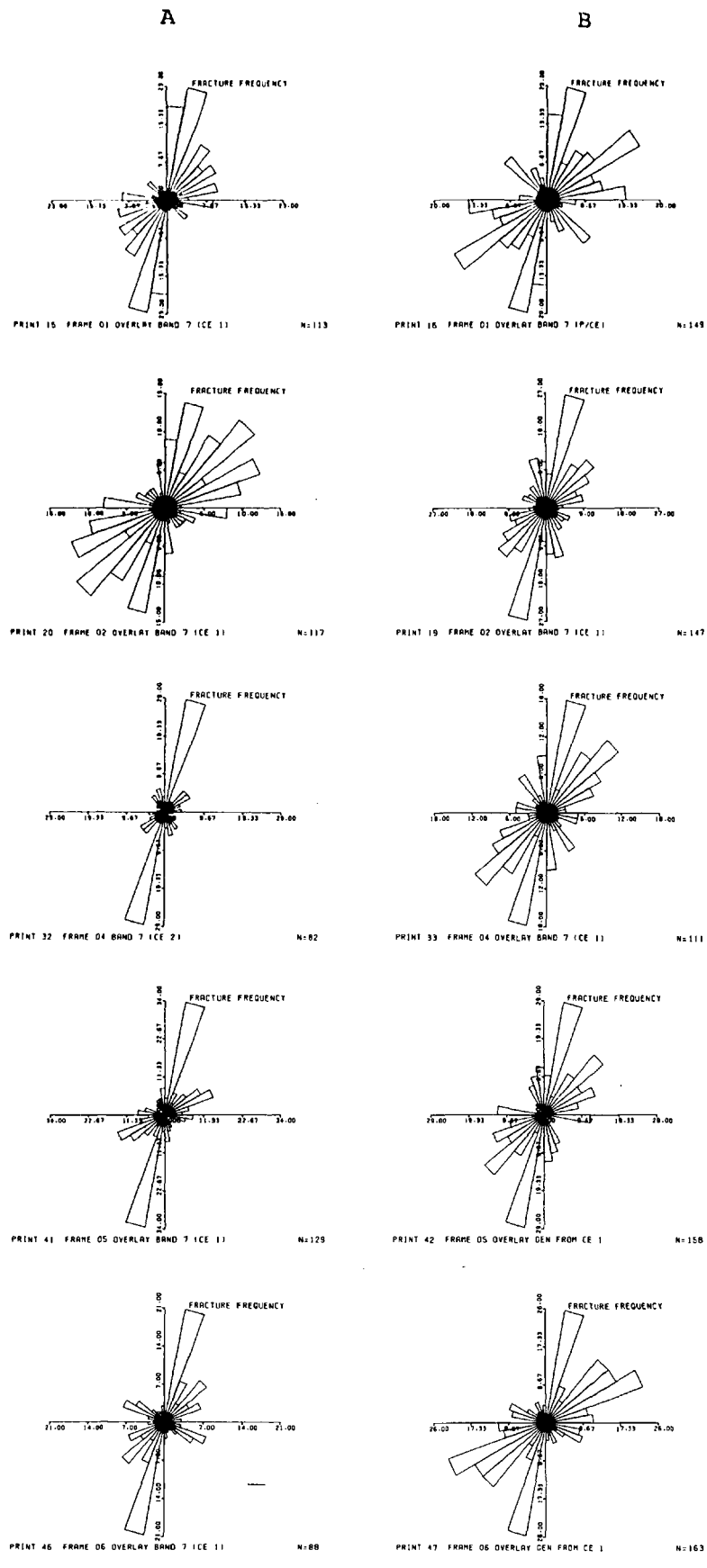


Figure (23) : Directional frequency rose diagrams of interpretations of ce_1 (A) and images generated by photographic processing (B) scale 1:1,000;000 (complementary to Table 6).

the DN values of the original scan lines pixels of the computer enhanced image. As a result a new distribution of DN values was established and the effect of the direction of placing the filter has been altered.

3.5.1.4 Computer Enhancement (High Pass Filter Band 7)

Table 7 represents correlation of interpreted data from seven H.P.F.B7 images of the two generations, and two S.p. images of Band 7. The latter being only two images giving an average measure but still can be referred to where differences between H.P.F.B.7 and s.p. images are required. Correlation of data in this section will be divided into:

(a) Correlation between the two generations of high pass filter images (Ce_1, Ce_2).

(b) Correlation between H.P.F.B.7 and s.p. images.

3.5.1.4.1

(a) The Two Generations of H.P.F.B.7 images are mainly produced by the same process, being stretched first and then subjected to high pass filtering. During the stretching process, different DN values were used to produce each type of image (See Section 2.3.2). Before correlating data interpreted from each type (Table 7), it is relevant to notice the following :

i) The relatively high value of both total frequency and percentage of the class interval N10°-20°E is due

Type of Imagery	Computer Enhanced HPFB7 1st Generation								Standard Production			Computer Enhanced HPFB7 Second Generation							
Path/Row	178/43	179/43	180/40	180/41	180/42	179/42	181/41		178/43	179/43									
Rose Diagram No.	15	20	32	41	46	51	65	Average	5	27	Average	17	22	36	43	48	54	68	Average
Exposure Date	10-1-73	6-12-72	19-10-72	19-10-72	14-10-72	6-12-72	20-11-72	wet sea sun	10-1-73	6-12-72	wet sea sun	10-1-73	6-12-72	14-10-72	14-10-72	14-10-72	6-12-72	20-11-72	wet sea. son
Interpretation Date	5-6-79	21-8-79	15-8-79	7-8-79	3-8-79	12-6-79	17-9-79	-8-79	5-6-79	13-9-79	6-9-79	5-6-79	10-6-79	9-7-79	4-7-79 17-9-79	9-7-79	12-6-79	17-9-79	7.79
Interpretation Time	1 pm	1 pm	11 am	12.30pm	11 am	10.30pm	4.30pm	day time	11 am	10 am	day time	5 pm	11 am	9 am	11 am	9.30 am	12.30 pm	3.30 pm	day inter-pretation
Illumination Source	sun light	artifi. sun light	sun light	artifi. light	sun light	sun light	artifi. light	sun light	sun light	good sun light	sun light	artifi. light	sun light	artifi. light	sun light	sun light	sun light	good sun light	sun + artifi. light
Total No. of Lineaments	113	117	82	129	88	187	127	124	102	34	118	92	134	89	130	108	131	138	117
Total ength of Lineaments (cm)	738.3	686.7	684.8	782.9	447.3	928.9	1110.7	768.5	636.5	742.2	689.3	640.7	843.1	588.7	746.3	560.7	687.1	1307.7	767.8
Average Length of Lineaments (cm)	6.5	5.9	8.4	6	5.1	5	8.7	6.5	6.2	5.5	5.9	7	6.3	6.6	5.7	5.2	5.2	9.5	6.5
NO° - 10E	16.8%	7.7%	2.4%	3.9%	2.3%	11.2%	9.7%	7%	9.8%	8.2%	9%	5.4%	10.4%	1.1%	7.7%	4.6%	25.2%	3.6%	8.3%
N10° 20°E Graphic Rep	max.	v.high	max	max	max.	v.high	max.	max.	max.	high	v.high	max.	high	max.	max.	max.	low	max.	max.
N10° 20°E Actual No.	23	14	29	34	21	26	24	25	15	19	17	21	16	17	16	24	10	17	17
N10° 20°E %	20%	12%	35.4%	26.5%	24%	14%	19%	22%	14.7%	14.2%	14.3%	22.8%	11.9%	19.1%	12.3%	22.2%	7.6%	12.3%	15.5%
N20° - 30°E	0.9%	4.3%	3.7%	5.4%	9.1%	6.4%	0.8%	4.8%	5.9%	2.2%	4%	1.1%	4.5%	5.6%	6.9%	10.2%	8.4%	2.9%	5.7
N30° - 40°E	11.5%	9.4%	3.7%	3.1%	4.5%	16.6%	3.9%	7.5%	12.7%	10.4%	11.5%	10.9%	3.7%	2.2%	11.5%	6.5%	12.2%	10.1%	8.2
N40° - 50°E	8%	12.8%	8.5%	6.2%	11.4%	9.1%	7.1%	9%	5.9%	11.2%	8.5%	10.9%	20.9%	14.6%	6.9%	13.9%	10.7%	10.1%	12.7
E - W	5.7%	4.2%	3.6%	5.1%	2.8%	2.1%	2.8%	3.8%	3.4%	3.7%	4%	4.8%	2.3%	4.5%	4.2%	2.8%	2.6%	3.2%	3.5
N40° - 50°W	4.5%	2.6%	1.2%	0%	3.4%	0.5%	3.1%	2.8%	5.9%	0.7%	3.3%	5.4%	0%	0%	0%	0%	0%	2.9%	1.2

TABLE (7) CORRELATION OF LINEAMENTS BASIC DATA ACQUIRED FROM INTERPRETATIONS OF CE_1 AND CE_2 IMAGES SCALE 1:1,000,000. (TWO S.P. IMAGES ARE INCLUDED FOR FURTHER CORRELATION.)

to the fact that this class interval lineament is being frequently obscured by Quaternary sediments, which apparently have increased the total number of these lineaments.

ii) The N40°-50°W is poorly represented or missing and the comparison of percentages might be misleading, so the value of these two directions will not be included in the correlation.

iii) In Rose diagram No.54 the value of 0°-10° class interval is higher than that of N10°-20°E. The reason for this might be the following:

The majority of lineaments of the class interval 0°-10° represent values of 8.5°-9° being very near to the class interval 10°-20°, since the H.P.F.B.7 images have a disadvantage of not having the co-ordinates, these co-ordinates were transfered from other images which most probably were responsible for this degree or two degrees variation which is limited to one or two cases.

Correlation of the two generations of H.P.F.B 7 (Table 7) agree on 98% of the data included in general, but only in two specific class intervals N40°-50°E and N20°-30°E agreement decreases to 71% and 84% respectively. This correlation indicates that the effect of two different stretching parameters (DN values) in general has no significant effect on data which can be obtained from both types.

3.5.1.4.2

(b) Since the two generations of H.P.F.B 7 agreed on 98% of the data, it is reasonable that the average of both types can be correlated with the S.P images. Both data indicate an agreement of 81%. The values of the S.P images show relatively lower percentages of agreement, in the following class intervals - $N20^{o}$-$30^{o}E$, $N30^{o}$-$40^{o}E$ and $N40^{o}$-$50^{o}W$ respectively.

It seems that H.P.F.B 7 images have improved the detectability of lineaments on images by at least 20%.

3.5.1.5 Effect of Illumination Source

In the majority of previous tables of correlation, the source of illumination and its nature was included because of the effect they may have on results.

Tables 4,5,6, 7, indicate certain relatively higher numbers of detected lineaments if the same images were interpreted using mainly an artificial light.

During the interpretation process clear transparent shining overlays were used. By interpreting the images under a relatively near source of artificial light, the smoothness of the overlays seemed to have affected the reflection and refraction of light thus creating an apparent frequency of lineaments or exagerating the presence of some others, apparently parallel or in the vicinity of relatively clear ones.

3.5.2 EFFECT OF SUBJECTIVE FACTORS

Since these factors are mainly dependent on human characteristics, agreement on their effect on interpretation is variable. In fact the effect of these factors has been referred to indirectly in the previous tables under effect of objective factors on results.. For better understanding and discussion of the effect of some of those important subjective factors they will be dealt with under certain classification where possible, since it is known that the effect has a great interference.

During the interpretation process the interpreter carried out most of the interpretations under the same physiological and psychological factors and which helped in applying relatively consistent procedures.

Memory of good quality images have subconsciously affected the result to some extent. Such a factor proved to be a difficult task to avoid when using multi-imagery techniques. On the other hand, the main factors of subjective nature which can be dealt with individually are human bias, experience, and repetition of interpretations.

3.5.2.1 Human Bias

This can be defined as stated by Burns, et. al. (1976). "The human observer is a variable detector of features and does not produce the same annotation on each occasion".

In this research few images 179/43 of 1:500,000 scale, 178/43 of 1:1000,000 scale,(Photo plate 6) , were interpreted

by 2 and 3 interpreters respectively. This multi-variate method of investigating Landsat image lineaments may give an idea of the human bias effect preferably by percentage of similarities and/or differences between various interpreters. In this correlation, the measure is the total number of lineaments, and their frequency and length in various class intervals.

3.5.2.1.1 Difference in Human Bias between two Interpreters

Image 179/43 band 7 scale 1:500,000 has been interpreted by interpreters A and B. The two interpretations and their representing frequency rose diagrams are shown in Figure 24. The data are included in(Table 8). The table also includes a background summary of both interpreters which may indicate their experiences and knowledge of the area, also it includes some of the subjective factors under which both interpretations have been carried out. To obtain more accurate results the actual number of each class interval lineament and their percentages are correlated. Also the average length of lineament is included to investigate the human bias on both factors. The table indicates that agreement on the actual number of lineaments is 44.4% while a relative number is 44.9% while these values increased in the average length to 73%. This means that despite the disagreement on 55% of the number of lineaments, the 45% lineaments were interpreted with more confidence regarding their length where this agreement is 73% in general, and in 50% of the class intervals the agreement increases up to 90%.

Rose Diagram No.	106	129	
Interpreter	A	B	Agreement %
Interpreter Background	Good	Good	100%
Background of the Area	Good	Average	70%
Previous Interpretations of the Same Scene	Many times in 2 scales	Interpreted occasionally both scales	50-60%
Interpretation Date	9.6.79	24.11.79.	
Illumination Source	Artificial light + sunlight	Mainly Artif. light	70%
Duration of Interpretation	One hour	1/2 hour	75%
Total No. of Lineaments	292	117	40%
Total Length of Lineaments in cm.	1381.3	570	41%
Average Length of Lineaments in cm.	4.7	4.87	97%

Direction	Frequency Act No.	%	Length in cms. Total	%	Frequency Act. No.	%	Length in cms. Total	%	Agreement Freq. Act. No.	%	Length %
N10°-10°E	17	5.8	63.1	3.7	7	6	39.3	5.6	41	97	66
N10°-20°E	60	20.5	299.6	5	9	7.7	36.3	4	15	38	80
N20°-30°E	12	4.1	46.5	3.9	4	3.4	14.9	3.7	33	83	95
N30°-40°E	23	7.9	97.8	4.25	6	5.1	28.5	4.75	25	65	90
N40°-50°E	50	17.1	242.2	4.84	6	5.1	31.6	5.26	12	30	92
N50°-60°E	35	12	169.1	4.83	5	4.3	18.3	3.7	14	36	77
N60°-70°E	35	12	185.7	5.3	13	11.1	67.2	5.2	37	93	98
N10°-80°E	27	9.2	143.3	5.3	15	12.8	87.7	5.8	56	72	91
N80°-90°E	3	1	14.9	5	2	1.7	9.1	4.6	67	59	92
N80°-90°W 90-100	9	3.1	35.2	3.9	11	9.4	59.7	5.4	82	33	72
N10°-80°W 100-110	2	0.7	4.4	2.2	3	2.6	12.5	4.2	67	27	52
N60°-70°W 110-120	2	0.7	15.1	7.55	4	3.4	13.6	3.4	50	21	45
N50°-60°W 120-130	0	0	0	0	4	3.4	19.4	4.9	0	0	0
N40°-50°W 130-140	4	1.4	19.5	4.9	4	3.4	19.3	4.8	100	41	98
N30°-40°W 140-150	6	2.1	19.4	3.2	4	3.4	11.2	2.8	67	62	88
N20°-30°W 150-160	3	1	8.8	2.9	12	10.3	65.7	5.5	25	9	53
N10°-20°W 100-170	2	0.7	4.9	2.5	5	4.3	25.1	5	40	16	50
N0°-10°W 170-180	2	0.7	11.6	5.8	3	2.6	10.9	3.63	67	27	73
									Average % = 44.4%	44.9%	73%

1 Agreement on frequency of lineament 44.9% = 45%

2 Agreement on length of lineaments 73%

3 Total Average agreemtn on interpretation = 59%

TABLE (8) BASIC DATA AND BACKGROUND CORRELATION SHOWING THE EFFECT OF HUMAN BIAS BETWEEN INTERPRETATIONS OF THE SAME IMAGE BY TWO INTERPRETERS (A,B).

Interpreter A

Interpreter B

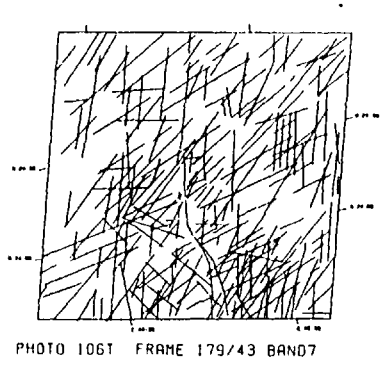


PHOTO 106T FRAME 179/43 BAND7

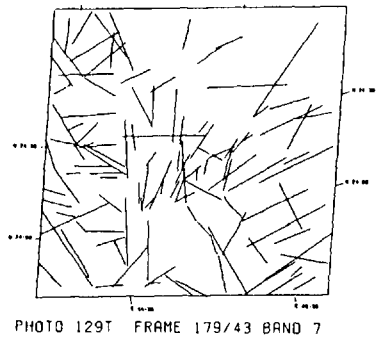
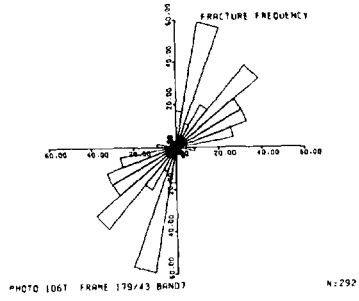


PHOTO 129T FRAME 179/43 BAND 7



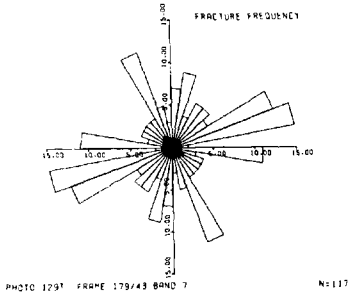


Figure (24) : Lineaments analyses and their directional frequency rose diagrams of image 179/43 band 7, scale 1:500,000 by two interpreters (A and B), showing human bias effect (complementary to Table 8).

This result disagrees with Huntington, Raiche (1978) since they believed that lengths show greater variability between interpreters than the number of lineaments. This might be due to the relatively good quality of the image and the clarity of these lineaments. On the contrary of the detailed contents of interpretation, when rose diagrams are included in the correlation they indicate much higher agreement where they have an average of 80%. The lineaments within the whole class intervals (except $N40^{\circ}-50^{\circ}W$) were observed by both interpreters with varying degrees of frequency.

3.5.2.1.2 Difference in Human Bias between Three Interpreters

For further understanding of the human bias on interpretation and the effect of scale, three interpreters, A, B and C, carried an interpretation of image 178/43 of Ce_2 H.P.F.B7 image of 1:1,000,000 scale. Rose diagrams and interpretations are presented in Figure 25 and the correlated data is presented in Table 9 . The table includes the background information which may have influenced the results.

The agreement between interpreter A, and B on the frequency of lineaments is 51% and on the lengths is 55%. An interesting point to be mentioned is that both interpreter A, and B, in both cases, of two and three interpreters, are the same. The relatively higher agreement is mainly due to the computer enhanced quality of the image and the fact that both backgrounds on this area are closer.

Interpreter B A and C

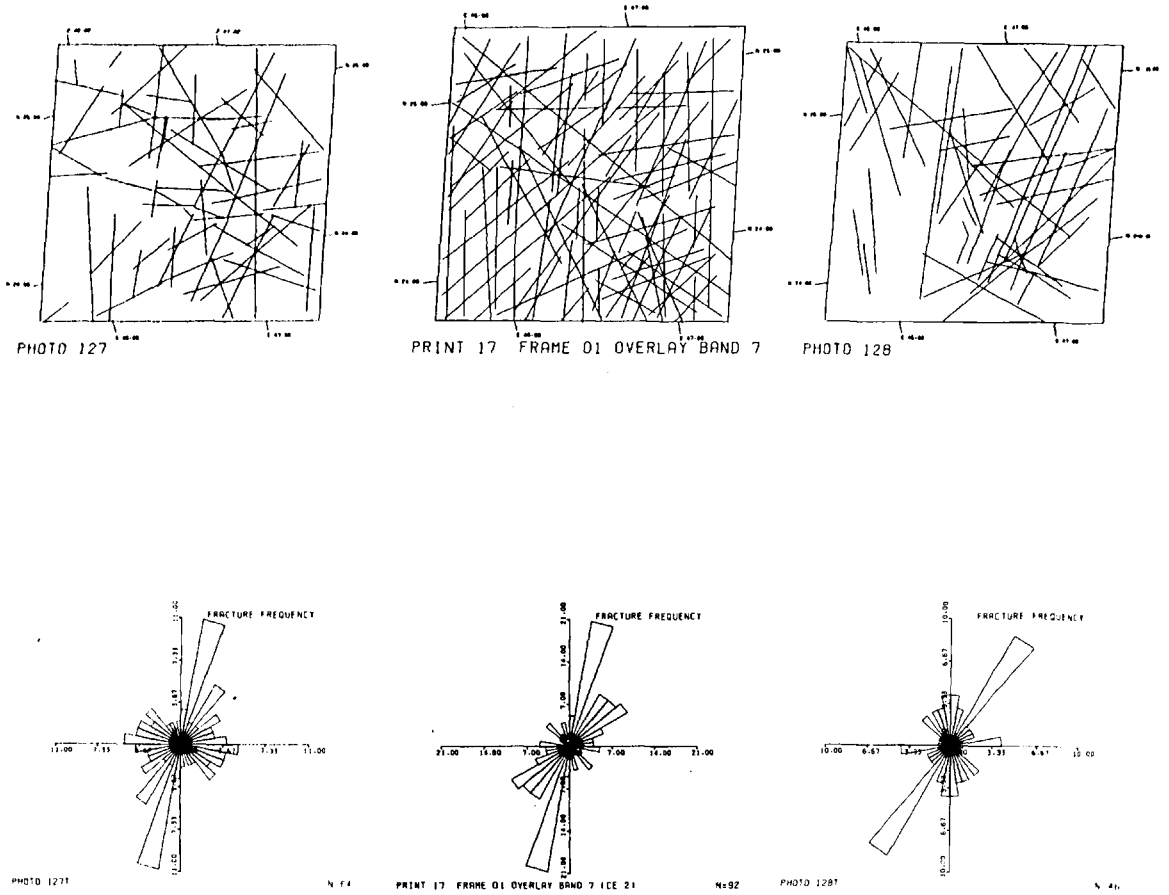


Figure (25) : Lineament analyses and rose diagrams of image 178/43 ce_2, scale 1:1,000,000 by three interpreters (B, A and C), showing human bias effect (complementary to Table 9).

Rose Diagram No.	127	17	128	Agreement In Percentage		
Interpretor	B	A	C	A/C	A/B	B/C
Interpretor Background	very good	good	average	10%	70% - 90%	60%
Background of the Area	average	good	not known	10%	70%	10%
Previous Interpretations of the Same Scene	Few times in two scales	Several times in two scales	Seen the image through discussions with A	0 - 10%	50%	40%
Interpretation Date	6-11-79	5-6-79	7-11-79			
Interpretation Time	8 pm	5 pm	4 pm	Afternoon interpretation		
Illumination Source	Artificial light	Artificial light	Artificial light	Mainly artificial light		
Visual Power	Uses glasses (slight stegmatism)	Don't use glasses (no stegmatism)	Use glasses (slight stegmatism)	60%	70%	50%
Duration of Interpretation	one hour	one hour	one hour (on separate occasions)			
Total Length of Lineaments in cms	640.9	640.7	662.9	97%	100%	97%
Total No. of Lineaments	64	92	46	50%	70%	72%
Observed Horizontal Displacement on Faults	Three	Four	Four	80%	75%	75%
Displacements	Riyadh fault system	Riyadh fault system and Awsat Graben	Riyadh fault system and Awsat Graben	100%	50%	60%
Curved Features	3 (not including 2 of A)	1	0	0%	30%	0%

Direction	Frequency		Length in cms		Frequency		Length in cms		Frequency		Length in cms		A/C			A/B			B/C		
	Act. No.	%	Total	Aver. of Lineam.	Act. No.	%	Total	Aver. of Lineam.	Act. No.	%	Total	Aver. of Lineam.	Act. No. Frequency	%	Average length	Act. No. Frequency	%	Average length	Act. No. Frequency	%	Average length
NO° - 10°E	3	4.7	29.7	9.9	5	5.4	28.3	5.7	4	8.7	37.2	9.3	80%	62%	61%	60%	87%	58%	75%	54%	94%
N 10° - 20°E	11	17.2	116.8	10.6	21	22.8	138.2	6.6	3	6.5	64.9	21.6	14%	29%	31%	52%	75%	62%	27%	38%	49%
N 20° - 30°E	2	3.1	12.3	6.2	1	1.1	11.3	11.3	1	2.2	15.2	15.2	100%	50%	74%	50%	36%	55%	50%	71%	41%
N 30° - 40°E	6	9.4	86.3	14.4	10	10.9	64	6.4	10	21.7	146.3	14.6	100%	50%	44%	60%	86%	44%	60%	43%	99%
N 40° - 50°E	2	3.1	13	6.5	10	10.9	70.3	7	2	4.3	38	19	20%	40%	37%	20%	28%	93%	100%	76%	39%
N 50° - 60°E	4	6.3	46.6	11.7	11	12	75.7	6.9	2	4.3	33.8	16.9	18%	36%	41%	36%	51%	59%	50%	69%	69%
N 60° - 70°E	3	4.7	26.3	8.8	6	6.5	34.3	5.8	2	4.3	34.7	17.3	33%	66%	34%	50%	72%	66%	66%	92%	51%
N 70° - 80°E	3	4.7	26.5	9	4	4.3	29.4	7.4	1	2.2	14	14	25%	51%	53%	75%	92%	82%	33%	47%	64%
N 80° - 90°E	4	6.3	45.7	11.4	4	4.3	26.9	6.7	4	8.7	57.7	14.4	100%	50%	47%	100%	68%	59%	100%	72%	79%
N 80° - 90°W 90° - 100°	5	7.8	46.2	9.2	5	5.4	30.9	6.2	1	2.2	18.1	18.1	20%	41%	34%	100%	69%	67%	20%	28%	51%
N 70° - 80°W 100° - 110°	4	6.3	30.8	7.7	1	1.1	8.9	8.9	0	0	0	0	0	0	0	25%	18%	86%	0	0	0
N 60° - 70°W 110° - 120°	4	6.3	33.9	8.5	0	0	0	0	1	2.2	14.5	14.5	0	0	0	0	0	0	25%	35%	57%
N 50° - 60°W 120° - 130°	3	4.7	20.8	6.9	2	2.2	8.8	4.4	1	2.2	17.5	17.5	50%	100%	25%	66%	53%	64%	33%	47%	39%
N 40° - 50°W 130° - 140°	4	6.3	54.5	13.6	5	5.4	60.4	12.1	3	6.5	57.3	19.1	60%	83%	63%	80%	88%	89%	75%	97%	71%
N 30° - 40°W 140° - 150°	2	3.1	8.8	4.4	0	0	0	0	1	2.2	10.3	10.3	0	0	0	0	0	0	50%	71%	43%
N 20° - 30°W 150° - 160°	2	3.1	29.8	14.9	1	1.1	9.9	9.9	3	6.5	36.1	12	33%	17%	83%	50%	35%	66%	66%	48%	80%
N 10° - 20°W 160° - 170°	0	0	0	0	4	4.3	37.6	9.4	3	6.5	22.2	7.4	75%	66%	79%	0	0	0	0	0	0
N 0° - 10°W 170° - 180°	2	3.1	12.9	6.5	2	2.2	5.9	3	4	8.7	45.1	11.3	50%	25%	27%	100%	71%	46%	50%	36%	58%
% Average													43%	42.5%	41%	51%	51.6%	55.3%	49%	48.5%	54%

	A/C	A/B	B/C
Agreement on average frequency	43%	51%	49%
Agreement on average length	41%	55%	54%
Total average agreement on interpretations	42%	53%	51%

TABLE (9) LINEAMENTS BASIC DATA AND BACKGROUND CORRELATION SHOWING THE EFFECT OF HUMAN BIAS ON INTERPRETATIONS OF THE SAME IMAGE 178/43 CE2 SCALE 1:1,000,000, BY THREE INTERPRETERS B, A, C.

Interpreters A and C agreed on an average of 42% of both frequency and length. This relatively higher disagreement is due to the relatively poor knowledge of interpreter C on the area. Interpreters B and C agreed on 49% of the frequency and 54% of the length with an average of 51% on both aspects. These results emphasize that previous experience of the area and the repetition and experience in interpreting the same images has a relatively important effect on the results.

3.5.2.2 Effect of Experience by the Same Interpreter

It has been noticed during the interpretation process that certain images, which were available early in the research and cover well known areas and important structures, were always interpreted and consulted. Later when the rest of the images covering the whole thesis area were available, they were not exactly subjected to the same repetition and consultation. This is not to be considered as a disadvantage. Instead, they were interpreted after the interpreter had established consistent methods and interpretations were carried out with more confidence.

According to these factors, relatively important areas with images of more than one scale were subjected to many interpretations. They indicated that experience gained over longer periods can either increase or occasionally decrease the total number of lineaments in some class intervals and may add few trends (Figure 26.a). In some other images which do not cover important structures and were subjected to fewer

Early interpretation

Late interpretation

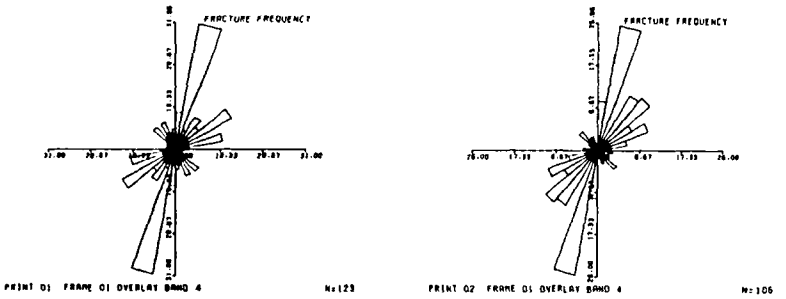


Figure (26 a) : Directional frequency rose diagrams from interpretations of an image, covering a well known and structurally important area; images were available in the early stages of research.

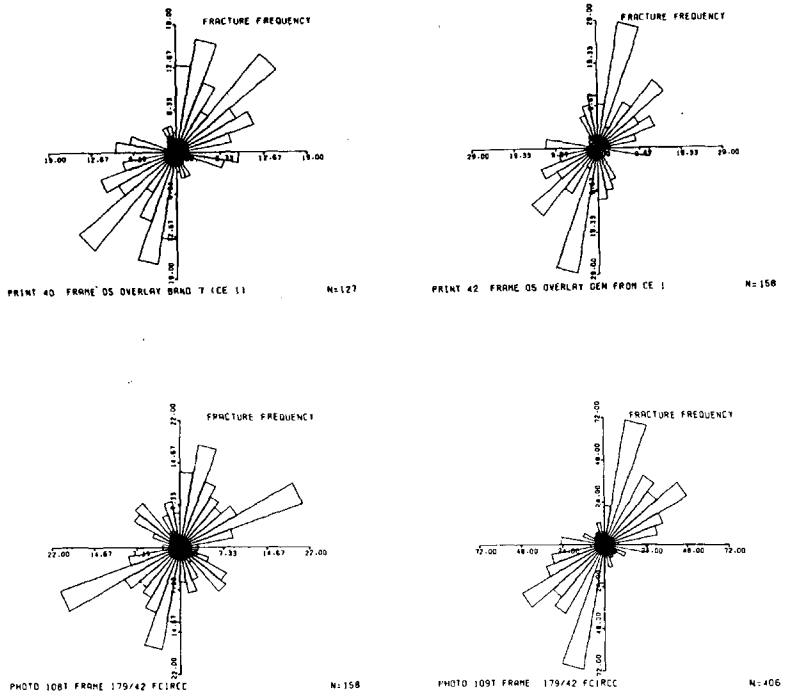


Figure (26 b) : Directional frequency rose diagrams from interpretations of an image: areas which do not include important structures, images were available later in the research.

interpretations on longer time intervals, new trends as well as more lineaments were added. (Figure 26.b).

Experience gained by Repetition and Interpretations by the same interpreter :-

This factor has a connection with the experience factor but does not, by necessity require the same longer time intervals. It is known that variations in lineament interpretation and their patterns of the same scene by the same observer on multiple occasions do occur.

In practice this factor was included in the interpretations of previous correlations of the various tables and plates included in the text.

Agreement between these various multiple interpretations range between 65% - 80%. This percentage of agreement varies according to band, quality and type of image as well as the time interval between interpretations, and to some extent on the nature and the experience of the area covered by this image.

The agreement between interpretations by the same observer in this research in general are higher than those between 2 or 3 observers of various backgrounds (Tables 8,9). This agreement is also higher than those values suggested by Burns and Brown (1979), while agreements achieved between 2 or 3 observers in this research agrees to a certain extent with Burns and Brown who suggested 0.1 to 0.3 (on their scale)* which is equivalent to an average of 51 - 53% agreement.

---

*Burns and Brown suggested an agreement scale of -1, 0, +1, between interpretations by the same observer and between two observers as well.

3.5.3 EFFECT OF ATMOSPHERIC FACTORS

Prevailing atmospheric conditions during the exposure time of multi-bands images is known to play an important role on the quality of images and the detectability of different bands. In some cases the clarity of some bands is minimal due to certain atmospheric factors. For example, bands 4, 5 in a dusty, hazy dry and hot day have a poor clarity relative to band 7. While this difference is minimised under the constant favourable conditions of the wet season.

All particles in the atmosphere scatter the E.M.R. energy which is the main source necessary for the M.S.S. during exposure. Wet atmosphere or dry atmosphere varies regarding their content of N_2, O_2 which are higher in the dry season. In the lower atmosphere and as a result of these contents scattering is much higher in dry than in the wet season (Valley, 1965). Beside these molecules, and relatively larger in size, are dust and haze particles which are of more concern in this section. Since the thesis area and the country in general falls in the arid region of the world, haze and dust to some extent affect or control the horizontal as well as vertical visibility in certain parts of the area. Beside haze and dust other important atmospheric factors are precipitation of rain, relative humidity, temperatures, wind speed, sun elevation and sun azimuth, (Figures 11,12,13,14 and 15) indicate the mean average values of these factors over the main part of Najd Plateau as measured in three different localities in the year 1972, 1973. The majority of images of this research

were made at different seasons. Most of the factors are strongly related either to each other or to a specific time of the year. For example, if an image of a relatively low sun angle is required for a certain project, this implies that it has to be a winter image and higher values of rain, relative humidity, lower temperatures and so on. If higher sun angles are involved this means summer images with almost the reverse of the winter atmospheric factors. Spring and Autumn images lie in between these two extremeties.

According to the atmospheric factors shown on Figures 12,13,14,15, the year can be roughly divided into two seasons; wet season, which extends from early April to late October and a dry season, extending from early May to early October. Unlike the wet season images, dry season images are obtained under more variable factors. The most effective are dust, haze, relatively higher E-W sun angles, low relative humidity and higher air temperatures. In the dry season, haze and dust, because of their small,size can remain suspended in the atmosphere for days and such a situation might be increased by prevailing wind speed and direction. In the thesis area and during helicopter field traversing, it was found that local and/or regional topography together with the distribution of sand dunes and sand belts have a direct effect on controlling haze and dust in the atmosphere(Photo plates 45, 46).

In the case of relatively wide grabens bounded on on one or two sides by cliff-forming rocks and are filled with sands,wind direction and speed were restricted to these

A B

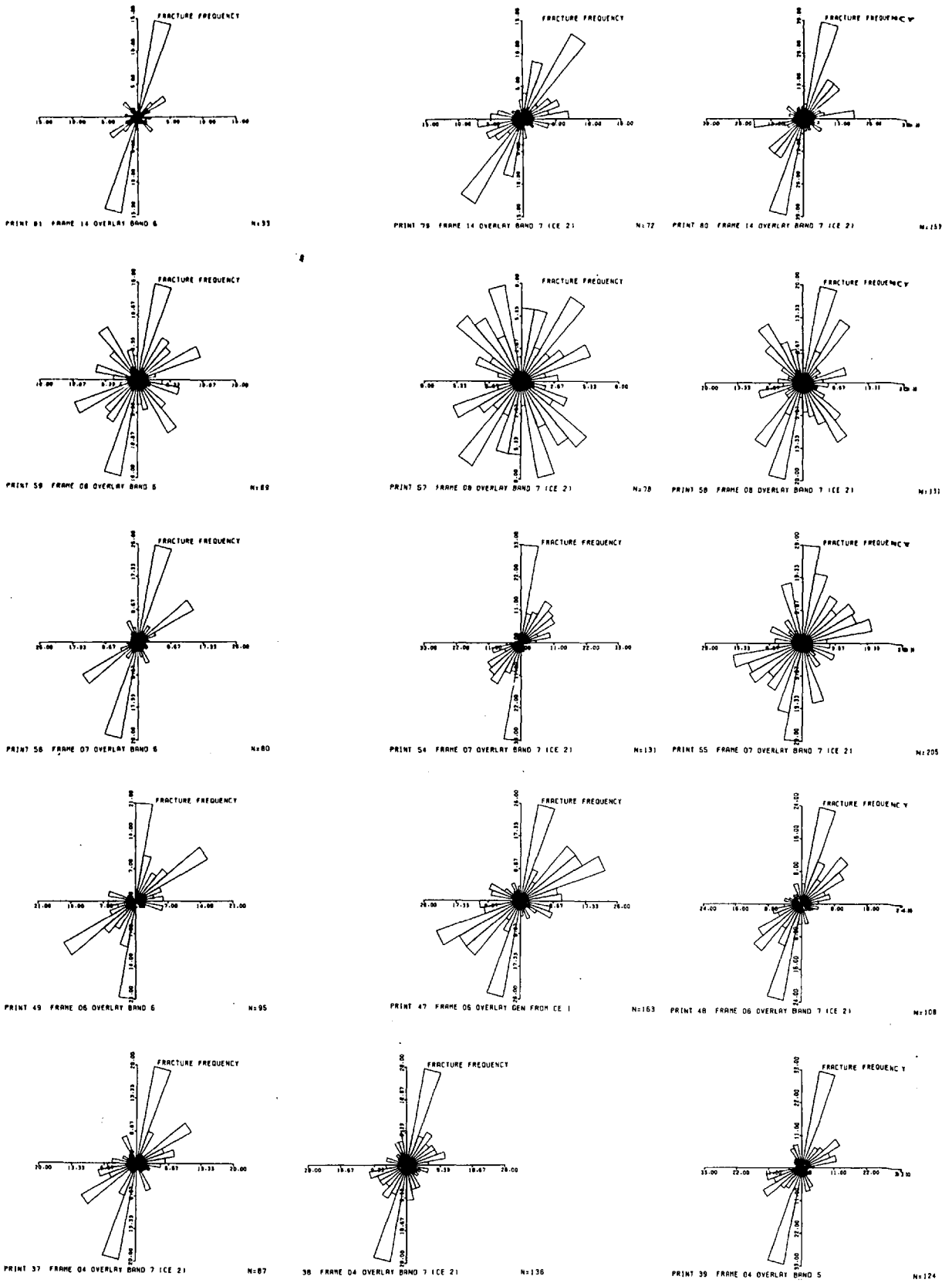


Figure (27) : Frequency rose diagrams from interpretations of images covering the same areas acquired in the dry season (A) and the wet season (B), (complementary to Table 10).

structures and dust and haze minimized both horizontal and vertical visibility. When crossing the area over the graben visibility in general improves (Photoplate 46). Such a phenomenon has its effect on the related image or parts of it depending on the band used.

Fortunately, the majority of images of both scales used in this research were acquired in the wet season which proved to be the best favourable season for images in this part of the world, the atmospheric effect on different bands was insignificant. Some of the S.P. images of band 5 and 6 and a few H.P.F.B7 of certain areas were exposed under both dry and wet season conditions. (Figure 27).

Images of both season are to be correlated, but since S.P. band 7 images were not available in both seasons, few H.P.F.B 7 images together with some S.P. images of the wet seasons were used in this correlation.

The dry season images,Table 10 were mainly interpreted later than the few H.P.F.B7 wet season images used in the correlation, which slightly influenced the effect of the subjective factors in favour of the S.P images of the dry season. Such a process will, to a certain extent, justify the correlation. Within the dry season images, the two H.P.F.B7 images used, exposed in mid-October, and the wet season images of the same scenes were exposed in late December, where atmospheric factors are expected to vary.

Because of the specific nature of this correlation, the average background frequencies of lineaments are to be used and

sun angles and sun azimuths are included in the table. Since the wet season images always indicate the higher values, these values will be referred to in correlation as expected values of 100%. Data shown in the table indicates the following:

1. Dry season images showed an average of 68% of the total lineaments, which may indicate that dust and haze beside sun angle have affected this result since band 7 was not used.

2. The slightly higher values 82% of the N10° - 20°E lineaments are a result of being normal to the dry season sun angle.

3. The dry season images have failed to indicate lineaments in some class intervals which were detected in the wet season images, especially those more or less parallel to the sun azimuth.

4. The N40°-50°W (i.e. 130° - 140°) is poorly represented in images of both seasons which may indicate that the actual presence of this direction is insignificant except in some specific areas.

5. The higher proportion of this direction N40°-50°W under column 2 of both types of images of the same scene 179/40 which is an exceptional case is probably due to the following: This scene represents an area in the Interior Homocline near wadi Al-Batin where

	Dry Season							Wet Season								
	1	2	3	4	5	6	7	1	2	3	4	5	6	7		
Path/Row	177/43	179/40	179/42	160/42	180/40	180/41		177/43	179/40	179/42	180/42	180/40	180/41		Agreement	Remarks
Rose Diagram No.	81	59	56	49	37+38	43+44	average	79+80	57+59	54+55	47+48	39	45	average		
Band	6	5	6	6	7	7	7	7	7	7	7	5	5 good	CE + S.P		Quality of S.P. images is good
Type of Image	S.P	S.P	S.P	S.P	CE 2	CE 2	S.P	CE 2	CE 2	CE 2	CE 2	S.P	S.P	CE + S.P		
Exposure Date	8-7-73	10-7-73	10-7-73	11-7-73	14-10-72	14-10-72	dry season	18-9-73	30-3-77	6-12-72	14-10-72	25-12-72	25-12-72	wet season		
Interp. Date (Memory of CE images)	26-9-79	21-9-79	20-9-79	20-9-79	21-9-79 / 17-9	4-7-79 / 13-8	9-79	4-8-79 / 25-9	8, 31 / 7-79	12, 19 / 9-79	6-9-79 / 9-7	20-9-79	20-9-79	9-79		
Sun Angle	60°	60°	61°	61°	48°	48°	high 56°	57°	42°	35°	48°	30°	30°	Low		
Sun Azimuth	85°	85°	93°	93°	138°	138°	E-W	115°	130°	147°	138°	148°	148°	SE-NW		
Total No. Lineaments	33	89	80	95	112	105	86	112	104	168	135	124	116	127	68%	Images used are CE, exposed in October
N0°-10°E	2	1	1	21[x]	2	9	6	5	5	31[x]	3	3	6	9	67%	[x] These higher values are average of 8° east of north.
N10°-20°E	15	16	26	10	24	16	18	20	13	15	25	33	26	22	82%	
N30°-40°E	0	8	5	7	7	10	6	17	12	16	7	8	11	12	50%	
N40°-50°E	3	7	2	9	5	9	6	10	3	14	17	9	8	10	60%	
E-W	0	2	1	4	5	5	3	8	4	6	5	3	3	5	60%	
N40°-50°W	3	6[x]	1	1	3	0	2	0	8[x]	2	1	3	0	2	100%	These values are due to very clear pattern in the vicinity of wadi Al-Batin
								Landsat 2 Images							68%	Total average agreement
Remarks	No lineam. in 10 classes	N30°-40°W missing	N70°-80°E missing	N50°-90°W missing	N70°-80°W N0°-10°W missing	N40°-70°W in both are missing		N30°-40°W is missing in 80	N30°-40°E trend is clear	N20°-50°W missing	N40°-70°W missing from 48		N20°-60°W missing			

TABLE (10) CORRELATION OF LINEAMENTS BASIC DATA ACQUIRED FROM INTERPRETATIONS OF IMAGES OF THE SAME SCENES EXPOSED UNDER DRY AND WET SEASON CONDITIONS. SCALE 1:1,000,000.

the general NW strike direction of the sedimentary sequence has vanished. Also this H.P.F.B7 image is the only image acquired by Landsat 2, probably with different quality.

6. The relatively higher values of NO°-$10^{\circ}E$ and the lower values of $N10^{\circ}$-$20^{\circ}E$ under line 4 and 3 in dry season and wet season images respectively are mainly not related to atmospheric factors but more likely are due to geological and photogeological reasons in these specific areas. Image 180/42 covers Precambrian areas, 179/42 represents the main part of Al-Majma'ah Graben and related structures.

For further detailed correlation two images of S.P band 5 obtained in late December are correlated with H.P.F.B7 images of the same area made in the middle of October, the first proved to have an advantage of 20% - 25% over the computer enhanced H.P.F.B7 images.

The previous correlation (Table 10) and the remarks made on the results together with many other interpretations during this research clearly indicate that images, whatever their quality, made in the wet season (mainly December-January-February) provide better information than those exposed in the dry season of areas dominated by arid or semi-arid atmospheric conditions. The correlation also indicates that enhancement of certain bands in the dry season can hardly achieve the same results obtained by standard production of other bands exposed

in the wet season. Enhancement of band 7 images made in the dry season, proved to modify and enhance the quality of image for some aspects and can overcome some effects of atmospheric factors such as haze, dust and relative humidity, but to overcome the effect of sun angle and sun azimuth is beyond enhancement capability.

3.6 CORRELATION OF DIRECTIONAL FREQUENCY AND LENGTH ROSE DIAGRAMS

On the same basis as frequency rose diagrams, length rose diagrams were prepared and are presented in Plates 2,4. Some raw data concerning the length of lineaments and the degree to which this length might be affected by some of the objective factors has been indicated in the previous tables.

The length of lineament, in this study, means"length visible on the image which may represent the actual total length in the field."

The extensive literature on the classification of lengths of fractures by several investigators is not of this sections concern, but from the scale of images used in this study, and size and nature of the area, the writer agrees with Blanchet's (1957) definition that lineaments of relatively greater lengths have generated at basement level. To minimize the confusion and noise in the data, lengths less than 1cm on the images were not included in the construction of rose diagrams. Long lineaments disconnected due to local superficial cover over certain parts were an exceptional case,

since a few areas on the images were covered by sand dunes and other alluvial deposits. This is supported by Norman (1967) who found an evidence for an "increased proportion of short lineations within the soil covered area of bedrock". Length as well as frequency of lineaments may serve as a good tool in geological investigations if the relationship is clearly established and understood. It is perhaps surprising that despite several assertions about the significance of lineament lengths, still little is known about their important parameters and little research is directed towards its possible usage and its relation with lineament frequency. The relationship of length and frequency of lineaments is the main concern of this section and has been carried out by a technique in which rose diagrams of frequency were superimposed on those of length of the same interpreted image. This procedure was carried out in two ways; graphically and statistically.

(a) Graphical method: This required the preparation of both lineament frequency and length rose diagrams of the same image into rose diagrams of the same scale and class intervals indicating actual or relative values. These rose diagrams were prepared on thin paper prints through which light can penetrate.

In each class interval, for example N10^{o}-20°E in a given rose diagram the number of lineaments which were included in the frequency rose diagram, their total lengths were also included together in the same class interval on the length rose diagram. Each of 129 frequency rose diagrams was

superimposed on the length rose diagram over a light table and the correlation was carried out visually. The remarks on the general agreement of each rose diagram or each class interval in specific cases were recorded. The total rose diagrams indicated that the frequency/length relationship have a general agreement by more than 90%. For further details of this correlation, the same six general aspects which have been discussed in the previous frequency presentations were also studied in the length presentations. Both length and frequency relationship indicated the following:

1. The prominent N10°-20°E direction is shown as a maximum in 68% of the length rose diagrams and indicated 97% agreement in frequency/length relationship.

2. The NE trends in length rose diagrams in general indicated a clear dominance over the NW direction and indicated 90% agreement in frequency/length relationship. The 10% disagreement is due to increase of length over frequency in 60% of roses and/or increase of the frequency over that length in the 40% of roses.

3. The NW direction is still represented as less dominant in the length rose diagrams and indicated about 85% agreement in frequency/length relationship. This direction indicated relatively much variable results among the six aspects of the

general remarks. In most cases of the 10%-15% disagreement, the few interpreted lineaments in this direction indicated higher values of lengths (65%), while in 35% the difference was due to more lineaments.

4. E-W directions:- This direction represents lower values of length, as in frequency, and they indicated 85% agreement in frequency/length relationship.

5. Roses indicating the radial pattern:- this pattern is presumed in the length rose diagrams with slight variations of the weight of the arcs in the rose diagrams. The frequency/length relationship in this characteristic pattern has a complete agreement of 100%.

6. The conjugate set:- Rose diagrams which indicate conjugate sets of an acute angle directed N-S indicated an agreement of 95 - 100%.

It can be concluded however, that the dominance of some directions which indicates higher values of both frequency and length may indicate a regional significance of these directions, for example the N10^{o}-20°E, N30^{o}-40°E, N40^{o}-50°E. Other directions which include relatively less frequency but indicate higher values of length are more likely to be related to a certain geological feature or affected by certain restrictions in the region, as for example the N40^{o}-50°W

direction. In the third case where few directions indicate few lineaments and shorter lengths, are possibly related to local events of both geological or non geological nature.

(b) The statistical method (frequency/length ratio)

For more detailed correlation and for the purpose of cross checking the previous graphical method, this statistical method was used. The method requires correlation of only the relative values of both frequency and length basic data of the 18 class intervals as given by a computer print-out (Figure 28). This technique was used to avoid the scale problems of the 1:500,000 and 1:1,000,000 interpretations. Being time consuming, this method was carried out by using the raw data of 32 rose diagrams which cover the majority of the effects of objective, subjective and atmospheric factors which have been discussed earlier in the Chapter. This method involved the frequency/length ratio in each of the 18 class intervals and was calculated by dividing the smaller value by the higher, and recording those responsible for the higher or lower ratios, and then the total average of the 18 values was calculated as a frequency/length ratio for each rose diagram. The frequency/length ratio in general indicated an agreement of 83% in both scales.

Using the average ratios of this method the results are relatively lower than that of the graphical method which indicated a higher agreement over 90%. This result agrees with what usually has been noticed before, that agreement

PRINT 66 FRAME 10 OVERLAY GEN FROM CE 1

SEARCH SECTOR (DEGREES) FROM	TO	NO. OF FRACTURES ACTUAL	RELATIVE	LENGTH OF FRACTURES ACTUAL	RELATIVE
0	10.0	5.0	3.7	31.1	2.9
10.0	20.0	20.0	14.8	117.3	10.8
20.0	30.0	8.0	5.9	69.9	6.5
30.0	40.0	4.0	3.0	40.8	3.8
40.0	50.0	19.0	14.1	152.0	14.0
50.0	60.0	9.0	6.7	84.3	7.8
60.0	70.0	0	0	0	0
70.0	80.0	17.0	12.6	199.0	18.4
80.0	90.0	8.0	5.9	41.4	3.8
90.0	100.0	2.0	1.5	16.7	1.5
100.0	110.0	5.0	3.7	34.4	3.2
110.0	120.0	2.0	1.5	9.1	.8
120.0	130.0	6.0	4.4	60.0	5.5
130.0	140.0	2.0	1.5	11.3	1.0
140.0	150.0	7.0	5.2	36.0	3.3
150.0	160.0	11.0	8.1	91.2	8.4
160.0	170.0	1.0	.7	3.3	.3
170.0	180.0	9.0	6.7	84.3	7.8
TOTALS		135.0	100.0	1082.1	100.0

PRINT 67 FRAME 10 OVERLAY BAND 7 (CE 2)

SEARCH SECTOR (DEGREES) FROM	TO	NO. OF FRACTURES ACTUAL	RELATIVE	LENGTH OF FRACTURES ACTUAL	RELATIVE
0	10.0	7.0	7.3	45.4	6.5
10.0	20.0	18.0	18.8	130.2	18.5
20.0	30.0	0	0	0	0
30.0	40.0	3.0	3.1	24.2	3.5
40.0	50.0	10.0	10.4	91.7	13.1
50.0	60.0	4.0	4.2	38.2	5.5
60.0	70.0	6.0	6.3	42.7	6.1
70.0	80.0	13.0	13.5	89.4	12.8
80.0	90.0	4.0	4.2	25.0	3.6
90.0	100.0	4.0	4.2	28.0	4.0
100.0	110.0	6.0	6.3	35.5	5.1
110.0	120.0	1.0	1.0	11.6	1.7
120.0	130.0	3.0	3.1	22.6	3.2
130.0	140.0	3.0	3.1	17.3	2.5
140.0	150.0	1.0	1.0	5.8	.8
150.0	160.0	6.0	6.3	39.9	5.7
160.0	170.0	5.0	5.2	34.4	4.9
170.0	180.0	2.0	2.1	17.5	2.5
TOTALS		96.0	100.0	699.4	100.0

Figure (28) : Basic data of lineament analysis as shown by a computer print-out.

between rose diagrams is higher than correlation of the same statistics of basic data.

From the writers point of view, this impression in fact is an apparent one based on the assumption that human brains can interpret information in graphical forms easier than great amounts of numbers.

In the statistical method it has been noticed that some class intervals include only one, two or three lineaments which in turn possess lengths of different values. This situation being a non representative sample, increases the inhomogenuity of the data and as a result the frequency/length ratio is decreased in the statistical method. This factor acts in favour of the graphical method in the following way:

The average total number of lineaments in the 1:1,000,000 imagery is 125 and 270 in the 1:500,000 images being regarded as the sample number. A given class interval in one of these scales which include 2, 3 or 4 lineaments will be given a relatively small or very small weight in the representation of its graphical arc , i.e. negligible when the rose diagram is constructed. Accordingly, the small arcs are overshadowed by those of the higher values due to the scale of the rose diagram, and the agreement becomes apparently higher in the rose diagrams. If these class intervals with lower values are in the same way eliminated from the data in case of statistical method on the basis being a non-representative samples, the frequency/length ratio will certainly increase to the same level of the graphical method. As a result,

the final frequency/length ratio in this study can be regarded as 90%. This result indicates that in this lineament analysis there is a clear frequency/length relationship which can be summarised as follows:

From correlation of frequency and length of lineaments under the same objective, subjective and atmospheric factors, it is expected that the effect of these factors on the interpretation of length are more or less the same as in frequency. This is supported by an average agreement in frequency/length relationship of around 90%.

On this basis, the previously discussed six general aspects under the frequency rose diagrams can also apply to the length rose diagrams (see section 3.3.1.1). This does not mean underestimating the importance of the length factor, but on the contrary length importance as a qualitative aspect can give some guidance and provide additional information and means of analysing a given pattern of lineaments, which may help in the understanding of the surface and subsurface nature of the rock sequence involved in the same geological events. According to this importance, the length factor is considered under the N-S periodically spaced lineaments and the process of propagation.

CHAPTER FOUR

DETECTED STRUCTURES

4.1 GENERAL DISCUSSION

The analysis of rose diagram maps,(plates 1, 2, 3, 4,) the interpretation of multi-imagery by various methods, and fieldwork integrated with existing supplementary surface and subsurface data, have all revealed the presence of some important structures which are neither shown on previous published maps nor described in reports of the area. These are shown in Figure 29,(in pocket).

To achieve the original intention of this study, it has been regarded desirable to study the lineament analysis of the Phanerozoic sedimentary rocks together with any existing or detected structures in the adjacent exposed Precambrian rocks. Through the lineament analysis it has been found easy to locate frequency highs or directional anomalies, but without studying their possible relation with some existing or interpreted geological structures and other events, the analysis will be of little significance and only tells a small part of the geological story. To avoid this situation, lineament analysis is not treated separately from other geological approaches and, in particular, from the tectonic activity in the area. It is hoped that the recording of these detected structures will assist materially in coming to an overall view of the subsurface structure and geological

development of the Phanerozoic Cover Rocks.

It is noticed, however, that whilst there is much evidence for some form of subsurface feature in the area, it is not always possible to make a fully detailed investigation of the nature of these features or of their possible original structure. It is the intention of the writer to state that the aim of this imagery interpretation, as it is of most photogeological studies and lineament analysis, is to pin-point targets which require more studies by some other geological techniques, such as geochemistry, geophysics, lithofacial studies and drilling. The best example of this is the interpretation of the extension of Al-Amar-Idsas basement fault and the later semi-detailed field investigations which supported its existence in the sedimentary rocks.

4.2 EXTENSION OF THE AL-AMAR-IDSAS BASEMENT FAULT UNDER THE PHANEROZOIC COVER ROCKS

One of the most important structures so far known in the eastern part of the Arabian Shield is the roughly N-S striking Al-Amar-Idsas Fault which, for reasons of structure and mineralization, is of regional significance. All the previously published maps, reports and technical papers on this fault suggested that it ends at the boundary of the Phanerozoic sedimentary rocks, but this proved to be misleading when structural interpretation of different types of Landsat images and aerial photographs was carried out,

using different interpretation methods. The discovery of Al-Amar-Idsas Fault extension was first sensed by applying the fishing method on 1:500,000 I.R.C.C.images. A computer enhanced H.P.F.B7 image of 1:1,000,000 scale, covering the same area, was later used with great advantage, for not only was the effect of the fault on the Jilh Formation detected as in the I.R.C.C. image, but also its extension through the alluvial and sand cover was clearly seen (Photo plates 1,2).

More evidence of the structure was collected from a photomosaic approximately of 1:120,000 scale(Photo plate 5) which had been prepared by the photographic scanning method from four 1:60,000 aerial photographs.

Later ground investigations and helicopter traverses proved the structures in the Jilh Formation at Khashm al-Juair to be a syncline and complementary anticline, the first with a clear plunge, (Khashm in Arabic). Figure 30 is a sketch, interpreted from the photomosaic, and the dip measurements are shown as collected in the field.

The scale of imagery used has some effect on the results. Although no extension of the fault into the sedimentary rocks could be seen on the 1:2,000,000 Landsat mosaic, the structure is detectable on 1:1,000,000 scale imagery and the 1:120,000 photomosaic with a variable degree of clarity depending, in the case of the images, on the band and on the processing of the images used (Photo plates 1,2,3 and 4)

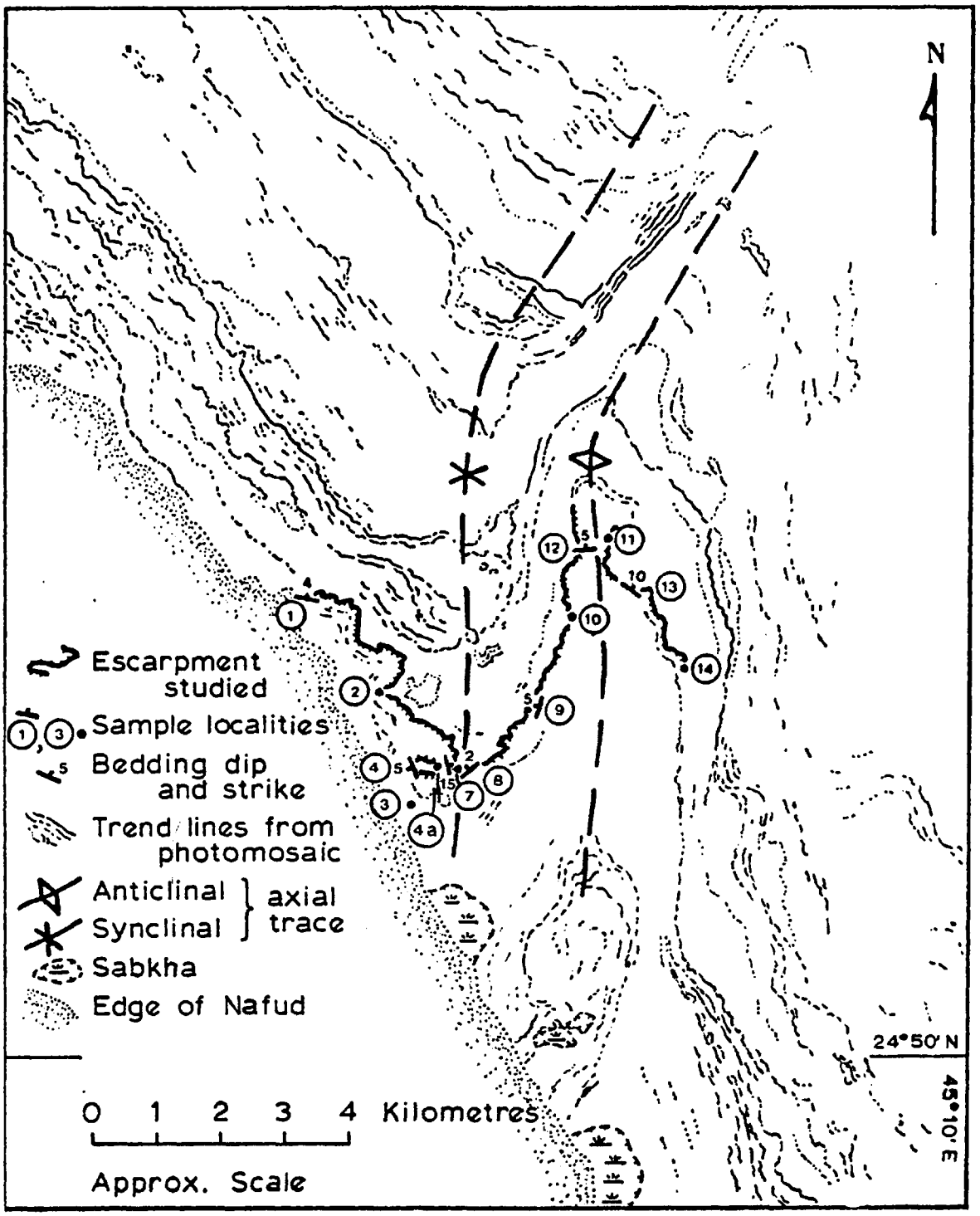


Figure (30) : Structures (syncline and anticline) in the Jilh Formation at Khashm Al-Juair Area: effect of Al-Amar Idsas Basement Fault Extension.

Rose diagrams constructed from interpreted lineaments on both Landsat imagery, 1:1,000,000 and photomosaic 1:120,000 (Figure 20.a) indicated the N10°E direction as a maximum, which is the average direction of the Al-Amar-Idsas Fault, while some other directions are incompletely represented on both types of images with different scales. This correlation of small scale Landsat images and large scale aerial photographs can be summarized as follows :

Except for major features, such as large wadis or prominent long lineaments, most tectonic information from the aerial photographs relates to features too small to be resolved in the Landsat imagery pixels. It can be concluded, however, that aerial photographs and Landsat images provide different and complementary types of geological information. Aerial photographs can provide a particularly useful method for independent corroboration of the existence, or ambiguity, of ill-defined features subjectively identified on Landsat images. The effect of the bands and multiple interpretations, however, has been examined when constructed rose diagrams of lineaments on both sides of the fault were correlated. In some roses significant differences do occur mainly in the basement while differences in the sedimentary rocks are not significant probably due to difference in band detectability as well as difference of the fault effect in both regions (Figure 31).

4.2.1 Al-Amar-Idsas Fault in the Basement

The Al-Amar-Idsas Fault has been previously investigated by a number of geologists and has also been referred to as The Marjan Line (Nebert, 1970) after a small oasis in the area.

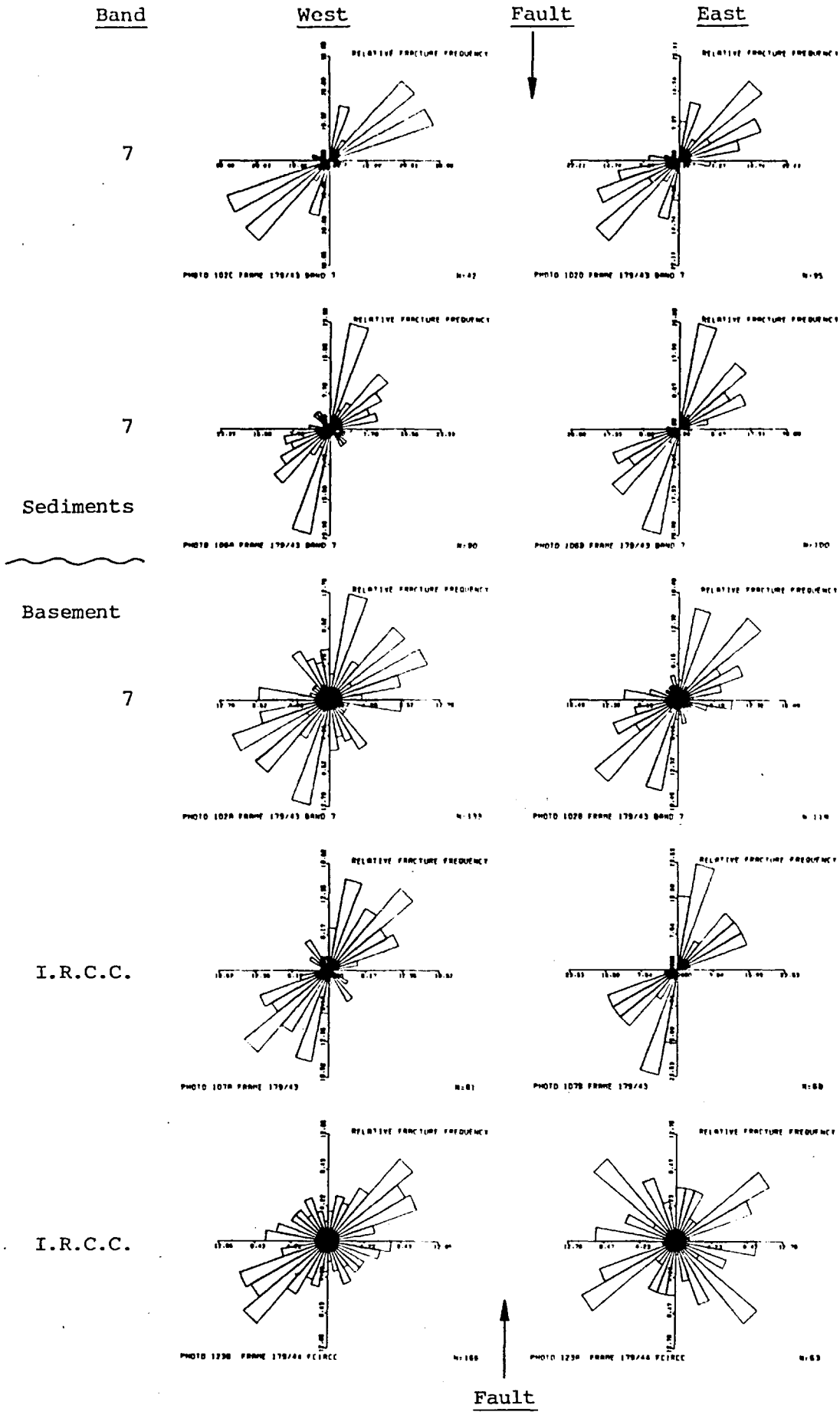


Figure (31): Relative frequency rose diagrams on both sides of Al-Amar Idsas Fault, showing relatively less disturbing effect in the sedimentary rocks than in the Basement.

It has been mapped as a thrust-wrench fault on the U.S.G.S. geological map 1:270-A. Its curved southern section is thought to be a thrust, while it is represented as a transcurrent fault in its northern part, which is also curved. On the same map, the fault separates two geologically different formations, the older Abt Schist to the west and the relatively younger Halaban Formation to the east (Figure 32).

Shanti and Mitchell (1976) indicated that the fault represents a late Precambrian subduction and collision zone. Nawab (1978) later supported Shanti and Mitchell's idea of its representing a subduction zone and added that it is a major tectonic discontinuity along which later movements were of transcurrent nature. Moore (1976) presented the relation of the fault to mineralization in the Arabian Shield, where metalliferous mineral deposits formed a mineral belt (Figure 33). Moore also indicated that the fault has been activated and moved (displaced) by sinistral slip (transcurrent) faulting during the Early Palaeozoic Najd Orogeny.

During the interpretation, the reason for the curved northern part of this fault in the basement has been deduced from study of Landsat image 179/43 generated from H.P.F.B7. The fault has followed part of a pre-existing arc before straightening again and heading towards the sedimentary rocks. Part of the continuation of this arc that has not been used in Al-Amar-Idsas movement is seen on Photo plate 3 . A second arcuate section is also seen along the recorded position of the fault. These arcuate features have been previously noted

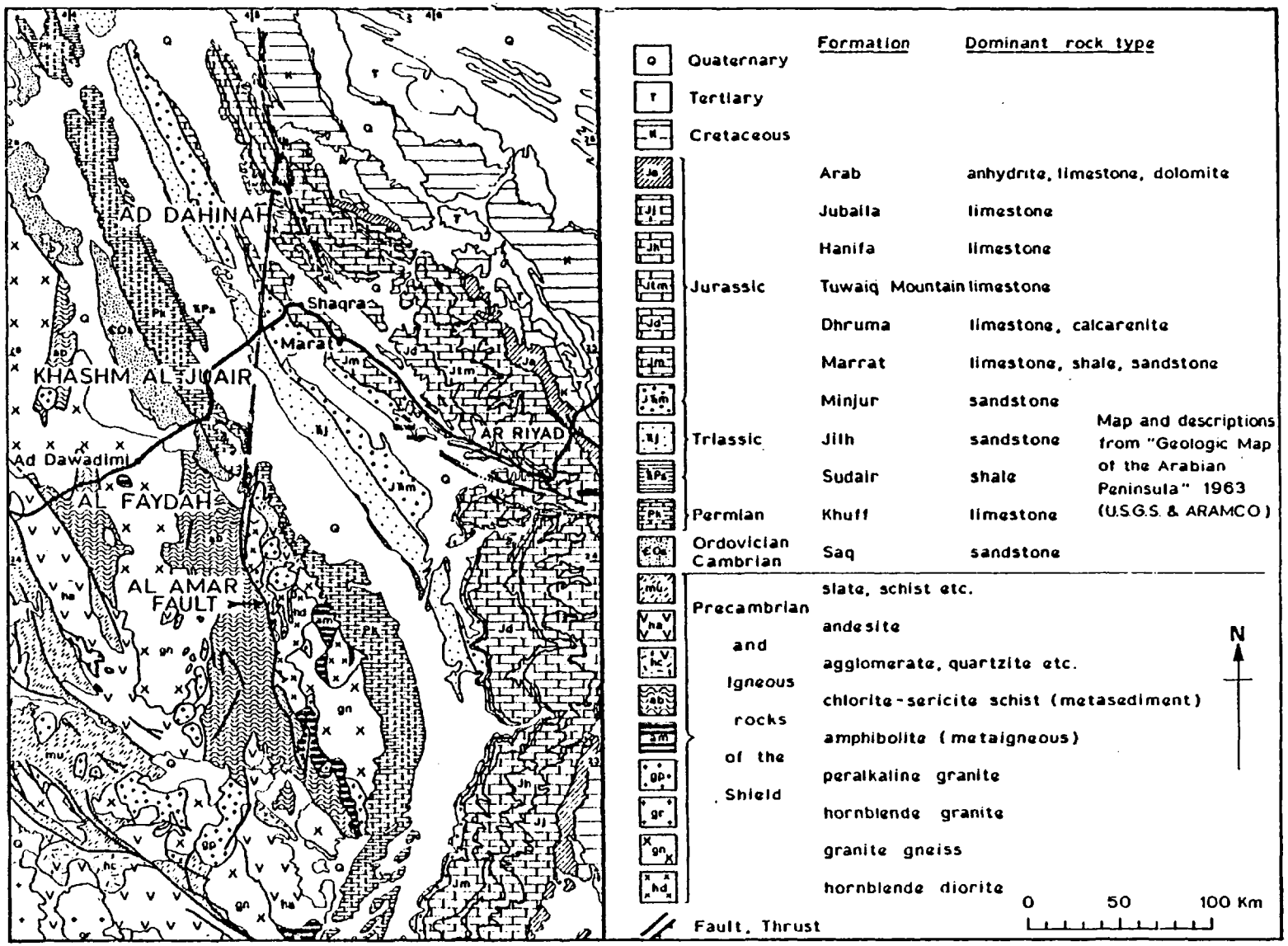


Figure (32) : Extension of Al-Amar Idsas Fault in the sedimentary Cover Rocks.

and appear to be the remaining evidence of large impact' phenomena; and not only are the arcs part of a peripheral phenomenon outside the old cratons, but the deeper rocks inside may have undergone sufficient heating and impact metamorphism to form resistent blocks (Norman, 1980). From this evidence it would appear that the Al-Amar-Idsas Fault is a response to later stresses, but exploiting part of the line of an old pre-existing roughly N-S failure zone or perhaps being deflected around circular resistant blocks. These N-S failure zones have been occupied by a Precambrian granites (Figure 57). From this, it can be deduced that there is a very old basement system of features in this direction which appears to have been rejuvinated in Phanerozoic times; and that, should that part of the fault under the sedimentary rocks exist, it is more likely to be in the same general N-S direction.

4.2.2 Evidence of Movement in the Sedimentary Rocks

If the Al-Amar-Idsas Fault is a line of collision and subduction along which later movements were of a transcurrent nature, such a movement within the Precambrian part has been propagated upward through the sedimentary cover and has affected them in a way that depends to some extent on their lithology and/or thickness as well as on the magnitude and continuity of activation. Nebert (1970) suggested reactivation a number of times, the last of which was in the Quaternary. It has been found, however, that the latest reactivation appears to have taken place in Early or Middle Cretaceous times,

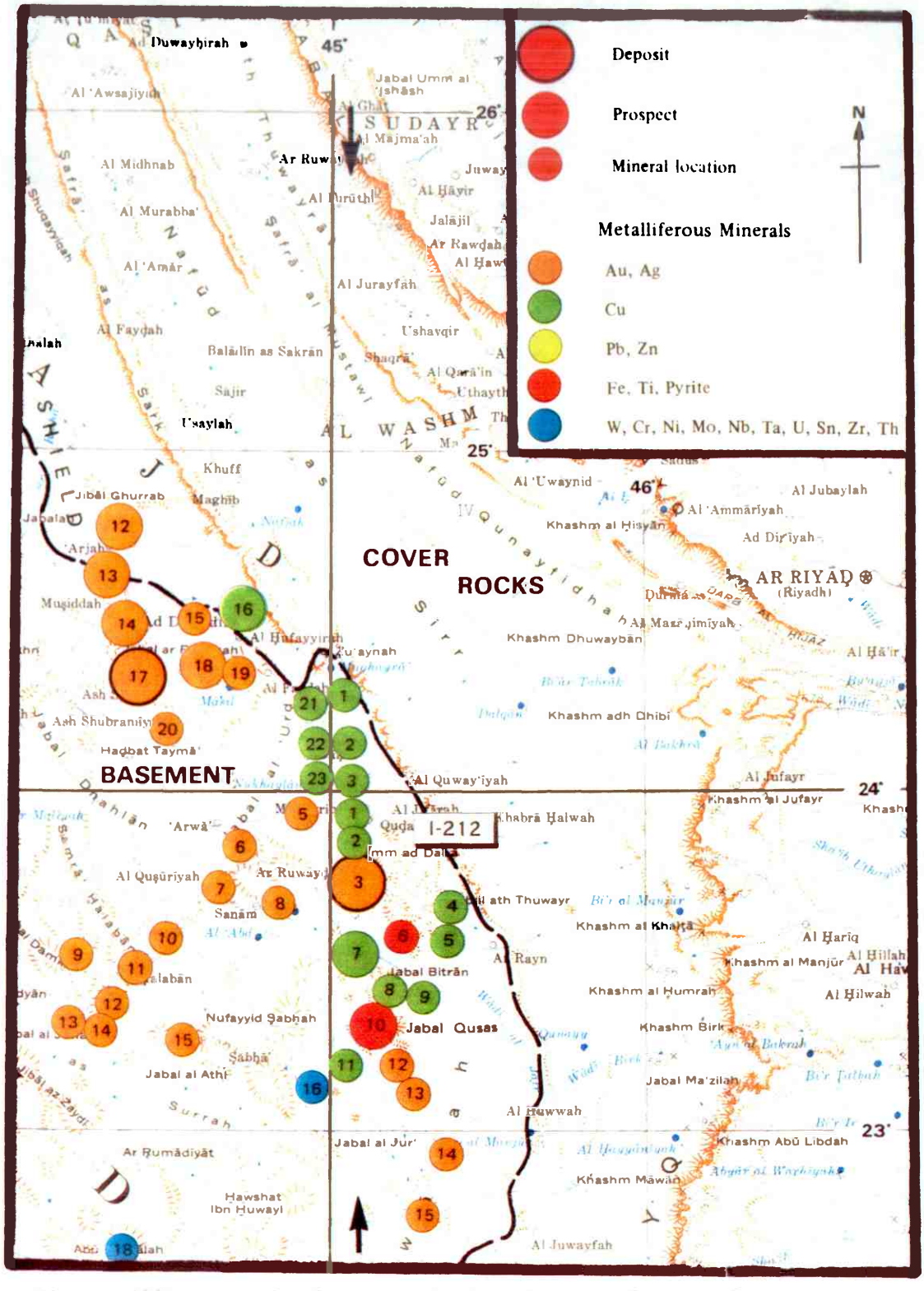


Figure (33) : Metalliferous belt in Al-Amar Idsas Fault Region scale 1:2,000,000 (modified after Van Daalhoff 1974). Approx. fault location is shown by arrows.

just about the time of the formation of the Al Majma'ah Graben (which is a part of the C.A.G.T.S.). The evidence of the clear extension of the fault within the sedimentary rocks is disturbed by the graben and some of its related structures. Evidence of movement within the rocks of the Jilh Formation is clearly visible on Landsat image 179/43, on both S.P and the H.P.F.B7(Photo plates 4,1)and can also be clearly seen on the 1:120,000 photomosaic (Photo plate 5).

Ground investigations were carried out, both by field traverses and helicopter reconnaissance. During the field work the dip measurements on the flanks of the syncline and anticline ranged from 12° to 2° on both sides (Figure 30). The syncline to the west is clearly plunging (Khashm Al Juair). Within the fault zone, shear joints occur trending more or less normal to the fault zone itself, while other N-S joints are parallel to the fault zone and are displaced by others of E-W direction (Photo plate 35).

Detailed stratigraphic sections within the Jilh Formation proved differences in the sedimentary horizons across the fault extension and clearly demonstrate the effect of the fault (Garrard, 1980). Here, in Khashm Al-Juair, after trending constantly southeast for tens of kilometers, the Jilh escarpment swings abruptly northeast and north for six kilometres, then sharply south for a further seven kilometres, before resuming its southeast trend again (Photo plate 5).

Dip measurements on Khashm Al-Juair show that the northerly re-entrant of the escarpment is not simply an

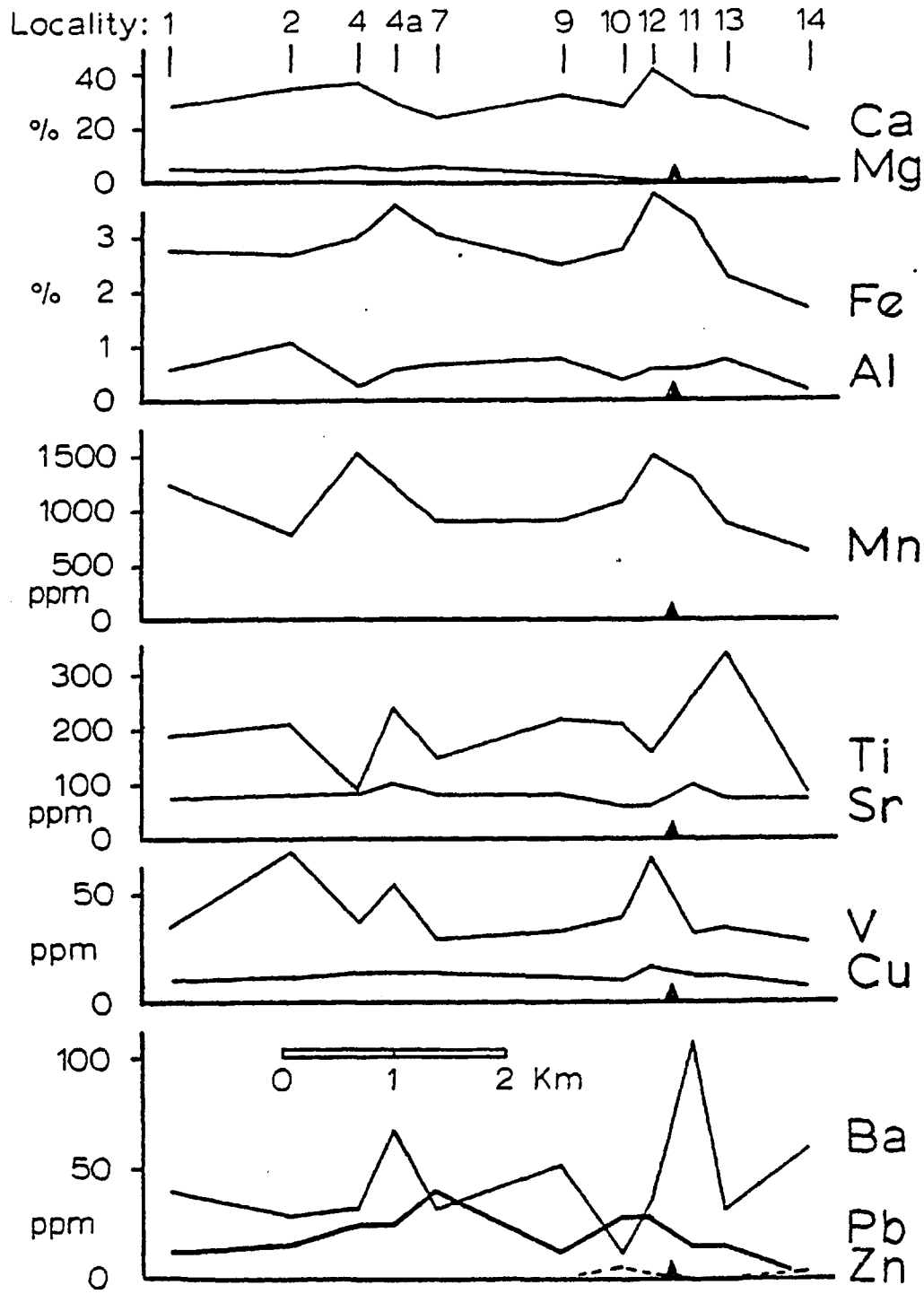


Figure 34 : Lithogeochemistry of the Jilh Formation carbonates of Khashm Al-Juair Structure. The axial trace of anticline ▲ (after Garrard 1980).

erosional feature cutting back into regularly dipping beds, but is in fact a reflection of horizontal transcurrent movement with a relatively smaller component of vertical movement indicated by the gentle dips on both flanks of the syncline and anticline (personal communication, Dr. J. Cosgrove). This is supported by investigation of the fault in the basement, which indicates that the latest movements along the fault were of a strike-slip nature. Further evidence of movement has been reported by Lozej (1979) who stated that "east of the fault there occurs a relatively smaller fault related to the Al-Amar-Idsas Fault, which has controlled the sedimentation in the area, and the overlying Khuff Formation suffered warping of its beds from 5 to 10 degrees. This related fault, which displays the same structural effect as the Al-Amar-Idsas Fault, can be considered as a splay of the main fault, such a phenomenon being characteristic of transcurrent faults in general (De Sitter, 1965).

After the extension of the fault in the sedimentary rocks had been detected and recorded by the writer, P. Garrard (1980) carried out a geochemical analysis of some samples collected across the anticlinal axis, which suggested a different pattern from that of the synclinal axis. When the analysed data were plotted, the anticlinal axis revealed itself as peaks on the plots for Ca, Mg, Fe, Mo, Ti, Sr, U, Cu and Ba (Figure 34).

The extension of the fault, where it is interrupted by the Al Majma'ah Graben, is located near Addahina village (longitude 45°17'E, Latitude 25°35'N), which lies about 35 kilometres north of Shaqra (Figure 32). East of this village is a prominent scarp, trending NNE. North of the village, the scarp swings northwest for a few kilometres before resuming its north-northwesterly direction. The sense of this directional change is in sympathy with that of the Jilh Formation escarpment of Khashm Al Juair, although the form is different (Photo plate 36). Immediately east of the swing and parallel to it, a normal fault has been detected with a downthrow to the NNE of about 30 to 35 metres (Photo plate 38). This fault and the main fault extension, together with other minor structures in this locality (Photo plate 38) appear to have been utilised as channelways for iron-bearing ground waters, and the carbonate sequence in this area contains a number of facies types which require further detailed investigations. (Photo plates 37,39).

4.3 RIYADH TILTED BLOCK

4.3.1 General Discussion

Imagery interpretations, fieldwork and later trend surface computer programmes all suggested the presence of a tilted block located NW of Riyadh and named after it. The block occupies the SW corner of the C.A.G.T.S. where is curves from EW to NW direction in en-echelon structure before

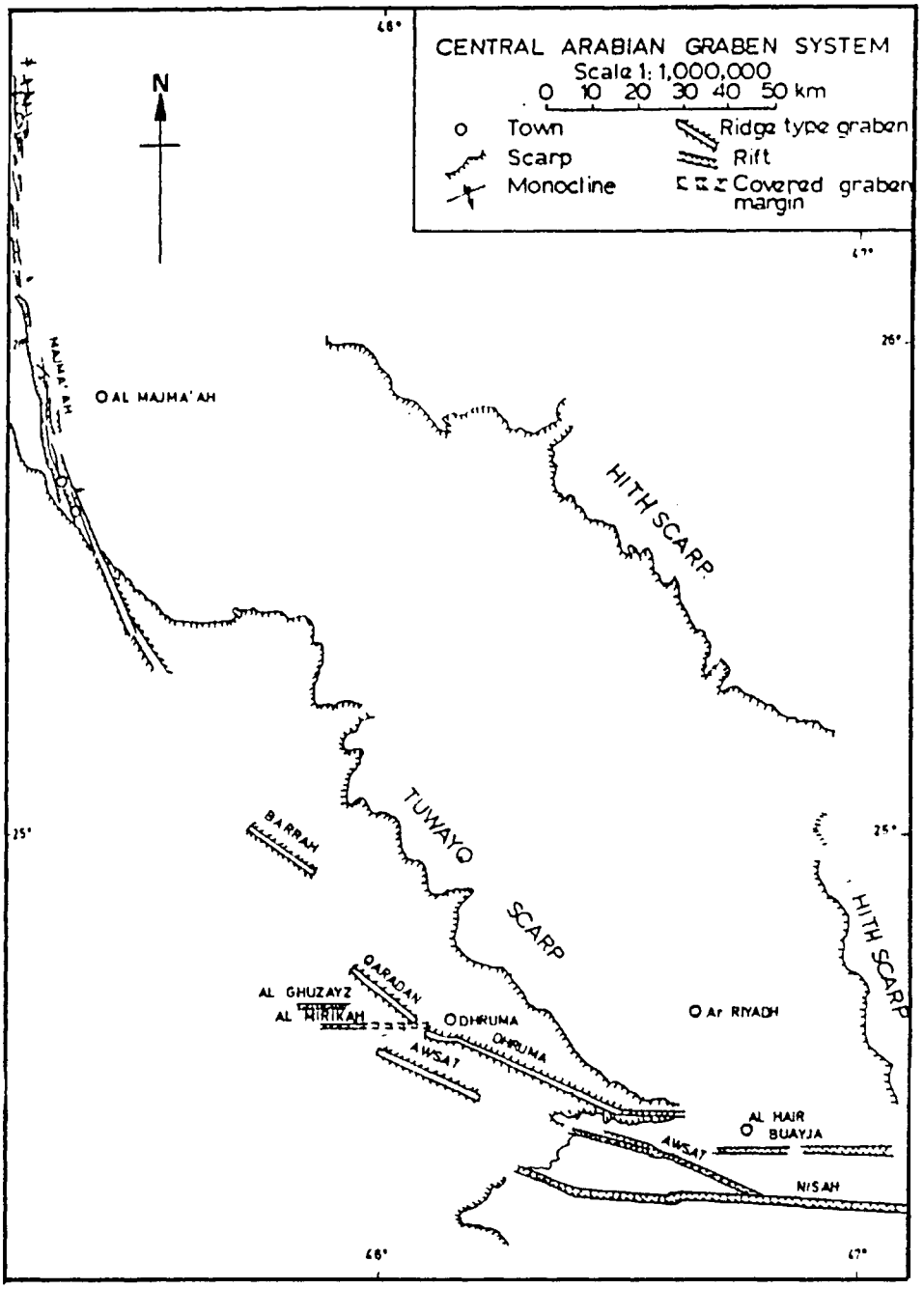


Figure (35) : The en-echelon shaped structures of the Central Arabian Graben and Trough System (modified after Kadhi 1976).

it straightens and extends NW (Figure 35).

It is bounded by two major NW lineaments; the eastern lineament A-B controls Wadi Hanifa, while the western lineament C-D is parallel with some of the faults bounding the grabens in that area. The block is also bounded by part of Nisah-Awsat Graben in the south and apparently Wadi Al-Atk lineament or one of its related structures in the north. The block lies within the following lines of latitude and longitude

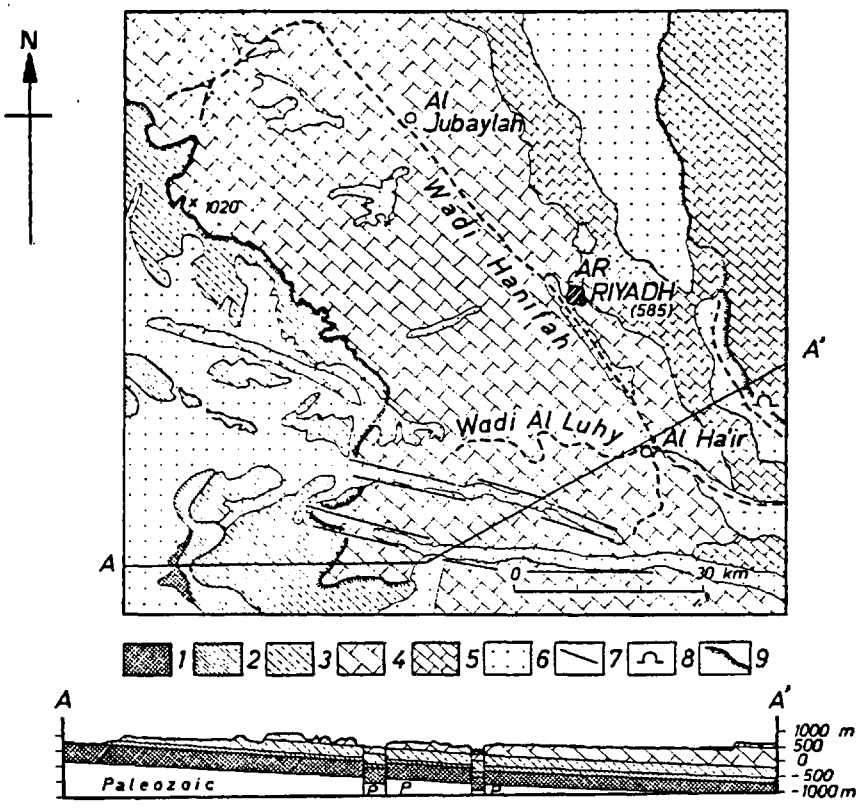
Lat. 24° 20' 25° 20'

Long. 45° 36' 46° 36'

in a diagonal NW direction.

In this text it will be referred to as the block. Regionally, the block is located in the central part of the Interior Homocline bordering the eastern margin of the Arabian Shield, the homocline is thought to be relatively stable. Despite this relative stability, significant structural interruptions do occur, but these appear to result from blocks of different sizes and shapes moving independently and without disturbing the adjacent parts of the homocline surface (Powers,et al, 1966).

The writer agrees to some extent with Power's observations, but adds that the magnitude of disturbances or interruptions in the homocline are more likely greater than have been thought before. This opinion is due to the availability of new devices such as small scale multi-imagery, multi-scale images processed by many different techniques which enhanced more regional views of some geological events that were not,



Generalized geological map of Tuwayq Mountains in the surroundings of Wadi Hanifah. *1* Triassic Minjur Sandstone, *2* Lower Jurassic Marrat Formation, *3* Middle Jurassic Dhruma Formation, *4* Upper Jurassic Tuwayq Mountain Limestone, Hanifa Formation, Jubaila Limestone, and Arab Formation, *5* Lower Cretaceous formations, *6* Upper Pliocene and Quaternary sediments, *7* fault, *8* cave, *9* dominant escarpment

Figure (36) : Riyadh Tilted Block with the structurally controlled drainage, approx scale 1:250,000. (The geological map is modified after Al-Sayari, Zotl 1978).

otherwise easy to detect, for example, images 178/43, 179/42,(Photo plate 3,6,13) which indicate the main parts of the C.A.G.T.S

It seems that the curvature of and the change of the general strike of the Interior Homocline around the Central Arabian Arch, related to the gentle flexing of the basement, tends to break the Homocline belt into several poorly defined segments, the main of which are the C.A.G.T.S., Hail Arch and several other basins and plateaus (Brown 1972). As a result of this process together with other local or regional geological events, other structures seem to have been formed such as Riyadh Tilted Block, while others have been initiated by these events. The block extends northwesterly from Riyadh for an approximate 160km with an average width of 40kms as shown on Figure 36 and on image 178/43(Photo plate 6) . It was detected through the fishing method after noticing its characteristic drainage pattern. Further field investigation and helicopter traverses across the block added more evidence. The availability of water well logs inside and outside the block with some topographic information provided a basis for a trend surface computer programme .

The results of the three phases of studies, imagery interpretation, fieldwork and computer programming, were integrated together to study the nature, characteristics and to prove the existence of this block.

4.3.2 The Photogeological Phase:

Interpretation of Riyadh image 178/43 in three scales of 1:250,000, 1:500,000 and 1:1000,000 high-lighted unusual drainage patterns over an area built up of massive limestone sequence including the Tuwaiq, Hanifa and Arab Formations of Jurassic Age. In the principles of photogeology it has been accepted for a long time that some drainage patterns such as dendritic, radial, annular and some other types are associated with certain land surface material and rock types (Parvis 1950, Mekel, 1971).

For detailed analysis of the unusual drainage pattern for massive limestone, large scale aerial photograph 1:60,000 covering a part of the western margin of the tilted block and outside it in the Dhruma Graben was interpreted, (Photo plate 32). In the Dhruma Region where Dhruma Formation rocks cover the main part of the area and varies from the Upper Tuwaiq-Jubaila massive limestone sequence including some clastic horizons within its stratigraphy. This photograph indicates noticeable differences in drainage patterns where the rocks are relatively bare over the block and covered with varying thickness of soil in the adjacent Dhruma Region. This also may indicate, likewise, that drainage patterns develop differently in horizontal than in the tilted rocks and the relatively more youthful topography and well defined drainage is mainly characteristic of areas undergoing tilting and uplifts.

From the previous literature and fieldwork in the area and over other limestone regions in different parts of the

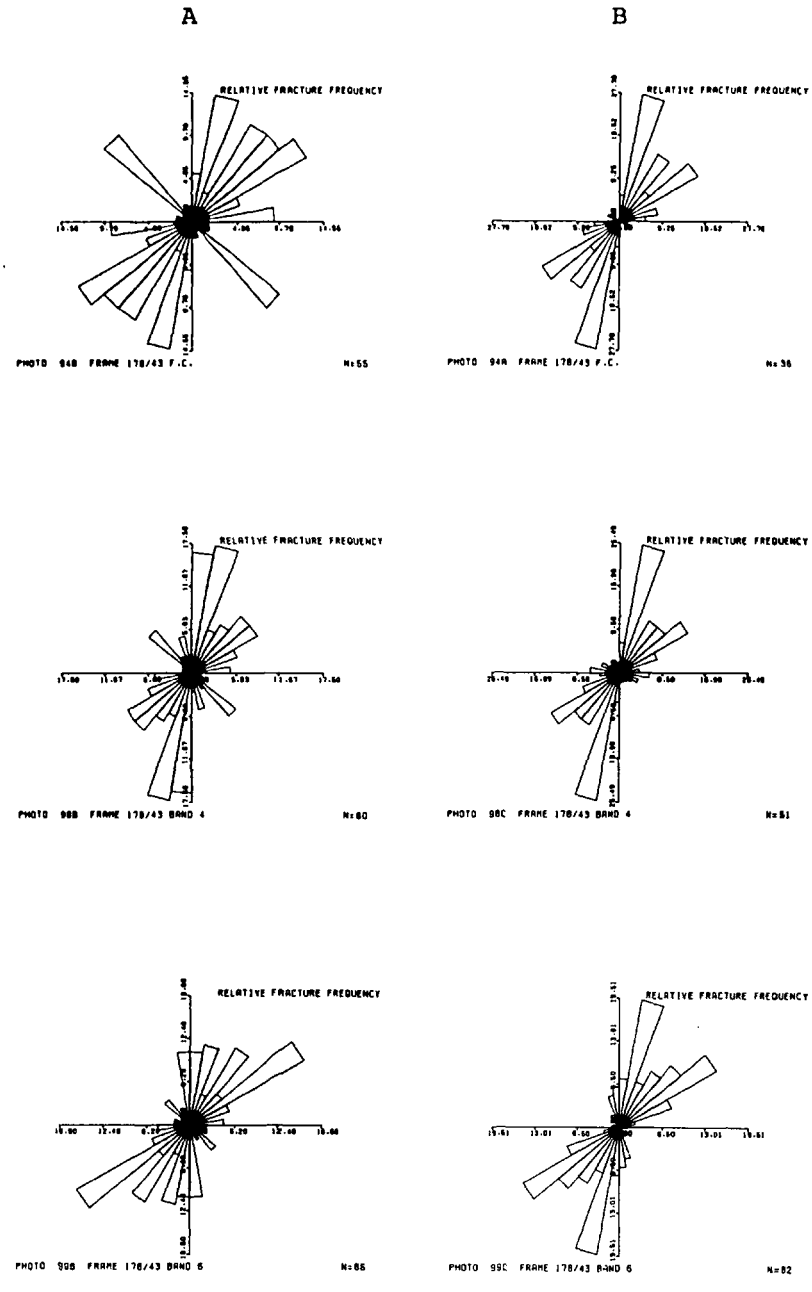


Figure (37) : Relative frequency rose diagrams showing lineament analysis of areas inside (A) and outside (B) the Riyadh Tilted Block.

world it has been found that limestones in general are usually characterized by a coarse, deeply incised surface and subsurface drainage, under the same prevailing atmospheric factors. The main factors producing the prevailing climatic changes in the area are altering conditions of precipitation, air temperature, humidity and wind directions, which are dependant on the seasonal changes which to a great extent affect the Landscape (Al Sayari-Zotl 1978). The present day landscape in the specific area and across Arabia in general is dominated by features typical of arid climates such as bare rocks, abrupt cliff-like scarps, butte and pinnacle rocks, (Photo plates 40,41) together with intervening flat floored wadis and flat open pediplanes. Although these features indicate that arid climate has prevailed for a long time, there is a wide spread evidence that the topography has been produced by at least two cycles of erosion, an earlier wet cycle and the later present arid cycle. The deep incisions of the great meandering antecedent river gorges in the area is perhaps the most striking evidence of a former dominating humid climate (Photo plate 32).

The effect of the humid period on the present topography possibly took place during the last Pluvial Period of the Quaternary Time when precipitation was considerably greater than at the present (Al-Sayari, Zotl 1978).

Ground investigations and field traverses across some major wadis in the area indicated the common presence of alluvial terraces along their sides. These terraces are often



Figure (38) : Wadi Waybayr Monocline (modified after map 1-207-A, scale 1:500,000 DGMR).

a few metres above the present wadi floors. Within these wadis around the tilted block as well as in the block itself there are a number of changes in the drainage regime which may have caused this terracing such as river capture (stream capture), tectonic earth movements or solution collapse in certain formations (Photo plate 8).

From the review of data and climatic conditions one can conclude that the block was tilted in pre-Quaternary Time. Other evidence is coming from the movements along faults and structures bounding the block on the Southern side in Wadi Nisah and Awsat Grabens (Hancock, Kadhi, 1980) and the nearby Amar-Idsas Fault has been reactivated in the Quaternary (Nebert, 1970). So during the heavy precipitation in the Late Quaternary, it seems that the massiv limestone rocks being already tilted, the expected deep V shaped drainage and subsurface drainage were not able to develop and instead this unusual dendritic youthful drainage pattern has developed. After the tilt, the tectonic boundaries of the block have presented an easy access for the coarser drainage to follow and the main wadis are controlled by the tectonic boundaries of the block (Figure 36). The water drained to the east through the newly formed drainage are trapped by the roughly NW-SE Wadi Hanifa which is controlled by the eastern, A-B NW lineament which seems to be responsible for dislocating Wadi Shuaiba before it joins Wadi Hanifa, as shown on image 178/43 (Photo plate 9). Detailed study of Landsat image 178/43 band 7 (Photo plate 8), also indicated the presence of

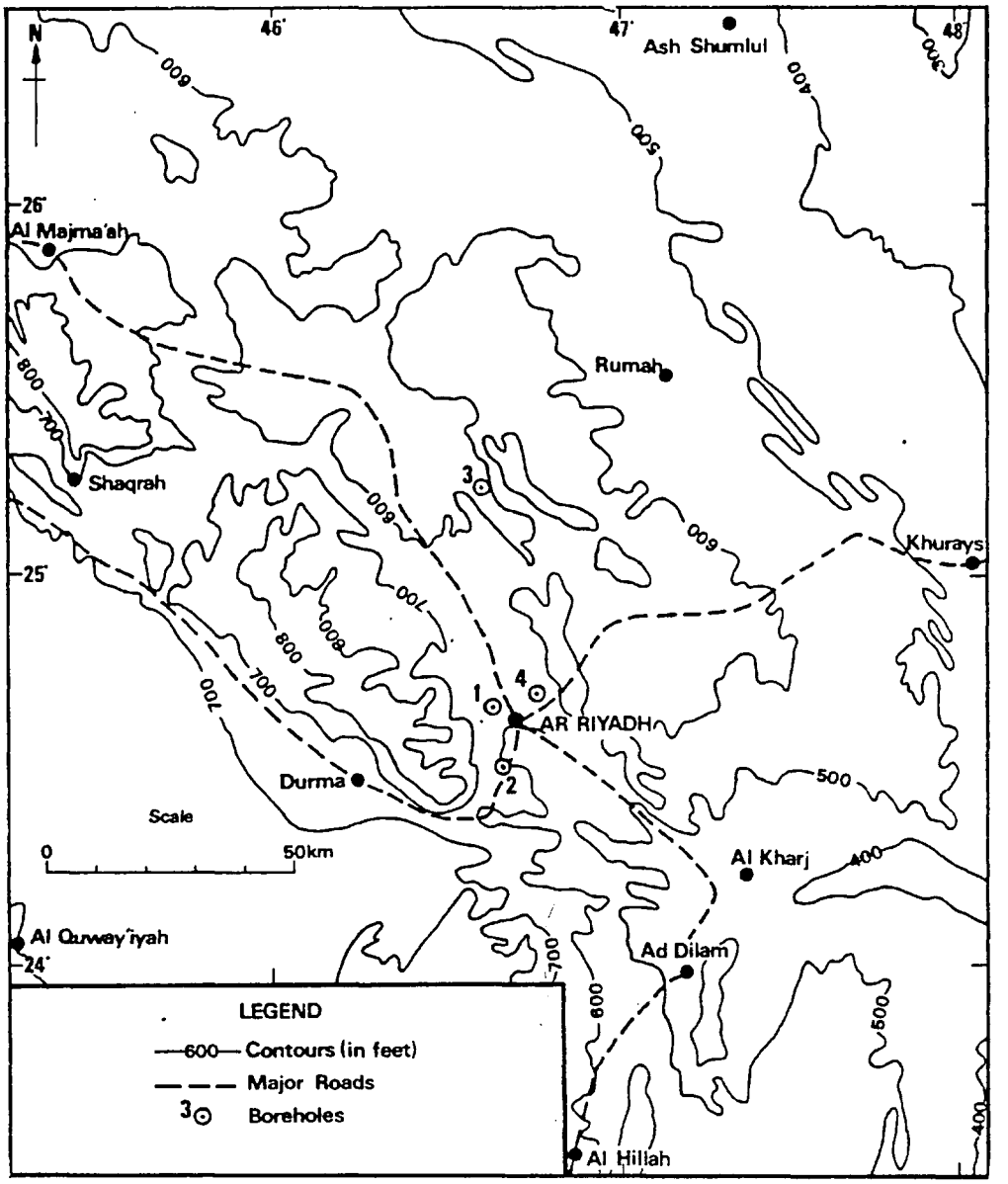
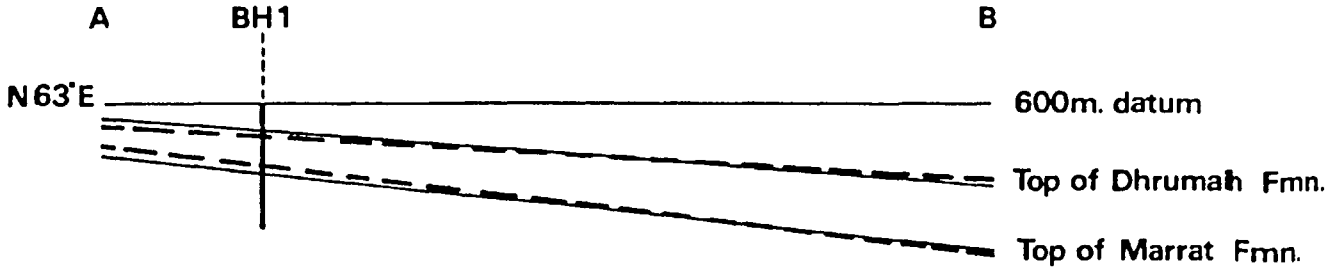


Figure (39) : Topographic contour map of the Riyadh Tilted Block and the surrounding areas (modified after Map AP-1 DGMR).

relatively small arcuate or crescent-like shape incisions with their opening facing the direction of tilting. These may represent a part of pre-existing circular features where this clear part was enhanced by the incision of water flowing to the east after the block has been tilted. The photogeological evidences of tilting can be summarized as follows :- unusual drainage pattern depending on the type of rock and soil cover involved, structurally controlled boundaries, stream capture and terraces, enhanced crescent-like arcuate features with their opening facing the tilting direction and some structural interruptions between the block and the surrounding crust to facilitate tilting. Another photogeological evidence was achieved by correlating frequency rose diagrams of lineaments inside and outside the block which indicated some differences preferably on the H.P.F.B7 images (Figure 37).

4.3.3 Field Investigations:

Later, the writer with his supervisor carried out a few helicopter traverses on various altitudes and some ground investigations; both indicated that the block in general reflects NNE dips with relatively higher values than the average one degree general dip of the region. Also indicated that within the Hanifa Formation there was some abnormalities of both strike and dip, these disturbances and/or abnormalities coincide with one of the structural features which is Wadi-Waubayr Monocline (Figure 38). Macdonald and Partners (1977-78) pointed out that this structure i.e. the monocline cannot



——— Surface predicted by linear T. S. Equ.

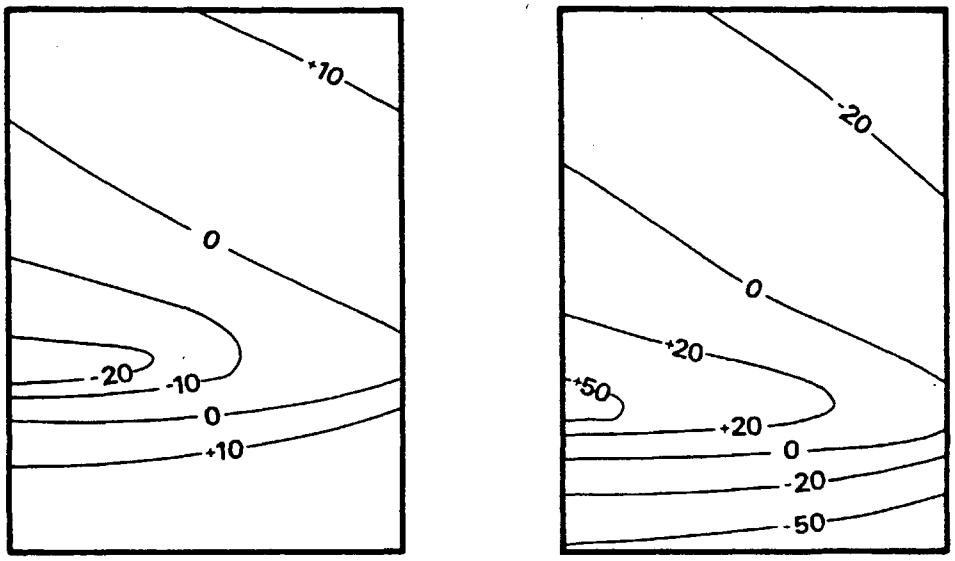
— — — Residual surface of T. S. analysis

Predicted direction of dip N63°E

Vertical Scale - 1mm. = 100 metres

Horizontal Scale - 1cm. = 7·1 km

Figure (40) : Predicted surface of top of Dhrumah and top of Marrat Formations indicating a tilt of 5° to N63°E. (as revealed by linear trend surface computer programme).



Top Dhrumah Fmn. Residual

Top Marrat Fmn. Residual

Figure (41) : Assymetrical contours of residual values on the top of Dhrumah and Marrat Formations due to tilting of the Riyadh Block.

easily be fitted into the framework of tectonic history compiled from the area. This NE-SW trending monocline is located completely in the tilted block and can be a direct or indirect effect of the block and its stratigraphic sequence. A possible explanation for the formation of this abnormal structure can be related to the thickness variations in the Dhruma and Marrat Formations. These formations include many incompetent layers of shales especially the Marrat Formation which is built up completely of red shales. Percolating solutions along the deeply penetrating structures surrounding the tilted block and the pressure of the overlying rocks seems to have caused draping of the overlying rocks and resulted in the strike and dip changes which produced this monocline. These variations in the thicknesses of the Dhruma and the Marrat Formations at depth have been supported by trend surface computer programme results.

4.3.4 Trend Surface Computer Programme :

The availability of water well logs inside and outside the tilted block together with a topographic map of the area, (Figure 39), initiated a trend surface programme. Both wells inside and outside the block if connected with a line are almost parallel to each other and to the eastern edge of the block.

The four wells No. 1, 2, 3 and 4 (Figure 39) started in Arab or Jubaila limestone Formations (Jurassic). The Riyadh deep well No.4 is an exception where the total depth

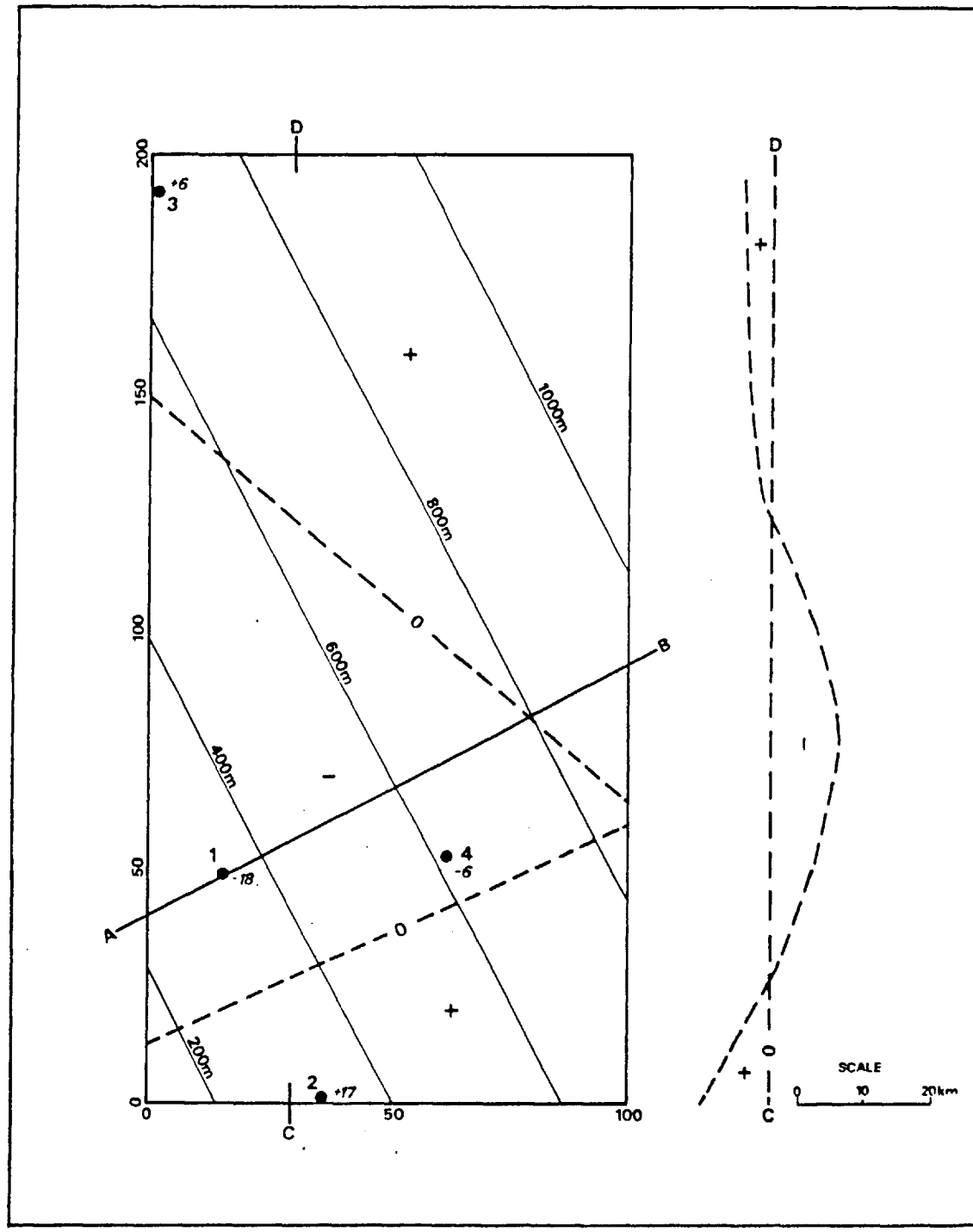


Figure (42) : Linear trend surface to top Dhrumah Formation.
Contours are depth below 600m Datum.

was around 3000 metres and ended very near to the top of the basement (unpublished reports of M.A.W.). The information from wells represented the basic raw data for the trend surface programme, the results of which indicated the following:-

The predicted surface indicates a regional tilt of about 5° dipping N63°E, (Figure 40), which is significantly greater if correlated with the average general dip of one degree in the area. The beds between the Top Dhruma, (Figure 42) and the Top Marrat, (Figure 43), thicken in the same direction about 300 metres along a line of section C-D where the two figures show the predicted contours to the top of each formation from a common 600 metres (above sea level) datum.

The residual values show that the central area of thinning (Figure 42) is calculated as 65 metres at the well No.1, approximately 10% of the total thickness and getting less eastward which seems probably to have minimized the effect of tilting in that direction.

The two wells No. 1, 2 in the southwest corner of the area are located in the tilted block, while the other two No.3, 4 are outside it. It would be predicted that the residual values of the two wells inside the block 1, 2 should be positive while those outside the block should be negative (personal communication, Dr. J. Ferguson) but because of the influence of the stratigraphic thinning in the Dhruma and Marrat Formations this has not been achieved.

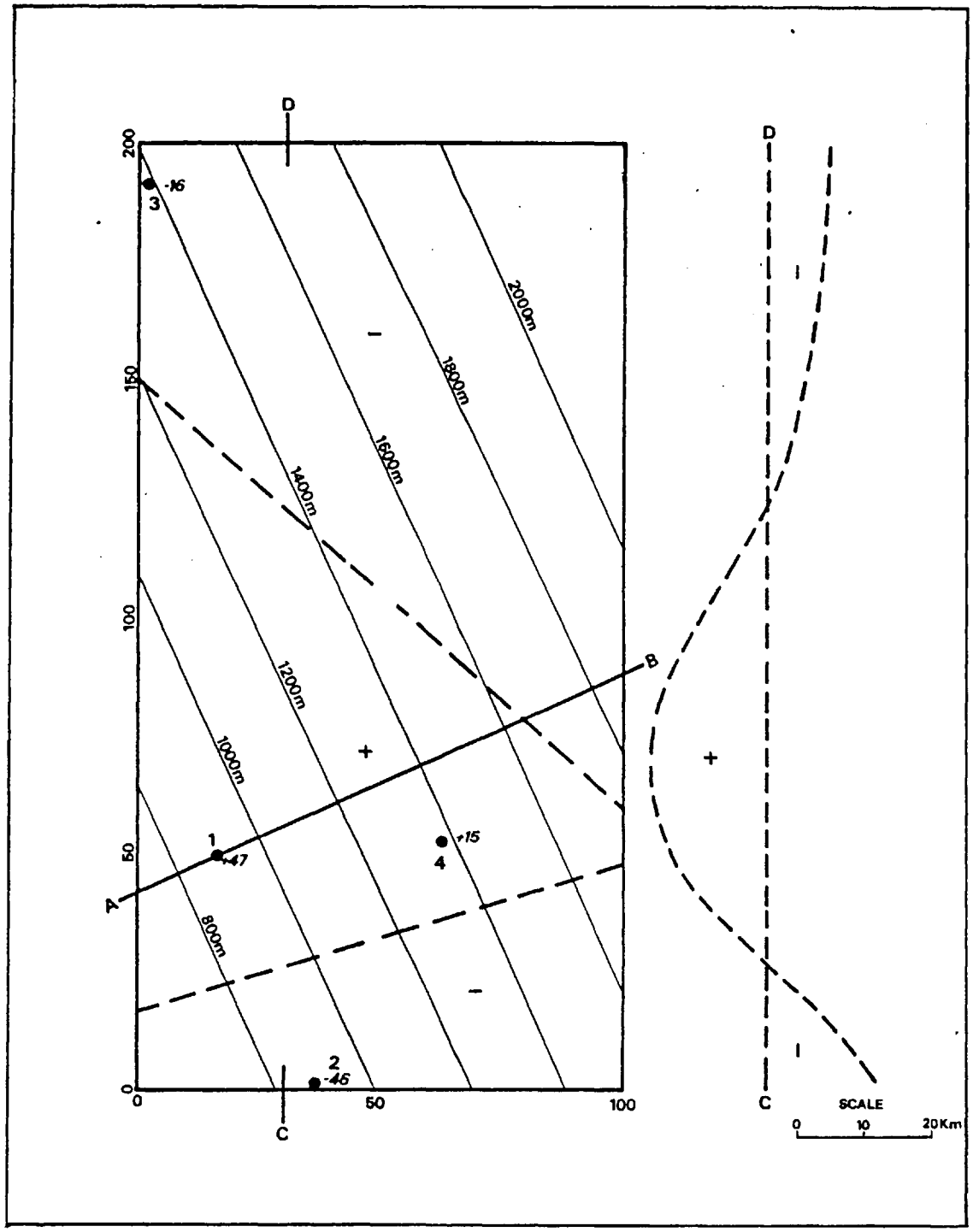


Figure (43) : Linear trend surface to top Marrat Formation.
Contours are depth below 600m Datum.

However, inspection of the residual value shows that in both cases the wells inside the block 1, 2 are three times the magnitude of those outside it. This difference in magnitude and the asymmetry of contour patterns of residual values, (Figure 41), substantiate the existence of a tilted block NW of Riyadh.

4.4 EAST ARABIAN BLOCK

(Central Arabian Graben System and Wadi Al-Batin Relationship)

The interpretation of a few computer enhanced H.P.F.B7 images which showed an arc of 80 km length, together with existing geological, structural and topographical maps, field traverses and ground investigations, revealed a continuous one thousand km arc of faults, troughs and grabens. The detection of this arc link allows continuation of C.A.G.T.S. and Wadi Al-Batin forming an arc cutting the Mesozoic-Cenzoic rocks of the Arabian Shelf. The main purpose in this section is to illustrate and present some photogeological surface evidence together with structural evidence which permit an arcuate zone to be recognised in the eastern part of the Arabian Plate, referred to as East Arabian Block (Figure 44,45).The block itself is a part of the Arabian Shelf, a region characterised by gently north easterly dipping Phanerozoic-sedimentary rocks of a range of half degree to one degree at the most. The sequence is composed of nonclastic and clastic rocks where the latter type include some incompetent layers of marls, shales

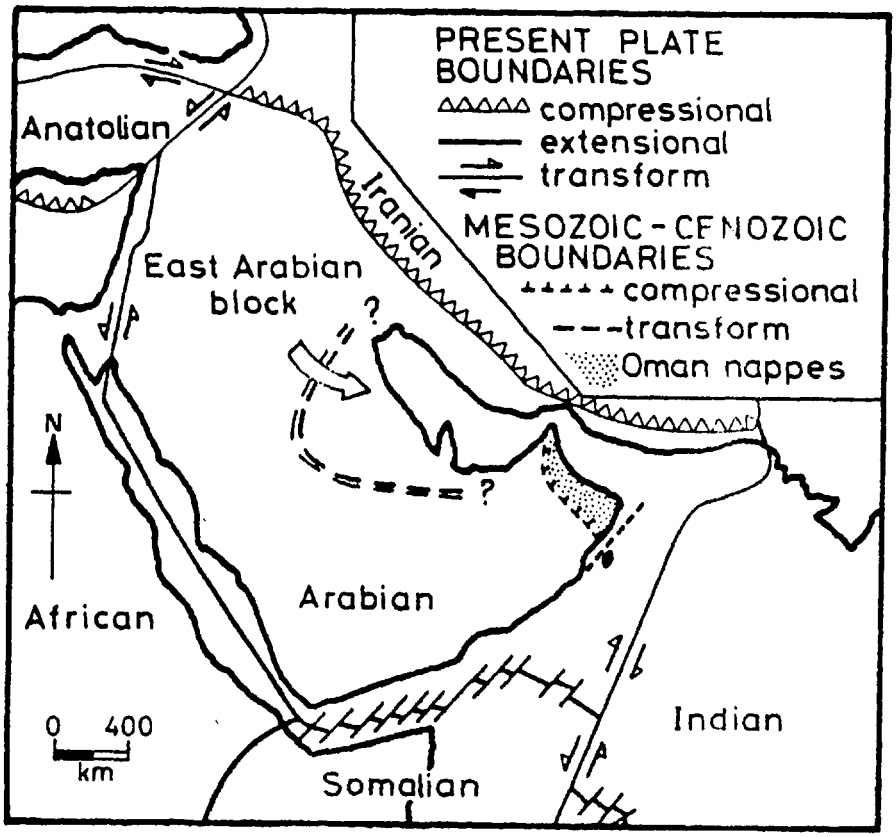


Figure (44) : East Arabian Block and its present boundaries in relation to Arabian Plate (after Hancock, Al-Khatieb and Kadhi 1980).

and evaporites which may have played a role in the regional structural history. The whole sequence is resting unconformably on a Precambrian crystalline basement, exposed in the west on the Arabian Sheild.

Figure 46 shows the three principal structural and phototectonic elements within the one thousand kms arc of structures, those segments are referred to as 1 - Wadi Al-Batin Segment, 2 - The Al-Hamudiyah Arcuate Lineament, 3 - The Central Arabian Graben and Trough System (C.A.G.T.S.).

4.4.1 Wadi Al-Batin Segment:

This is mainly rectilinear and partly curvilinear wadi which possesses a width of 2 - 10 km and trends N40^{o}E, and can be traced southwest from the Mesopotamian Plain, in Kuwait, for a distance of 300 kms. Most of the low plateau which it dissects is underlain by nearly horizontal Neogene sedimentary rocks, although Palaeogene rocks of the Umm Er-Rhuduma Formation crop on both sides of the wadi in the extreme southwest (Figure 47). A cover of Quaternary sediment obscures much of the bed rock geology of the plateau surfaces and much of the wadi floor. South of latitude 28°N the outcrop of the contact between the Paleogene and Neogene succession is sinistrally offset to the southwest on the northern side of the wadi. This offset and another NW-SE faults cutting through the main wadi are most likely to be related to sinistral strike slip which is sympathy with the NE-SW Riyadh Fault System (Figure 53). Although existing maps (Bram-Kamp and Ramirez

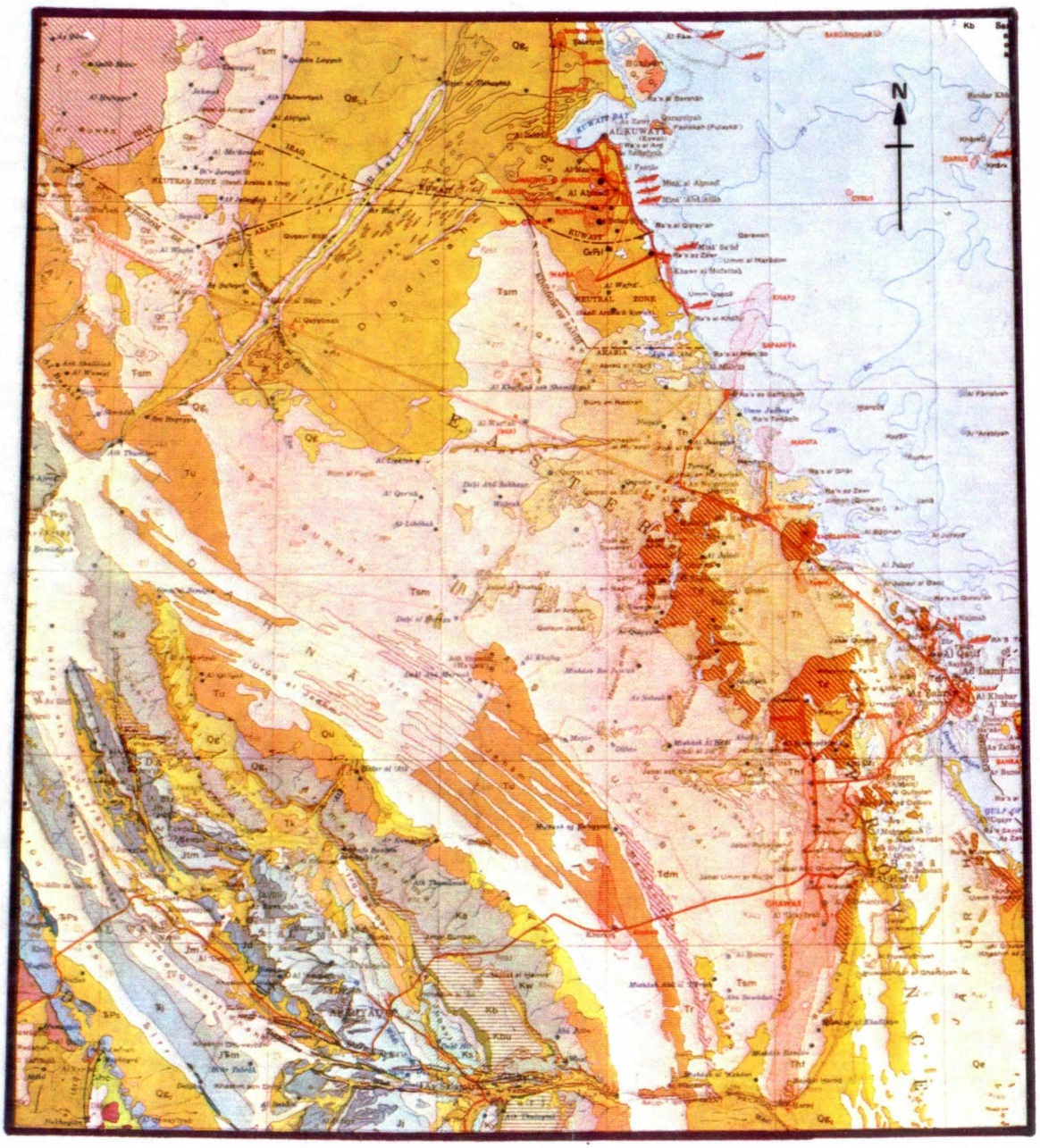


Figure (45) : Geology of East Arabian Block, scale 1:4,000,000 (after map 1-270 A DGMR).

1958, 1959) do not show a fault cutting the rocks of the wadi, its remarkable straightness and great length are suggestive of an underlying tectonic control (Hancock, Al-Khatieb and Kadhi 1980 in press - geological magazine). This inference is supported by the geophysical evidence presented by Al-Sarawi (1978) who concluded that Eocene rocks beneath the Neogene Quaternary Cover are cut by a major fault zone of graben-like form which is coincidental with the wadi where it passes through the Kuwait Territory.

In addition to this geophysical evidence, interpretation of H.P.F.B7 Landsat image 179/40(Photo plate 16) revealed a few NW-SE lineaments cutting through and slightly dislocating the Neogene rocks of the wadi. The presence of these structures probably remained undetected by conventional reconnaissance geological mapping. These faults can be interpreted as minor rejuvinated expressions of the older faults underlying wadi which in the Kuwaiti Region were detected by geophysical research (Al-Sarawi, 1978).

4.4.2 Al-Hamudiyah Arcuate Lineament:

Although the location of Wadi Al-Batin and the C.A.G.T.S have been known for a long time, there has been no published discussions about whether they are connected. In part, this may be related to much of the bed rock geology of the intervening terrain being obscured by a cover of Quaternary Sediments.

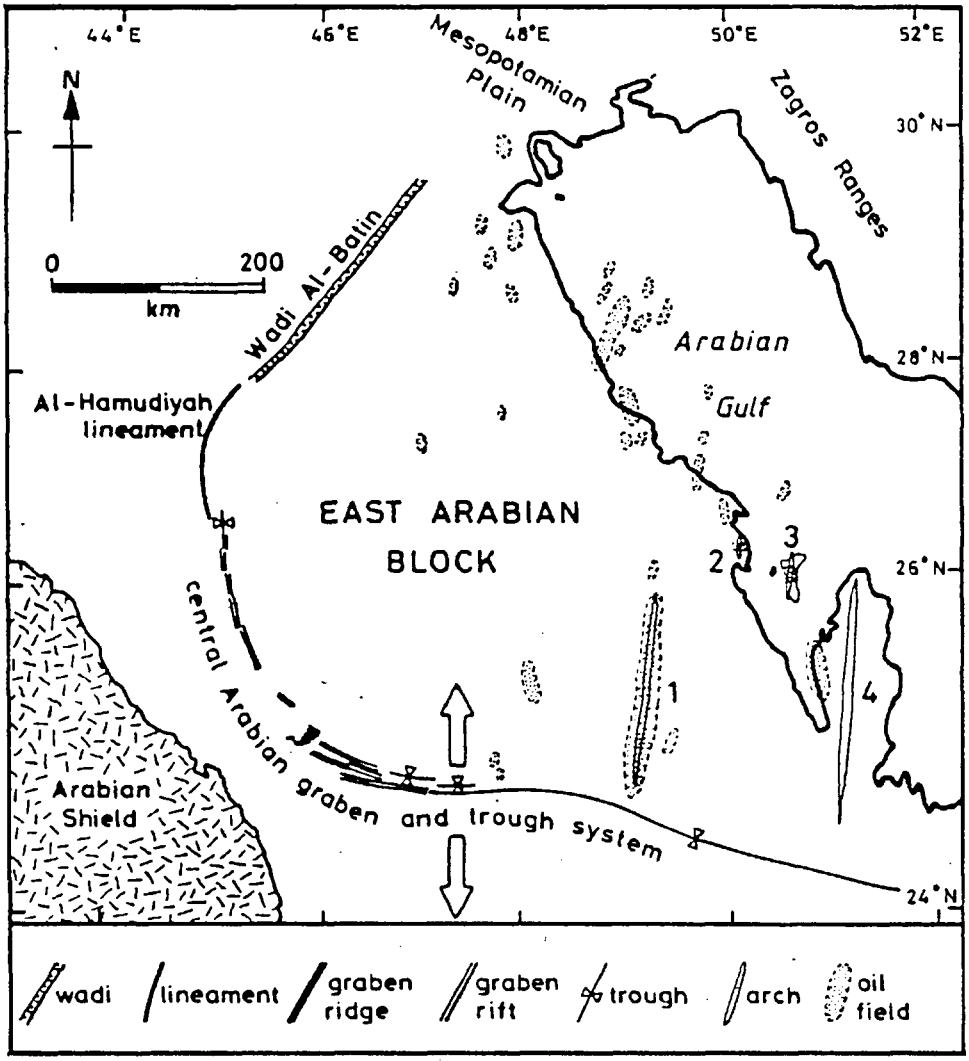


Figure (46) : Principal structural and photo-tectonic elements of the East Arabian Block (after Hancock, Al-Khatieb and Kadhi 1980).

The availability of computer enhanced Landsat images of H.P.F.B7 with relatively small scales, allowed the large scale morphotectonic features of the region to be identified, as for example the near meridional N-S lineaments of a few hundred kilometres length, which the majority in the sedimentary sequence, are located in this block (Figures 29,57)

H.P.F.B7 image 180/41(Photo plate 14) and Figure 48 shows the interpretation of the principle lineaments visible on the image. The generalized areas of outcrop of pre-Quaternary rocks are closely distinguishable from the Quaternary Cover, much of which comprises sand dunes. In the southeast of the image and the interpretation sheet, the arc of the approximately 80 km long of Al-Hamudiyah lineament A-B separates a plateau underlain by rocks of the Aruma Formation (Upper Cretaceous) from an area of sand cover. The Al-Hamudiyah Arcuate Lineament also interrupts an almost straight NE-SW trending lineament C-D which is probably a surface reflection of a major subsurface structural zone influencing sedimentary patterns in the Quaternary Cover. This is supported by the fact that the southwest extension of the NE-SW lineament corresponds to Wadi Arumah known to have a geophysical anomaly in the adjacent Precambrian rocks. The change of sand dune textures across this NE-SW lineament probably reflects a change in the direction and/or force of the locally prevailing wind, itself influenced by a subdued physiographic expression of the buried structure, probably a negative feature and might represent one of the NE-SW

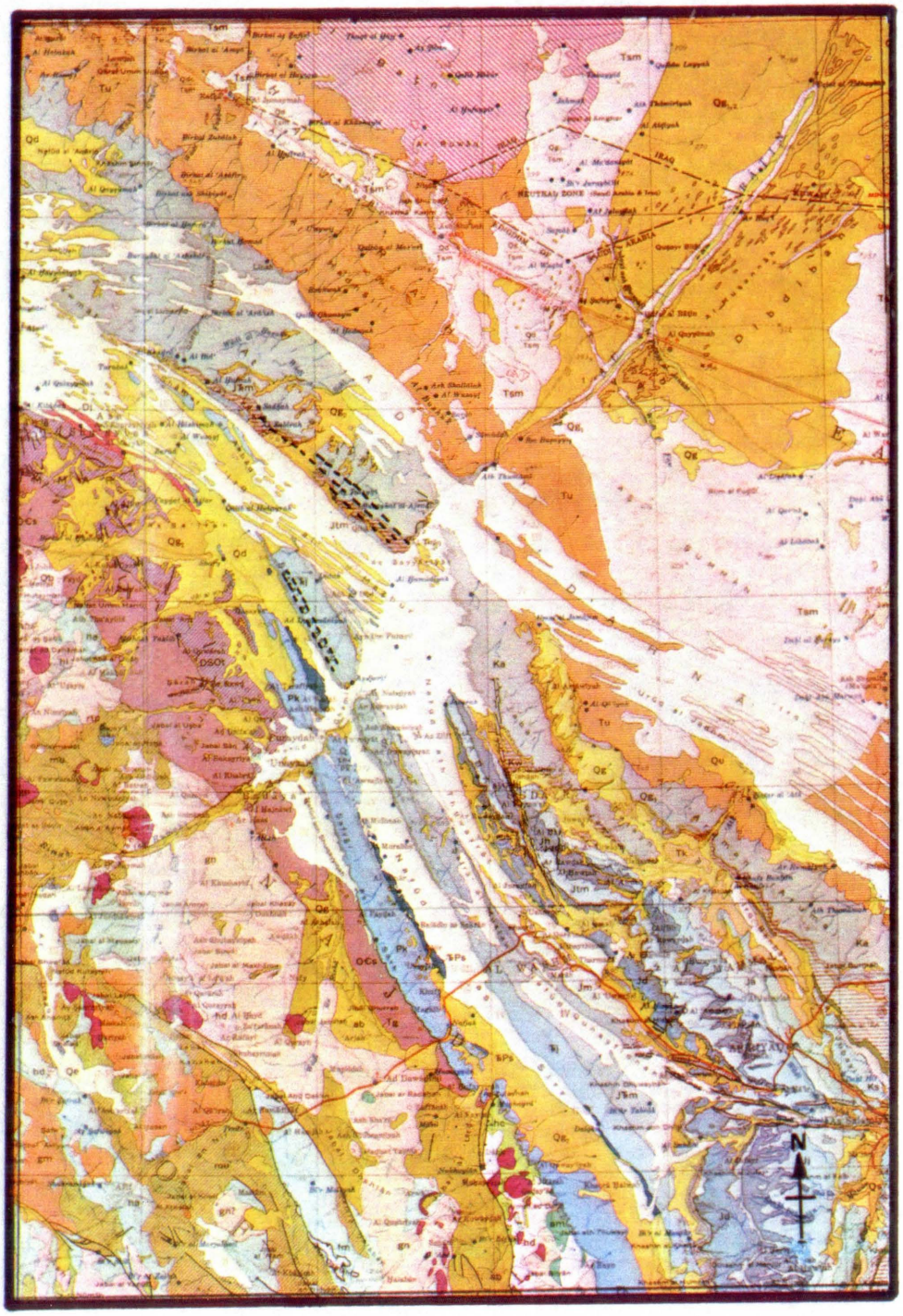


Figure (47) : Wadi Al Batin linear feature and its possible effect on the surrounding geology (modified after map 1-270 A scale 1:4,000,000 DGMR) showing the convergence of the strike on the NW side of the Wadi.

Riyadh Fault System.

To the west of this Lineament there is a noticeable divergence of strike in the Mezozoic bed rocks. Interpretation of image 180/41 (Photo plate 14) and the U.S.G.S. geological map (Figure 46) reveals such a divergence is not present east of this lineament, further evidence of the structural importance of these NE lineaments.

4.4.3 Central Arabian Graben and Trough System (C.A.G.T.S.)

The 560 km arc of grabens and troughs which defines this segment has been known from previous geological mapping by Bramkamp and Ramirez (1958), Steinke et al (1958), Powers et al (1966), Brown (1972), Hancock and Kadhi (1978, 1980). This segment is also visible on Landsat images 178/43, 177/43 179/42 (Photo plates 6, 17, 19). This relatively wide zone of structures displaces an Upper-Triassic to Eocene succession and comprises six major grabens and three major troughs. Where grabens cut escarpment and back slopes they are expressed by rift valleys, but where they cross plains they form ridges bounded by obsequent fault line scarps (Hancock and Kadhi, 1980). Although most grabens and troughs are arranged en echelon of 25 km width they do not display a consistent sense of offset or overlap. Some grabens are themselves compound structures comprising overlapping segments. (Figure 35).

Powers et al (1966) believed the C.A.G.T.S. is related to regional tension but Brown (1972), while accepting the plausibility of the tensional hypothesis, proposed that the system might also be a reflection in the Mesozoic-Cenozoic

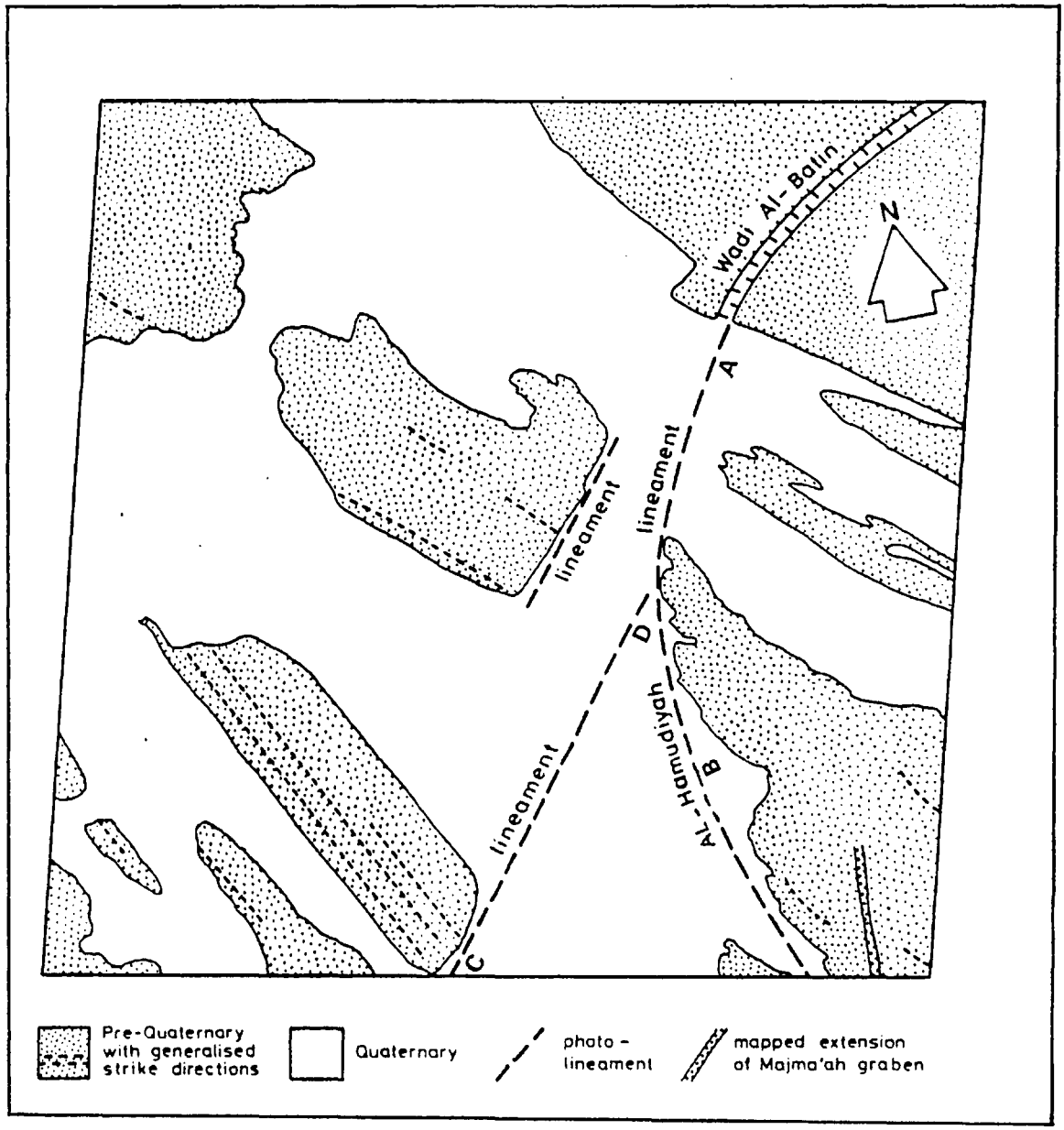


Figure (48) : Al-Hamudiyah lineaments A-B, C-D with relation to Wadi Al-Batin. (Approx. scale 1:1,250,000).

cover of left lateral (sinistral)shear along a fault zone in the crystalline basement. Hancock, Kadhi (1978) using Paleostress trajectories inferred from mesofracture sets concluded that the southwestern part (Awsat-Dhruma Grabens) of the system is probably related to N-S stretching of a cover succession above an arcuate basement fault zone.

This conclusion of an arcuate basement structure propagated to the surface and affected sediments is in good agreement with some of the arcuate features interpreted from Landsat images and geological maps as interpreted by Norman (1980) (Figure 49). These arcuate features of a few hundred kms. radius are not uncommon in the exposed Precambrian adjacent to the C.A.G.T.S image 180/43(Photo plates 29,30). Norman (1980) indicated that these features are a result of the effect of great impacts on the earth surface in the early times, later propagated to the surface.

Stratigraphical relationships in the vicinity of the C.A.G.T.S indicate that the system began to develop in the Cretaceous time between relatively stable upland in the south and a sinking shelf in the north, and that displacement along the system were largely complete by the Mid-Miocene (Powers et al, 1966) indicating that movement along this segment of the block were active from Cretaceous to Eocene.

Other evidence which supports the idea of the Eastern Arabian Block:

1. The majority of the principal hydrocarbon fields of the Arabian Peninsula lie within the block

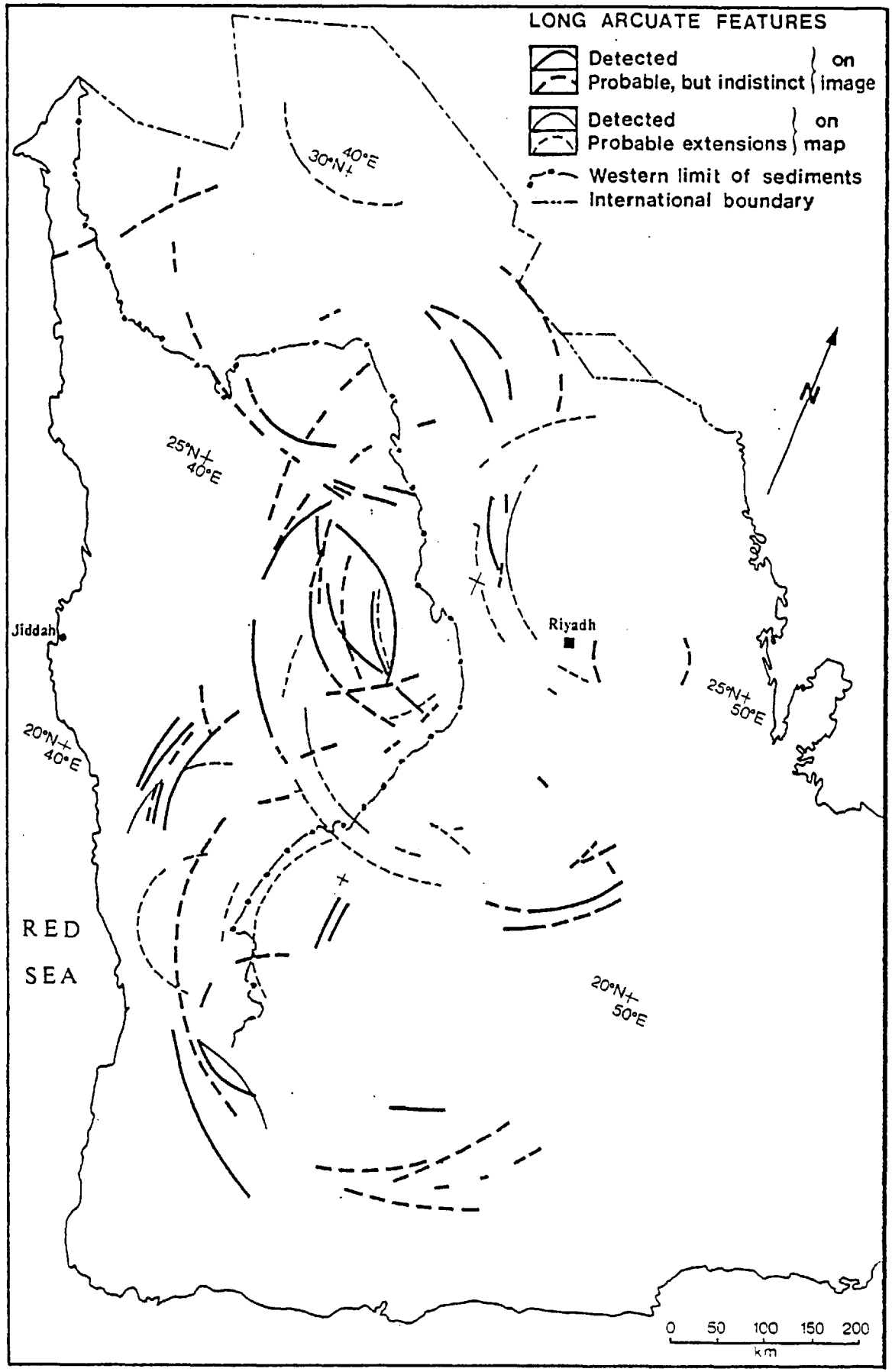


Figure (49) : Long arcuate features as interpreted from landsat imagery and geological maps (after Norman 1980).

(Al-Khatieb, 1978), and the giant Ghawwar oil field terminates exactly at its southern end along Wadi Nisah Graben extension, Brown (1972). (Figures 45,57).

2. The presence of a few arches directed N-S parallel to the Ghawwar oil field such as Qatar Arch and Bahrain Arch. (Figure 46).

3. The extension of Al-Majmaa'h Graben to join Barrah Graben, known before to be obscured by Quaternary sand cover.. (Photo plates 13, 19).

4. Interpretations of Landsat images of Wadi Al-Batin indicated that because of its length, straightness and some dislocations along its course it is a more likely area of structural significance.

Point 1 seems to present a relation between the oil field locations and the plate. This has been supported by Norman, Price, Ike, (1977) who have noticed "that there is a relationship between astrons and distribution of minerals and oil fields in areas where astron grabens have been rejuvinated and filled with Post-Carboniferous sediment younger than 300 million years, thus the astrons could provide astratigraphic guide to prospecting".

This statement by Norman, Price, Ike, (1977) is in full agreement with the East Arabain Block being a result of an old astron arcuate structure, surrounded by grabens, and including

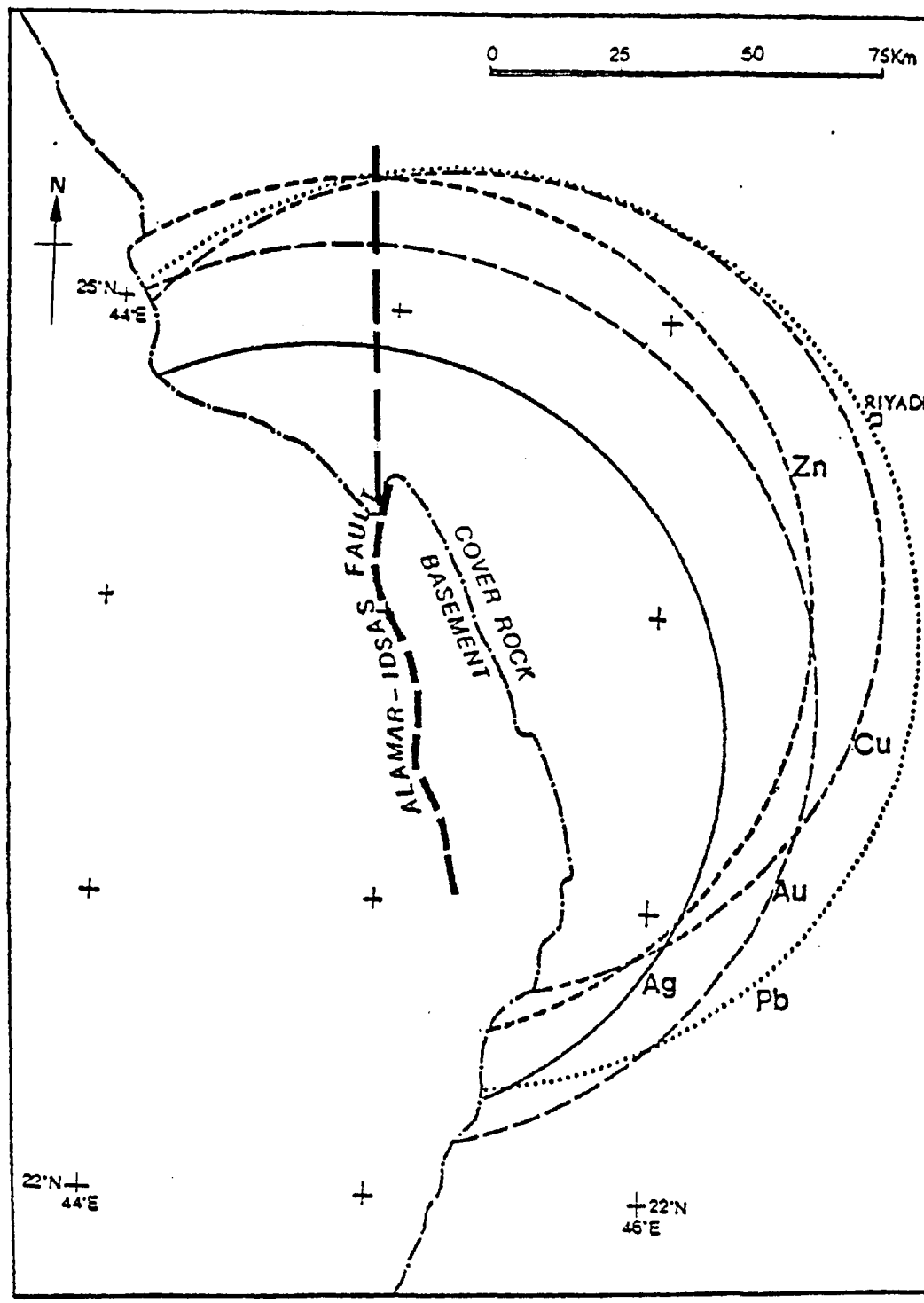


Figure (50) : Possible mineralized basement areas under Cover Rocks in the vicinity of Al-Amar-Idsas Fault (modified after Norman 1980).

sedimentary sequence younger than 300 million years and includes the majority of the Arabian oil fields. Norman (1980) also indicated that the distribution of minerals in the Arabian Shield follow to some extent circular patterns which, if extrapolated, will cover the main parts of the block (Figure 50).

In the case of the E.A.B. and the Norman, Price, Ike statement; both agree to an extent that seems they have been referring to this block without being in physical knowledge of its existence in the Arabian Peninsula.

4.5 WADI AL-ATK AND RELATED STRUCTURES

4.5.1 Wadi Al-Atk

Wadi Al-Atk is one of the important wadi systems in the region whose catchment areas reach back into the Shield. The constancy of the general direction of its gradient can also be observed in the existing wide wadi system which represents morphogenetically the result of an early-formed drainage system (Figure 51).

In the main course of the wadi Miocene sedimentary rocks can be found on the present floor, the drainage of the main wadi cutting relatively deeply through the Jurassic and Cretaceous cuestas which must have existed even at that time if not earlier (Sayari, Zotl, 1978). The wadi in the Tertiary and Cretaceous rocks seems to be structurally controlled, being



Figure (51) : Wadi Al-Atk and Khashm Al-Haqaqa Structures (modified after map 1-207A scale 1:500,000 DGMR).

divided into two segments, image 178/42, (Photo plate 18).

The eastern segment A-B, directed NNE,is controlled by a roughly N-S lineament C-D, the western segment by two NE-SW lineaments of the Riyadh Fault System, E-F and G-H cutting deeply through the northern side of the wadi, forming escarpments of the Aruma Formation (Photo plate 51). The wadi, as the majority of the main NE-SW drainage, extends from the west near Al-Udayniyat in the Jurassic rocks to Hafr Al-Atk in the Tertiary Umm Ar-Rhudema Formation. The SW extension of Wadi Al-Atk delineates the NE side of the Riyadh Tilted Block before it is lost under the Quaternary cover; here the area is overshadowed by NE-SW lineaments, seen in image 179/42, Photo plate 13)and the wadis direction may match that of a major NE-SW lineament. Later, the ground investigations and helicopter traverses indicated some other structures, possibly related to the Atk lineament itself.(Photo plates 52,53 and 54).

On the SW side of the wadi near the wide open flood plain and on the top of the Cretaceous Aruma there is found a series of alternating ridges probably representing a tight sequence of horsts and graben, parallel to the main course of the major wadi. These are intersected by NNW lineaments normal to the direction of the main wadi,(Photo plates 47,49 and 50). Because of the strong erosional effect and surface deposits, these lineaments do not show any observed movement.

A review of the existing literature supported data acquired from the image interpretation and field work.

First, Powers et al (1966) indicated that the truncation of the base of the Biyadh Sandstone Formation in the region in general is one meter per kilometer. Northwestwards, in the direction of Wadi Al-Atk, the amount of truncation increases to about three metres per kilometer, and the Biyadh Sandstone Formation is completely overlapped near Wadi Al-Atk.

Second, U.S.G.S. geological map 1:207-A indicates that certain formations, such as the Sulaiy and Buwaib Limestone Formations are present in the southern side of the wadi and missing from the northern side. Third, the general dip in the area is to the NE, the formations should be thickening eastwards, but this is not the case in the Wadi Al-Atk area. The Triassic Minjur Formation within the Wadi Al-Atk region and its sandstone vicinity is behaving differently from what might be expected and is thinning. Unpublished hydrological information from M.A.W. also reflects this situation (personal communication, S. Abo Mustafa and H. Helly). Fourth, interpretation of the stratigraphic log of Umm Erojoom water-well (lat. 26°03'00"; long.46°10'30"), of a total depth of 2575 metres, indicated that a characteristic horizon of shales in the Minjur Formation was reached approximately 80 metres earlier

than expected. This was later supported by personal communication, Heley (1980).

Fifth, structural "happenings"also appear to be responsible for interruptions at Wadi Al-Atk and along Al-Butayn (lat. 26°52'N, long. 45°18'E; Powers, et al., 1966). Powers and his colleagues did not specify these structural"happenings"but it seems that the data now available supported to some extent that there is a geological significance in this structure.

Lastly, in the vicinity of the SW part of the wadi near the flood plain (Figure 51) the strike of the Cretaceous Wasia Formation changes abruptly from NW to NE. These lines of evidence, ground investigation and traverses together with the interpretation of image 178/42,(Photo plate 18) , all suggest that this structure bounded as it is by two NE-SW lineaments with clear escarpments, is most likely to be a surface expression of a subsurface structure. Its development has affected sedimentation, as witness the thinning of the Triassic Minjur Formation in the region.

During the interpretation of images, pre-existing geological maps and later fieldwork and traverses, the presence of other structures emerged within the vicinity of Wadi Al-Atk. These structures seem to be related to the structural evolution of the Wadi Al-Atk Region.

4.5.2 Khashm Al-Haqaqa Lineament:

This NE-SW lineament seen on the 1:500,000 scale geologic map 1;207 A, in the area north of Wadi Al-Atk, (Figure 51) and can be seen by a study of image 178/42 and 179/42,(Photo plates 18,13) , supporting evidence was provided by the following:

First,the Cretaceous Aruma Formation on the NW side of Wadi Al-Atk is represented by a rectangular geomorphological shape forming a Khashm, a feature which indicates structural control (Figure 51). This can be correlated with Khashm Al-Juair in Al-Amar-Idsas Fault zone(Figure 30).

Second, the structure seems to have dislocated a monoclinal axis, which is clear on Figure 31 .

Third, on the same figure, the lineament seems to have a control on a main tributary of the drainage running to the NE side of the area.

Fourth, on the NW side of this lineament, the Aruma Formation is represented by two belts, the SW of which is terminated by the lineament near the village of Khazza (Figure 51).

Fifth, near the sinistrally dislocated monocline this lineament seems to have controlled the migration of both surface and subsurface ground solutions. As a result of dissolution of the underlying evaporites, a large collapse structure has been formed and huge blocks have dropped into the lower valleys and new failure zones have started to develop. (Photo plates 55,56).

This process may have resulted in the evaporites migrating and were responsible for the formation of some domal feature in the graben structure (Figure 52).

Sixth, field investigations near the SW extension of this lineament indicated a fault with clear vertical displacement, roughly normal to the general direction of the lineament. This fault, and other minor structures in the vicinity, are possibly related to the tectonic events responsible for the formation of Khashm Al-Haqaqa and related structures (Photo plates 57,58).

Lastly, both the extension of this lineament to the SW and the roughly parallel Wadi Al-Atk appear to have terminated the main NW lineaments (faults) of the Riyadh Tilted Block at its northern end. At this point, the Khashm Al-Haqaqa lineament coincides with a relatively clear NE lineament slightly obscured by the Quaternary cover of Nafud Al-Buldan and other dominant NE lineaments, image 179/42 (Photo plate 19).

These points suggest that it might be a NE fault with a sinistral transcurrent movement. It is possibly representative of the Riyadh Fault System (Figure 53).

4.5.3 Al-Butayn-Himar Sabha Structure

This graben-like structure is bounded on its southern side by the Khashm Al-Haqaqa lineament and extends northwesterly for 160 kilometres to the Umm Al Jamjim area, where outcrops are completely covered by the Great Nafud of A Dahina. The structure width is about 40 kilometres and is

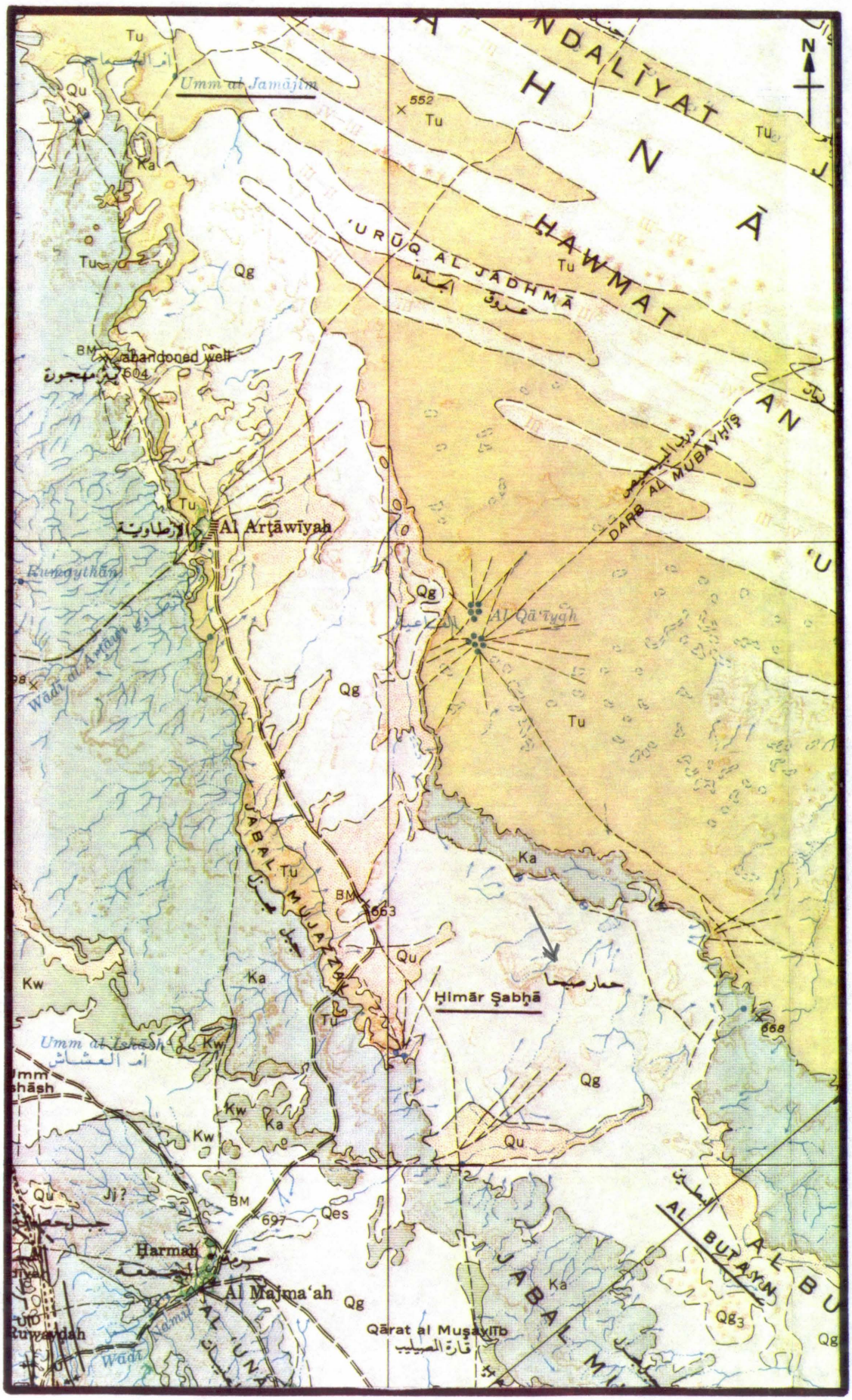


Figure (52) : Al-Butayn-Himar Sabha Structures (after map 1-207A scale 1:500,000 DGMR).

bounded on both sides by the Cretaceous Aruma Limestone (Figure 52).

The western side, as expected follows the regional dip to the east or northeast. On the eastern side, the Aruma limestones are dipping in the opposite direction to the southwest. Where these rocks change their dip direction, they clearly indicate a well-established faulting and fracturing pattern (Photo plate 48).

In the middle of the graben-like structure, the Himar Sabha domal feature is located with both clear radial and annular drainage patterns, shown by interpretation of 1:500,000 Landsat images and 1:60,000 aerial photographs, (Figure 19) and later seen from high altitude helicopter traverses.

Ground investigations within the area of this domal feature indicated that the basal Aruma limestone on the near escarpment was dropped in the Himar Sabha area in the graben with a stratigraphical variation of 30-50 metres. The interpretation of image 179/42, (Photo plate 19) of the data base quality (contract stretch) and the H.P.F.B7 image of the same scene show the graben-like structure bounded by two major NW lineaments. A regional cross section in the area U.S.G.S. geological map 1:207-A indicates that the Aruma limestones on the eastern side of the structure are reversed from their normal dip and are dipping to the SW, in the three upper formations.

The structural "happenings" which Powers, et al, considers to be responsible for the interruptions at Wadi

Al-Atk extend along Al-Butayn to Umm Al-Jamajim (lat. 26°52', long. 45°18') (Figure 52). This area of structural complications mainly corresponds to the Al-Butayn graben-like structure. This structure is further demarcated by a NW trending sheet of locally derived gravel which is banked on the east against a sharp monocline involving Aruma rocks.

Support for the presence of a graben-like structure is that it is completely parallel to the nearby Majmaah Graben and to the general arcuate structure of the Tuwaiq escarpment, image 179/42 (Photo plate 19).

This graben-like structure can be correlated with the Riyadh Tilted Block for the following reasons:

- both represent blocks which seem to have moved independently. Such phenomena are not uncommon in the area
- both have a general NW direction;
- both are more or less 160 kilometres in length, and around 40 kilometres in width;
- within each, the surface and subsurface rocks have a flexural or monoclinal structure, and
- both are bounded by major NW lineaments (faults).

Support can therefore be found from the imagery, geological maps, interpretation, field data and the surface and subsurface data for the presence of the Wadi Al-Atk, Khasm Al-Haqaqa and Al-Butayn graben-like structure.

These lines of evidence in general show a tectonic

complication in the area. Further support is provided by the aeromagnetic data of the Ministry of Petroleum and Mineral Resources as summarised by Davis, Morrisey, (1976). Measurements on a pair of EW test lines flown near latitude 25°30'N indicated "Two magnetic blocks that may coincide with basement highs between 45°20', and 46°30'E, with one block apparently centred near 45°45'E. The geometry of the magnetic blocks was not established".

It is however, interesting to note that the two basement highs between 45°20' and 46°30'E cover the Wadi Al-Atk, the Khashm Al-Haqaqa and the Al-Butayn Graben structures. More significant is that the block centred near 45°45' exactly coincides with the centre of the Himar-Sabha structure in the middle of the interpreted Butayn Graben.

These various points all seem to suggest that the Wadi Al-Atk and its related structures seems to be a surface manifestation of a subsurface (basement) structure which can be correlated with the well known C.A.G.T.S. being a surface evidence of a basement structure (Brown, 1972).

Also, the Wadi Al-Atk, and the Khasm Al-Haqaqa lineaments striking northeast and possibly indicating sinistral horizontal movement, can be considered as a part of the Riyadh Fault System and may present more structural evidence for this system in general.

4.6 THE RIYADH FAULT SYSTEM

4.6.1 General Discussion

The tectonic history after the Precambrian reached a climax in the Cretaceous Period, which marked a period of remarkable structural unrest in the history of the Arabian Shield, the Arabian Shelf and the surrounding geological provinces. The destruction of the ancient Tethys seaway began in the Late Cretaceous, with orogenic movements recorded from Turkey through Iran and extending to Oman (Powers et al, 1966). In Arabia, it reached its climax during the separation of the Arabian Subplate from Africa in Tertiary times.

The formation of the C.A.G.T.S , other structural elements and basins, such as the Arabian Gulf and the Rub' Al-Khali, are all related. The latter is known to have been a positive feature until Tertiary times, when it became a negative feature for the first time (Brown, 1972). Accordingly, it seems that the Arabian Shield and Shelf have been subjected to a history of structural events, despite the fact that the latter has been protected by the underlying rigid basement blocks of the Shield.

These structural disturbances, together with other local tectonic events, seem to have initiated the formation of other structures in the Phanerozoic sedimentary rocks than that the initially published mapping has revealed. Amongst them is the formation of a conjugate set of relatively long lineaments, where the NE ($N30^{\circ}$-$40^{\circ}E$) is dominant over the

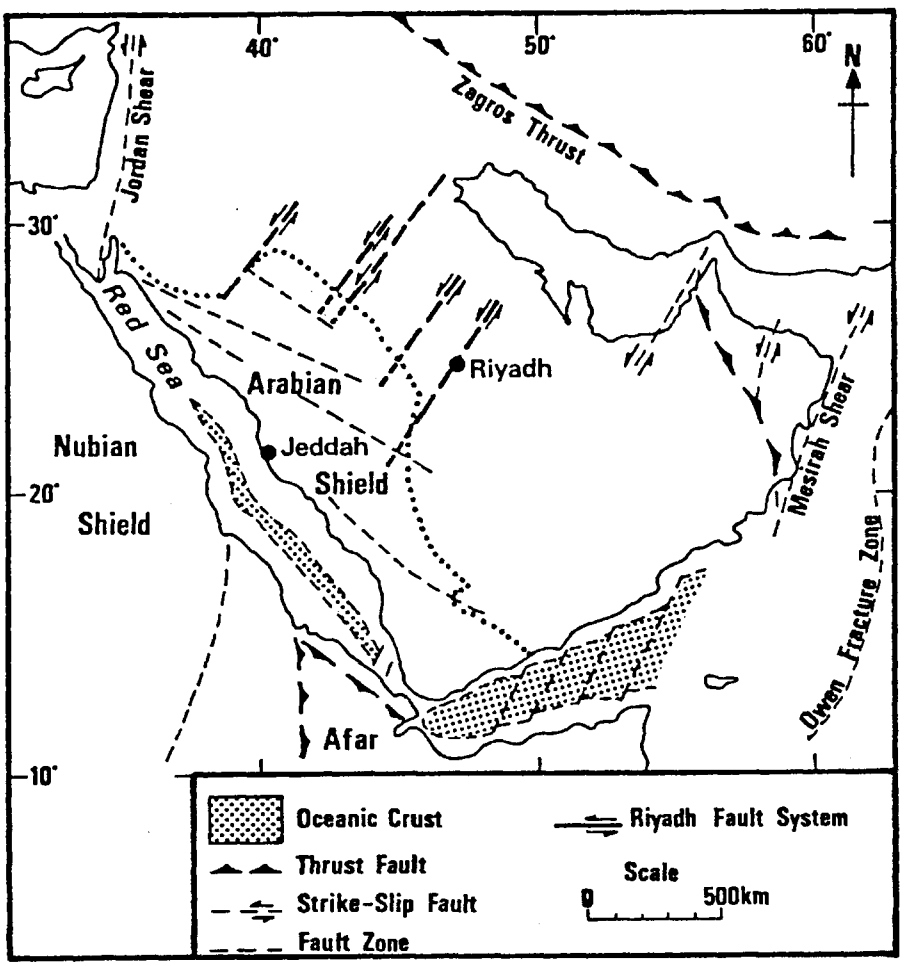


Figure (53) : Riyadh Fault System (modified after Gass and Gibson 1977).

NW (N40°-50°W) direction (plates 1, 2, 3 and 4). These directions intersect to form an acute angle of 75°-80°, the bisectrix of which is aligned N-S, almost parallel to the near meridional N-S lineament system. Existing geological and structural maps are dominated by the NW Najd and the N-S Hijaz structures, while the NE direction is poorly represented in the Precambrian rocks and is almost completely missing from the Phanerozoic sedimentary cover.

4.6.2 Interpretation Phase

It has been possible, however, by applying the previously mentioned interpretation methods and types of imagery, to detect many NE and fewer NW lineaments, the majority of which are over 100km. in length within the sedimentary cover and the eastern part of the Shield (Photo plates 6,10,18,20,22,26 and Figure 16).

The NW lineaments in the sedimentary rocks almost coincide with the basement NW Najd fault system and may represent a surface propagation of some of these faults with some modifications of original length, direction and nature. Because of the dominance of the N30°-40°E direction within the N20°-70°E sector in the majority of the rose diagrams, and the evidence of its structural significance, it will be discussed in some detail.

Generally, these almost straight lineaments, with a considerable length and frequency across the area, have been interpreted mainly from Landsat images supplemented, locally,

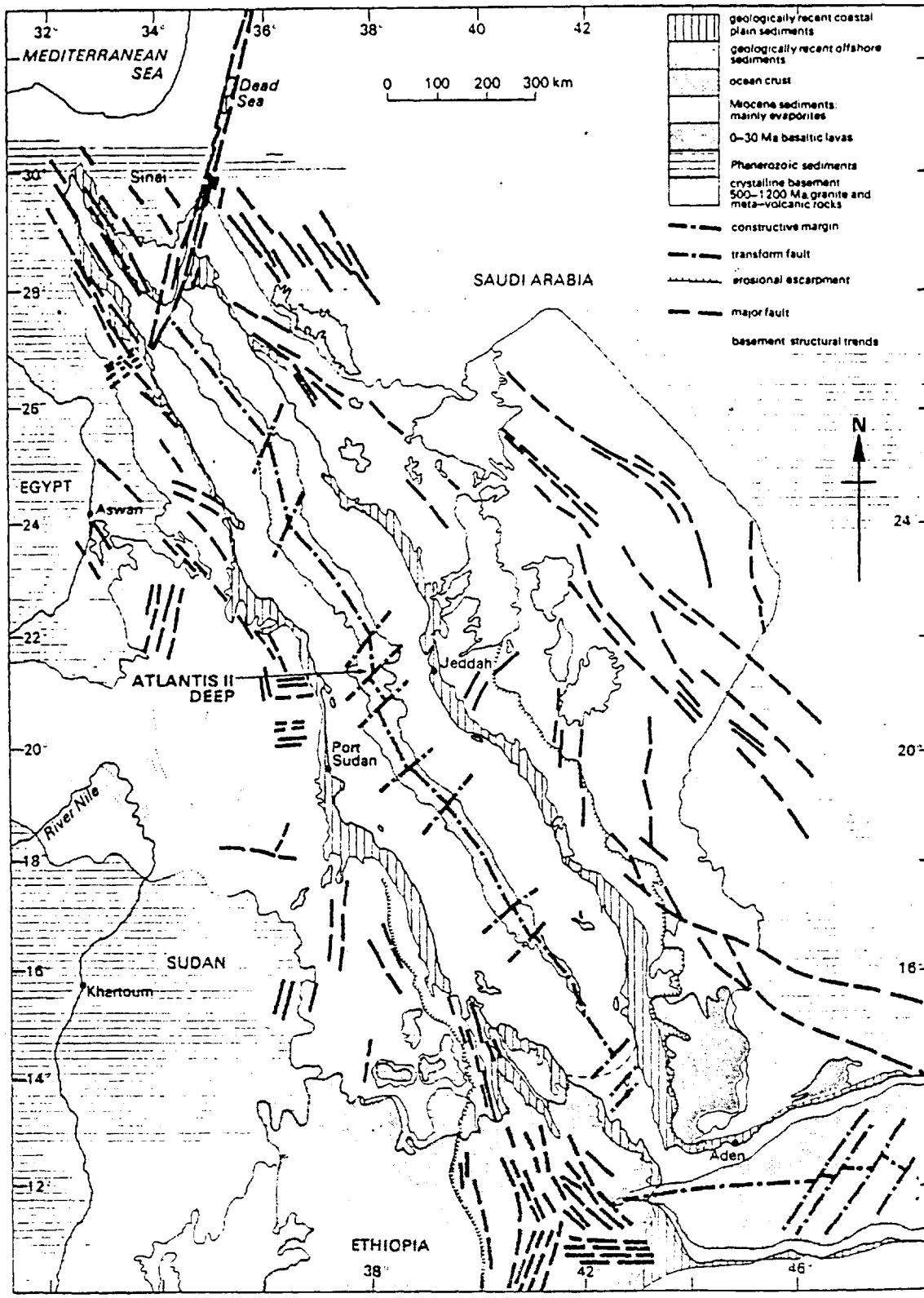


Figure (54) : Arabian Shield and Red Sea Structures (after Red Sea Case Study - Open University 1980).

be existing information. According to their length and straightness they may represent features likely to have penetrated the crust or a significant portion of it. The majority of these lineaments on the surface do not show a conclusive sense of horizontal movement of any feature which, if it occurs, may have been lost during the process of propagation.

The few lineaments which indicate horizontal movements (sinistral faults), are parallel to or coinciding with the hypothetical NE conjugate trend of the Najd System but with the opposite sense of theoretical shearing movement. Since this event has been detected only in the relatively younger Phanerozoic rocks, it implied the existence of another large (N-S) horizontal principal stress at a different time, some 90° or so from that E-W principal compressive stress which caused the Najd movement, and it took advantage of the pre-existing Najd failures and reversed their sense of movement.

The analysis of surface lineaments in this case may highlight some deep crustal features which, after rejuvenation and upward propagation through a pile of covering sedimentary rocks, mostly lost the evidence of their movement. The original nature of these structures and any sense of movement may be difficult to ascertain, except with many integrated processes where ground information and/or existing maps might be available. One of the simplest methods of determining this is to relate them to the main regional stress system which was possibly responsible for their formation.

4.6.3 Current and Previous Ground Investigation:

Ground data were collected from Khashm Addughum area (NE of Riyadh), where a NE lineament fault (Photo plates 23, 60) indicated a relatively clear sinistral horizontal movement by dislocation of the Biyad and Buwaib Formations. This structure was also detected on different versions of image 178/43 (Photo plates 6,7,8,9,10,11). In fact, this was the first clear NE fault with displacement to be detected near Riyadh and this led to its being referred to as the Riyadh Fault System. Some other important interpreted NE structures in the area are prominent directions, namely, Wadi Al-Atk, Khasham Al-Haqaqa, Wadi Al-Batin, Wadi Asshallalah and the Hail Fault (Figure 53) where the latter was inferred from the U.N.E.S.C.O. structural maps of the world.

It has been proved by different means that the Al-Amar-Idsas basement fault zone and other N-S structures exist at a considerable distance into the sedimentary rocks (Section 4.2), and on the same basis one can expect that other NE structures are more likely to be propagated to the surface by later events, although parts of their original nature now may be obscured at the surface and consequently on images. The significance of the obscure traces of the subsurface structures become clearer when the possible course and nature can be inferred from the other regional structures established in the adjacent areas. Sayari and Zotl (1978) pointed out that there is a prominent drainage pattern of NE direction with enormous channels back from the Precambrian shield, and

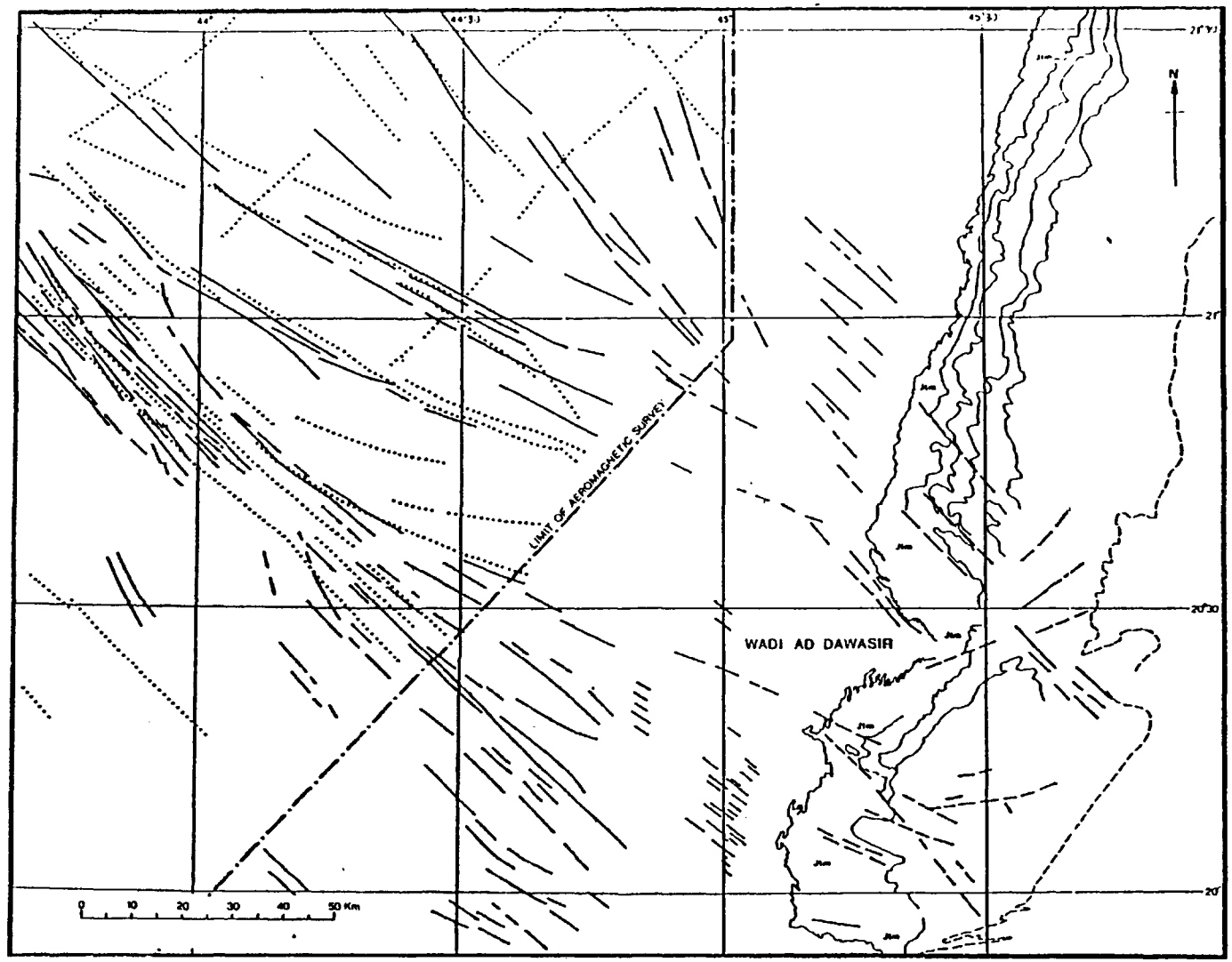


Figure (55) : Linear fault traces in Basement and Cover Rocks as revealed from landsat imagery interpretations and the aeromagnetic map of Addawasir Area (after Moore 1980).

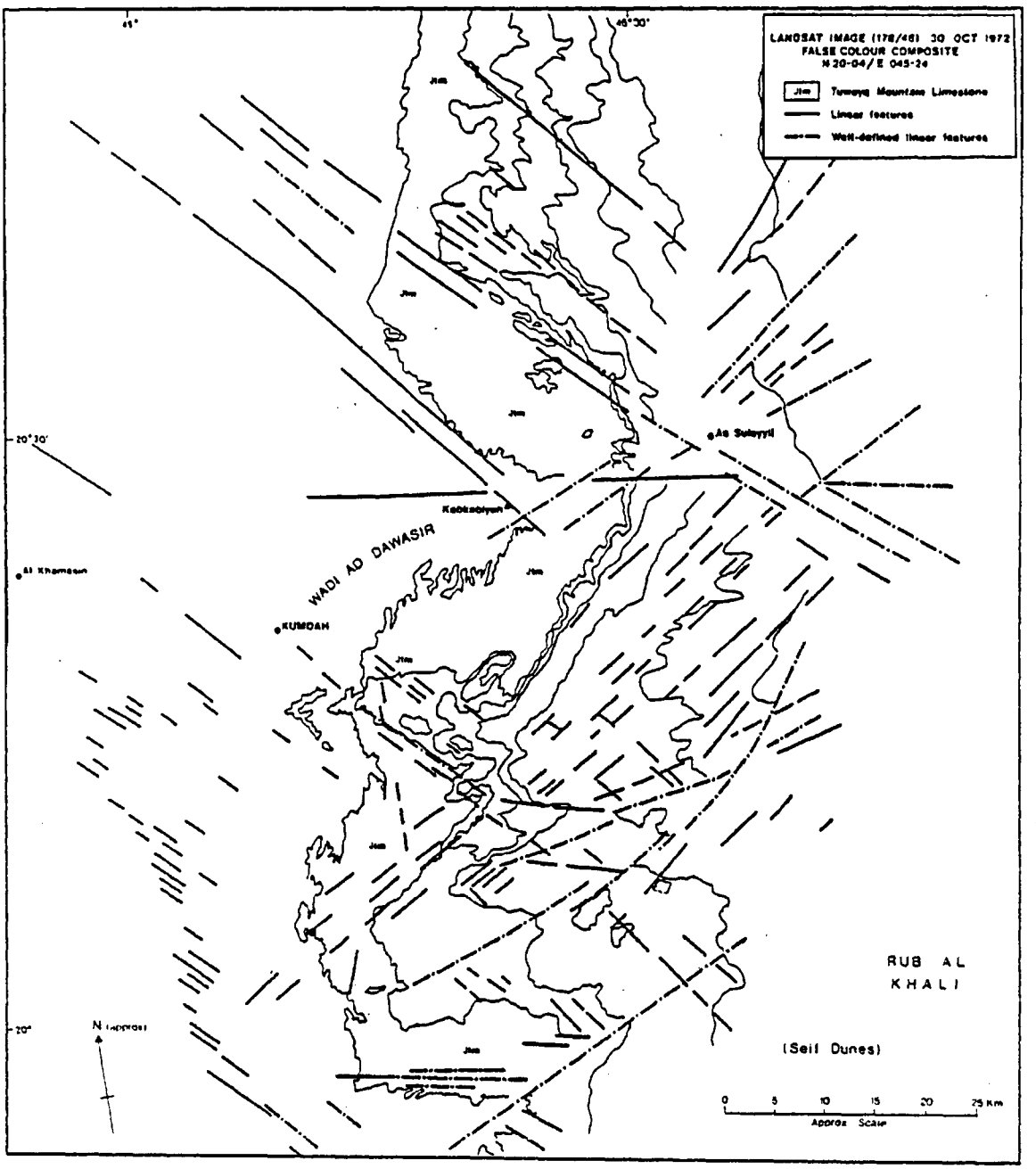


Figure (56) : Lineaments interpreted from landsat images showing clear NE pattern in the Wadi Addawasir Area (after Moore 1980).

cutting across the Arabian Cuesta landscape, as well as the ample gravel fans with their high percentage of crystalline rocks that extend all the way towards the Arabian Gulf coast. Some of the old channels which Sayari and Zotl mentioned are Wadi Arimah, Al-Batin and Wadi Al-Atk (Figure 53). The Wadi Arimah is a major NE channel-way extending mainly in the Precambrian and only partly in the sedimentary cover at its NE extension before it is interrupted by surface cover and other structures. This lineament is known to display a geophysical anomaly in the Precambrian. The Wadi Al-Batin (see section 4.4 for more details) is a major wadi in the region and extends N35°-40°E with a possible sinistral horizontal movement indicated by apparent dislocation of some geological formations.(Figure 47). Al-Sarawi (1978), by applying geophysical data, indicated sinistral horizontal movement as well as some vertical component, either along the main structure or its related elements at the extension of this wadi into the Kuwaiti Territories. Wadi Al-Atk is described in detail in section 4.5.

Nawab (1978) indicated the presence of faults aligned N35°E, N45°W in a Precambrian area northwest of Riyadh (Al-Amar region) and which are in full agreement with the set aligned N30°-40°E, N40°-50°W interpreted as a conjugate set of lineaments in this area.

Gass and Gibson (1977, cited by Nawab, 1978), in their work on the regional tectonics of Arabia, indicated a group of NE faults with sinistral horizontal movement, in a good agreement with the interpreted NE lineaments in the area (Figure 53).

Gass (1980), in the Open University Red Sea case study, agreed on a sinistral fault in the Gulf of Aqaba, the main part of which and its sinistral movement are almost parallel to the NE lineament direction (Figure 54).

Moore (1980) interpreting both aerial photographs and Landsat images, supplemented by geophysical (aeromagnetic) data, in the Wadi Addawasir Arean pointed out the presence of NE lineaments, some being faults (Figures 55,56). These lineaments or faults, if extended NE, mostly coincide with the interpreted NE lineaments in this area.

Another clear line of evidence of these NE faults detected in the area, is a NE fault with another N-S fault forming a scissor-shaped structure which are dislocating the Awsat Graben, Image 178/43 (Photo plates 6,8). The scissor-like structure is not an uncommon phenomenon in this area, especially around or within the C.A.G.T.S. region.

4.7 NORTH-SOUTH PERIODICALLY SPACED LINEAMENTS

Analysis of the directional frequency and length rose diagrams (plates 1, 2, 3 and 4) strongly indicates that over the study area there exists a characteristic pattern of lineaments of considerable regional consistency. These lineaments fall within the 10° - 20° class interval, but individual measurements indicated that the majority has a N10°E direction which (locally) swings a few degrees either to the east or to the west and is referred to as the roughly N-S

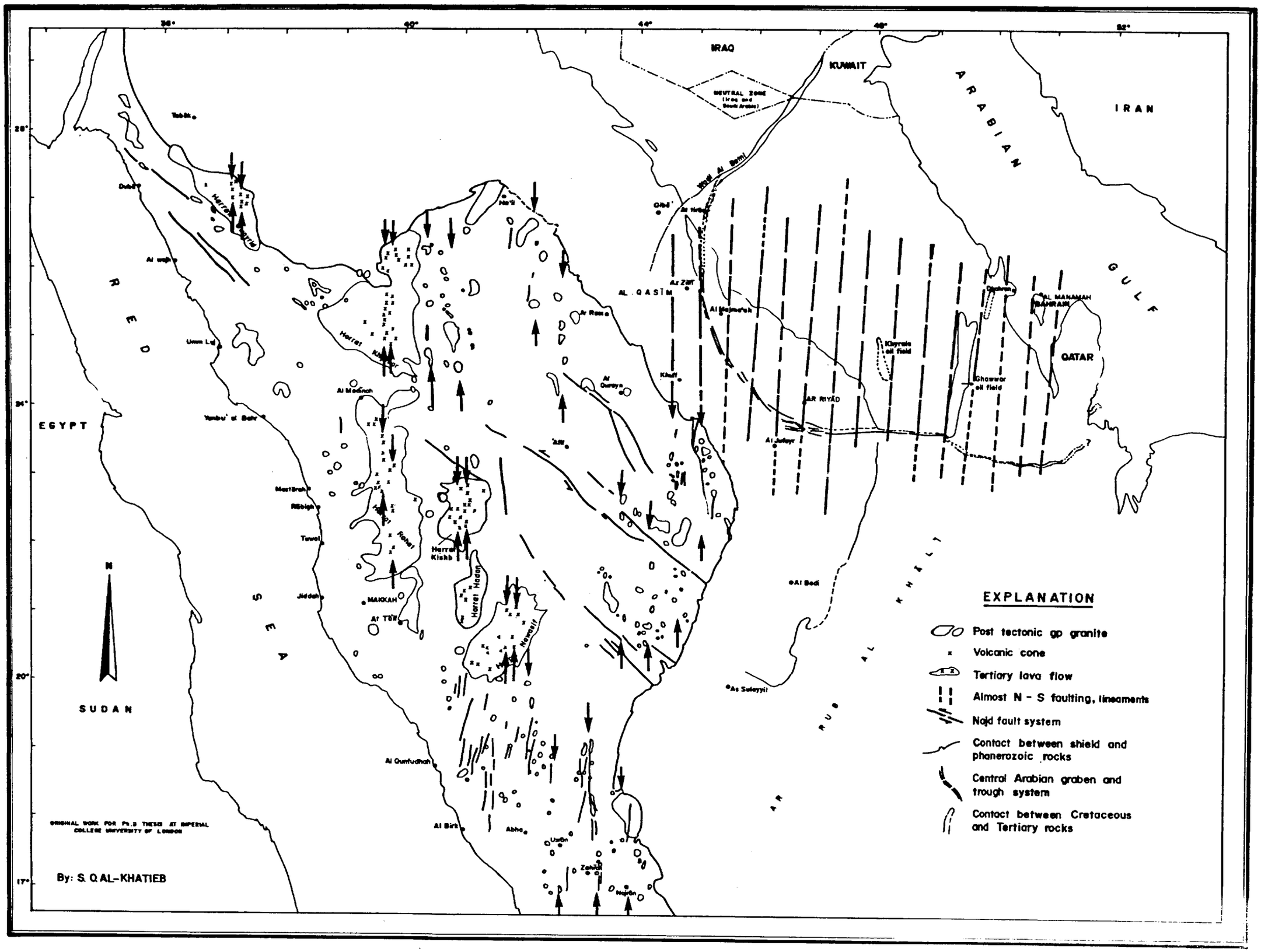
lineaments (rose diagrams are discussed in Chapter Three). The prominent and consistent distribution of this N-S regularly spaced pattern in the basement, where it is followed by Precambrian intrusions, as well as in the sedimentary rocks rose diagrams, indicate that this system of failures has been partially rejuvenated through the sedimentary cover.

The almost regular spacing and parallelism of certain physiographic features within the Precambrian, together with the alignment of the Precambrian granitic intrusions, of around 40 km spacing,(Figure 57), in this N-S direction, emphasize that this must be a fairly old system. Locally, it has acted as a passage for late volcanic activity, the latest of which is of Tertiary Age and which is mainly related to the opening of the Red Sea which is dominant along the western margin of Arabia (Figure 57).

These N-S lineaments display lengths of a few hundred kilometres, ranging from 200 - 500 km. despite being locally disconnected or obscured by superficial cover or due to subsurface complexities and have not been shown on any existing maps.

This length is significant, since there is a general acceptance among earth scientists that there is a probable relationship between the length and the depth of origin of lineaments as well as a relation between length and spacing. There is,however, no complete agreement on the nature of these relations.

FIGURE 57: MAP SHOWING APPROXIMATE N - S TREND AND CHARACTERISTIC SPACING PATTERN OF POST- TECTONIC GP GRANITES AND TERTIARY VOLCANIC CONES



Pamenter (1968) mentioned Haman's contention that as a rule of thumb, fracture length and depth are roughly equal; others indicate that the dpeth of a lineament is almost one half of its length. The latter is accepted by the writer as the more likely. No relation between length and spacing has been established, but Norman, Ike (1977), in a similar study of N-S regularly spaced parallel lineaments in Nigeria, suggested a spacing of the order of the thickness of the earth's crust. The nature of long lineaments has been discussed by different authors, although the evaluation of these large scale features is far from complete (Collins, et al., 1974 cited by Huntington (1977). Later, Rowan et al., (1975) indicated that long lineaments may represent some previously undetected zones of crustal weakness, while many others almost certainly have similar origins, and added that the discovery of these features is already having significant impact on regional geologic investigations. Frisch et al., (1977) cited by Nawab (1978), identified what could be the largest ophiolitic belt in the central part of the Arabian Shield and concluded that the Shield is built up of several closely spaced volcanic arcs of late Proterozoic Age. Such pre-existing old failures have given access to the post-tectonic Precambrian alkalic granites which preferentially followed these regularly spaced N-S lineaments (Figure 57). This conclusion agrees with that by Gass (1977) in Nawab (1978), who concluded that the alkali granites in the Arabian Shield formed above a Proterozoic Age Benioff zone.

These basement linear structures seem to have been propagated upwards through the sedimentary cover, since there is no reason to believe that the exposed basement rocks behaved differently from those covered under the sedimentary cover, where many surface structures are known to be a reflection of those in the basement. A good example of this, is the formation of C.A.G.T.S. (Brown, 1972; Hancock and Kadli, 1980). Khain and Muratov (1969) also indicated that platforms are characterized by gradual changes, from uplifts to depressions. This is the case with the Central Arabian Arch, where the northern part is subsiding and the southern part appears to be stable or an uplifted segment. This situation may have existed for a long geological time and divide the earth's crust in these platforms into blocks with fixed boundaries that move relative to one another. A good example of this situation in the area is the Gharwar oil field, which represents the southern part of the Anaala N-S anticline. This rises above the general level of the platform and is known to be surface reflection of the horst-like uplift over rigid block of the basement at great depths which has relatively resisted deformation (Powers et al., 1966).

The clarity and regularity of spacing of these N-S lineaments both on the ground or on Landsat images vary slightly across the area. This variation can be related to the geologic province in which these lineament fall, that is, the Arabian Shield or the Arabian Shelf.

These long lineaments, which cut through the crust as block-forming structures affect the vertical movement of the earth's crust in the different geological provinces. At depths these structures remain temporarily healed and manifest themselves but little, depending however on many surface and subsurface factors. The most important of these is the tectonic activation of platforms; when propagated to the surface, these lineaments do not necessarily indicate vertical movement, which seems to be the common case in this area (after Khain and Muartov, 1969 with modification).

This conclusion is supported by many geologists, who maintain that relatively long, deep faults, may not originate entirely in contrasting vertical movements of the earth's crust but are an initial result of strains in the earth caused by some "phenomenon" related to the planet as a whole. But what is this phenomenon, which must be of great magnitude to bring about the development of a system of such long, parallel and closely and regularly spaced features ?

The first glimpse of this phenomenon was given by Saul (1977), Norman, Price and Ike (1977); Norman, Ike (1977); Norman (1980) who put forward the idea of meteoritic impact or near miss. These authors largely agree that the change of the earth's speed of rotation, due to bombardment by huge meteors, led initially to a wrinkling of the crust, followed by later failure along the lines of the incipient wrinkles thereby resulting in N-S lineaments.

These periodically spaced lineaments detected in the area indicate that the failures show through the surface rocks of the sedimentary cover image 178/43, 180/40,(Photo plates 7,11,20, 21) and would therefore at first sight appear to be younger than the rocks themselves. However, the sedimentary formations seem to be less disturbed along the lineaments than rocks of the older underlying Precambrian basement, which is explained by evidence in the western part of Arabia, both can be seen with varying degree of clarity on images 181/41, 181/42, 182/41,(Photo plates 22,24,25).

The alignment of(gp)post-tectonic granites and the basic and ultrabasic intrusions,(Figures 57,58) indicate that the relatively older or deep seated failure zones had provided the main conduits for uprising magma, and the alignments are shown on Figure 57 , as a system of regularly spaced lineaments approximately 40km apart connecting the intrusions.

Norman, Ike (1977) suggested that the spacing between the N-S lineaments in Nigeria is of the order of the thickness of the earth's crust. They did not mention a figure, but from the scale of the map showing these lineaments,(Figure 59) it can be concluded to be 40 - 50 km.

The Saudi Arabian case, however, supports Norman, Ike's assumption and it is interesting to observe that the average $\pm$ 40 km spacing between the N-S lineaments closely corresponds to the thickness of the earth's crust of an average of 35 - 45 km as proved by a seismic study carried out by the Sauid Arabian Directorate General of Mineral Resources (Blank et al., 1979).

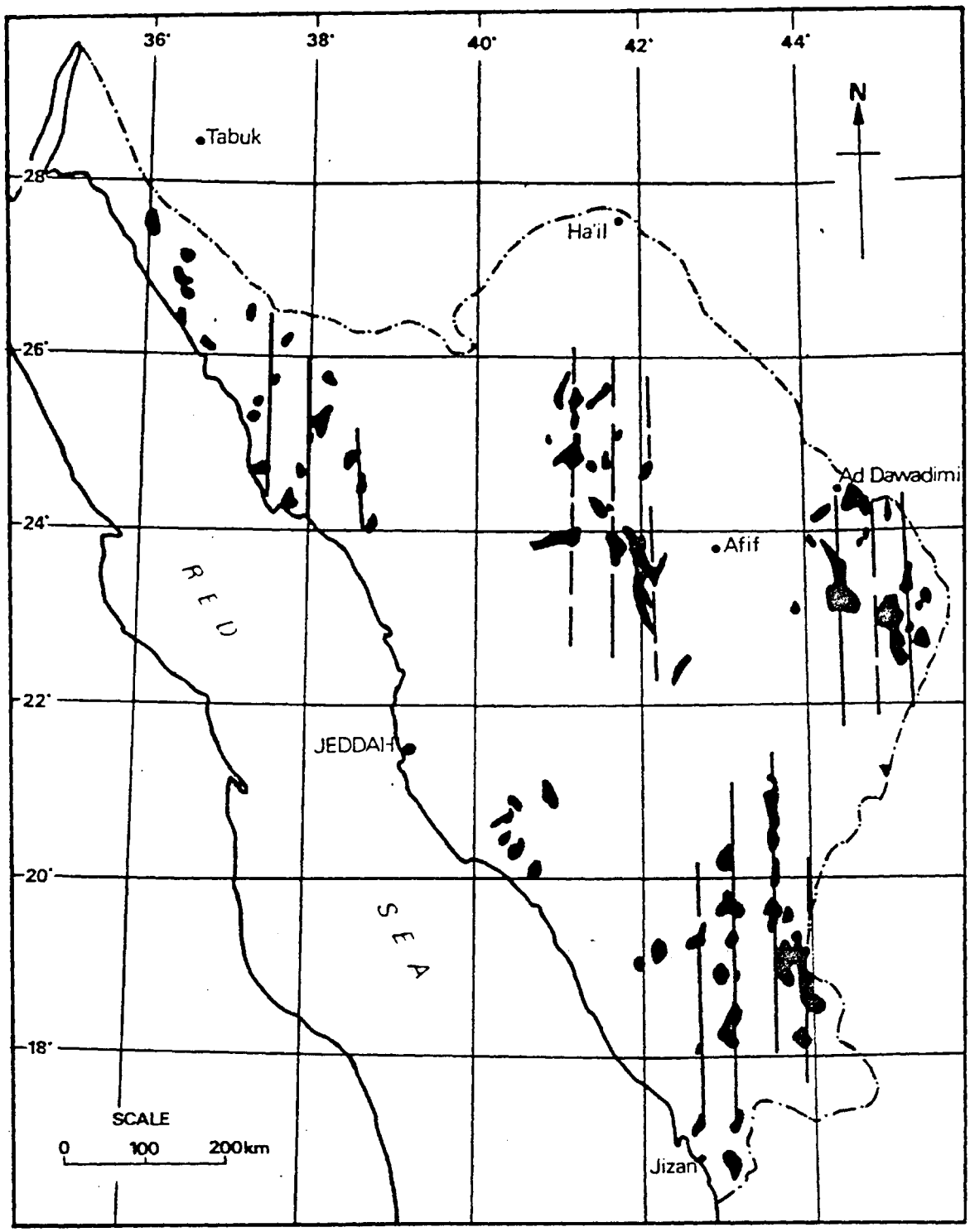


Figure (58) : N-S alignment of Basic and Ultra-basic intrusions with characteristic spacing pattern (modified after Kanaaan, Baghdadi 1979).

This conclusion can also highlight the relationship between the length and depth to an extent.

Statistical analysis of the interpreted N-S lineaments in the sedimentary rocks (Ferguson, 1980) supports the fourty kilometre spacing and shows up as well the less dominant 15 km. spacing. The latter, as previously mentioned, has controlled volcanic activity in Tertiary times and is restricted to the western part of the Shield, in the Red Sea vicinity (Figure 57, Plate 7 and Photo plate 61). The whole pattern as shown by the distribution of Tertiary lava flows, the alignment of volcanic cones at depth being related to Red Sea tectonics (Van Padang, 1963; Coleman et al., 1977 and Blank, 1977) cited by Barazangi (1980), failed to allow movement to concentrate in a few widely spaced lineaments. Instead, it is believed that movement was disseminated into many closely spaced lines. The presence of some faint N-S lineaments within the relatively clearer 40 km. spaced system is possibly due to the influence in the sedimentary rocks of these deep seated volcanic eruptions, or other relatively uncommon structures of these depths.

Imagery interpretation, existing maps, and field investigation across the Arabian Shield, Interior Homocline and Interior Platform (the two latter known as the Arabian Shelf) indicated the occurrence of some geological and physiographical features which can be regarded as evidence of the N-S fc rty km. spaced lineaments.

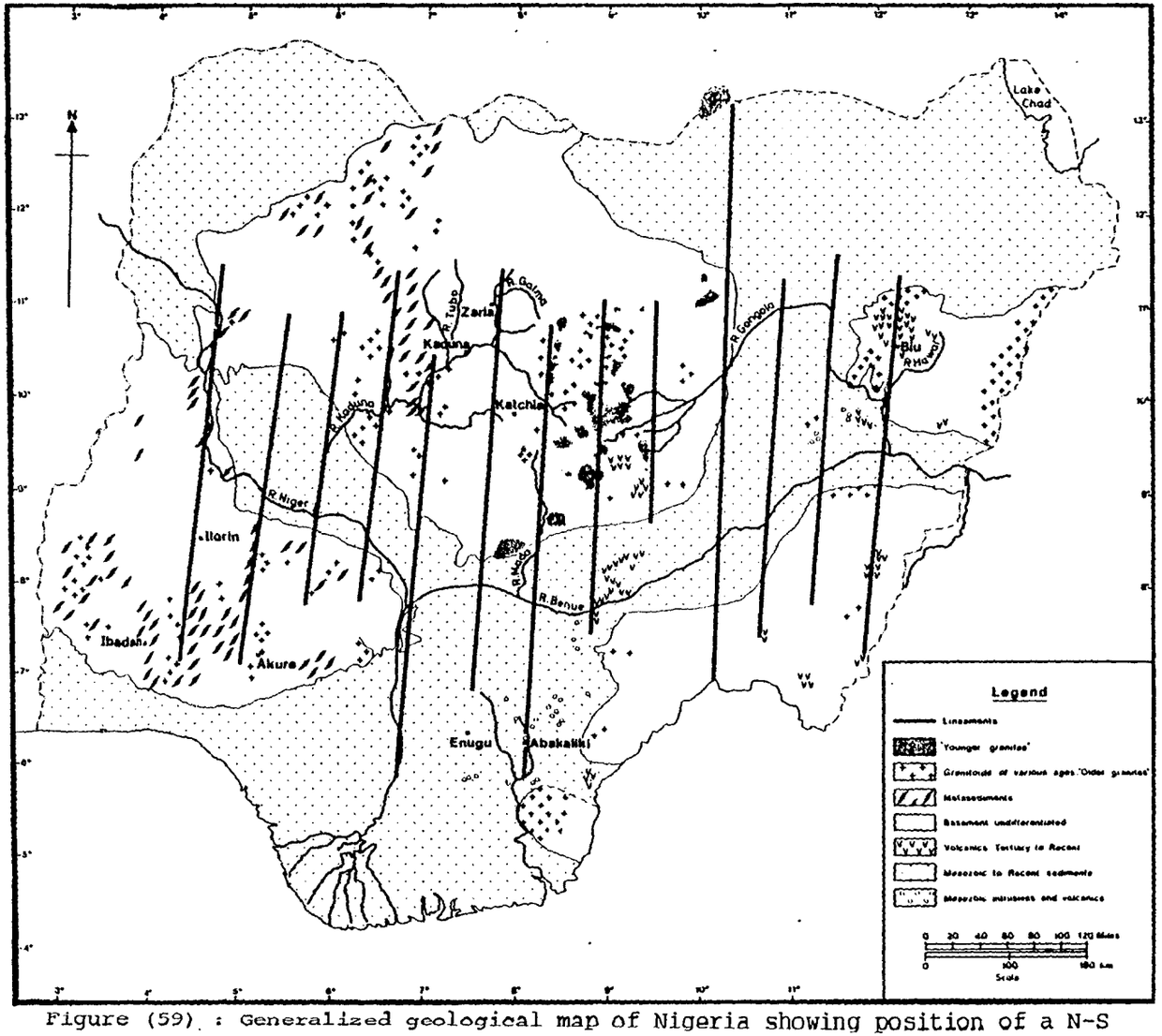


Figure (59) : Generalized geological map of Nigeria showing position of a N-S periodically spaced directions (after Chukwi - Ike 1977).

4.7.1 Evidence in the Shield

1. The Post-tectonic peralkalic granites (gp) (Figure 57) dated about 520 million years, are mainly aligned in a N-S direction with an average 40 km. spacing as detected on the 1:4,000,000 geological map (in pocket). Later field work proved that these gp granitic intrusions are more frequent than shown on the geologic map (scale factor) and all sizes are aligned in a N-S direction.(Photo plates 24,25).

2. The Al-Amar Idsas Fault and other important structures of the relatively old Hijaz Orogeny are oriented N-S. In the case of the Al-Amar Idsas Fault, it has been found that this important paleo-suture (Moore 1979) and other Hijaz folds have been displaced by the Precambrian Najd structures. Greenwood (1980) indicated the very old history of this direction. The fault itself is occupied by(gp)granites (Figure 57). It has been proved that this important basement fault maintains the same direction when extended through the overlying sedimentary rocks (Al-Khatieb, Norman, 1980 in preparation); an item of evidence of the propagation of the deep-seated structures in the overlying sedimentary rocks.

3. The distribution of the basic and ultrabasic rocks suggests their alignment in a N-S direction and indicates spacing with a slight variation from the gp granites; they are shown on Figure 58. The Al-Amar Idsas Fault, beside being occupied by (gp) granites, is also followed by an alignment of these basic and ultra-basic rocks.

4. The Hail Arch, being a significant feature in the geologic history of the area (Brown 1972), is directed N-S. Figure 57 indicates the characteristic alignment of gp granites on both sides of the Hail Arch.

5. Fischer et al (1977), concluded that the Arabian Shield is built up of relatively closely spaced volcanic arcs of late Proterozoic Age, this was agreed by Gass, Naseef (1977) cited by Nawab (1978). According to these authors the trench sediments between these N-S volcanic arcs have been squeezed out as a result of collision. The Al-Amar-Idsas Fault supports these conclusions (Nawab, 1978).

6. Some of the present NNW directed early Hijaz structures, which are dominant in the southern parts of the Shield, were originally directed N-S but because of their location near the NW Najd shear zones they were rotated into

parallelism with the shear zones themselves (Greenwood, et al., 1980). This supports the early assumption that some lineaments deviate or swing from the N-S direction, probably due to local or regional tectonic events and propagation through the overlying sedimentary rocks.

The extension of the Al-Amar-Idsas basement fault in the overlying sedimentary rocks, the statistics of the interpreted N-S lineament spacing, the presence of some N-S lineaments seen with a variable degree of clarity on images 178/43, 178/42, 182/41, 180/40, 181/42,(Photo plates 11,18,24, 21 and 25) and some existing known structures all indicate that these N-S periodically spaced lineaments,although of basement origin, have been propagated upward and are now detectable in the sedimentary rocks.

4.7.2 Evidence in the Sedimentary Rocks of the Arabian Shelf:

1. One of the important lines of evidence can be interpreted from the tectonic map prepared by Brown (1972). The structural contours of the base of the Tertiary, the base of the Mesozoic and the top of the Basement (at depths of a few thousand metres) indicate alignment in this pattern. These features or sharp deflections in most of the sedimentary region, are aligned N-S and the plunge-like patterns of alternating 'highs' and 'lows' display spacings of approximately the

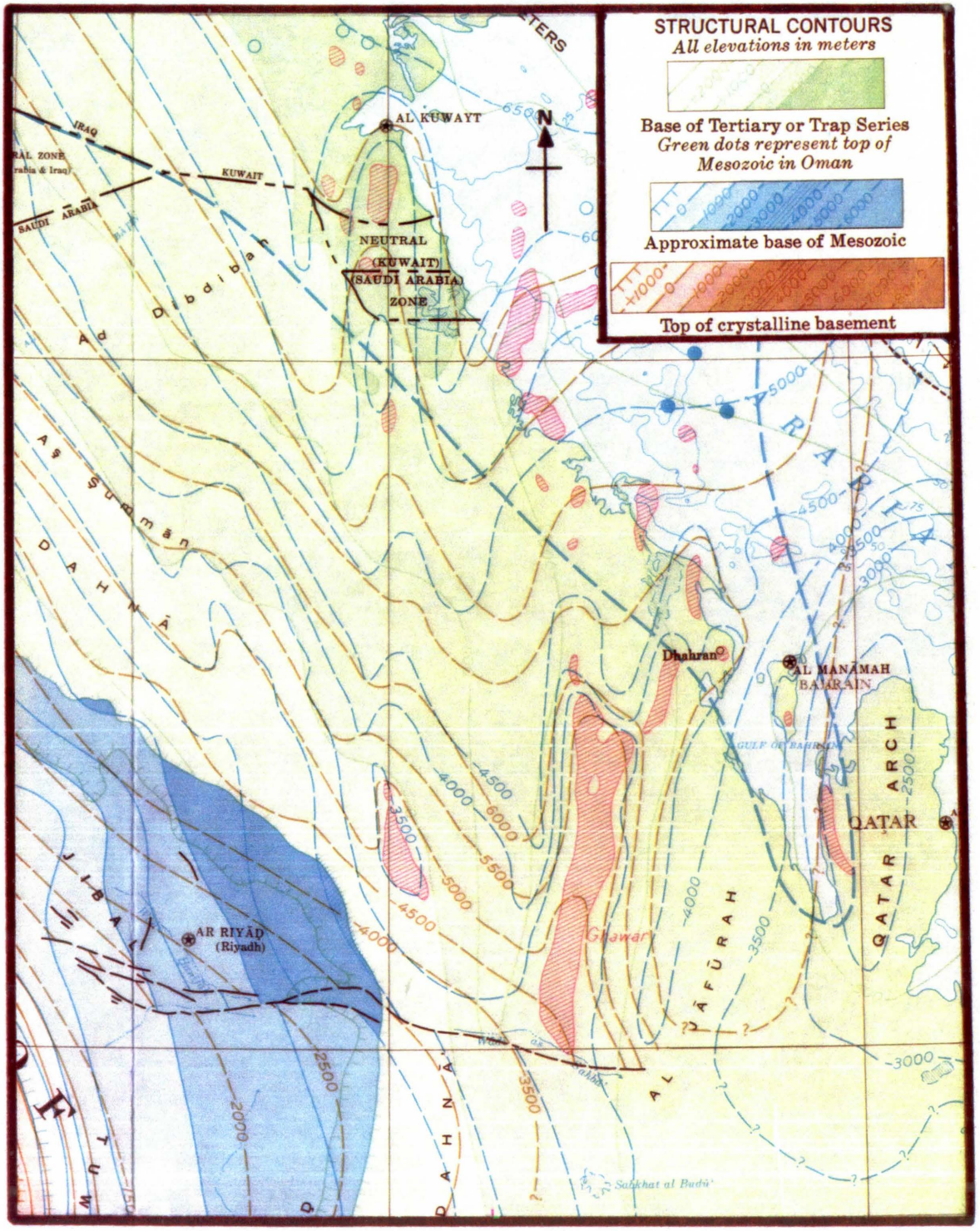


Figure (60) : Alternating 'highs' and 'lows' in the structural contours in the Arabian Shelf Region (after Brown 1972).

same order) as the lineaments in the Precambrian rocks (Figure 60). This is tangible evidence of the presence of these lineaments in the basement and propagated through the overlying sediments.

2. One of the major oil fields in the area (and in the world), the Al-Ghawwar Oil Field, which represents the southern part of Ana'ala Anticline, is directed N-S with a width of about 40 km. and is bounded by two of the N-S lineaments (Figure 57) The structure is known to be a surface expression of a host structure in the basement (Power, et al., 1966). The Khyrais Oil Field, on the same figure, is bounded by two of these N-S lineaments.

3. The Qatar and Bahrain Arches are direction N-S, parallel to the Ghawar Oil Field.

4. The clear N-S lineaments around Riyadh, image 178/43 (Photo plate 6,7)coincide with the 'highs' and 'lows' of contours in the tectonic map.

5. Hancock and Kadhi (1980) indicated a clear N-S extensional direction responsible for the formation of the C.A.G.T.S

It has been noticed from both the structural contour map and evidence in the Arabian Shelf, that the majority of examples of the N-S lineaments are restricted to the East Arabian Block (Hancock, Al-Khatieb, Kadhi in press, geological magazine).

Similar regular N-S lineaments have been detected in Nigeria by Norman, Ike (1977); many of the details of this study have their parallel in Saudi Arabia (Table 11).

Thus it can be concluded that these may have been a significant system in the Afro-Arabian Plate before separation by the Red Sea opening. The separation may have initiated the opening of some of these lineaments, mainly in the vicinity of the Red Sea itself. The correlation of these regional N-S structures in Nigeria and Saudi Arabia has been initiated by the great resemblance of the geological history of the African and Arabian Sub-plates, as discussed by many authors.

The summary of the relevant literature may highlight these resemblances. It is known that the Arabian Shield appears to be the northern extension of the Late Precambrian zone of deposition and deformation in Africa: the Mozambique Belt of Holmes (1951). Bloomfield (1970); Kazmin (1971); and Black and Girod (1970) cited by Brown (1972), considered that the Najd and Hijaz tectonic events represent a time span and tectonic history closely parallel to the events in the Central African Hoggar. It is interesting to note that both the older Hijaz and the relatively younger Najd are structural elements which have a direct relationship to these N-S lineaments.

Recently Anderson and Greenwood (1976) and Anderson, et al (1980) have indicated that the structural zones and lineaments of the Arabian Shield continue directly into the

ASPECT	SAUDI ARABIA	NIGERIA
General Direction	N-S swings 5°-10° mainly to the East.	N-S swings few degrees to the East and West.
Average Spacing	Approx. 40 km	apparently 40 - 50 km
Average Thickness of earth's crust	35 - 45 km as proved by seismic survey.	principles as in Saudi Arabia.
Length of Lineament	200 - 500 km	200 - 550 km
Nature of Movement	not clear on surface, but as being bounding horsts and grabens in the basement vertical movement is expected.	some vertical movement
Age	cannot be exactly determined, but older than 550 m.y.	over 520 m.y.
Linear Pattern	all lineament are surprisingly straight except locally where some have followed preexisting arcuate feature.	mainly straight, locally obliterated by later intrusions.
Nature of Dislocation	dislocated by NW sinistral trans-current faults (Najd fault system).	dislocated by NW sinistral trans-current faults.
Origin of Force of Dislocation	The Najd system is produced by E-W compressive stress field.	produced by E-W compressive stress field.
Magnitude of Dislocation	locally 2 - 25 km, but regionally increase to tens of kilometers.	tens of kilometres.
Nature of Rocks Occupying the Lineament	mainly followed by gp granites and to less extent volcanic rocks.	followed by granites and volcanic rocks.
Age of Intrusive Rocks.	$\pm$ 520 - 530 m.y.	$\pm$ 520 - 540 m.y. and 180 m.y.
Mineralization	most of the mineralized belt are following N-S direction.	Mineralization of base metals and tin, tungsten and copper

TABLE (11) CORRELATION OF THE NATURE OF N-S PERIODICALLY SPACED LINEAMENTS IN SAUDI ARABIA AND NIGERIA

African Shield if the Red Sea is hypothetically closed, they added that the continuity of these structural belt and patterns, and the suggested lithologic correlation across the Red Sea suggest that both were involved in the same cratonization events. To summarize the general structural resemblance of both Arabia and Africa, Gass (1980), in the Open University Red Sea Case Study, pointed out that "across the Red Sea, the Arabian Structure is almost a mirror image of that on the African side."

The data presented in the table summarize the geologic history and the current nature of these near-meridional lineaments and suggest that this system adds other evidence of the strong geological relationship between Arabia and Africa in the early geological periods.

It is surprising to find that these major near meridional lineaments in Arabia remain parallel and almost straight across the different geological provinces from the Arabian Shield in the west as far as the Arabian Gulf coast in the east. (Figures 29,57).

The presence of some Tertiary volcanic cones along some of these N-S lineaments,(Photo plate 61) and the reactivation of some old structures, such as the Al-Amar-Idsas Fault, in the Quaternary times (Nebert 1972) indicates that reactivation of these lineaments has been going on from Precambrian times on.

The movement along some of these (old failure zones) lineaments seems to have been initiated by the stress acting

during the separation of the Arabian Plate from the surrounding plates and the disturbance of major structural events within the Arabian Plate itself.

The straightness, parallelism, and regular spacing of these old crustal failures found in Nigeria (Africa) Saudi Arabia (ASIA) and similar style have been found in Brazil (South America) by Norman, Ike (1977) indicate that they are more widely spread than has been realised.

Both studies (in Arabia, Nigeria) may present some photo-geological and field measures of these near meridional periodically spaced lineaments.

4.8 CIRCULAR, ELLIPTICAL AND ARCUATE FEATURES

During the interpretation process a considerable number of circular, elliptical and arcuate features were noticed. Different types of images and certain aerial photographs display such features, of various sizes and frequency, in different parts of the thesis area. Amongst these features, certain genetic differences can be inferred, depending on their size, shape, position in the stratigraphic sequence and the geological province. Accordingly they can be divided into two main categories:

First, semicircular or elliptical features, ranging in size from one to tens of kilometres in radius, were detected on 1:1,000,000 scale images and some on 1:60,000 aerial photographs or field photographs. These are very common within all geological provinces, for they are found in both Precambrian and Phanerozoic rocks. In the latter they represent either domal features or settling over Precambrian topographic highs or collapse features.

The second category includes the great circular or arcuate features, which are observed more clearly in the Precambrian rocks and less so in the overlying sedimentary rocks, where thicker sequences are involved. These features were detected only on Landsat images of 1:1,000,000 and on some existing geological maps of 1:2,000,000 scale (Figure 49). These arcuate features vary in size from tens to hundreds of kilometres in radius and are thought to be mainly the result of meteoritic impact (Saul, 1978; Norman, 1980).

Because of the geological importance of both types as well as their significance in controlling certain mineralized regions, they will be discussed in some detail.

4.8.1 Circular, Semicircular and Elliptical Features:

4.8.1.1 Detectability of circular features on Landsat images

The interpretation of different types of images and utilising different bands, revealed variable sizes and distribution of these features. The majority of the images used exhibits faint circular and elliptical features locally grouped, which have not been reported before from the area. Some of these features are characterized by the presence of topographic rims along parts of their circumference, where drainage is preferably deviated thereby enhancing part of the circumference by relatively deep incisions, images 178/41, 179/41 (Photo plates 27,15). Many are discontinuous along thier rims, although this may reflect only the different degrees of detectability along their circumferences.

During the interpretation of images, it has been noticed that a circle which is in general clearly and readily visible along a great portion of its circumference, will be then easily or readily visible over the whole circumference; whereas, on the other hand, the majority of the faint circles are almost uniformly faint. These faint circular features are indeed indistinct and there has been some difficulty in

reproducing the same circle using different images of the same scene, although some parts of their circumferences were detected on more than one image.

Detection of parts of circumferences was relatively more easy where two or more circles intersect. Such intersection results in the enhancement of two arcuate rim features due to some erosional and topographic factors, and during interpretation attention has been paid to these relatively clearer intersections. Some other circular features are readily detected because of their characteristic lineament and drainage patterns. Lineaments are mainly radial with radial drainage over the area of the feature and annular drainage around it. Again, they may be detected because of their deflecting or disturbing effect on other clear, straight lineaments. Locally, these change their direction by following a part of the circumference of the circular feature before straightening again image 179/41 and 179/43 (Photo plate 15,3). In some cases, circular features can be observed on images which are defined by distinctive tonal, textural and pattern elements resulting probably from the integration of some lithological, structural, topographical and drainage characteristics images 179/41, 178/41 (Photo plates 15,27). Some of these characteristic patterns seem to be the result of circular features which are bordered by major lineaments or which are located in graben-like structures as, for example, the Himar-Sabha domal structure, image 179/42 (Photo plate 19).

The area studied covers a part of the Arabian Shield

and the Arabian Shelf. The shape, size and distribution of the circular features differ somewhat in these two subdivisions, and redundant features in each geological province will be discussed in brief.

4.8.1.1.1 Circular Features in the Arabian Shield:

Interpretation of the few images which cover part of the eastern edge of the Shield image 182/41, 181/42, 180/43, (photo plates 24,25,29) clearly indicate the sizes, shapes and abundance of circular features. Size and location of these in the shield are mainly related to high-level, post-tectonic granitic intrusives and their effect on the older metavolcanic rocks. The intrusives are mainly represented by different types of granitic rocks and to a lesser extent, by mafic and ultramafic rocks.

The intrusive rocks generally form circular plugs, stocks and ring dykes ranging in size from a few to 30km. in radius. Some of these rocks have been easily eroded and have left few exposed remnants in a larger circular feature which indicates the original size of the plug. In some cases only the effect of the intrusion on the country rock is left behind as a semicircular feature, with no intrusive rocks left exposed. The degree of surface erosion therefore seems to be responsible for the variations in size and to a smaller extent in shape , (Photo plate 26).

The fact that the majority of these granitic or mafic intrusions is structurally controlled also affects the

general pattern of their distribution image 182/41,(Photo plate 24) and accordingly will affect their upward propagation through the overlying sedimentary rocks.

4.8.1.1.2 Circular Features in Sedimentary Rocks Near to the Basement

The sedimentary rocks bordering the eastern edge of the Arabian Shield are referred to as the Interior Homocline. Images covering part of the Homocline include 178/43, 179/42 and the NE corner of image 179/43 (Photo plates 10,13,2). The thicknesses of the formations forming the homocline range from a few hundred metres close to the contact with the shield to some 3000m (Powers et al, 1966).

The irregularity of shape and size of circular features within the sedimentary rocks is, to a great extent, the same as in the underlying basement with a lesser degree of clarity with respect to their circumferences. It is known from previous literature that there is no dominant horizon of evaporite within this stratigraphic sequence, so that the majority of the circular features included are inferred to be the result of settling over a Precambrian topography.

One phenomenon has been noticed, that some relatively clear circular features are in fact represented by two circular features, one within the other, and where the circumference of the inner is slightly clearer than the outer rim. This feature can probably be interpreted as the result of upward propagation of both the top and the bottom of almost conical

features on the Precambrian surface. This is more likely to take place where substantial thicknesses of overlying sedimentary rocks are occurring. On the other hand, relatively thinner sedimentary sequences, near the edge of the shield, seem to produce drag or warping over the Precambrian irregularities. (Photo plates 9, 28).

The slightly different sizes and shapes of these faint circular features in the homocline are probably a result of settling not only over the circular plutonic rocks but also over the other irregularities in the Precambrian rocks in general which do not follow any regular pattern.

4.8.1.1.3 Circular Features in Relatively Thick Sedimentary Rocks

These include those surface features over the relatively thick sedimentary sequence of the Interior Platform bordering the eastern side of the homocline. Thicknesses of sedimentary rocks reach a maximum of 5,500m (Powers et al., 1966). The stratigraphic sequence is variable within the homocline in that a few evaporite horizons are included in the sequence within the Cretaceous and the Tertiary rocks which to some extent have resulted in the formation of salt diapiric structures known to occur in the Eastern Province of Saudi Arabia. Images 180/40, 181/40, Photo plates 21,28) cover parts of the platform. The interpretation of circular features indicates more persistent shapes and sizes of these features, mainly represented in two

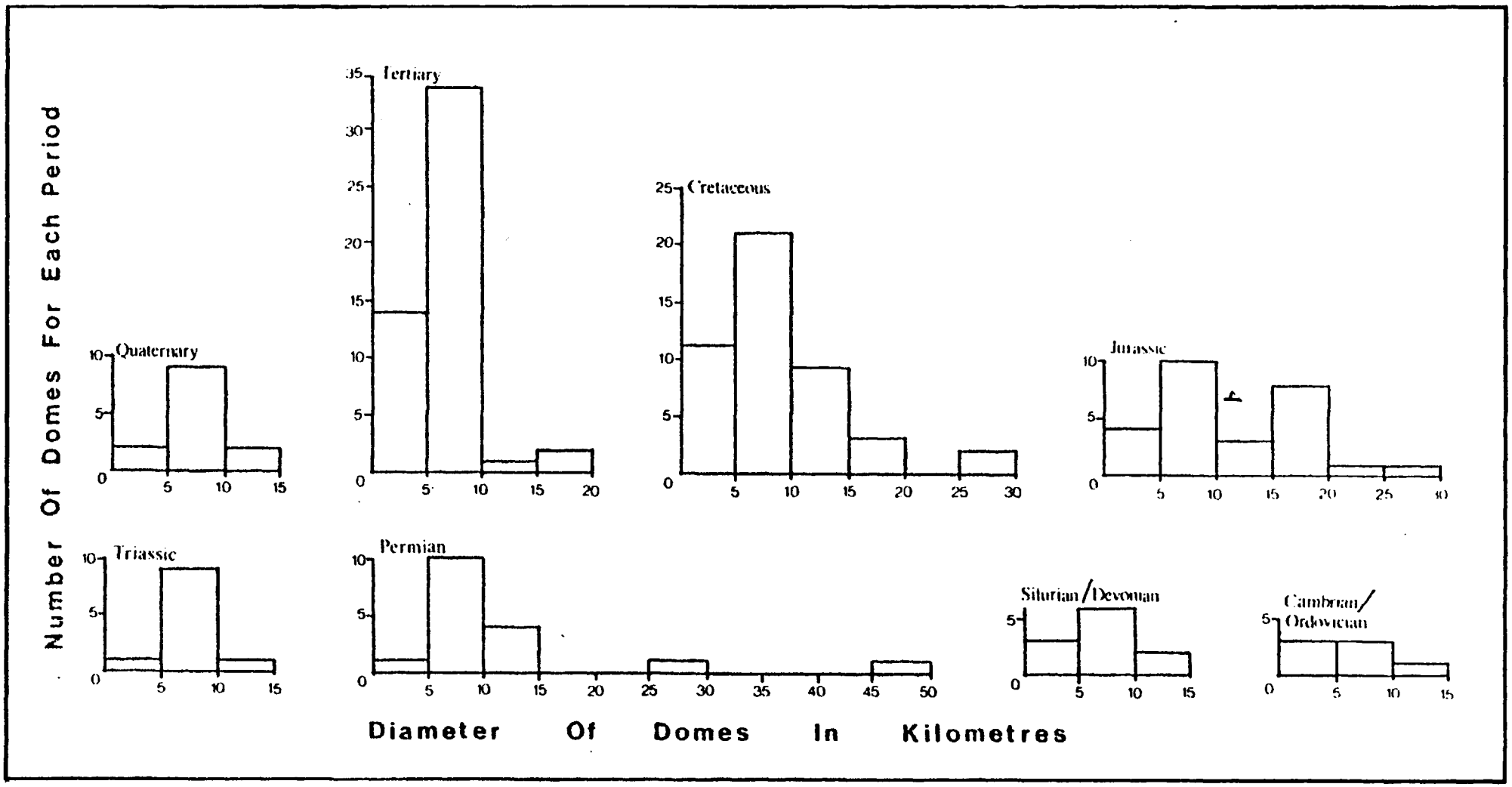


Figure (61) : Diameters of domal features related to bedrock in the Cover Rocks (after Norman 1980).

major classes: relatively smaller ones around 5 - 10km in radius and larger features of about 15 - 30 km in radius. This classification agrees to a certain degree with the statistical analysis of these features carried out by Norman, 1980, (Figure 61), and both are to be discussed in detail.

4.8.1.1.3.1

5 - 10km radius:-

It is possible however to suggest numerous causes for such domal features, but some would appear to rule themselves out by the nature of the environment. Circular features of 5 - 10km diameter are mostly to be found in the Cretaceous and the Tertiary Formations, where both are well known to be underlain by evaporites (Powers et al., 1966,Table 1) This is supported by the fact that some of these domes, where detected on images, appear to have white material exuding from their sides, where anhydrite is known to occur in the subsurface. Some calcium sulphate powder, moreover, has been found at some of these features,during field work (Shearman, Norman, 1980). An example of these features is Himar-Sabha (Figure 19). Ground investigations and helicopter traverses at different altitudes indicated the domal nature of this feature, with clear radial and annular drainage. (Photo plate 19).

4.8.1.1.3.2

10 - 30km radius:-

The other dominant type of circular features ranges in size from 10 - 30km in radius, with some exceeding these

dimensions. The existence of these features, with generally faint circumferences, seems to be characteristic of the Interior Platform, where the thicknesses of the overlying rocks are relatively greater than in the homoclinal region. These great thicknesses seem to have supressed the propagation of relatively smaller sizes of features in the Precambrian topography at this great depth. On the other hand, it seems that the larger prominent subsurface features are the only features to have been propagated to the surface.

It may not be a coincidence, however, that the width of these circular features, 40 - 60km, agrees with the spacing between the prominent N-S pattern which has been proved to be representing deep seated basement failure. Possibly these 40 - 60km diameter features can represent the surface propagation of the subsurface structures bounded by the N-S lineaments which at depth may indicate variable topography.

Another possibility is that these surface semicircular features are first, a surface manifestation of a persistant basement topography which was brought to the surface through the sedimentary cover during millions of years of upward propagation, enhanced by being relatively near to the seismically active region of the Arabian Gulf. Second, a salt diapers of great size, a phenomenon which is not uncommon in the region for example Dammam Dome. (Powers et al, 1966).

4.8.1.2 Detectability of Circular Feature on Different Images:-

Unlike lineaments, the detection of circular features requires the study of relatively greater areas to facilitate

the study of tonal variations across the features. Because of the nature of the process by which H.P.F.B7 images were prepared, one can detect lineaments better than areas. Accordingly, they did not prove to be of much advantage over the other types of images, apart from exceptional cases where the circumference of some circles is displayed as arcuate lineaments. Generated images, in which the effect of high pass filtering was obliterated, proved to show circular features with more clarity image 179/43 (Photo plate 3).

Fortunately, beside the complete coverage of H.P.F.B7 images, a few parts of the area were also covered by S.P images of different bands. Through the interpretation of circular features S.P. images of bands 5, 6, 7 and I.R.C.C exposed under the wet season conditions, proved to be more useful in this case than it has been in interpreting lineaments. S.P band 4 is the least recommended band, if circular features are to be investigated. Exceptional cases are seen where parts of the circumference, deeply incised in the rocks, are filled with water during some showery day in the season, and this proved to enhance the detection of these parts of the circle. (Photo plate 11).

4.8.1.3 Small Circular Features on Aerial Photographs:-

The interpretation of aerial photographs, together with later field traverses and ground investigations, indicated the presence of relatively smaller circular or elliptical features ranging from 0.5 - 2km in radius and a few metres in

height. These circles gave the impression of small volcanic cones, being dark in contrast with their surroundings (Photo plates 23,59).

The field work proved that this phenomenon is restricted to the Biyadh Sandstone Formation, where the black colour is due to a desert varnish weathering. Accordingly they have been referred to as pseudovolcanic cones, because of their very close apparent similarity to true volcanoes (Unpublished reports of M.A.W., 1978). They have outward dipping flanks surrounding a crater, and at first sight it might be thought that they were caused by diapirism of some kind. Detailed field investigation however, frequently reveals in the 'crater' characteristic blocks of Biyadh Sandstone which belong higher in the sedimentary succession than the Lower Sulaiy limestones which are characterised by collapse features. These features,(Photo plate 59) lie in the vicinity of a NE lineament which may have brought about collapse of the Lower Sulaiy Formation by solutions percolating along it at different depths. When the Sulaiy limestones collapsed the overlying black (desert varnished) sandstones seem then to have been let down forming these circular features. The circles themselves then became filled with rubble and wind-blown material.

4.8.2 Arcuate Features

The present appearance, on Landsat imagery, of evidence of large arcuate features is clearly demonstrated on

certain images, the most significant being 180/43 (Photo plate 29) such features are also depicted on the existing 1:4,000,000 geological map. These features range in size and clarity on images covering both the Precambrian and Phanerozoic rocks. Their size ranges from tens to hundreds of kilometres, while their clarity ranges from clear and sharp to faint (Figure 49). The large size of these features and their persistence through geologic history suggest that they are a result of old impact and meteoritic effect in the early Precambrian times which were later propagated upward in the overlying sediments (Norman, 1980).

4.8.2.1 Arcuate Features in Precambrian Rocks:

The interpretation of images covering Precambrian areas reveals some arcuate sections of numerous former circular failures that seem locally to overlap. In general, arcuate features with clear geological definition such as those associated intrusion or mineralization, are more obvious in Precambrian rocks than in the overlying Phanerozoic. Norman (1980) suggested that "it seems unlikely that the earth received many very large impacts since the start of the Phanerozoic, and major crustal failures due to large impact effects are likely to be Precambrian."

Despite the fact that age interpretation can be confused when later events have exploited parts of some of these failures, the relationship can be demonstrated if other existing information is taken into account. For example, interpretation of image 180/43(Photo plate30), which is represented by both

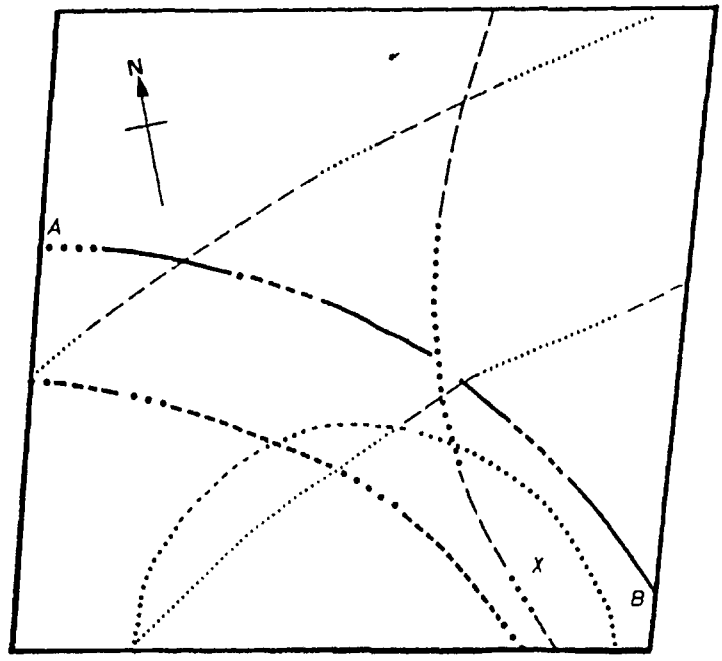


Figure (62) : Arcuate features interpreted from S.P. band 5, showing several overlapping impact effects. Dotted sections are geometrical extrapolations and are not seen on original image (after Norman 1980).

H.P.F.B7 and a data base image, can highlight some of the history of the very clear E-W arcuate features (Photo plates 29, 30). Both images indicate that the western part of this arcuate feature is clearly dislocated by a NW-SE sinistral transcurrent fault (GH), probably of the Najd System. One can then infer that the arcuate structure is older than the Najd Fault System (540 - 510 million years).

Another line of evidence that Norman (1980) has noticed is that the Najd Fault System itself seems to have taken advantage of some of these existing arcuate features and exploited parts of them. Study of imate 180/43, (Photo plage 29), also indicates that some intrusions exploited parts of arcuate features. All these lines of argument suggest an age older than 540 - 510 million years.

Image 179/43 (Photo plate 3) on the other hand, indicates that the N-S Al-Amar-Idsas Fault, known to be of the older Hijaz Orogeny (over 1000 million years), has exploited part of an existing arcuate feature before it has straightened again heading north to the Phanerozoic rocks. This relationship suggests an age of older than 1000 million years for some arcuate features in the area.

The clarity of these features on images, and the confidence with which they can be mapped, depend, not only on geological provinces, but also on the various rock types of different ages, type, quality and on processing techniques by which these Landsat images are produced. Interpretation of image 180/43 using S.p. band 5 of average quality, (Figure 62)

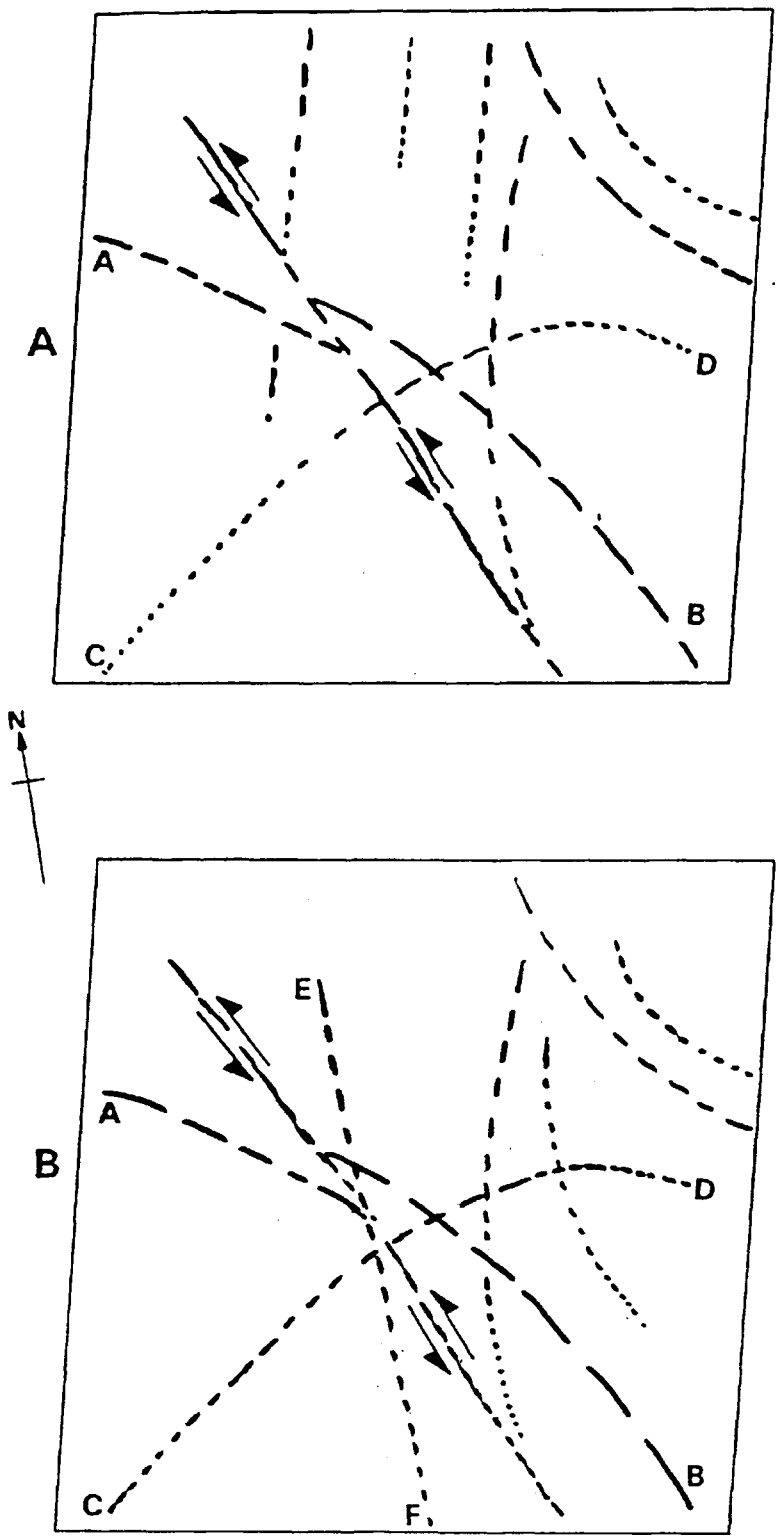


Figure (63) : Arcuate features interpreted from ce$_1$ (A) and contrast stretch (B) images covering the same area as figure 62, showing the effects of quality, band and processing on interpretation.

and the interpretation of both H.P.F.B.7 and data base of band 7 of the same scene,(Figures 63)clearly indicates the difference in detectability of the same arcuate features and their structural relationship with other geological events, which cannot be established by interpretation of band 5 only.

4.8.2.2 Arcuate Features in Sedimentary Rocks

Although most of the relatively clearer circular features or parts of their circumference (that is, arcuate features) can be taken as possible old Precambrian in origin, they may become rejuvenated and propagated through much later sedimentary cover of various thicknesses and competence. The best example of this is the great arcuate feature of the C.A.G.T.S. in the Mesozoic-Cenozoic rocks (Figure 45). This system has been proved to be a surface result of subsurface arcuate basement structures (Brown, 1972; Hancock and Kadhi, 1980). This arcuate structure together with the Wadi Al-Batin and Al-Hamudiyah Arcuate Lineament, seems to represent parts of a great semicircular feature referred to as the East Arabian Block (Hancock, Al-Khatieb and Kadhi, in press, geological magazine). Interpretation of 1:2,000,000 Landsat mosaic and existing geological maps of the same scale by Norman (1979) indicated some arcuate features in the sedimentary rocks which mainly coincide with the E.A.B. boundaries (Figure 55).

The western part of image 179/42,(Photo plate 19) clearly indicates another arcuate feature of more than one hundred kilometres in length, which is almost parallel to the

margin of Al Majmaah Graben, being a part of the C.A.G.T.S Arcuate Structure. It intersects the general NW-SE strike of the sedimentary sequence at both extremities. This arcuate feature is also mapped on the 1:4,000,000 geological map (Plate 7 in pocket). It is also noticeable on this image, other field photographs and maps that sand dunes and sand steaks are almost represented as an arcuate feature in the majority of cases in the area, (Photo plate 34).

The Tertiary sedimentary rocks of the Arabian Platform, however, despite being relatively thicker than those of the homocline, still indicate some relatively clear arcuate features of relatively smaller size. Image 178/41 (Photo plate 27), in its central part includes a clear arcuate feature which represents two thids of an elliptical circular feature(A). Because of the clarity of the main portions of this feature the other faint parts can be extrapolated easier than if the whole feature is faint.

4.9 DETECTION OF LINEAMENTS THROUGH SURFACE SAND COVER

One third of the Arabian Peninsula as well as the thesis area is covered by a mobile sand in one form or another. In this part of the country the term "Nafud" is applied to areas of deep sand and wind built dunes. Few of these Nafuds or parts of them are represented in the area as:

1. Ad-Dahna is one of the dominant physiographic features of the Arabian Peninsula in general and

its northern part is included in the thesis area. It is represented by a long narrow belt of shifting sand and dunes. The sands of Ad-Dahna are bright red orange due to a coating of iron oxide on the quartz grains and are detected as yellow or yellowish on the I.R.C.C. images of the region.

2. In the western part of the area and roughly parallel to Ad-Dahna, which follows along the western edge of the Tuwaiq and Aruma escarpments, are a few types of Nafud: Nafud Assir, Nafud Ath-Thuwayrat, Nafud Qunaifdah. The sand here is not continuous but occurs in elongate patches strung out in a chain. The significance of this type of sand is that it tends to lie in low areas and its distribution and movement appear to be influenced in part by the relatively high escarpments (see geological map in pocket, Plate 7).

3. A third, and less dominant type is Uruq (plural of IRQ): an example is IRQ Banban parallel to the Aruma Cretaceous Escarpment in the Central Part of the area; it is composed of the same type of sand as Ad-Dahna. These URUQ are the resultant of a system of two dominant wind directions and are identical to graben structures. They represent parallel, sharp-crested narrow sand ridge dune chains (Photo plate 45).

The movements of eolian sands is controlled by regional wind patterns, source of sand and the characteristics of local

topography, among other less dominant factors such as precipitation of rain, vegetation, other atmospheric factors which often partly help in stabilizing the sand dunes. Beside this eolian sand coverage in regional areas, locally there exists another type of Quaternary Coverage known as Qu, and Qg referred to as Quaternary fans composed of gravels of transported or local origin, silt and associated fine sediments including caliche-like deposits in undrained depressions (sabkhas).

In some specific areas such as around Wadi Al-Batin and the Al-Amar Idsas fault extention, the Quaternary loose deposits are composed of limestone, quartz and some igneous gravels, at places forming mixed terraces related to present or recent drainage.

Discussing Saudi Arabian sands, one cannot avoid mentioning the great Sand Sea of the Empty Quarter(Photo plate 31).. It is not included in the thesis area but still represents the major source of sands when the SE or Southern winds are dominant, especially in summer (for more details of the Arabian Peninsula Sands and Sand Seas please refer to U.S.G.S. Professional Paper 1052 A Study of Global Sand Seas (Mackee, E.C., 1979).

What concerns this research is the effect of different types and probably different depths of the superficial cover on lineament analysis of the imagery used in the study. Some specific images for example 178/42, 180/41 represent areas covered with 30 - 40% sand coverage.(Photo plates 18,14).

The superficial cover or more specifically Quaternary Sand Dunes and Sand Cover are known to obscure or mask the underlying structures or other geologic features. In this research however, and during the interpretation phase of Landsat images of H.P.F.B7 and a few aerial photographs it has been found that the previous statement is not always right. On the contrary some sand cover of specific characteristics seems to have recorded the surface propagation of some subsurface geologic features. For the better understanding of this process a few examples are to be discussed and very simple field tests will be summarized.

4.9.1 The Northern Extension of Al-Amar Idsas Basement Fault:-

This well known structure in the Arabian Shield has been found to extend northward where its effect on the Triassic Jilh limestone was clear as a plunging syncline and complementary anticline (Photo plate 5).

Interpretation of H.P.F.B7 image 179/43, (Photo plate 1) indicated not only the effect of the fault on the Jilh Formation but also the extension of the fault through the surface coverage of the Qg and the edge of Nafud Assir sand dunes.

The fault is known to be a zone of active movement through parts of the geologic history (Nebert, 1972; Nawab, 1978). Due and during this movement the fault zone was probably refilled by the overlying loose silt, sands and gravels. Later perculating hydrothermal solutions (Moore, 1978) or surface water conditions where the image was exposed in the wet season, seems to have increased the moisture content of the

new fillings, creating a heterogeneous filling which is different from the surroundings not only by composition but also by physiographic nature and moisture content. Such a phenomenon was detected by H.P.F.B 7 images being sensitive for such a change along the lineament.

On aerial photomosaic scale, (Photo plate 5) , which shows sand dunes of part of Nafud Assir, indicate few NE and NS lineaments in the outcrop of the Triassic Jilh Limestones and their extension in the sands can be detected with some degree of confidence.

4.9.2 Barrah and Majma'ah Grabens continuity:-

Powerset al (1966) "Suggested" that the extension of Al-Majma'ah Graben southeastward under URUQ Al-Buldan is possible and added that the presence of Jabal Fahda outcrop, (Photo plate 44) , in the middle of the sand dunes may support this. In fact interpretation of I.R.C.C. images scale 1:500,000 and H.P.F.B 7 1:1,000,000, ground investigation and helicopter traverses showed that Majma'ah Graben and Barrah Graben to the south are connected and were only apparently separated by the sand dunes cover. The overlying sand cover in general are characterized by sharp crested narrow sand ridges directed N-S in Urauq-Al Buldan, image 179/42 (Photo plate 13). Detailed interpretation of these sands indicated the presence of two almost parallel NNW lineaments crossing the sand ridges direction and joining Al-Majma'ah Graben. The spacing between the two lineaments corresponds to the graben width.

Jabal Al-Fahda, (Photo plate 44), and another relatively smaller outcrop mainly buried in the sand are located in between these two lineaments too. The two NNW lineaments seem to represent two faults bounding the Tuwaiq limestone blocks under the sand cover.

These features may prove the connection of the grabens by evidence detected through a sand cover by the interpretation of different types of images.

4.9.3 Al-Hamudiyah Arcuate and Straight Lineaments:-

Under the discussion of the E.A.B. the second segment which is Al-Hamudiyah arcuate lineament has been interpreted as a possible connection between Wadi Al-Batin and Al-Majma'ah Graben, image 180/41 (Photo plate 41). Although the main part of this arcuate feature is covered by sand it still can be seen and interpreted with some confidence, more clear than this arcuate feature is the NE-SW straight lineament C-D which has been interrupted in the northeastern corner of the image by the arcuate feature A-B. The two lineaments probably represent subsurface structures which have propagated to the surface through the sand cover. The projection of the C-D straight lineament to the southwest corner of the image coincides with the NE basement wadi Arumah known to possess a geophysical anomaly. Further evidence of this lineament, as shown on image 180/41, is that it probably caused a prominent change in the direction and/or force of the locally prevailing wind which has been influenced

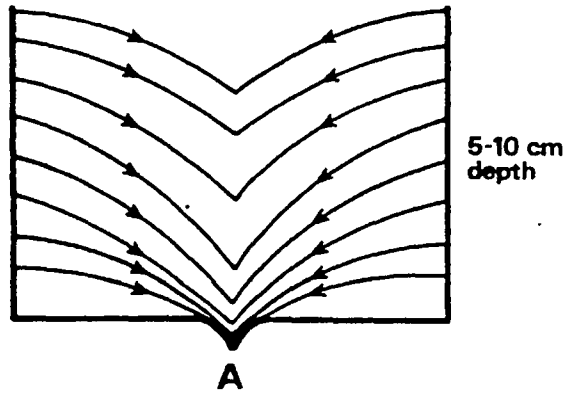
by a subdued physiographic expression of the buried structure.

So the probable extension of this known sub-surface linear feature was not obscured by the sand, but the constant seismic movement in the earth caused its upward propagation through this sand cover.

To understand the behaviour of sands during the possible upward propagation of any subsurface feature a simple test has been carried out in one of the sand dunes in the area.

A simple wooden board with a longitudinal crack in its upper surface was inserted through the top few centimetres of a sand dune and it was subjected to a simple continuous vibration. After a few minutes the upper surface of the sand indicated a negative or a concave line which corresponded to the crack at the bottom (Figure 64.A). The test was repeated again with relatively coarser sands and gravels of variable size. The result under the same constant factors took more time and partly failed to indicate the same pattern. The reason for this might be that the sphericity, roundness and homogenity of the 95% quartz grains forming the dunes facilitate the mobility or the rolling of these grains over each other much easier than heterogeneous shape, size and composition of the silt, sands and gravels in the second case.

Another test was carried out with a similar wooden board but with a steel bar with relatively sharp edge fixed on the surface of the board. The board, with the bar, was inserted again through the sand dune and the same procedure was



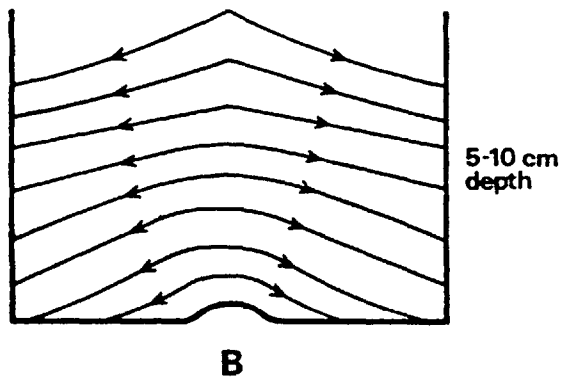


Figure (64) : Schematic cross section illustrating the behaviour of well rounded quartz grain sands during the upward propagation of a subsurface linear feature in a simple field test.

A. linear feature of a negative physiographic nature.

B. linear feature of a positive physiographic nature.

repeated. It was noticed that after more or less the same time the sand grains started to roll away from the centre line leaving an apparent positive alignment probably reflecting the steel bar, but was not as clear as in the first test with a negative crack (Figure 64B). This can be equated on a much larger scale with positive and negative subsurface features propagated upward through the sands under the much longer time interval of tens and hundreds of millions of years. These simple tests may help to understand the different behaviour of well rounded homogeneous sand grains forming the dunes, and the other angular illsorted heterogeneous surface cover i.e. Quaternary fans, when they are covering a subsurface feature. On the basis of this experiment it can be suggested however,that the relatively clear lineaments on images through surface sand cover are more likely to represent subsurface features with negative physiographic nature. As a good example is the NE, C-D, lineament in image 180/41 (Photo plate 14).

From the interpretation of specific quality of images and both field observations and the field simple tests it is clear that certain types of sand cover do not always obscure subsurface features, but on the other hand may enhance their surface propagation depending on various factors under frequent disturbances:

1. The nature of the cover
2. The nature of the buried structure and its physiographic pattern
3. The atmospheric factors.

Details of propagation and the factors which control it are discussed in detail in Chapter Five.

CHAPTER FIVE

PROPAGATION OF SUBSURFACE FAILURES

5.1 GENERAL DISCUSSION

Propagation in this research is defined as the process or processes by which subsurface failures, through many variable processes of various parameters of either internal or external nature, are manifested at the surface not necessarily with the same length, form and direction. By the term propagation in this text is meant upward propagation.

Multi-imagery interpretation, analysis of both frequency and length rose diagrams, detected structures, ground investigation and existing data of surface and subsurface nature indicated that there is a definite relationship between these surface lineaments and the subsurface structures in the studied area.

The main causes of the majority of these lineaments appear to be one or more of the following:-

1. Regional horizontal stress due to tectonic forces, for example, the E-W compressive stress which produced the older Hijaz structures and the relatively younger Najd structures and the possibly N-S stress which produced the Riyadh Fault System.

2. Reactivation of old failure zones in deeper basement rocks (mainly basement blocks). The cause of this phenomenon is possibly related to variation in rotation of earth due to a large impact or a near miss effect (Norman, 1977), for example, the prominant N-S periodically spaced lineaments.
3. Influence of intrusion of a dome or diapir.
4. Adjustment to a buried relief during and after the period of sedimentation and compaction, for example, the C.A.G.T.S. and related structures.

The present surface lineaments are probably a result of these processes together with the effect of other internal and external factors.

The propagation of fractures (lineaments) through indurated rocks or the controlled re-establishment of an older pattern in younger rocks has been discovered by a number of writers and has been mentioned early in the history of geology.

Dana (1847, cited by Rumsey and Bostronn (1971), was one of the first to do so when he said that "there is a predetermined tendency to fracture in a certain direction". This is stated after more than a hundred years in a different way by Price (1974) who wrote "rocks have memories".

Later, Closs (1948) cited by Rumsey and Bostronn (1971), and Meinesz (1974) amongst many, have discussed the continual rejuvination of ancient shear systems. Rendal and Briggs (1933) cited by Rumsey and Bostronn (1971), said that "in the majority, the roofs of the coal seams have been jointed in the same

direction as the cleat in the Coal". Blanchet (1957) claims to be able to detect buried reef bioherms by analysing fractures as seen on aerial photographs.

Hodgson (1961), cited by Rumsey and Bostronn (1971), has shown that fracture patterns and trends cross and pass up through major unconformities in rocks ranging from Pennsylvanian to late Jurassic in Arizona and Utah. Hodgson also indicated that the same dominant joint trends persist all the way from the Precambrian to Triassic. Rumsey (1971) stated that "some obvious fractures that pass from the basement granites to the Ordovician sandstones although those of the granites may be faults they are not faults in the sediments.

Norman (1968, 1975, 1977, 1980), and Norman and Partridge (1977), in various publications explained the idea of detection of subsurface conditions by photogeology, i.e. the surface fracture evidences of subsurface structures. Later Al-Khatieb, Norman (1980), under preparation, proved that a basement fault in the Arabian Shield was detected as far as the Cretaceous in the overlying sedimentary rocks (Figure 32).

The generation and propagation of these features is a subject of many factors. Classification and/or separation of these factors, is difficult to achieve. Those factors enhancing propagation can also, to some extent, generate and affect the lineaments and their propagation. For better and systematic discussion of these factors, the following procedure has been followed.

5.2 FACTORS ENHANCING GENERATION AND PROPAGATION OF LINEAMENTS

It has been agreed among earth scientists that generation and upward propagation of subsurface rock failure is due to one or more of the following effects.

5.2.1 Tectonic Effect

The generation and propagation in some extent is mainly a result of tectonic events which may represent horizontal stress field, local or regional orogenic movements in the tectonic history.

5.2.2 Fatigue Effects

Fatigue theory is mainly concerned with the generation and propagation of regional lineaments of crustal scale which nowadays can be detected on small scale Landsat images. These effects are mainly based on the concept of fatigue as an accumulated strain in the earth's crust which has been produced by an internal and/or external factors.

5.2.2.1 Earth Tides:-

The Arabian Plate is a peninsula surrounded by the Red Sea in the west, Gulf of Aden and the Arabian Sea in the south and the Arabian Gulf in the east. Accordingly the periodic rise and fall of the water in these seas caused by the tidal attraction of the sun and moon, where the effect of the latter is much stronger, and exerts an effect on the generation and propagation of failures. There is a similar

tide in the crust which is relatively more significant. The effect of this tidal stress on the earth's crust lies not only in the relatively low magnitude of the stress produced by the tide but in the repetition of these stresses twice a day for millions of years. Such an effect is probably capable of creating tremendous geological strain.

5.2.2.2 Seismic Activity:-

Seismic activity generated by earthquakes resulting from the release of stored energy which can cause failure in the earth depending on the magnitude and duration. Repeated seismic tremors tend to prevent the cracks or failures from sealing up (Mollard, 1959), cited by Barazangi (1980), and most likely enhance their propagation.

The Arabian Plate being a relatively smaller lithospheric plate surrounded by other plates,(Figure 3), which indicates active movement on these boundaries. Because of this seismic activity around the Arabian Plate and its importance to propagation in this area, it will be discussed in some detail.

The Red Sea and Gulf of Aden in the west southwest and south of Arabia, represent an area of active sea-floor spreading along their axial troughs (MacKenzie, 1970; Hall et al 1977), cited by Barazangi, (1980). To the southeast lies the Owen Fracture Zone, a relatively active transform type boundary (Matthews, 1966). The Arabian Plate is colliding with the Persian Plateau to the east and the Turkish Plateau to the north along the Zagros and Taurus mountains respectively

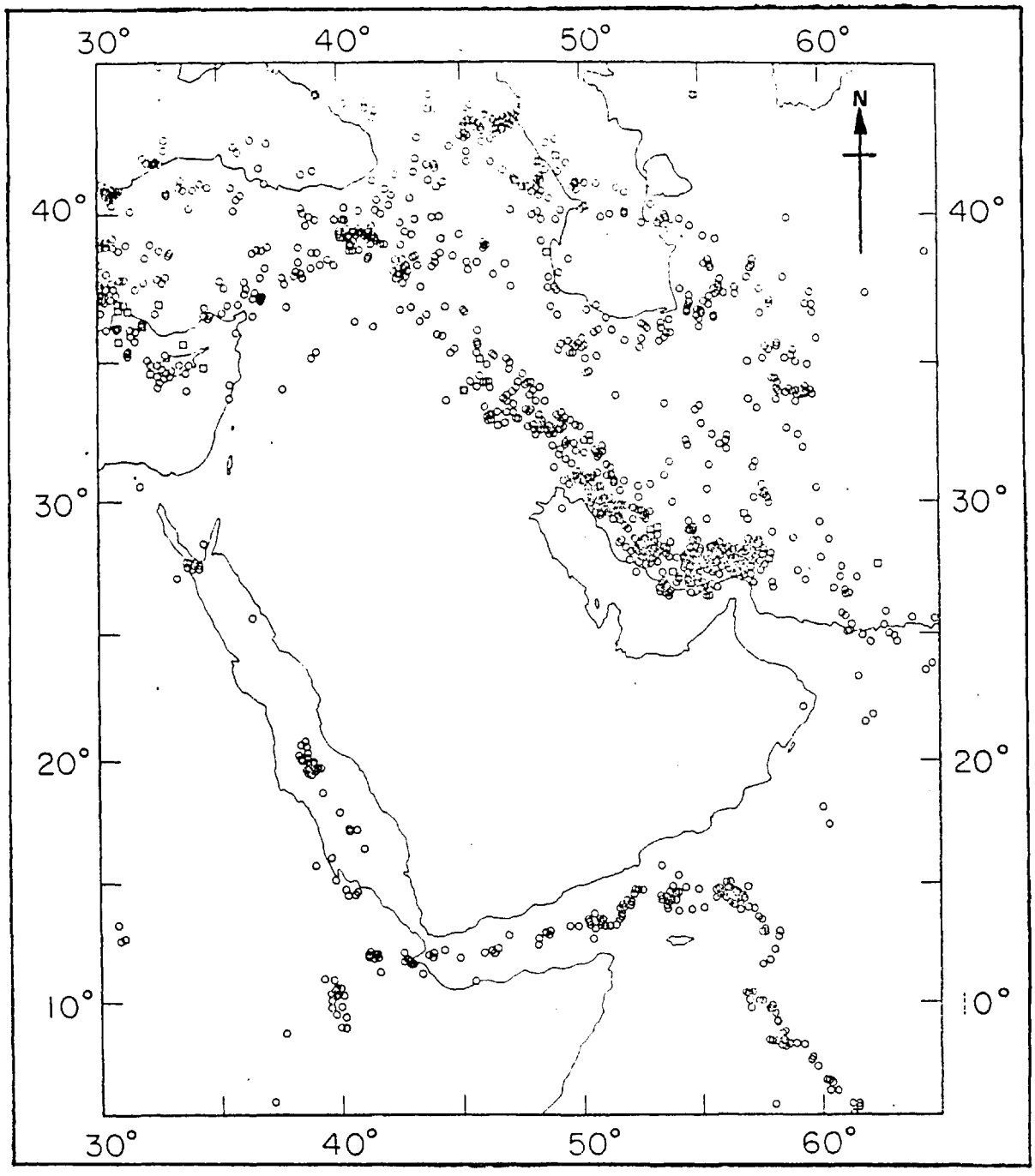


Figure (65) : Seismic activity (distribution of earthquakes) around the Arabian Plate boundaries recorded between 1961-1975 (after Barazangi 1980).

(MacKenzie, 1972), Nowroozi, 1972; Stocklin, 1974 and others). To the northeast, the boundary of the Arabian Plate is along the Dead Sea Fault System, which is a complex transform boundary (Freund et al, 1968; Ben-Menahem, 1976; Shearman, 1979), cited by Barazangi (1980).

As a result of these active boundaries the Arabian Plate seems to have been subjected to almost continuous seismic vibration since it has been separated from the surroundings 18 - 30 million years ago (Barazangi, 1980). This is shown by Figure 65, which shows the distribution of earthquakes in the region that occurred only between 1961 - 1975 and are restricted mainly to the Plate boundaries.

Another relatively less effective process is the Tertiary(Upper Cenezoic) volcanism. Most of it is related to the period from about Lower Oligocene up to historical time (Coleman et al, 1977), cited in Barazangi (1980). Volcanic dykes of Miocene and possibly younger age are also prominent along the western margin of Arabia which is apparently related to the opening history of the Red Sea Rift System and appears to be controlled by deep seated fracture system in the crust (Bland, 1977). This conclusion is in complete agreement with the N-S alignment of volcanic cones representing failures on the basement which provided the main conduits for episodically rising magma to the surface. (Figure 57 and Photo plate 61).

Recent seismic investigations carried out by D.G.M.R. indicated that a few earthquakes in the Red Sea near Jeddah and in the southern side near Yemen have been recorded recently

in 1948, 1976, and 1978 of various magnitude (Marghalani, 1980). This recent information and the earthquakes recorded from 1961 - 1975 (Figure 65) may explain the phenomenon of propagation of some subsurface failures through the very recent sands and sand dunes.

5.2.2.3 Rotational Effect:-

This is based on the assumption that the earth is subjected to two major stresses N-S and E-W caused by the earth spinning around its axis, the precession of the earth axis and the rotation of the earth around the sun. This process is believed to be responsible for the regional crustal failure (N-S lineaments of hundred of kms in length) in Nigeria, Brazil (Norman, Ike, 1977) and in Saudi Arabia. It has been assumed that the rate of rotation of the earth was sometimes decreased whether by "tidal friction" (Zwain, 1976) or the earth rotation, i.e. rate of spin may have been changed due to bombardment of cosmic bodies, i.e., impacts effect (Norman, 1977, 1979, 1980).

5.2.3 The Gravitational Effects

The gravity force at the earth crust is regarded by many geologists as an important effect in causing failure in rock masses as well as influencing the existing subsurface structures to be propagated into the overlying relatively younger rocks.

5.2.3.1 Differential Consolidation:-

It has been proposed that the differential consolidation and compaction of sedimentary rocks with a sufficient magnitude can lead to shear and other types of failures especially in the early stage of consolidation (Belcher, et al, 1965), cited in Zwain (1976). Compressive forces can start from above as the weight of the overburden, or from below as force generated by igneous intrusions or salt domes activity. These failures resulting from differential consolidation are more likely to be spaced limited at distances forming a failure zone. Later in the process they propagate to the surface. This spacing will depend to some extent on the slope of the buried surface. Thus steep slopes will generate more closely spaced failures and gentle slopes on the other hand are more likely to produce widely spaced failures (Zwain, 1976). The developing of these failure zones and their propagation will be accelerated if they are underlain by firm basement blocks (Wilcox, 1973) or particularly consolidated older formations, Khain, Muratov (1969).

During consolidation and compaction, the thesis area being of generally gentle dips underlain by the basement may have undergone down-warping, uplifting and concomitent dewatering which may have the same effect on both generation and propagation of lineaments, which as a result, may modify the prevailing stress system (Price, 1966).

This process of dewatering will affect the propagation especially when incompetent clays, shales and muds are included in the stratigraphic sequence. Sparoule (1962) has offered a hypothesis, that clays and muds are known to be

compressible to less than 40% of their original volume. On the other hand, if shales are hydrated they can increase 25 - 30% of their volume (personnel communication with Professor D. J. Shearman). Such decrease or increase of rock volumes have a definite effect on propagation.

5.2.3.2 Isostatic Adjustment:-

Isostacy is the tendency of the earth's crust to attain an equilibrium. During geological history, the strong erosion of surface rocks in some areas causes a reduction of loads and results in uplifting. Sedimentation on the other hand adds more load and results in subsidence. This effect, together with other tectonic events, seems to be responsible for the suggested propagation of the Central Arabian Arch, up to the surface forming the C.A.G.T.S., (Power, et al, 1966; Brown, 1972; Hancock and Kadli, 1980). The earth surface, after an earthquake shock, undergoes a process of isostatic balance which helps to propagate the failure through the overlying sediments or on unconsolidated material, in this case of isostatic adjustment the propagation is more likely to take place along the original failure. This agrees with Price (1966) who indicated that rocks possess "a memory" so that stresses induced are relatively little changed by relaxation.

5.3. FACTORS AFFECTING AND CONTROLLING PROPAGATION

Multi imagery interpretation, field investigations and traverses, existing surface and subsurface data and review

of the literature concerning the thesis area highlighted some relatively important factors which can affect and control, i.e. activate or render, propagation of lineaments and other sub-surface structures amongst them are the following:

5.3.1 Inhomogenuity of Tectonic History

The area being mainly located in the Arabian Shelf overlying the Shield thus directly or indirectly affected by some of the tectonic events which have prevailed in the geologic history. Another important feature of the Arabian Shelf is the fact that not all parts of this shelf had the same geological history. Some areas were more active than others, some were depressed and some elevated either persistently or for short periods. Thus the shelf is divisible into several provinces such as Interior Homocline, Interior Platform and several basinal areas that have from time to time collected more sediments (Powers et al, 1966).

5.3.2 The General Stratigraphy of the Overlying Rocks

It has been indicated that the majority of lineaments, and detected structures are regarded as an upward propagation from basement structures or failure zones, through the overlying sedimentary sequence which may have exercised an effect on these lineaments during their propagation. It is important however, to know the nature and interrelationship of these sedimentary rocks.

5.3.2.1 Summary of the stratigraphic sequence:

Table 1 is a brief descriptive summary of the different types of rocks which build up the stratigraphy from the unconformable surface of the basement upward. The rocks consist of a variety of compositions ranging from nonclastics, mainly limestone, to clastics as sandstones and shales and are ranging in age from Palaeozoic to Cenezoic sediments.

The variety of composition is related to the different environments of deposition from continental to shallow water shelf sediments were beds certainly reflecting buried basement configuration and dipping gently to the E, NE. Dominating these types of rocks are the relatively resistant limestones which when exposed are forming parallel, west facing strike escarpments. Sandstones and shales are less resistant to arid weathering. The great variety of these rock types as shown in the Table, have exerted an effect on the propagation of subsurface failures.

The rock strata react differently to stress and strain, depending mainly on their rock type especially their competency among some other less important factors. Accordingly, if there is major fracture at certain depth covered in one part with shales and in the other by limestones, and it is later subjected to reactivation the propagated part in the limestones, under the same conditions, is expected to reach the surface relatively earlier than the other end. In this case affecting not only the propagation of the form of the lineament but most

important its length and the degree of detectability in general. This explains differences between the two terms, actual length and the manifested length on the surface.

5.3.2.2 Nature and relations of rock types in a vertical succession:

The propagation is not only affected by the difference in rock types but also the nature of repetition of the sedimentary succession. Systematic disturbed rythmic sedimentation might be expected to affect the propagation in a way different if the whole sequence was made up of either 50% of shales and limestones in general. A linear feature propagating through a sequence of two types of rocks,for example shales and limestones is subjected to relatively more homogenous factors exerted by these two rock types together with other internal or external factors. On the other hand a structure propagating through the same total thickness but built of many systematic and irregular repetition of rock types is subjected to various and multiple effects during its upward trip.

5.3.2.3 Thickness of overlying sediment:

The total thickness of the sedimentary sequence in Table 1, is about 5,500 meters, ranging from a few hundred meters lying on the eastern edge of the shield and increasing eastward. According to this thickness variation, basement topography, isostacy, compaction and other local or regional tectonic events, the generation and the nature of

propagation of subsurface failures may vary from one region to another.

According to this variation in thickness and possible effect on the propagation, the area is mainly divided into three subareas, namely the Precambrian Basement, sediments near the basement, and the sediments. This classification corresponds to some degree with the Arabian Shield , Interior Homocline and Interior Platform by Powers et al (1966).

5.3.3 Unconformities

One may expect that unconformities and the associated sedimentalogical history may affect propagation.

With reference to the thesis area, the stratigraphic sequence indicate eight major unconformities together with many hiatus and periods of non deposition, Table1). A regional stratigraphic cross section also indicates these major unconformities and showing formation relationship such as thinning, thickening directions, facial changes and truncation (Figure 66). These interrelationships are mainly a result of both structural control, i.e. uplifting where the rocks are subjected to strong erosion, and subsidence where rocks are deposited. Each of these environments has its own different erosion, nature of sediments, i.e. their competency, grain size, cement. During the regression phase the prevailing conditions are mainly of continental nature and characterised by strong erosion or peniplanation which may enhance or

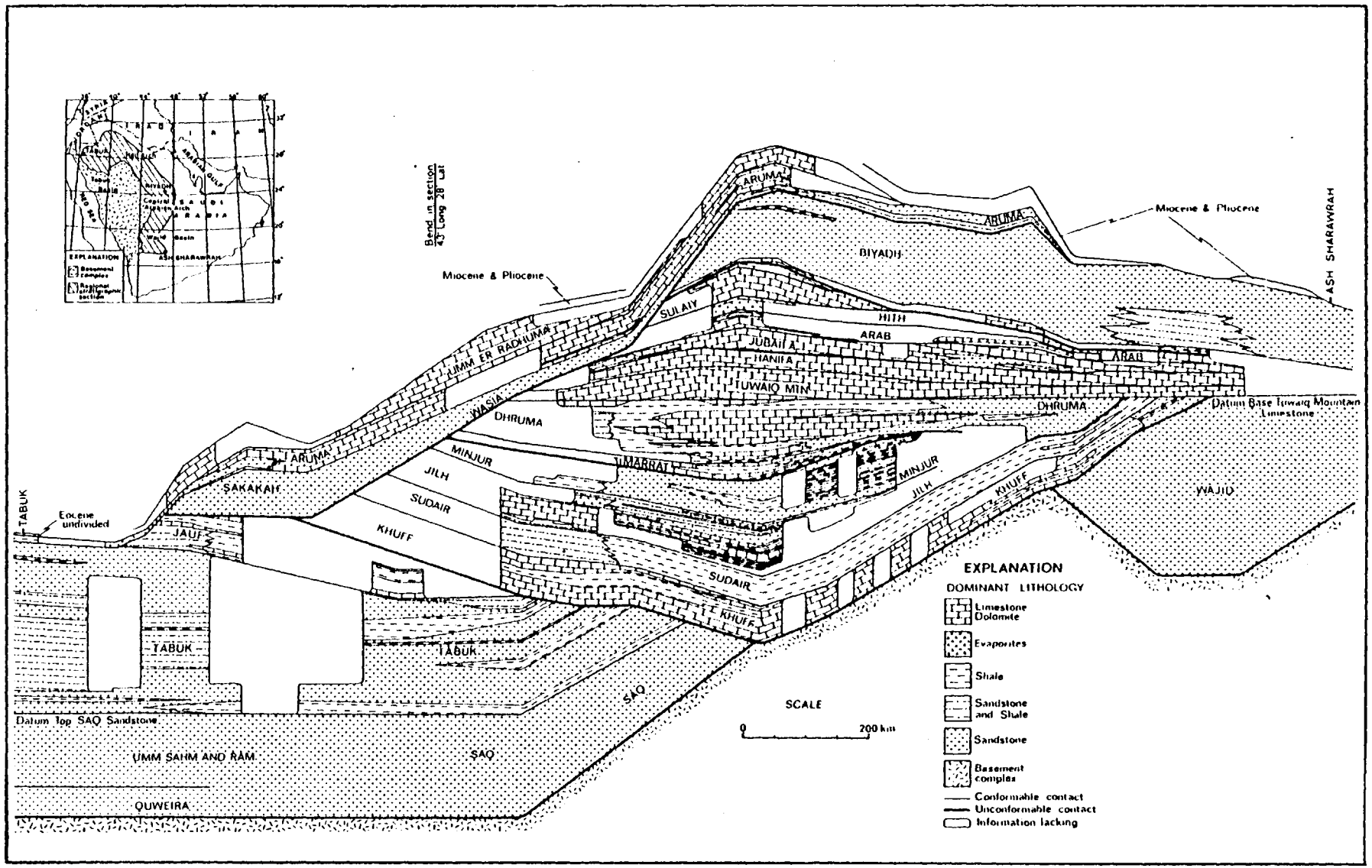


Figure (66) : Generalized cross-section in the sedimentary Cover Rocks (after Davis-Morrissey 1976. Powers etal 1966).

generate isostatic adjustment. The regression phase, on the other hand, is mainly characterised by sedimentation and some minor structures such as cross bedding, turbidity and this sedimentation may enhance compaction.

So if features which were undergoing the process of propagation through the sediments under the marine environment are suddenly exposed to the surface during uplifting or regression. The prevailing environment is then of continental nature, the exposed structure or zone of failure is expected to be subjected to the following factors, depending on the time span of the unconformity:

1 - Strong, variable erosion which may change the physiographic nature.

2 - These features may be followed by a newly developed drainage changing its nature and depth of incision.

3 - Refilled with continental sediments and is subjected to variable compaction.

4 - Some region or local continental sediments may have been accumulating thus changing the nature of the cover through which the linear feature was supposed to propagate. Later, under another stage of subsidence this propagating lineament is expected to be affected by some other factors of this environment for example:

   1. Compaction of the continental filling of the continental sediments overlying it.
   2. Deposition of marine sediments of either clastic or non clastic nature.

3. Isostatic adjustment may take place.

These alternating factors acting for variable periods of the geological history will to some extent have their effect on the propagation of the feature or parts of it as well as on the physiographic nature of the feature itself.

These variations are expected to be relatively higher if the features are propagating through shales (personnel communication with J. Ferguson and D. Shearman).

5.3.4 Logged Aquifers : (Hydraulic Effect)

Some specific formations of different ages in the sedimentary sequence represent the main aquifers supplying most of the water resources in the region, for example, the Triassic Minjur Sandstone, Cretaceous Wasia Sandstone Formations.

The large volumes of water in these horizons, affected by many other factors of internal or external nature will have some effect on the propagation process. This may result in slight alterations of the general picture by the newly produced hydraulic fractures (Dunlap, 1963 and Bredhoeft et al 1973). This is also known to be the case in the thesis area where hydraulic factors are complicated by stratigraphic changes, (Powers et al, 1966). This effect is not only restricted to aquifers but can be expected along some structures at various depths. An example of this has been observed in the field where such structures with the effect of solutions affected and enhanced the collapse and/or slumping of relatively huge

blocks in Khashm Al-Haqaqa collapse structure (Photo plate 55).

5.4 SUMMARY OF PROPAGATION :

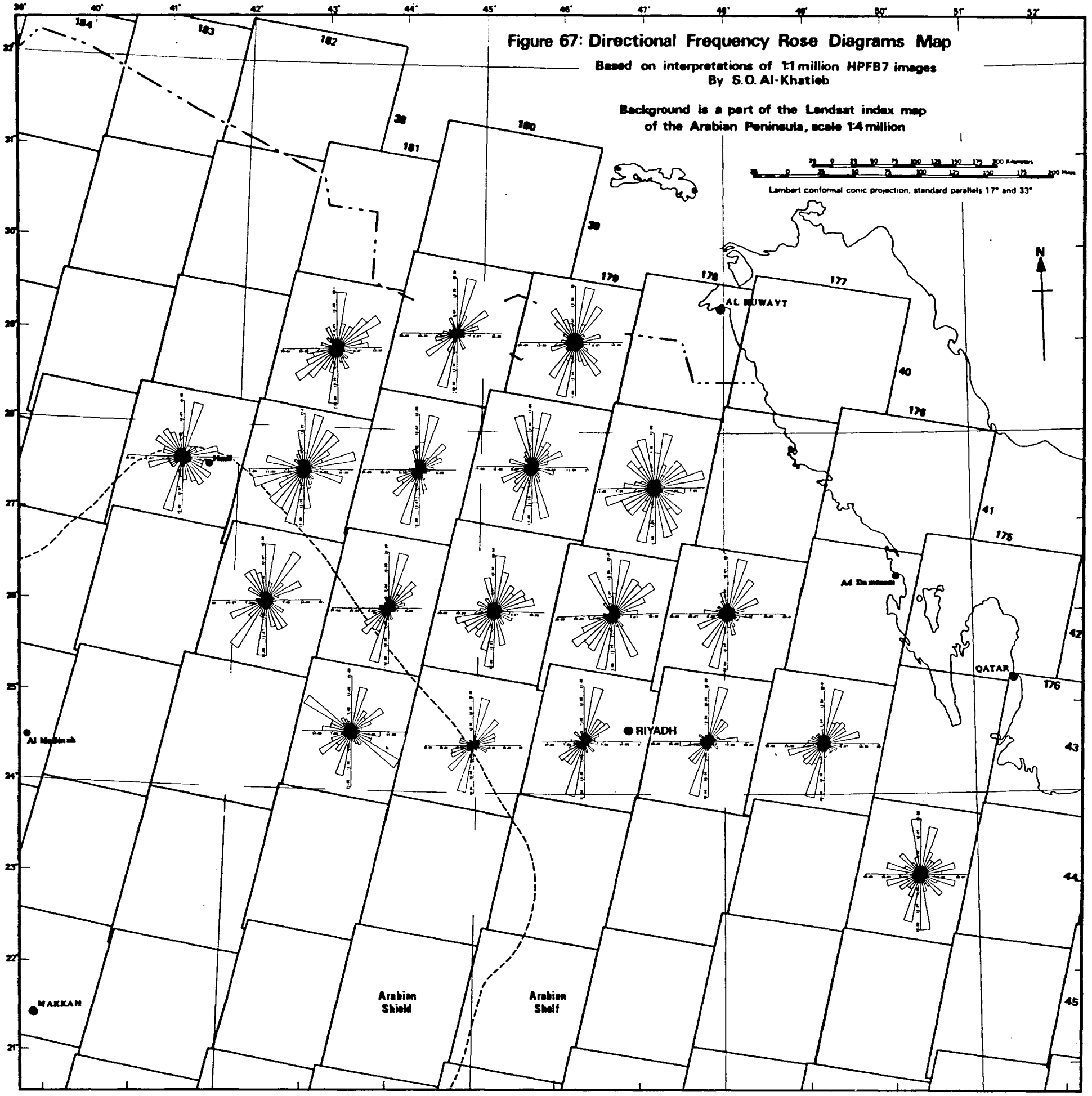
The previous review of the multiple factors affecting in various degrees the generation and propagation of subsurface structures indicate the expected interference of the processes involved. This seems to justify the definition of propagation as stated in this research. As a result of the discussed influences together with other minor surface and subsurface effects one therefore can reasonably assume the following. In a given area, the surface manifestations of the relatively long, disconnected interrupted structure (failure zone) with a few degrees of swing in direction, known in adjacent areas to be continuous and straight, are not to be regarded always as a simple result of surface superficial deposits or a result of human bias during interpretation, but also can be regarded as surface evidence relaying a message about a possibly complicated subsurface nature.

This conclusion is to a great extent in agreement with Norman (1980) who stated "old crustal failures, when propagating upwards through a cover of sediments, can commonly be manifested at the surface in a quite different, and possibly more dispersed form compared with the original feature".

5.5 CORRELATION OF BASEMENT AND SEDIMENTARY ROCK LINEAMENTS

5.5.1 General Discussion

The lineament analysis of the sedimentary cover and the exposed Precambrian shield rocks together with the detected structures both indicated that they mainly represent a surface propagation of a deep seated and/or basement level structure. On the basis of their host rock type and their location in different sedimentary environments the area can be divided into three sub-areas, i.e. Precambrian rocks; sedimentary rocks near Precambrian and sedimentary rocks away from Precambrian. This classification almost agrees with the classification of the structural provinces, i.e. Shield, Interior Homocline and Interior Platform respectively. Analysis of both frequency and length rose diagrams across the area indicate that each geological province possesses some characteristic patterns. For the purpose of detailed correlation between these geological provinces, a few representative rose diagrams were selected and the basic raw data of both relative frequency and length are presented in Table12 . The data in this table show that rose diagrams of the three provinces indicate some points of agreement as well as others which disagree. To demonstrate the possible relation of these three provinces rose diagram maps,(Figures 67,68), were prepared where rose diagrams are located according to their geographical position on a background of Landsat images index of the area as shown by Path/row. The maps are

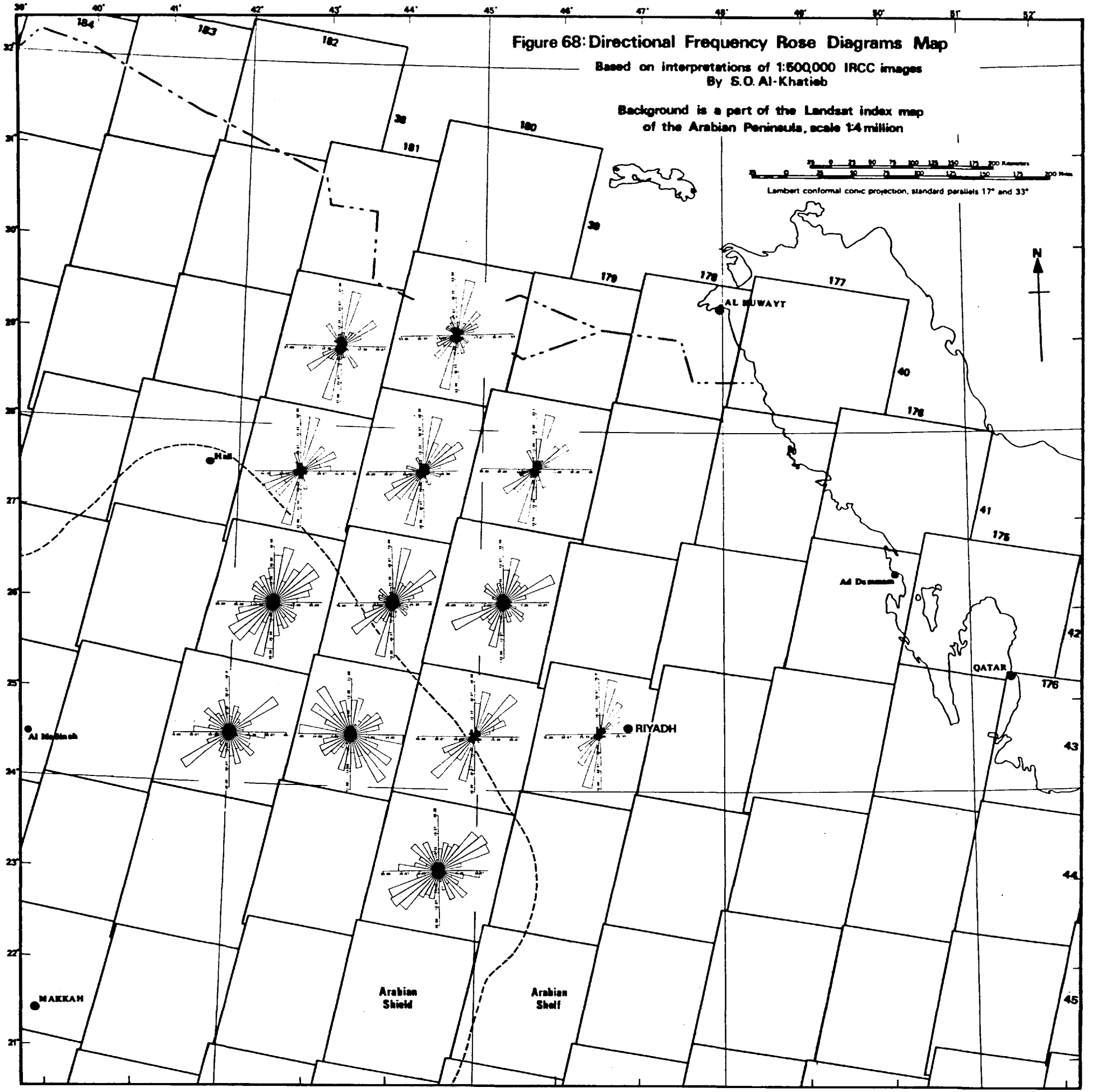

Figure 67: Directional Frequency Rose Diagrams Map
Based on interpretations of 1:1 million HPFB7 images
By S.O. Al-Khatieb
Background is a part of the Landsat index map
of the Arabian Peninsula, scale 1:4 million
Lambert conformal conic projection, standard parallels 17° and 33°
N
AL KUWAYT
QATAR
RIYADH
Al Madinah
MAKKAH
Arabian Shield
Arabian Shelf
184
183
182
181
180
179
178
177
176
175
38
39
40
41
42
43
44
45
46
47
48
49
50
51
52
30
29
28
27
26
25
24
23
22
21

presented from results in both scales 1:1,000,000 (Figure 67) and 1:500,000, (Figure 68), where rose diagrams are constructed from data acquired from H.P.F.B.7 and I.R.C.C. images respectively. The lineament patterns of each category are to be discussed in some detail.

5.5.2 Lineaments in Precambrian Rocks

The exposed Precambrian rocks in the area represent the central eastern part of the Arabian Shield. The majority of rose diagrams which represent this area possess a clear radial shape (Figures 67,68). The contact between the shield and the sediments can be drawn on the radial shape basis with more confidence on Figure 68 of the 1:500,000 scale, as it includes more rose diagrams constructed from images covering Precambrian areas. This seems to add another advantage to lineament analysis from Landsat images on the basis of which one might be able to delineate contacts between structurally different provinces. This characteristic radial pattern of lineaments in the shield rocks is a reason of one or more of the following factors :-

1. The dominance of the NW Najd Fault System and the NE Riyadh Fault System.
2. The radial effect introduced by the plutonic and volcanic intrusions of both basic and acidic rocks.


Figure 68: Directional Frequency Rose Diagrams Map
Based on interpretations of 1:500,000 IRCC images
By S.O. Al-Khatieb
Background is a part of the Landsat index map
of the Arabian Peninsula, scale 1:4 million
Lambert conformal conic projection, standard parallels 17° and 33°
N
AL KUWAYT
Hail
RIYADH
Al Madinah
MAKKAH
Arabian Shield
Arabian Shelf
Ad Dammam
QATAR
184
183
182
181
180
179
178
177
176
175
40
41
42
43
44
45

3. The regional radial effect is expected as a result of the old and relatively large impacts (Norman, 1980) mainly in the Precambrian times.

Another point of interest which is indicated by the rose diagrams of this province is that the roughly N-S lineaments although originated in the basement, are relatively less preserved inside the Precambrian part of the area. This is probably due to one or both of the following :

1. The exposed shield rocks have been subjected to strong erosional cycles where thick portions have been eroded and transported to the east in the early history of the formation of the sedimentary cover rocks.
2. The N-S lineaments have been rejuvenated many times in the geological history of the area providing an access for later plutonic or volcanic rocks which obliterated their physiographic surface and alignment nature. During some reactivation periods these lineaments have followed pre-existing arcuate features thus deviating from the general N-S direction. The direction has also been changed by the effect of later tectonic forces and has, for example, been offset by the Najd Fault System.

   The lineament analysis of images covering Precambrian areas, in general, indicated higher frequencies and relatively longer lineaments and higher frequency/length ratio (for more details please refer to Table 12)

	(BASEMENT) SHIELD										(SEDIMENT NEAR BASEMENT) INTERIOR HOMOCLINE										(SEDIMENT AWAY FROM BASEMENT) INTERIOR PLATFORM									
Image	182/41		181/42		181/41		180/43		Average		181/40		180/41		179/42		178/43		Average		177/42		176/43		175/41		175/40		Average	
Rose Diagram No.	70		73		68		87				63		92		54		17				82		85		91		58			
Structure	Granite Batholith		Wadi Rumah Lineament		Contact shield/ Cover Rock		Arcuate Feature + Clear Najd Faulting				Near Hail Arch		Part of E.A.E		Near Hail Arch		C.A.G.T.S + Riyadh F.S.				Circular Features		Ghawar Oil Field		Clear Arcuate Features		Wadi Al-Batin			
Total No. Of Lineaments	134		130		138		138		135		140		122		131		92		121		152		105		105		131		123	
Total Length Of Lineaments In km.	7632		6876		13077		10446		9507		9221		9181		6871		6400		7912		13503		9305		11044		7585		10359	
Average Length Of Lineament In km.	57		53		95		76		70		66		5		53		70		66		89		89		105		58		84	
Relative Values	F	L	F	L	F	L	F	L	F	L	F	L	F	L	F	L	F	L	F	L	F	L	F	L	F	L	F	L	F	L
N0°-10°%	6.7	6.9	9.2	11.6	3.6	2.7	5.1	9.5	6.2	6.4	14.3	15.2	4.1	3.2	25.2	20	5.4	4.4	12.3	10.7	3.3	2	1.9	2	6.7	5.4	2.3	2.3	3.6	2.9
10°-20°%	8.2	7.8	3.1	2.3	12.3	14	12.3	12.8	9	9.2	6.4	5.6	18.9	20.1	7.6	6.1	22.8	21.6	13.9	13.4	18.4	16.7	19	20.2	10.5	14.7	15.3	13.3	15.8	16.2
20°-30°%	7.5	7.5	3.8	3.1	2.9	1.7	0.7	0.7	3.7	3.3	2.9	2	9.8	6.1	8.9	6.5	1.1	1.8	5.6	4.1	1.3	0.6	7.6	6.6	4.8	4	5.3	5	4.8	4
30°-40°%	3.7	3.2	11.5	11.6	10.1	9.3	6.5	6.7	8	7.7	6.4	7.5	7.4	7.3	12.2	10.5	10.9	10	9.2	8.8	13.2	12.2	8.6	8.5	2.9	4.4	11.5	10.2	9	8.8
40°-50°%	6	6.2	6.2	3.9	10.1	13	5.1	5.3	6.9	7.1	10	9.1	9.8	10.1	10.7	13	11.9	11	10.4	10.8	2.6	2.5	9.5	8.8	6.7	5.8	3.1	2	5.5	4.8
50°-60°%	6	5.8	8.5	7.5	6.5	5.9	10.1	10.2	7.8	8.4	12.9	12.9	6.6	5.9	9.9	10.7	12	11.8	10.4	10.3	.6	5.4	8.6	12.9	6.7	8.7	3.1	2.3	5.3	7.3
60°-70°%	7.5	5.8	6.2	8.3	4.3	4.5	5.8	7.1	6	6.4	8.6	8.4	8.2	8.4	4.6	5.3	6.5	5.4	7	6.9	10.3	11.3	1.9	2	6.7	7.1	2.3	1.7	5.3	5.5
70°-80°%	12.7	14.2	5.9	6.6	11.6	13.9	2.9	2.6	8.2	9	6.4	6.4	6.6	10.2	7.6	9.9	4.3	4.8	6.2	7.7	5.3	4.6	12.4	11.8	9.5	12.2	6.9	7.8	8.5	9.1
80°-90°%	0.7	0.6	1.5	1.6	3.6	4.2	2.2	2.4	2	2.2	7.9	7.4	0.8	0.2	3.8	7	4.3	4.2	9.2	9.7	3.3	3.9	3.8	3.8	1.9	1.4	3.1	5.3	3	3.6
90°-100°%	2.2	1.7	0	0	2.9	1.7	8	7.9	3.3	2.8	0.7	0.6	5.7	5.8	1.5	1.6	5.4	4.8	3.3	3.2	7.9	6.8	5.7	4.7	5.7	5.4	3.8	3.7	5.8	5.2
100°-110°%	3	4.7	3.1	3.5	8.7	8.3	5.8	5.4	5.2	5.5	4.3	4.4	2.5	1.9	0.8	1.5	1.1	1.4	2.2	2.3	3.9	5.6	1	0.9	3.8	2.3	2.3	1.3	2.8	2.5
110°-120°%	3	3.3	3.8	2.2	0	0	5.8	7.5	3.2	3.3	7	1.2	0	0	0	0	0	0	0.2	0.3	2.6	3.2	4.8	5.8	2.9	2.1	2.3	3	3.2	3.5
120°-130°%	3.7	3.7	5.4	4.9	1.4	1.9	15.2	11.3	6.4	5.5	1.4	1.9	0	0	0	0	2.2	1.9	0.9	0.8	3.9	3.8	0	0	1	0.6	3.8	4.6	2.2	2.3
130°-140°%	2.2	4.1	9.2	12	2.9	3.1	2.9	2.7	4	5.5	3.6	3.3	0.8	0.8	0	0	5.4	9.4	2.5	3.4	2	2	3.8	1.5	6.7	7.2	7.6	8.7	5	4.9
140°-150°%	3.7	4.7	3.1	3.6	2.2	1.1	4.3	4.2	4.3	3.4	2.9	2.9	0.8	0.9	1.5	2.3	0	0	1.3	1.5	2.6	3.3	3.8	4.3	4.8	3.4	10.7	12.1	5.5	5.8
150°-160°%	6.7	5.4	6.2	3.3	3.6	3.6	3.6	4.7	5	4.3	5.7	7.2	6.6	6.3	1.5	2.2	1.1	1.5	3.7	4.3	4.6	4.7	0	0	8.6	8.2	6.4	6.5	5	4.9
160°-170°%	9.7	7.8	8.5	9.2	4.3	2.7	2.9	3	6.4	5.7	3.6	3.4	9	9.4	2.3	2.3	4.3	5.9	4.8	5.3	7.2	7.7	2.9	3.1	9.5	6.6	5.3	5.3	6.2	5.7
170°-180°%	6.7	6.8	5.4	4.9	8.7	8.9	7	1.1	5.4	5.3	1.4	6	2.5	3.5	2.3	1.8	2.2	9	2.1	2	4.6	3.8	4.8	3.2	1	0.6	4.6	4.8	3.8	3.1
Frequency/length Ratio	86%		81%		81%		90%		84%		88%		83%		78%		80%		82%		83%		86%		77%		84%		82.5%	

TABLE (12) CORRELATION OF LINEAMENTS BASIC DATA ACQUIRED FROM INTERPRETATIONS OF H.P.F.B7 IMAGES COVERING AREAS IN DIFFERENT GEOLOGIGAL PROVINCES.

F = frequency

L = length

5.5.3 Lineaments in Sedimentary Rocks near the Basement

The sequence of these sedimentary rocks are unconformably resting on the shield rocks and have a thickness ranging from hundreds of meters to an average of two thousand meters. The lower part is mainly composed of clastic rocks, while non-clastic carbonate rocks are relatively dominant in the upper part. The thickness and composition variations are some of the important factors affecting the propagation of the underlying structures. In other words there is a relation between thickness, (which generates vertical pressure), composition and the speed by which propagation proceeds under the other effective factors. Such factors seem to have affected both frequency and length of the propagated features.

The rose diagrams representing this province possess the following characteristics:

1. Relatively less frequent and shorter lineaments.
2. The roughly N-S lineament direction is represented as the maximum in the majority of rose diagrams.
3. The NE quadrant in general is dominant over the NW direction and represents around 80% of the total number of lineaments.
4. The radial pattern is almost missing except locally in an area where the Majma'ah, Butayn Grabens and other domal structures as Himar-Sabha seem to be responsible for such a pattern.

(Details of general aspects of the analysis are given in Chapter Three).

On this basis, and as revealed by Figure 67 a rough contact between the two sedimentary provinces, i.e. Interior Homocline and Interior Platform, can be inferred.

5.5.4 Lineaments in Sedimentary Rocks away from Basement

This province of sedimentary rocks has a relatively thicker sequence ranging from 2,000 - 5,500m and is almost homogeneous in composition, being a non-clastic carbonate rock. The characteristics of these rocks seem to have enhanced the propagation of some subsurface prominent structures.

The data in Table 12 indicates an average of low frequency but longer lineaments. The radial shape in both raw data and rose diagrams,(Figure 67), starts to show itself again in some areas as well as conjugate set with an intersection angle directed almost N-S.

The presence of these patterns seems to be due to one or more of the following:

1. The NW strike restriction is insignificant.
2. The presence of known domal salt structures in the region (Powers, et al, 1966).
3. The presence of some structures as for example the main part of the E.A.B. and related structures.

The relatively longer but less frequent lineaments, than other provinces, is possibly due to one or more of the following :-

1. The effect of relatively thick sequence (higher pressure and compaction) in enhancing propagation

more likely on selective basis, i.e. prominent, long deep seated structures, which can persist, for example, the long N-S lineaments and the Ghawwar oil field and other N-S aligned structures.

2. The homogeniuity of this thick sequence where it is mainly composed of non-clastic carbonates which have played a role in enhancing propagation specially the length of the subsurface structures.

3. The province in general being in the vicinity of the Arabian Gulf Basin known to be seismically very active (Figure 65) and being near the boundary between the Arabian and the Persian Plates.

4. The presence of some radial pattern in the rose diagrams beside the effect of salt domed structures, may be caused by the NW Najd fault system, or its rejuvenated part due to the Riyadh Fault System.

5.5.5 Summary of Correlation

The correlation of rose diagram maps (Figures 67,68) and the data in Table 12 both indicate that contacts between different geological provinces can be inferred with some degree of confidence from lineament analysis using Landsat images.

The correlation also indicates that there is an obvious disparity as well as some degree of agreement between lineament analysis of different geological provinces as revealed from Landsat image interpretations. The results highlighted that some of the interpretted prominent directions in the shield

rose diagrams which are not represented in those of the sedimentary region seems to be an old regional failure direction in the basement which has not been activated subsequent to the establishment of the sedimentary sequence during the Phanerozoic. Also they may represent relatively younger activity which took place in the basement and has not been able to propagate upward properly in the overlying thick sequence of sediments, for example, the roughly N-S alignment of Tertiary volcanic cones. On the other hand the lineaments which are represented in the sedimentary rose diagrams while poorly represented or missing from the Shield rose diagrams, may indicate that they have originated at deep seated horizons not necessarily from the basement level. For example, the thinning of the Marrat and Dhruma Formations (Jurassic) which seems to have played a role in the tilting of Riyadh Block, and the effect of Salt dome structures in the upper part of the Phanerozoic rocks specially in the Interior Platform.

The complexity of the directions of the lineaments, in general, mainly in the basement and partly in the sedimentary sequency, suggests that beside the known regional stresses of Hijaz and Najd cycles, there may be a possible additional regional principal stress direction. The cause of which, among some other possibilities, might be a major radial brittle failure related to impacts (Norman, 1979).

REFERENCES

AL-KHATIEB, S.O., (1977) Progress Report on Cover Rock project (5.9), Open file Report, Ministry of Petroleum and Mineral Resources, Jeddah, Saudi Arabia.

AL-KHATIEB, S.O., (1978) Summary on the Progress of Ph.D. Research Work. Cover Rock project, central part of Sauid Arabia. Open File Report. Ministry of Petroleum and Mineral Resources, Jeddah, Saudi Arabia.

AL-KHATIEB, S.O., NORMAN, J.W., (1980). Photogeological evidence of the continuation of Al-Amar-Idsas Basement Fault under the Phaerozoic Rocks, Central Saudi Arabia. In preparation

AL-SARAWI, M., (1978) Geomorphology and general geology of Wadi Al Batin, Kuwait. Unpublished Ph.D. thesis, Ohio University, 88p.

AL-SAYARI, S.S., ZOTL, Y.G., (1978). Quaternary Period in Sauid Arabia. Springer-Verlag Wein. New York.

AL-SHANTI, A.M.A., and MITCHELL, A.H.G., (1976). Late Precambrian subduction and collision in Al-Amar-Idsas region, Arabian Shield, Kingdom of Saudi Arabia. Tectonophysics., Vol.30, T41-T47.

ABRAMS, M.J., (1978). Computer image processing in: Geologic Applications. NASA Jet Propulsion Laboratory Publications, NASA Cr 157347, 36 pages.

AMERICAN SOCIETY OF PHOTOGRAMMETRY (1974). Manual of Remote Sensing. Vol.I.II.

ARABIAN AMERICAL OIL COMPANY STAFF (1959). Ghawwar Oil Field. Saudi Arabia. Bull.Am.Ass.Pet.Geol., Vol.43, N.12, pp 434-454.

BARAZANGI, M., (1980). On the evaluation of seismic risk along the western part of the Arabian Plate. CES Bull.I, King Abdul Aziz University, Jeddah, Saudi Arabia.

BARRETT, E.C., CURTIS, L.F., (1976). Environmental remote sensing. Chapman and Hill, London.

BLANCHET, P.H., (1957). Development of fracture analysis as exploration method. Bull.Am.Ass.Pet.Geol.Vol.41,No.8.

BLANCHET, P.H., (1960). Theoretical basis of fracture analysis, manual of photointerpretation. Am.Soc.Photogramm., Washington, 1960.

BLANK, H.R., et al, (1979). Seismic refraction profile, Kingdom of Saudi Arabia. Field operations, instrumentation and initial results. U.S. Geol.Survey, Saudi Arabian Project Report 259. Ministry of Petroleum and Mineral Resources,Jeddah, Saudi Arabia.

BLODGET, H.W., et al, (1978). Discrimination of rock classes and alteration products in south western Saudi Arabia with a computer enhanced Landsat data. NASA Technical Paper, 1327.

BRAMKAMP, R.A. and RAMIREZ, L.F., (1958). Geology of the Northern Tuwaiq Quadrangle, Kingdom of Saudi Arabia, Map 1 - 207A. Ministry of Petroleum and Mineral Resources.

BREED, C.S., GROW, T., (1979). Morphology and distribution of dunes in sand seas observed by remote sensing. U.S. Geol. Survey Professsional Paper 1052.

BROWN, G.F., (1972). Tectonic map of Arabian Peninsula. Map AP-2 Ministry of Petroleum and Mineral Resources, Jeddah, Saudi Arabia.

BULLETIN of Am.Ass.Pet.Geol. (1959) V.43, No.2.

BURNS, K.L., BROWN, G.H., (1978). The human perception of geological lineaments and other discrete features in remote sensing imagery: signal strengths, noise levels and quality, remote sensing of environment 7, 163-176 (1978)

CHUKWU-IKE, I.M., (1977). Regional photogeological interpretation of the tectonic features of the Central Nigerian basement complex: A satellite imagery based study. Unpublished Ph.D. thesis, Geol.Dept. Imperial College, London.

CONDIT, C.D., CHAVEZ, P.S.J.R., (1979). Basic concepts of computerized digital image processing for geologists. U.S. Geol. Survey.Bull.1462.

DAVIS, G.R., MORRISSEY, C.J., (1976). Target feasibility report, Cover Rock project. Kingdom of Saudi Arabia. Ministry of Petroleum and Mineral Resources, Jeddah, Saudi Arabia.

DESITTER, L.U., (1964). Structural geology. MacGraw-Hill,New York,1964.

FARHOUDI, G., (1978). Jour.of Geol.,Vol.86 p.323-334.

GARRARD, P., (1980). Report on reconnaissance of the Al-Amar-Idsas fault extension. Open File Report. CRC/IC4. Ministry of Petroleum and Mineral Resources, Jeddah, Saudi Arabia.

GIRDIER, R.W., (1967). The role of translational and rotational movements in the formation of the Red Sea and Gulf of Aden. Canadian Geol.Soc.Vol.66, No.14.

GODDARD SPACE FLIGHT CENTER (1974). Third ERTS Symposium.Vol.I., NASA sp-351.

GOETZ, A.F.H., BILINGSIEY, F.C., (1974). Digital image enhancement techniques used in some ERTS application. Contribution to geology Vol.12, No.2.

GREENWOOD, W.R., et al., (1980). Precambrian geologic history and plate tectonics evolution of the Arabian Shield. Mineral Resources Bull.No.24. Ministry of Petroleum and Mineral Resources, Jeddah, Saudi Arabia.

GREENWOOD, W.R., and ANDERSON, R.E., (1976). Palinspastic map of the Red Sea area prior to Miocene sea floor spreading. U.S.Geol.Survey. Saudi Arabian Project Report 197. Ministry of Petroleum and Mineral Resources, Open File Report 23p.

HAMAN, P.J., (1964). Geomechanics applied to fracture analysis on aerial photographs. West Canadian Research Publication, series 2, No.2., 1964.

HANCOCK, P.L., (1968). Joints and faults. The morphological aspects of their origin. Proc.Geol.Assoc.Vol.79, part 2. pp. 141 - 151.

HANCOCK, P.L., KADHI, A., (1978). Analysis of Mesoscopic fractures in the Dhruma Nisah segments of the Central Arabian Graben System. Geol.Soc.Lond.V.135, pp 339 - 347.

HANCOCK, P.L., AL-KHATIEB, S.O., KADHI, A., (1980). East Arabian Block. Geol.Magazine in press.

HARRIS, J.F., TAYLOR, G.L. and WALPER, J.L., (1960). Relation to deformational fractures in sedimentary rocks to regional and local structures. Bull.Amer. Petr.Geol.Vol.44, No.12 pp 1853 - 1973.

HUNTINGTON, J.F., (1975). A photogeological study of fracture trace patterns using data processing techniques. Unpublished Ph.D thesis, Dept.Geol. Imperial College, Lond. 1975.

HUNTINGTON, J.F., and RAICHE, A.P., (1978). A multi-attribute method for comparing geological lineament interpretation. Remote sensing of environ.7, 145 - 161 (1978).

JOSEPH, L.Jr., SIMONETT, D.S., (1976). Remote sensing of environment. Addison's-Wesley Publication Company, Reading - Massachustts.

KADHI, A., (1976). Analysis of Mesoscopic fractures in the Dhruma Nisah Segments of the Central Arabian Graben System. Unpublished Ph.D thesis, Dept.Geol.Bristol University.

KHAIN, V.E., MURATOV, M.V., (1969). Crustal movements and tectonic structure of continents. The earth's crust and upper mantle. Amer.Geophysical. Monograph 13.

LATTMAN, L.H., (1958). Technique for mapping geologic fracture traces and lineaments on aerial photographs. Photogramm.Eng., Vol.24, No.4.

LLOYD-LAWRENCE, L.A.H., (1977). The characteristics of plutonic rocks in various climatic zones as shown on multiband satellite imagery. Unpublished Ph.D thesis, Dept.Geol., Imperial College, 1977.

MACKENZIE, D.P., (1970). Plate tectonics of the Mediterranean Region. Nature, Vol.226, 239 - 243. April, 1970.

MCDONALD and PARTNERS., (1978). Unpublished reports of M.A.W. Riyadh, Saudi Arabia.

MCKEE, E.D., BREED, C.S., (1976). Sand seas of the World. U.S.Geol.Surv. Professional paper 929.

MEKEL, F., (1971). Lectures in photogeology for postgraduate students. I.T.C. Delft, Netherlands.

MINISTRY OF AGRICULTURE AND WATER, (1980). Unpublished reports and hydrogeological data of central Arabia, Riyadh, Saudi Arabia.

MOORE, M.J., (1976). A major lineament in the Arabian Shield and its relationship to mineralization. Mineralium Deposita, 11, pp 323; 328.

MOORE, M.J., (1979). Primary and secondary faulting in the Najd Fault System, Kingdom of Saudi Arabia.U.S. Geol.Surv.Project Report 292. Ministry of Petroleum and Mineral Resources, Jeddah, Saudi Arabia.

MOORE, M.J., (1980). Interpretation of tectonic structures in Wadi Addawasir district from satellite imagery and aerial photographs. Open File Report, CRC/IC8, Ministry of Petroleum and Mineral Resources, Jeddah, Saudi Arabia.

NAWAB, Z., (1978). Al-Amar Idsas Fault. Unpublished, Ph.D thesis Ontario University, Canada.

NEBERT, K., (1970). Geology of western Al-Quway'iyah Region, Saudi Arabia. N.Jb.Geol.Palaont.Abh., 135,2. pp 150-170.

NORMAN, J.W., (1968). The geological significance of natural linear features occurring in areas of superficial deposits, as revealed by air photographs. Unpublished Ph.D thesis. Imperial College, University of London.

NORMAN, J.W., (1969). Linear geological fractures as an aid to photogeological research. Photogramm. 25.pp 177-187.

NORMAN, J.W., WATSON, I., (1975). Detection of subsidence conditions by photogeology. Eng.Geol.9.pp 359 - 381.

NORMAN, J.W., IKE, M.C., (1977). The world is a bit cracked. New Scientist, Vol.73. p.320.

NORMAN, J.W., PRICE, N., IKE, M.C., (1977). Astrons - the earth's oldest scars ?. New Scientist. Vol.72. March 1977.

NORMAN, J.W., (1977). Photogeological fracture trace study of controls of kimberlite intrusion in Lesotho basalts. Trans.I.M.M., Vol.86.

NORMAN, J.W., (1979). Regional tectonic structures of the Cover Rocks. Open File Report CRC/IC.1, Ministry of Petroleum and Mineral Resources, Jeddah, Saudi Arabia.

NORMAN, J.W., (1980). Causes of some old crustal failure zones interpretted from Landsat images and their significance in regional mineral exploration. Trans.I.M.M.,Vol.89.

NORMAN, J.W., (1980). Regional tectonic structures of Cover Rocks. Open File Report CRC/IC.5, Ministry of Petroleum and Mineral Resources, Jeddah, Saudi Arabia.

OPEN UNIVERSITY (1980). Crustal and mantle processes - Red Sea Case Study.

PARKER, and DAUNA., (1973). Some basic consideration related to the problem of remote sensing. Inst.Science and Techno., University of Michigan.

PAMENTER, C.B., (1968). Air photo analysis outline structures. Canadian Petroleum, February, pp.18 - 19.

PARVIS, M., (1949). Drainage pattern significance in air photo identification of soils and bedrocks. Joint Highway Res.Project., Purdue University.

POWERS, R.W., et al., (1966). Geology of the Arabian Peninsula. U.S. Geol.Surv.Professional Paper 560D.

PRICE, N.J., (1974). The development of stress systems and fracture patterns in undeformed sediments. Adv.Rock Mecha.proce. 3rd Congress Intern. Soci. for Rock Mechanics., V.I.A.

ROWAN, L.C., et al., (1975). Application of satellites to geologic exploration. Amer.Scien., Vol.63.

RUMSEY, I.A., BOSTRONN, R.C., (1971). Relationships of fractures in unconsolidated superficial deposits to those in the underlying rocks. Modern Geology. Vol.3, No.1., pp 25 - 41.

SABIN, F.F. Jr., (1978). Remote sensing principles and interpretations. Freeman and Company.

SAUL, J.M., (1978). Circular structures of large scale and great age on the earth's surface. Nature Vol.271.

TRAINER, F.W., (1967). Measurement of the abundance of fracture traces on aerial photographs. U.S.Geol.Surv. Professional Paper, 575-C.

U.S.G.S. (1963) Geologic map of the Arabian Peninsula. Map 1-270A., Ministry of Petroleum and Mineral Resources, Jeddah, Saudi Arabia.

WILLIAMS, R.S. Jr., CARTER, W.D., (1976). A new window on our planet. U.S.Geol.Surv., Professional Paper 929.

ZWAIN, J.A., (1976). Analysis from air photographs of fracture trace in Northern Iraq. A structural geology study with reference to oil exploration. Unpublished Ph.D thesis. Dept.Geol.Imperial College, London, 1976.

A P P E N D I X

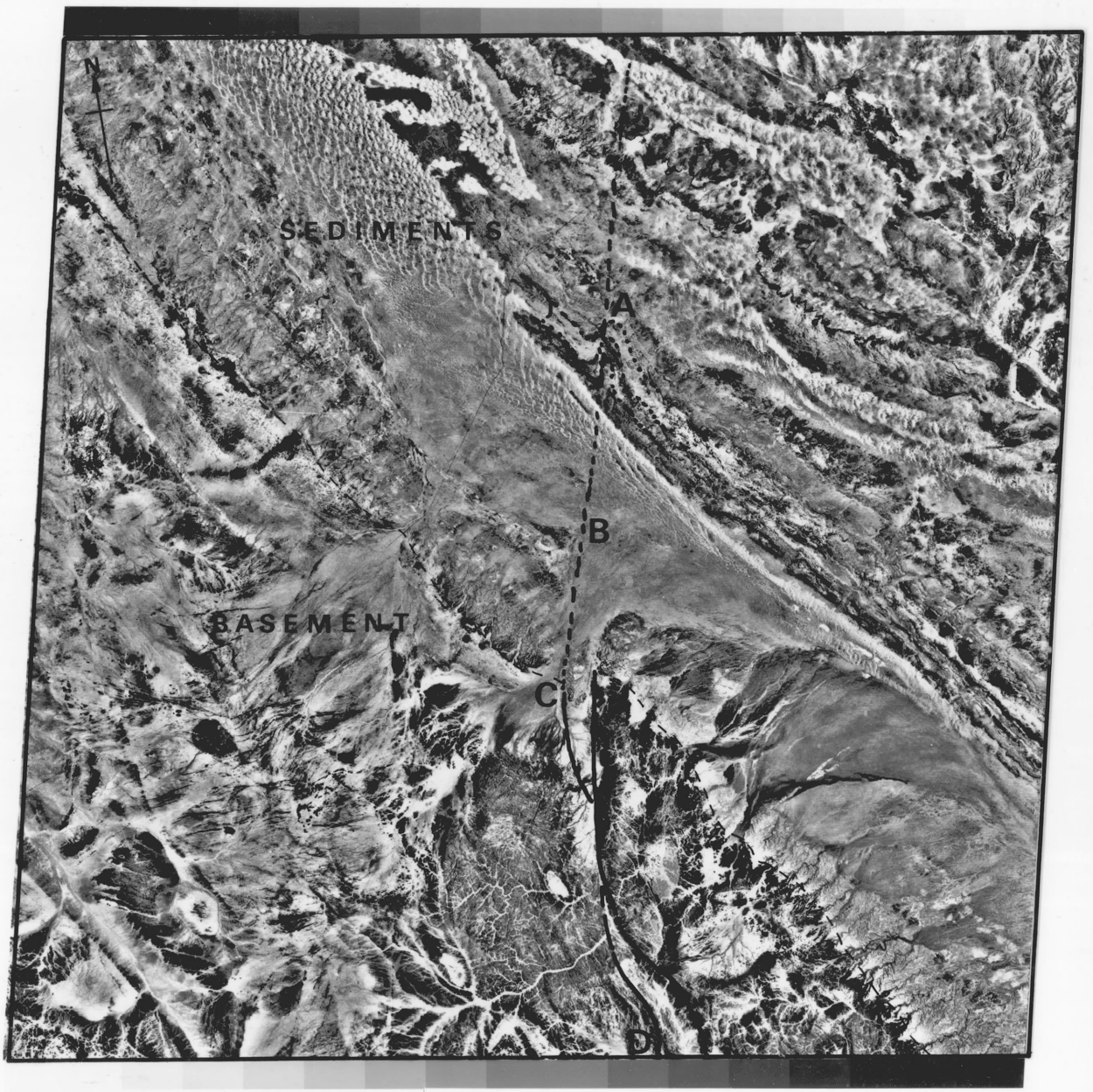
LANDSAT IMAGES AND SOME AERIAL PHOTOGRAPHS

GENERAL REMARKS

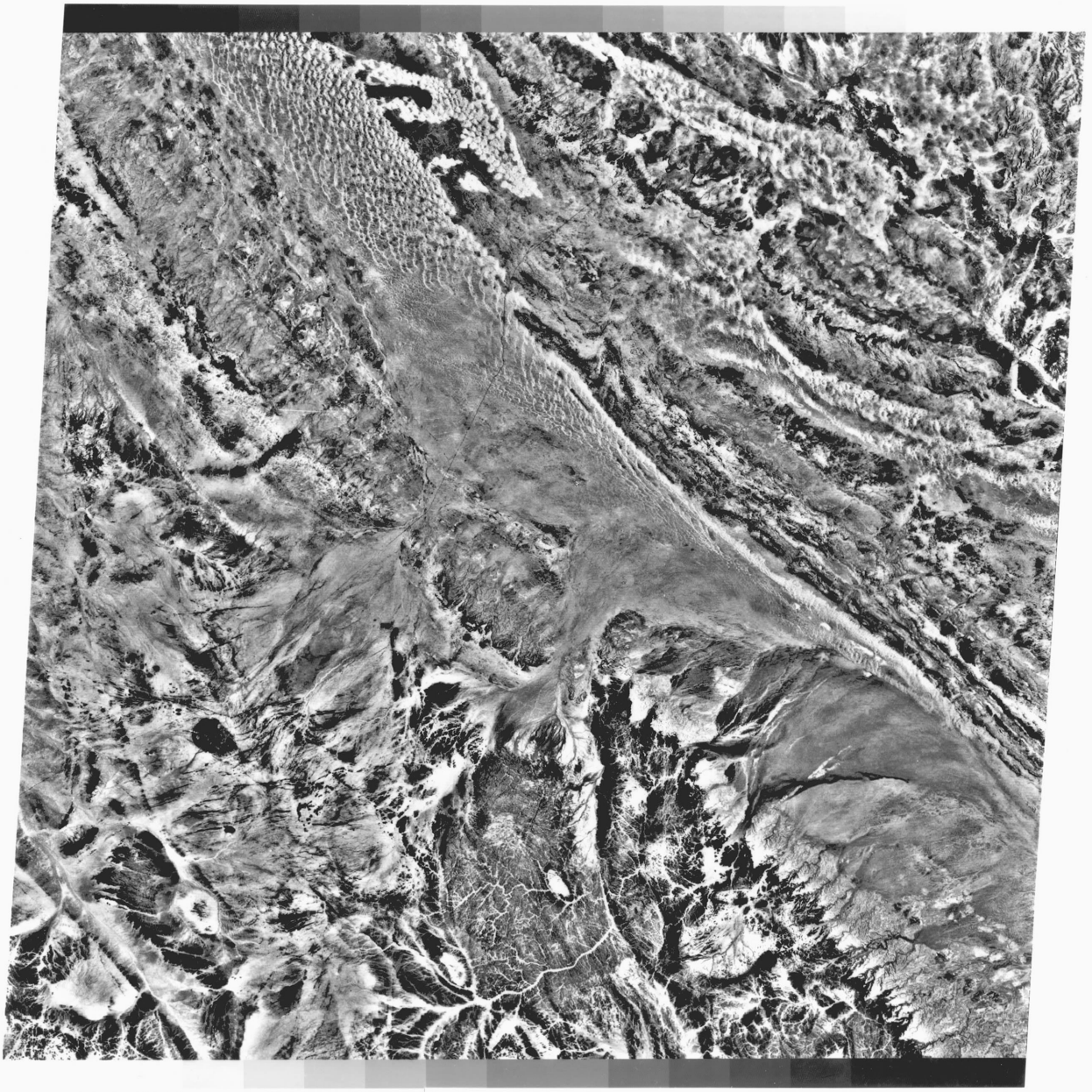
Certain key areas, in the study area, are important from the structural and/or photogeological points of view, for example Al-Amar-Idsas area (Photo plates 1 - 5) and Riyadh area (Photo plates 6 - 12A). Such areas are covered by a number of images of different bands, types or processed by different processing techniques. The multi-images of such areas and some others are included in this appendix. This procedure may help one to correlate and sense the differences between these images and their possible effect on interpretation. On the attached overlays, only a few structural features or lineaments are interpreted where reference has been made in the text. The detailed lineament interpretation of multi-images of different scales have been dealt with early in the research prior to the rose diagram preparation, these rose diagrams are shown on Plates 1, 2, 3, 4, 5 and 6. Some examples of the detailed lineament interpretations can be seen in the text (Figures 16, 24-A and 25-A). The interpreted features on the overlays are drawn with different dashed and dotted lines relative to their clarity on images as much as possible. The majority of Landsat images included are of an approximate scale 1:1,120,000 unless otherwise stated.

Photo plate (1) Image 179/43 Ce_1 of band 7 showing :-

1. The Al-Amar Idsas fault in the Basement (C-D)
2. Its extension under the alluvial sand cover (B)
3. Its effect on the sedimentary rocks of the Jilh Formation (A)



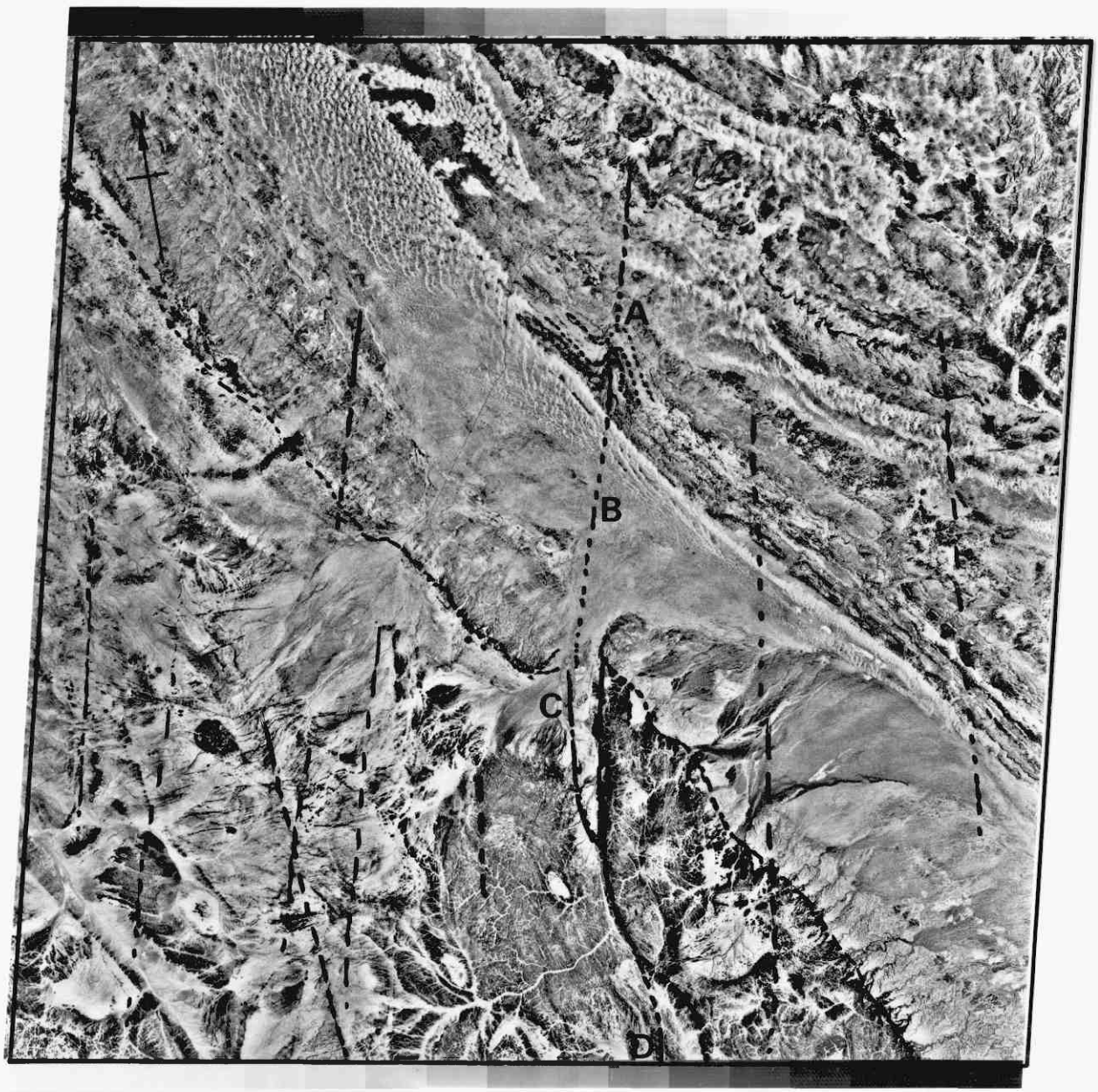
SAUDI ARABIA MOSAIC PATH 179 ROW 43 SCENE ID 10334-0658 C
BITS 4 EXPOSURE DATE 22-JUN-73 PATH 179 ROW 43 C
SBRZA FILE 2 SAUDI ARABIA PATH 179 ROW 43 BAND 7 101X101 MPF
STRETCH1 0- 0.112- 0.142-255 255-255
ED /SRAS 9TRACK 8BIT 800BPI FILE 2 NL 2340 NS 2484
03-JUN-80 18:55:42 U.S.G.S. FLAGSTAFF IMAGE PROCESSING FACILITY



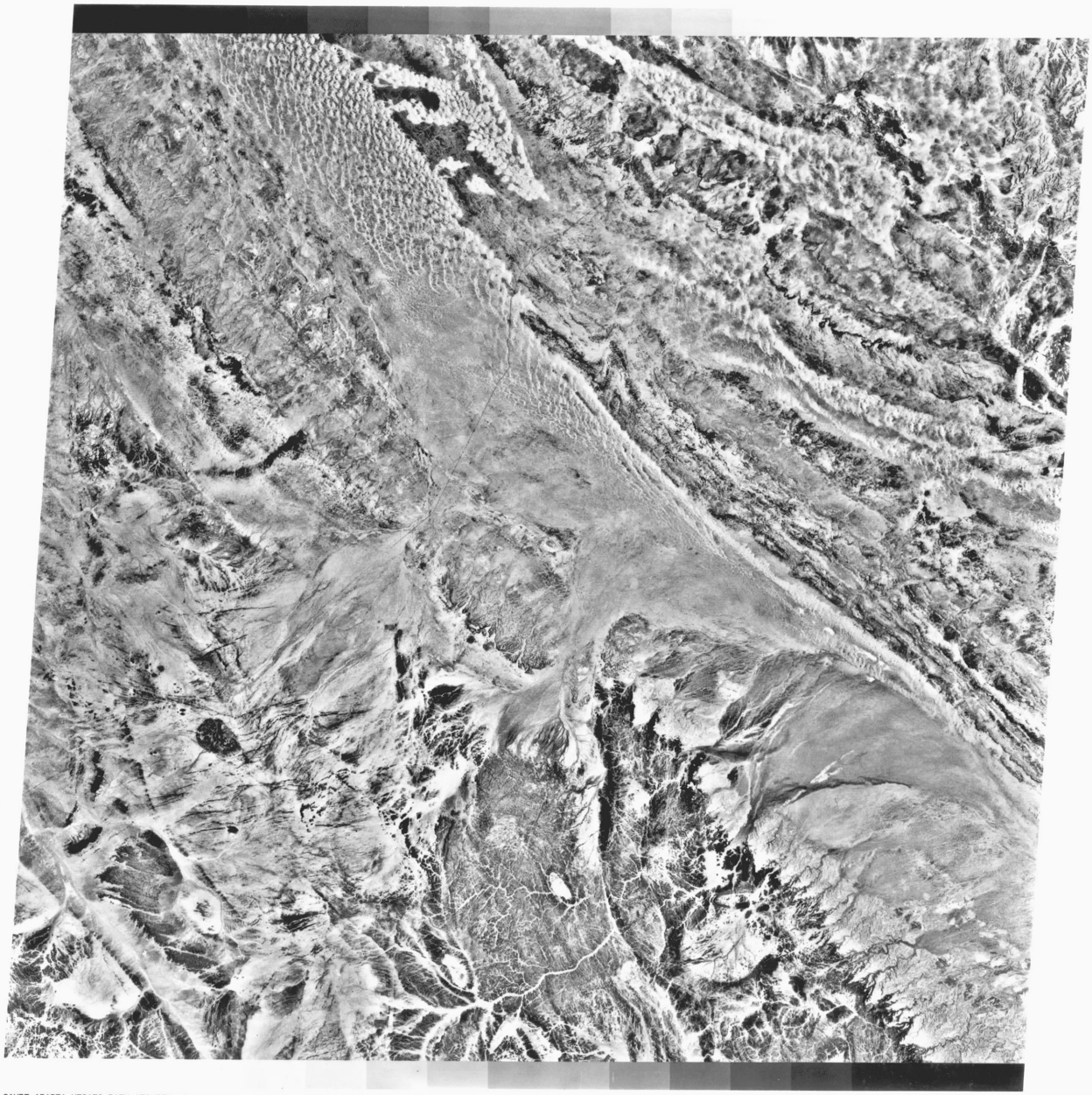
;SAUDI ARABIA MOSAIC PATH 179 ROW 43 SCENE ID 10334-0658 C
;RTS-1 EXPOSURE DATE 22-JUN-73 PATH 179 ROW 43 C
;GRID TILE 2 SAUDI ARABIA PATH 179 ROW 43 BAND 7 101X101 MPF
;STRETCH 0- 0.112- 0.142-255 255-255
;EOF 7SRAS 9TRACK 8BIT 800BPI FILE 2 NL 2340 NS 2484
03-JUN-80 18:55:42 U.S.G.S. FLAGSTAFF IMAGE PROCESSING FACILITY

Photo plate (2) Image 179/43 Ce_2 of band 7 showing :-

1. The same details as Photo plate (1) with varying degree of clarity mainly due to change in contrast stretch parameters
2. Some approximately N-S Lineaments parallel to Al-Amar Idsas Fault which can be observed on Photo plates 1, 3 and 4 in different degrees of clarity



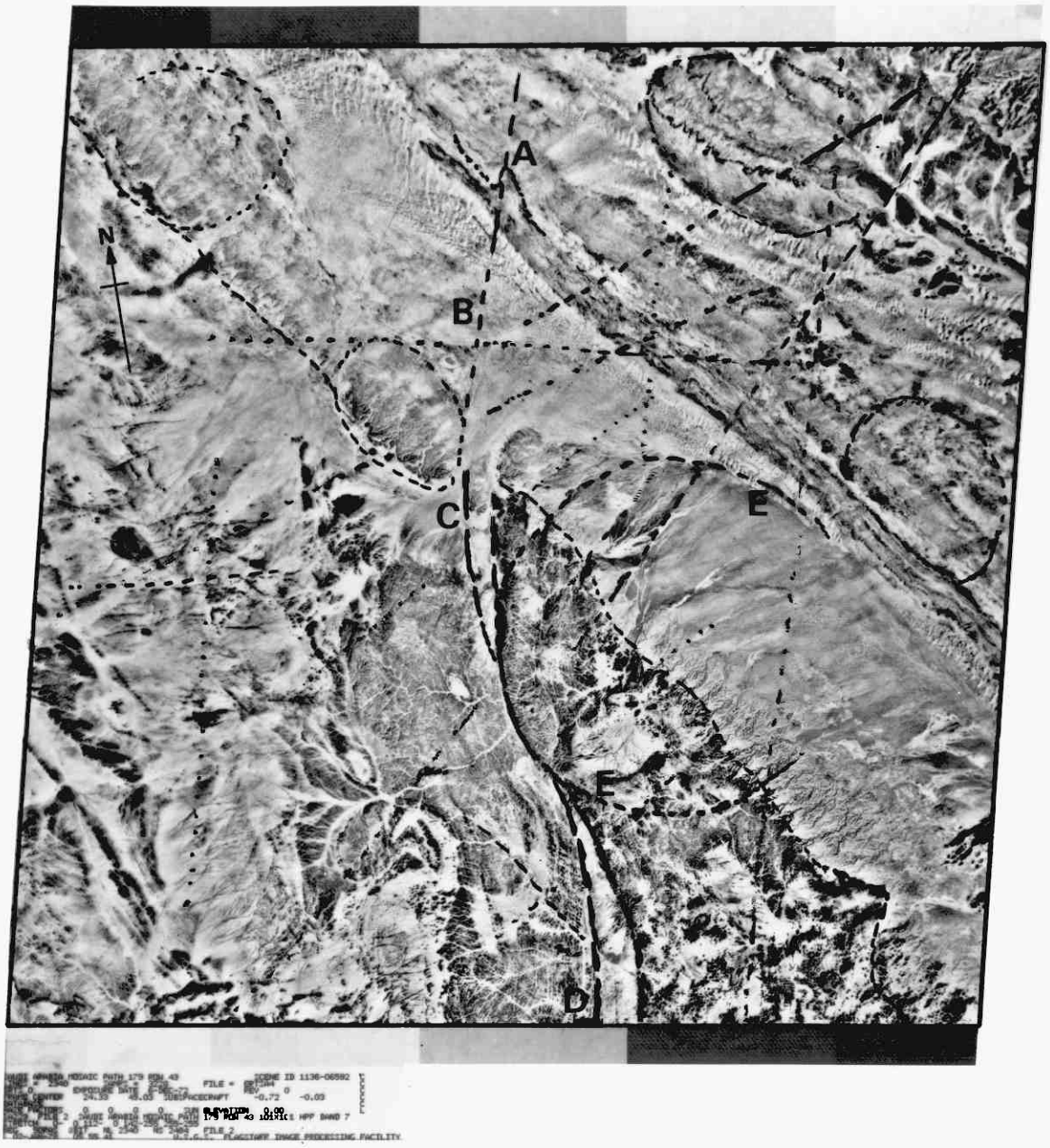
SAUDI ARABIA MOSAIC PATH 179 ROW 43 SCENE ID 10334-0658 C
BPIS 1 EXPOSURE DATE 22-JUN-73 PATH 179 ROW 43 C
20673 FILE 2 SAUDI ARABIA Path 179 ROW 43 BAND 7 101X101 HPF
STRETCH 0- 70 102- 98 185-235 236-255
NEG CSRQS 8BIT NL 2340 NS 2404 FILE 2
15-DEC-79 13:42:15 U.S.G.S. FLAGSTAFF IMAGE PROCESSING FACILITY



SAUDI ARABIA MOSAIC PATH 179 ROW 43 SCENE ID 10334-0658 C
BITS 1 EXPOSURE DATE 22-JUN-73 PATH 179 ROW 43 C
X982/3 FILE_2 SAUDI ARABIA PATH 179 ROW 43 BAND 7 101X101 HPF
STRETCH! 0- 20 102- 20 152-235 255-235
NEG 75ROS 8BIT NL 2340 NS 2484 FILE_2
15-DEC-79 13:42:15 U.S.G.S. FLAGSTAFF IMAGE PROCESSING FACILITY

Photo plate (3) Image 179/43 generated from Ce_1 of band 7 by a photographic process showing :-

1. The Al-Amar-Idsas Fault in the Basement (C-D)
2. The fault extension under the alluvial sand cover (B)
3. The effect of the fault on the Jilh Formation (A) is less clear relative to Photo plates 1 and 2.
4. The fault in the Basement (C-D) has followed part of a circular feature (E) (Impact effect) before it straightened again to the north. This is more clear in this image than Photo plates 1 and 2.
5. Some semicircular features in the basement and sediments.
6. Same clear N-S and N-E Lineaments.


A
B
C
D
E
F
N

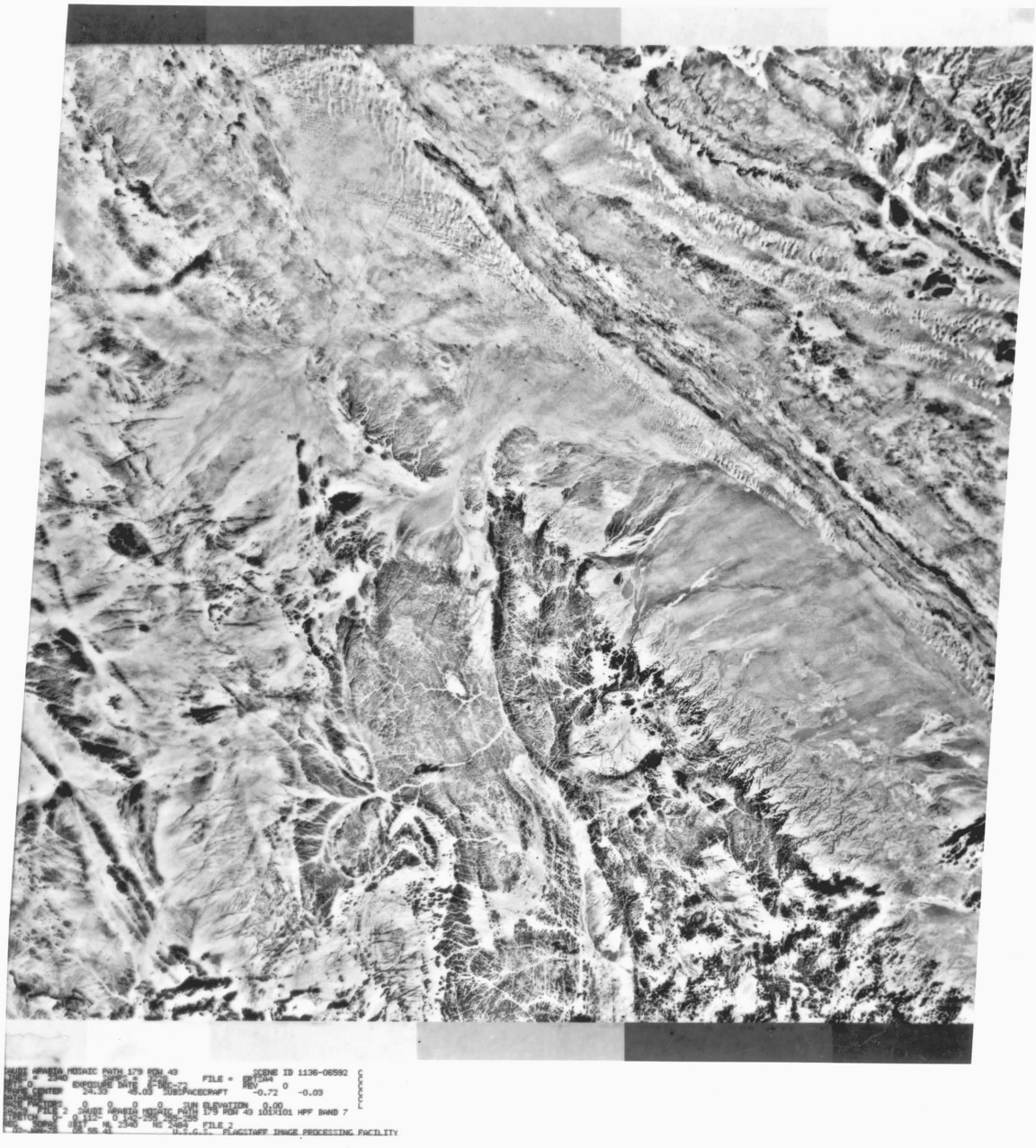
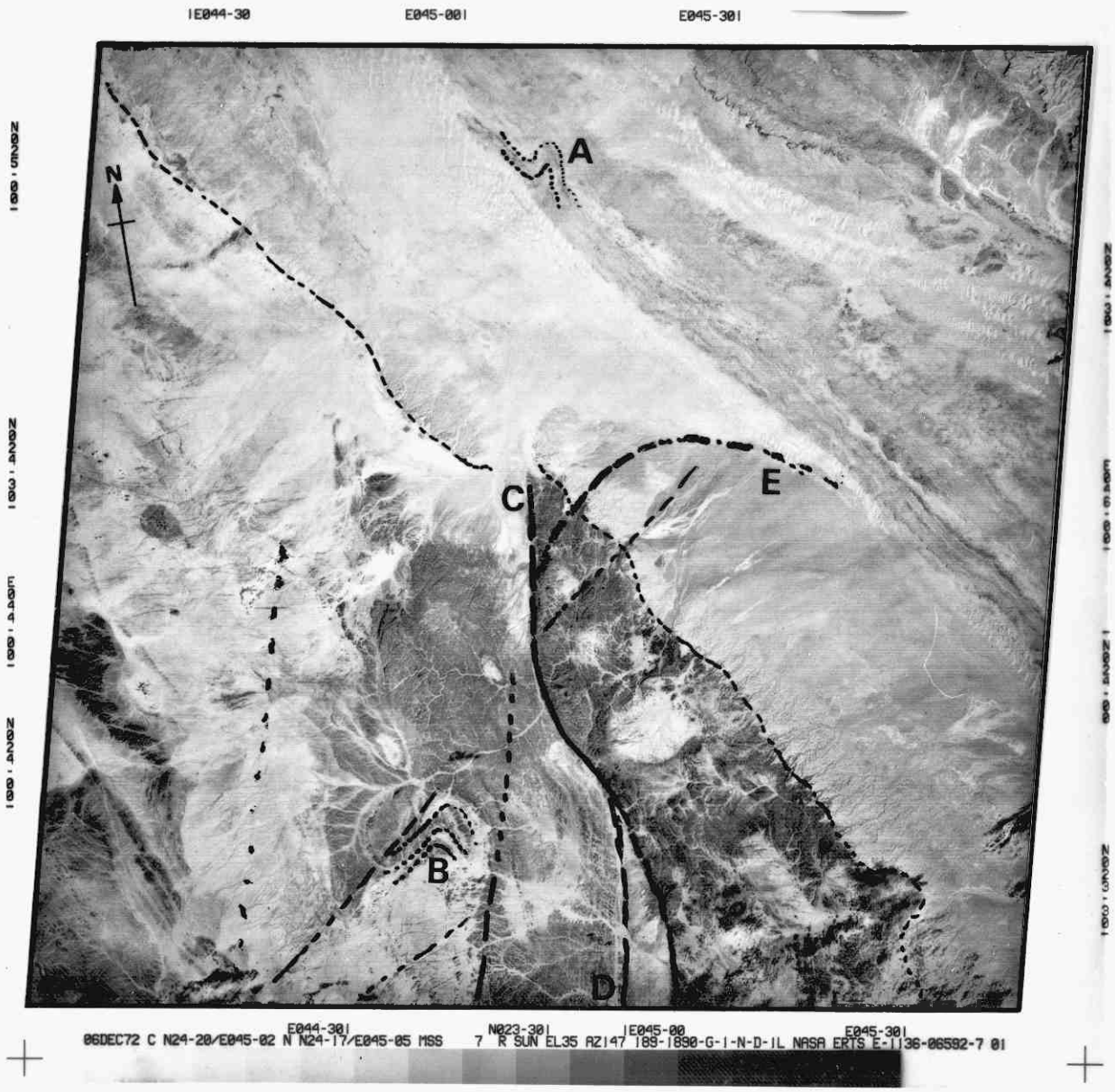

LANDSAT ARABIA MOSAIC PATH 179 ROW 43 SCENE ID 1136-06592
FILE = ARABIA
EXPOSURE DATE = DEC 73 REV 0
SUBSPACECRAFT -0.72 -0.03
SUN ELEVATION 0.00
LANDSAT ARABIA MOSAIC PATH 179 ROW 43 101X101 MPF BAND 7
FILE_2
U.S.G.S. FLAGSTAFF IMAGE PROCESSING FACILITY

Photo plate (4) Image 179/43 S.p. of band 7 showing :

1. Only the Al-Amar-Idsas Fault in the Basement (C-D).
2. To some extent its effect on the Jilh Formation (A).
3. The extension of the fault under the alluvial sediments is not clear.
4. The circular feature (E).
5. Relatively small fold (B).
6. Two approximately N-S Lineaments.


E044-30
E045-001
E045-301
N
A
B
C
D
E
E044-301
N023-301
E045-00
E045-301
06DEC72 C N24-20/E045-02 N N24-17/E045-05 MSS 7 R SUN EL35 AZ147 189-1890-G-1-N-D-IL NASA ERTS E-1136-06592-7 01

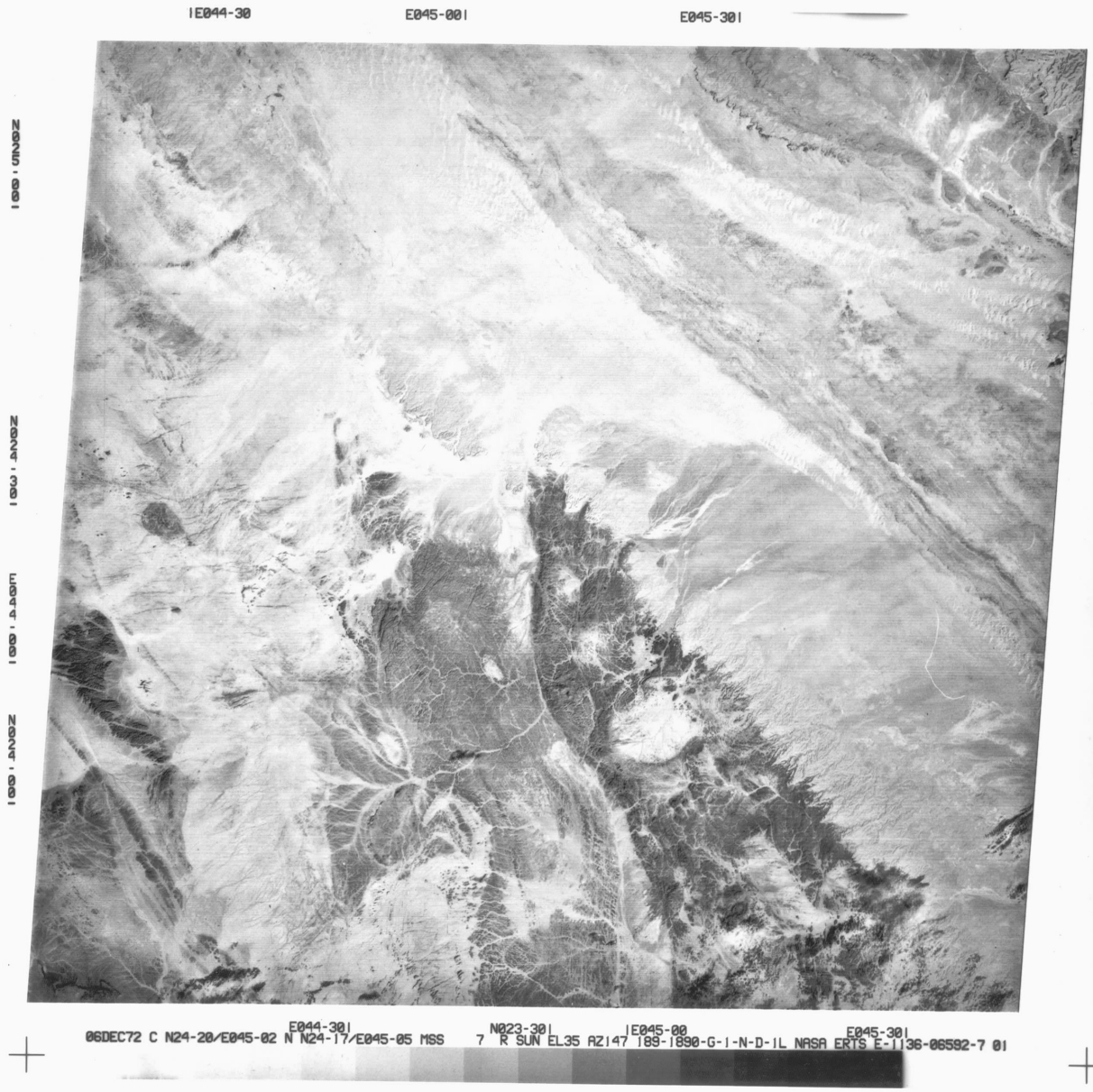

!E044-30
E045-001
E045-301
E044-301
N023-301
!E045-00
E045-301
06DEC72 C N24-20/E045-02 N N24-17/E045-05 MSS 7 R SUN EL35 AZ147 189-1890-G-1-N-D-1L NASA ERTS E-1136-06592-7 01

Photo plate (5) Aerial photomosaic, approximate scale 1:120,000 showing :

1. The structures of Khashm Al-Juair Area, Syncline (A) and Anticline (B) as an effect of Al-Amar Idsas Fault on the Jilh Formation (complementary to Figure 30 which shows the detailed field measurements).
2. Same NE Lineaments which extend from the outcrop through the sand cover and are relatively clear as well.
3. Some N-S Lineaments parallel to the main fault zone.


N
B
A

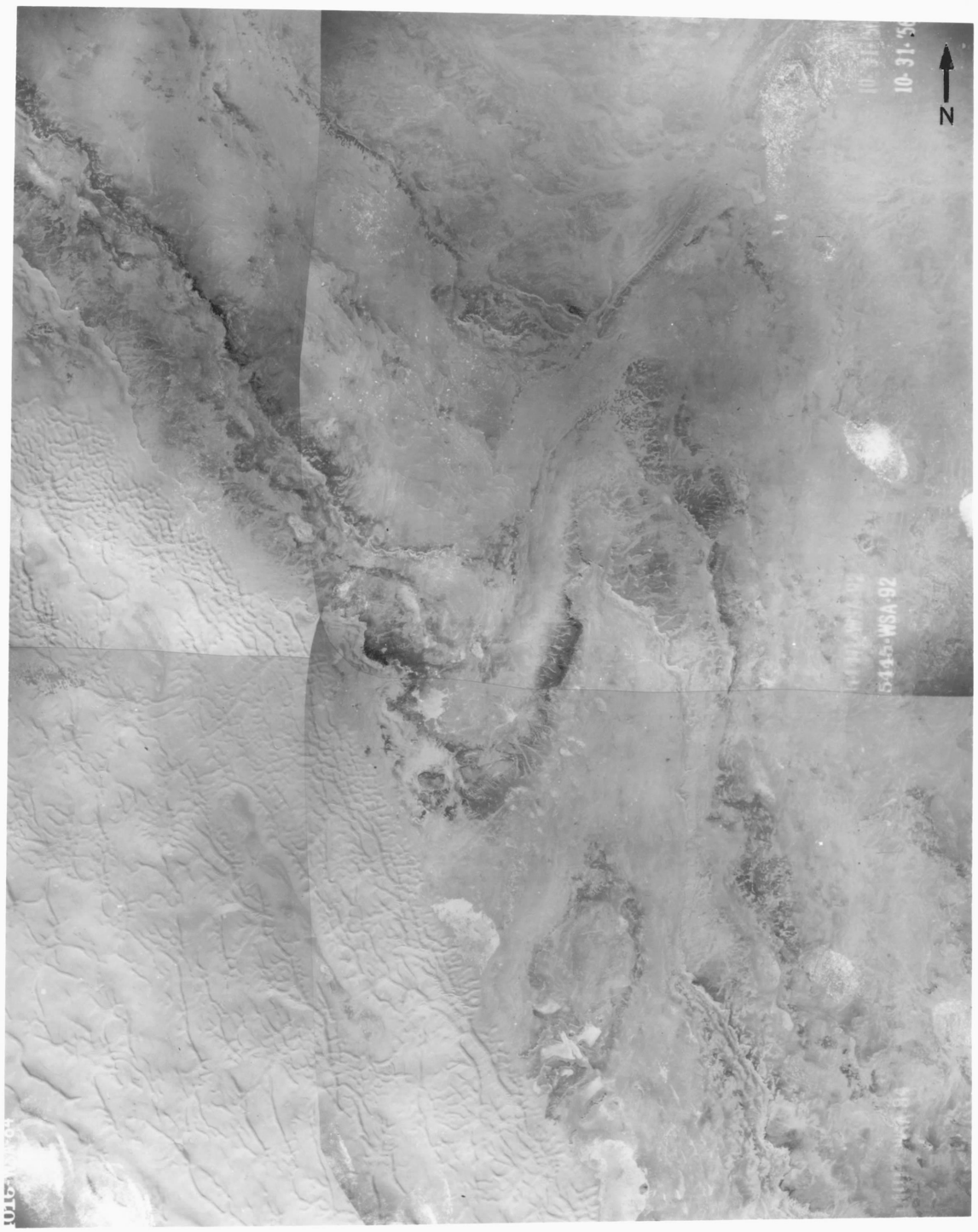
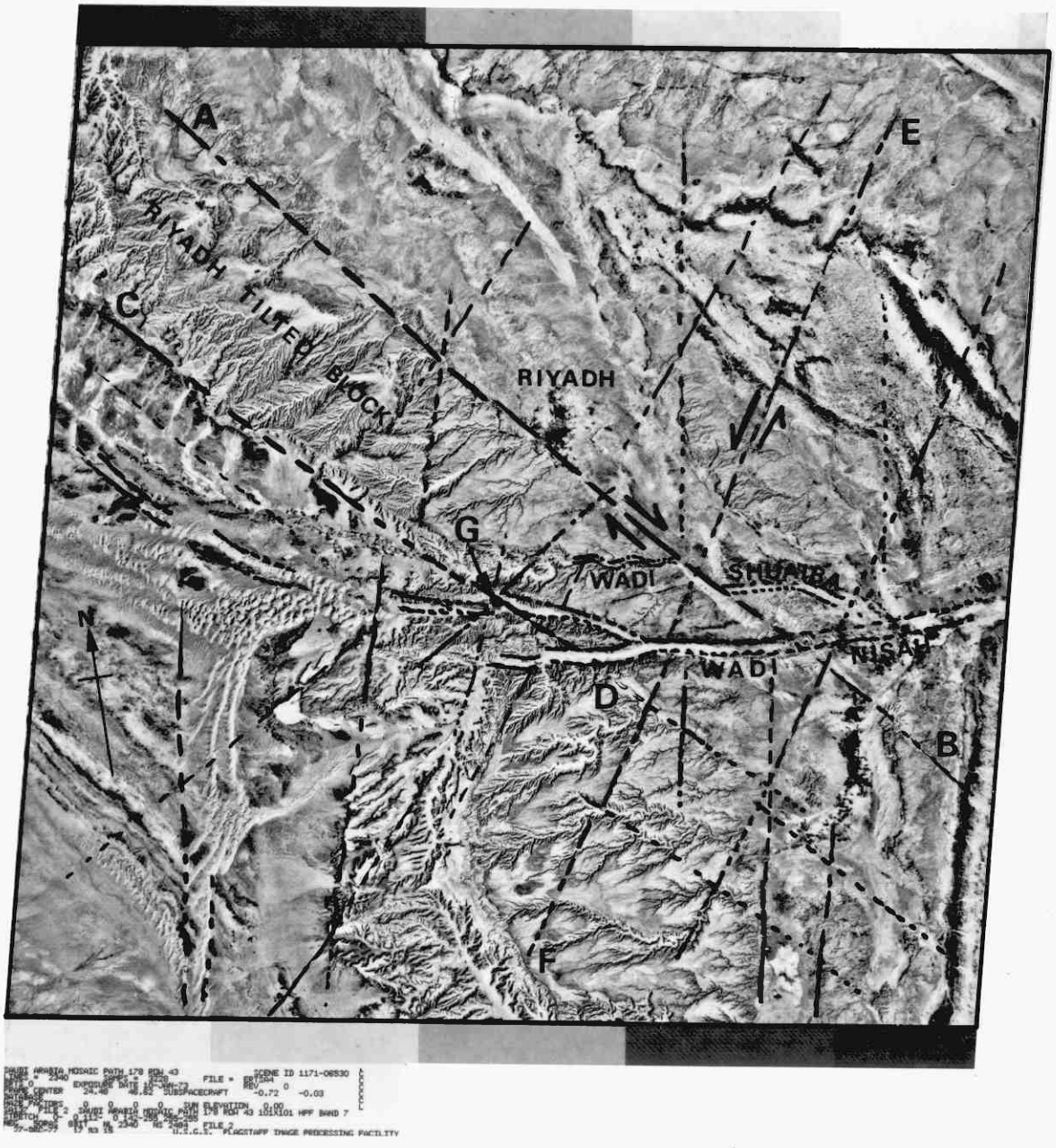

N

Photo plate (6) Image 178/43 Ce_1 of band 7 showing :

1. Parts of the C.A.G.T.S
2. Riyadh Tilted Block and its characteristic drainage pattern.
3. Two NW faults (A-B), (C-D) of the Riyadh Fault System bordering the block.
4. Some other lineaments of the Riyadh Fault System.
5. Khashm Addingham (E-F) fault with its horizontal sinistral movement.
6. Displacement of Wadi Awsat Graben (G).
7. Displacement of Wadi Shuaiba by the (A-B) fault.


A
E
RIYADH FILTED BLOCK
C
RIYADH
G
WADI
SHUAIBA
N
WADI
NISAH
D
B
F

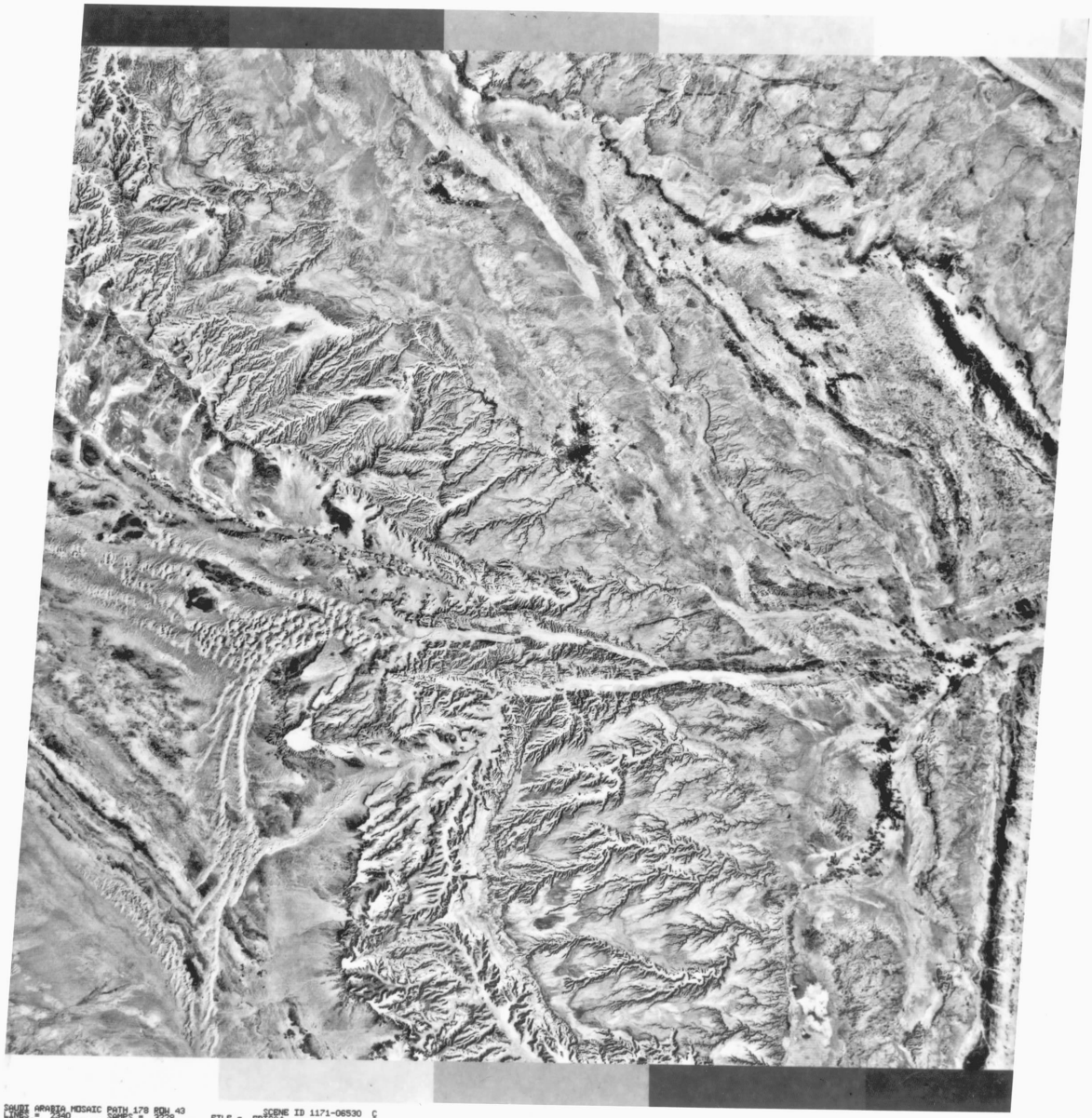
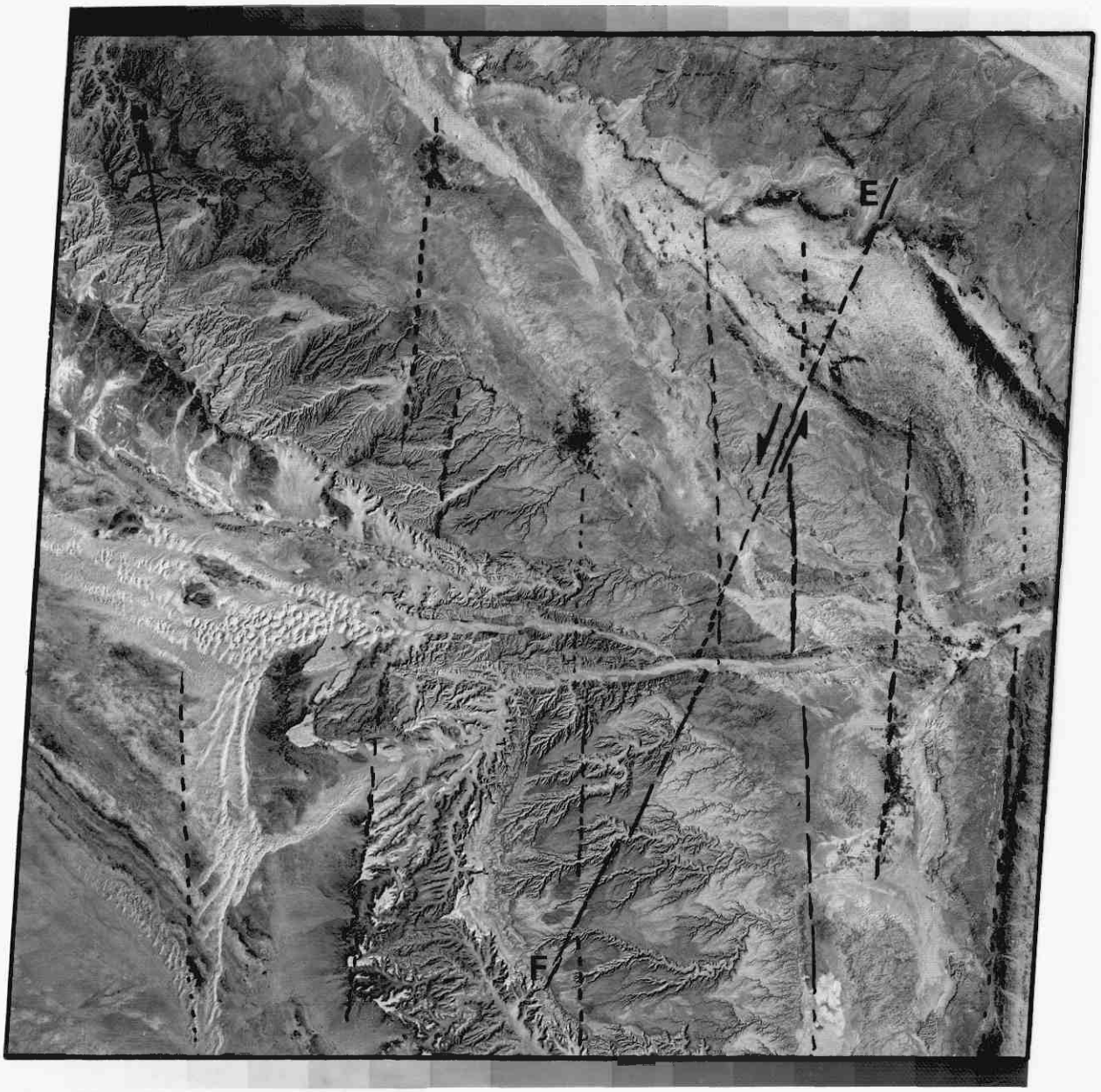

SAUDI ARABIA MOSAIC PATH 178 ROW 43
LINES = 2340 SAMPS = 2259
SCENE ID 1171-08530
FILE = SAUDI
BAND4
EXPOSURE DATE 10-JUN-72
REV 0
SCENE CENTER 24.48 46.62 SUBSPACECRAFT -0.72 -0.03
RECTIFIED
RASE PIXTIDES 0 0 0 0 SUN ELEVATION 0.00
SAUDI FILE 2 SAUDI ARABIA MOSAIC PATH 178 ROW 43 1011101 MPF BAND 7
STRETCH 0- 0.112- 0.132- 255 256- 299
NDS SAMPS 8BIT- NL 2340 NS 2404 FILE 2
17 93 IN U.S.G.S. FLAGSTAFF IMAGE PROCESSING FACILITY

Photo plate (7) Image 178/43 Data Base (contrast stretch) of band 7 showing :

1. Khashm Addughum Fault (E-F).
2. Some relatively clear approximate N-S lineaments if correlated with other types of images of the same scene.
   Notice the change in tonal contrast being sharper than Photo plates 6, 8, 9, 10,11.



SAUDI ARABIA MOSAIC PATH 178 ROW 43 SCENE ID 1171-06530 C
ERTS-0 EXPOSURE DATE 10-JAN-73 REV 0 C
SAUDI FILE 1 SAUDI MOSAIC DATABASE BAND 7 PATH 178 ROW 43
STRETCH1 0. 20 14. 20 36. 230 256. 256
NEG /SPOS BEIT NL 2340 NS 2563 FILE 1
21-AUG-79 08:18:00 U.S.G.S. FLAGSTAFF IMAGE PROCESSING FACILITY



SAUDI ARABIA MOSAIC PATH 178 ROW 43 SCENE ID 1171-06530 C
BRIS.D EXPOSURE DATE 10-JAN-73 REV 0 C
SA137 FILE 1 SAUDI ARABIA DATABASE BAND 7 PATH 178 ROW 43
STRETCH1 0- 20 14- 20 35-235 255-255
NEG 7SRAS 8BIT NL 2340 NS 2404 FILE 1
21-AUG-79 06:18:00 U.S.G.S. FLAGSTAFF IMAGE PROCESSING FACILITY

Photo plate (8) Image 178/43 S.p of band 7 showing :

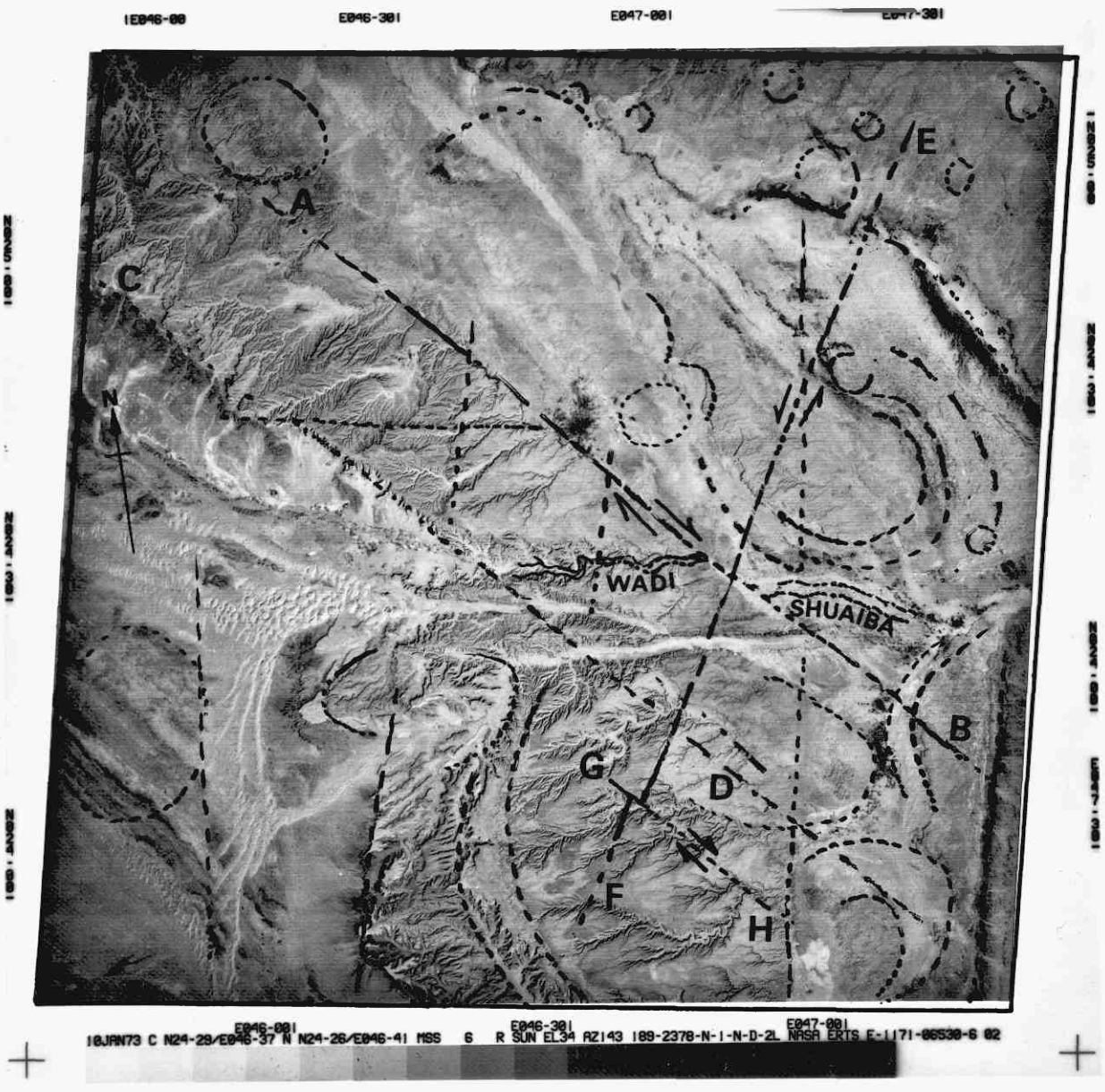
1. The stream capture (A) in the region of the Riyadh Tilted Block.
2. Some crescent-like shapes (arcuate features) with their openings facing opposite to the direction of tilting shown in area B.
3. Khashm Addughum Fault (E-F).
4. Wadi Awsat Graben displacement.


E046-00
E046-301
E047-001
E047-301
A
B
A
B
E
A
N
WADI AWSAT
F
E046-001
E046-301
E047-001
10JAN73 C N24-29/E046-37 N N24-26/E046-41 MSS 7 R SUN EL34 AZ143 189-2378-N-1-N-D-1L NASA ERTS E-1171-08538-7 02


1E046-00
E046-301
E047-001
E047-301
E046-001
E046-301
E047-001
10JAN73 C N24-29/E046-37 N N24-26/E046-41 MSS 7 R SUN EL34 AZ143 189-2378-N-1-N-D-IL NASA ERTS E-1171-06530-7 02

Photo plate (9) Image 178/43 S.p of band 6 showing :

1. Displacement of Wadi Shuaiba by the A-B fault of the Riyadh Fault System.
2. Khashm Addughum Fault (E-F).
3. Riyadh Tilted Block and the faults bordering it (A-B), (C-D).
4. The southern part of the fault (E-F) possess clear tonal contrast on both sides if correlated with Photo plates 10, 11 and it is displaced by a relatively smaller fault (G-H).


E046-00
E046-301
E047-001
E047-301
A
C
E
N
WADI
SHUAIBA
B
G
D
F
H
E046-001
E046-301
E047-001
18JAN73 C N24-29/E046-37 N N24-26/E046-41 MSS 6 R SUN EL34 AZ143 189-2378-N-1-N-D-2L NASA ERTS E-1171-08530-6 02

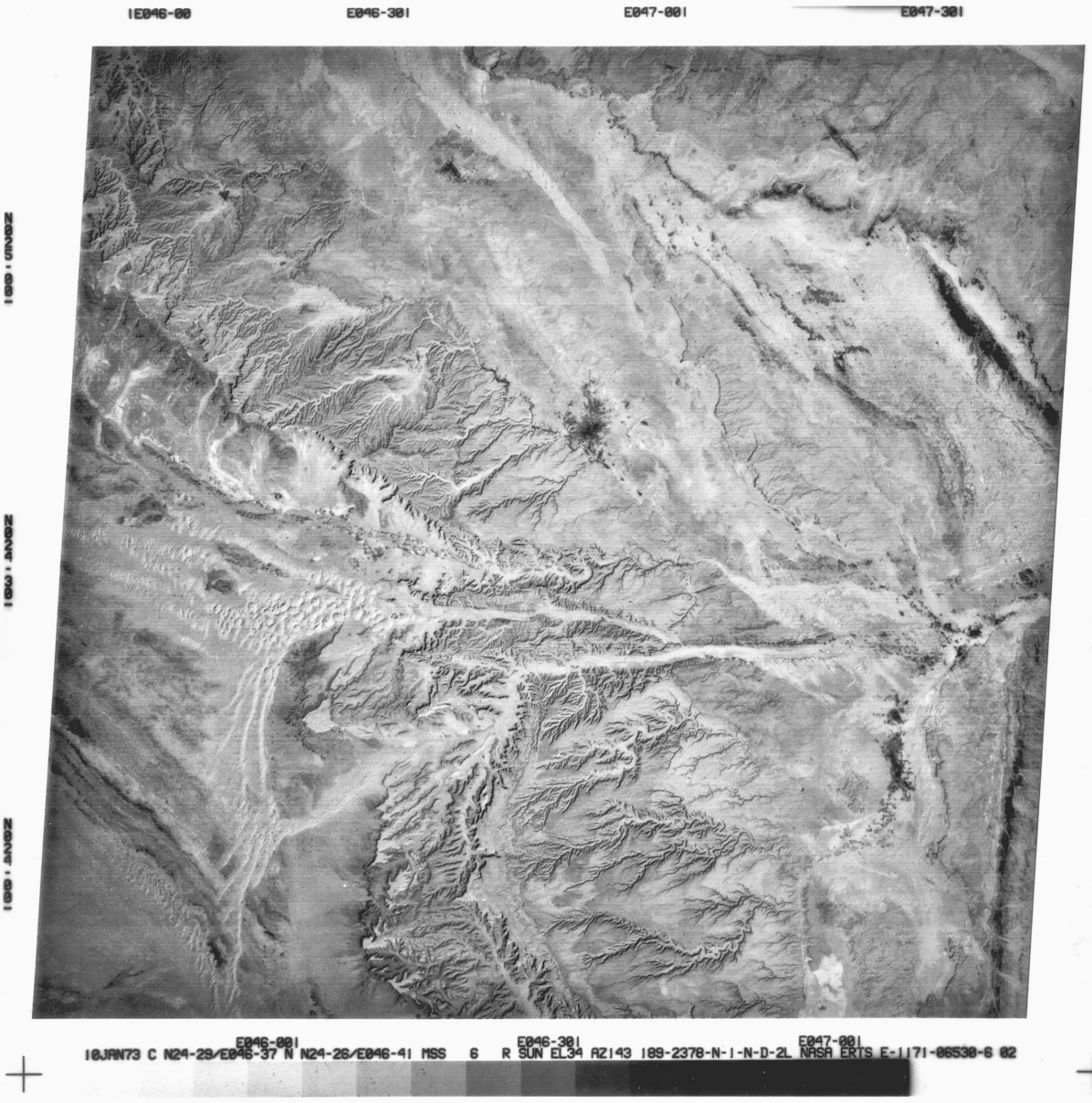
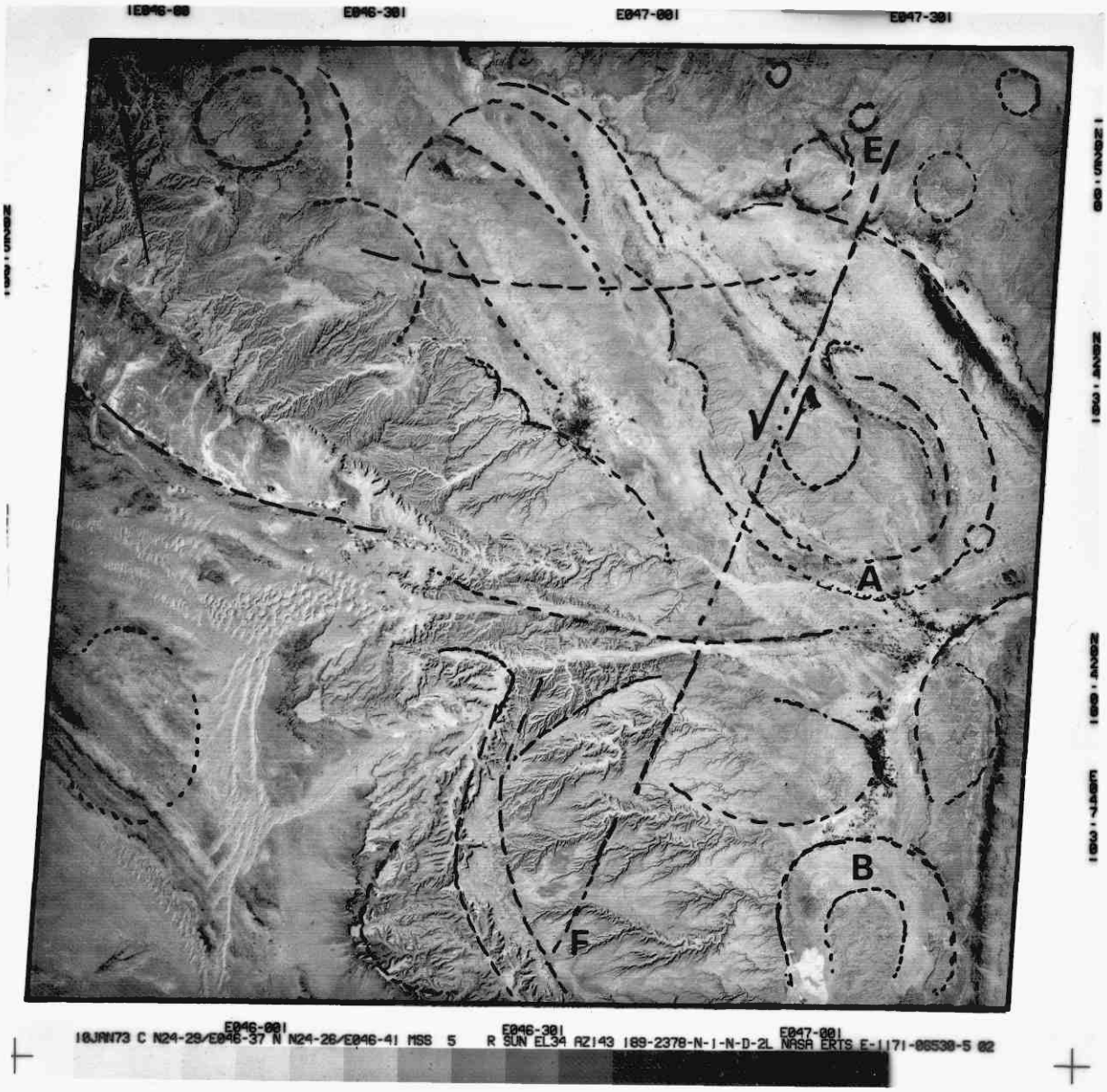

1E046-00
E046-301
E047-001
E047-301
E046-001
E046-301
E047-001
10JAN73 C N24-29/E046-37 N N24-26/E046-41 MSS 6 R SUN EL34 AZ143 189-2378-N-1-N-D-2L NASA ERTS E-1171-06530-6 02

Photo plate (10) Image 178/43 S.p of band 5 showing :

1. Some circular features of different sizes.
2. Long arcuate features
3. Khashm Addughum Fault (E-F).
4. Some of the circular features are represented by two circles inside each other (A and B).


E046-00
E046-301
E047-001
E047-301
E
A
B
F
E046-001
18JAN73 C N24-29/E046-37 N N24-26/E046-41 MSS 5
E046-301
R SUN EL34 AZ143 189-2378-N-1-N-D-2L
E047-001
NASA ERTS E-1171-08530-5 02

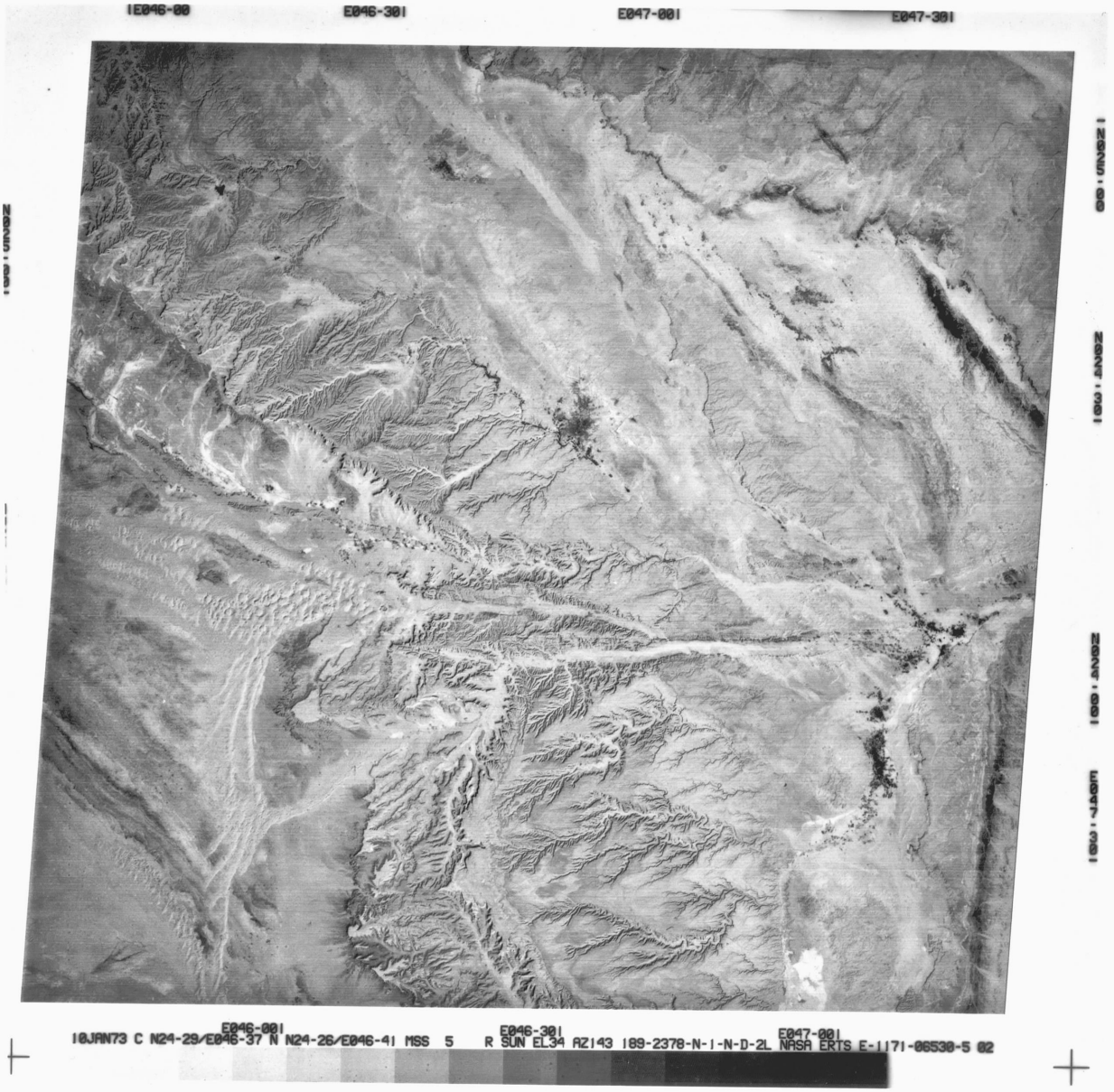
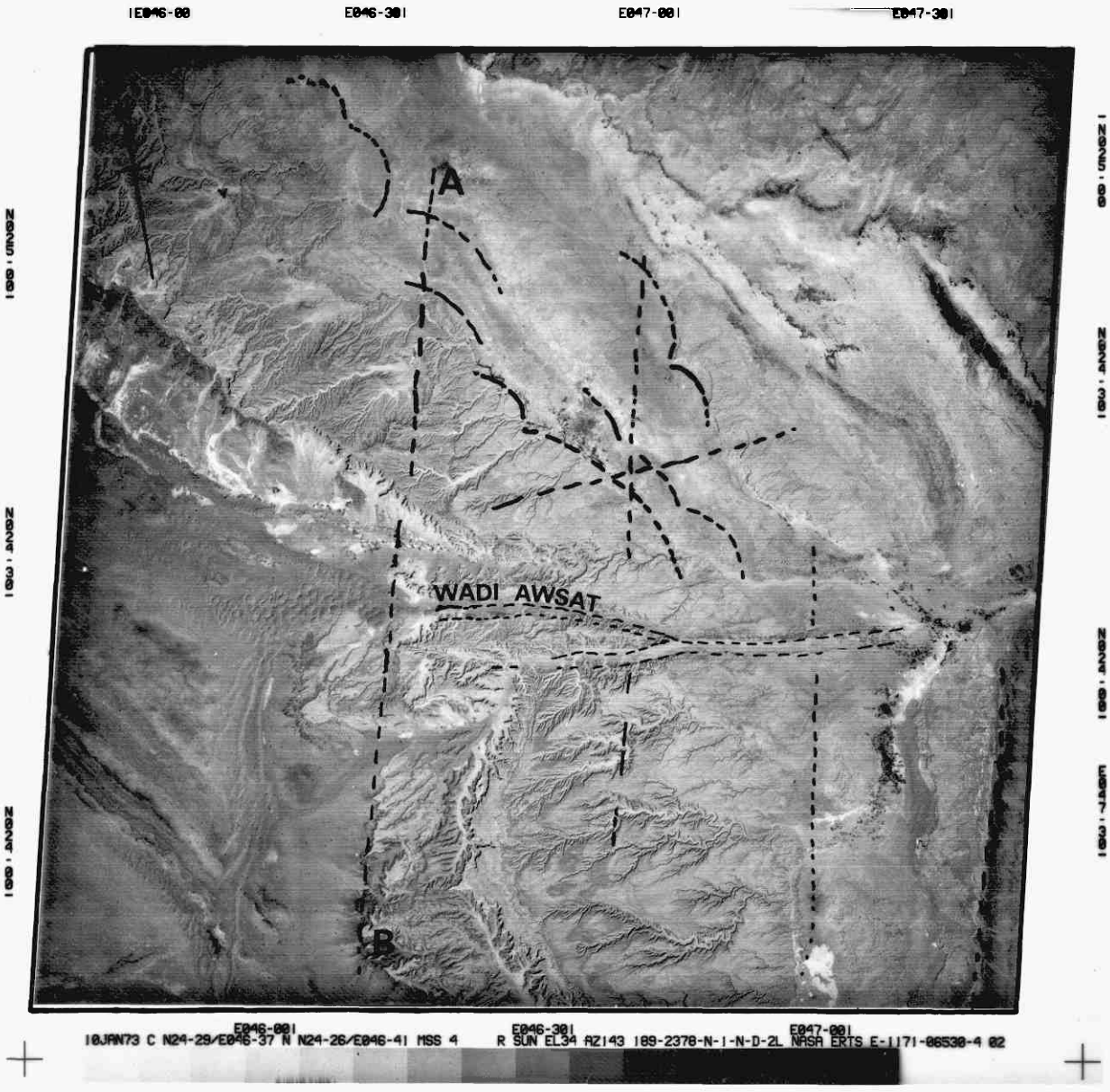

1E046-00
E046-301
E047-001
E047-301
18JAN73 C N24-29/E046-37 N N24-26/E046-41 MSS 5
E046-001
R SUN EL34 AZ143 189-2378-N-1-N-D-2L
E046-301
E047-001
NASA ERTS E-1171-06530-5 02

Photo plate (11) Image 178/43 S.p of band 4 showing :

1. Some of the approximate N-S lineaments where lineament A-B is relatively more clearer.
2. Crescent-like small arcuate features facing the Riyadh Tilted Block.
3. Displacement of the Awsat Graben is not shown on this image (for details see Photo plate 12).
4. The tonal contrast between white and black areas is minimally related to other bands, shown on Photo plate 8, 9.


E046-00
E046-30
E047-00
E047-30
A
WADI AWSAT
B
E046-00
E046-30
E047-00
10JAN73 C N24-29/E046-37 N N24-26/E046-41 MSS 4
R SUN EL34 AZ143 189-2378-N-1-N-D-2L NASA ERTS E-1171-08530-4 02

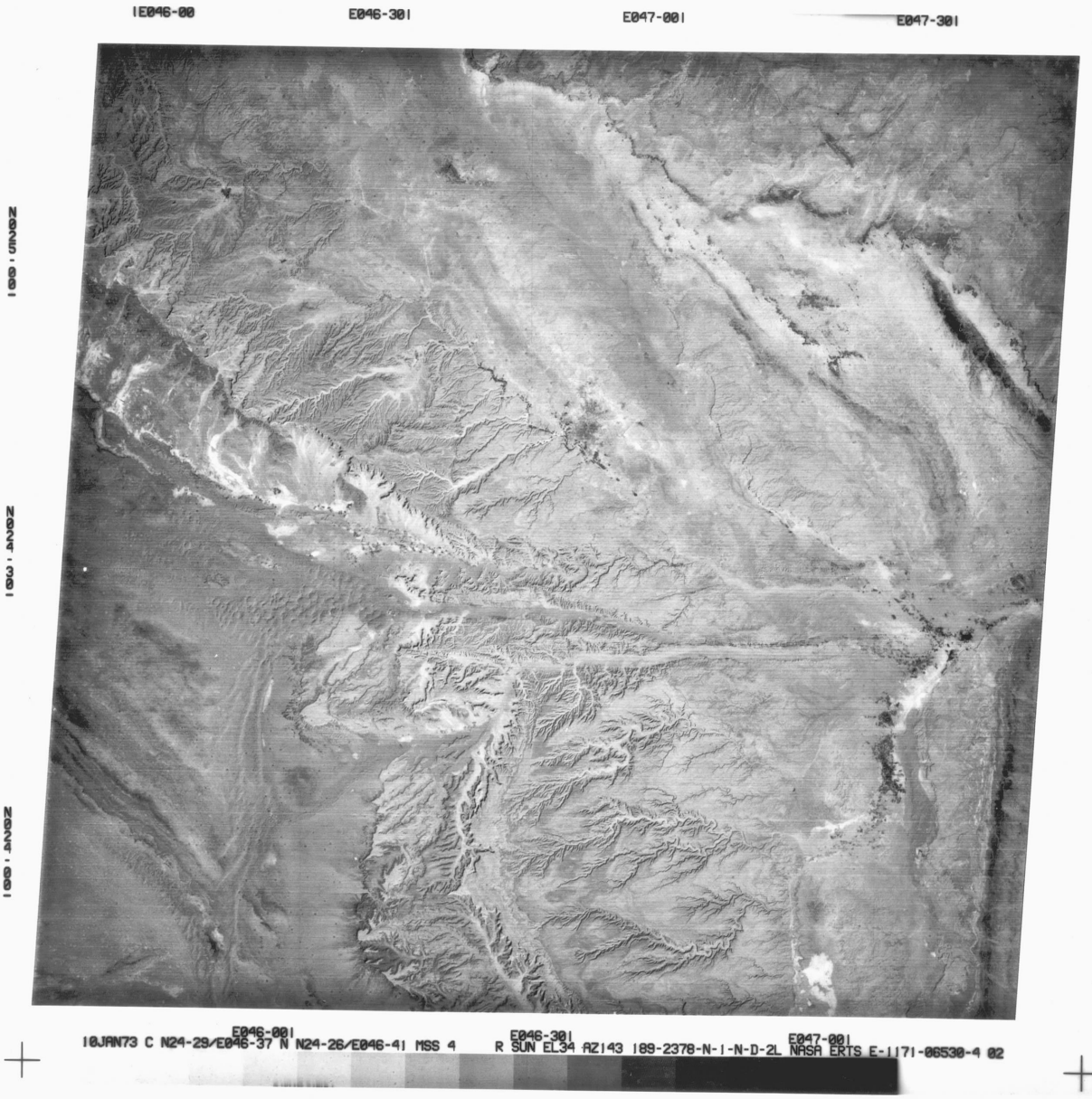
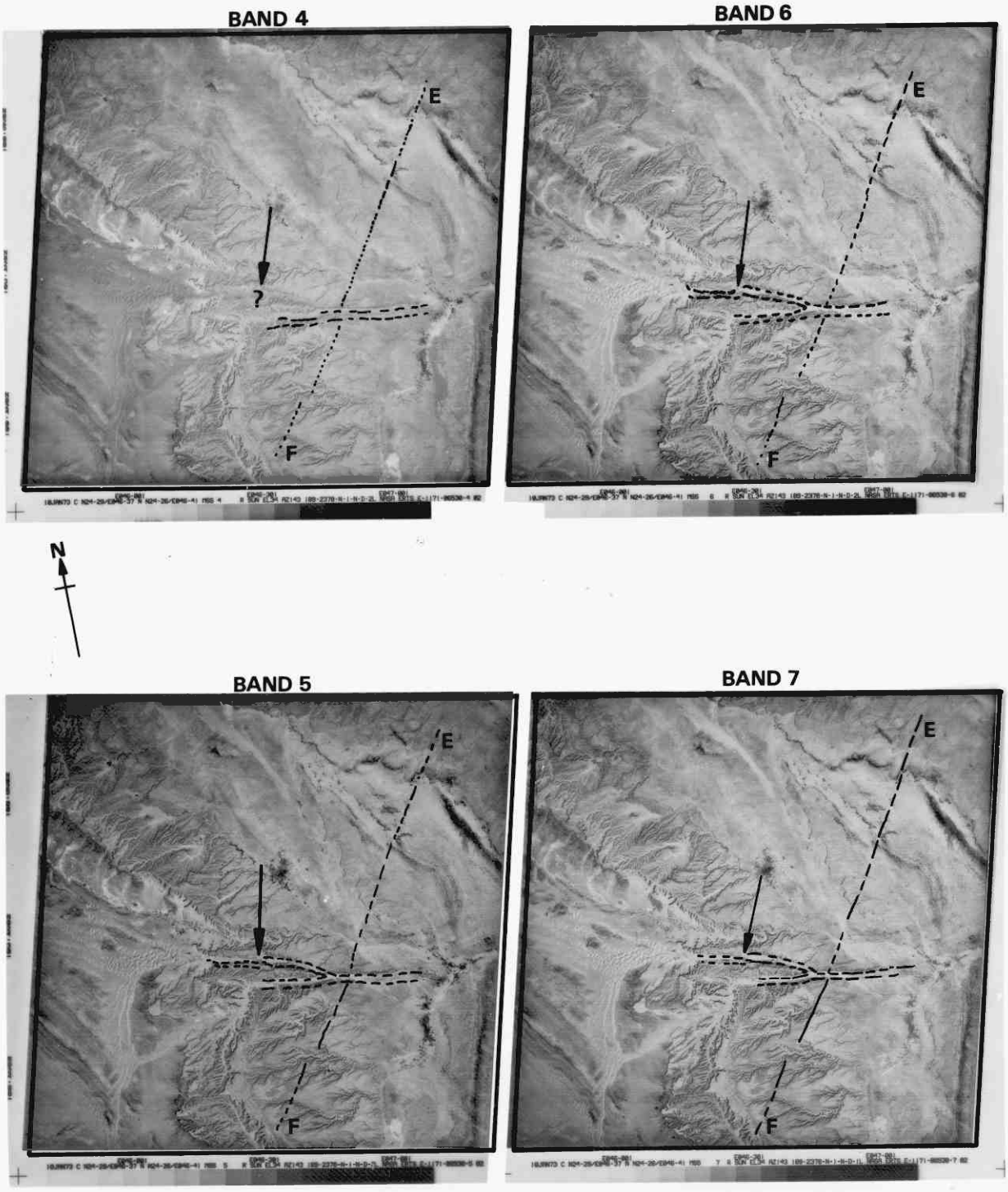

1E046-00
E046-301
E047-001
E047-301
10JAN73 C N24-29/E046-37 N N24-26/E046-41 MSS 4
E046-001
E046-301
R SUN EL34 AZ143 189-2378-N-1-N-D-2L
E047-001
NASA ERTS E-1171-06530-4 02

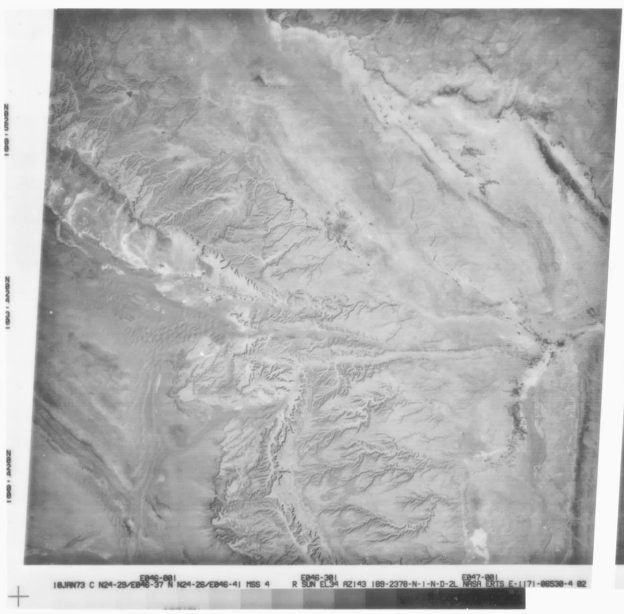
Photo plate (12) Images of scene 178/43 (Riyadh area) of S.p bands 4, 5, 6 and 7 exposed in the wet season, approximate scale 1:4,000,000

Bands 7, 6 and to a lesser extent 5, show the Wadi Awsat Graben and its displacement (shown by arrows) as well as the drainage pattern of the Riyadh Tilted Block in various degrees of clarity.

Band 4 failed to show these features clear enough especially the displacement of Wadi Awsat Graben. The variations in detectability are mainly due to differences in sensitivity of the various MSS bands (wave lengths) to moisture content (water) along the course of these features (please refer to Sections 2.4.2 and 3.5.1.2 in text).

Notice the tonal differences on both sides of the southern part of the E-F fault in the different bands.


BAND 4
BAND 6
BAND 5
BAND 7
E
F
?
N


E046-08|
E046-38|
E047-08|
18JAN73 C N24-25/E046-37 N N24-26/E046-41 MSS 4 R SUN EL34 AZ143 189-2378-N-1-N-D-2L NASA ERTS E-1171-08538-4 82


E046-08|
E046-38|
E047-08|
18JAN73 C N24-25/E046-37 N N24-26/E046-41 MSS 6 R SUN EL34 AZ143 189-2378-N-1-N-D-2L NASA ERTS E-1171-08538-6 82


E046-08|
E046-38|
E047-08|
18JAN73 C N24-25/E046-37 N N24-26/E046-41 MSS 5 R SUN EL34 AZ143 189-2378-N-1-N-D-2L NASA ERTS E-1171-08538-5 82

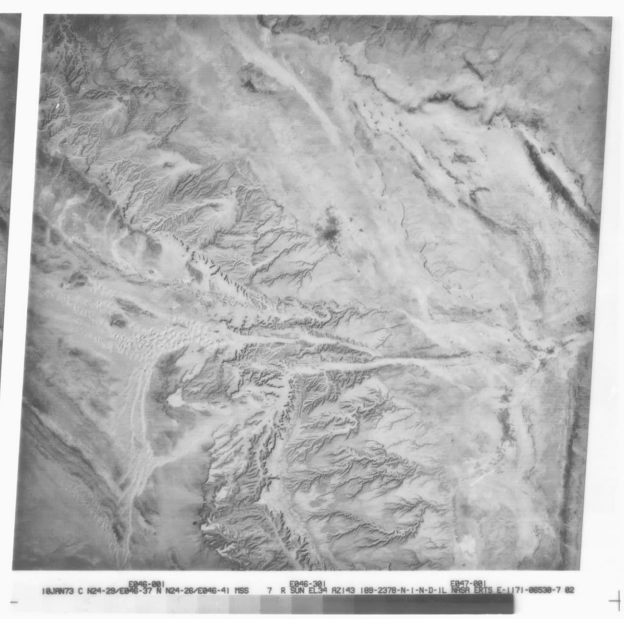

E046-08|
E046-38|
E047-08|
18JAN73 C N24-25/E046-37 N N24-26/E046-41 MSS 7 R SUN EL34 AZ143 189-2378-N-1-N-D-1L NASA ERTS E-1171-08538-7 82

Photo plate (12.A) Image 178/43 Negative print of band 7

Included for correlation with the other images of the same scene (Riyadh Area) Photo plates from 6 - 12. Most of the structures can also be observed on this type of image with varying degrees of clarity.

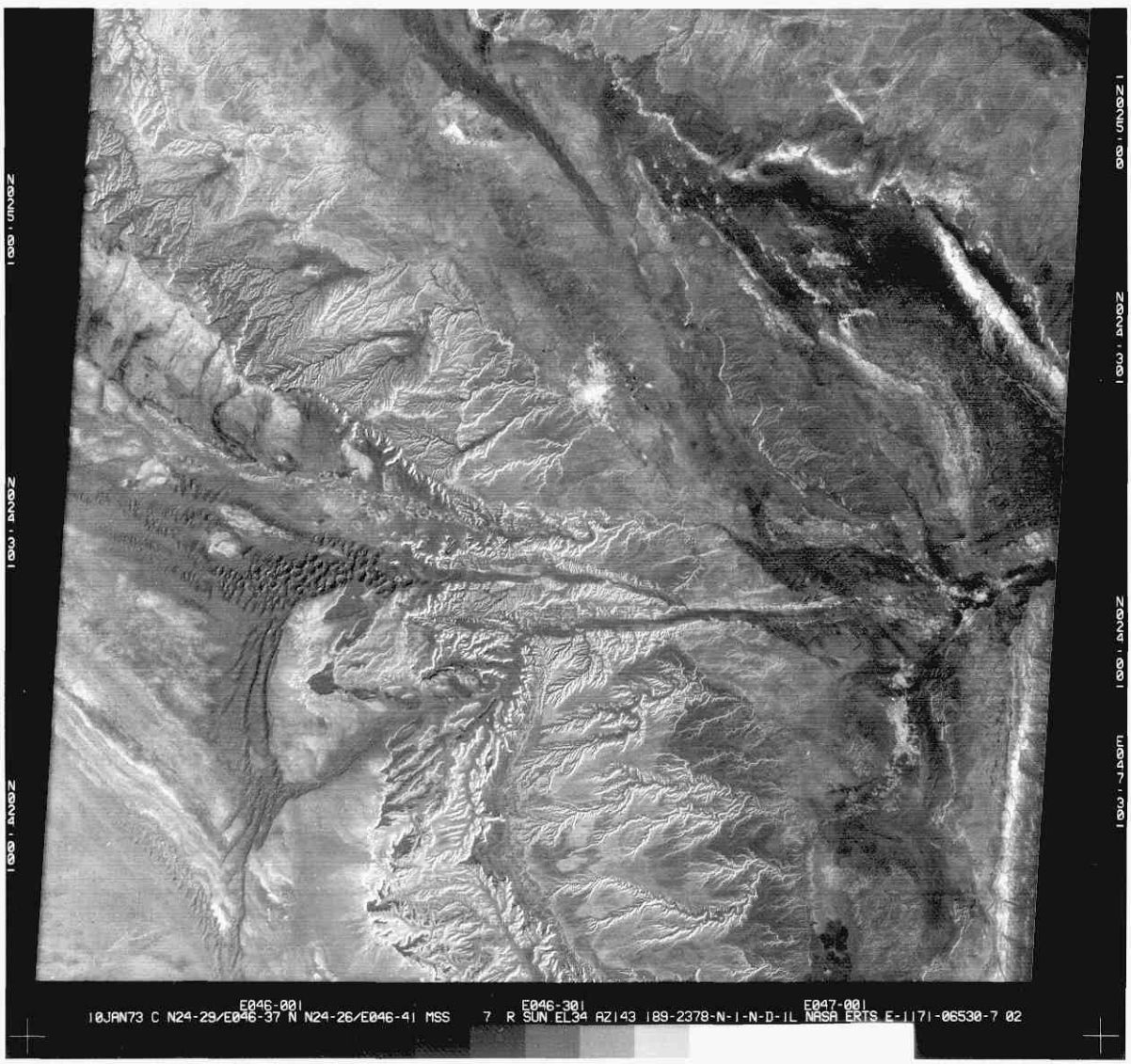
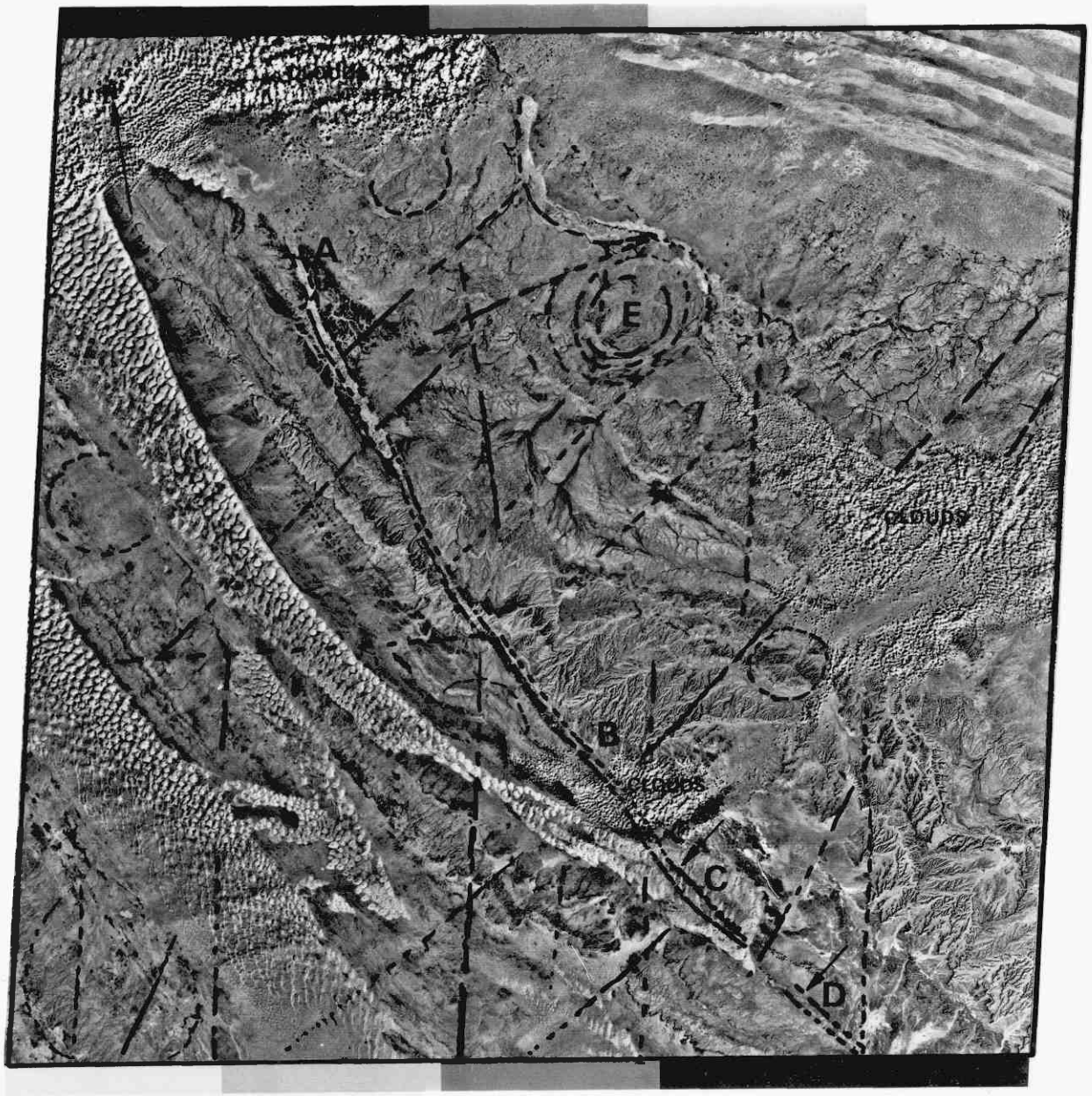
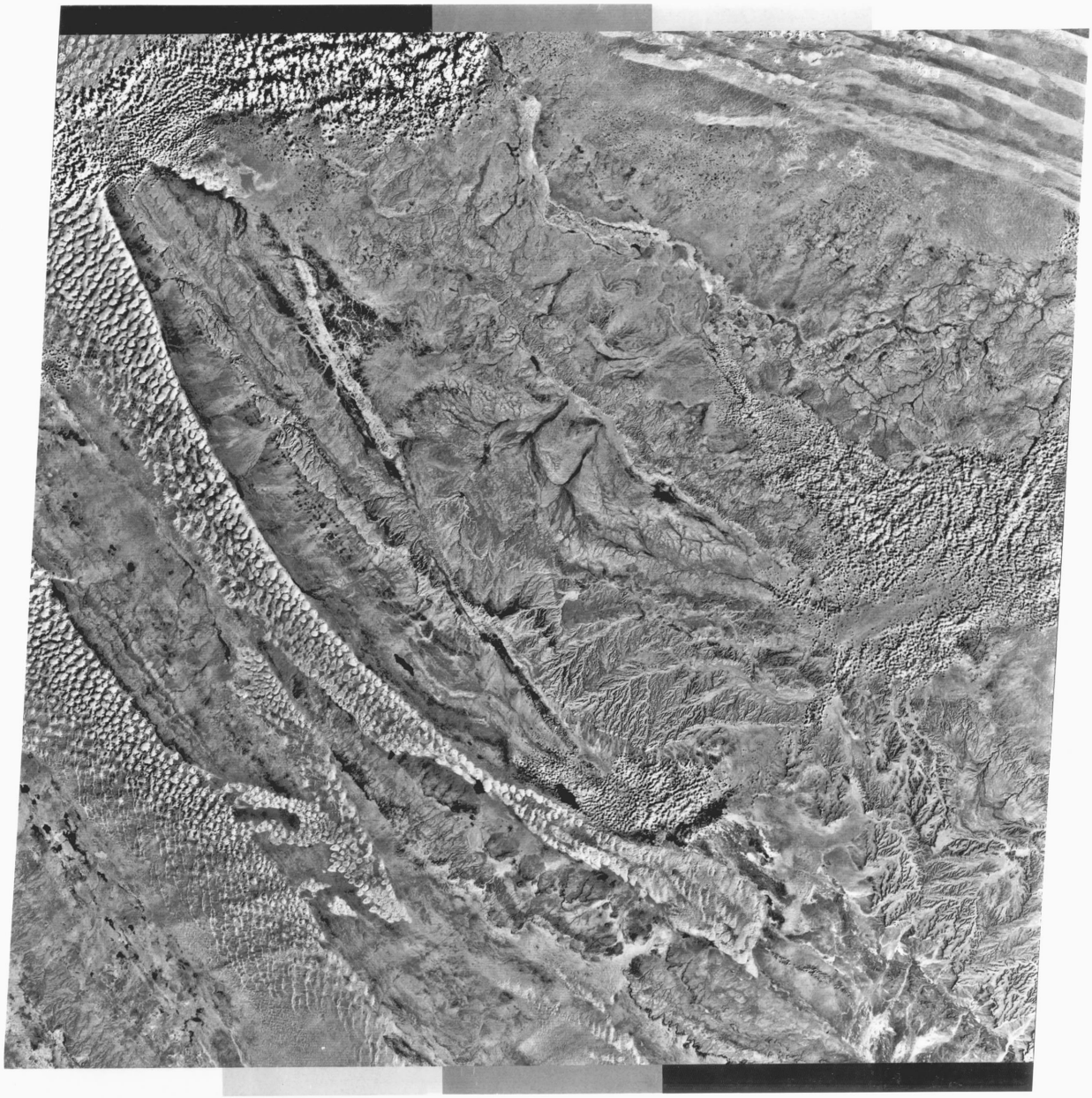

E046-001
10JAN73 C N24-29/E046-37 N N24-26/E046-41 MSS
E046-301
7 R SUN EL34 AZ143 189-2378-N-1-N-D-1L NASA ERTS E-1171-06530-7 02
E047-001

Photo plate (13) Image 179/42 Ce_2 of band 7 showing :

1. The Majma'ah Graben (A-B).
2. Part of Barrah Graben (D).
3. The possible continuation of both Majma'ah and Burrah Grabens as propagated through the sand cover in area (C).
4. Himar-Sabha domal feature (E).
5. Some circular features of different sizes.
6. A few approximate N-S lineaments.
7. Some NE lineaments of the Riyadh Fault System .
8. Clouds of approximately 20% coverage over Khashm Al-Haqaqa and Al-Majma'ah Graben.



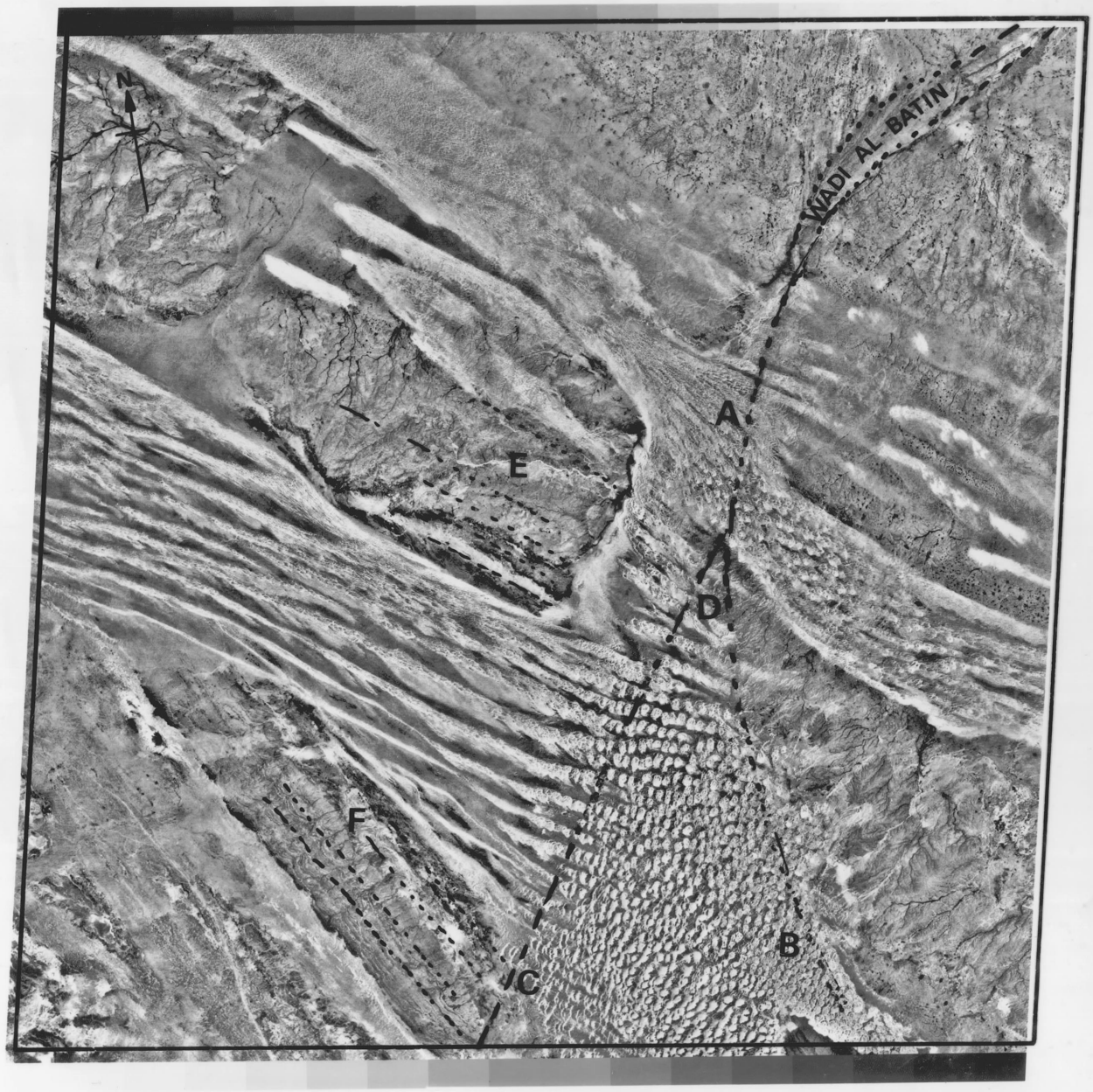
SAUDI ARABIA MOSAIC PATH 179 ROW 42 SCENE ID 1136-06585
SR14 U EXPOSURE DATE 8-DEC-72 REV 11
SR226 FILE 2 SAUDI ARABIA MOSAIC PATH 179 ROW 42 101X101 HPF BAND 7
STRETCH 0- 20 102- 20 182- 238 255- 295
SEV 1 SUN EL 01:17 AZ 2340 NS 3265 FILE 2
18-JUN-78 17 51 58 U.S.G.S. FLAGSTAFF IMAGE PROCESSING FACILITY



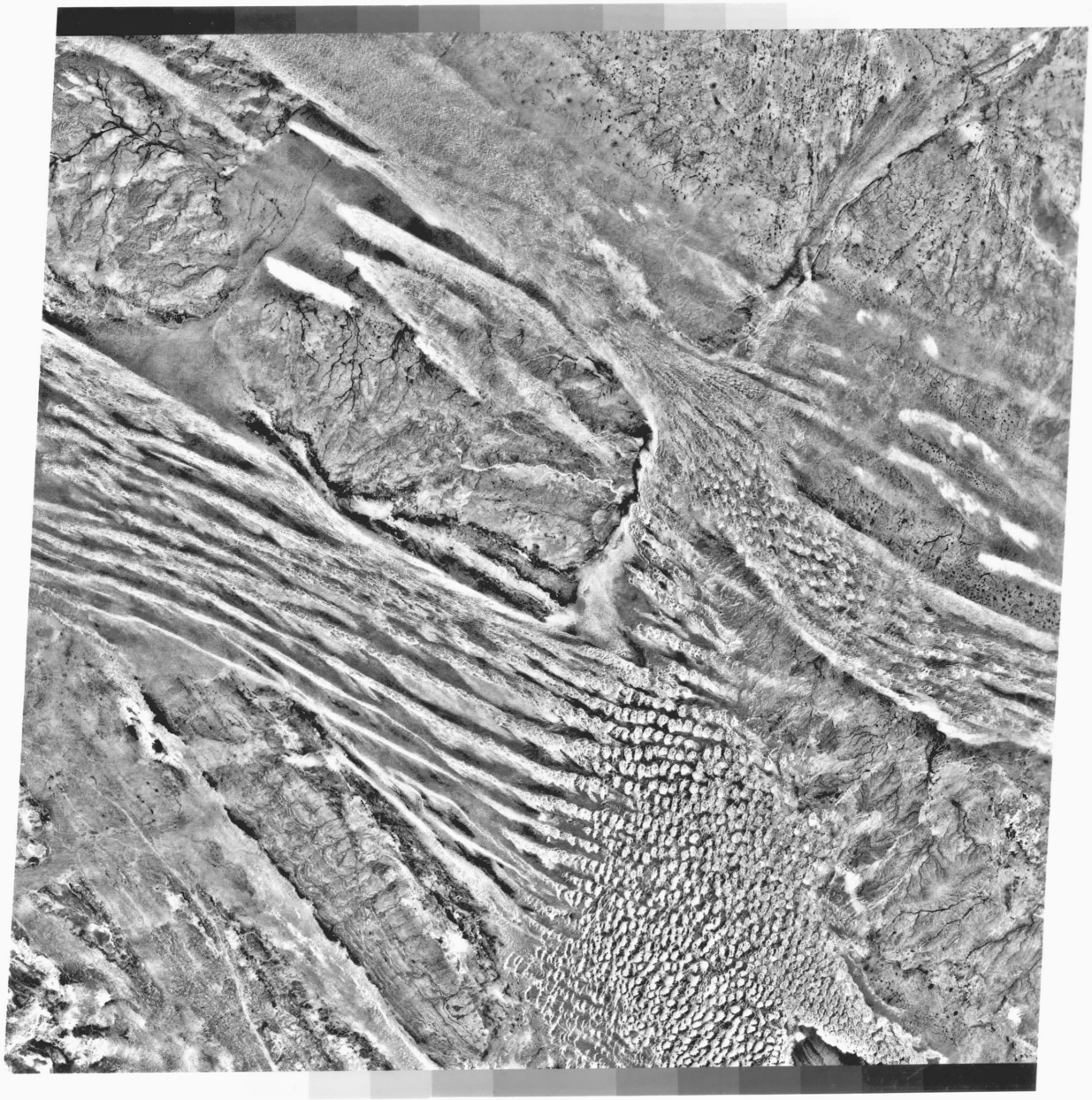
SAUDI ARABIA MOSAIC PATH 179 ROW 42 SCENE ID 1136-06585 C
BITS 0 EXPOSURE DATE 6-DEC-72 REV 0 C
IMAGE FILE 2 SAUDI ARABIA MOSAIC PATH 179 ROW 42 101X101 HPF BAND 7
STRETCH 0- 20 102- 20 154-235 255-235
WEG 75R6S 8BIT NL 2340 NS 2482 FILE 2
18-JUN-78 17 51 58 U.S.G.S. FLAGSTAFF IMAGE PROCESSING FACILITY

Photo plate (14) Image 180/41 Ce_1 of band 7 showing :

1. The SW end of Wadi Al-Batin.
2. The Al-Hamudiyah arcuate lineament (A-B) which allow the connection of Wadi Al-Batin to Al-Majma'ah Graben end of C.A.G.T.S to form the East Arabian Block.
3. Al-Hamudiyah straight NE lineament (C-D) possibly representing a subsurface failure zone with negative physiographic nature. Its clear effect on the distribution and texture of sand dunes on both sides is well shown (sands cover 30 - 40% of the area).
4. Convergence of the strike in the Aruma Formation (E) and the Jilh Formation (F). The last two points substantiate its structural significance.



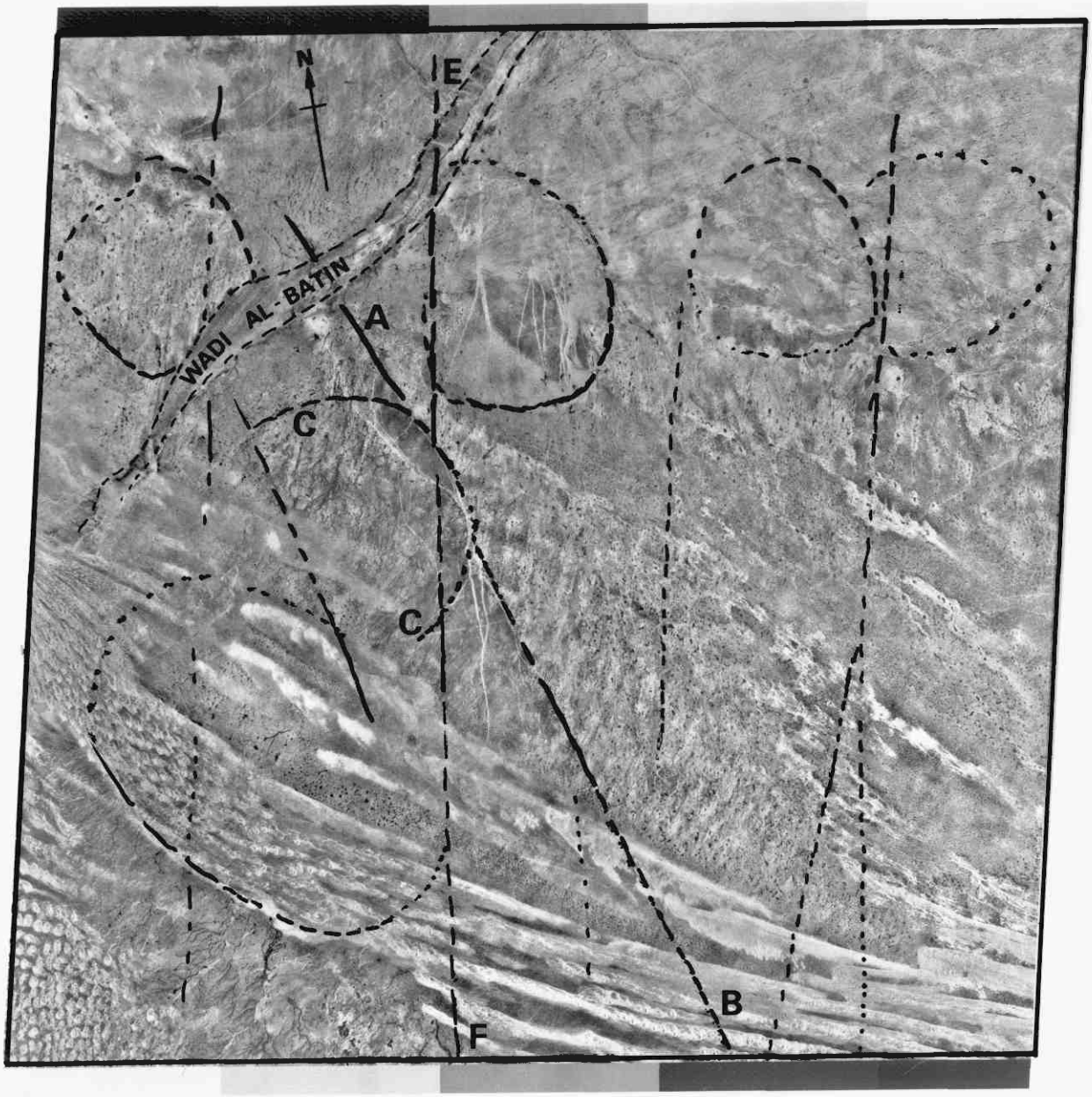
SAUDI ARABIA MOSAIC PATH 180 ROW 41 SCENE ID 1083-07033 C
BYTE 0 EXPOSURE DATE 14-OCT-72 REV 0 C
SC288 FILE 2 SAUDI ARABIA PATH 180 ROW 41 BAND 7 101X101 HPF
STRETCH: 0- 112- 0 142-255 255-255
460 75PRS 7TRACK 8BIT 800BPI FILE 2 NL 2340 NS 2480
04-JUN-80 00:05:08 U.S.G.S. FLAGSTAFF IMAGE PROCESSING FACILITY



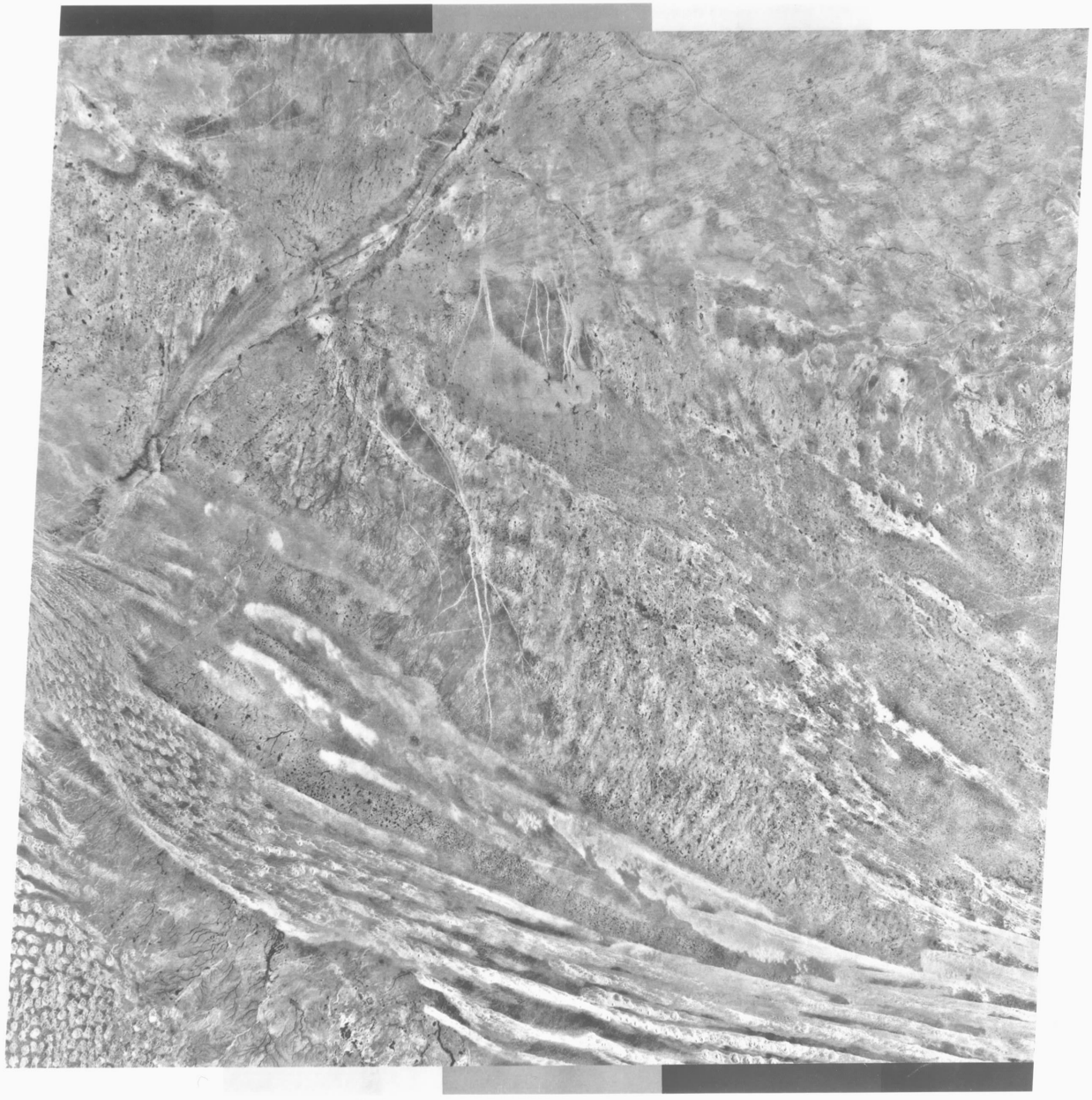
SAUDI ARABIA MOSAIC PATH 180 ROW 41 SCENE ID 1083-07033 C
BITS 0 EXPOSURE DATE 14-OCT-72 REV 0 C
IMAGE FILE 2 SAUDI ARABIA PATH 180 ROW 41 BAND 7 101X101 HPF
STRETCH 0= 0.112- 0.142=255 255=255
MAG 75RAS 7TRACK 8BIT 800BPI FILE 2 NL 2340 NS 2480
04-JUN-80 00:05:08 U.S.G.S. FLAGSTAFF IMAGE PROCESSING FACILITY

Photo plate (15) Image 179/41 Ce_2 of band 7 showing :

1. Some semi-circular-elliptical features.
2. A NW lineament (A-B) has followed part of a pre-existing arcuate feature (C) before it straightened again to cross Wadi Al-Batin.
3. Some approximate N-S periodically spaced lineaments.



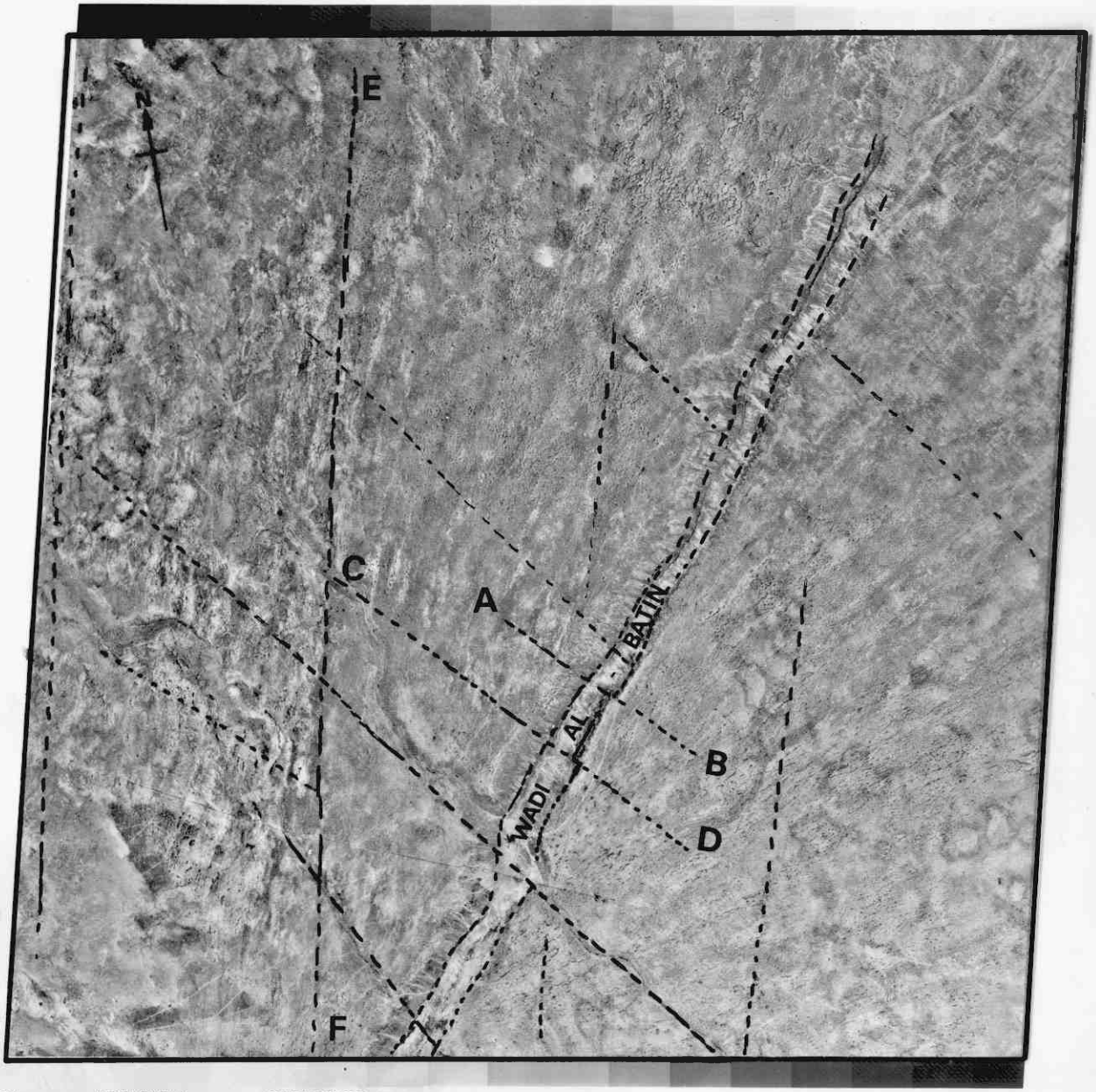
SAUDI ARABIA MOSAIC PATH 179 ROW 41 SCENE ID 1370-06574
EROS FILE 2 EXPOSURE DATE 28-JUL-73 PRODUCT ID
SAUDI ARABIA MOSAIC PATH 179 ROW 41 BAND 7 101X101 HPF
ATRACK 35
NEDHS FILE 2
16-JUL-76 23 13 59 U.S.G.S. FLAGSTAFF IMAGE PROCESSING FACILITY



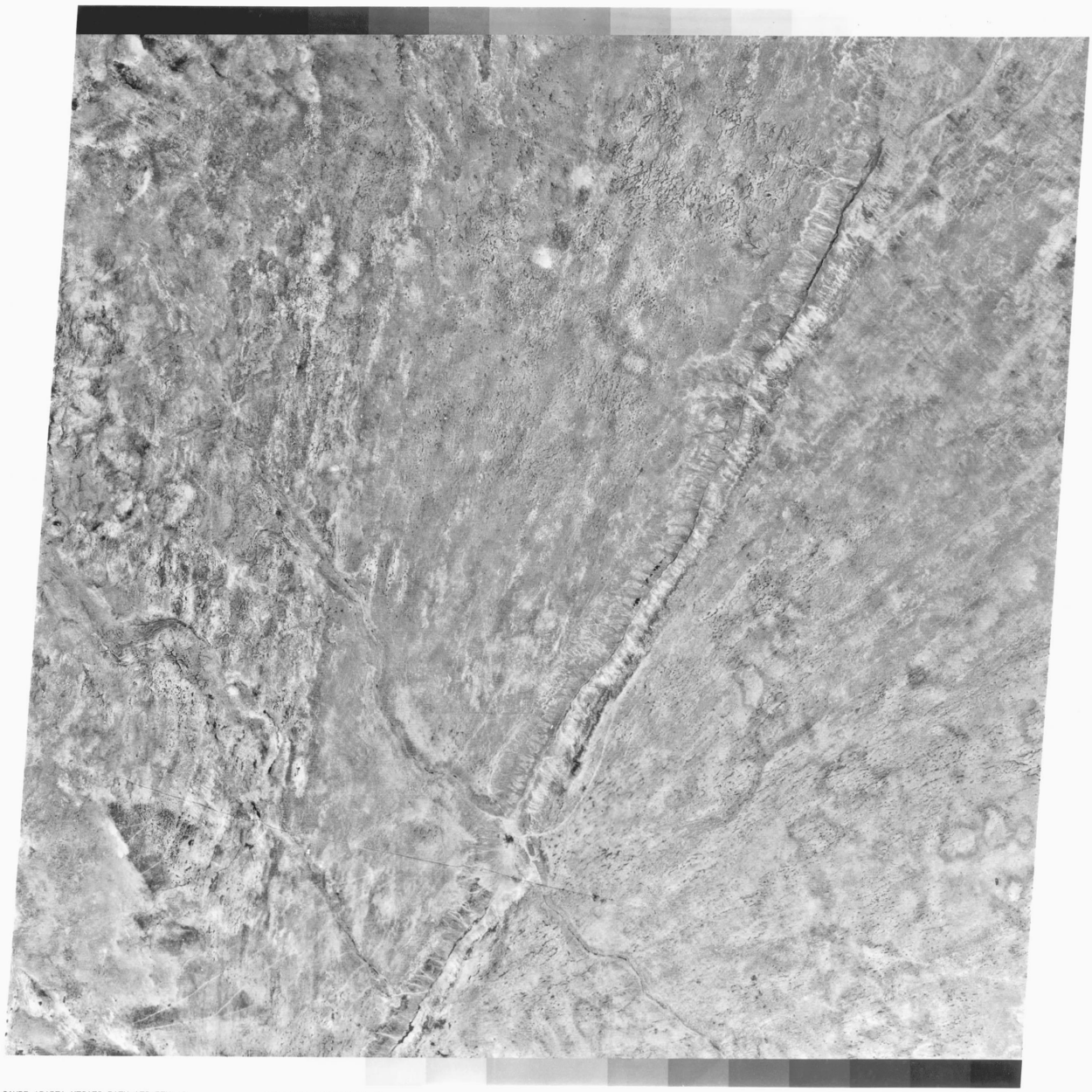
SAUDI ARABIA MOSAIC PATH 179 ROW 41 SCENE ID 1370-06574 C
BRIS-O EXPOSURE DATE 28-JA-73 REV 0 C
SAUDI FILE 2 SAUDI ARABIA MOSAIC PATH 179 ROW 41 BAND 7 101X101 HPF
STRETCH O- 20 102- 20 452-235 255-235
NEG 75R6S 8B1T NL 2340 NS 2480 FILE 2
16-JUL-78 23 13 58 U.S.G.S. FLAGSTAFF IMAGE PROCESSING FACILITY

Photo plate (16) Image 179/40 Ce_2 of band 7 showing :

1. The main part of the almost straight and NE trending Wadi Al-Batin.
2. Some NW lineaments cutting across the Wadi where two of them (A-B), (C-D) are displacing the Neogene rocks of the Wadi.
3. Some approximate N-S periodically spaced lineaments with different degree of clarity. The clearest is E-F. More evidence of this clarity is shown on Image 179/41 (Photo plate 15) which overlaps with 15%. The extension of the same lineament E-F if connected on both images will indicate a total length of approximately 300 kms.



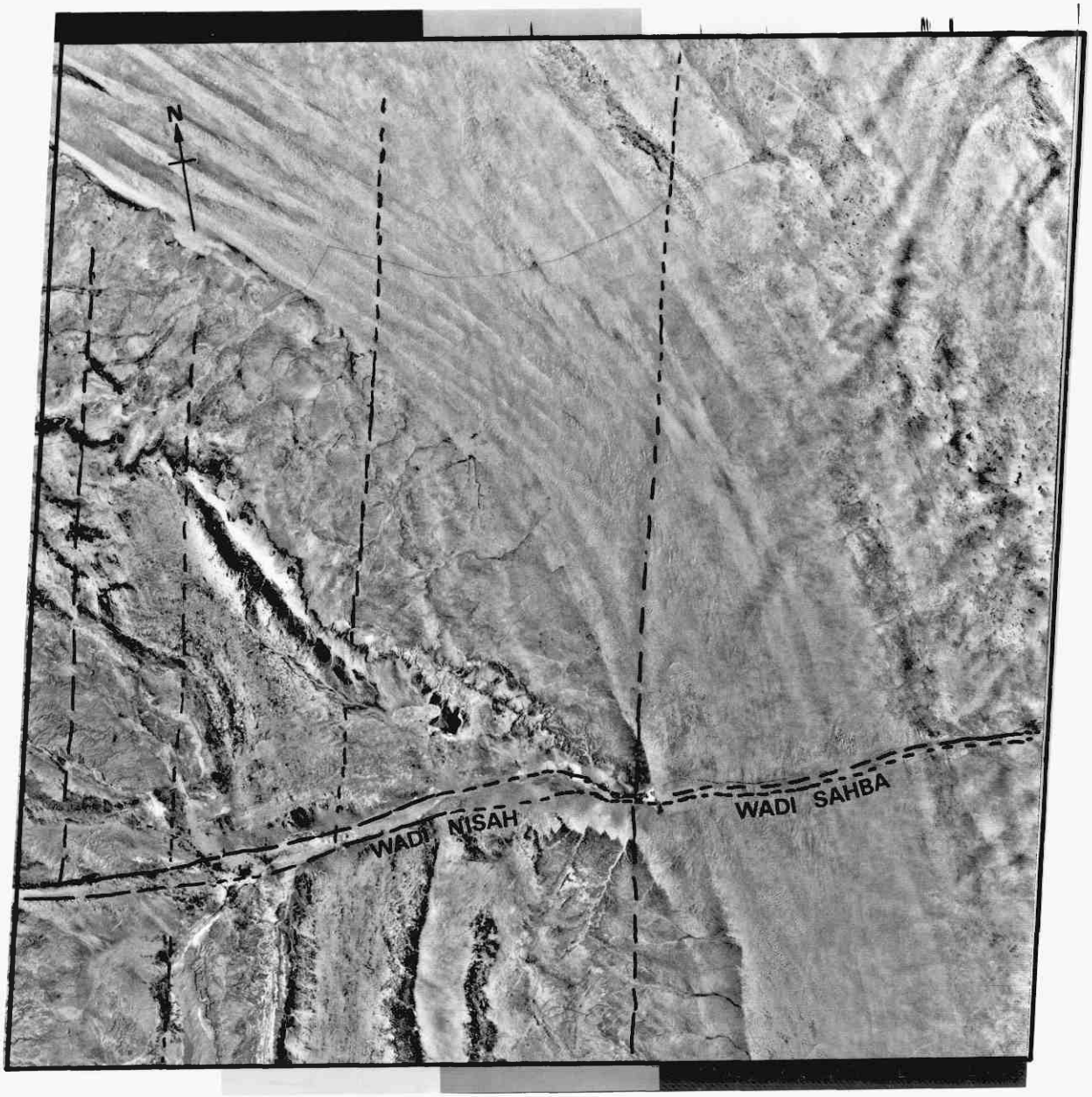
SAUDI ARABIA MOSAIC PATH 179 ROW 40 SCENE ID 1370-08571 C
BAND 1 WAVELENGTH DATE 28-JUL-73 PATH 0 ROW 0 C
SAUDI FILE 2 SAUDI ARABIA PATH 179 ROW 40 BAND 7 101X101 MAP
STRETCH: L= 6 U= 102 CO 152-238 235-245
NDC FORM: BIT NL 2340 NS 2478 FILE 2
15-DEC-79 14:40:07 U.S.G.S. FLAGSTAFF IMAGE PROCESSING FACILITY



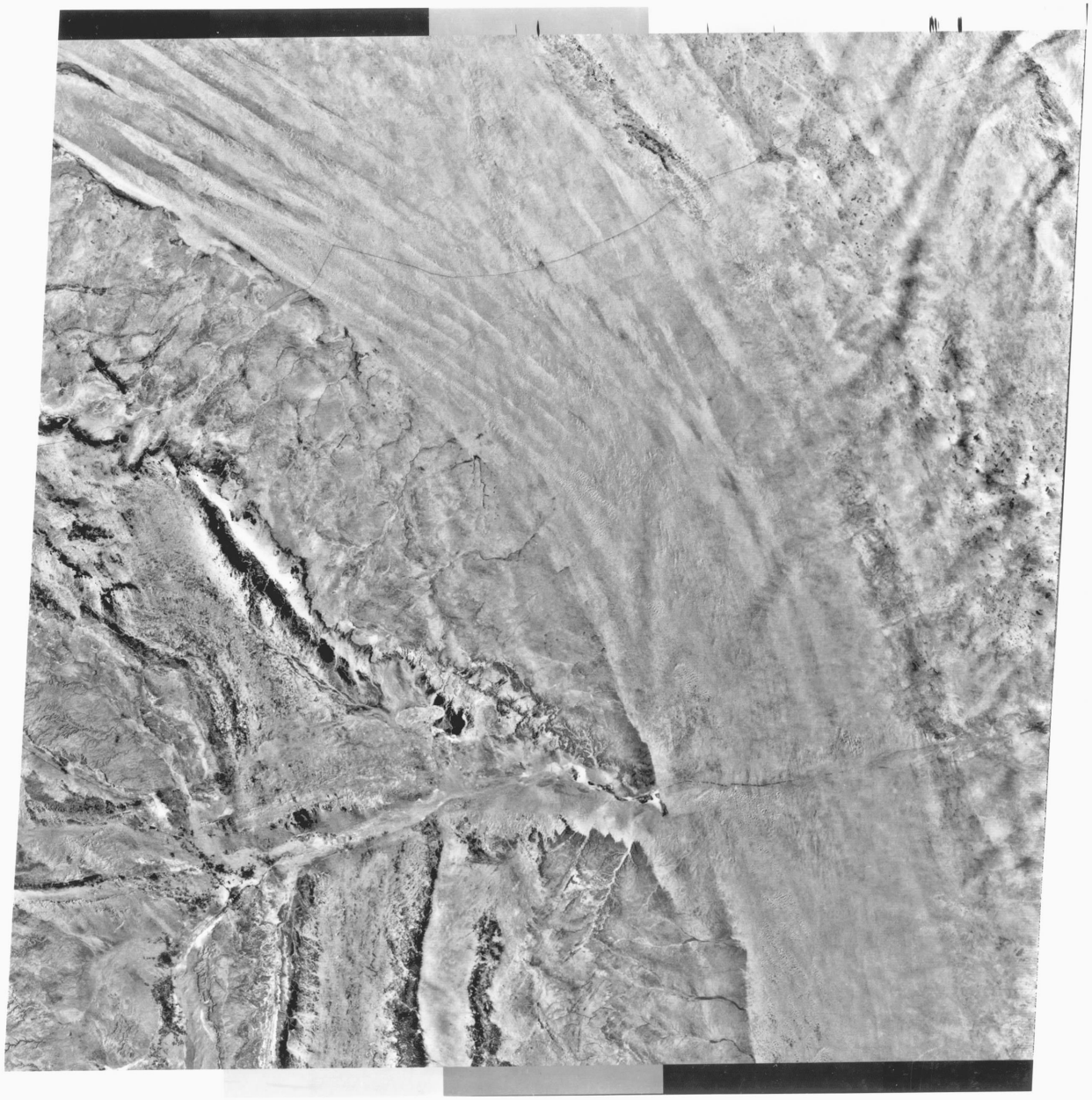
SAUDI ARABIA MOSAIC PATH 179 ROW 40 SCENE ID 1370-06571 C
EBYE 1 EXPOSURE DATE 28 JUL 73 PATH 0 ROW 0 C
XRBS1 FILE_2 SAUDI ARABIA PATH 179 ROW 40 BAND 7 101X101 HPF
STRETCH: Q= 20 102= 20 152=235 255=235
NDC 7SR8S 8BIT NL 2340 NS 2428 FILE_2
15-DEC-79 14:40:07 U.S.G.S. FLAGSTAFF IMAGE PROCESSING FACILITY

Photo plate (17) Image 177/43 Ce_2 of band 7 showing :

1. The extension of Wadi Nisah Graben to join Wadi Sahba to the east (part of the C.A.G.T.S).
2. Some approximate N-S lineaments.



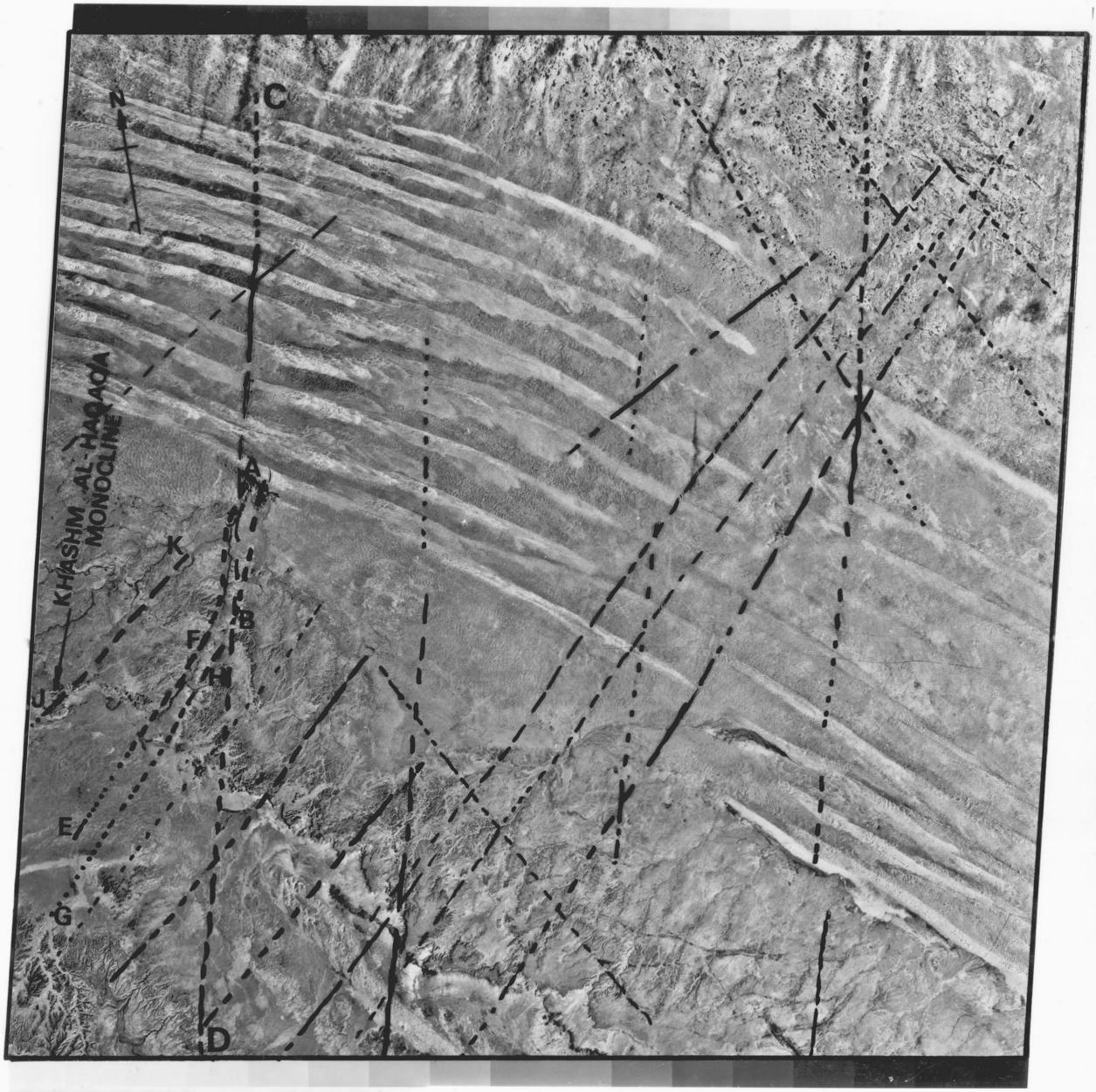
SAUDI ARABIA MOSAIC PATH 177 ROW 43 SCENE ID 10422-0646 C
ERTS 1 EXPOSURE DATE 18-SEP-73 REV 0 C
SKIDO FILE 2 SAUDI ARABIA MOSAIC PATH 177 ROW 43 101X101 HPF BAND 7
STRETCH 0- 20 102- 20 142- 238 255- 235
NEG 75095 6811 NL 2340 NS 2484 FILE 2
11-AUG-78 22 28 46 U.S.G.S. FLAGSTAFF IMAGE PROCESSING FACILITY



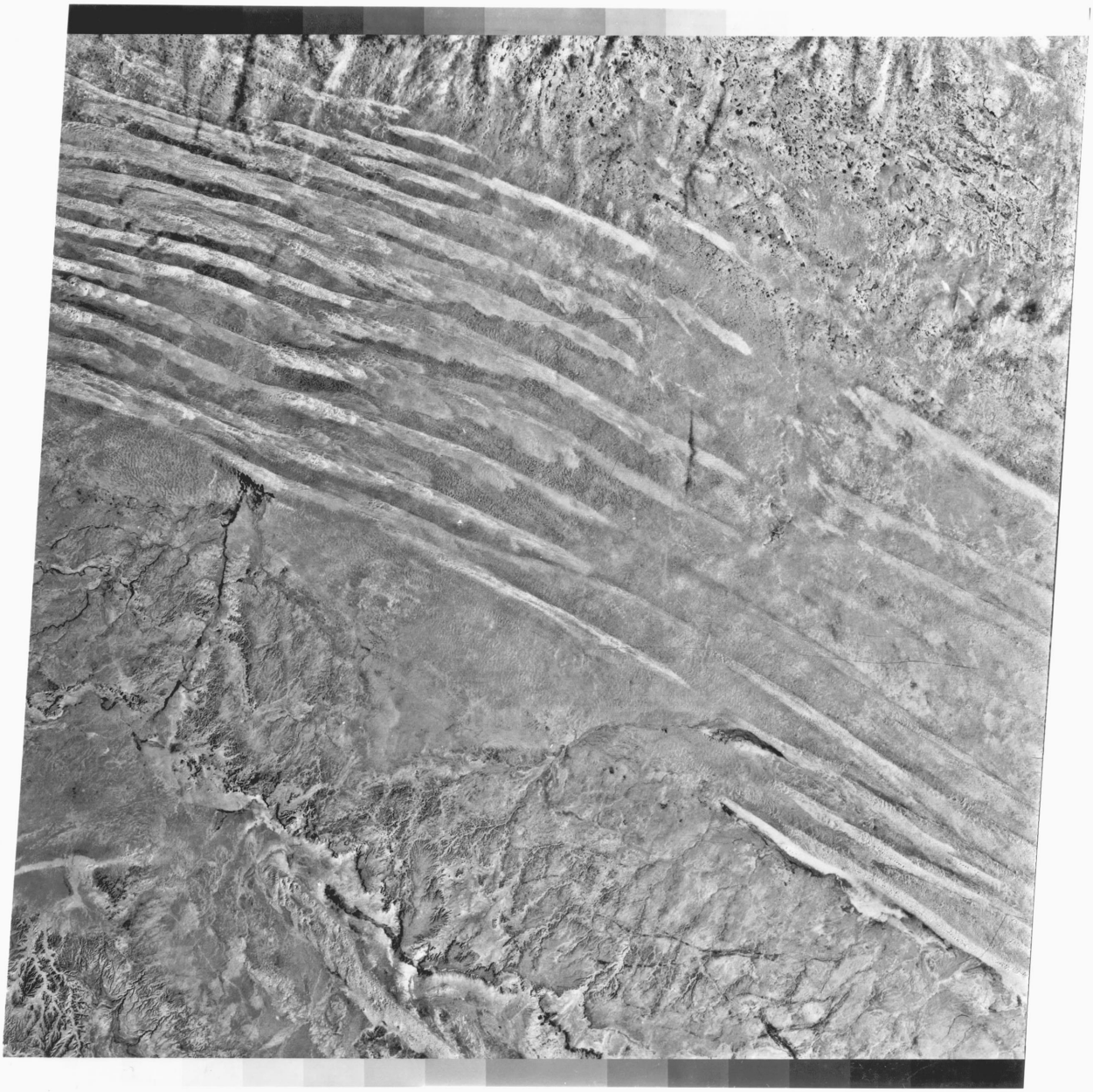
SAUDI ARABIA MOSAIC PATH 177 ROW 43 SCENE ID 10422-0646 C
ERTS 1 EXPOSURE DATE 18-SEP-73 REV 0 C
SK303 FILE 2 SAUDI ARABIA MOSAIC PATH 177 ROW 43 101X101 HPF BAND 7
STRETCH 0- 20 102- 20 152-235 255-235
NES 2560 8BIT NL 2340 NS 2384 FILE 2
11-AUG-78 22 28 46 U.S.G.S. FLAGSTAFF IMAGE PROCESSING FACILITY

Photo plate (18) Image 178/42 Ce_2 of band 7 showing :

1. Wadi Al-Atk segments.
2. The first segment (A-B) is almost controlled by an approximate N-S lineament (C-D).
3. The second segment is bounded by two NE lineaments (E-F) and (G-H).
4. Part of Khashm Al-Haqaqa lineament (J-K) controlling a main drainage tributary.
5. Some NE and NW lineaments of the Riyadh Fault System
6. Some approximate N-S lineaments.



SAUDI ARABIA MOSAIC PATH 178 ROW 42 SCENE ID 10171-0652 C
SITS 1 EXPOSURE DATE 10-JAN-73 PATH 178 ROW 42 C
VERSZ FILE 2 SAUDI ARABIA PATH 178 ROW 42 BAND 7 101X101 HPF
STRETCH1 0- 20 102- 20 132-235 255-235
VDC 75DAS 8BIT NL 2340 NS 2482 FILE 2
15-DEC-78 15:03:30 U.S.G.S. FLAGSTAFF IMAGE PROCESSING FACILITY



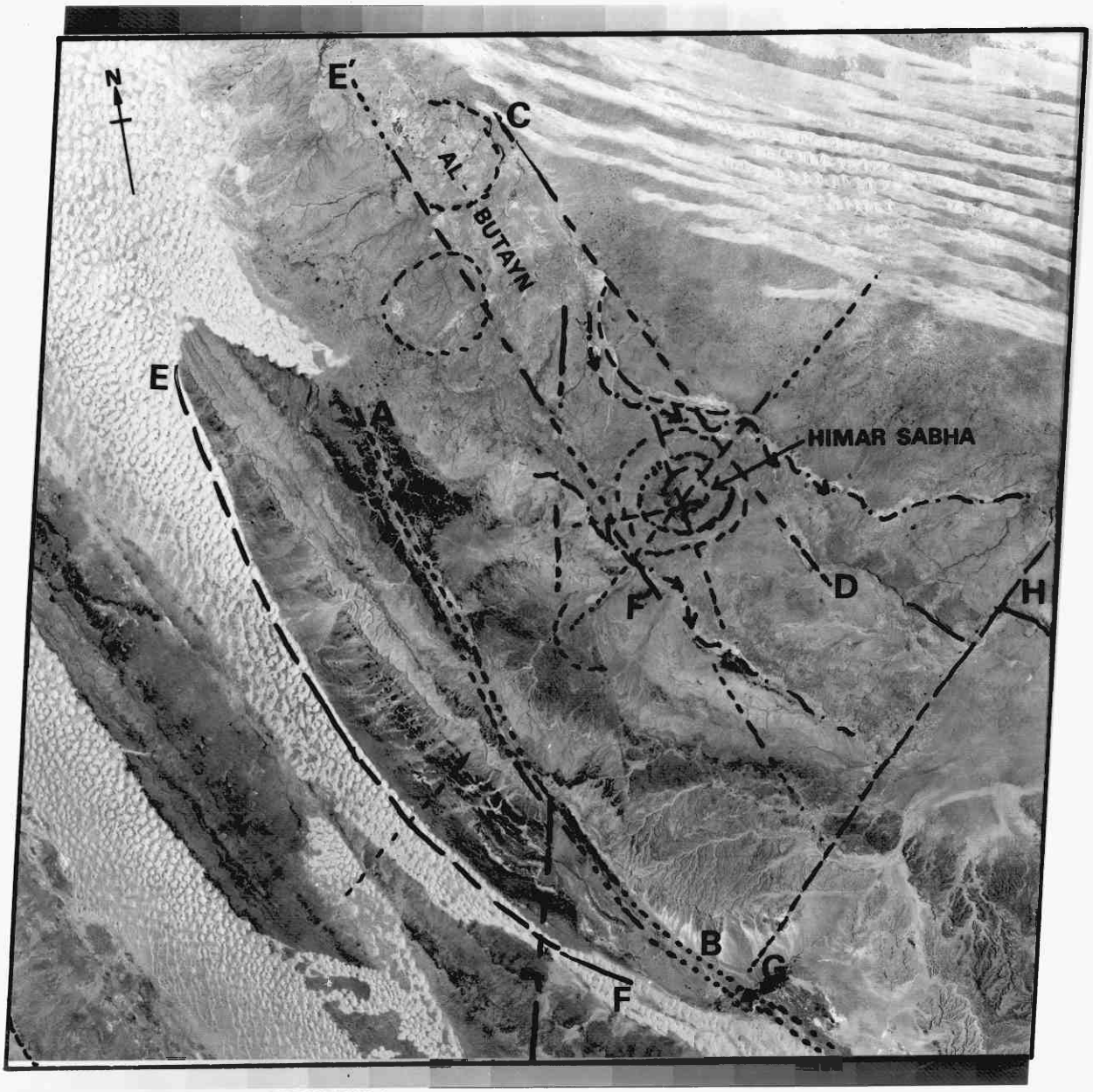
SAUDI ARABIA MOSAIC PATH 178 ROW 42 SCENE ID 10171-0652 C
SITS 1 EXPOSURE DATE 10-JAN-73 PATH 178 ROW 42 C
IMAGE FILE 2 SAUDI ARABIA PATH 178 ROW 42 BAND 7 101X101 HPF
STRETCH1 0- 20 102- 20 152-235 255-235
IMAGE 2560S 8BIT NL 2340 NS 2482 FILE 2
15-DEC-78 15:03:30 U.S.G.S. FLAGSTAFF IMAGE PROCESSING FACILITY

Photo plate (19) Image 179/42 Data base (Contrast stretch of band 7) showing :

1. Two NW lineaments (C-D), (E-F) bounding the Himar Sabha- Al-Butayn structure.
2. The main drainage in the area (wadis) deviate around Himar Sabha which shows lineaments of radial pattern.
3. Majma'ah Graben (A-B).
4. Part of Khashm Al-Haqaqa Fault (G-H)

   The last two areas are free of cloud coverage shown on Photo plate (13). because of the difference in the exposure dates of the two images.
5. The long arcuate feature of the Tuwaiq Escarpment (E-F) cutting the Aruma strike at its extremeties E and F.
6. This image (data base) and the image 179/42 Ce_2 were exposed with almost one year interval as a result they are not covering exactly the same ground area. This is due to Satellite Orbit Decay.

   (Exposure dates are shown on each image).



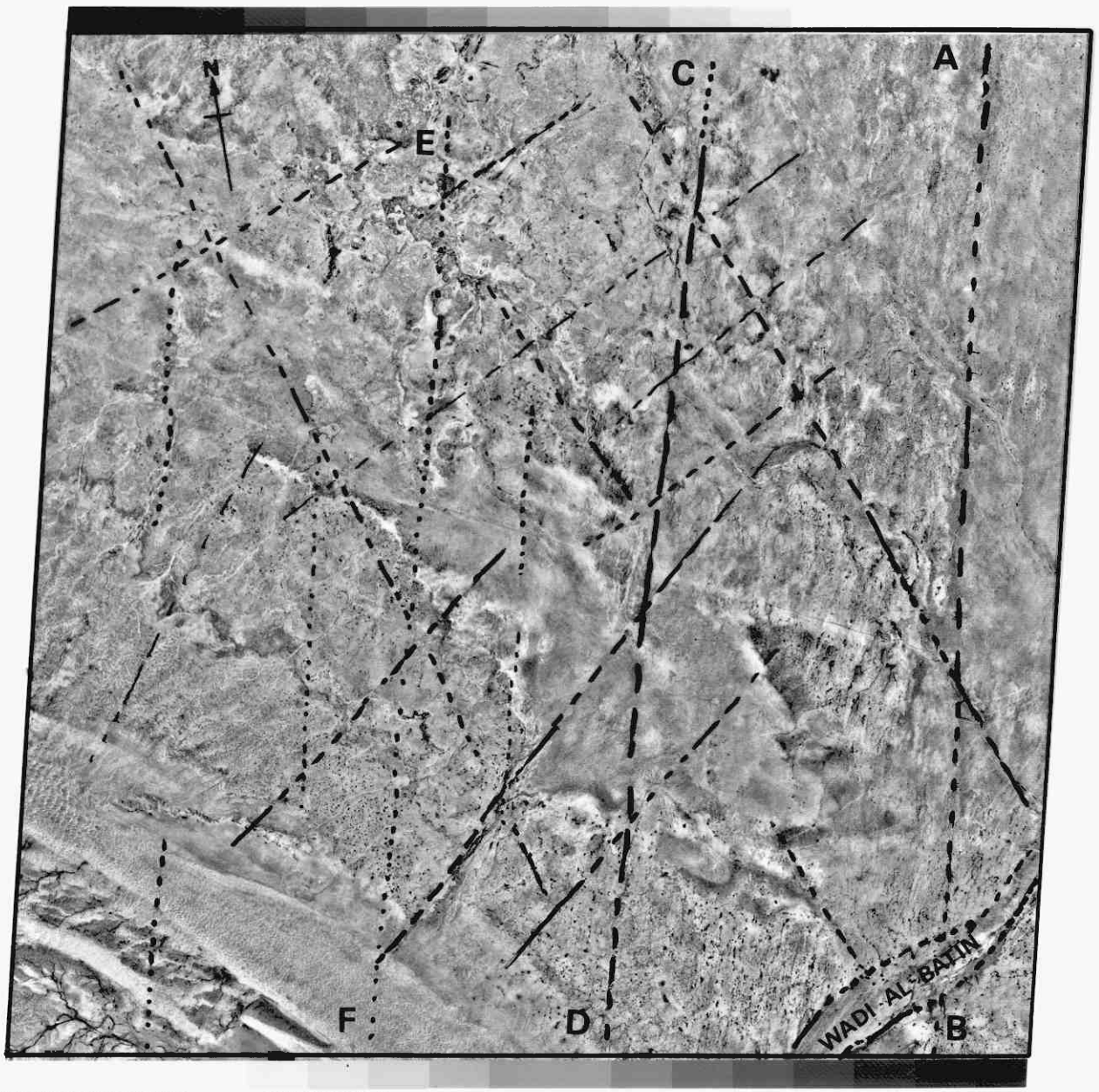
SAUDI ARABIA MOSAIC PATH 179 ROW 42 SCENE ID 10370-0858 C
ORIG 1 EXPOSURE DATE 28-JUL-73 PATH 179 ROW 42 C
30696 FILE 1 SAUDI ARABIA DATABASE BAND 7 PATH 179 ROW 42
LITBTCHI 0- 20 27- 20 54-235 208-235
NEG 75RQS 8BIT ML 2340 NS 2402 FILE 1
13-SEP-79 21:25:16 U.S.G.S. FLAGSTAFF IMAGE PROCESSING FACILITY



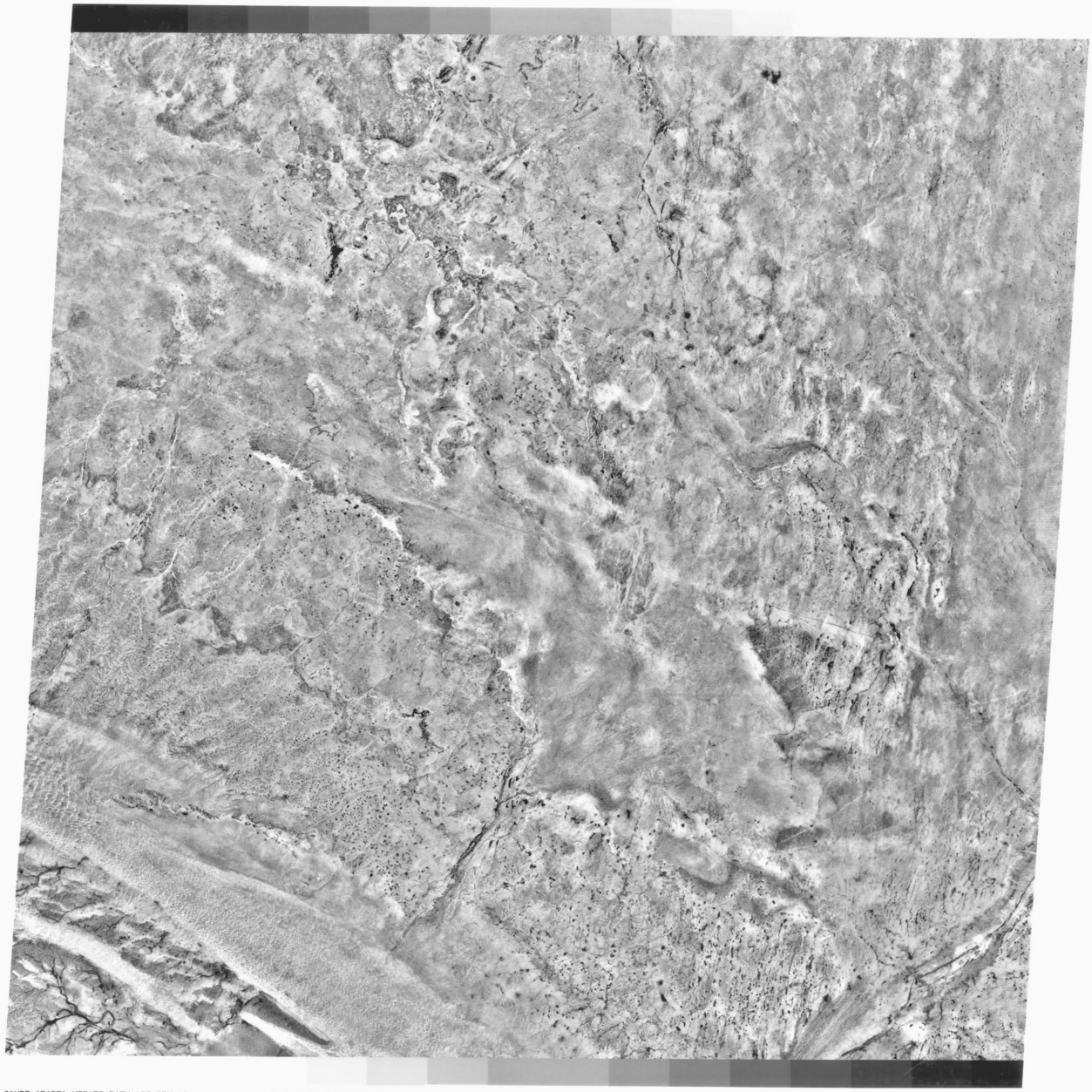
SAUDI ARABIA MOSAIC PATH 179 ROW 42 SCENE ID 10370-0658 C
EDTS 1 EXPOSURE DATE 28-JUL-73 PATH 179 ROW 42 C
XRGB FILE 1 SAUDI ARABIA DATABASE BAND 7 PATH 179 ROW 42
STRETCH: 0- 20 27- 20 34-235 255-235
NEG 7SR8S 8BIT NL 2340 NS 2482 FILE 1
13-SEP-79 21:25:18 U.S.G.S. FLAGSTAFF IMAGE PROCESSING FACILITY

Photo plate (20) Image 180/40 Ce_1 of band 7 showing :

1. Relatively clear approximate N-S, A-B, C-D, E-F, lineaments with 35 - 45 (average 40) km spacing (see Photo plate 21 for details).
2. Some NE lineaments of the Riyadh Fault System.



SAUDI ARABIA MOSAIC PATH 180 ROW 40 SCENE ID 1083-07031 C
SPIB.1 EXPOSURE DATE 14-OCT-72 REV 1151 C
SAUDI FILE 2 SAUDI ARABIA PATH 180 ROW 40 BAND 7 101X101 HPF
STRETCH Q- 0.112- 0.142-255 255-255
VEG 7SRGS 7TRACK 8BIT 800BPI FILE 2 NL 2340 NS 2428
04-JUN-80 23:42:27 U.S.G.S. FLAGSTAFF IMAGE PROCESSING FACILITY



SAUDI ARABIA MOSAIC PATH 180 ROW 40 SCENE ID 1083-07031 C
SITE 1 EXPOSURE DATE 14-OCT-72 REV 1151 C
SAVE/ FILE_2 SAUDI ARABIA PATH 180 ROW 40 BAND 7 101X101 HPF
STRETCH! 0: 0.112- 0.142~255 255-255
WSG 75PAS 7TRACK 8BIT 800BPI FILE 2 NL 2340 NS 2478
04-JUN-80 23:42:29 U.S.G.S. FLAGSTAFF IMAGE PROCESSING FACILITY

Photo plate (21) Image 180/40 generated from Ce_1 of band 7, by a photographic process showing :

1. The approximate N-S lineaments with the approximate 35 - 45 km. spacing are relatively clear in this image than in the original Ce_1 image (Photo plate 20). These lineaments seem to represent sub-surface failure zones rather than individual linear feature. This is mainly shwon by the lineaments (A-B), (C-D) to a lesser extent (E-F).
2. Circular, semi-circular and arcuate features of variable sizes.
3. One of these semi-circular features (G) is located between two of the approximate N-S lineaments and part of its circumference is followed by one or two NE lineaments of the Riyadh Fault System.
4. The wadi is following the main part of the semi-circular feature (G) which may enhance this part of the circumference.
5. These circular and semi-circular features are shown with varying degrees of clarity along their circumferences.


N
E
CI
A
G
F
D
WADI AL BATIN
B

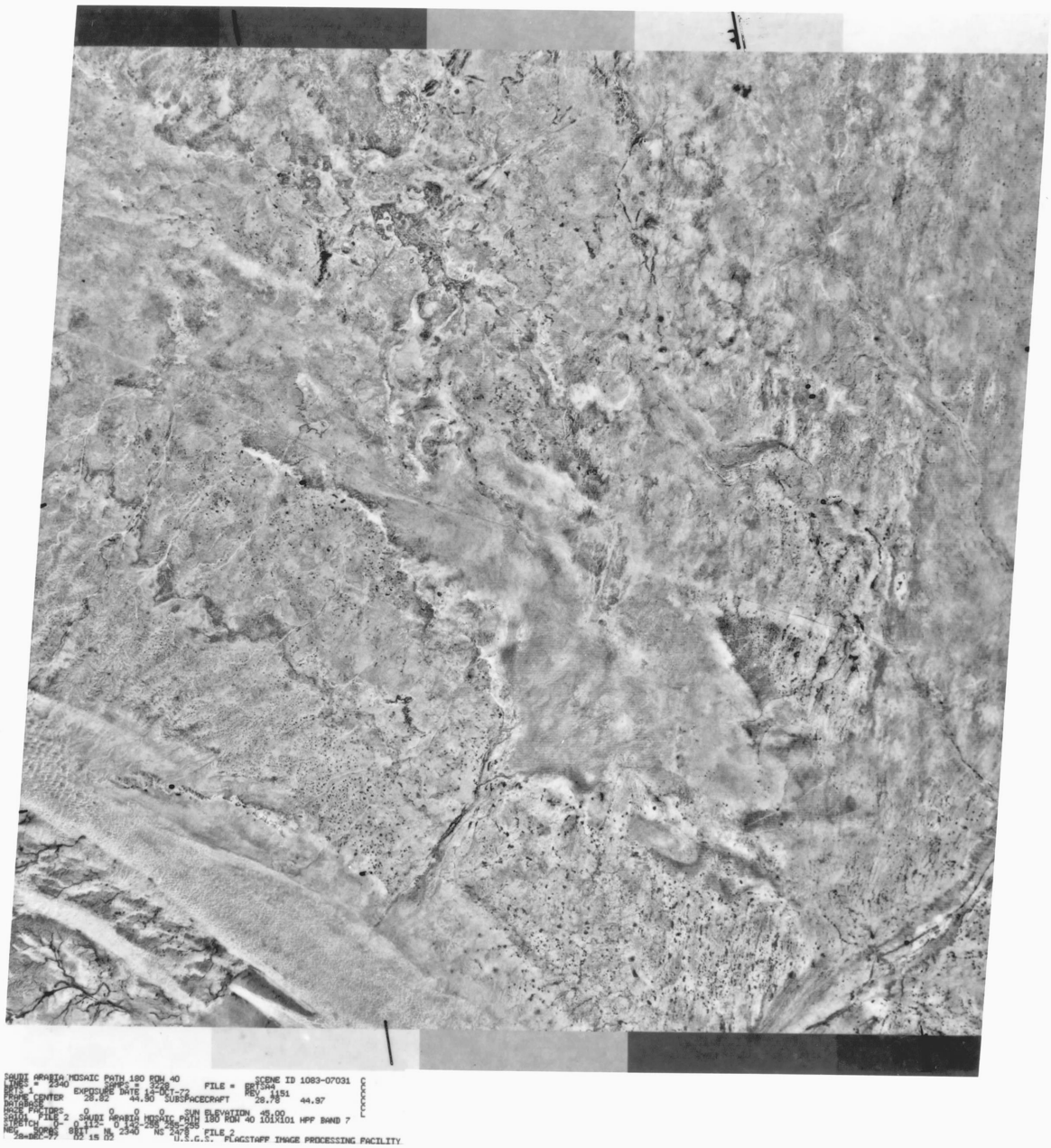
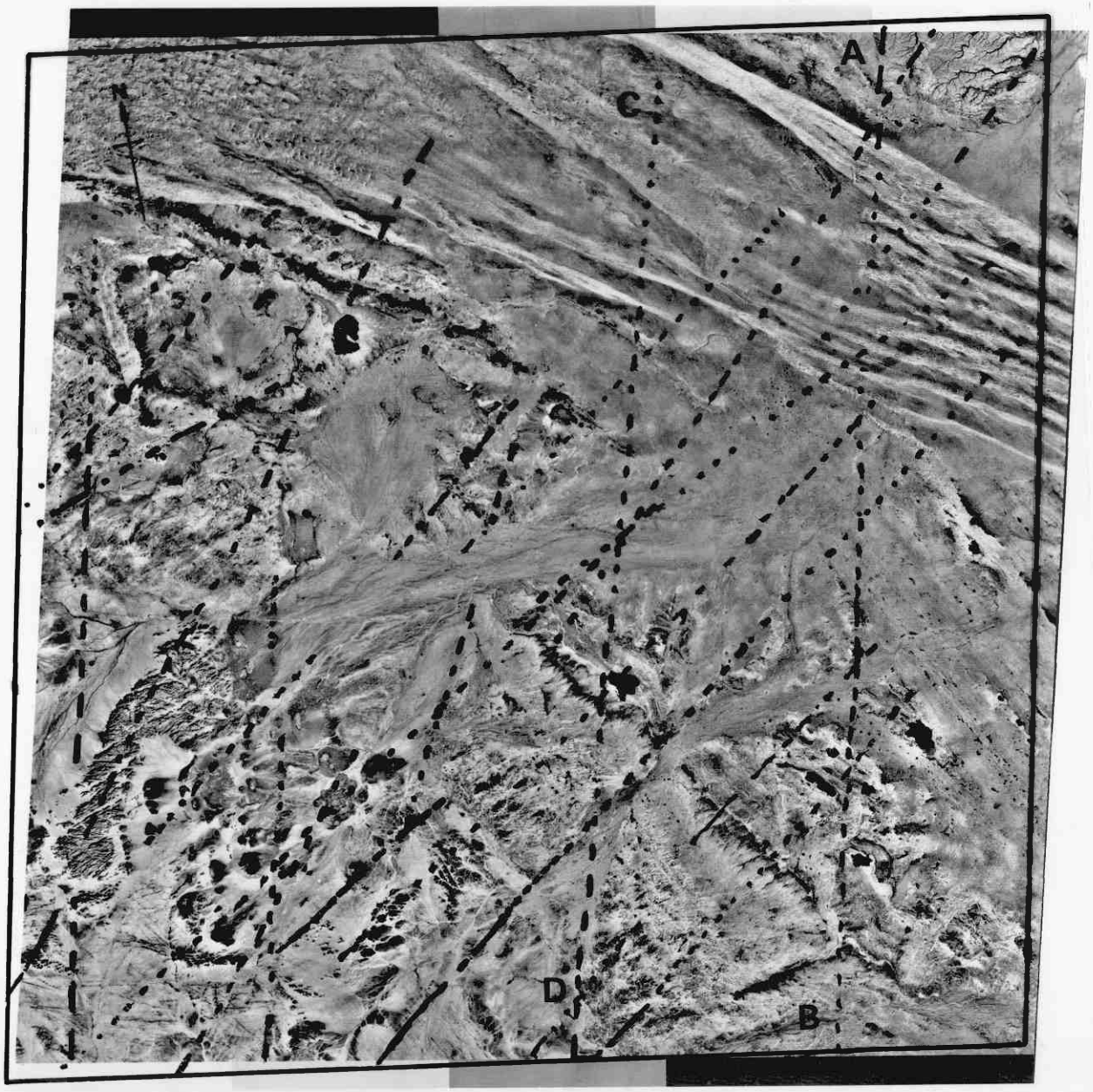
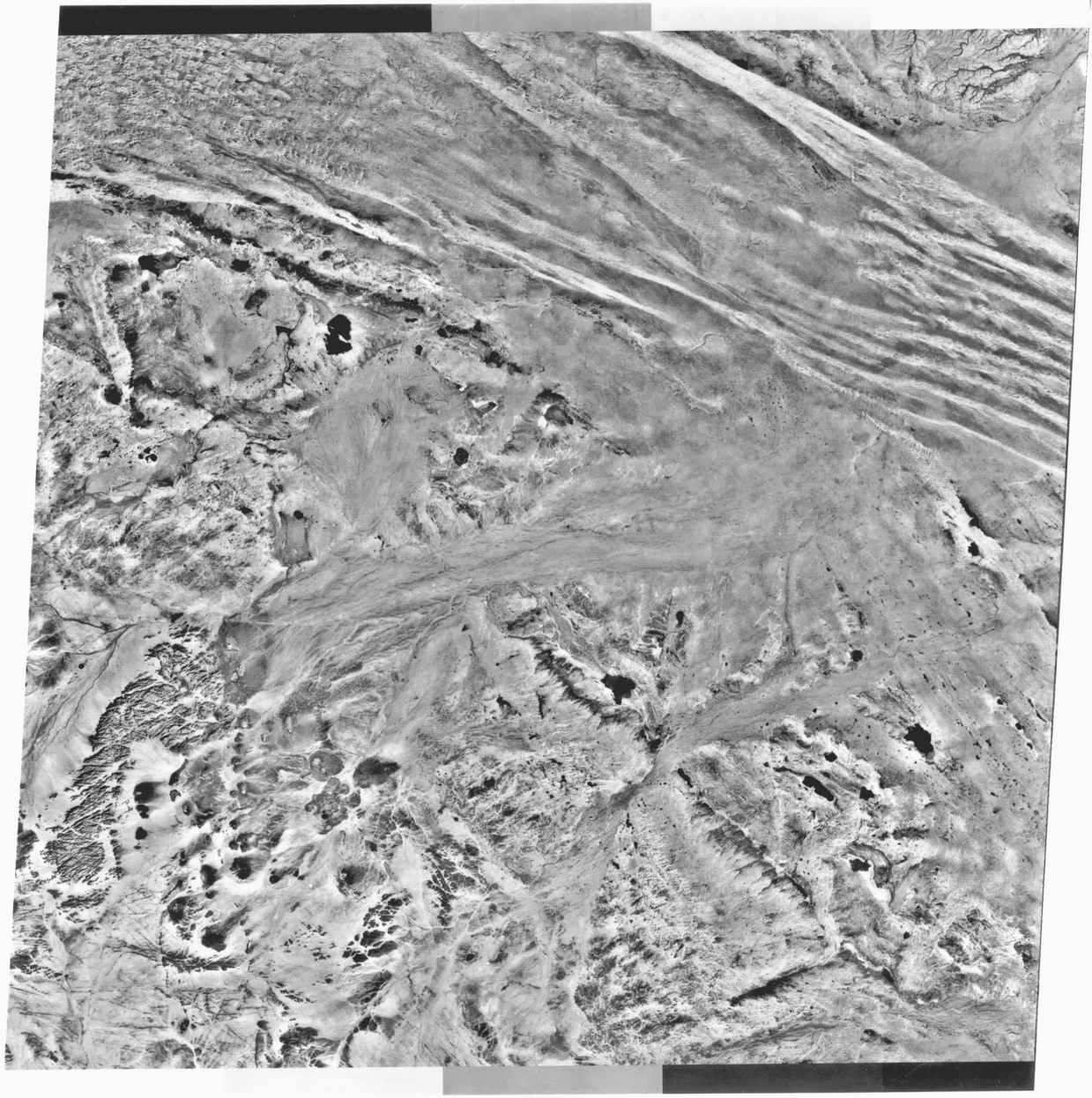

SCENE ID 1083-07031
FILE = 2
EXPOSURE DATE 14-OCT-72
28.82 44.90 SUBSPACECRAFT 28.78 44.97
0 0 0 0 SUN ELEVATION 45.00
0.112- 0.142-
0 1 2340 NS 2478
02 15 82
U.S.G.S. FLAGSTAFF IMAGE PROCESSING FACILITY

Photo plate (22) Image 181/41 Ce_2 of band 7 covering part of the contact between the eastern edge of the Arabian Shield and Cover Rock sediments showing :

1. The approximate N-S lineaments with an average 40 km spacing across the Shield and the sedimentary rocks with varying degrees of clarity.
2. Two N-S lineaments A-B and C-D shown across the Shield-Cover Rocks contact as well as through the sand dunes (which cover 20% of the area) with different degrees of clarity.
3. Some NE lineaments extending from the basement across the sedimentary rocks and parts of them are showing through surface sand cover in the NE corner of the image.



SAUDI ARABIA MOSAIC PATH 181 ROW 41 SCENE ID 1120-07095 C
SRI3 0 EXPOSURE DATE 20-NOV-?? REV 0 C
SRI4 FILE 2 SAUDI ARABIA MOSAIC PATH 181 ROW 41 101X101 HPF BAND 7
SIDELAP LP 20.4U2 20.182 235 235 235
VBC /SRO3 8BIT NL 2340 NS 2401 FILE 2
14-NOV-78 00 00 00 U.S.G.S. FLAGSTAFF IMAGE PROCESSING FACILITY



SAUDI ARABIA MOSAIC PATH 181 ROW 41 SCENE ID 1120-07095 C
SRTS O EXPOSURE DATE 20-NOV-72 REV 0 C
SA014 FILE 2 SAUDI ARABIA MOSAIC PATH 181 ROW 41 101X101 HPF BAND 7
STRETCH 0- 20 102- 20 152-235 255-235
VEC 75RGS 8BIT NL 2340 NS 2480 FILE 2
14-NOV-78 00 00 00 U.S.G.S. FLAGSTAFF IMAGE PROCESSING FACILITY

Photo plate (23) Aerial photograph of approximate scale 1:120,000 showing :

1. The Biyadh Formation (sandstone) is displaced by part of Khashm Addughum Fault (A-B) (Riyadh Fault System) which part of it are also shown on Landsat images (Photo plates 6 to 12) and field photograph (Photo plate 60).
2. Some relatively small size circular - elliptical features with varying degrees of clarity.

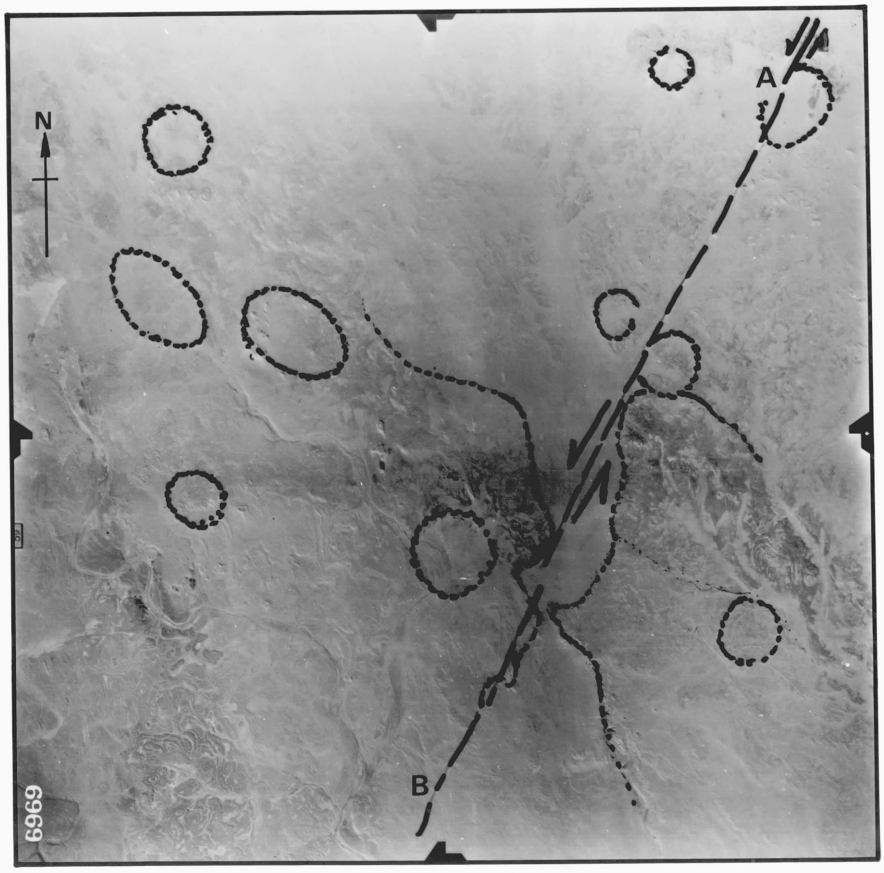
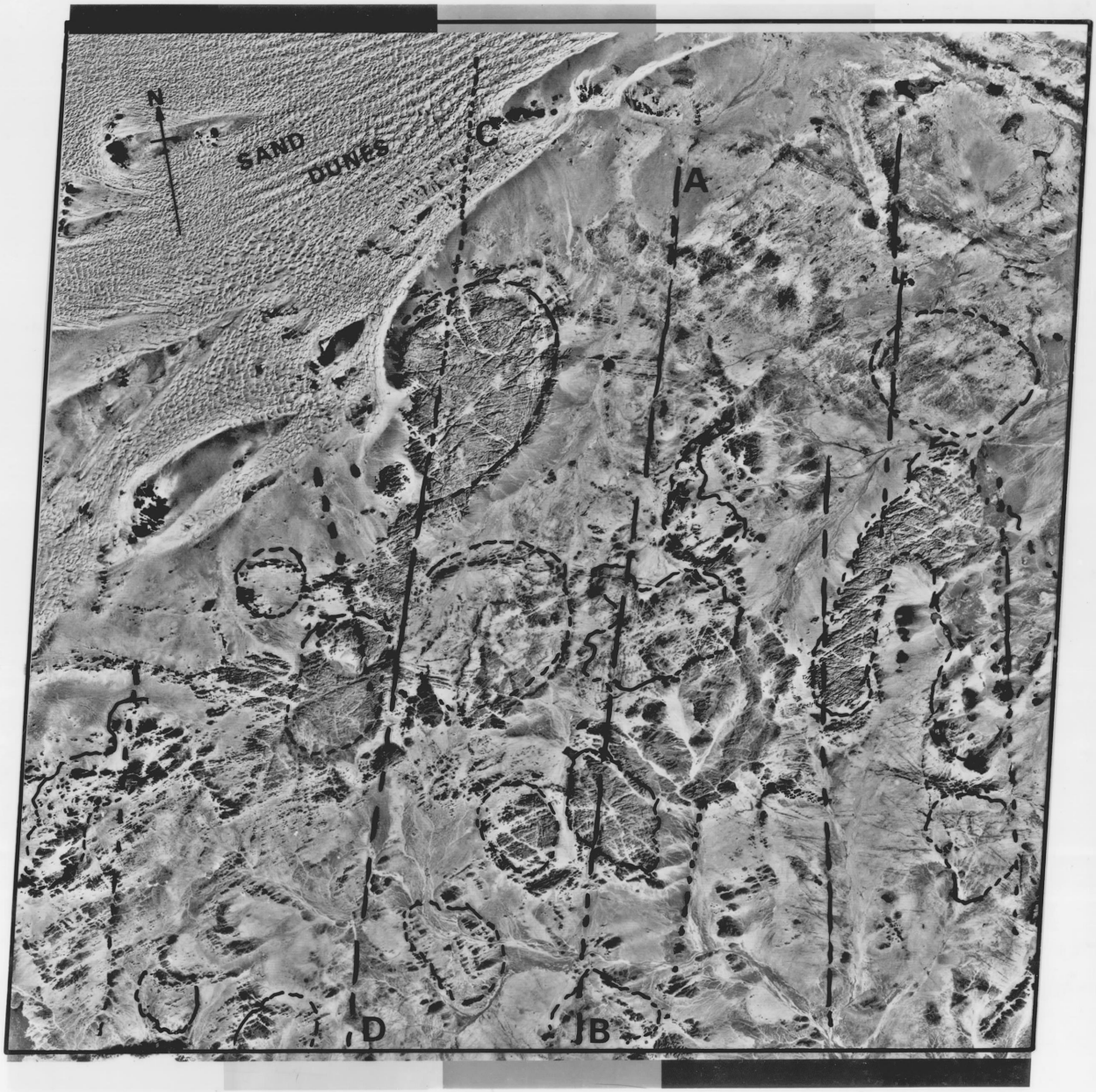
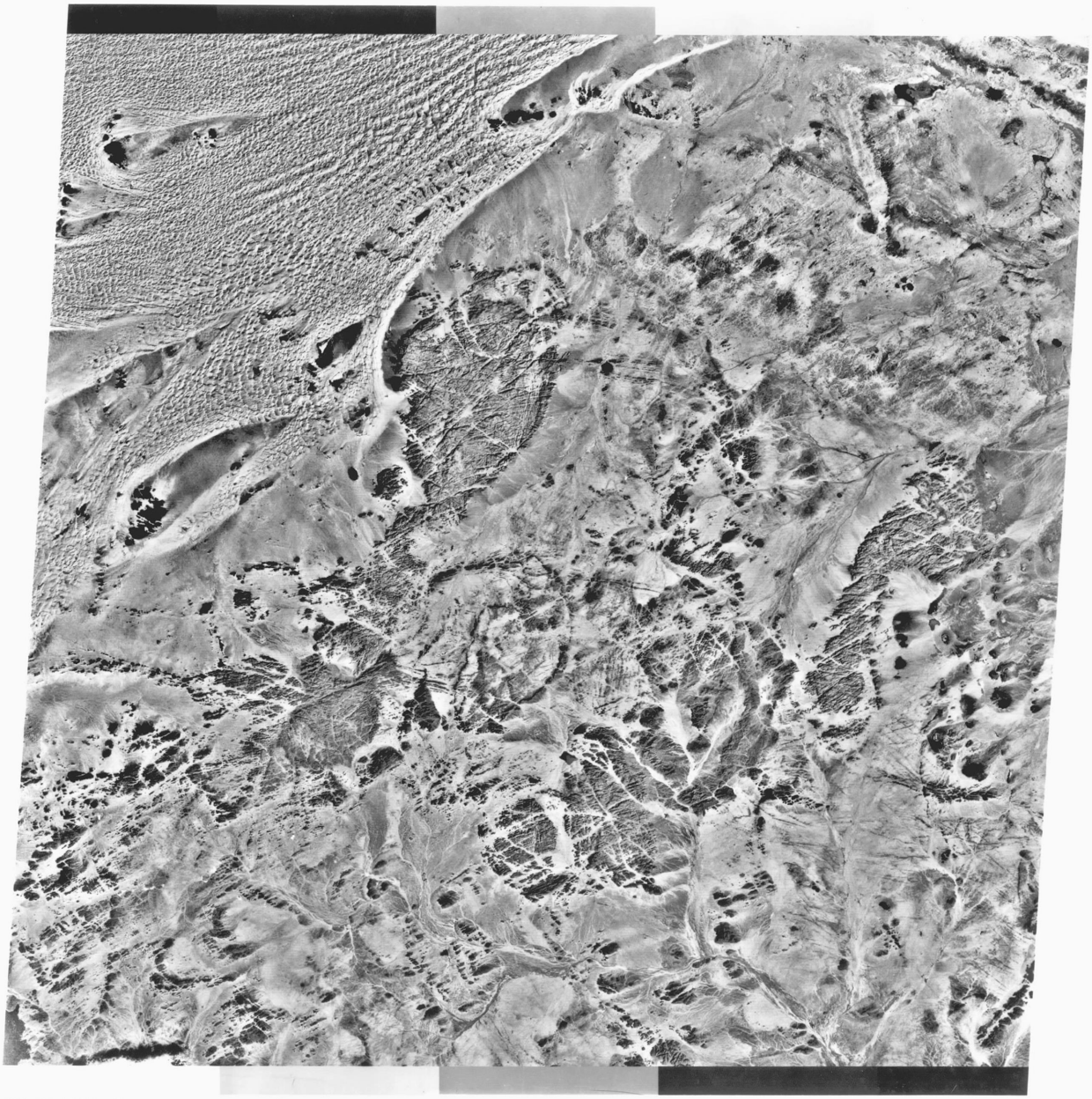

N
A
B
6969

Photo plate (24) Image 182/41 Ce_2 of band 7 covering part of the eastern edge of the Arabian Shield showing :

1. Precambrian granitic intrusions of variable sizes are mainly following general N-S trend with approximately 35 - 40 km spacing.
2. Some N-S lineaments mainly (A-B), (C-D), which is shown through the sand dunes, represent failure zones rather than a single linear feature. Such a phenomenon is also shown on images covering the sedimentary rocks with almost the same spacing pattern (Photo plate 21).



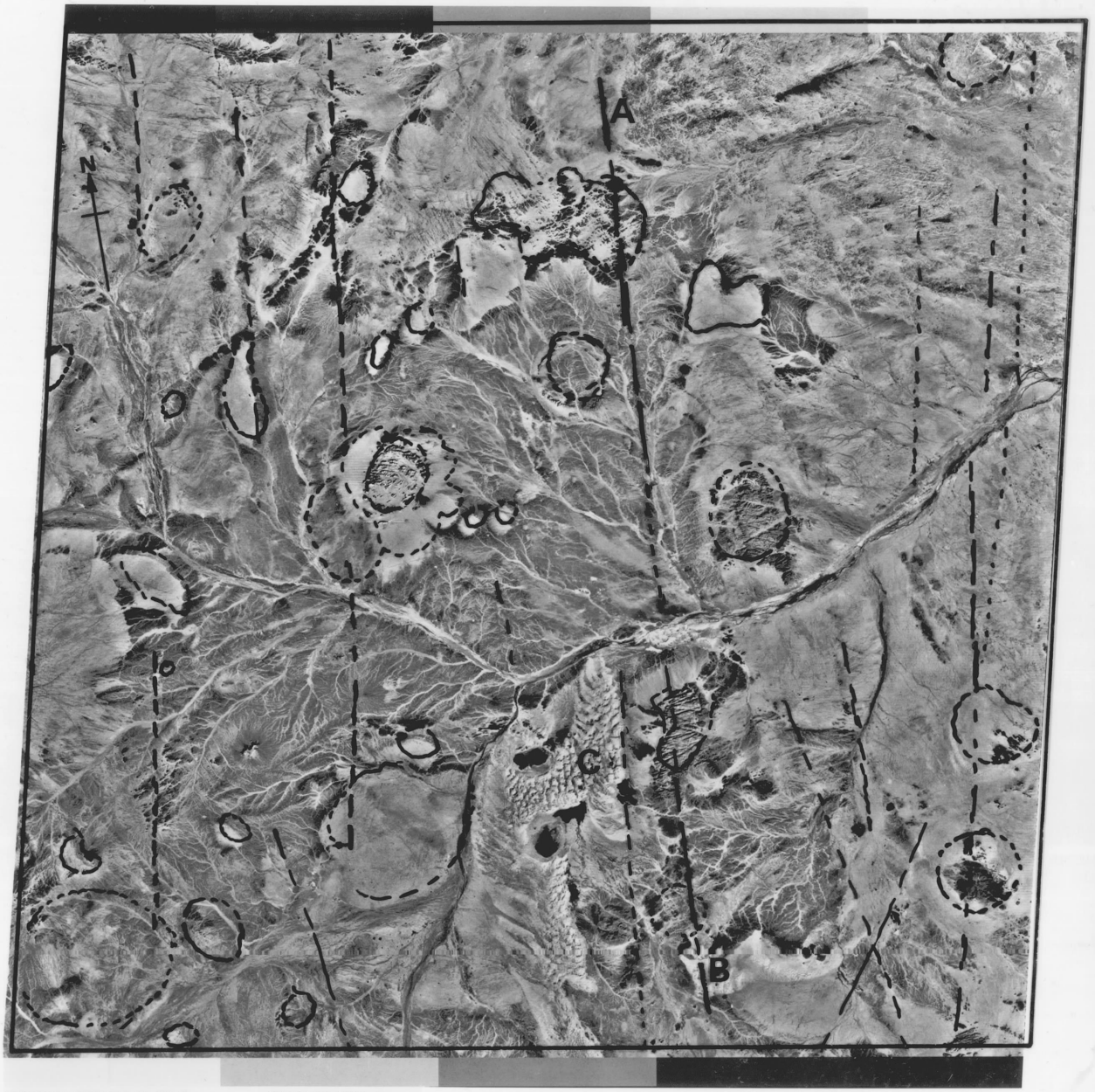
SAUDI ARABIA MOSAIC PATH 182 ROW 41 SCENE ID 1121-07153 C
ERTS-D EXPOSURE DATE 21-NOV-72 REV 0 C
29075 FILE 2 SAUDI ARABIA MOSAIC PATH 182 ROW 41 101X101 HPF BAND 7
STRETCH O- 20 102- 20 152-235 255-235
NDC 7SR6S 8BIT NL 2340 NS 2480 FILE 2
12-NOV-78 00 00 00 U.S.G.S. FLAGSTAFF IMAGE PROCESSING FACILITY



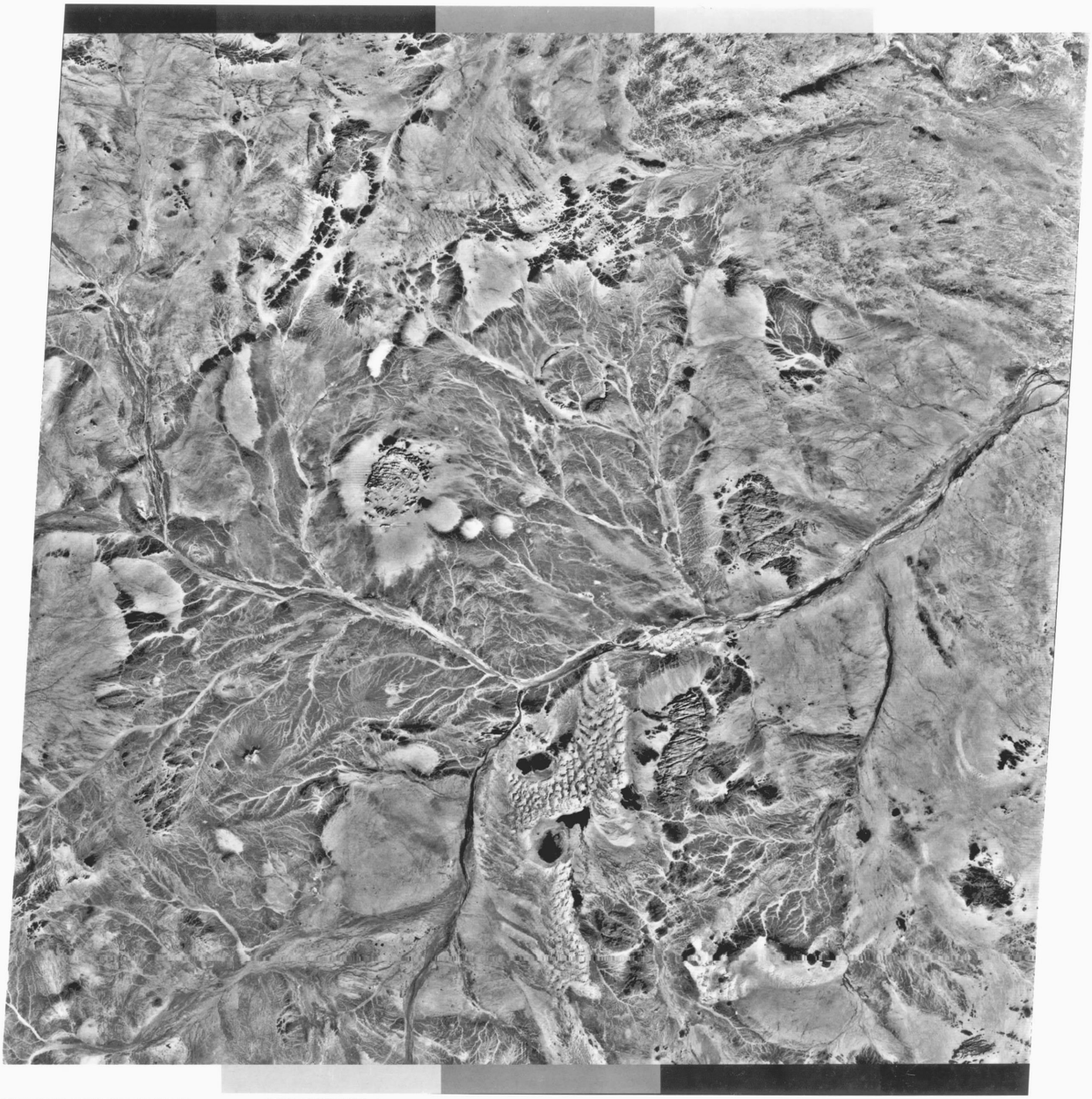
SAUDI ARABIA MOSAIC PATH 182 ROW 41 SCENE ID 1121-07153 C
ERTS-D EXPOSURE DATE 21-NOV-72 REV 0 C
SOUTH FILE 2 SAUDI ARABIA MOSAIC PATH 182 ROW 41 101X101 HPF BAND 7
STRETCH 0- 20 102- 20 152-255 255-235
NEG 7SRAS 8BIT NL 2340 NS 2480 FILE 2
12-NOV-78 00 00 00 U.S.G.S. FLAGSTAFF IMAGE PROCESSING FACILITY

Photo plate (25) Image 181/42 Ce_2 of band 7 mainly covering part of the eastern edge of the Arabian Shield and partly its contact with the Cover Rock Sediment in Wadi Arumah Region, showing :

1. Some approximate N-S lineaments (mainly failure zones) across the Arabian Shield with an approximately 35 - 45 km spacing, with varying degrees of clarity, the clearest is A-B.
2. Some Precambrian granitic intrusions of different shapes and sizes are following the approximate N-S trend show the original size of the intrusion and the present remnant due to strong erosion. In the field these granites (gp) are coarse grained and friable, easily eroded and broken as a result. A white/pinkish blanket of quartz and potash feldspar is dominant in the area.



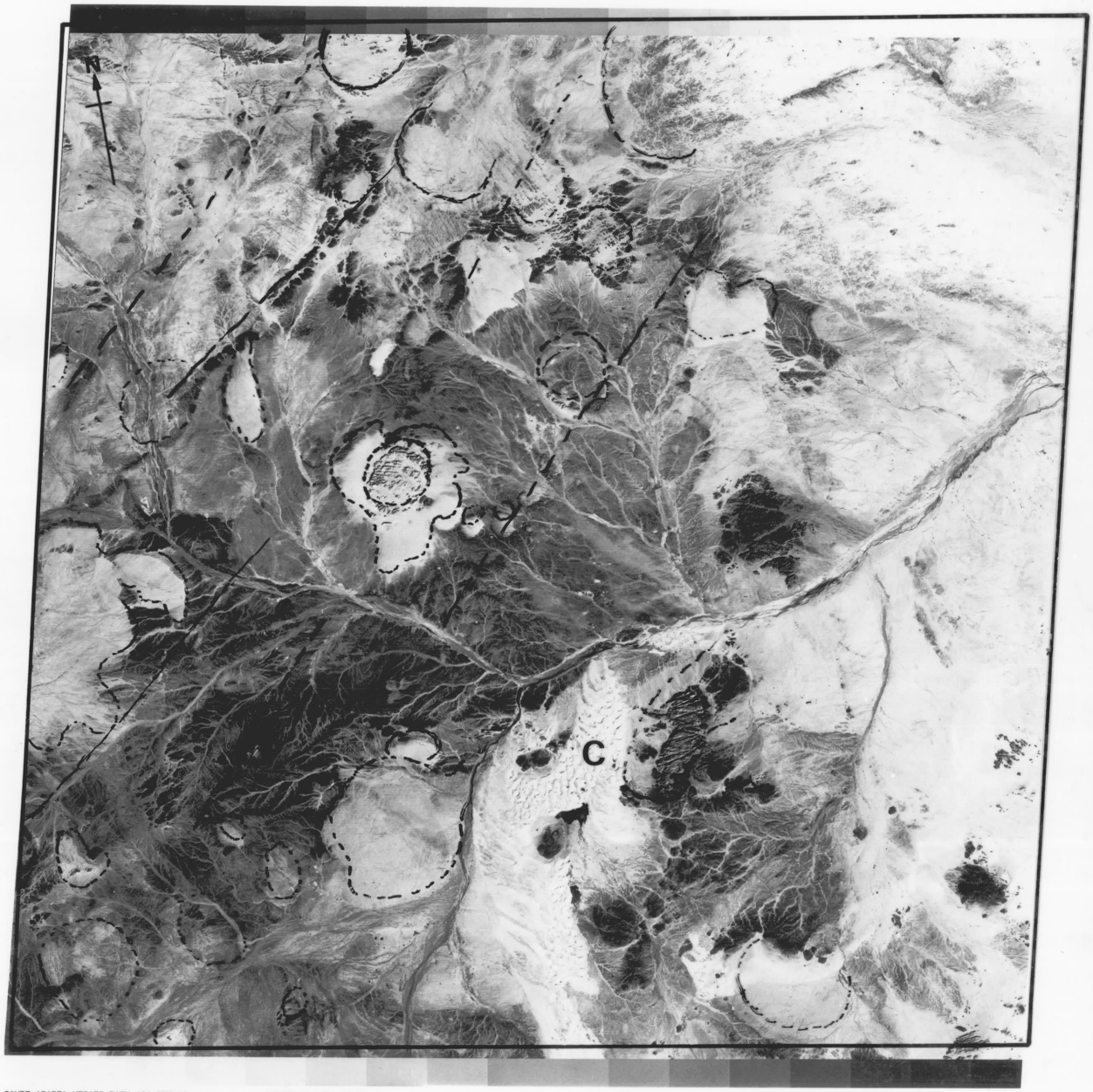
SAUDI ARABIA MOSAIC PATH 181 ROW 42 SCENE ID 1120-07101 C
ORTS 0 EXPOSURE DATE 20-NOV-72 REV 0 C
SA42Q FILE 2 SAUDI ARABIA MOSAIC PATH 181 ROW 42 BAND 7 101X101 HPF
STRETCH Q= 20 102= 20 152=235 255=235
NDS 7SR8S 8BIT NL 2340 NS 2482 FILE 2
11-OCT-78 00 00 00 U.S.G.S. FLAGSTAFF IMAGE PROCESSING FACILITY



SAUDI ARABIA MOSAIC PATH 181 ROW 42 SCENE ID 1120-07101 C
ERTS O EXPOSURE DATE 20-NOV-72 REV 0 C
SA040 FILE 2 SAUDI ARABIA MOSAIC PATH 181 ROW 42 BAND 7 101X101 HPF
STRETCH 0- 20 102- 20 152-238 255-238
NEG 7SRGS 8BIT NL 2340 NS 2402 FILE 2
11-OCT-78 00 00 00 U.S.G.S. FLAGSTAFF IMAGE PROCESSING FACILITY

Photo plate (26) Image 181/42 Data base (contrast stretch) of band 7 covering the same area as Photo plate (25).

Notice the difference in tonal contrast distribution within the granitic intrusions and over the sand dunes area (c) and the other lineaments across the country rocks (mainly metavolcanics).



SAUDI ARABIA MOSAIC PATH 181 ROW 42 SCENE ID 1120-07101 C
ERTS O EXPOSURE DATE 20-NOV-72 REV 0 C
XHRS FILE 1 SAUDI ARABIA DATABASE BAND 7 PATH 181 ROW 42
STRETCH: 0 20 7 20 36 236 255 235
NEG 25805 BIT NL 2340 NS 2462 FILE 1
17-DEC-79 04:30:16 U.S.G.S. FLAGSTAFF IMAGE PROCESSING FACILITY



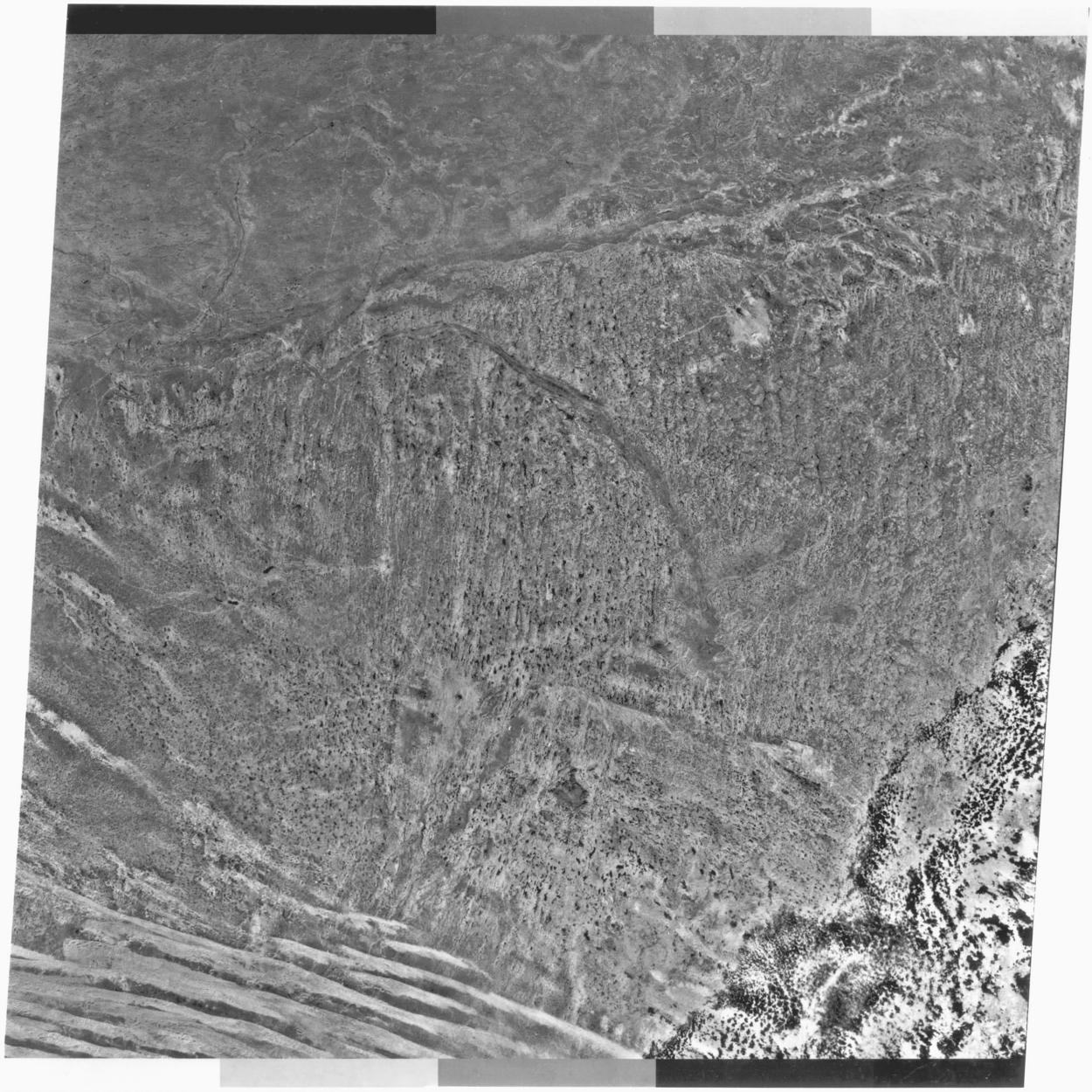
SAUDI ARABIA MOSAIC PATH 181 ROW 42 SCENE ID 1120-07101 C
ERTS O EXPOSURE DATE 20-NOV-72 REV 0 C
S9489 FILE 1 SAUDI ARABIA DATABASE BAND 7 PATH 181 ROW 42
STRETCH: 0-20 7- 20 36-236 255-235
NEG CROS BIT NL 2340 NS 2482 FILE 1
17-DEC-79 04130:18 U.S.G.S. FLAGSTAFF IMAGE PROCESSING FACILITY

Photo plate (27) Image 178/41 Ce_2 of band 7 covering an area in the Interior Platform showing :

1. A relatively clear elliptical feature (A) of approximately 30 - 40 km radius and other smaller arcuate or circular features of different sizes.
2. Drainage in the area deviates around and enhances parts of its circumference.
3. The general pattern of this feature (A) is probably a result of combinations of lithostratigraphic, topographical and atmospheric factors.
4. The image in its SE corner is obscured by 10 - 15% cloud coverage.



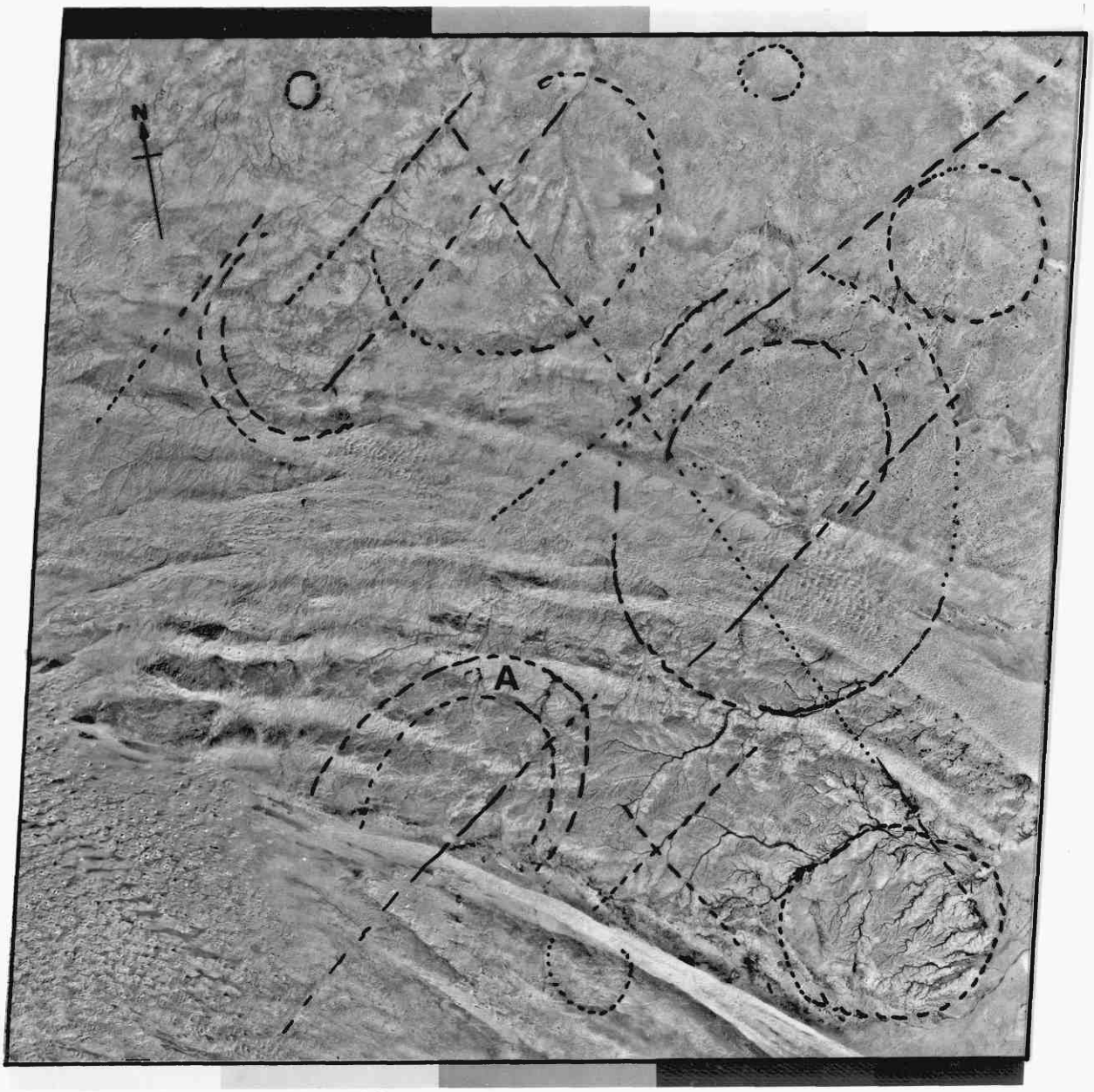
SAUDI ARABIA MOSAIC PATH 178 ROW 41 SCENE ID 1099-06522 C
SPIS 1 EXPOSURE DATE 30-OCT-72 REV 0 C
SPIA FILE 2 SAUDI ARABIA MOSAIC PATH 178 ROW 41 101X101 HPF BAND 7
STRETCH 0 30 102 20 152 236 255 238
WDC 7SR05 BIT NL 2340 NS 2400 FILE 2
18-JUN-78 11 59 28 U.S.G.S. FLAGSTAFF IMAGE PROCESSING FACILITY



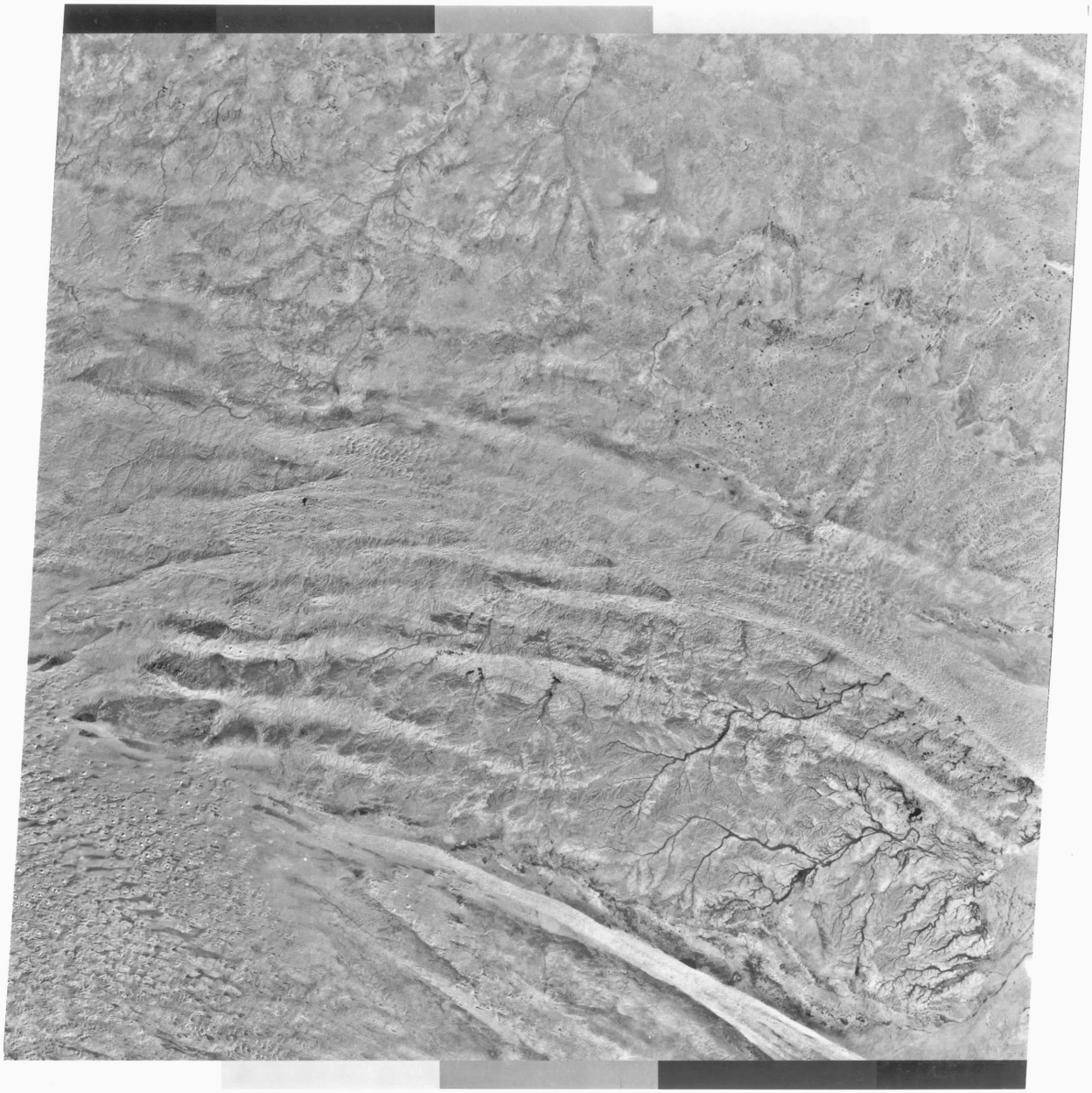
SAUDI ARABIA MOSAIC PATH 178 ROW 41 SCENE ID 1099-06522 C
SITE 1 EXPOSURE DATE 30-OCT-72 REV 0 C
AREA FILE_2 SAUDI ARABIA MOSAIC PATH 178 ROW 41 101X101 HPF BAND 7
STRETCH Q= 20 102= 20 152=238 255=235
WDC 7SRAS 8BIT NL 2340 NS 2480 FILE_2
18-JUN-78 11 59 28 U.S.G.S. FLAGSTAFF IMAGE PROCESSING FACILITY

Photo plate (28) Image 181/40 Ce_2 of band 7 covering sedimentary area in the Interior Homocline showing :

1. Some circular, semi-circular or arcuate features, the circular features are mainly with 15 - 25 km radius and to a lesser extent smaller sizes shown with varying degrees of clarity along their circumferences.
2. Some of the 15 - 25 km radius are represented by two circles or arcuate features one inside the other (A) (the same phenomenon is shown on Photo plates 9,10).
3. Some NE and less NW lineaments



SAUDI ARABIA MOSAIC PATH 181 ROW 40 SCENE ID 1120-07082 C
ERTS-1 EXPOSURE DATE 20-NOV-72 REV 1867 C
SAUDI FILE 2 SAUDI ARABIA MOSAIC PATH 181 ROW 40 101X101 MPP BAND 7
STRETCH G 20 10DB -20 10DB 255-235 255-235
NEG /SPAS 8BIT NL 2340 NS 2478 FILE 2
05-AUG-78 09 36 19 U.S.G.S. FLAGSTAFF IMAGE PROCESSING FACILITY



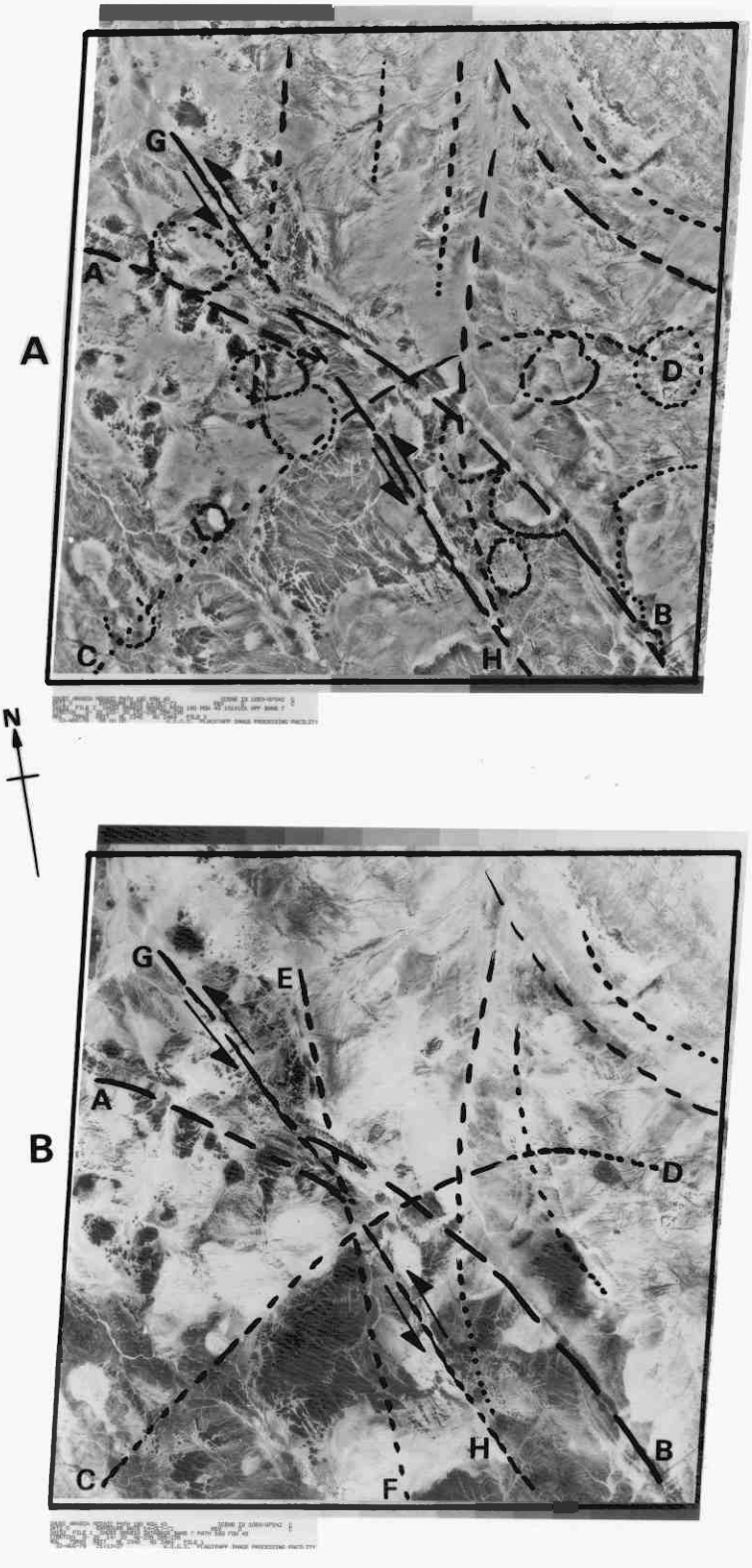
SAUDI ARABIA MOSAIC PATH 181 ROW 40 SCENE ID 1120-07092 C
ERTS-1 EXPOSURE DATE 20-NOV-72 REV 1667 C
2A2I7 FILE 2 SAUDI ARABIA MOSAIC PATH 181 ROW 40 101X101 HPF BAND 7
STRETCH 0- 20 102- 20 152-235 255-235
NBC 7SR0S 6817 NL 2340 NS 2476 FILE 2
05-AUG-78 08 36 15 U.S.G.S. FLAGSTAFF IMAGE PROCESSING FACILITY

Photo plate (29) Image 180/43 Ce_2 of band 7 approximate scale 1:3,000,000 showing :

1. Some long arcuate features which may represent impact effects in the Arabian Shield.
2. The arcuate feature (A-B), which is relatively clearer than (C-D), is displaced by a fault of the Najd Fault System (G-H).
3. Few intrusions (mainly granitic) are following parts of the arcuate features.
4. Some other arcuate features with varying degrees of clarity.
5. A few N-S lineaments.

Photo plate (30) Image 180/43 Data base of band 7 approximate scale 1:3,000,000 covering the same area as Photo plate (29) showing :

1. Different tonal contrast from 29.
2. Another NNE lineament (E-F) clearer than in 29.
3. In the NE corner of the image two relatively small arcuate features are shown across the shield-sedimentary rocks contact with varying degrees of clarity. (Please refer to Figures 62 and 63 A-B for more details).


A
G
A
D
D
C
H
B
N
B
G
E
A
D
C
F
H
B

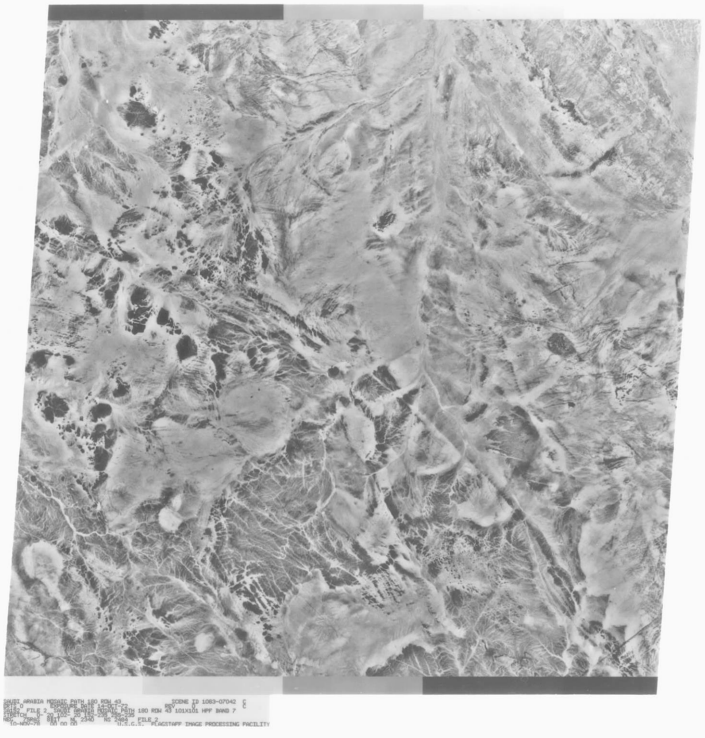
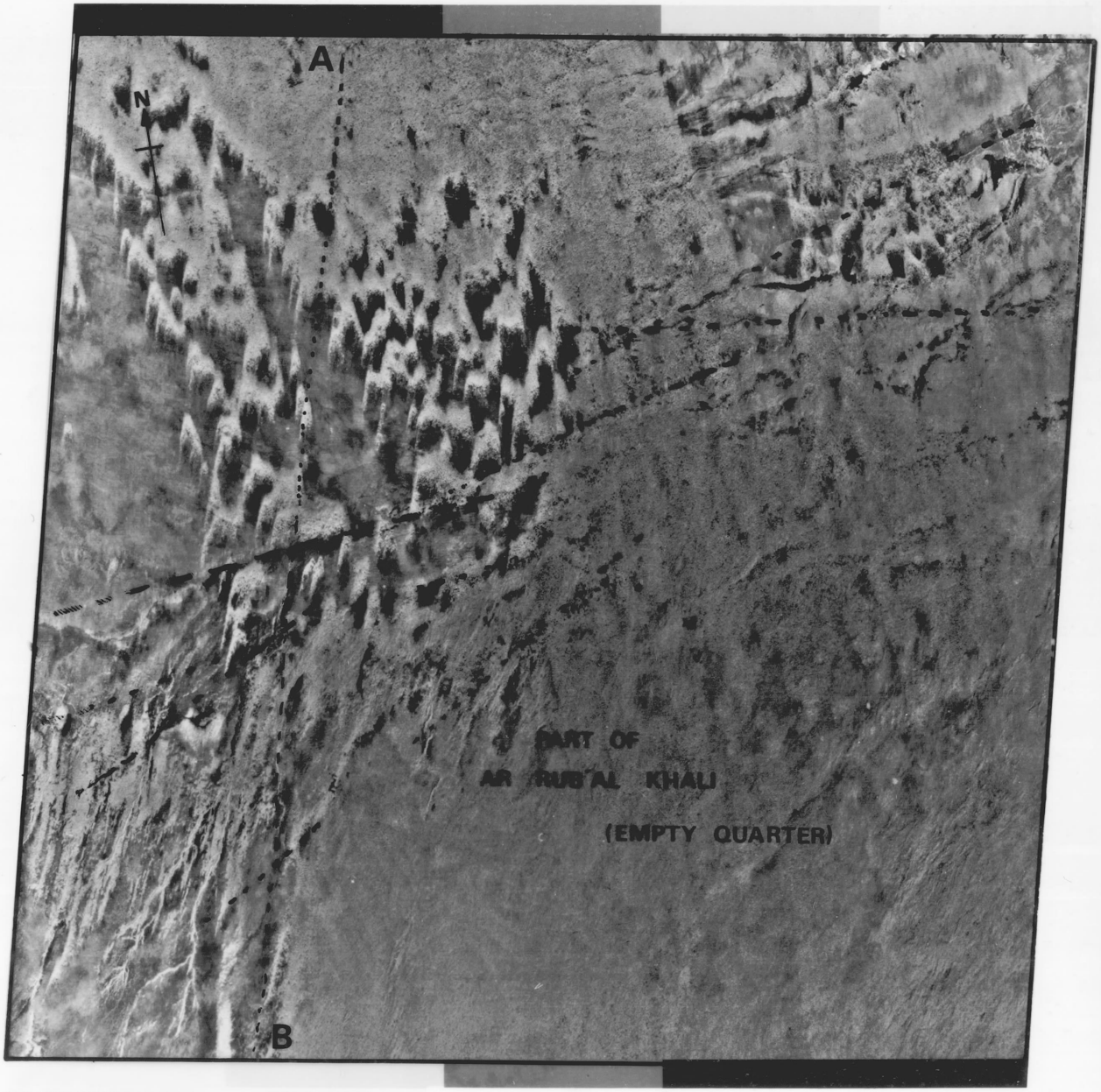




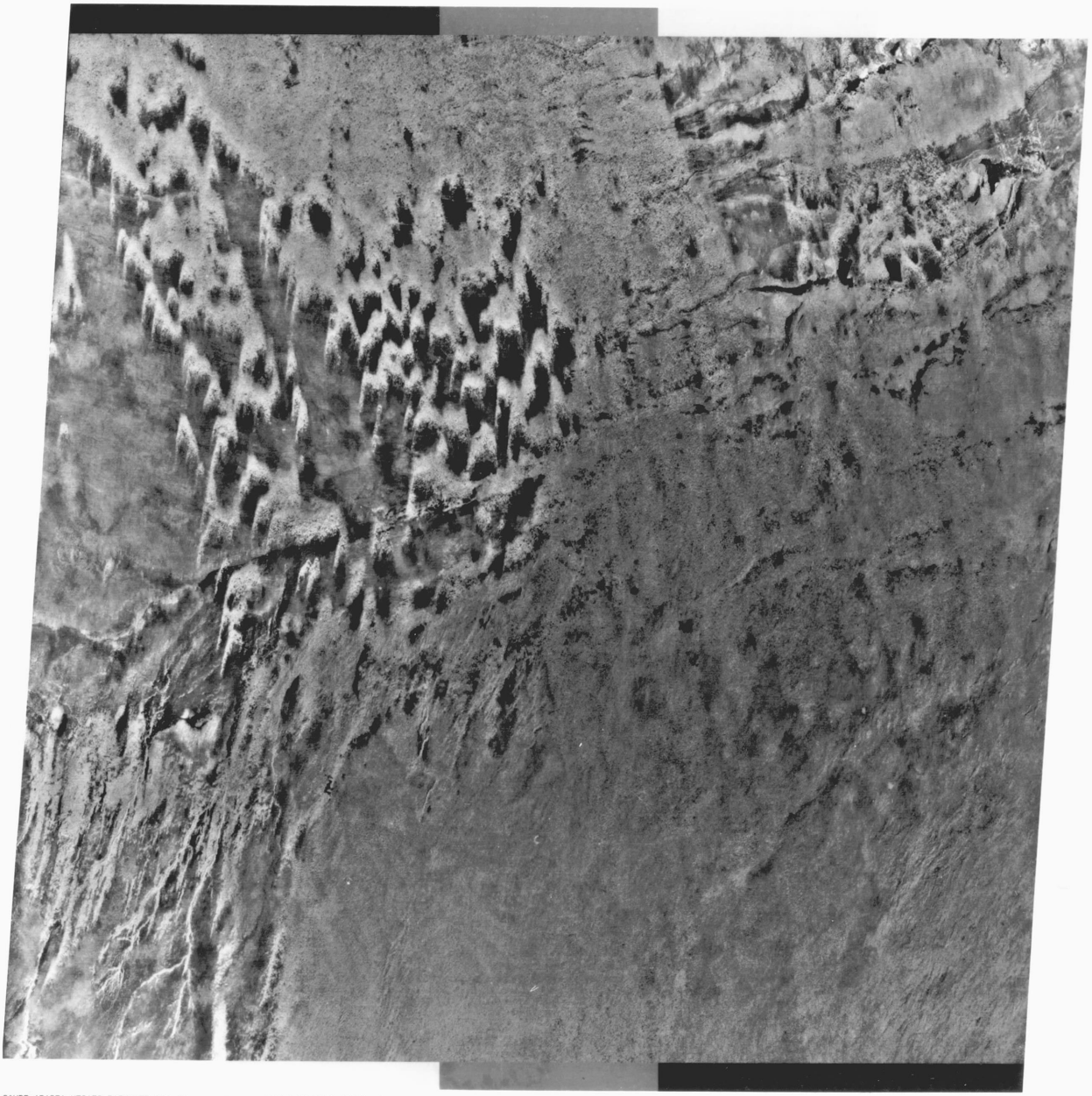
Photo plate (31) Image 175/44 Ce_2 of band 7 covering part of the great sand sea in Arabia i.e. The Empty Quarter (Rub'Al-Khali) - showing :

1. Different patterns and textures of relatively large sand dunes.
2. Their shape and distribution seems to be affected by the prevailing wind directions and local physiographic nature of some lineaments which may represent sub-surface linear features and/or failure zones.
3. N-S lineament (A-B) shown across different patterns of sand dunes.

This image and the image in Photo plate 14 substantiates the idea that subsurface features can be detected even through sands and sand dune coverage of specific nature.



SAUDI ARABIA MOSAIC PATH 175 ROW 44 SCENE ID 1438-06344 C
BPTF 0 EXPOSURE DATE 4-OCT-73 REV A C
>RQDB FILE 2 SAUDI ARABIA MOSAIC PATH 175 ROW 44 101X101 HPF BAND 7
STRETCH 0- 20 102- 20 152-235 255-235
NEG 75R8S 8BIT NL 2340 NS 2486 FILE 2
05-AUG-78 16 40 22 U.S.G.S. FLAGSTAFF IMAGE PROCESSING FACILITY



SAUDI ARABIA MOSAIC PATH 175 ROW 44 SCENE ID 1438-06344 C
ERTS-0 EXPOSURE DATE 4-OCT-73 REV 0 C
SMOOS FILE 2 SAUDI ARABIA MOSAIC PATH 175 ROW 44 101X101 HPF BAND 7
STRETCH 0- 20 102- 20 152-235 255-235
NEG 7596 8BIT ML 2340 NS 2408 FILE 2
05-AUG-78 16 40 22 U.S.G.S. FLAGSTAFF IMAGE PROCESSING FACILITY

Photo plate (32) Aerial photograph approximate scale 1:120,000 covering part of the western edge of the Riyadh Tilted Block, showing :

1. Different types of drainage pattern(A-B) due to variation in rock composition and possibly structural control.
2. The meandering drainage routes in the southern and western parts of the photograph (A) indicate a wet climate which had prevailed in the Pluvial Period before the present arid climate had dominated the area.


N
6093
A
A
B

FIELD AERIAL VIEWS

AND GROUND PHOTOGRAPHS

Photo plate (33) Aerial view of non-geological lineaments which resulted from Bedouin vehicular traffic. They cause vegetation alignments in the wet season, and can be misleading in high alititude photography.

Photo plate (34) Aerial view showing the effect of the prevailing wind which produces an arcuate feature probably affected by the local topography.





Photo plate (35) Jointing and faulting (probably of second order) in the vicinity of Al-Amar-Idsas Fault at Khashm Al-Juair Area.

(Notice the displacement of the vertical joint A-B by two E-W faults C-D, E.F, the hammer head points to the north).

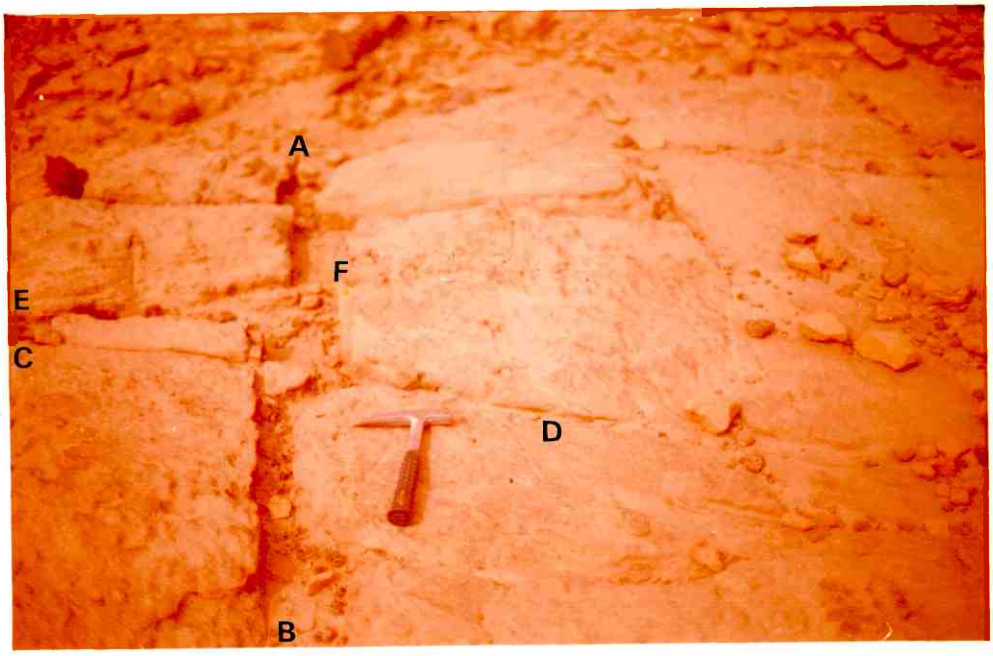
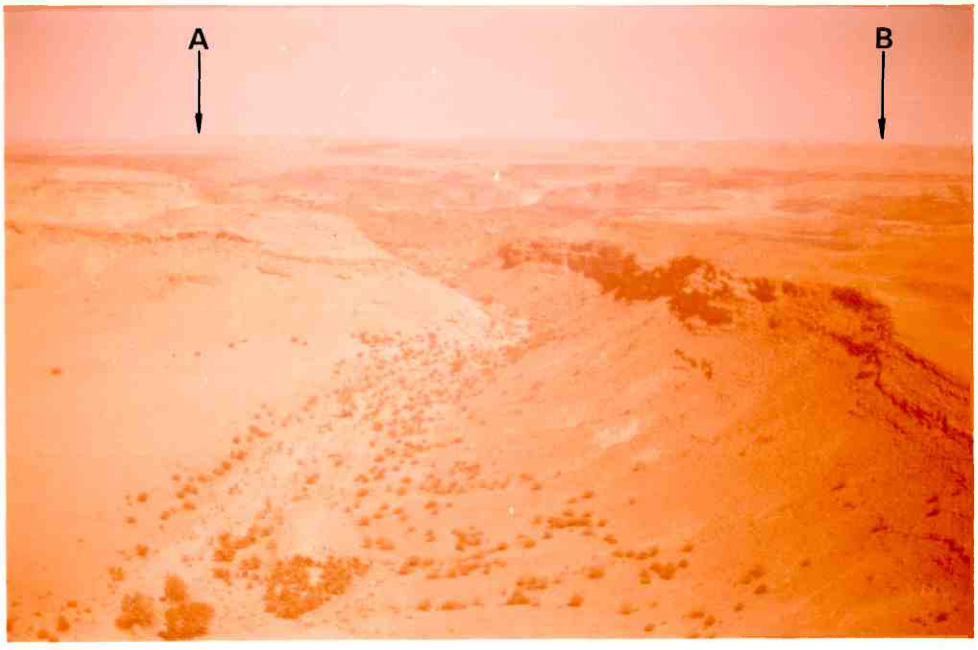

A
F
E
C
D
B

Photo plate (36) Aerial view(looking approximately North) showing the sudden change in the strike of the Tuwaiq Escarpment limestone where Al-Amar-Idsas Fault extension is interrupted by Al-Majma'ah Graben part of it is shown on A-B, near Addahina Village.

Photo plate (37) Aerial view (looking approximately North) of part of Tuwaiq Escarpment limestone where some rock horizons have started to collapse in a syncline-like structure (A). This is in the vicinity of a normal fault of 35m vertical displacement (Photo plate 38).

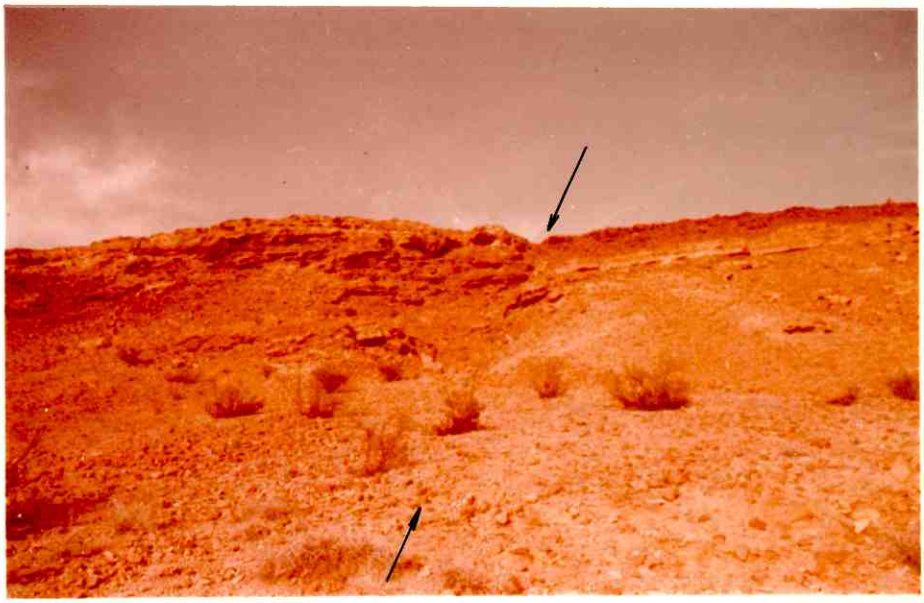

A
B


A

Photo plate (38) Normal fault with approximately 35 m. vertical displacement across the Tuwaiq Escarpment in Addahina Area (looking approximately east).

Photo plate (39) Vertical section across the Tuwaiq-Dhruma limestone contact showing :

1. Dolomitic dyke (A-B)
2. Pockets of manganese, iron oxides and black calcite (C) along Al-Amar-Idsas Fault extension in Addahina Area.



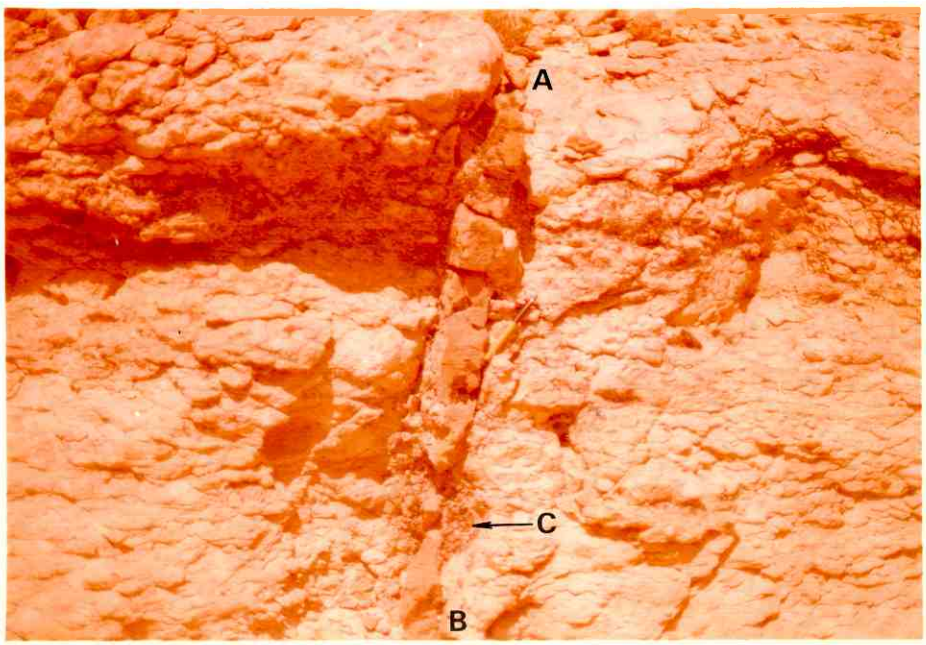

A
C
B

Photo plate (40) Aerial view showing a butte-Mesa of isolated Tuwaiq limestone on the top of Dhruma dropped in the Dhruma Graben (Cathedral-like shape).

Photo plate (41) Aerial view of the same feature (Photo plate 40) from different altitude and angle. Showing the abrupt Turwaiq cliff-like scarp.

Both photographs strongly indicate the effect of the erosion in this arid/semi-arid region (Saudi Arabian desert).





Photo plate (42) Aerial view (looking approximately North), Tuwaiq limestone outcrop in the Dhruma Graben showing approximately 6° - 10° SW dip.



Photo plate (43) Field photograph west of Al-Majma'ah Graben shows the enhancement of vegetation in variable degrees along lineaments due to the water content. Such a feature on large scale is better detected on I.R.C.C. images exposed in the wet season.

Photo plate (44) Aerial view (looking approximately North) of Jabal Al-Fahda in the middle of URUQ Al-Buldan sand dunes (looking north), represents an outcrop of the Tuwaiq segments which substantiate the connection of Majma'ah and Barrah Grabens. The dip can be correlated with the same SW dip of 6° - 10° in the Tuwaiq limestone in Photo plate 42.
(refer to Photo plates 13 and 19).





Photo plate (45) Aerial view of part of IRQ-Banban sand belt (see Plate 7) where the individual sand dunes are represented by sharp crested, narrow ridge dune chains. Notice the haze over the sand dune area.

Photo plate (46) Aerial view of part of Aruma Formation cliff forming rocks (A) bounding IRQ-Banban and controlling the haze and dust. Notice the clear sky over the cliff and the dusty, hazy part over the sands as a result of topographic control.




A

Photo plate (47) Aerial view (looking north) of set of tight sequence of horst and graben like lineaments intersected by other NW lineaments near the flood plain of Wadi Al-Atk (complimentary to Figure 51). (The haze in the photograph is due to sun reflection on the helicopter cabinet).

Photo plate (48) Aerial view (looking north) of the Aruma Formation limestone rocks near Khashm Al-Haqaqa Monocline showing the well established jointing pattern, mainly due to change of dip and the effect of Wadi Al-Atk and its related structures.





Photo plate (49) Aerial view of the Aruma Formation limestone with clear ridges and sink hole (A).

Photo plate (50) Aerial view (looking approximately N40^{o}E) of approximately the same area as (Photo plate 47) with different altitude and angle beside 47 it shows the Aruma Escarpment at Wadi Al-Atk.


A



Photo plate (51) Vertical jointing of Aruma Formation rocks on the northern escarpment of Wadi Al-Atk (looking approximately north). (Lineament E-F in Photo plate 18).

Photo plate (52) Jointing in the Base of Aruma Formation in Wadi Al-Atk.



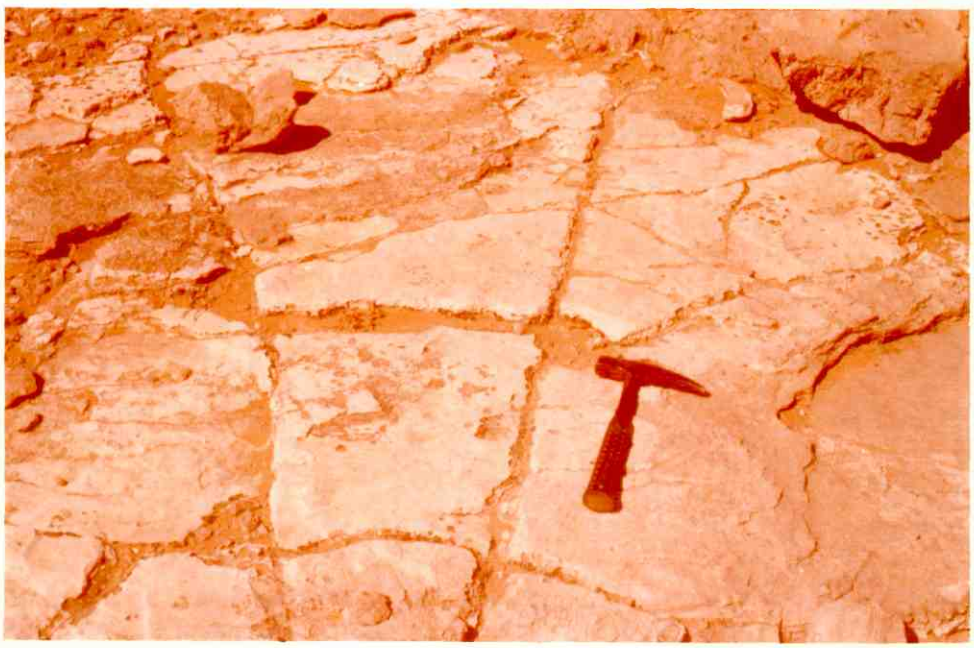


Photo plate (53) Displacement on small faults in the base of Aruma Formation in Wadi Al-Atk (looking north).

Photo plate (54) Sigmoidal, S shaped joint, (A) and microfolding (shown by arrows) in the Aruma Formation Escarpment (limestone) in Wadi Al-Atk. (looking north).




A

Photo plate (55) Irregular tension opening in the vicinity of Khashm Al-Haqaqa collapse structure. This shows the edge of the block expected to collapse.

Photo plate (56) Detailed photograph of part of the tension opening in (55) showing the arcuate shape of the newly formed failure zone along which water was flowing at a few meters depth.





Photo plate (57) Fault affecting the dip of the Aruma Formation rocks (limestone) in the vicinity of Khashm Al-Haqaqa structure (indicated by arrow).

Photo plate (58) Detailed photograph of the same fault in (57) clearly showing the difference in the amount of dip on both sides of the fault. Relatively steep dip to the west shown by arrow. (The man is standing on the fault line).



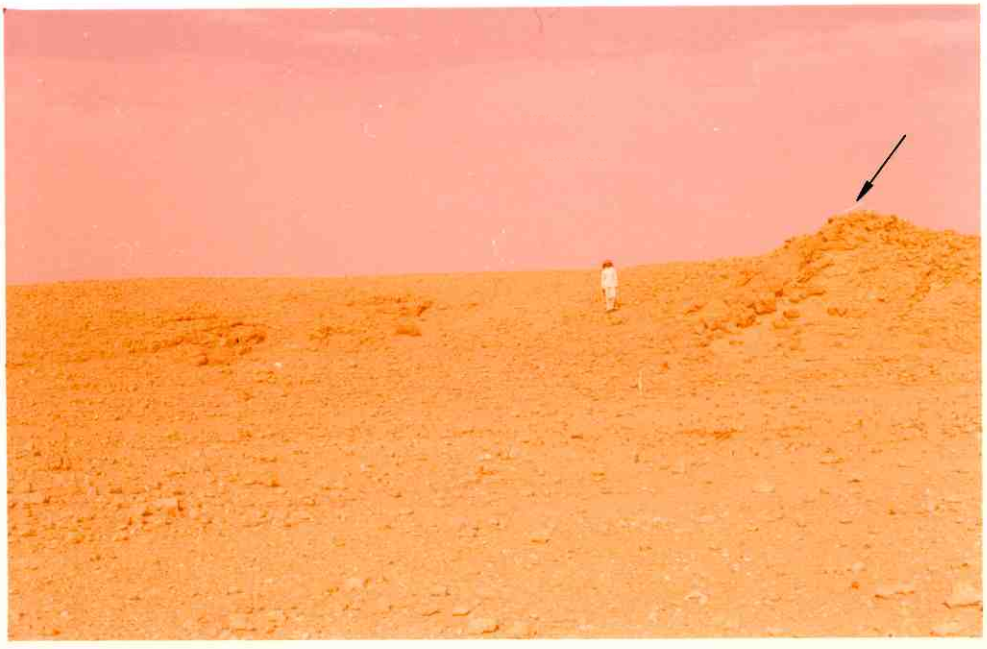
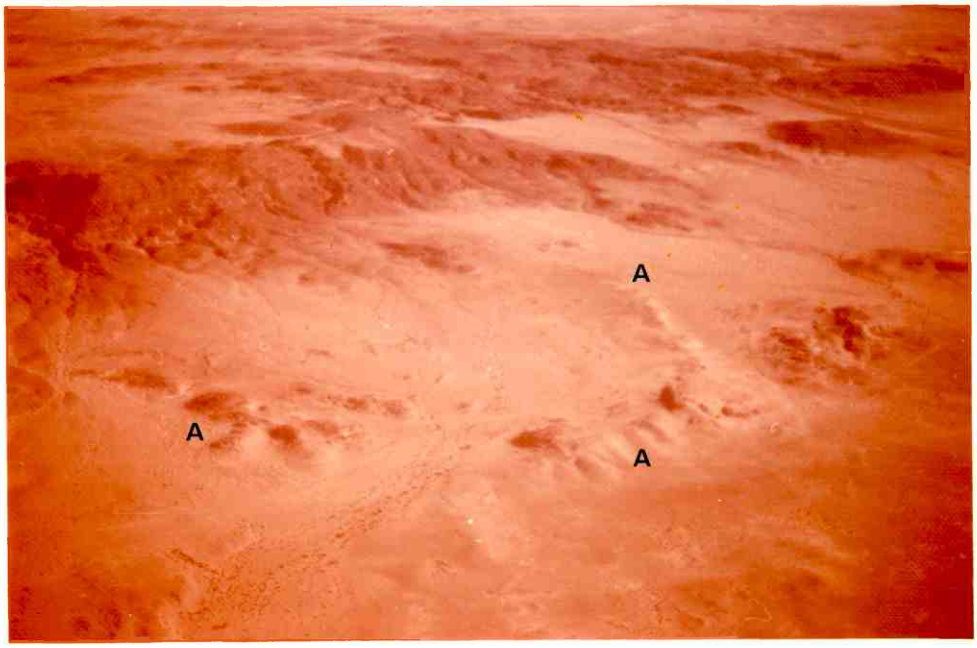


Photo plate (59) Aerial view of part of the Biyadh sandstone Formation showing one of the pseudovolcano features in the vicinity of Khashm Addughum Area. (A)

Photo plate (60) Aerial view (looking west) showing part of Khashm Addughum fault line (A-B) (complementary to Photo plate 23).


A
A
A

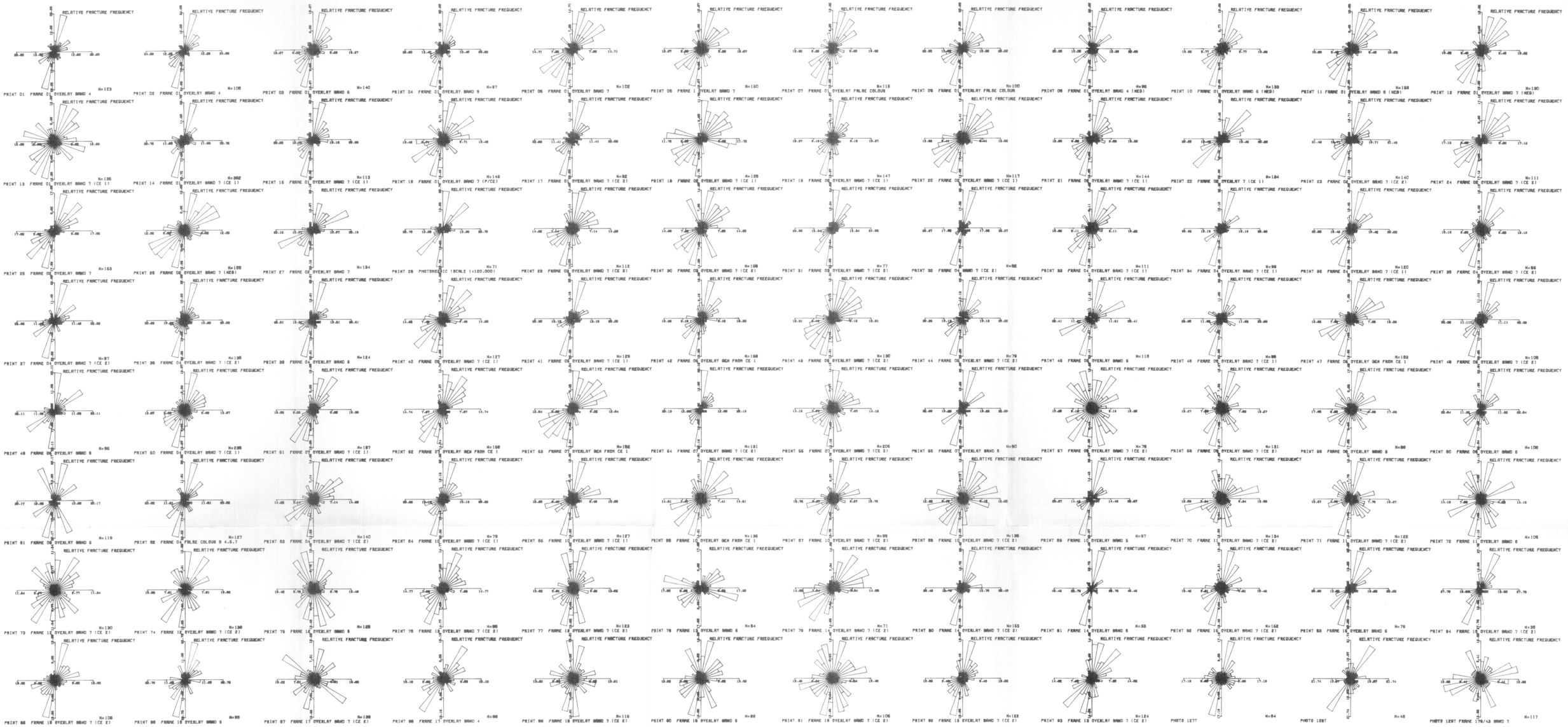

A
B

Photo plate (61) Aerial view over Harrat Khaybar (refer to Plate 7) showing the approximate N-S alignment of Tertiary volcanic cones (with permission of Elias Khoghandi DGMR).


N

PLATE 1. GENERAL ROSE DIAGRAMS (relative fracture frequency)

A. 1:1,000,000 interpretation overlays (multi-imagery)



B. 1:500,000 interpretation overlays (multi-imagery)

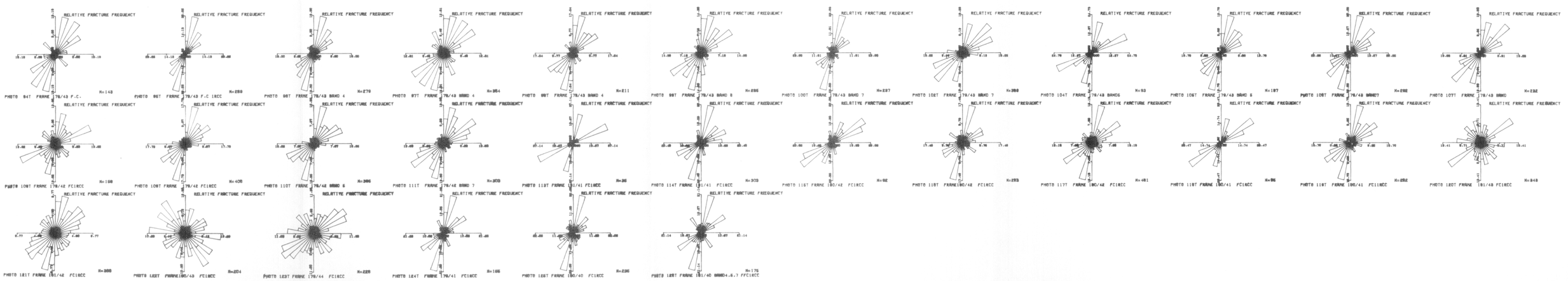
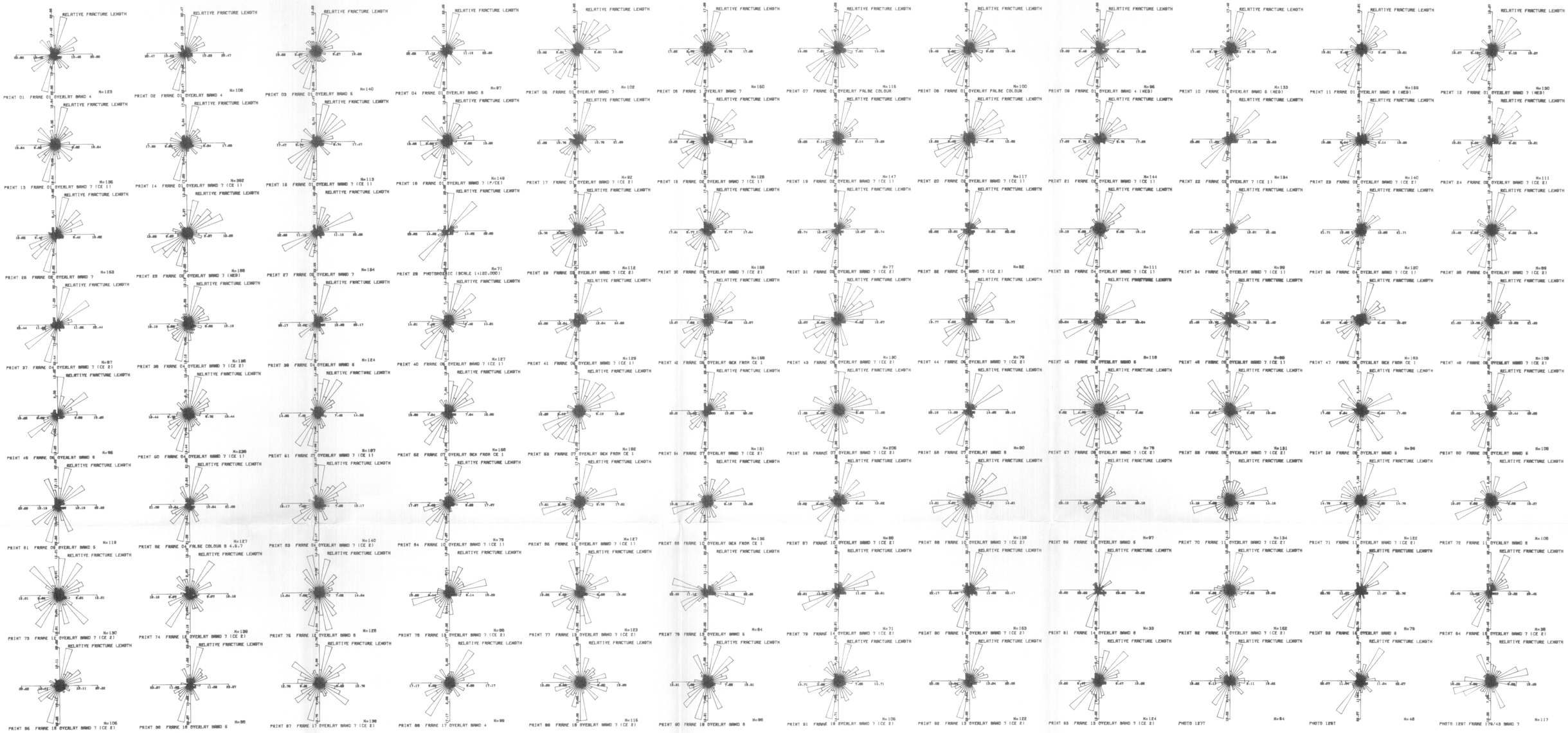


PLATE 2. GENERAL ROSE DIAGRAMS (relative fracture length)

A. 1:1,000,000 interpretation overlays (multi-imagery)



B. 1:500,000 interpretation overlays (multi-imagery)

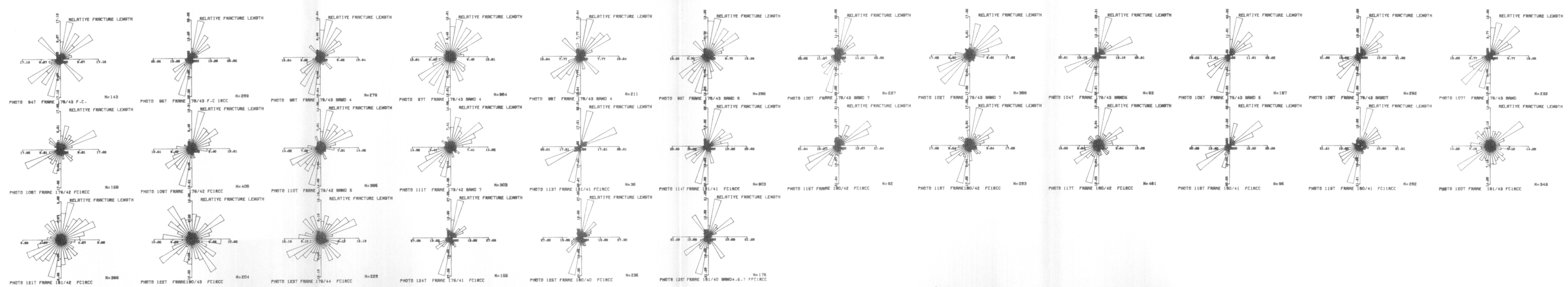
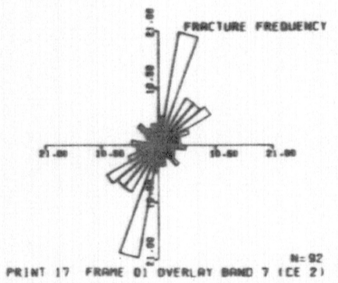
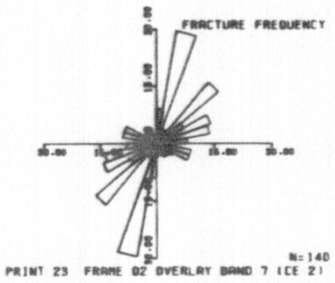


PLATE 3. SELECTED ROSE DIAGRAMS (fracture frequency)

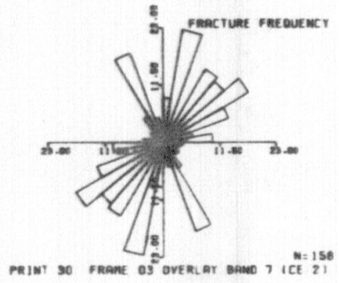
A. 1:1,000,000 C.E. Second Generation



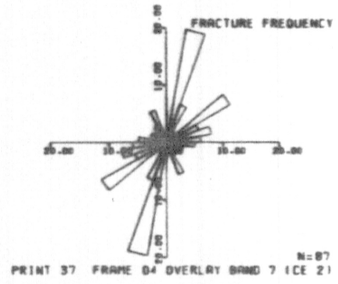
PRINT 17 FRAME 01 OVERLAY BAND 7 (CE 2)



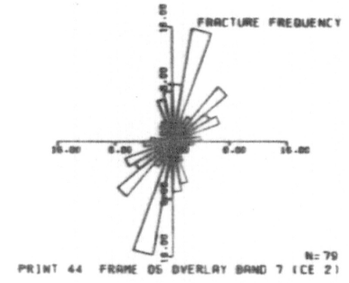
PRINT 23 FRAME 02 OVERLAY BAND 7 (CE 2)



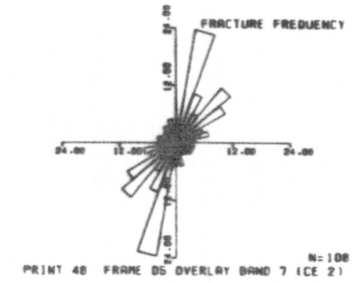
PRINT 30 FRAME 03 OVERLAY BAND 7 (CE 2)



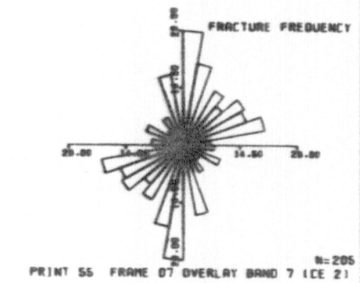
PRINT 37 FRAME 04 OVERLAY BAND 7 (CE 2)



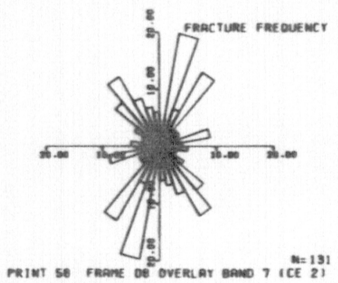
PRINT 44 FRAME 05 OVERLAY BAND 7 (CE 2)



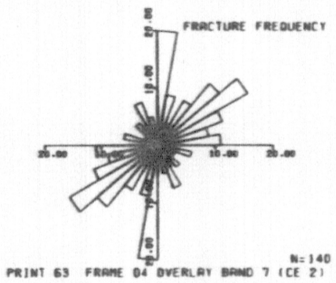
PRINT 48 FRAME 06 OVERLAY BAND 7 (CE 2)



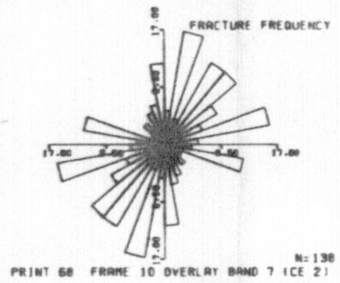
PRINT 55 FRAME 07 OVERLAY BAND 7 (CE 2)



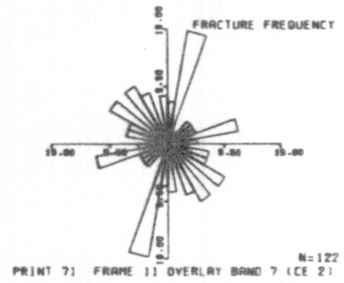
PRINT 58 FRAME 08 OVERLAY BAND 7 (CE 2)



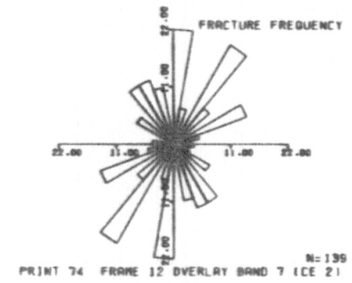
PRINT 63 FRAME 04 OVERLAY BAND 7 (CE 2)



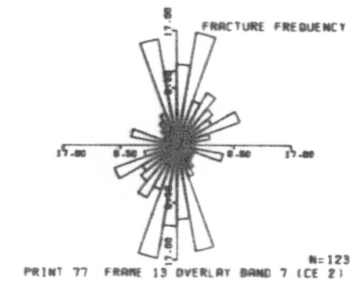
PRINT 68 FRAME 10 OVERLAY BAND 7 (CE 2)



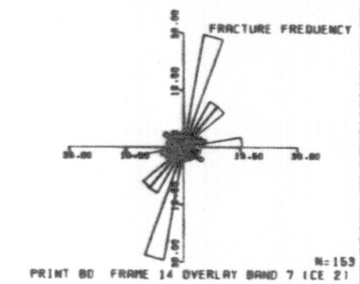
PRINT 71 FRAME 11 OVERLAY BAND 7 (CE 2)



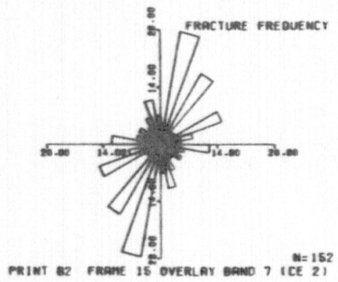
PRINT 74 FRAME 12 OVERLAY BAND 7 (CE 2)



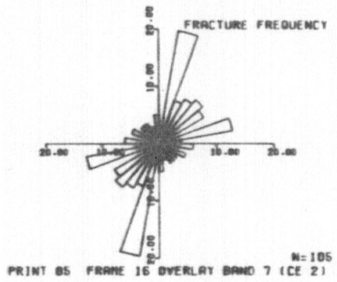
PRINT 77 FRAME 13 OVERLAY BAND 7 (CE 2)



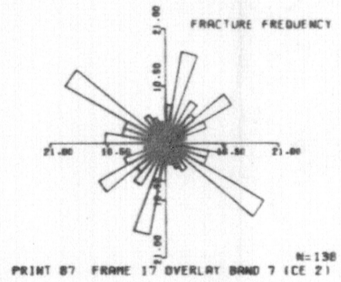
PRINT 80 FRAME 14 OVERLAY BAND 7 (CE 2)



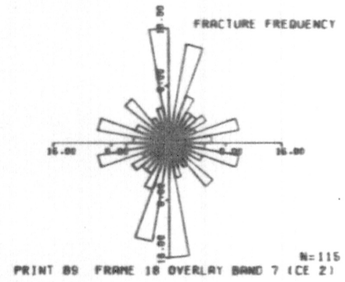
PRINT 82 FRAME 15 OVERLAY BAND 7 (CE 2)



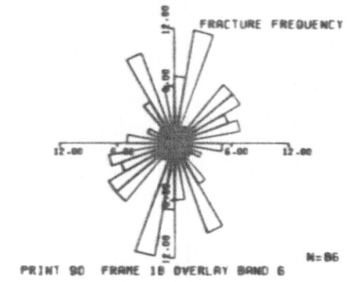
PRINT 85 FRAME 16 OVERLAY BAND 7 (CE 2)



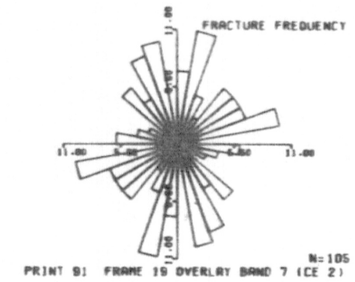
PRINT 87 FRAME 17 OVERLAY BAND 7 (CE 2)



PRINT 89 FRAME 18 OVERLAY BAND 7 (CE 2)



PRINT 90 FRAME 18 OVERLAY BAND 6



PRINT 91 FRAME 19 OVERLAY BAND 7 (CE 2)

B. 1:500,000 infra-red colour composite

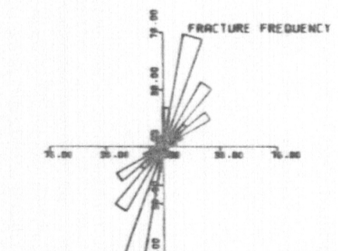


PHOTO 96T FRAME 178/43 F.C 1RCC

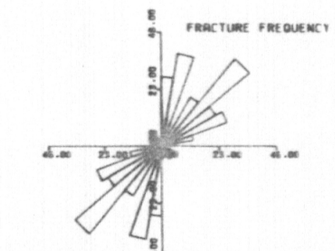


PHOTO 107T FRAME 179/43 BAND

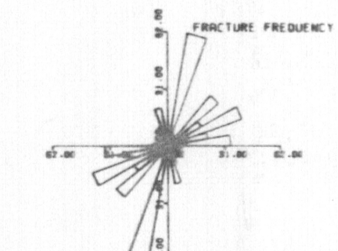


PHOTO 114T FRAME 181/41 FC1RCC

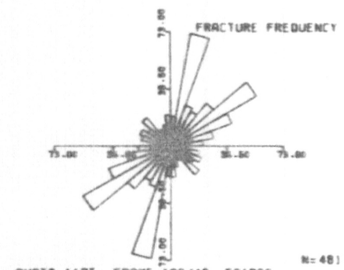


PHOTO 117T FRAME 180/42 FC1RCC

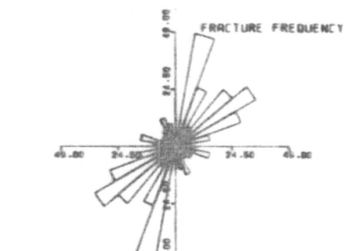


PHOTO 119T FRAME 180/41 FC1RCC

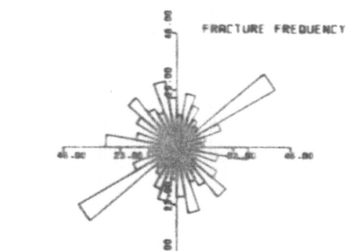


PHOTO 120T FRAME 181/43 FC1RCC

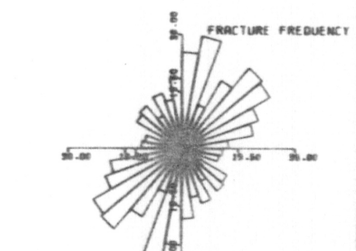


PHOTO 121T FRAME 181/42 FC1RCC

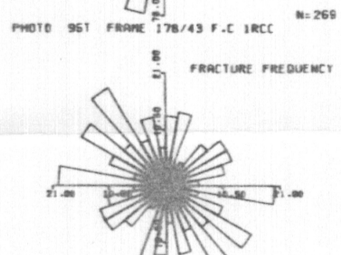


PHOTO 122T FRAME 180/43 FC1RCC

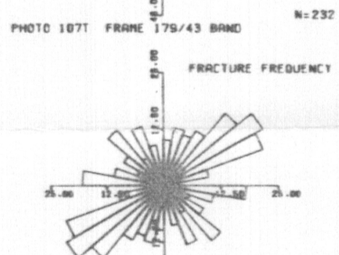


PHOTO 123T FRAME 179/44 FC1RCC

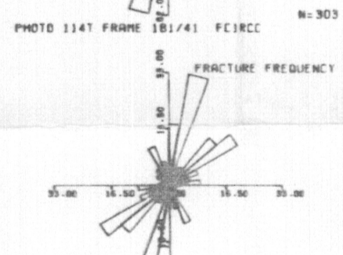


PHOTO 124T FRAME 179/41 FC1RCC

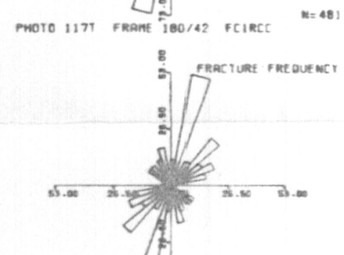


PHOTO 125T FRAME 180/40 FC1RCC

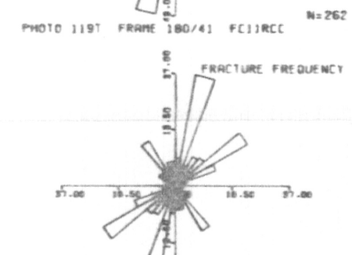
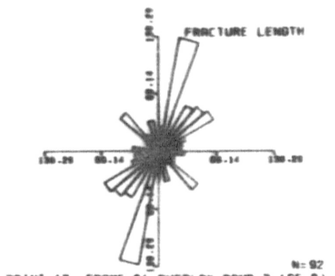


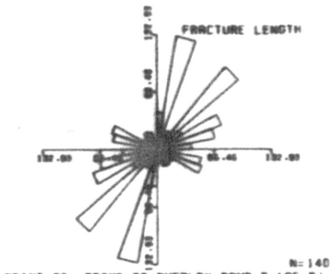
PHOTO 126T FRAME 181/40 BAND4.5.7 FFC1RCC

PLATE 4. SELECTED ROSE DIAGRAMS (fracture length)

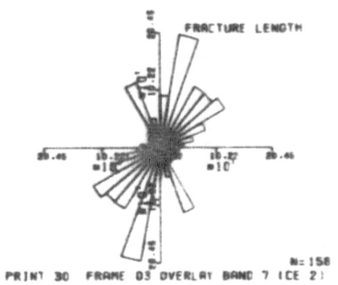
A. 1:1,000,000 C.E. Second Generation



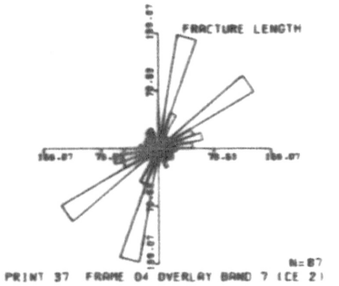
PRINT 17 FRAME 01 OVERLAY BAND 7 (CE 2)



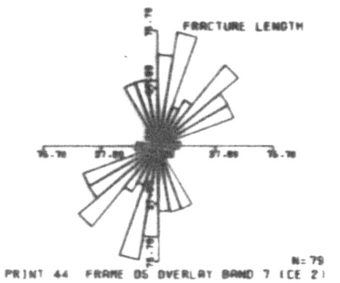
PRINT 23 FRAME 02 OVERLAY BAND 7 (CE 2)



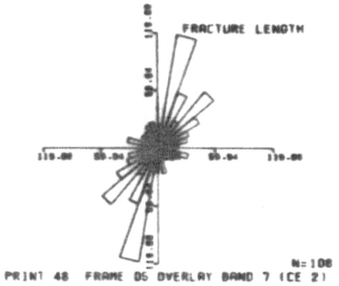
PRINT 30 FRAME 03 OVERLAY BAND 7 (CE 2)



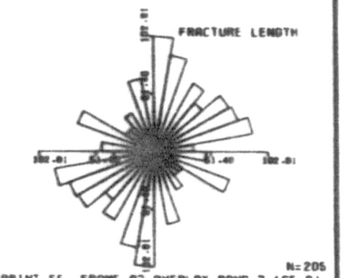
PRINT 37 FRAME 04 OVERLAY BAND 7 (CE 2)



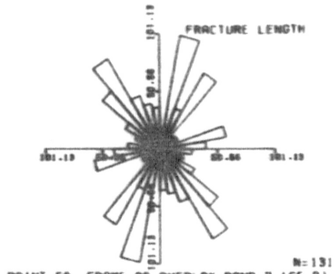
PRINT 44 FRAME 05 OVERLAY BAND 7 (CE 2)



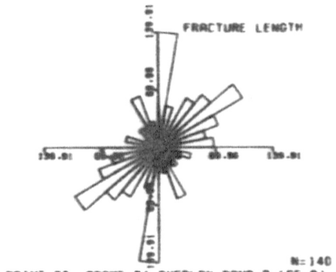
PRINT 48 FRAME 06 OVERLAY BAND 7 (CE 2)



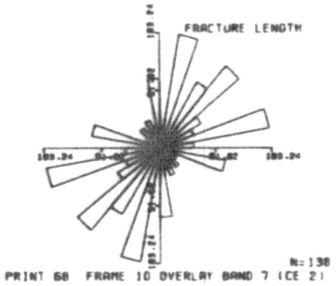
PRINT 56 FRAME 07 OVERLAY BAND 7 (CE 2)



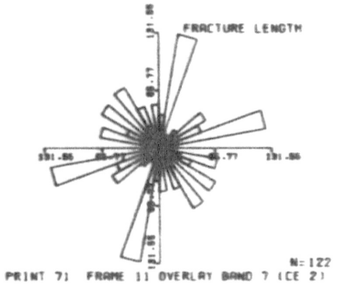
PRINT 58 FRAME 08 OVERLAY BAND 7 (CE 2)



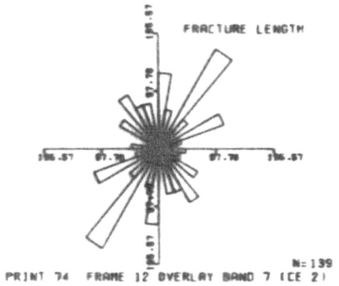
PRINT 63 FRAME 04 OVERLAY BAND 7 (CE 2)



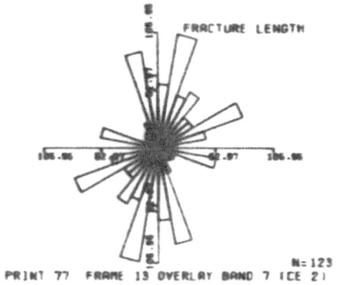
PRINT 68 FRAME 10 OVERLAY BAND 7 (CE 2)



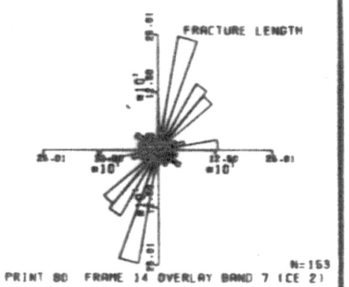
PRINT 71 FRAME 11 OVERLAY BAND 7 (CE 2)



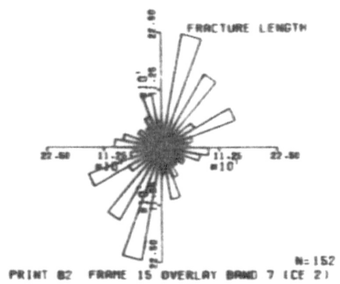
PRINT 74 FRAME 12 OVERLAY BAND 7 (CE 2)



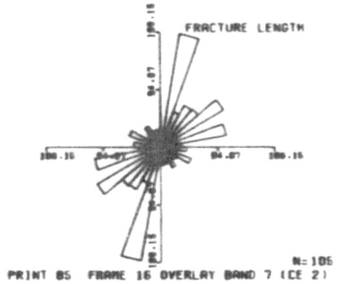
PRINT 77 FRAME 13 OVERLAY BAND 7 (CE 2)



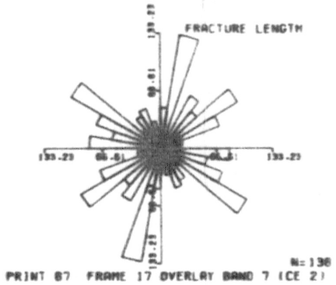
PRINT 80 FRAME 14 OVERLAY BAND 7 (CE 2)



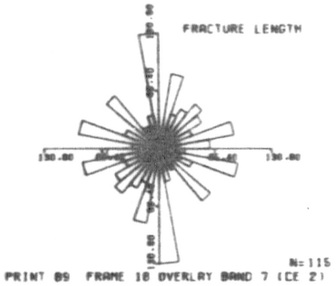
PRINT 82 FRAME 15 OVERLAY BAND 7 (CE 2)



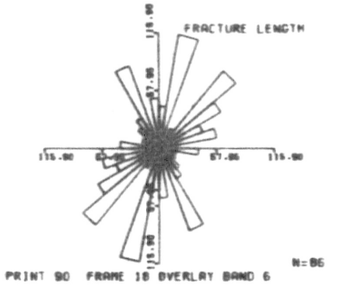
PRINT 85 FRAME 16 OVERLAY BAND 7 (CE 2)



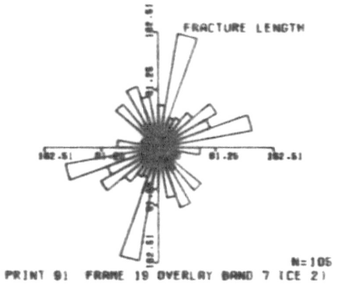
PRINT 87 FRAME 17 OVERLAY BAND 7 (CE 2)



PRINT 89 FRAME 18 OVERLAY BAND 7 (CE 2)



PRINT 90 FRAME 18 OVERLAY BAND 6



PRINT 91 FRAME 19 OVERLAY BAND 7 (CE 2)

B. 1:500,000 infra-red colour composite

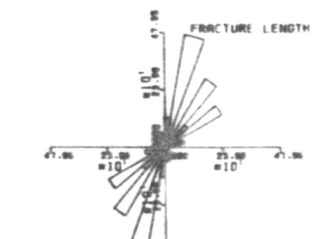


PHOTO 96T FRAME 178/43 F.C IRCC

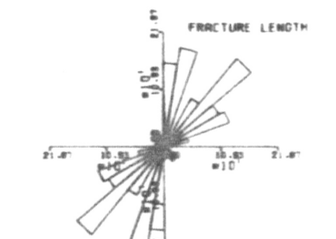


PHOTO 107T FRAME 179/43 BAND

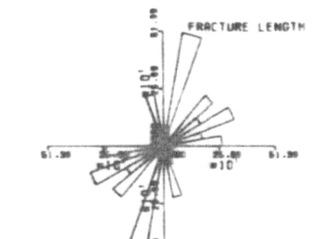


PHOTO 114T FRAME 181/41 FC)RCC

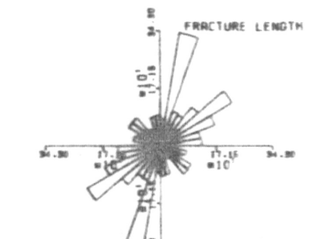


PHOTO 117T FRAME 180/42 FC)RCC

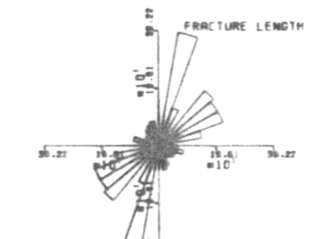


PHOTO 119T FRAME 180/41 FC)RCC

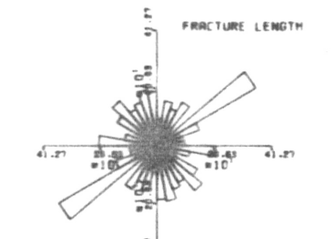


PHOTO 120T FRAME 181/43 FC)RCC

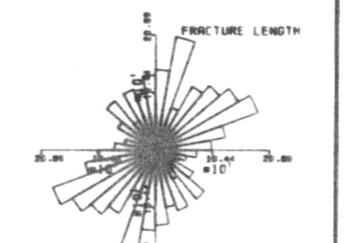


PHOTO 121T FRAME 181/42 FC)RCC

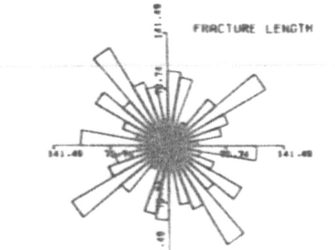


PHOTO 122T FRAME 180/43 FC)RCC

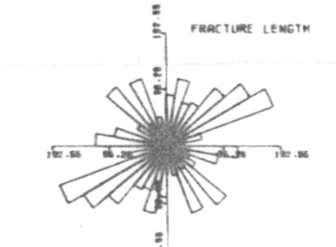


PHOTO 123T FRAME 179/44 FC)RCC

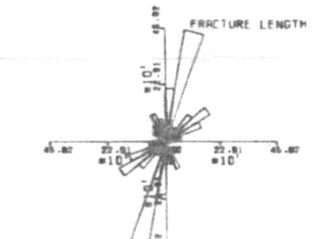


PHOTO 124T FRAME 179/41 FC)RCC

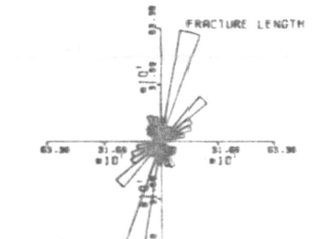


PHOTO 125T FRAME 180/40 FC)RCC

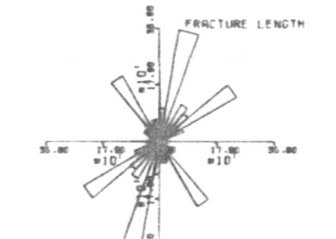
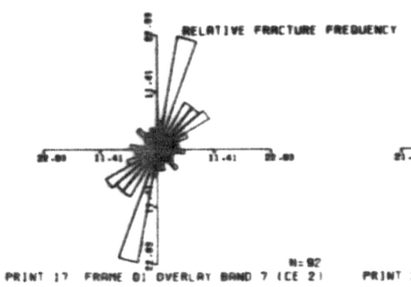
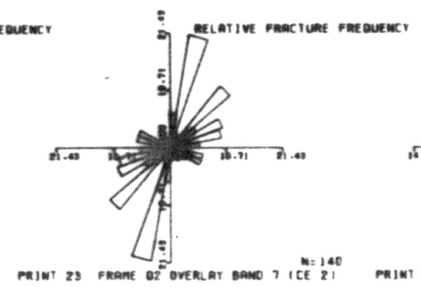


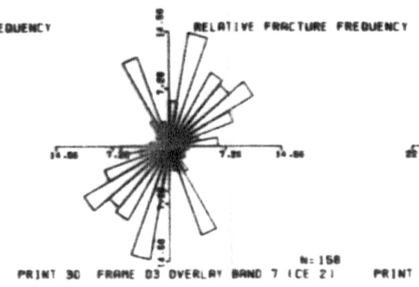
PHOTO 126T FRAME 181/40 BAND4,5,7 FC)RCC

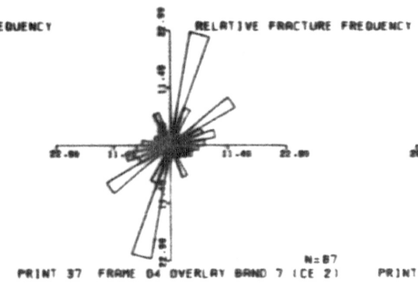
PLATE 5. SELECTED ROSE DIAGRAMS (relative fracture frequency)

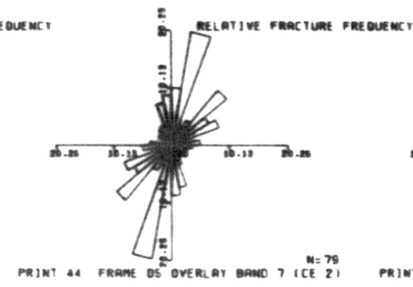
A. 1:1,000,000 C.E. Second Generation

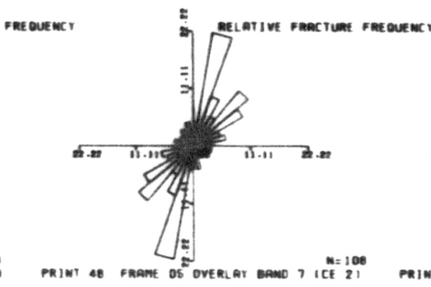


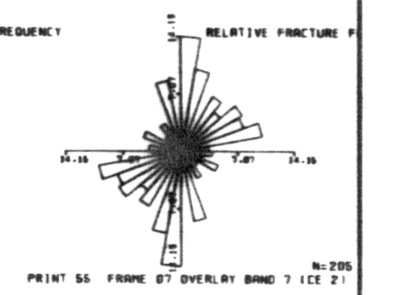


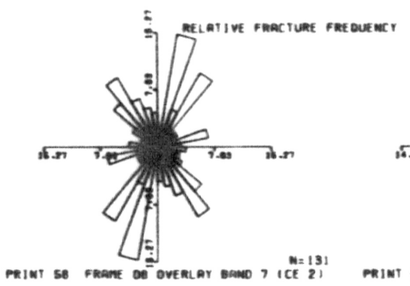


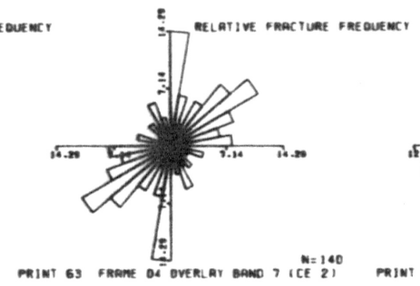


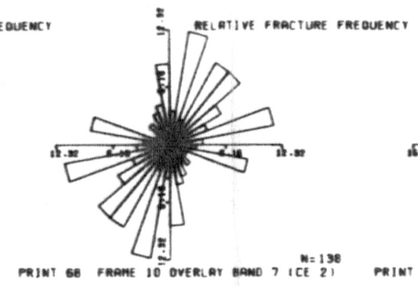


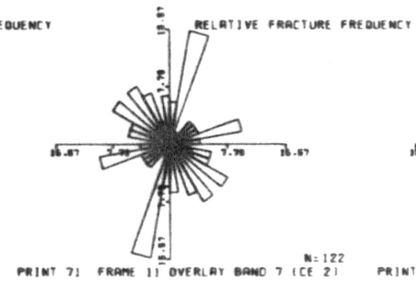


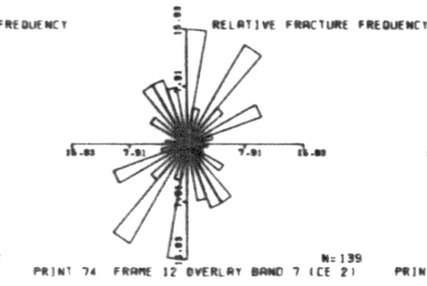


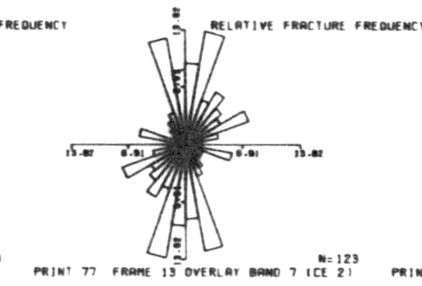


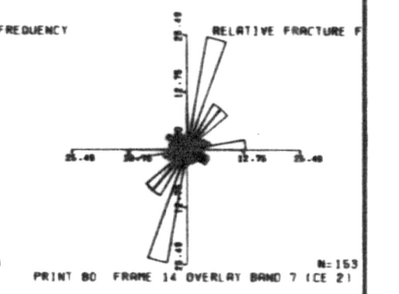


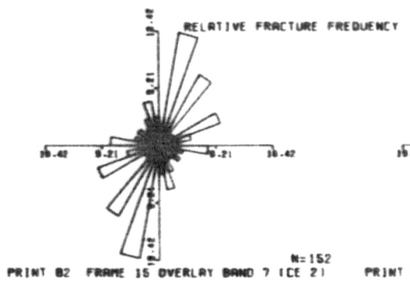


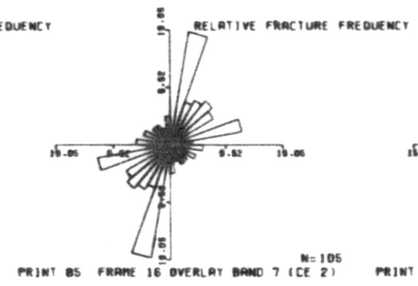


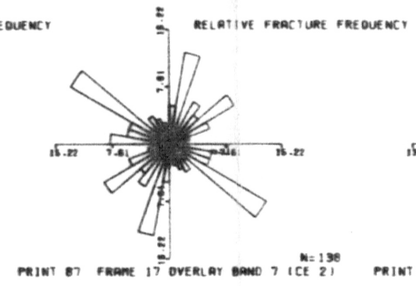


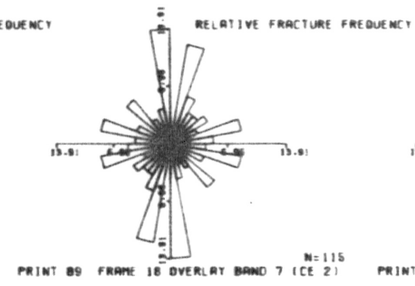


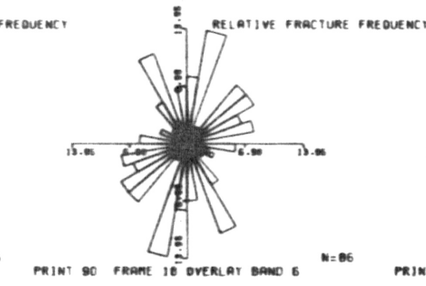


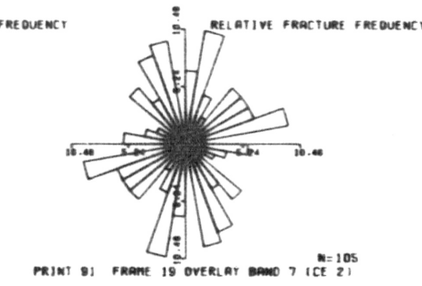




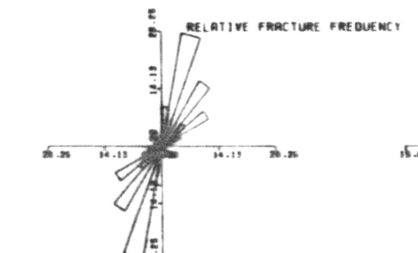


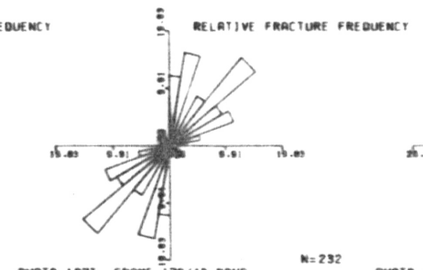


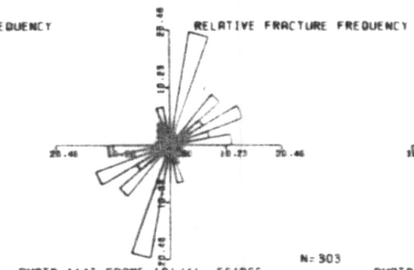


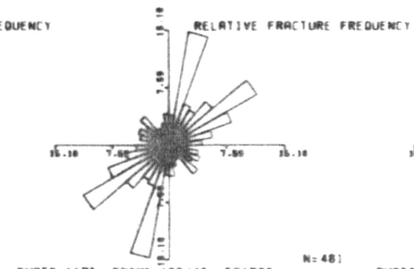


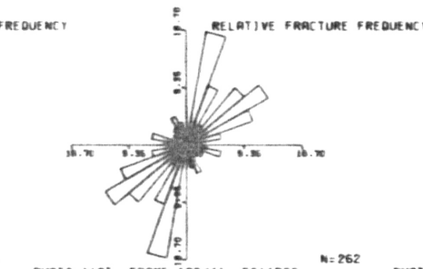
B. 1:500,000 infra-red colour composite

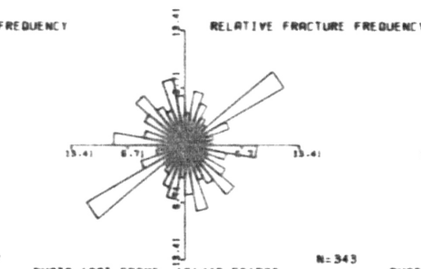


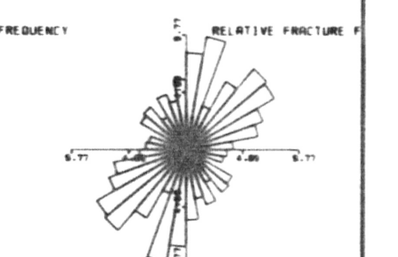


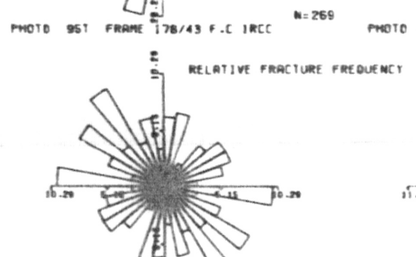


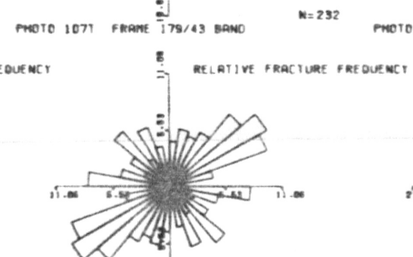


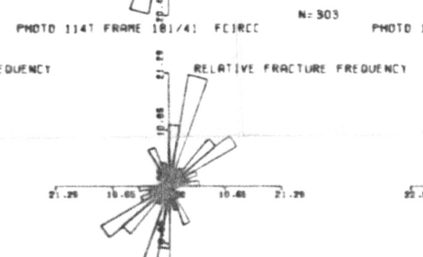


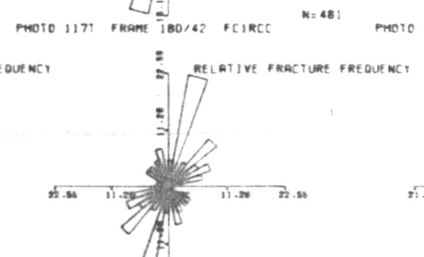












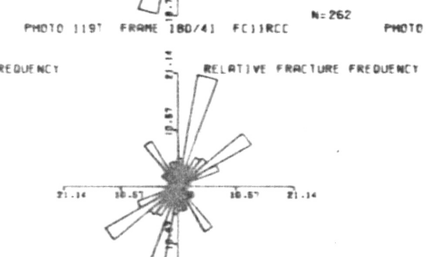
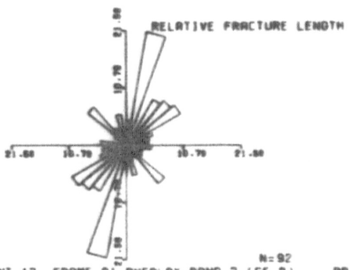
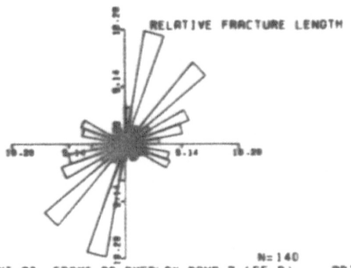


PLATE 6. SELECTED ROSE DIAGRAMS (relative fracture length)

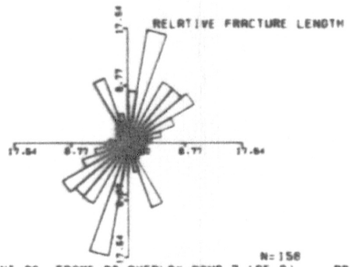
A. 1:1,000,000 C.E. Second Generation



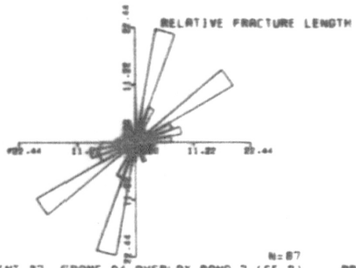
PRINT 17 FRAME 01 OVERLAY BAND 7 (CE 2)



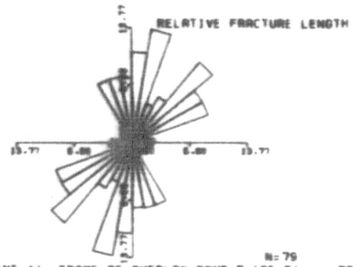
PRINT 23 FRAME 02 OVERLAY BAND 7 (CE 2)



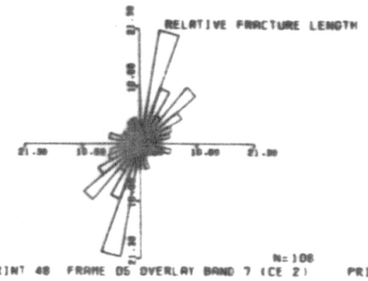
PRINT 30 FRAME 03 OVERLAY BAND 7 (CE 2)



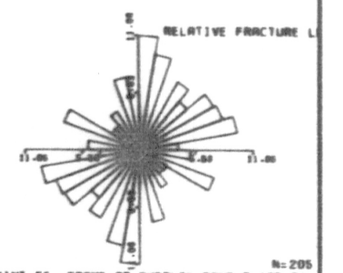
PRINT 37 FRAME 04 OVERLAY BAND 7 (CE 2)



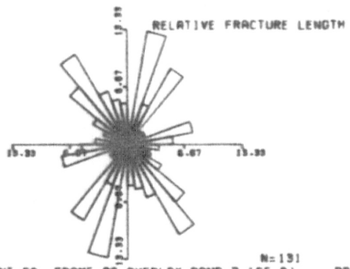
PRINT 44 FRAME 05 OVERLAY BAND 7 (CE 2)



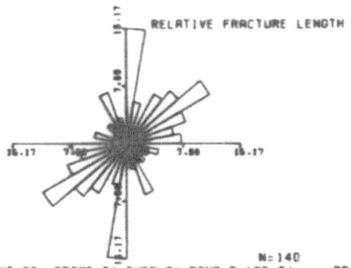
PRINT 48 FRAME 06 OVERLAY BAND 7 (CE 2)



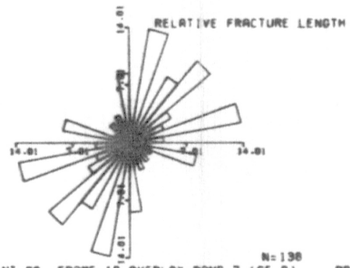
PRINT 56 FRAME 07 OVERLAY BAND 7 (CE 2)



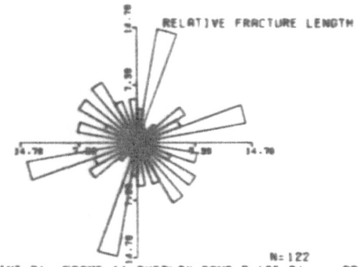
PRINT 58 FRAME 08 OVERLAY BAND 7 (CE 2)



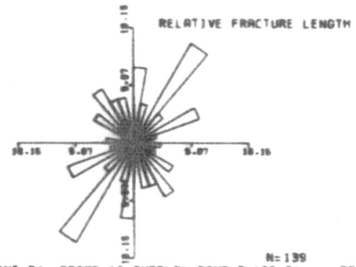
PRINT 63 FRAME 04 OVERLAY BAND 7 (CE 2)



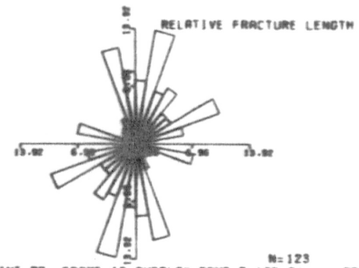
PRINT 68 FRAME 10 OVERLAY BAND 7 (CE 2)



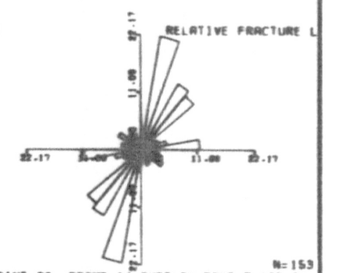
PRINT 71 FRAME 11 OVERLAY BAND 7 (CE 2)



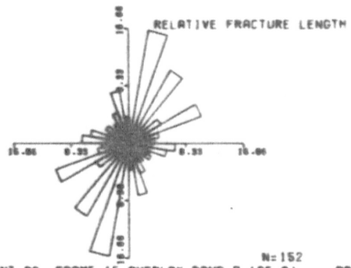
PRINT 74 FRAME 12 OVERLAY BAND 7 (CE 2)



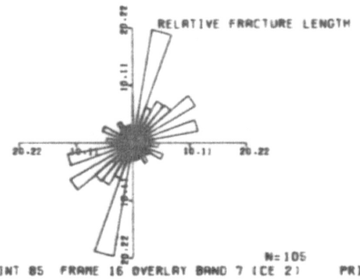
PRINT 77 FRAME 13 OVERLAY BAND 7 (CE 2)



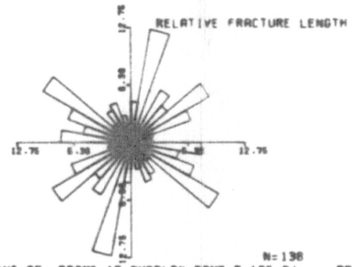
PRINT 80 FRAME 14 OVERLAY BAND 7 (CE 2)



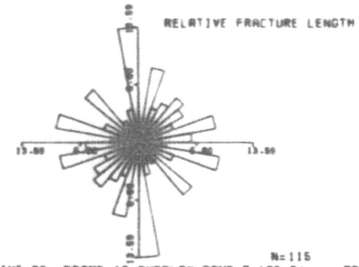
PRINT 82 FRAME 15 OVERLAY BAND 7 (CE 2)



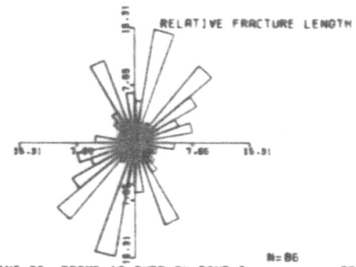
PRINT 85 FRAME 16 OVERLAY BAND 7 (CE 2)



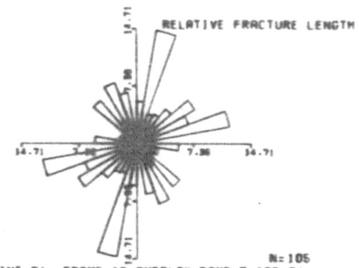
PRINT 87 FRAME 17 OVERLAY BAND 7 (CE 2)



PRINT 89 FRAME 18 OVERLAY BAND 7 (CE 2)



PRINT 90 FRAME 18 OVERLAY BAND 6



PRINT 91 FRAME 19 OVERLAY BAND 7 (CE 2)

B. 1:500,000 infra-red colour composite

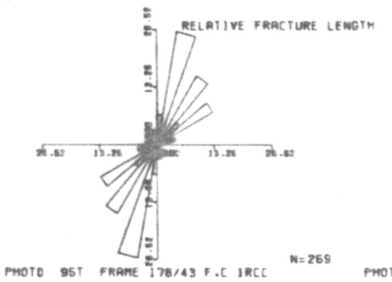


PHOTO 95T FRAME 178/43 F.C 1RCC

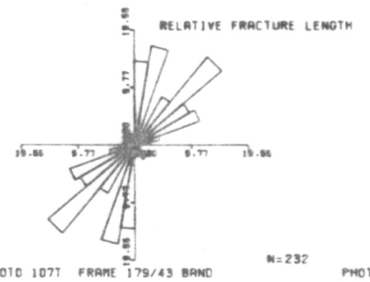


PHOTO 107T FRAME 179/43 BAND

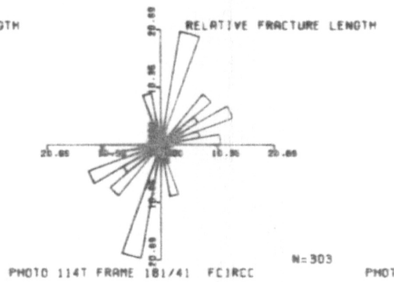


PHOTO 114T FRAME 181/41 FC1RCC

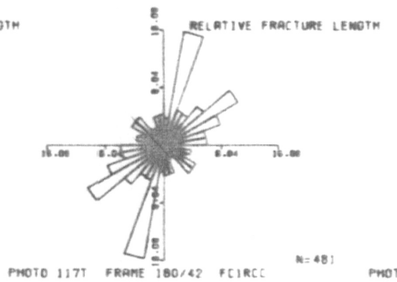


PHOTO 117T FRAME 180/42 FC1RCC

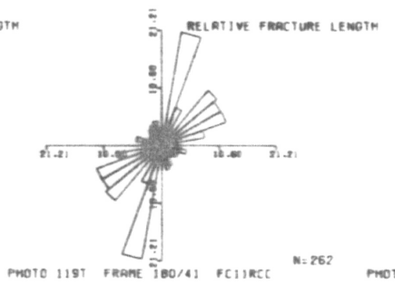


PHOTO 119T FRAME 180/41 FC11RCC

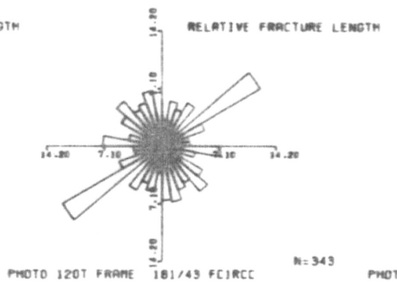


PHOTO 120T FRAME 181/43 FC1RCC

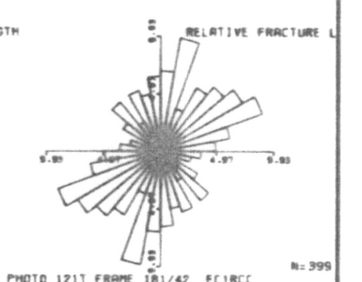


PHOTO 121T FRAME 181/42 FC1RCC

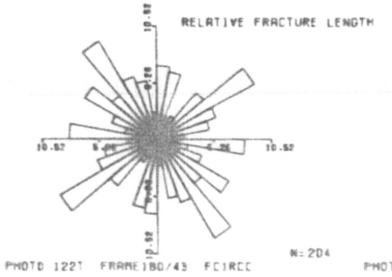


PHOTO 122T FRAME180/43 FC1RCC

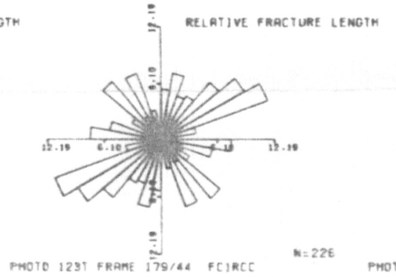


PHOTO 123T FRAME 179/44 FC1RCC

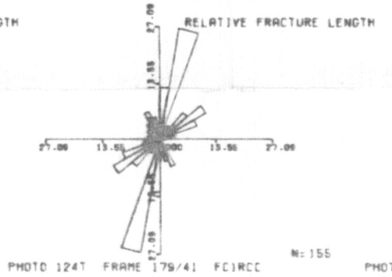


PHOTO 124T FRAME 179/41 FC1RCC

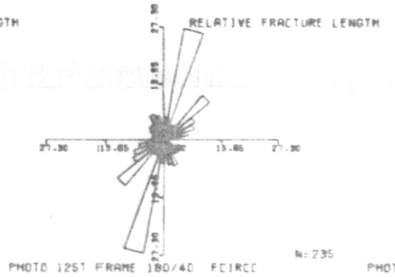


PHOTO 125T FRAME 180/40 FC1RCC

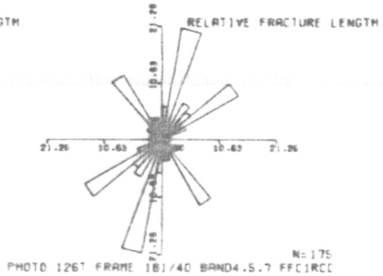


PHOTO 126T FRAME 181/40 BAND4.5.7 FFC1RCC

KINGDOM OF SAUDI ARABIA

Plate 7 (This geological map clarifies figure numbers 37, 45, 47, 51 and 52).

GEOLOGIC EXPLANATION

Double or fractional symbols indicate grouped formations; color-pattern of dominant formation shown. Symbols queried where identification doubtful.

SAUDI ARABIA (Includes western Saudi Arabia and northern Yemen) — **YEMEN** — **WESTERN ADEN PROTECTORATE**

QUATERNARY
- Qe Eolian sand — Qe Eolian sand — Qe Eolian sand
- Qu Alluvium and related surficial deposits — Qu Alluvium and related surficial deposits — Qu Alluvium and related surficial deposits *May include rocks of Pliocene age*
- Qsb Qs Sabkhah and silt deposits
- Qb Basalt and pyroclastic rocks — Qa Aden Volcanic Series *May include rocks of Pliocene age* — Qa Aden Volcanic Series *May include rocks of Pliocene age*

TERTIARY AND QUATERNARY
- Qt Terrace sand and gravel
- QTb Basalt and andesite

TERTIARY(?) — *Pliocene(?)*
- Tuc/Tc Molasse-like clastic rocks

TERTIARY — *Miocene or Pliocene*
- Tlb Lacustrine sediments
- Tb Basalt and andesite
- Ta Andesite and diabase — TERTIARY(?): Tla Laccoliths *May include intrusive rocks of Late Cretaceous age*

Miocene
- Tba/Tra Baid and Raghama Formations — Tgr Granite

Eocene
- Tsh Shumaysi Formation — Tr Rus Formation

Paleocene and Eocene
- Tus Usfan Formation — Tj Jeza Formation
- Tm Medj-zir Series — Tu Umm er Radhuma Formation

CRETACEOUS
- TKt Trap Series in places upper part overlies Medj-zir Series — TKt Trap Series
- Kk Khurma Formation — Kt Tawilah Group — Kt Tawilah Group

JURASSIC
- Jh Hanifa Formation — Jam Amran Series — Ju Jurassic rocks, undivided
- Jk Khums Formation — Jko Kohlan Series

PERMIAN OR OLDER
- Pw Wajid Sandstone — Pw Wajid Sandstone

PRECAMBRIAN(?) TO PALEOZOIC
- ag Albite-muscovite granite — PRECAMBRIAN(?) AND PALEOZOIC: Pp&Cg Precambrian(?) synkinematic and Paleozoic postkinematic granitic rocks
- rtp Rhyolite, trachyte and phonolite

PRECAMBRIAN
- sr Shammar Rhyolite — PRECAMBRIAN(?): gh Granitic and hybrid rocks
- gp/sy Peralkaline granite and syenite — hr Hybrid rocks
- di Diorite — dr Dioritic rock
- a/fa Abla and Fatima Formations
- fm Farida Marble
- sc Sericite and chlorite schist
- mu/h Murdama and Hadiyah Formations
- hi Hibshi Formation
- gm Calc-alkaline granite — ur Precambrian rocks undivided — mr Precambrian metamorphic rocks
- hd Diorite and quartz diorite
- ub/s Ultrabasic rocks and serpentinite
- ha/hc Halaban Formation *ha, andesite hc, clastic rocks*
- gr Calc-alkaline granite
- qd Quartz diorite and adamellite
- gn/gg Granite gneiss and granite *gn, mapped only north of Najd fault zone*
- dg Granodiorite and diorite
- d/gb Diorite and gabbro
- bu Altered basic igneous rocks
- bg/bs Baish Greenstone *bs, greenschist. as, amphibolite schist*
- gd/gds Jiddah Greenstone *gds, greenschist*
- sl Silasia Formation
- am Amphibolite
- ab Abt Schist
- wh Hali Schist
- wl Lith Complex

Geologic contact

Fault, showing dip *Dashed where approximately located; dotted where concealed*

Thrust fault *Dashed where approximately located*

Anticline *Showing trace of axial plane and bearing and plunge of axis. Dashed where approximately located*

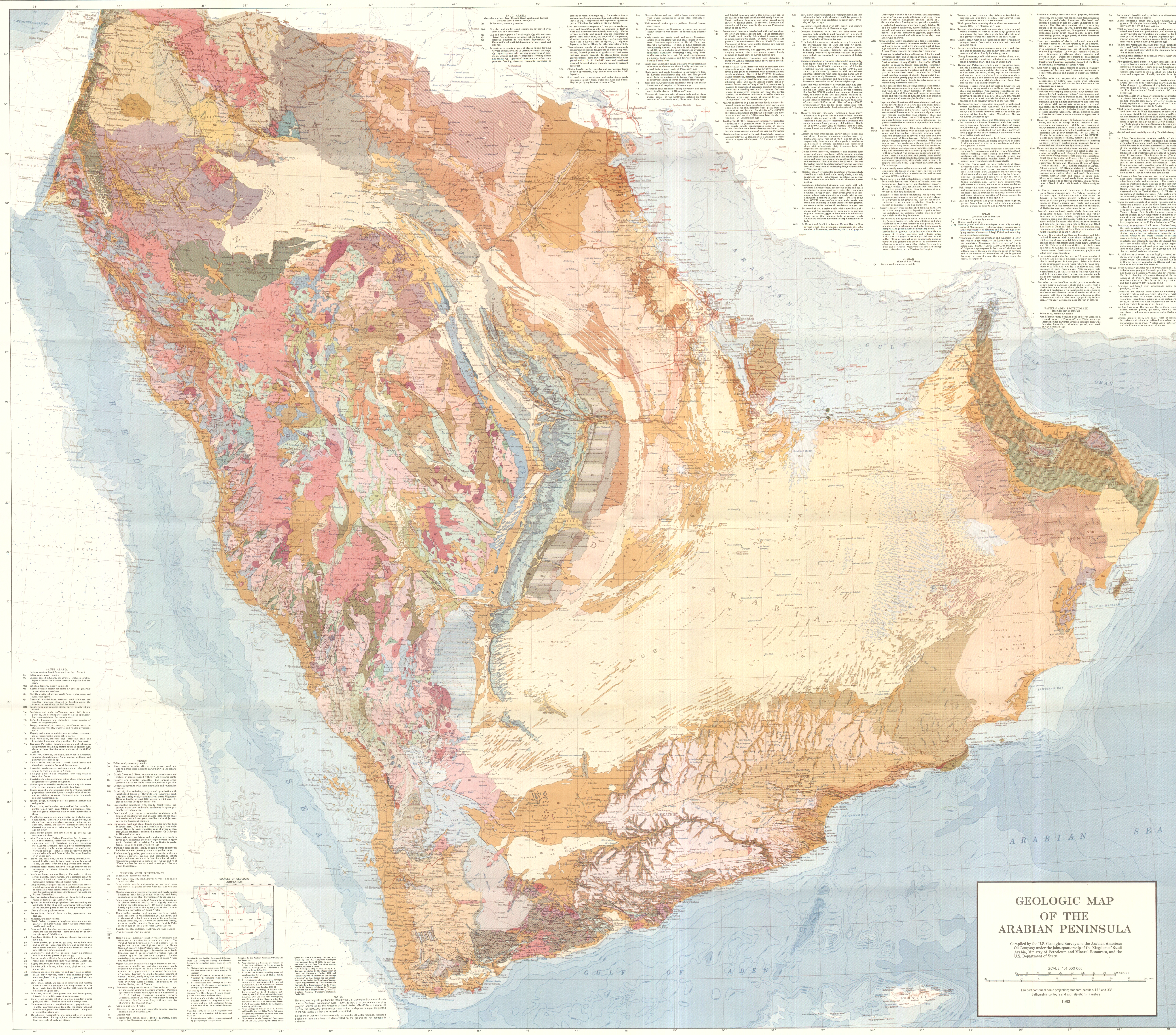
Syncline *Showing trace of axial plane and bearing and plunge of axis. Dashed where approximately located*

Monocline *Trace of axis dashed where approximately located; arrows indicate downfolded side*

Dug well

Drilled well

Dahl



GEOLOGIC EXPLANATION

Double or fractional symbols indicate grouped formations; color-pattern of dominant formation shown. Symbols queried where identification doubtful.

SAUDI ARABIA (Includes southern Iraq, Kuwait, Saudi Arabia and Kuwait Neutral Zone, Bahrain, and Qatar) — **JORDAN (East of Rift Valley)** — **OMAN (Includes part of Dhufar)** — **EASTERN ADEN PROTECTORATE (Includes part of Dhufar)**

QUATERNARY
- Qe Eolian Sand — Qe Eolian sand — Qe Eolian Sand — Qe Eolian sand
- Qsb Sabkhah deposits
- Qg/Qs Gravel, sand, and silt — Qu Gravel, sand, and clay — Qu Gravel, sand, and silt — Qu Alluvium and related surficial deposits *May include rocks of Pliocene age*
- Qg Gravel — Qg Gravel
- Terrace, mud flat and gypsum deposits — Qlm Lisan Series
- Qd Calcareous duricrust — Qa Aden Volcanic Series *May include rocks of Pliocene age*

TERTIARY AND QUATERNARY
- QTb Basalt — QTb Basalt
- QTm Marl and sandstone — QTag Alluvium and gravel

TERTIARY — *Miocene and Pliocene*
- Tag Terrace sand and gravel
- Tg Gravel
- Tk Kharj Formation
- Tam Sandstone, marl, and limestone — Tam Sandstone, marl, and limestone — Tam Sandstone, marl, and conglomerate
- Thf Hofuf Formation
- Tf Lower Fars Formation
- Td Dam Formation
- Th Hadrukh Formation

Oligocene: Tl Limestone, chalk, marl, and evaporite; To Limestone and marl — *Oligocene and Miocene*: Ts Shihr Group and equivalents

Eocene
- Tdm Dammam Formation — Tha Habshiya Formation — Tdr Dammam and Rus Formations
- Tdr Dammam and Rus Formations — SAUDI ARABIA AND JORDAN: Tlc Limestone and chalk — Thj Habshiya and Jeza Formations
- Tr Rus Formation — Tj Jeza Formation — Tr Rus Formation

Paleocene
- Tu Umm er Radhuma Formation — Tml Marl and limestone — Tu Umm er Radhuma Formation

CRETACEOUS — *Upper Cretaceous*
- Ka Aruma Formation — *Upper Cretaceous to Eocene*: TKb Belqa Series — CRETACEOUS AND TERTIARY: TKs Sedimentary rocks; Kse Semail Igneous Complex; Kh Hawasina Complex
- Kw Wasia Formation

Middle Cretaceous
- Kwb Wasia and Biyadh Formations — Kaj Ajlun Series

Lower Cretaceous
- Kb Biyadh Sandstone — CRETACEOUS: Klm Limestone, marl, and sandstone — Kt Tawilah Group — Km Mahra Group
- Kbu Buwaib Formation — Kha Hathira Sandstone
- Ky Yamama Formation
- Ks Sulaiy Formation

JURASSIC — *Upper Jurassic*
- Jhi/Ja Hith Anhydrite and Arab Formation — JURASSIC TO CRETACEOUS: KJm Musandam Limestone
- Jl Jubaila Limestone
- Jh Hanifa Formation
- Jtm Tuwaiq Mountain Limestone

Middle Jurassic
- Jd Dhruma Formation — Ju Jurassic rocks — Ju Jurassic rocks

Lower Jurassic
- Jm Marrat Formation
- JTkm Minjur Sandstone — JTkz Zarqa Group

TRIASSIC
- Tkj Jilh Formation — SAUDI ARABIA — PALEOZOIC, MESOZOIC AND CENOZOIC: CzPzl Limestone, chert and sandstone — PERMIAN AND TRIASSIC: TkP Triassic and Permian rocks
- TkPs Sudair Shale — MzPzs Sakaka Sandstone

PERMIAN
- Pk Khuff Formation

PERMIAN OR OLDER
- Pw Wajid Sandstone

DEVONIAN
- Dj Jauf Formation

ORDOVICIAN, SILURIAN AND DEVONIAN
- Dt/DSOt Tabuk Formation *Dt, Tawil Sandstone Member* — DSOt Tabuk Formation — PALEOZOIC: Pzu Limestone, dolomite, and shale; Pzm Murbat Sandstone — PALEOZOIC(?): Pzg Ghabar and Gharish Groups; Pzhs El Hota and Ain Sarit Groups

CAMBRIAN AND ORDOVICIAN
- OCs Saq Sandstone
- OCur Umm Sahm and Ram Sandstones — OCur Umm Sahm and Ram Sandstones

CAMBRIAN
- Cq Quweira Sandstone — Cq Quweira Sandstone
- Cs Siq Sandstone
- Ch Hormuz Complex equivalents

PRECAMBRIAN(?) TO PALEOZOIC
- Pp&Cg Precambrian(?) synkinematic and Paleozoic postkinematic granitic rocks

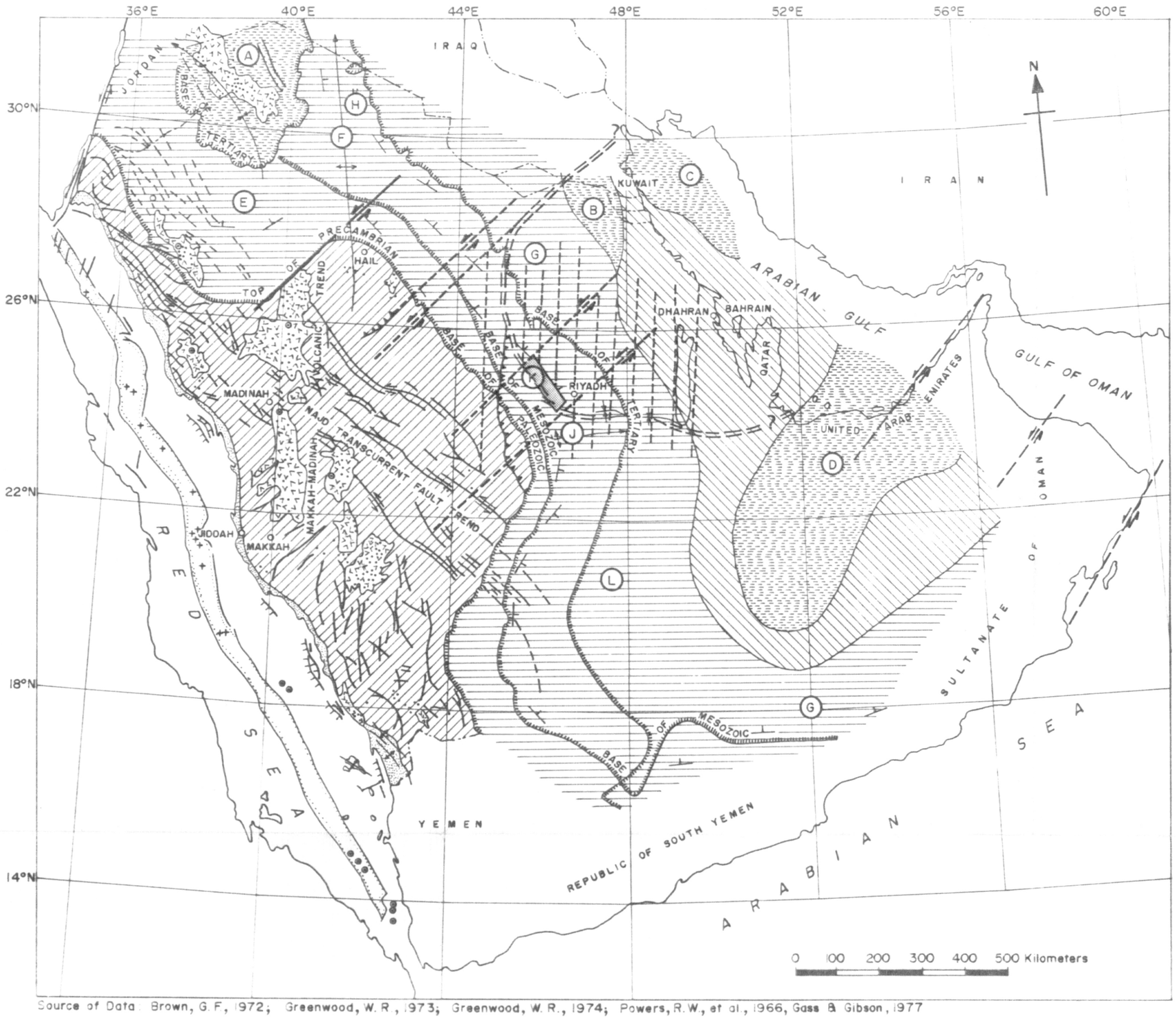
PRECAMBRIAN(?)
- vs Volcanic Series

PRECAMBRIAN
- ss Saramuj Series — th Thaniya Group
- pCa Aqaba Granite Complex — gs Gneiss and schist
- ggs Gneiss, granitic rock and schist

This map is a photographically reduced version of the 1963 edition of the U.S. Geological Survey Miscellaneous Geologic Investigations Map I-270A. Copies of this map are available from the Ministry of Petroleum and Mineral Resources, Directorate General of Mineral Resources, P.O. Box 345, Jiddah, Saudi Arabia.

FIGURE 29: MODIFIED TECTONIC MAP
KINGDOM OF SAUDI ARABIA

by S.O. Al-Khatieb (1980)



Source of Data: Brown, G.F., 1972; Greenwood, W.R., 1973; Greenwood, W.R., 1974; Powers, R.W., et al., 1966, Gass & Gibson, 1977

EXPLANATION

PHANEROZOIC (not in chronological order)

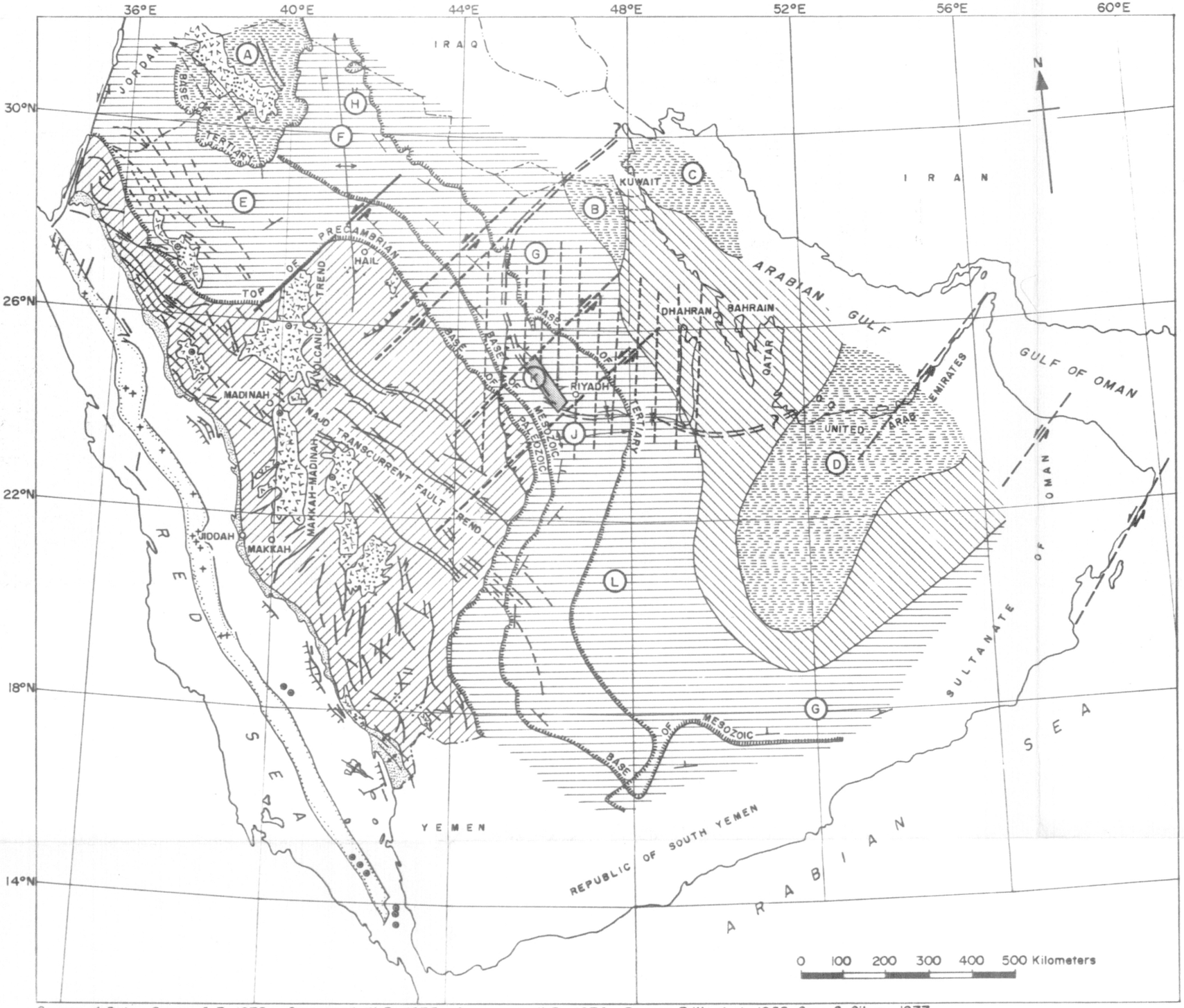
- CENOZOIC VOLCANIC ROCKS (basalt)
- UPPER MESOZOIC – CENOZOIC Sedimentary Rocks Paralleling Red Sea Structure
- PALEOZOIC – MESOZOIC – CENOZOIC (not in chronological order)
- ARABIAN SHELF BASINS
  - A. Wadi Sirhan Basin
  - B. Dibdiba Basin
  - C. Northern Arabian Gulf Basin
  - D. Rubal Khali Basin
- INTERIOR PLATFORM
- INTERIOR HOMOCLINE
  - E. Tabuk Segment
  - F. Ha'il Arch
  - G. Northern Tuwaiq Segment
  - H. Widyan Basin Margin
  - J. Central Arabian Arch
  - K. Central Arabian Graben and Trough System
  - L. Southern Tuwaiq Segment

PRECAMBRIAN

- PROTEROZOIC ARABIAN SHIELD
- Cinder cones and isolated volcanic pipes
- Historic cinder cones
- Strike and dip of beds
- Synclinal axis, arrow indicates plung
- Anticlinal axis, arrow indicates plung
- Fault / or lineament
- Transcurrent Fault — Riyadh fault system
- High angle Faults, hatchures show downdropped side
- Thrust Fault
- Graben
- Axial trough, Pliocene and Quaternary generated oceanic crust
- Riyadh tilted block
- N-S failure zones

FIGURE 29: MODIFIED TECTONIC MAP
KINGDOM OF SAUDI ARABIA

by S.O. Al-Khatieb (1980)



Source of Data: Brown, G.F., 1972; Greenwood, W.R., 1973; Greenwood, W.R., 1974; Powers, R.W., et al., 1966, Gass & Gibson, 1977

EXPLANATION

PHANEROZOIC (not in chronological order)

- CENOZOIC
  VOLCANIC ROCKS (basalt)
- UPPER MESOZOIC – CENOZOIC
  Sedimentary Rocks Paralleling Red Sea Structure
- PALEOZOIC – MESOZOIC – CENOZOIC
  (not in chronological order)
- ARABIAN SHELF
  BASINS
  - A. Wadi Sirhan Basin
  - B. Dibdiba Basin
  - C. Northern Arabian Gulf Basin
  - D. Rubal Khali Basin
- INTERIOR PLATFORM
- INTERIOR HOMOCLINE
  - E. Tabuk Segment
  - F. Ha'il Arch
  - G. Northern Tuwaiq Segment
  - H. Widyan Basin Margin
  - J. Central Arabian Arch
  - K. Central Arabian Graben and Trough System
  - L. Southern Tuwaiq Segment

PRECAMBRIAN

- PROTEROZOIC
  ARABIAN SHIELD
- Cinder cones and isolated volcanic pipes
- Historic cinder cones
- Strike and dip of beds
- Synclinal axis, arrow indicates plung
- Anticlinal axis, arrow indicates plung
- Fault / or lineament
- Transcurrent Fault — Riyadh fault system
- High angle Faults, hatchures show downdropped side
- Thrust Fault
- Graben
- Axial trough, Pliocene and Quaternary generated oceanic crust
- Riyadh tilted block
- N-S failure zones